Appendix D
ISFSI Safety Analysis Report

LIST OF EFFECTIVE PAGES

LIST OF EFFECTIVE PAGES

Page	Rev.	AR Number
SECTION 2	NA	
2.1-1 through 2.1-2	12	
2.2-1 through 2.2-2	17	
2.3-1 through 2.3-4	9	
2.4-1 through 2.5-9	9	
2.5-1 through 2.6-2	21	604000000330
2.6-1	21	604000000330
Table 2.1-1	17	
Table 2.3-1	9	
Table 2.3-2	9	
Figure 2.1-1	0	
Figure 2.1-2	3	
Figure 2.1-3	3	
Figure 2.3-1	0	
Figure 2.3-2	0	
Figure 2.4-1	0	
Figure 2.4-2	0	
Figure 2.4-3	0	
Figure 2.4-4	0	
Figure 2.5-1	0	
Figure 2.5-2	0	
Figure 2.5-3	0	
Figure 2.5-4	0	
Figure 2.5-5	2	
Figure 2.5-6	21	604000000330
Figure 2.5-7	3	
Figure 2.5-7A	21	604000000330
Figure 2.5-8	3	
Figure 2.5-9	2	

LIST OF EFFECTIVE PAGES

Page	Rev.	AR Number
APPENDIX 2A	NA	
2A-1 through 2A-27	2	
APPENDIX 2B	NA	
2B-1 through 2B-28	2	
APPENDIX 2C	NA	
2C-1 through 2C-38	21	604000000330
SECTION 3	NA	
3.1-1 through 3.1-4	21	604000000330
3.2-1 through 3.2-20	21	604000000330
3.3-1 through 3.3-24	21	604000000330
3.4-1 through 3.4-2	17	
3.5-1 through 3.5-4	17	
Table 3.1-1	9	
Table 3.1-2	9	
Table 3.2-1	9	
Table 3.2-2	9	
Table 3.2-3	9	
Table 3.2-4	9	
Table 3.2-5	9	
Table 3.2-6	9	
Table 3.2-7	9	
Table 3.2-8	9	
Table 3.2-9	9	
Table 3.3-1	9	

LIST OF EFFECTIVE PAGES

Page	Rev.	AR Number
SECTION 3 (continued)	NA	
Table 3.3-2	9	
Table 3.3-3	9	
Table 3.3-4	9	
Table 3.3-5	9	
Table 3.3-6	9	
Table 3.3-7	9	
Table 3.3-8	9	
Table 3.4-1	17	
Table 3.4-2	13	
Figure 3.1-1	0	
Figure 3.1-2	0	
Figure 3.1-3	0	
Figure 3.1-4	2	
Figure 3.2-1	0	
Figure 3.2-2	0	
Figure 3.2-3	0	
Figure 3.2-4	0	
Figure 3.3-1	3	
Figure 3.3-2	2	
Figure 3.3-3	0	
Figure 3.3-4	0	
Figure 3.3-5	0	
Figure 3.3-6	0	
Figure 3.3-7	0	
Figure 3.3-8	0	
Figure 3.3-9	3	
Figure 3.3-10	3	
Figure 3.3-11	3	
Figure 3.3-12	3	

LIST OF EFFECTIVE PAGES

Page	Rev.	AR Number
SECTION 3 (continued)	NA	
Figure 3.3-13	3	
Figure 3.3-14	3	
Figure 3.3-15	0	
Figure 3.3-16	0	
Figure 3.3-17	3	
Figure 3.3-18	0	
Figure 3.3-19	0	
Figure 3.3-20	3	
Figure 3.3-21	3	
APPENDIX 3A	NA	
Cover page, 3A-1 – 3A-16	14	
SECTION 4	NA	
4.1-1 through 4.1-2	21	604000000330
4.2-1 through 4.2-12	21	604000000330
4.3-1 through 4.3-13	21	604000000330
4.4-1 through 4.4-3	21	604000000330
4.5-1 through 4.5-3	21	604000000330
4.6-1 through 4.6-3	17	
4.7-1 through 4.7-2	13	
Table 4.2-1	12	
Table 4.2-2	9	
Table 4.2-3	9	
Table 4.2-4	9	
Table 4.2-5	9	

LIST OF EFFECTIVE PAGES

Page	Rev.	AR Number
SECTION 4 (continued)	NA	
Table 4.2-6	9	
Table 4.2-6a	9	
Table 4.2-7	9	
Table 4.2-8	9	
Table 4.2-9	9	
Table 4.2-10	9	
Table 4.2-11	9	
Table 4.2-12	9	
Table 4.2-13	9	
Table 4.2-14	9	
Table 4.2-15	12	
Table 4.5-1	13	
Table 4.6-1	9	
Table 4.6-2	17	
Table 4.6-3	17	
Figure 4.1-1 (DELETED)	21	604000000330
Figure 4.2-1	21	604000000330
Figure 4.2-1A	21	604000000330
Figure 4.2-2	21	604000000330
Figure 4.2-3 (DELETED)	1	
Figure 4.2-4 (DELETED)	1	
Figure 4.2-5 (DELETED)	1	
Figure 4.2-6	0	
Figure 4.3-1	3	
Figure 4.3-2	3	
Figure 4.3-3	3	
Figure 4.3-4	3	
Figure 4.3-5	3	
Figure 4.3-6	3	

LIST OF EFFECTIVE PAGES

Page	Rev.	AR Number
SECTION 4 (continued)	NA	
Figure 4.3-7	3	
Figure 4.4-1	0	
Figure 4.4-2	0	
Figure 4.4-3	0	
APPENDIX 4A	NA	
4A-1 through 4A-22	12	
Table 4A.2-1	10	
Table 4A.2-2	11	
Table 4A.2-3	9	
Table 4A.3.3-1	9	
Table 4A.3.3-2	9	
Table 4A.3.3-3	9	
Table 4A.3.3-4	9	
Table 4A.3.3-5	9	
Table 4A.3.3-6	9	
Table 4A.3.3-7	9	
Table 4A.3.4.1-1	9	
Table 4A.3.4.1-2	9	
Table 4A.3.4.1-3	9	
Table 4A.3.5-1	9	
Table 4A.3.5-2	9	
Table 4A.3.5-3	9	
Table 4A.3.5-4	9	
Table 4A.3.5-5	9	
Table 4A.3.5-6	9	
Table 4A.3.5-7	9	
Table 4A.3.5-8	9	
Table 4A.6-1	9	

LIST OF EFFECTIVE PAGES

LIST OF EFFECTIVE PAGES

Page	Rev.	AR Number
APPENDIX 4A (continued)	NA	
Figure 4A.7-1	0	
Figure 4A.7-2	0	
APPENDIX 4B	NA	
4B-1 through 4B-12	9	
Table 4B.1-1	9	
Table 4B.1-2	9	
Table 4B.1-3	9	
Table 4B.1-4	9	
Figure 4B.2-1	8	
Figure 4B.2-2	1	
Figure 4B.2-3	1	
Figure 4B.2-4	1	
Figure 4B.2-5	1	
Figure 4B.2-6	1	
Figure 4B.2-7	1	
Figure 4B.2-8	1	
Figure 4B.2-9	1	
Figure 4B.3-12	1	
Figure 4B.3-13	1	
Figure 4B.6-1	1	
Figure 4B.6-2	1	
Figure 4B.6-3	8	
Figure 4B.6-4	8	
Figure 4B.6-5	1	
Figure 4B.6-6	8	
Figure 4B.6-7	8	
Figure 4B.7-1	8	

LIST OF EFFECTIVE PAGES

Page	Rev.	AR Number
APPENDIX 4C	NA	
4C-1 through 4C-4	9	
Figure 4C.1-1	1	
Figure 4C.1-2	1	
Figure 4C.1-3	1	
Figure 4C.1-4	1	
Figure 4C.1-5	1	
Figure 4C.1-6	1	
Figure 4C.2-1	1	
SECTION 5	NA	
5.1-1 through 5.1-3	21	604000000330
5.2-1	9	
5.3-1	9	
5.4-1	21	604000000330
5.5-1	9	
5.6-1	9	
Table 5.1-1	11	
Table 5.1-2	17	
Figure 5.1-1	20	
Figure 5.4-1	20	
SECTION 6	NA	
6.1-1 through 6.1-2	9	
6.2-1 through 6.2-2	9	

LIST OF EFFECTIVE PAGES

Page	Rev.	AR Number
SECTION 7	NA	
7.1-1 through 7.1-6	12	
7.2-1 through 7.2-2	9	
7.3-1 through 7.3-2	21	604000000330
7.4-1 through 7.4-2	21	604000000330
7.5-1 through 7.5-2	13	
7.6-1 through 7.6-2	11	
7.7-1 through 7.7-2	9	
7.8-1 through 7.8-2	9	
Table 7.2-1	9	
Table 7.2-2	9	
Table 7.2-3	9	
Table 7.2-3a	9	
Table 7.2-4	9	
Table 7.2-5	9	
Table 7.2-6	9	
Table 7.2-7	9	
Table 7.4-1	9	
Table 7.4-2	9	
Table 7.4-3 (DELETED)	13	
Table 7.4-4 (DELETED)	13	
Table 7.4-6 (DELETED)	13	
Figure 7.4-1 (DELETED)	13	

LIST OF EFFECTIVE PAGES

Page	Rev.	AR Number
APPENDIX 7A	NA	
7A-1 through 7A-4	13	
Table 7A-1	9	
Table 7A-2	9	
Table 7A-3	9	
Table 7A-4	9	
Table 7A-5 (DELETED)	13	
Table 7A-5a (DELETED)	13	
Table 7A-5b (DELETED)	13	
Table 7A-6 (DELETED)	13	
Table 7A-7 (DELETED)	21	604000000330
Table 7A-8 (DELETED)	13	
Figure 7A-1	3	
Figure 7A-2	3	
Figure 7A-3	0	
Figure 7A-4	0	
Figure 7A-5	0	
Figure 7A-6	2	
Figure 7A-7 (DELETED)	13	
Figure 7A-8 (DELETED)	2	
Figure 7A-9 (DELETED)	2	
Figure 7A-10 (DELETED)	13	
Figure 7A-11 (DELETED)	13	
APPENDIX 7B	NA	
Cover page, 7B-1 – 7B-5	14	

LIST OF EFFECTIVE PAGES

Page	Rev.	AR Number
SECTION 8	NA	
8.1-1 through 8.1-2	9	
8.2-1 through 8.2-14	21	604000000330
8.3-1 through 8.3-2	9	
8.4-1 through 8.4-2	9	
Table 8.2-1	9	
Figure 8.2.1 (DELETED)	1	
Figure 8.2-1A	3	
Figure 8.2-1B	5	
Figure 8.2-1C	3	
Figure 8.2-1D	3	
Figure 8.2.2 (DELETED)	1	
Figure 8.2-5	8	
Figure 8.2.20 (DELETED)	1	
Figure 8.2.21 (DELETED)	1	
Figure 8.2.22 (DELETED)	1	
Figure 8.2-33	0	
SECTION 9	NA	
9.1-1 through 9.1-3	21	604000000330
9.2-1 through 9.2-2	18	
9.3-1	9	
9.4-1 through 9.4-2	15	
9.5-1	11	
9.6-1	15	
9.7-1	9	
9.8-1 through 9.8-3	17	
9.9-1	18	

LIST OF EFFECTIVE PAGES

Page	Rev.	AR Number
SECTION 9 (continued)		
Table 9.8-1	17	
Figure 9.1-1 (DELETED)	21	60400000860
Figure 9.1-2 (DELETED)	21	60400000860
Figure 9.1-3 (DELETED)	21	60400000860
Figure 9.1-4 (DELETED)	18	
SECTION 10	NA	
10.1-1 through 10.1-4	9	
10.2-1	9	
10.3-1 through 10.3-2	9	
10.4-1 through 10.4-2	21	604000000330
10.5-1 through 10.5-2	9	
10.6-1 through 10.6-2	9	
SECTION 11	NA	
11.1-1 through 11.1-6	20	
11.2-1 through 11.2-2	21	604000000330
11.3-1 through 11.3-2	21	604000000330

ADDENDUM
LIST OF EFFECTIVE PAGES

ADDENDUM
LIST OF EFFECTIVE PAGES

Page	Rev.	AR Number
SECTION A1 (continued)	NA	
Figure TN-40HT-72-21 Figure TN-40HT-72-21 (2 of 7 pages)	19 17	
Figure TN-40HT-72-21 Figure TN-40HT-72NP-21 (3 of 7 pages)	19 13	
Figure TN-40HT-72-21 Figure TN-40HT-72NP-21 (4 of 7 pages)	19 13	
Figure TN-40HT-72-21 Figure TN-40HT-72NP-21 (5 of 7 pages)	19 13	
Figure TN-40HT-72-21 Figure TN-40HT-72NP-21 (6 of 7 pages)	19 13	
Figure TN-40HT-72-21 Figure TN-40HT-72NP-21 (7 of 7 pages)	19 13	
Figure TN-40HT-72-22 Figure TN-40HT-72NP-22 (1 of 8 pages)	19 13	
Figure TN-40HT-72-22 Figure TN-40HT-72NP-22 (2 of 8 pages)	19 13	
Figure TN-40HT-72-22 (3 of 8 pages)	19	
Figure TN-40HT-72-22 (4 of 8 pages)	19	
Figure TN-40HT-72-22 (5 of 8 pages)	19	
Figure TN-40HT-72-22 (6 of 8 pages)	19	
Figure TN-40HT-72-22 (7 of 8 pages)	19	

ADDENDUM
LIST OF EFFECTIVE PAGES

Page	Rev.	AR Number
SECTION A1 (continued)	NA	
Figure TN-40HT-72-22 (8 of 8 pages)	19	
SECTION A2	NA	
A2.1-1 through A2.1-2	13	
A2.2-1 through A2.2-2	13	
A2.3-1 through A2.3-2	13	
A2.4-1 through A2.4-2	13	
A2.5-1 through A2.5-2	13	
A2.6-1 through A2.6-2	13	
SECTION A2A	NA	
A2A-1 through A2A-2	13	
SECTION A2B	NA	
A2B-1 through A2B-2	13	

ADDENDUM
LIST OF EFFECTIVE PAGES

Page	Rev.	AR Number
SECTION A3	NA	
A3.1-1 through A3.1-3	20	
A3.2-1 through A3.2-24	21	604000000330
A3.3-1 through A3.3-64	21	604000000330
A3.4-1	17	
A3.5-1 through A3.5-3	13	
A3.6-1 through A3.6-4	21	604000000330
Table A3.1-1	13	
Table A3.1-2	13	
Table A3.1-3	13	
Table A3.2-1	13	
Table A3.2-2	15	
Table A3.2-3	13	
Table A3.2-4	13	
Table A3.2-5	13	
Table A3.2-6	13	
Table A3.2-7	13	
Table A3.2-8	13	
Table A3.2-9	13	
Table A3.2-10	13	
Table A3.3-1	13	
Table A3.3-2	13	
Table A3.3-3	21	604000000330
Table A3.3-4	21	604000000330
Table A3.3-5	21	604000000330
Table A3.3-6	21	604000000330
Table A3.3-7	21	604000000330
Table A3.3-8	13	
Table A3.3-9	13	

ADDENDUM
LIST OF EFFECTIVE PAGES

Page	Rev.	AR Number
SECTION A3 (continued)	NA	
Table A3.3-10	13	
Table A3.3-10A	21	604000000330
Table A3.3-11	13	
Table A3.3-12	13	
Table A3.3-13	15	
Table A3.3-14	15	
Table A3.3-15	21	604000000330
Table A3.3-16	21	604000000330
Table A3.3-17	13	
Table A3.3-18	13	
Table A3.3-19	13	
Table A3.3-20	13	
Table A3.3-21	13	
Table A3.3-22	18	
Table A3.3-23	18	
Table A3.3-24	13	
Table A3.3-25	13	
Table A3.3-26	13	
Table A3.3-27	13	
Table A3.3-28	13	
Table A3.3-29	13	
Table A3.3-30	13	
Table A3.3-31	13	
Table A3.3-32	13	
Table A3.3-33	15	
Table A3.3-34	16	
Table A3.3-35	16	
Table A3.3-36	21	604000000330

ADDENDUM
LIST OF EFFECTIVE PAGES

Page	Rev.	AR Number
SECTION A3 (continued)	NA	
Table A3.3-37	21	604000000330
Table A3.3-38	21	604000000330
Table A3.3-39	16	
Table A3.4-1	17	
Table A3.4-2	16	
Figure A3.2-1	13	
Figure A3.2-2	13	
Figure A3.2-3	13	
Figure A3.3-1	13	
Figure A3.3-2	13	
Figure A3.3-3	13	
Figure A3.3-4	13	
Figure A3.3-5	15	
Figure A3.3-6	13	
Figure A3.3-7	13	
Figure A3.3-8	13	
Figure A3.3-9	13	
Figure A3.3-10	13	
Figure A3.3-11	15	
Figure A3.3-12	15	
Figure A3.3-13	13	
Figure A3.3-14	15	
Figure A3.3-15	15	
Figure A3.3-16	13	
Figure A3.3-17	13	
Figure A3.3-18	13	
Figure A3.3-19	13	
Figure A3.3-20	13	

ADDENDUM
LIST OF EFFECTIVE PAGES

Page	Rev.	AR Number
SECTION A3 (continued)	NA	
Figure A3.3-21	13	
Figure A3.3-21A	21	604000000330
Figure A3.3-22	13	
Figure A3.3-23	13	
Figure A3.3-24	13	
Figure A3.3-25	13	
Figure A3.3-26	15	
Figure A3.3-27	15	
Figure A3.3-28	13	
Figure A3.3-29	13	
Figure A3.3-30	13	
Figure A3.3-31	13	
Figure A3.3-32	13	
Figure A3.3-33	13	
Figure A3.3-34	13	
Figure A3.3-35	13	
Figure A3.3-36	13	
Figure A3.3-37	13	
Figure A3.3-38	13	
Figure A3.3-39	13	
Figure A3.3-40	13	
Figure A3.3-41	13	
Figure A3.3-42	16	
Figure A3.3-43	16	
Figure A3.3-44	16	

ADDENDUM
LIST OF EFFECTIVE PAGES

Page	Rev.	AR Number
SECTION A3A	NA	
A3A-1 through A3A-2	21	604000000330
A3A.1-1 through A3A.1-10	13	
A3A.2-1 through A3A.2-10	13	
SECTION A4	NA	
A4.1-1 through A4.1-2	21	604000000330
A4.2-1 through A4.2-28	21	604000000330
A4.3-1 through A4.3-2	21	604000000330
A4.4-1 through A4.4-2	13	
A4.5-1 through A4.5-2	13	
A4.6-1 through A4.6-3	17	
A4.7-1 through A4.7-3	21	604000000330
Table A4.2-1	13	
Table A4.2-2	13	
Table A4.2-3	13	
Table A4.2-4	13	
Table A4.2-5	13	
Table A4.2-6	13	
Table A4.2-7	13	
Table A4.2-8	13	
Table A4.2-9	13	
Table A4.2-10	13	
Table A4.2-11	13	
Table A4.2-12	13	
Table A4.2-13	13	
Table A4.2-14	13	
Table A4.2-15	13	

ADDENDUM
LIST OF EFFECTIVE PAGES

Page	Rev.	AR Number
SECTION A4 (continued)	NA	
Table A4.2-16	13	
Table A4.2-17	13	
Table A4.2-18	13	
Table A4.2-19	13	
Table A4.2-20	15	
Table A4.2-21	15	
Table A4.2-22	15	
Table A4.2-23	15	
Table A4.2-24	15	
Table A4.2-25	13	
Table A4.2-26	13	
Table A4.5-1	13	
Table A4.6-1	17	
Table A4.6-2	17	
Figure A4.2-1	13	
Figure A4.2-2	13	
Figure A4.2-3	13	
Figure A4.2-4	13	
Figure A4.2-5	13	
Figure A4.2-6	13	
Figure A4.2-7	13	
Figure A4.2-8	13	
Figure A4.2-9	13	
Figure A4.2-10	13	
Figure A4.2-11	13	
Figure A4.2-12	13	
Figure A4.2-13	13	
Figure A4.2-14	13	

ADDENDUM
LIST OF EFFECTIVE PAGES

Page	Rev.	AR Number
SECTION A4 (continued)	NA	
Figure A4.2-15	13	
Figure A4.2-16	13	
SECTION A4A	NA	
A4A.1-1 through A4A.1-2	13	
A4A.2-1 through A4A.2-2	13	
A4A.3-1 through A4A.3-10	13	
A4A.4-1 through A4A.4-10	13	
A4A.5-1 through A4A.5-8	15	
A4A.6-1 through A4A.6-6	13	
A4A.7-1 through A4A.7-4	13	
A4A.8-1 through A4A.8-4	13	
A4A.9-1 through A4A.9-4	13	
A4A.10-1 through A4A.10-6	13	
A4A.11-1 through A4A.11-2	13	
Table A4A.2-1	13	
Table A4A.3-1	13	
Table A4A.3-2	13	
Table A4A.4-1	15	
Table A4A.4-2	13	
Table A4A.4-3	13	
Table A4A.4-4	13	
Table A4A.4-5	13	
Table A4A.4-6	13	
Table A4A.4-7	13	
Table A4A.5-1	13	
Table A4A.5-2	13	

ADDENDUM
LIST OF EFFECTIVE PAGES

Page	Rev.	AR Number
SECTION A4A (continued)	NA	
Table A4A.5-3	21	604000000330
Table A4A.5-4	15	
Table A4A.5-5	15	
Table A4A.6-1	13	
Table A4A.6-2	13	
Table A4A.6-3	13	
Table A4A.6-4	13	
Table A4A.7-1	13	
Table A4A.7-2	13	
Table A4A.8-1	13	
Table A4A.8-2	13	
Table A4A.8-3	13	
Table A4A.9-1	13	
Table A4A.9-2	13	
Table A4A.9-3	13	
Table A4A.9-4	13	
Figure A4A.3-1	13	
Figure A4A.3-2	13	
Figure A4A.3-3	13	
Figure A4A.3-4	13	
Figure A4A.3-5	13	
Figure A4A.3-6	13	
Figure A4A.3-7	13	
Figure A4A.3-8	13	
Figure A4A.3-9	13	
Figure A4A.3-10	13	
Figure A4A3-11	13	
Figure A4A.3-12	13	

ADDENDUM
LIST OF EFFECTIVE PAGES

Page	Rev.	AR Number
SECTION A4A (continued)	NA	
Figure A4A.3-13	13	
Figure A4A.3-14	13	
Figure A4A.3-15	13	
Figure A4A.6-1	13	
Figure A4A.6-2	13	
Figure A4A.7-1	13	
Figure A4A.7-2	13	
Figure A4A.9-1	13	
Figure A4A.9-2	13	
Figure A4A.10-1	13	
Figure A4A.10-2	13	
Figure A4A.10-3	13	
Figure A4A.10-4	13	
Figure A4A.10-5	13	
Figure A4A.10-6	13	
SECTION A4B	NA	
A4B.1-1 through A4B.1-12	13	
A4B.2-1 through A4B.2-2	13	
Table A4B.1-1	13	
Table A4B.1-2	13	
Table A4B.1-3	13	
Table A4B.1-4	13	
Table A4B.1-5	13	
Table A4B.1-6	13	
Figure A4B.1-1	13	
Figure A4B.1-2	13	

ADDENDUM
LIST OF EFFECTIVE PAGES

Page	Rev.	AR Number
SECTION A4B (continued)	NA	
Figure A4B.1-3	13	
Figure A4B.1-4	13	
Figure A4B.1-5	13	
Figure A4B.1-6	13	
Figure A4B.1-7	13	
Figure A4B.1-8	13	
Figure A4B.1-9	13	
Figure A4B.1-10	13	
Figure A4B.1-11	13	
Figure A4B.1-12	13	
Figure A4B.1-13	13	
Figure A4B.1-14	13	
Figure A4B.1-15	13	
Figure A4B.1-16	13	
Figure A4B.1-17	13	
Figure A4B.1-18	13	
Figure A4B.1-19	13	
Figure A4B.1-20	13	
Figure A4B.1-21	13	
Figure A4B.1-22	13	
SECTION A5	NA	
A5.1-1 through A5.1-2	13	
A5.2-1 through A5.2-2	13	
A5.3-1 through A5.3-2	13	
A5.4-1 through A5.4-2	13	
A5.5-1 through A5.5-2	13	
A5.6-1 through A5.6-2	13	

ADDENDUM
LIST OF EFFECTIVE PAGES

Page	Rev.	AR Number
SECTION A6	NA	
A6.1-1 through A6.1-2	13	
SECTION A7	NA	
A7.1-1	13	
A7.2-1 through A7.2-9	13	
A7.3-1 through A7.3-2	13	
A7.4-1 through A7.4-2	21	604000000330
A7.5-1	21	604000000330
A7.6-1	13	
A7.7-1	13	
A7.8-1	17	
Table A7.2-1	13	
Table A7.2-2	13	
Table A7.2-3	13	
Table A7.2-4	13	
Table A7.2-5	13	
Table A7.2-6	13	
Table A7.2-7	13	
Table A7.2-8	13	
Table A7.2-9	13	
Table A7.2-10	13	
Table A7.2-11	13	
Table A7.2-12	13	
Table A7.4-1	13	
Table A7.4-2	13	
Table A7.4-3	21	604000000330

ADDENDUM
LIST OF EFFECTIVE PAGES

ADDENDUM
LIST OF EFFECTIVE PAGES

Page	Rev.	AR Number
SECTION A7A (continued)	NA	
Table A7A.6-1	13	
Table A7A.7-1	13	
Table A7A.7-2	21	604000000330
Table A7A.7-3	21	604000000330
Table A7A.7-4	13	
Table A7A.8-1	13	
Table A7A.8-2	13	
Table A7A.8-3	13	
Table A7A.8-4	13	
Table A7A.8-5	13	
Table A7A.8-6	13	
Figure A7A.1-1	13	
Figure A7A.2-1	13	
Figure A7A.4-1	13	
Figure A7A.4-2	13	
Figure A7A.4-3	13	
Figure A7A.4-4	13	
Figure A7A.5-1	13	
Figure A7A.5-2	13	
Figure A7A.5-3	13	
Figure A7A.5-4	13	
Figure A7A.5-5	13	
Figure A7A.5-6	13	
Figure A7A.5-7	13	
Figure A7A.5-8	13	
Figure A7A.5-9	13	
Figure A7A.6-1	13	
Figure A7A.7-1	13	

ADDENDUM
LIST OF EFFECTIVE PAGES

Page	Rev.	AR Number
SECTION A7A (continued)	NA	
Figure A7A.8-1	13	
Figure A7A.8-2	13	
SECTION A7B	NA	
A7B-1 through A7B-2	13	
A7B.1-1 through A7B.1-4	13	
A7B.2-1 through A7B.2-18	13	
A7B.3-1 through A7B.3-18	13	
A7B.4-1 through A7B.4-24	13	
SECTION A8	NA	
A8.1-1 through A8.1-2	13	
A8.2-1 through A8.2-10	21	604000000330
A8.3-1 through A8.3-2	13	
A8.4-1 through A8.4-2	13	
SECTION A9	NA	
A9.1-1	13	
A9.2-1	13	
A9.3-1	13	
A9.4-1	13	
A9.5-1	13	
A9.6-1	13	
A9.7-1 through A9.7-12	16	
A9.8-1 through A9.8-4	17	

ADDENDUM
LIST OF EFFECTIVE PAGES

Page	Rev.	AR Number
SECTION A9 (continued)	NA	
A9.9-1 through A9.9-2	17	
Table A9.7-1	13	
Table A9.7-2	16	
SECTION A10	NA	
A10-1 through A10-2	13	
SECTION A11	NA	
A11.1-1 through A11.1-4	13	
A11.2-1 through A11.2-2	13	
A11.3-1 through A11.3-2	13	

LIST OF EFFECTIVE PAGES

RECORD OF REVISIONS

Revision (Rev) No.	Effective Date	Date of Issue	Remarks
ORIGINAL	8/90	8/31/90	
1	4/91	4/2/91	
2	9/91	9/26/91	
3	4/94	4/18/94	
4	10/95	10/19/95	
5	10/96	10/21/96	
6	10/97	10/20/97	
7	10/98	10/19/98	
8	10/99	10/19/99	
9	10/01	10/01	
10	10/05	10/05	
11	10/07	10/07	
12	10/09	10/09	
13	8/10	10/10	
14	9/11	9/11	
15	2/14	2/14	
16	11/15	11/15	
17	3/8/16	3/8/16	
18	10/13/17	10/13/17	
19	10/6/19	10/6/19	
20	10/8/21	10/8/21	
21	10/9/23	10/9/23	

INDEX
ADDENDUM

SECTION 1 – INTRODUCTION AND GENERAL DESCRIPTION OF STORAGE SYSTEM

SECTION 1 TABLES

SECTION 1 FIGURES

INDEX (Cont'd)

SECTION 2 – SITE CHARACTERISTICS

INDEX (Cont'd)

SECTION 2 – SITE CHARACTERISTICS (CONT'D)

SECTION 2 TABLES

SECTION 2 FIGURES

INDEX (Cont'd)

INDEX (Cont'd)

SECTION 3 – PRINCIPAL CASK DESIGN CRITERIA (CONT'D)

SECTION 3 TABLES

INDEX (Cont'd)

SECTION 3 – PRINCIPAL CASK DESIGN CRITERIA (CONT'D)

SECTION 3 FIGURES

INDEX (Cont'd)

SECTION 3 – PRINCIPAL CASK DESIGN CRITERIA (CONT'D)

SECTION 3 FIGURES (CONT'D)

INDEX (Cont'd)

INDEX (Cont'd)

SECTION 4 – STORAGE SYSTEM (CONT'D)

SECTION 4 TABLES

INDEX (Cont'd)

SECTION 4 – STORAGE SYSTEM (CONT'D)

SECTION 4 TABLES (CONT'D)

SECTION 4 FIGURES

INDEX (Cont'd)

INDEX (Cont'd)

APPENDIX 4A – STRUCTURAL ANALYSIS OF THE TN-40 CASK BODY (CONT'D)

APPENDIX 4A TABLES (CONT'D)

INDEX (Cont'd)

APPENDIX 4A – STRUCTURAL ANALYSIS OF THE TN-40 CASK BODY (CONT'D)

APPENDIX 4A TABLES (CONT'D)

APPENDIX 4A FIGURES

INDEX (Cont'd)

APPENDIX 4A – STRUCTURAL ANALYSIS OF THE TN-40 CASK BODY (CONT'D)

APPENDIX 4A FIGURES (CONT'D)

INDEX (Cont'd)

INDEX (Cont'd)

APPENDIX 4B – STRUCTURAL ANALYSIS OF THE TN-40 BASKET (CONT'D)

APPENDIX 4B FIGURES (CONT'D)

INDEX (Cont'd)

INDEX (Cont'd)

INDEX (Cont'd)

SECTION 7 – RADIATION PROTECTION

SECTION 7 TABLES

INDEX (Cont'd)

SECTION 7 – RADIATION PROTECTION (CONT'D)

SECTION 7 TABLES (CONT'D)

SECTION 7 FIGURES

INDEX (Cont'd)

APPENDIX 7A – TN-40 CASK DOSE ANALYSIS

APPENDIX 7A TABLES

INDEX (Cont'd)

INDEX (Cont'd)

SECTION 8 – ACCIDENT ANALYSIS

SECTION 8 TABLES

INDEX (Cont'd)

SECTION 8 – ACCIDENT ANALYSIS (CONT'D)

SECTION 8 FIGURES

INDEX (Cont'd)

INDEX (Cont'd)

INDEX (Cont'd)

SECTION 11 – QUALITY ASSURANCE

INDEX
ADDENDUM

SECTION A1 – INTRODUCTION AND GENERAL DESCRIPTION OF STORAGE SYSTEM

INDEX (Cont'd)
ADDENDUM

SECTION A1 – INTRODUCTION AND GENERAL DESCRIPTION OF STORAGE SYSTEM (CONT'D)

SECTION A1 FIGURES (CONT'D)

INDEX (Cont'd)
ADDENDUM

INDEX (Cont'd)
ADDENDUM

SECTION A3 – PRINCIPAL TN-40HT CASK DESIGN CRITERIA

INDEX (Cont'd)
ADDENDUM

SECTION A3 – PRINCIPAL TN-40HT CASK DESIGN CRITERIA (CONT'D)

SECTION A3 TABLES

INDEX (Cont'd)
ADDENDUM

SECTION A3 – PRINCIPAL TN-40HT CASK DESIGN CRITERIA (CONT'D)

SECTION A3 TABLES (CONT'D)

INDEX (Cont'd)
ADDENDUM

SECTION A3 – PRINCIPAL TN-40HT CASK DESIGN CRITERIA (CONT'D)

SECTION A3 TABLES (CONT'D**)**

INDEX (Cont'd)
ADDENDUM

SECTION A3 – PRINCIPAL TN-40HT CASK DESIGN CRITERIA (CONT'D)

SECTION A3 FIGURES

INDEX (Cont'd)
ADDENDUM

SECTION A3 – PRINCIPAL TN-40HT CASK DESIGN CRITERIA (CONT'D)

SECTION A3 FIGURES (CONT'D)

INDEX (Cont'd)
ADDENDUM

SECTION A3 – PRINCIPAL TN-40HT CASK DESIGN CRITERIA (CONT'D)

SECTION A3 FIGURES (CONT'D)

INDEX (Cont'd)
ADDENDUM

INDEX (Cont'd)
ADDENDUM

SECTION A4 – STORAGE SYSTEM (CONT'D)

SECTION A4 TABLES

INDEX (Cont'd)
ADDENDUM

SECTION A4 – STORAGE SYSTEM (CONT'D)

SECTION A4 TABLES (CONT'D)

INDEX (Cont'd)
ADDENDUM

SECTION A4 – STORAGE SYSTEM (CONT'D)

SECTION A4 TABLES (CONT'D)

SECTION A4 FIGURES

INDEX (Cont'd)
ADDENDUM

INDEX (Cont'd)
ADDENDUM

APPENDIX A4A – STRUCTURAL ANALYSIS OF THE TN-40HT CASK BODY (CONT'D)

INDEX (Cont'd)
ADDENDUM

INDEX (Cont'd)
ADDENDUM

APPENDIX A4A – STRUCTURAL ANALYSIS OF THE TN-40HT CASK BODY (CONT'D)

APPENDIX A4A TABLES

INDEX (Cont'd)
ADDENDUM

APPENDIX 4A – STRUCTURAL ANALYSIS OF THE TN-40 CASK BODY (CONT'D)

APPENDIX A4A TABLES (CONT'D)

INDEX (Cont'd)
ADDENDUM

APPENDIX A4A – STRUCTURAL ANALYSIS OF THE TN-40 CASK BODY (CONT'D)

APPENDIX A4A FIGURES

INDEX (Cont'd)
ADDENDUM

APPENDIX A4A – STRUCTURAL ANALYSIS OF THE TN-40 CASK BODY (CONT'D)

APPENDIX A4A FIGURES (CONT'D)

INDEX (Cont'd)
ADDENDUM

APPENDIX A4B – STRUCTURAL ANALYSIS OF THE TN-40HT BASKET

APPENDIX A4B TABLES

APPENDIX A4B FIGURES

INDEX (Cont'd)
ADDENDUM

APPENDIX A4B – STRUCTURAL ANALYSIS OF THE TN-40HT BASKET (CONT'D)

APPENDIX A4B FIGURES (CONT'D)

INDEX (Cont'd)
ADDENDUM

APPENDIX A4B – STRUCTURAL ANALYSIS OF THE TN-40HT BASKET (CONT'D)

APPENDIX A4B FIGURES (CONT'D)

SECTION A5 – STORAGE SYSTEM OPERATIONS

INDEX (Cont'd)
ADDENDUM

INDEX (Cont'd)
ADDENDUM

SECTION A7 – RADIATION PROTECTION (CONT'D)

SECTION A7 TABLES

INDEX (Cont'd)
ADDENDUM

SECTION A7 – RADIATION PROTECTION (CONT'D)

SECTION A7 TABLES (CONT'D)

SECTION A7 FIGURES

INDEX (Cont'd)
ADDENDUM

INDEX (Cont'd)
ADDENDUM

APPENDIX A7A – TN-40HT CASK DOSE ANALYSIS (CONT'D)

APPENDIX A7A TABLES

INDEX (Cont'd)
ADDENDUM

APPENDIX A7A – TN-40HT CASK DOSE ANALYSIS (CONT'D)

APPENDIX A7A TABLES (CONT'D)

APPENDIX A7A FIGURES

INDEX (Cont'd)
ADDENDUM

APPENDIX A7A – TN-40HT CASK DOSE ANALYSIS (CONT'D)

APPENDIX A7A FIGURES (CONT'D)

INDEX (Cont'd)
ADDENDUM

APPENDIX A7B – TN-40HT SHIELDING EVALUATION COMPUTER INPUT

INDEX (Cont'd)
ADDENDUM

INDEX (Cont'd)
ADDENDUM

INDEX (Cont'd)
ADDENDUM

INDEX (Cont'd)
ADDENDUM

SECTION A1

INTRODUCTION AND GENERAL DESCRIPTION OF STORAGE SYSTEM

A1.1 INTRODUCTION

Section 1.1 provides historical information regarding the need to provide dry storage at the Prairie Island Independent Spent fuel Storage Installation. The information in Section 1.1 remains relevant and is applicable for storage utilizing the TN-40HT dry casks with the exception that the descriptions of the fuel to be stored and the description of the TN-40HT dry cask is contained within this Addendum. The TN-40HT cask is a modified version of the TN-40 dry cask and is designed for high enrichment and high burnup fuel.

A1.2 GENERAL DESCRIPTION OF LOCATION

The information in Section 1.2 is independent of cask design.

A1.3 GENERAL STORAGE SYSTEM DESCRIPTION

The description of the ISFSI site including the storage building contained in Section 1.3 is independent of the cask design. A general description of the TN-40HT casks is contained in the following sections.

A1.3.1 TN-40HT General Description

The TN-40HT cask is very similar in design to the TN-40 cask. The major difference is that the TN-40HT cask is designed to store higher enrichment and higher burnup fuel. In order to accomplish this, the heat transfer capability of the basket design was enhanced. Additionally, to accommodate the enhanced basket, some minor changes were made to the cask body. The TN-40HT cask employs a slightly thinner lid, shield shell and cask bottom shield. However, the radial neutron shield thickness is increased to offset the higher neutron source of the high burnup fuel.

The TN-40HT cask accommodates up to 40, 14x14 PWR fuel assemblies with or without fuel inserts. It consists of the following components:

- A basket assembly which locates and supports the fuel assemblies, transfers heat to the cask body wall, and provides neutron absorption to satisfy nuclear criticality requirements.

- A containment vessel including a bolted closure lid and seals which provides radioactive material confinement and a cavity with an inert gas atmosphere.

- Gamma shielding surrounding the containment vessel.

- Radial neutron shielding surrounding the shield shell which provides additional radiation shielding. This neutron shielding is enclosed in an outer steel shell.

- A top neutron shield which is attached to the outer surface of the cask lid and provides additional neutron shielding.

- An overpressure system which monitors and maintains the pressure between the cask closure seals and provides a positive pressure differential across the inner seals so that any inner seal leak will result in inleakage to the cask cavity.

- A protective cover which provides weather protection for the closure lid, top neutron shield and overpressure system.

- Sets of upper and lower trunnions which provide the means for lifting and rotating the cask.

The maximum allowable initial enrichment of the fuel to be stored in a TN-40HT cask is 5.0 wt% U^{235}. The maximum bundle average burnup, maximum decay heat, and minimum cooling time are 60 GWd/MTU, 0.80 kW/assembly, and 12 years, respectively. The cask is designed for a maximum heat load of 32 kW.

A1.3.2 TN-40HT cask Characteristics

Each TN-40HT cask consists of a fuel basket, a cask body (shell, shell flange, bottom, and lid), a protective cover, an overpressure system, four trunnions, penetrations with bolted and sealed covers for leak detection and venting, closure bolts and locating pins.

A set of reference drawings is presented in Section A1.5. The cask is a self-supporting cylindrical vessel. Dimensions and the estimated weight of the cask are shown in Table A1.3-1. Where more than one material has been specified for a component, the most limiting properties are used in the analyses in the subsequent sections of this addendum.

The TN-40HT containment boundary components are shown in Figure A1.3-1. The containment vessel for the TN-40HT cask consists of: an inner shell (1) which is a welded, low alloy steel cylinder with a low alloy steel bottom closure; a welded shell flange (3); a low alloy steel lid with bolts and metal seals (2); and vent and drain covers with bolts and metal seals (4 and 5). The overall containment vessel length, wall thickness, cask cavity diameter, and length are shown in Table A1.3-1.

There are two penetrations through the lid. One is for draining and the other is for venting. A double-seal mechanical closure is provided for each penetration. The lid is fastened to the flange by 48 bolts. A double metal seal with interspace leakage monitoring is provided for the lid closure. To preclude air in-leakage, the cask cavity is pressurized above atmospheric pressure with helium.

The pressure monitoring system is the same as the TN-40 cask system. The interspace between the metal seals is connected to an overpressure tank and a pressure monitoring system. The overpressure tank and the interspace between the metal seals are pressurized with helium to a higher level than the cavity so that any seal leakage would result in flow into the cavity. A decrease in the pressure of the monitoring system would be signaled by a pressure transducer/switch wired to a monitoring/alarm panel.

For weather protection, a steel torispherical weather cover with an elastomeric seal is installed over the lid and bolted to the shell flange.

The materials used for neutron and gamma shielding are the same as those used for the TN-40 cask. A gamma shield is provided around the walls and bottom of the containment vessel by an independent shell and bottom shield of carbon steel which is welded to the shell flange. The gamma shield surrounds the containment vessel inner shell and bottom closure. A lid shield plate is also welded to the inside of the containment lid.

Neutron shielding is provided by a borated polyester resin compound surrounding the cask body. The resin compound is cast into long, slender aluminum containers. The array of resin-filled containers is enclosed within a smooth outer steel shell. In addition to serving as resin containers, the aluminum provides a heat conduction path from the cask body to the outer shell. A pressure relief valve is mounted on the top of the resin enclosure for venting pressure due to heating of the resin and entrapped air after fuel loading.

A 4.0 inch thick nominal disc of polypropylene enclosed by steel plates is attached to the cask lid to provide neutron shielding during storage.

The basket structure consists of an assembly of rectangular stainless steel tubes joined by a proprietary fusion welding process to 1.75 in. wide stainless steel bars. Above and below the bars are slotted Boral®, borated aluminum or boron carbide/aluminum metal matrix composite plates (neutron poison plates) and aluminum plates which form an egg-crate structure. The poison plates provide the necessary criticality control and aluminum plates provide the heat conduction paths from the fuel assemblies to the cask cavity wall. This method of construction forms a very strong honeycomb-like structure of cell liners which provide compartments for 40 fuel assemblies. The nominal open dimension of each cell is 8.05 in. x 8.05 in. which provides clearance around the fuel assemblies. The overall basket length is less than the cask cavity length to allow for thermal expansion and fuel assembly handling.

The cask cavity surfaces and outer shell have a sprayed metallic coating of Zn/Al for corrosion protection similar to the TN-40 cask. The external surfaces of the cask are also painted for ease of decontamination.

A stainless steel overlay is applied to the cask and lid wherever sealing surfaces for the metallic seals are required.

Four trunnions are attached to the cask for lifting and rotation of the cask. Two of the trunnions are located near the top of the cask and two near the bottom. The upper trunnions are sized for lifting. The lower trunnions are used for rotating the cask between vertical and horizontal positions.

Threaded holes are provided in the lid and top neutron shield for attachment of component lifting devices.

During dry storage of the spent fuel, no active systems are required for the removal and dissipation of the decay heat from the fuel. The TN-40HT cask is designed to transfer the decay heat from the fuel to the basket, from the basket to the cask body and ultimately to the environment by radiation and natural convection. The cask is capable of removing 32 kW of decay heat without external fins, thus providing a smooth outer surface for ease of decontamination.

A1.4 IDENTIFICATION OF AGENTS AND CONTRACTORS

The agents and contractors associated with the TN-40HT casks are the same as those described in Section 1.4 for the TN-40 casks.

A1.5 SUPPLEMENTAL DATA

The following TN Drawings are enclosed:

- TN-40HT Cask (Drawings TN40HT-72-1 through 10)
- TN-40HT Basket (Drawings TN40HT-72-21, sheets 1 through 7)
- TN-40HT Basket Rails (Drawings TN40HT-72-22, sheets 1 and 2)

A1.6 REFERENCES

None.

TABLE A1.3-1
NOMINAL DIMENSIONS AND WEIGHT OF THE TN-40HT CASK

Overall length (with protective cover, in)	199.6
Outside diameter (in)	101
Cavity diameter (in)	72.0
Cavity length (in)	163
Containment shell thickness (in)	1.5
Containment vessel length (in)	170
Cask wall thickness (in)	8.75
Containment Lid thickness (in)	4.5
Lid thickness (in)	10.0
Bottom thickness (in)	8.75
Resin and aluminum box thickness (in)	5.25
Outer shell thickness (in)	0.50
Overall basket length (in)	160
Top neutron shield thickness (in)	4
Protective cover thickness (in)	0.38
Nominal Cask weight:	
Loaded on storage pad (tons)	121.2

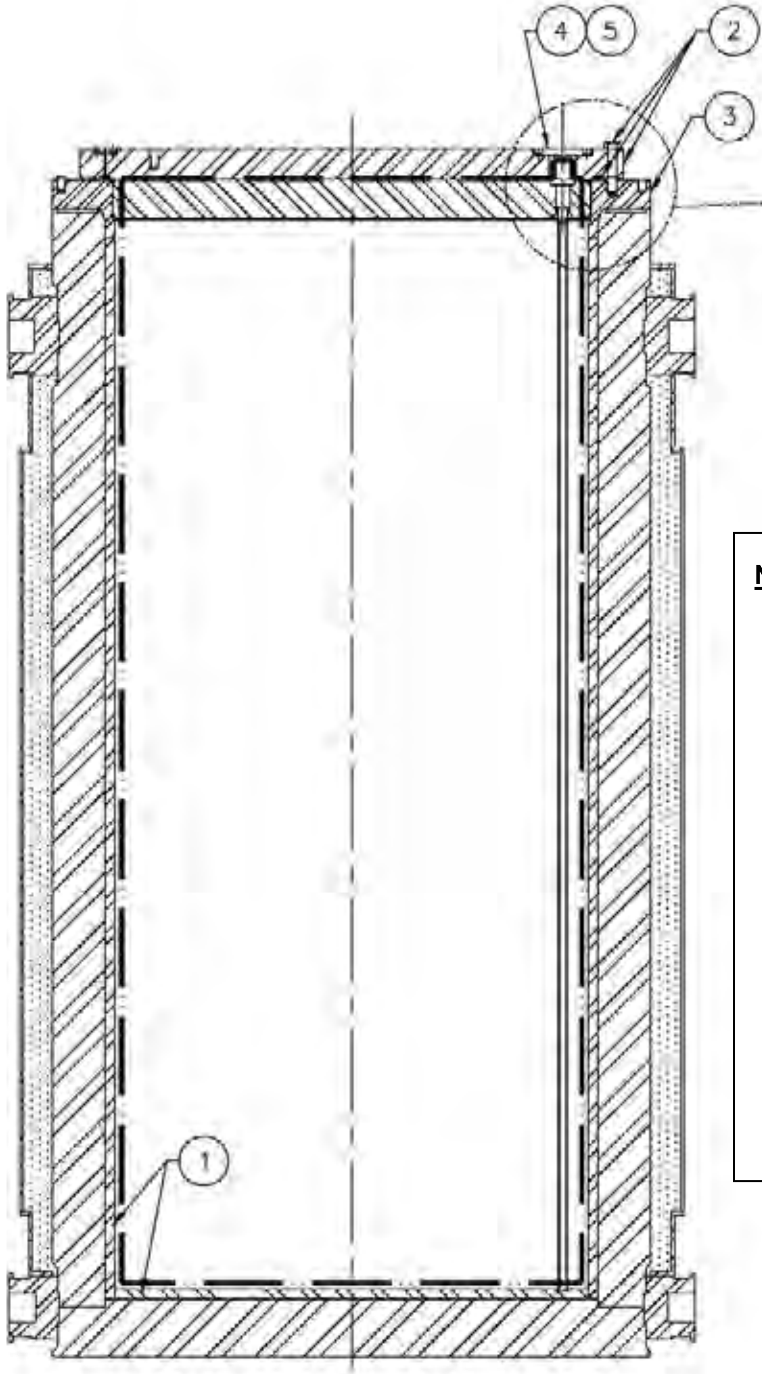

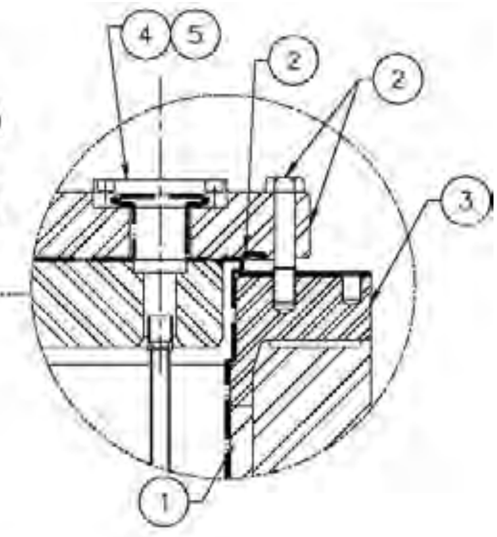

Notes:

- Figure not to scale. Features exaggerated for clarity.
- Phantom line (--- - --- -) indicates containment boundary.
- Containment boundary components are listed below:
  1. Cask body inner shell
  2. Lid assembly outer plate, closure bolts and inner metal seal
  3. Shell flange
  4. Vent port cover plate, bolts and seals
  5. Drain port cover plate, bolts and seals

FIGURE A1.3-1
TN-40HT CONTAINMENT BOUNDARY COMPONENTS

PROPRIETARY AND SECURITY RELATED INFORMATION WITHHELD UNDER 10 CFR 2.390

REVISION	DESCRIPTION	DATE
8	REVISED PER DCR 10426-13	01/08/15
7	REVISED PER DCR TN40HT-027	05/03/13
6	REVISED PER DCR TN40HT-022	07/18/12
5	REVISED PER DCR'S TN40HT-014, 017, 018 & 019	05/14/12
4	REVISED PER DCR TN40HT-010	04/23/10
3	REVISED PER DCR TN40HT-009	03/24/10
2	REVISED PER NRC RAI	02/04/10
1	REVISED PER DCR 10421-18	12/15/09
0	INITIAL ISSUE	05/03/07

AREVA

TN-40HT HIGH BURNUP DRY STORAGE CASK PARTS LIST AND NOTES

TN40HT-72NP-1 | NONE | 1 OF 1

UNCONTROLLED
FOR INFORMATION ONLY

PROPRIETARY AND SECURITY RELATED INFORMATION WITHHELD UNDER 10 CFR 2.390

REVISION	DESCRIPTION	DATE
4	REVISED PER ECR 10428-13	01/08/15
3	REVISED PER TN40HT-022	07/18/12
2	REVISED PER TN40HT-014	05/14/12
1	REVISED PER RAI ROUND 1 QUESTION A1.1	04/24/09
0	INITIAL ISSUE	05/03/07

AREVA

SAFETY ANALYSIS REPORT
TN-40HT HIGH BURNUP DRY STORAGE CASK ASSEMBLY

TN40HT-72NP-2 NONE 1 OF 1

FIGURE: TN40HT-72NP-2, SHT. 1 REV. 4

TN40HT-72NP-2.DGN NSP GENERATION CAD

UNCONTROLLED
FOR INFORMATION ONLY

PROPRIETARY AND SECURITY RELATED INFORMATION WITHHELD UNDER 10 CFR 2.390

REVISION	DESCRIPTION	DATE
3	REVISED PER 10428-13	0?/0?/15
2	REVISED PER TN40HT-022	07/18/12
1	REVISED PER TN40HT-014	05/14/12
0	INITIAL ISSUE	05/03/07

AREVA

SAFETY ANALYSIS REPORT
TN-40HT HIGH BURNUP DRY STORAGE CASK SHELL ASSEMBLY

TN40HT-72NP-3 | NONE | 1 OF 1

FIGURE: TN40HT-72NP-3, SHT. 1 REV. 3

TN40HT-72NP-3.DGN NSP GENERATION CAD

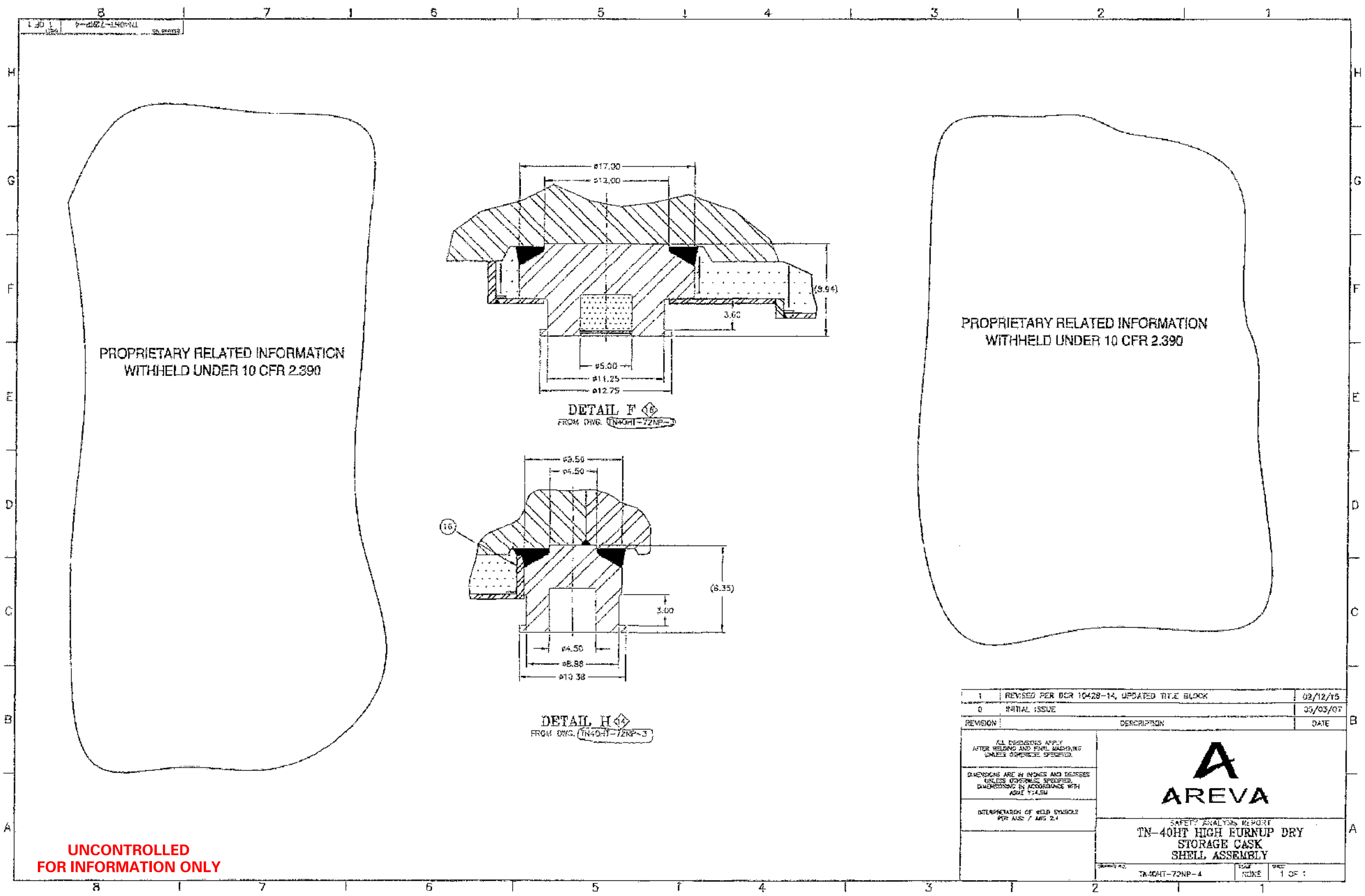

FIGURE: TN40HT-72NP-4, SHT. 1 REV. 1

TN40HT-72NP-4.DGN NSP GENERATION CAD

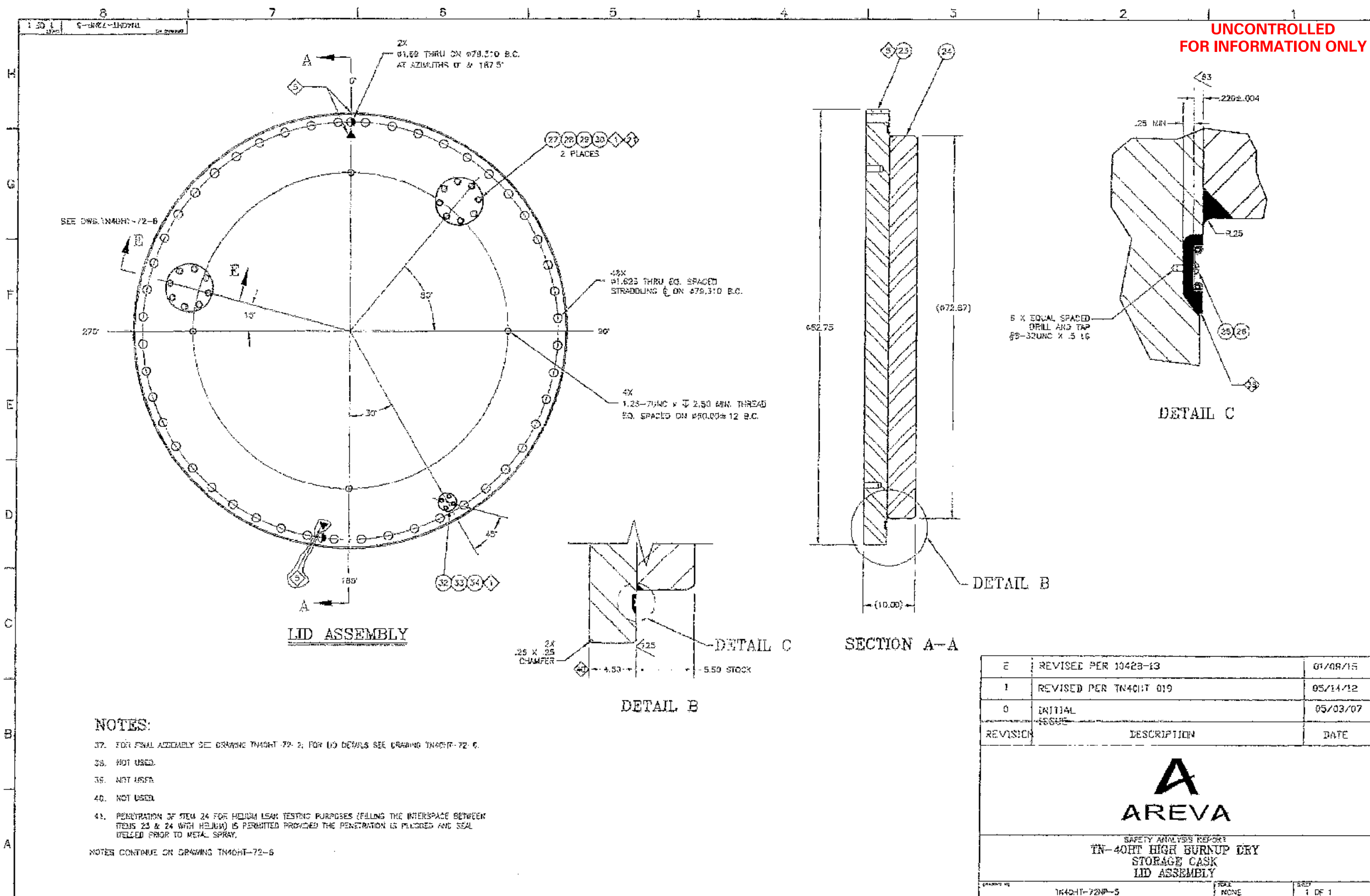

FIGURE: TN40HT-72NP-5, SHT. 1 REV. 2

TN40HT-72NP-5.DGN NSP GENERATION CAD

01500070

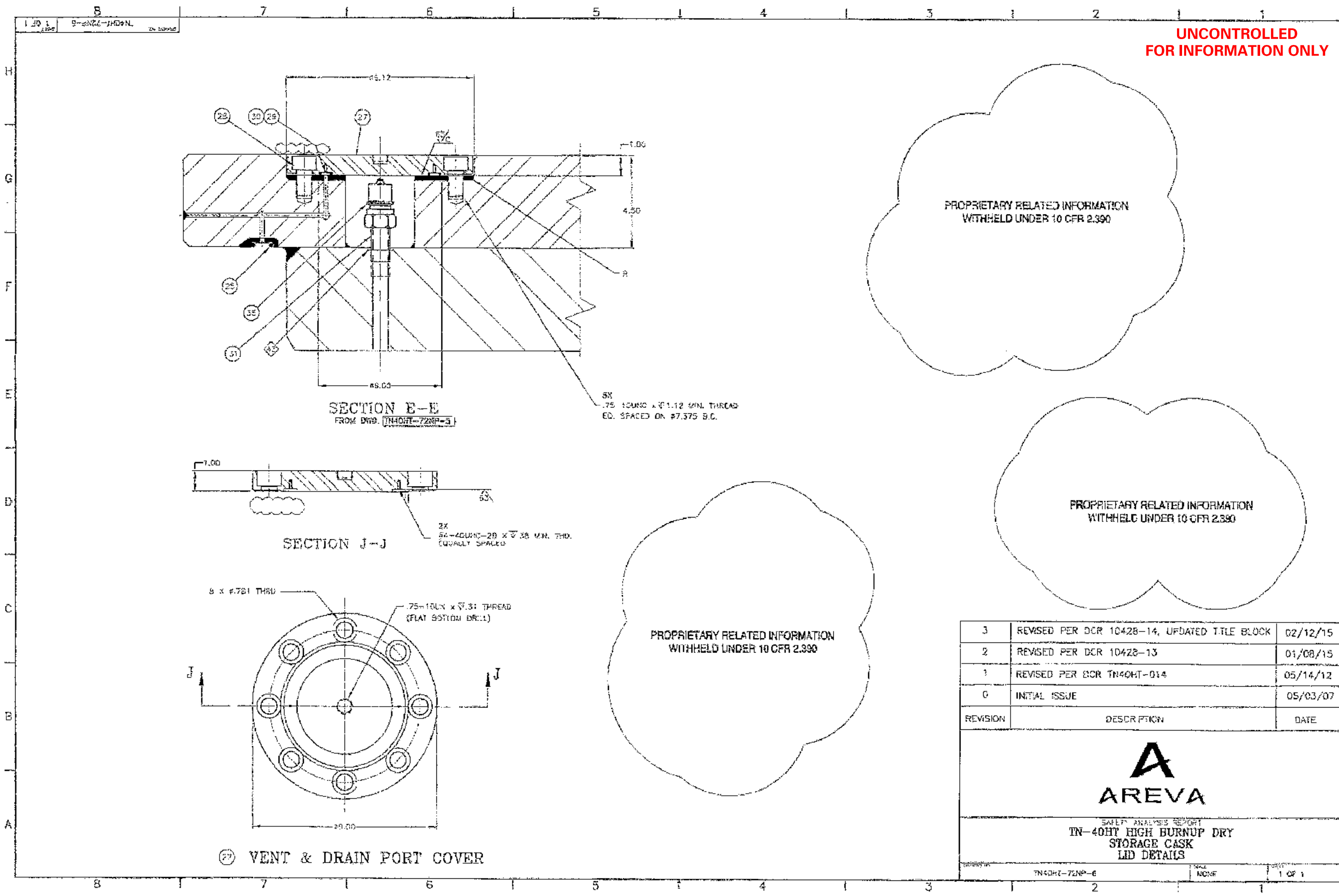

REVISION	DESCRIPTION	DATE
3	REVISED PER DCR 10428-14, UPDATED TITLE BLOCK	02/12/15
2	REVISED PER DCR 10428-13	01/08/15
1	REVISED PER DCR TN40HT-014	05/14/12
0	INITIAL ISSUE	05/03/07

FIGURE: TN40HT-72NP-6, SHT. 1 REV. 3

TN40HT-72NP-6.DGN NSP GENERATION CAD

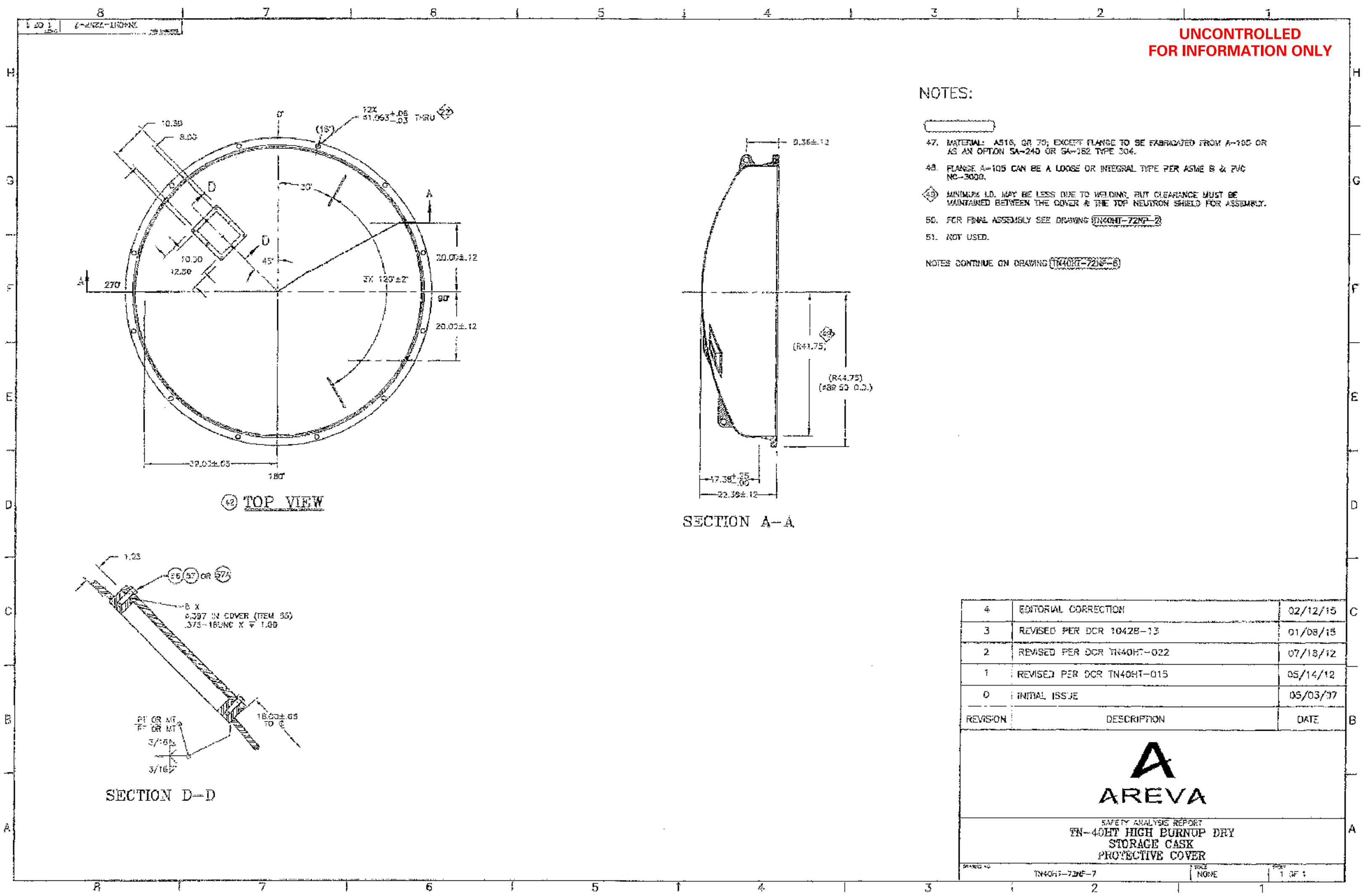

FIGURE: TN40HT-72NP-7, SHT. 1 REV. 4

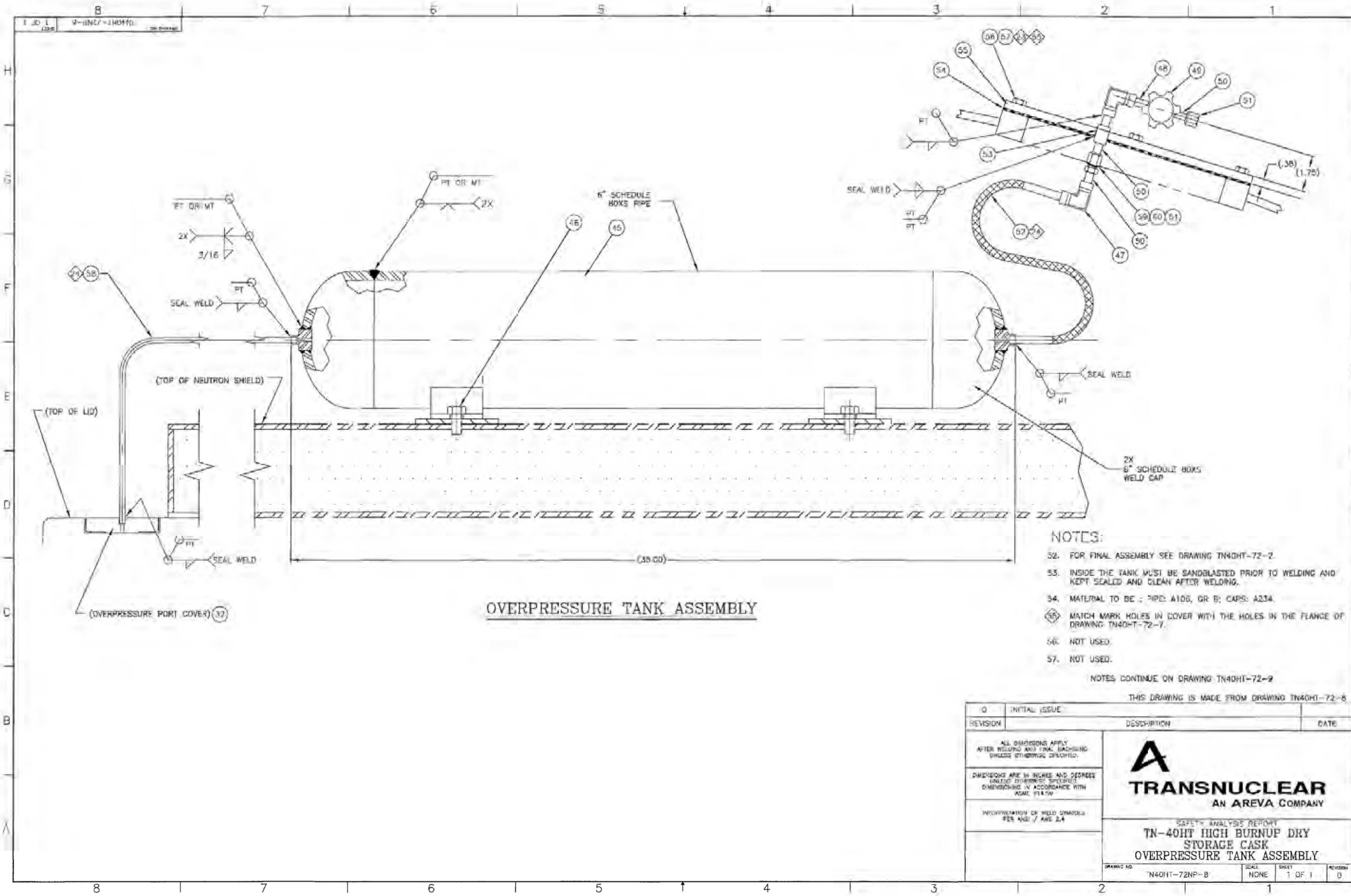
6" SCHEDULE 80XS PIPE
PT OR MT
2X
3/16
SEAL WELD
PT
(TOP OF NEUTRON SHIELD)
(TOP OF LID)
(OVERPRESSURE PORT COVER)
2X
6" SCHEDULE 80XS WELD CAP
(.38)
(1.75)
(35.00)
OVERPRESSURE TANK ASSEMBLY
NOTES:
52. FOR FINAL ASSEMBLY SEE DRAWING TN40HT-72-2.
53. INSIDE THE TANK MUST BE SANDBLASTED PRIOR TO WELDING AND KEPT SEALED AND CLEAN AFTER WELDING.
54. MATERIAL TO BE : PIPE: A106, GR B; CAPS: A234.
55. MATCH MARK HOLES IN COVER WITH THE HOLES IN THE FLANGE OF DRAWING TN40HT-72-7.
56. NOT USED.
57. NOT USED.
NOTES CONTINUE ON DRAWING TN40HT-72-9
THIS DRAWING IS MADE FROM DRAWING TN40HT-72-8
0
INITIAL ISSUE
REVISION
DESCRIPTION
DATE
TRANSNUCLEAR
AN AREVA COMPANY
SAFETY ANALYSIS REPORT
TN-40HT HIGH BURNUP DRY STORAGE CASK
OVERPRESSURE TANK ASSEMBLY
TN40HT-72NP-8
NONE
1 OF 1
0

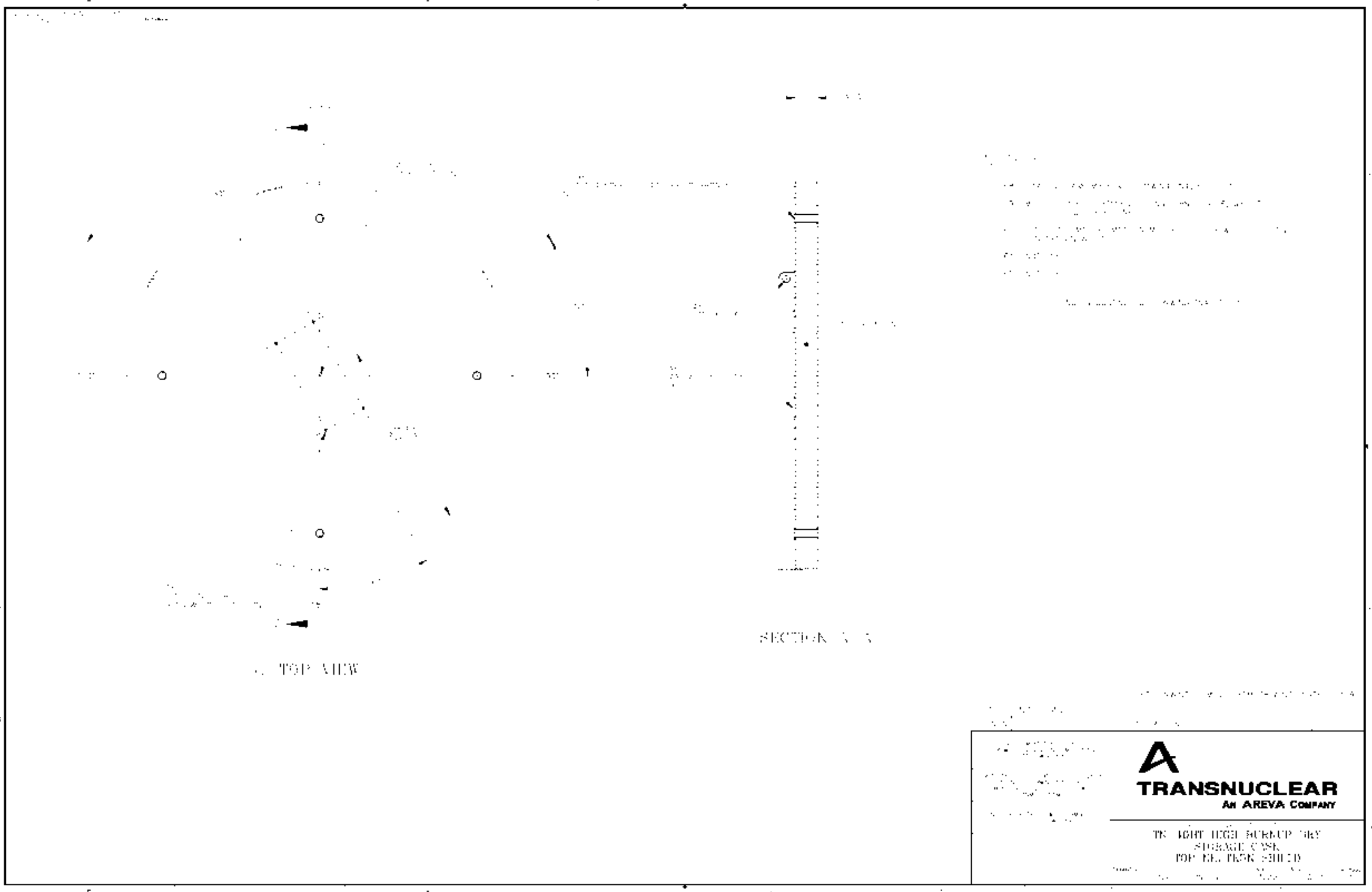
TOP VIEW
SECTION
TRANSNUCLEAR
AN AREVA COMPANY
TN-40HT HIGH BURNUP DRY
STORAGE CASK
TOP NEUTRON SHIELD

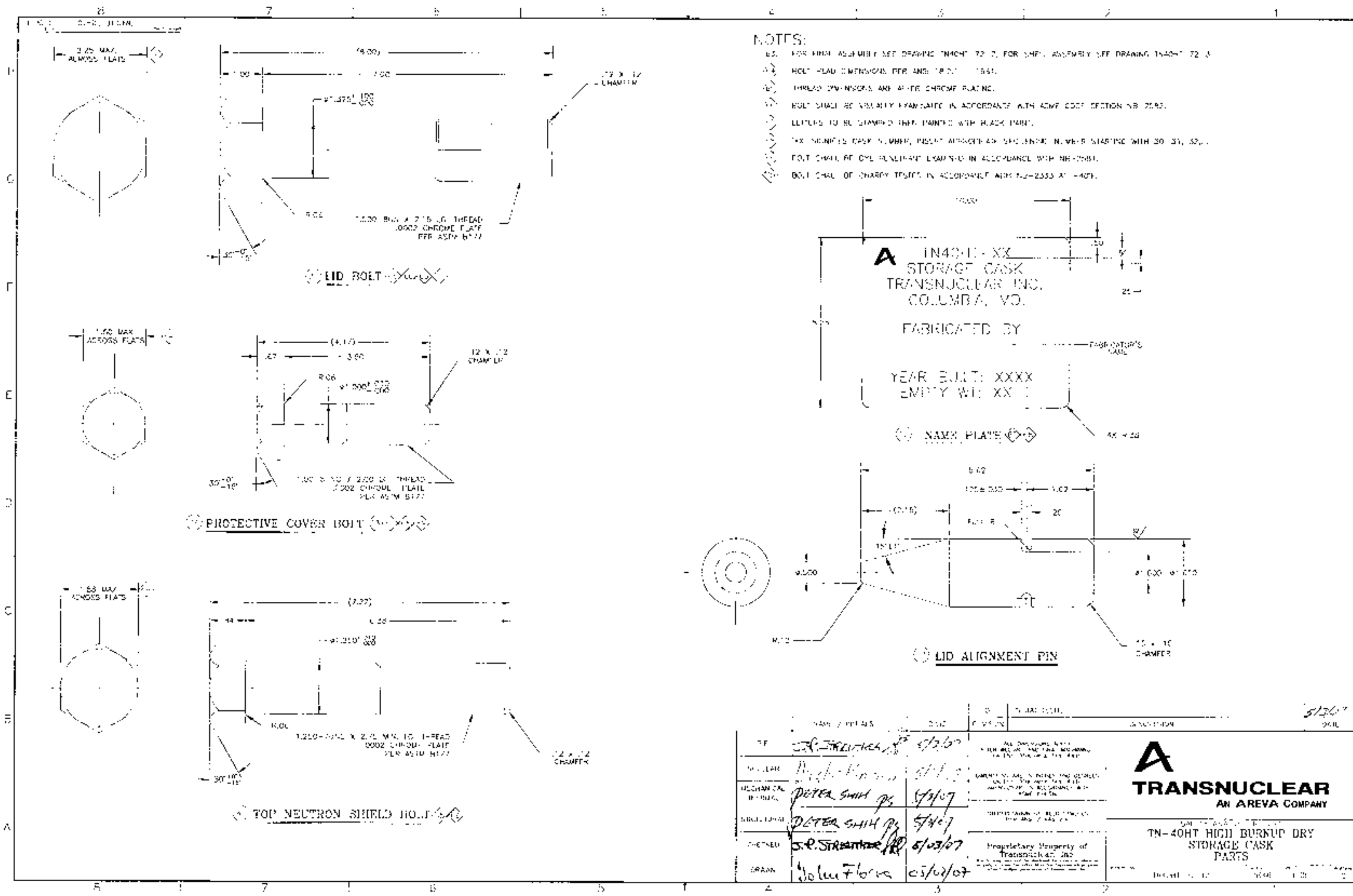
NOTES:
LID BOLT
PROTECTIVE COVER BOLT
TOP NEUTRON SHIELD BOLT
NAME PLATE
LID ALIGNMENT PIN
TN40HT-XX
STORAGE CASK
TRANSNUCLEAR INC.
COLUMBIA, MD.
FABRICATED BY
YEAR BUILT: XXXX
EMPTY WT: XX
TRANSNUCLEAR
AN AREVA COMPANY
TN-40HT HIGH BURNUP DRY
STORAGE CASK
PARTS
Proprietary Property of
Transnuclear, Inc.

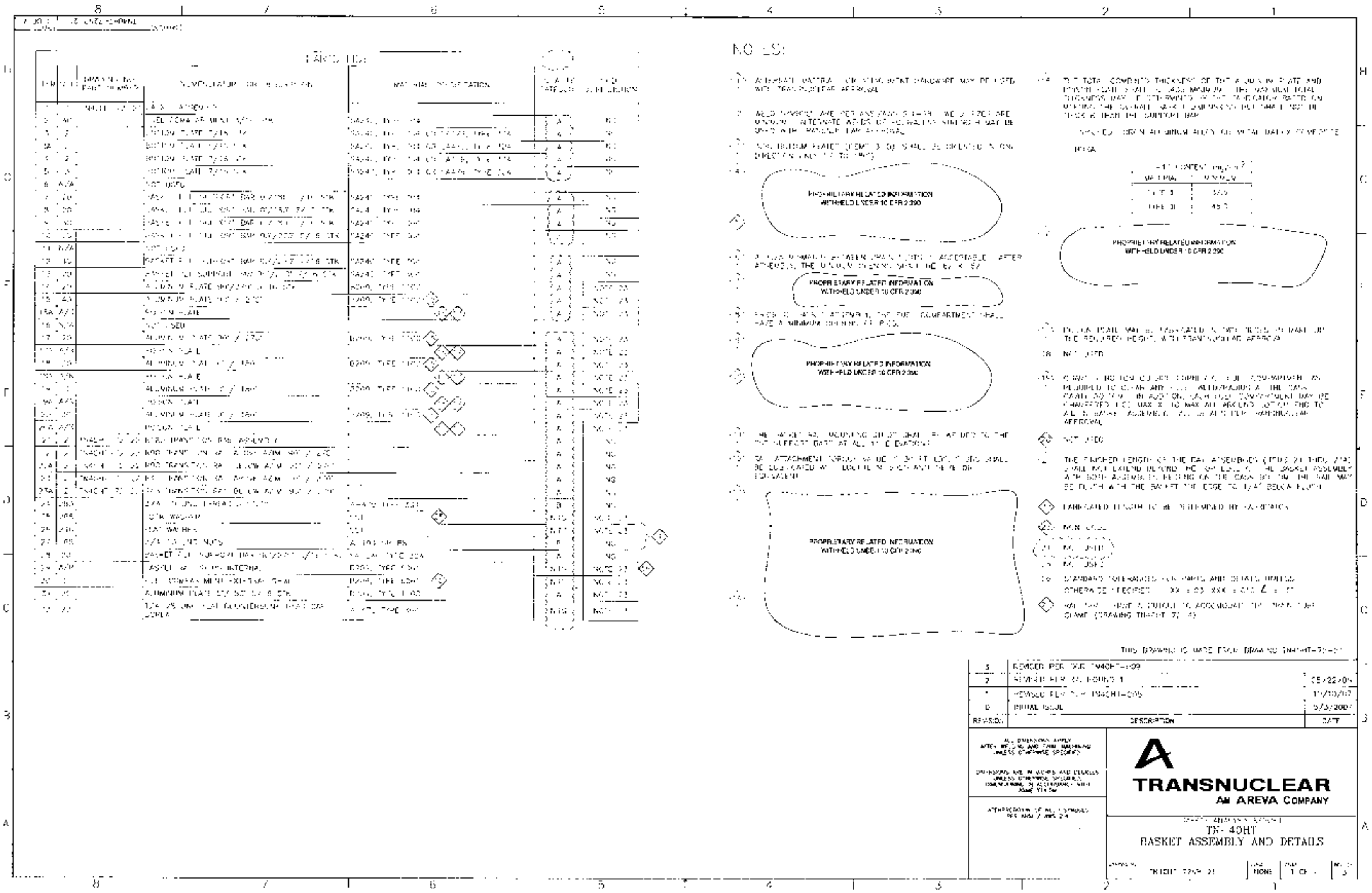
NOTES:
PARTS LIST
PROPRIETARY RELATED INFORMATION WITHHELD UNDER 10 CFR 2.390
INITIAL ISSUE
REVISION
DESCRIPTION
DATE
TRANSNUCLEAR
AN AREVA COMPANY
TN-40HT
BASKET ASSEMBLY AND DETAILS

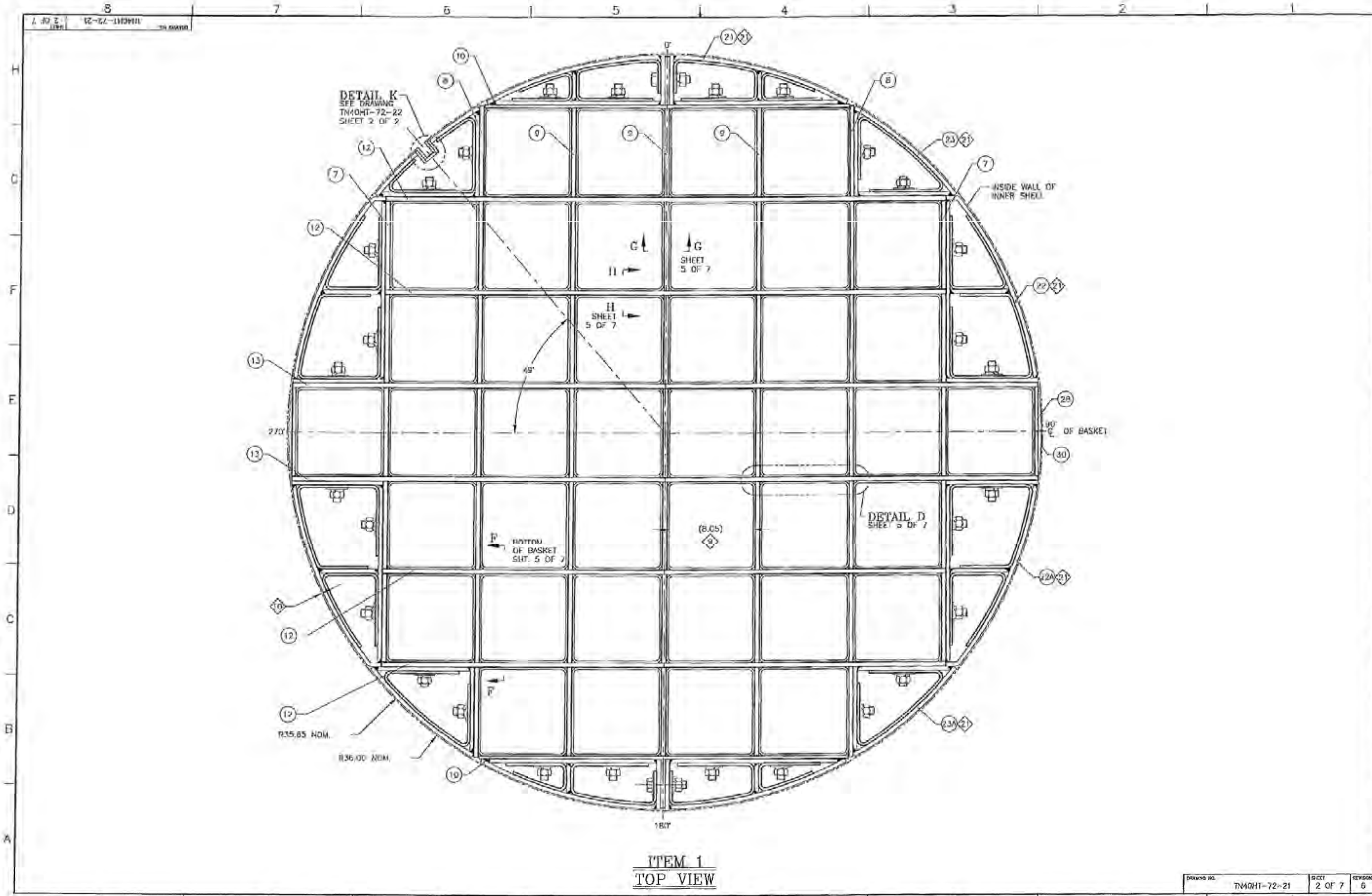
DETAIL K
SEE DRAWING
TN40HT-72-22
SHEET 2 OF 2
INSIDE WALL OF
INNER SHELL
OF BASKET
DETAIL D
BOTTOM
OF BASKET
SHT. 5 OF 7
SHEET
5 OF 7
R35.85 NOM.
R36.00 NOM.
0°
90°
180°
270°
45°
(8.05)
ITEM 1
TOP VIEW
TN40HT-72-21
2 OF 7
6

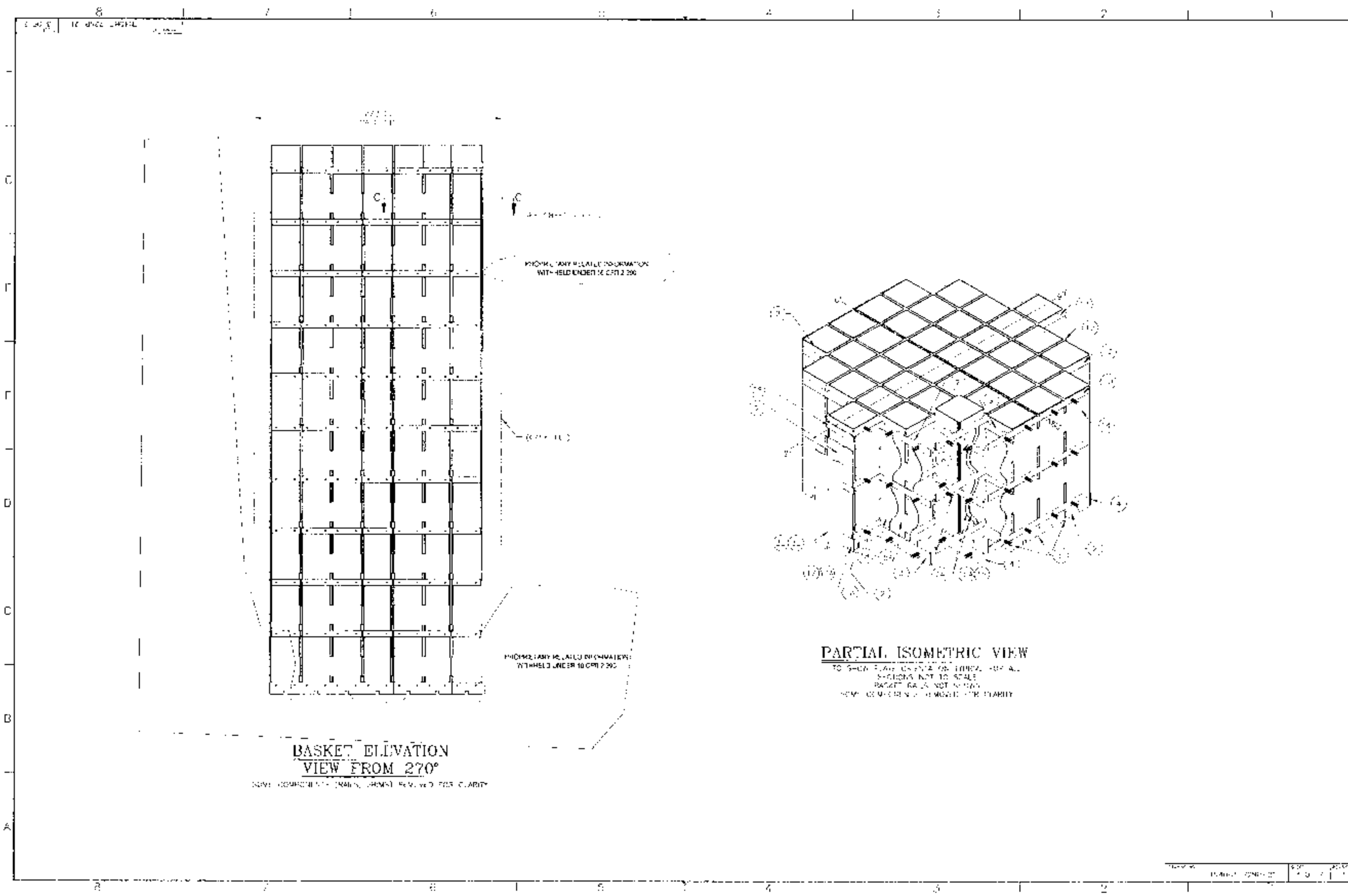
BASKET ELEVATION
VIEW FROM 270°
PARTIAL ISOMETRIC VIEW

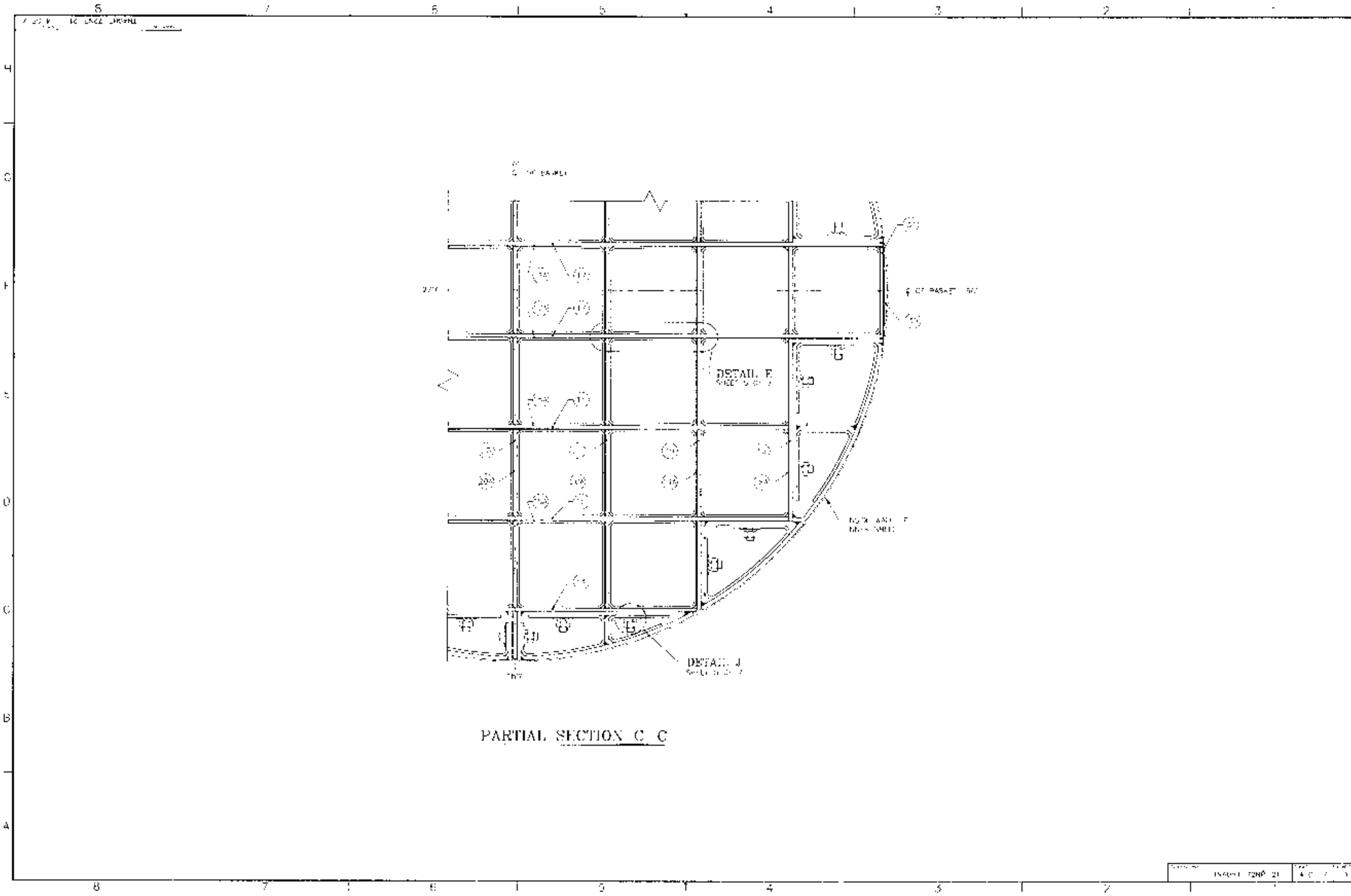
DETAIL E
DETAIL J
PARTIAL SECTION C-C

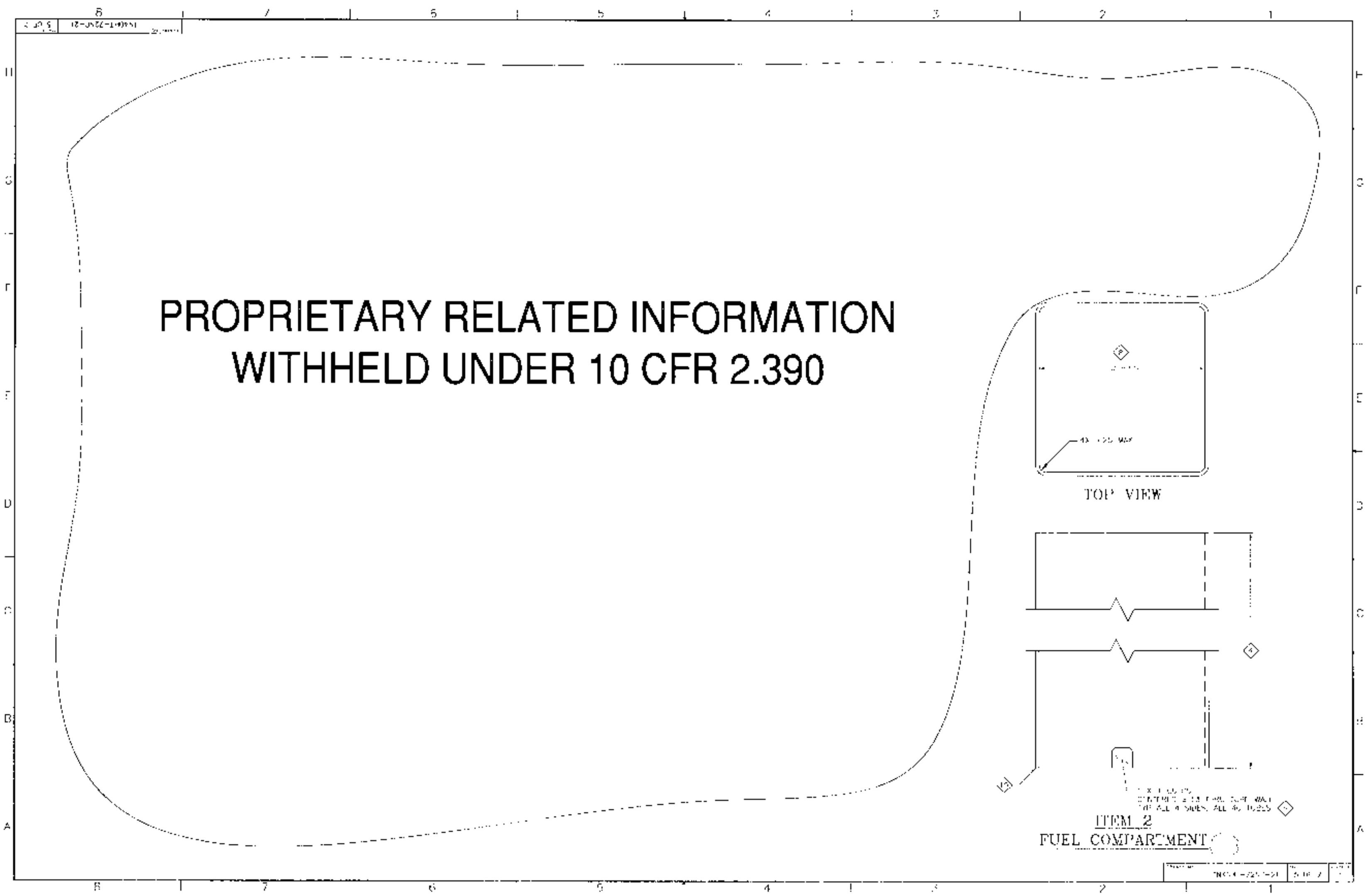
PROPRIETARY RELATED INFORMATION
WITHHELD UNDER 10 CFR 2.390
TOP VIEW
ITEM 2
FUEL COMPARTMENT

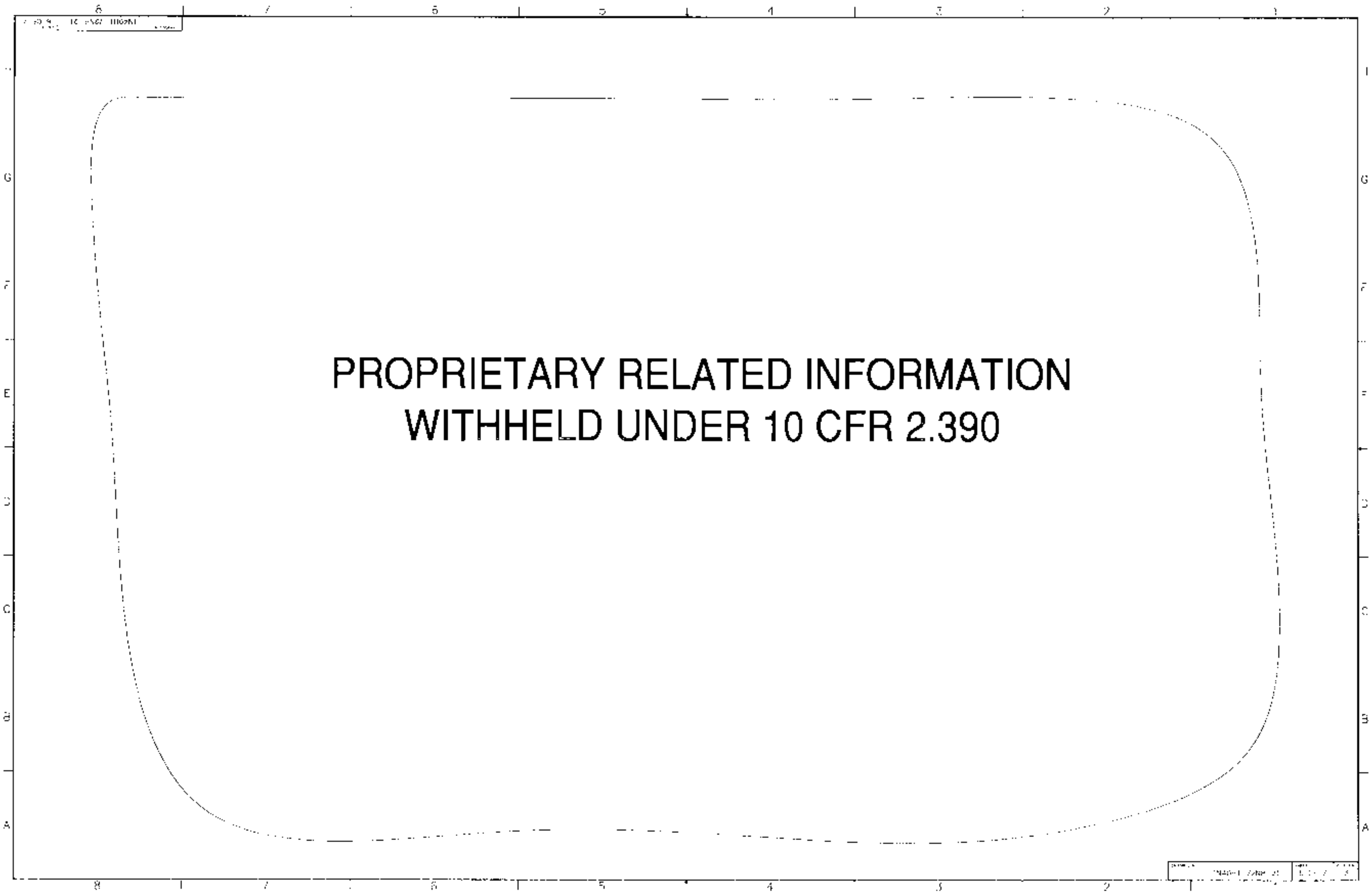

PROPRIETARY RELATED INFORMATION
WITHHELD UNDER 10 CFR 2.390

PROPRIETARY RELATED INFORMATION
WITHHELD UNDER 10 CFR 2.390

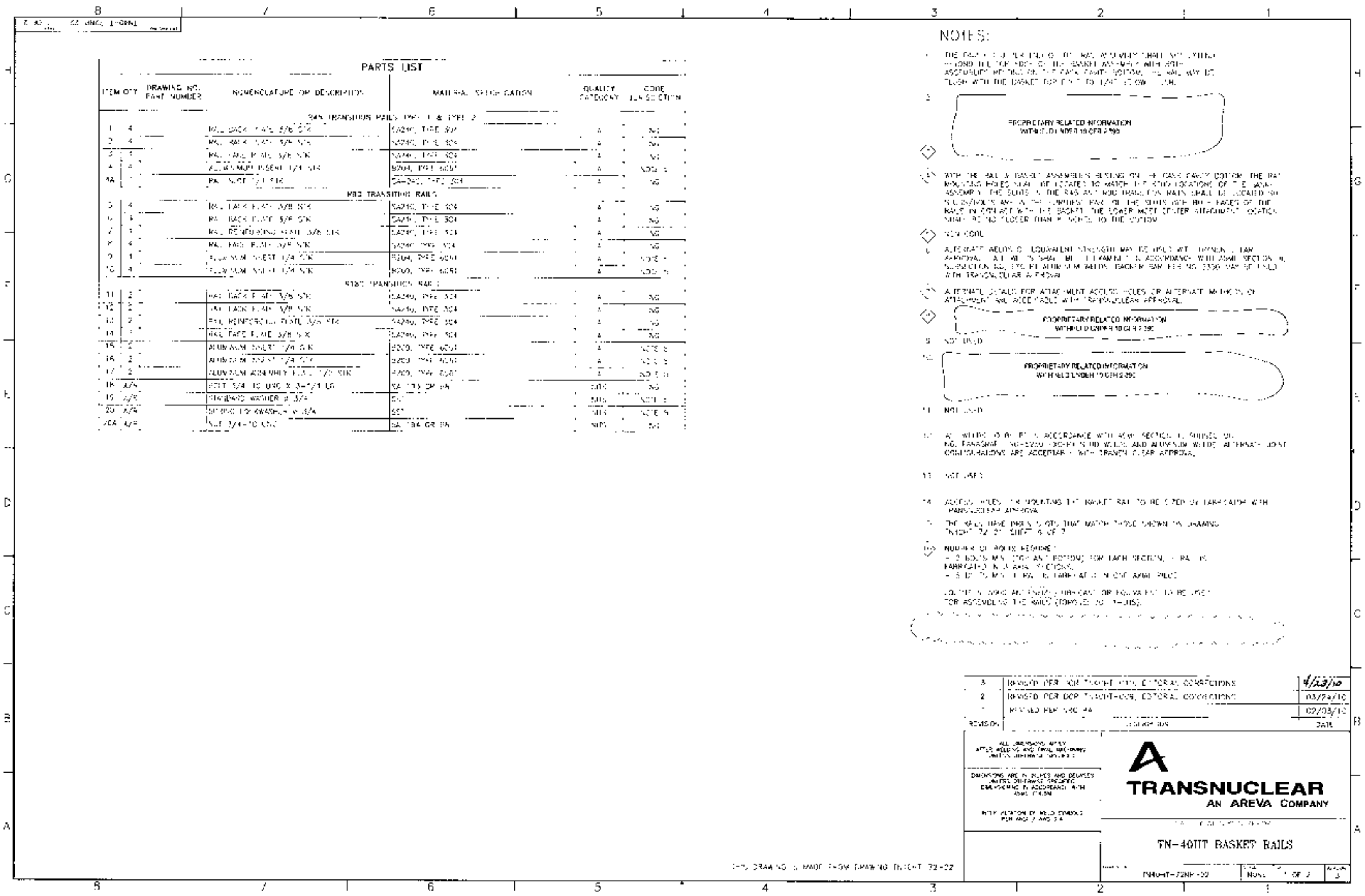
PARTS LIST
NOTES:
PROPRIETARY RELATED INFORMATION WITHHELD UNDER 10 CFR 2.390
TRANSNUCLEAR
AN AREVA COMPANY
TN-40HT BASKET RAILS

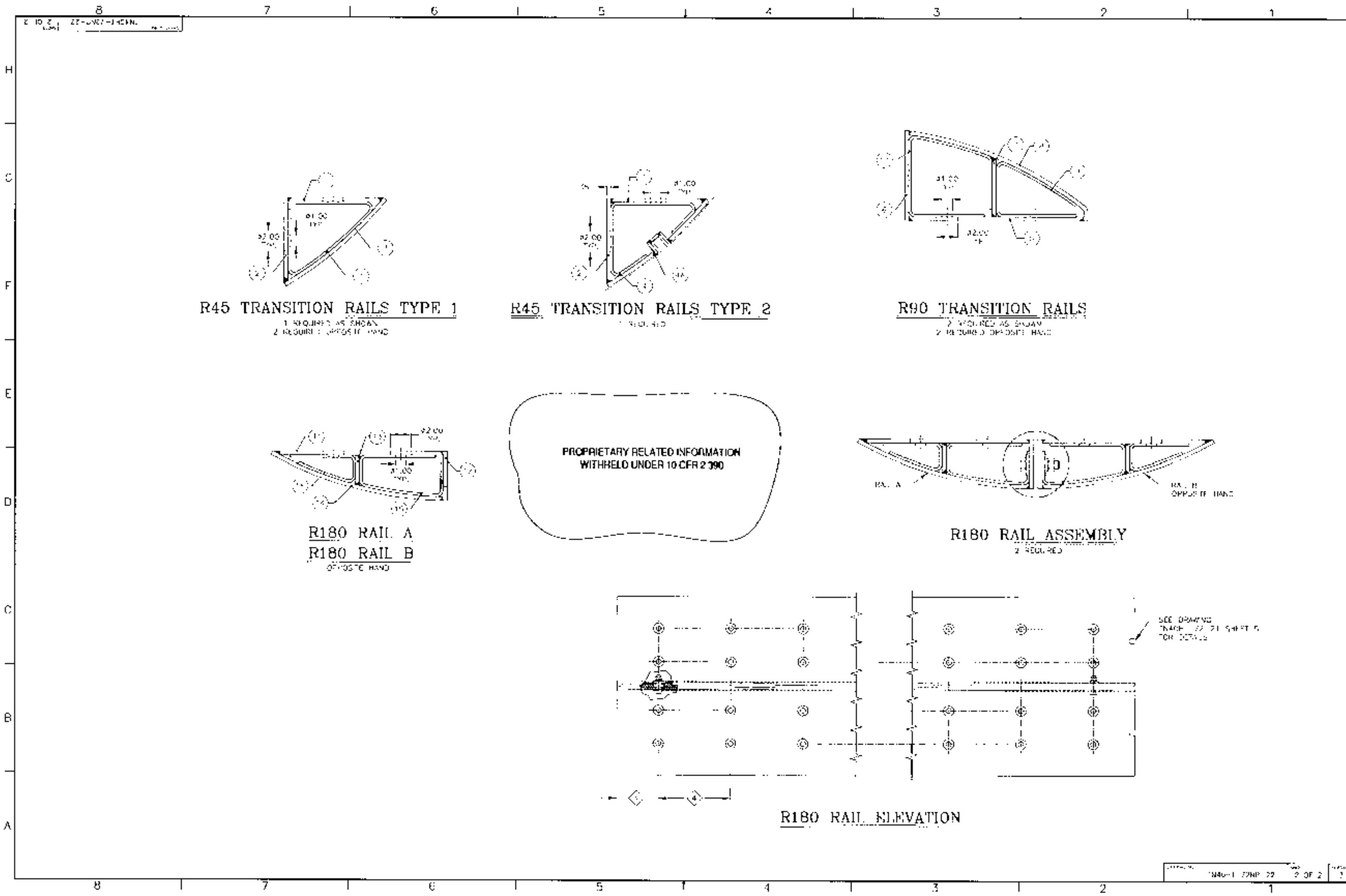
R45 TRANSITION RAILS TYPE 1
R45 TRANSITION RAILS TYPE 2
R90 TRANSITION RAILS
R180 RAIL A
R180 RAIL B
PROPRIETARY RELATED INFORMATION
WITHHELD UNDER 10 CFR 2.390
R180 RAIL ASSEMBLY
R180 RAIL ELEVATION

PROPRIETARY RELATED INFORMATION
WITHHELD UNDER 10 CFR 2.390
TN40HT-72NP-22-3

PROPRIETARY RELATED INFORMATION
WITHHELD UNDER 10 CFR 2.390
TN40HT-72NP-22-4

PROPRIETARY RELATED INFORMATION
WITHHELD UNDER 10 CFR 2.390
TN40HT-72NP-22-5

PROPRIETARY RELATED INFORMATION
WITHHELD UNDER 10 CFR 2.390
TN40HT-72NP-22-6

PROPRIETARY RELATED INFORMATION
WITHHELD UNDER 10 CFR 2.390
TN40HT-72NP-22-7

PROPRIETARY RELATED INFORMATION
WITHHELD UNDER 10 CFR 2.390
TN40HT-72NP-22-8

SECTION A2

SITE CHARACTERISTICS

A2.1 GEOGRAPHY AND DEMOGRAPHY OF SITE SELECTED

A2.1.1 SITE LOCATION

The information in Section 2.1.1 is independent of cask design.

A2.1.2 SITE DESCRIPTION

The information in Section 2.1.2 is independent of cask design.

A2.1.3 POPULATION DISTRIBUTION AND TRENDS

The information in Section 2.1.3 is independent of cask design.

A2.1.4 USES OF NEARBY LAND AND WATERS

The information in Section 2.1.4 is independent of cask design.

A2.2 NEARBY INDUSTRIAL, TRANSPORTATION AND MILITARY FACILITIES

The information in Section 2.2 is independent of cask design.

A2.3 METEOROLOGY

A2.3.1 REGIONAL CLIMATOLOGY

The information in Section 2.3.1 is independent of cask design.

A2.3.2 LOCAL METEOROLOGY

A2.3.2.1 DATA SOURCE

The information in Section 2.3.2.1 is independent of cask design.

A2.3.2.2 TOPOGRAPHY

The information in Section 2.3.2.2 is independent of cask design.

A2.3.3 ONSITE METEOROLOGICAL MEASUREMENT PROGRAM

The information in Section 2.3.3 is independent of cask design.

A2.3.4 DIFFUSION ESTIMATES

A2.3.4.1 BASIS

The information in Section 2.3.4.1 is independent of cask design.

A2.3.4.2 CALCULATIONS

The information in Section 2.3.4.2 is independent of cask design.

A2.4 HYDROLOGY

The information in Section 2.4 is independent of cask design.

A2.4.1 SURFACE WATER

The information in Section 2.4.1 is independent of cask design.

A2.4.2 GROUND WATER

The information in Section 2.4.2 is independent of cask design.

A2.5 GEOLOGY AND SEISMOLOGY

A2.5.1 BASIC GEOLOGIC AND SEISMIC INFORMATION

The information in Section 2.5.1 is independent of cask design.

A2.5.1.1 STORAGE SITE GEOMORPHOLOGY

The information in Section 2.5.1.1 is independent of cask design.

A2.5.1.2 GEOLOGIC HISTORY OF STORAGE SITE AND SURROUNDING REGION

The information in Section 2.5.1.2 is independent of cask design.

A2.5.1.3 SPECIFIC STRUCTURAL FEATURES OF SIGNIFICANCE

The information in Section 2.5.1.3 is independent of cask design.

A2.5.1.4 LARGE SCALE GEOLOGIC MAP

The information in Section 2.5.1.4 is independent of cask design.

A2.5.1.5 PLOT PLAN AND SITE INVESTIGATIONS

The information in Section 2.5.1.5 is independent of cask design.

A2.5.1.6 GEOLOGIC PROFILES

The information in Section 2.5.1.6 is independent of cask design.

A2.5.1.7 PLAN AND PROFILE DRAWINGS

The information in Section 2.5.1.7 is independent of cask design.

A2.5.1.8 LOCAL GEOLOGIC FEATURES AFFECTING SITE LOCATION

The information in Section 2.5.1.8 is independent of cask design.

A2.5.1.9 SITE GROUNDWATER CONDITIONS

The information in Section 2.5.1.9 is independent of cask design.

A2.5.1.10 GEOPHYSICAL SURVEYS AND STUDIES

The information in Section 2.5.1.10 is independent of cask design.

A2.5.1.11 SOIL AND ROCK PROPERTIES

The information in Section 2.5.1.11 is independent of cask design.

A2.5.1.12 ANALYSIS TECHNIQUES

The information in Section 2.5.1.12 is independent of cask design.

A2.5.2 VIBRATING GROUND MOTION

The information in Section 2.5.2 is independent of cask design.

A2.5.3 SURFACE FAULTING

The information in Section 2.5.3 is independent of cask design.

A2.5.4 STABILITY OF SUBSURFACE MATERIALS

The information in Section 2.5.4 is independent of cask design.

A2.5.5 SLOPE STABILITY

The information in Section 2.5.5 is independent of cask design.

A2.6 REFERENCES

The references listed in Section 2.6 are independent of cask design and there are no additional references associated with Section A2.

A2A BORING LOGS

The information in Appendix 2A is independent of cask design.

A2B GRAIN SIZE DISTRIBUTION TEST REPORTS

The information in Appendix 2B is independent of cask design.

SECTION A3

PRINCIPAL TN-40HT CASK DESIGN CRITERIA

A3.1 PURPOSES OF CASK

A3.1.1 SPENT FUEL TO BE STORED

The TN-40HT cask is designed to store 40 Westinghouse and Exxon 14x14 Pressurized Water Reactor (PWR) spent fuel assemblies with or without fuel inserts. The maximum allowable initial enrichment is 5.0 wt % U-235. The maximum bundle average burnup, maximum decay heat, and minimum cooling time for the fuel assembly are 60 GWd/MTU, 0.80 kW/assembly (including heat from inserts), and 12 years, respectively. The cask is designed for a maximum heat load of 32 kW.

Sensitivity analyses were performed to determine the fuel assembly type which was the most limiting for each of the analyses including shielding, criticality, heat load and confinement. The fuel assemblies considered are listed in Table A3.1-1. The design basis fuel for decay heat, shielding and confinement is the Westinghouse Standard 14x14 assembly with 179 fuel rods and with burnup, bundle average enrichment, and cooling time of 60 GWd/MTU, 3.4 wt% U-235, and 18 years, respectively. The fuel qualification screening which is developed based on this fuel type is conservative when applied to other fuel types with lower mass of uranium. For the criticality analysis, all fuel assembly types are analyzed with 5.0% lattice enrichment. The Westinghouse Standard 14x14 assembly is the most reactive and is evaluated for configurations which bound all normal, off-normal and accident conditions. The thermal and radiological characteristics for the PWR spent fuel were generated using the SAS2H/ORIGEN S modules of SCALE (Reference 14). These characteristics for the design basis Westinghouse Standard 14x14 assembly are shown in Table A3.1-2. The thermal analysis uses bounding fuel rod parameters for the fuel assembly model with the maximum allowable decay heat.

Fuel with various combinations of burnup, enrichment, and cooling time can be stored in the TN-40HT cask as long as the combination results in decay heat, surface dose rates, and radioactive sources for confinement that are bounded by the design basis fuel. As discussed in Section A7, an evaluation was performed to determine various combinations of burnup, enrichment, and cooling time that would result in acceptable dose rates for the TN-40HT. Table A3.1-3 provides information for determining the qualification of fuel assemblies for storage in the TN-40HT cask. This table also shows a parametric equation that can be utilized to qualify spent fuel assemblies for the allowable decay heat load. The decay heat load can be calculated based on a fuel assembly’s burnup, cooling time, and initial enrichment parameters. This table ensures that the fuel assembly decay heat load is less than the maximum allowable. The development of this equation is provided in Section A3.3.2.2.8.

Assemblies containing fuel inserts (TPAs and BPRAs) may be stored in the TN-40HT cask. Reconstituted assemblies, (natural uranium dioxide replacement rods, Zirconium inert rods, or stainless steel rods replacing fuel rods), may also be stored in the cask. The decay heat of a reconstituted assembly with stainless steel rods is bounded by an intact assembly. However, the irradiated stainless steel rods do increase the gamma source term for a period of time after irradiation. This period is shorter than the 12 year minimum cooling time required and thus no additional cooling time is required for these reconstituted assemblies.

The maximum combined weight of any fuel assembly and insert is limited to 1,330 lbs and the total weight of all fuel assemblies and inserts is limited to 52,000 lbs.

Within the population of assemblies that meet the criteria for storage in a TN-40HT as described above, there are three regions of fuel, Regions 4, 5 and 6 (assemblies identified as D, E and F) that were found to have compromised top nozzle to fuel skeleton connections due to stress corrosion cracking at the thimble tube joints (bulge joints). A fourth region of fuel, Region 14 (assemblies identified as N), was identified as potentially being subject to the condition. This condition could lead to top nozzle separation during assembly movement. The condition is addressed in one of three ways: visual inspection of the joints just prior to each movement of the assembly to insure integrity followed by movement with the standard spent fuel handling tool; the use of a thimble grip handling tool; permanent modification of the suspect assembly with anchors in the thimble tubes (Reference 45). The first two approaches do not modify the assembly. In the permanent modification approach anchors are mounted in at least six of the thimble tubes which secures the top nozzle of the assembly by bypassing the potentially compromised bulge joints. The anchors consist of two parts; a tapered pin and barbed sleeve which are stainless steel and do not extend into the active fuel (Reference 46)· A thimble plug insert or BPRA insert cannot be placed in the assembly once anchors are mounted. The anchors are designed and tested for structural integrity relative to assembly movement. Each anchor is load tested upon installation.

The presence of the anchors in the cask does not invalidate any safety analyses (Reference 47). The anchors are not irradiated and do not produce any internal heat and do not add to the source term for the cask dose analysis. They do not extend into the active fuel of the assembly and do not impact the criticality analysis. The anchors weigh less than the limiting insert (16-pin BPRA) and are not a source of gas that would affect cask internal pressure. After the installation of the anchors the assembly is moved with the standard spent fuel handling tool assuring retrieveability of the assemblies from the cask.

A3.1.2 GENERAL OPERATING FUNCTIONS

The fuel assemblies will be stored unconsolidated and dry in sealed storage casks. The casks will rest on a reinforced concrete pad, and provide safe storage by ensuring a reliable decay heat path from the spent fuel to the environment and by providing appropriate shielding and confinement of the fission product inventory. Storage of spent fuel in storage casks is a totally passive function, with no active systems required to function. Cooling of the casks is accomplished by radiant and convective cooling.

Each cask will be handled with a lifting yoke, the 125 ton capacity auxiliary building crane, a transport vehicle, or other appropriate equipment. The crane will lift the cask from the spent fuel pool, in the spent fuel pool enclosure, move the cask laterally through an access door, and lower the cask to ground level in the rail bay of the Auxiliary Building. The cask will then be picked up by a transport vehicle which will transit to the ISFSI. After the cask has been maneuvered to its storage position at the ISFSI, the transport vehicle will set the cask down.

All the handling equipment to be used outside the Auxiliary Building will be designed according to appropriate commercial codes and standards, and will be operated, maintained, and inspected in accordance with the supplier's recommendations. Documentation will be maintained to substantiate conformance with all applicable standards.

A3.2 DESIGN CRITERIA FOR ENVIRONMENTAL CONDITIONS AND NATURAL PHENOMENA

The storage casks are designed with the objectives of ensuring that fuel criticality is prevented, cask integrity is maintained, and fuel is not damaged so as to preclude its ultimate removal from the cask. The conditions under which these objectives are met are described below.

The safe storage of the spent fuel assemblies must depend only on the capability of the storage casks to fulfill their design functions. The casks are self-contained, independent, passive systems, which do not rely on any other systems or components for their operation. Therefore, the casks are important to safety. The criteria used in the design of the casks ensure that their exposure to credible site hazards will not impair their safety functions. Because the ISFSI is located on the plant site, all ISFSI design criteria for environmental conditions and natural phenomena are the same as the plant design basis, as found in the USAR (Reference 15).

The design criteria satisfy the requirements of 10 CFR Part 72 (Reference 1). They consider the effects of normal operation, natural phenomena and postulated man-made accidents. The criteria are defined in terms of loading conditions imposed on the storage cask. The loading conditions are evaluated to determine the type and magnitude of loads induced on the storage cask. The combinations of these loads are then established based on the number of conditions that can superimpose. The load combinations are then classified as Design and/or Service Conditions consistent with Section III of the ASME Boiler and Pressure Vessel Code (Reference 2). The stresses resulting from the application of these loads are then evaluated based on the rules of the ASME Code as defined herein.

A3.2.1 TORNADO AND WIND LOADINGS

Tornado loadings specified in Section 12.2.1.3.2 of the Prairie Island USAR were used in the design of the TN-40HT cask. These loads consist of the following:

- A differential pressure equal to 3 psi. This pressure is assumed to build up from normal atmospheric pressure in 3 seconds.
- A lateral force caused by a funnel of wind having a peripheral tangential velocity of 300 mph and a forward progression of 60 mph.
- The design tornado driven missile was assumed equivalent to an airborne 4″ x 12″ x 12′0″ plank traveling end-on 300 mph, or a 4000 lb. automobile flying through the air at 50 mph and at not more than 25 ft. above ground level.

An analysis of impact on the cask of tornado missiles in accordance with Table 12.2-9 of the Prairie Island USAR (Reference 15) is presented below. Wind loading is not significant in comparison to that due to tornados; therefore, the wind loading is conservatively taken to be the same as the tornado loading.

A3.2.1.1 APPLICABLE DESIGN PARAMETERS

The external pressure drop of 3 psi associated with passing of the tornado is small and, when combined with the other internal pressure loads, is far exceeded by the design internal pressure (22 psig normal design rating, 100 psig analyzed) for the cask. Its effect is included in the effects of the other internal pressure loadings listed in Table A3.2-2.

A3.2.1.2 DETERMINATION OF FORCES ON STRUCTURES

The 360 mph tornado wind loading is converted to a dynamic pressure (psf) acting on the cask by multiplying the square of the wind velocity (in mph) by a coefficient (0.002558 at ambient sea level condition) dependent on the air density, based on data presented in a paper by T.W. Singell (Reference 5). The result is a pressure of 332 psf (Figure A3.2-1).

The net force acting on the cask is obtained by multiplying this pressure by the product of the area of the cask projected onto a plane normal to the direction of wind times a drag coefficient. A drag coefficient of 1.0 is used based on the geometric proportions of the cask (i.e., length to diameter ratio of approximately 2) and the conservative assumption that the cask surface is rough.

An additional load on the structure is that created by the impact of tornado missiles on the cask. These impacts are analyzed for 2 types of missiles specified in the Prairie Island USAR (Reference 15):

- Missile A: High energy deformable missile (4000 lb. automobile) impacting the cask
    - a) horizontally at normal incidence at 50 mph.
- Missile B: A 4 inch thick by 12 inch wide by 12 foot long wood plank weighing 200 lbs:
    - a) horizontally at normal incidence at 300 mph.
    - b) vertically at normal incidence at 80% of the horizontal velocity.

The tornado missiles are summarized in the following table:

Missiles		Mass (lbs)	Horizontal Velocity (mph)	Vertical Velocity (mph)
A	Automobile	4,000	50	-
B	4" Thick Wood Plank 12" Wide × 12' Long	200	300	240

A3.2.1.2.1 STABILITY OF THE CASK IN THE VERTICAL POSITION UNDER WIND LOADING

The cask stands in an upright position on a concrete pad. The coefficient of friction between the steel cask and the concrete is taken as 0.25 for dry concrete. This coefficient is conservatively low based on data in Marks Handbook (Reference 6) which gives a value of 0.29 for steel on sandstone. Steel on concrete would be similar. A wind velocity of 409 mph would then be required to cause the cask to slide.

Cask Sliding

The wind loading on the cask body is:

$q = 0.002558\ V^2$

$q = F/A$
F = force to overcome the friction force, F_f
A = projected area of cask, ft^2

and the projected area is:

$A = (199.63\text{ in.} \times 101.0\text{ in.})/144 = 140.00\ ft^2$ (conservatively use the overall dimension for the cask height)

The friction force at the cask base is:

$F_f = W_{cask} \times \mu = 240{,}000 \times 0.25 = 60{,}000$ lbs.

(A conservatively low cask weight of 240,000 lbs is used for the stability analyses.)

Therefore: $0.002558\ V^2 = \dfrac{60{,}000}{140.0}$

$V = 409$ mph

The velocity to produce cask sliding is 409 mph which is greater than the 360 mph tornado wind velocity. Thus, the tornado wind will not slide the cask.

<u>Cask Tipping</u>

If the cask does not slide the force of the wind may cause the cask to tip. The minimum wind velocity required to tip the cask is calculated below:

M_c = the tipping moment about the bottom edge of the cask

$$M_c = \frac{d_b}{2} W - w \times \frac{l_c^2}{2}$$

where:

W = cask weight = 240,000 lb.
w = distributed load to tip cask, lb/in.
d_b = cask diameter at base = 89.5 in.
l_c = cask length = 199.63 in.

Therefore:

$$w = \frac{89.5}{2} 240{,}000 \; \frac{2}{199.63^2}$$

$$= 539 \; lb/in$$

The corresponding pressure load q, is:

$$q = \frac{539}{101.0} \times 144 = 768 \;\; psf$$

The corresponding wind speed, V, is:

$$V = \sqrt{\frac{768}{.002558}}$$

$$= 548 \; mph$$

Therefore the design basis tornado wind velocity of 360 mph will neither slide nor tip the cask.

A3.2.1.2.2 STABILITY OF THE CASK IN THE VERTICAL POSITION UNDER MISSILE IMPACT

It is assumed that Missiles A and B impact inelastically on the cask as shown in Figure A3.2-2. Both Missile A (the automobile) and Missile B (the wood plank) are assumed to crush. The cask will tend to slide if the missile strikes it below the CG (unless it is blocked in position) or tilt if the missile strikes it above the CG. Conservation of momentum is assumed for both sliding and tipping with a coefficient of restitution of zero. The energy transferred to the cask is dissipated by friction in the sliding case or transformed into potential energy as the cask CG lifts in the tipping case. When a missile strikes the side of the cask at an elevation near the CG, the following velocities are calculated:

In the sliding case: $$V = \frac{m\mathrm{V_o}}{M+m}$$

In the tipping case: $$\omega_p = \frac{m d_{CG}\mathrm{V_o}}{m(d_{CG})^2 + I_p}$$

Where:

V = cask translational velocity after impact
V_0 = missile initial velocity
m = mass of missile, lbf/386.4
M = cask mass, 240,000 lbf/386.4

ω_p = cask angular velocity about P after impact

d_{CG} = distance from center of gravity to pivot point P
= $(91.58^2 + 44.75^2)^{0.5}$ = 101.93 in.

I_p = mass moment of inertia of cask about pivot point P
= $(2{,}281{,}240 + 240{,}000 \times 101.93^2)/386.4 = 2.496 \times 10^9$ lbf.in./386.4

When the appropriate substitutions are performed for Missile A (automobile) impact, the cask translational velocity after impact, *V*, in the sliding case is found to be 14.4 in/sec (1.20 ft/sec). The rotational velocity, ω_p, about P is found to be 0.141 rad/sec for impact at the top. Missile B impact produces lower cask translational and rotational velocities because of its lower initial momentum. Vertical impact of Missile B has no effect on cask stability.

Cask Sliding

The cask may slide if the missile strikes it below the CG. Assuming no rotation and ignoring friction, the cask velocity could reach 14.4 in/sec after the impact. Therefore, the final kinetic energy is:

$$KE = 1/2(W_{cask} \times V^2)/g = 1/2\ (240{,}000 \times 14.4^2)/386.4 = 6.44 \times 10^4 \text{ in-lb}$$

If the cask slides on the concrete pad, the cask kinetic energy after impact is absorbed by friction. The friction work can be equated to the kinetic energy. Assuming a coefficient of friction of 0.25:

$$F_{friction} = \mu\ W_{cask} = 0.25 \times 240{,}000 = 6.00 \times 10^4 \text{ lbs}$$

Where:

$F_{friction}$ = friction force
μ = coefficient of friction

The sliding distance is determined by:

$$\text{Sliding Distance } L = KE/\ F_{friction} = 6.44 \times 10^4/6.00 \times 10^4 \approx 1.1 \text{ in.}$$

Given the above assumptions, the cask will slide 1.1 in. if the missile strikes it below the CG of the cask.

Cask Tipping

When the cask tips or pivots about point P after impact, the kinetic energy is transformed into potential energy as the center of gravity rises:

$E_{tipping}$ = increase in potential energy = kinetic energy

$$E_{tipping} = Mgd_{CG}\left[\cos(\beta + \alpha - \pi/2) - \cos\beta\right] = \frac{1}{2} I_p \omega_p{}^2$$

where:

$E_{tipping}$ = the increase in potential energy of the cask since the center of gravity rises as the cask pivots about the corner.

$ß = 90^o - \sin^{-1} (B/d_{cg}) = 26.0°$

α and $ß$ are indicated in Figure A3.2-2

The angle α is determined to be 89.7º for impact at the top of the cask (the cask tilts 0.3º and the c.g. lifts about 0.3 in.). The cask is stable and will not tip over since it will return to the vertical position as long as α is greater than about 64.0º.

Even at this 89.7º angle, wind will not tip over the cask (if the wind force occurs simultaneously with Missile A impact). At an 89.7º angle, the tipping moment about point P due to the 360 mph wind is less than 44% of the restoring moment due to the weight. Therefore the cask is stable in the vertical orientation under simultaneous tornado wind and tornado missile loadings.

A3.2.1.3 LOCAL EFFECT ON CONTAINMENT OF MISSILE IMPACT

Forces Applied to the Cask Due to Missile Impact

The impact forces applied to the cask as it is struck by the missiles are determined as follows:

- Missile A (automobile) is assumed to crush 1.5 ft (18 in.) under a constant force during the impact. The loss of kinetic energy is assumed to be dissipated by crushing of the missile.

Average Impact Force, F_a of missile A can be calculated from the relation:

(Average Impact Force) x (Crush Length) = (Initial Kinetic of Missile A)

The initial kinetic energy, KE, of the missile can be determined from the relation:

$$KE = \frac{1}{2}(\text{Missile A Mass}) \times (\text{Missile A Velocity})^2$$

$$KE = \frac{1}{2}\frac{4000}{32.2*12} \times (50*5280*12/3600)^2 = 4.008 \text{ x } 10^6 \text{ in. lb.}$$

Therefore, the Average Impact force (F_a) can be estimated as:

$$F_a = \frac{KE}{L} = \frac{4.008\text{x}10^6}{18} = 222{,}682 \text{ lb.}$$

Frontal area of the automobile is assumed to be 3 ft. x 6 ft. = 18 ft.^{2}, therefore the impact pressure on cask pa caused by Missile A is:

$$p_a = \frac{222{,}682}{18} \times \frac{1}{144} = 85.9\, psi$$

- Missile B (Wood Plank) will crush under impact. The highest crush strength S_{crush} of any wood listed (Reference 6) is 9210 psi (hickory). The contact force required for the plank to start crushing is:

$$F_c = S_{crush} \times A = 9210 \times (4 \times 12) = 442{,}080 \ lb.$$

The kinetic energy of the plank is dissipated as the plank crushes against the cask wall. The kinetic energy, *KE*, of the plank is:

$$KE = \frac{1}{2} m v_O^{\ 2} = \frac{12}{2} \times \frac{200}{32.2} \times \left(\frac{300 \times 5280}{3600} \right)^2 = 7.215 \times 10^6 \ in.lb.$$

The crush length, L, of the plank, for a constant force, is evaluated as:

$$L = \frac{KE}{F_c} = \frac{7.215 \times 10^6}{442{,}080} = 16.3 \ in.$$

For the case of the plank striking the top of the cask, the velocity is 80% of the horizontal case. Hence the kinetic energy would be $4.618 \text{x} 10^6$ in.lb. and the crush length of the plank is 10.4 in.

Missile A

Missile A (automobile) deforms and is crushed during the impact. The local pressure on the cask structure is less than 1% of the body yield strength. Therefore, no local penetration occurs. The shear stress in the cask wall is conservatively calculated below. It is assumed that the impact force is concentrated on a small curved section of the cask wall having rectangular dimensions. It is also assumed that only two edges are tending to shear (above and below the curved section). The impact force, F_a, above is used in the calculation. It is assumed that only 3 foot sections are shearing. Then:

Shear Area = 2 x 36 x the thickness of the gamma shielding

= 2 x 36 x 7.25 = 522.0 in^2

The shear stress, τ = Force/area = 222,682/522 = 426.6 psi.

The level D allowable shear stress for the gamma shielding is 0.42 S_u = 0.42 x 70,000 = 29,400 psi. The shear stress is well below the allowable shear stress.

Assuming that the impact on the side of the cask is reacted by a 3 foot high section of shielding, Case 15, Table 9.2, of Reference 17 is used to model the impact as shown below.

$|M_{max}| = 3/2(wR^2)$

The $2\pi Rw$ (from Table 9.2, case 15, Reference 17) is the side impact force = 222,682 lbs.

R = 41.125 inches (mean radius of gamma shield)

Therefore, $w = F/2\pi R$ = 861.8 lbs/in.

And, $|M_{max}| = 3/2(wR^2) = 2.1863 \times 10^6$ in lbs.

The bending stress on the section is:

$\sigma b = M \times c/I = 2.1863 \times 10^6 \times (7.25/2)/(36 \times 7.25^3/12) = 6{,}932$ psi

Where: I denotes moment of inertia of cylindrical slab

c is the maximum normal distance from neutral surface

A conservative estimate of the stress intensity is:

$(\sigma^2 + 4 \times \tau^2)^{0.5} = (6932^2 + 4 \times 426.6^2)^{0.5} = 6985$ psi

The Level D allowable for membrane plus bending stress is S_u. For SA-266 Cl. 2 shielding material at 300 °F, S_u = 70,000 psi. Thus the allowable stress is 70,000 psi. Therefore, the membrane plus bending stress is acceptable.

Missile B (wood plank, Horizontal Impact)

The shear stress is calculated using the contact force (F_c above), the perimeter of the plank, and the thickness of the shield shell.

Shear Area = (plank perimeter) x (thickness of shield shell)

Shear Area = (4+12+4+12) x 7.25 = 232 in^2

Shear Stress, τ = Force/area = 442,080/232 = 1,905 psi.

The Level D allowable shear stress for the gamma shielding is 0.42 S_u = 0.42 x 70,000 = 29,400 psi. The shear stress is well below the allowable shear stress.

Assuming that the impact on the side of the cask is reacted by a 36 inch high section of shielding, the impact is modeled as in missile A above. The height of the section is a conservative estimate of the portion of the shield shell that reacts to the impact. In reality, the entire shell would be affected.

$|M_{max}| = 3/2(wR^2)$

The $2\pi Rw$ (from Table 9.2, Case 15, Reference 17) is the side impact force = 442,080 lbs.

R = 41.125 inches (mean radius of gamma shield)

Therefore, $w = F/2\pi R$ = 1711 lbs/in.

And, $|M_{max}| = 3/2(wR^2) = 4.34 \times 10^6$ in lbs.

The bending stress on the section is:

$\sigma_b = M \times c/I = 4.34 \times 10^6 \times (7.25/2)/(36 \times 7.25^3/12) = 13,762$ psi

Where: I denotes moment of inertia of cylindrical slab

c is the maximum normal distance from neutral surface

A conservative estimate of the stress intensity is:

$(\sigma^2 + 4 \times \tau^2)^{0.5} = (13762^2 + 4 \times 1905^2)^{0.5} = 14280$ psi

From above, the Level D allowable stress is 70,000 psi. Therefore, the membrane plus bending stress is acceptable.

Missile B (wood plank, Vertical Impact)

The shear stress is calculated using the contact force, F_c, above, the perimeter of the plank, and the thickness of the lid.

Shear Area = (plank perimeter) x (thickness of shield shell)

Shear Area = (4+12+4+12) x 4.5 = 144 in^2

Shear Stress, τ = Force/area = 442,080/144 = 3,070 psi.

The Level D allowable shear stress for the gamma shielding is 0.42 S_u = 0.42 x 70,000 = 29,400 psi. The shear stress is well below the allowable shear stress.

The bending stress of the lid outer plate is calculated ignoring the protective cover and top neutron shield and assuming that the lid is simply supported circular plate. The bending stress is estimated using the analytic relation from Reference 17, Table 11.2, Case 18: the flat circular plate of constant thickness T, with uniform load over a small eccentric circular area of radius R_o, simply supported.

The equivalent radius of wood plank contact area is calculated as:

R_o = ((contact area)/π)$^{1/2}$ = ((4 x 12)/π)$^{1/2}$ = 3.91 in.

The lid model assumes that the inner radius of shell flange, R=36 inch, is the effective radius of the lid circular support and its outer radius.

To maximize bending the center of load is assumed to be at the center of the circular plate (p=0). The Poisson's ratio is assumed to be v = 0.3.

Per Reference 17, the maximum bending moment for this case can be expressed as:

$$M = \frac{CrushForce}{4\times\pi}\times\left[1+(1+\nu)\times\ln(\frac{R-p}{R_o})-(1-\nu)\times(\frac{R_o{}^2}{4\times(R-p)^2})\right]$$

$$M = \frac{442080}{4\times\pi}\times\left[1+(1+0.3)\times\ln(\frac{36-0}{3.91})-(1-0.3)\times(\frac{3.91^2}{4\times(36-0)^2})\right]$$

= 1.37 x 10^5 in-lb.

The bending stress on the section is:

σ_b = 6 x M / T^2 = 6 x (1.37 x 10^5) / 4.5^2 = 40,593 psi

A conservative estimate of the stress intensity is:

$(\sigma^2 + 4 \times \tau^2)^{0.5} = (40593^2 + 4 \times 3070^2)^{0.5}$ = 41,055 psi

This stress is much below the Level D allowable stress of 70,000 psi.

A3.2.2 WATER LEVEL (FLOOD) DESIGN

The design basis flood for the Prairie Island ISFSI is described in Section 2.4.1. The probable maximum flood level is calculated to occur at the ISFSI is 706.7 ft above mean sea level (msl) with a water velocity of 6.2 ft/sec. This includes wave run-up. The ISFSI is designed and sited such that the lowest point of potential leakage into the cask is above the level of the probable maximum flood.

The casks are designed to withstand loads from forces developed by the probable maximum flood including hydrostatic effects and dynamic phenomena such as momentum and drag.

The TN-40HT cask is designed for an external pressure of 25 psig which is equivalent to a static head of water of approximately 56 ft. This is greater than would be anticipated due to the probable maximum flood.

The drag force (F) exerted on the cask by the flowing water is:

$$F = C_D A \rho \frac{V^2}{2g}$$

Where:

F = Drag force
C_D = Drag coefficient $\approx$1.0
A = Projected area, 140.0 ft^2
ρ = 62.4 lb/ft^3
V = 6.2 ft/sec
g = 32.2 ft/sec^2

Therefore, F = 5,214 lbs

The drag force is applied to the cask in the same manner as the wind force discussed in Section A3.2.1. Since the wind force did not move the cask and the drag force is less than 20% of the wind force (0.2 * 332 psf * 140ft^2 = 9,296 lbs), the postulated flood will not cause the cask to slide or tip.

As mentioned previously, the maximum flood height including wave run-up does not exceed the height of the cask seals. Therefore no inleakage of water can occur. Also, the interspace between the containment seals and the containment vessel cavity are pressurized to further preclude any possibility of water inleakage.

A3.2.3 SEISMIC DESIGN

Seismic design criteria are set forth in 10 CFR Part 72.102. The design earthquake for use in the design of the casks must be equivalent to the safe shutdown earthquake (SSE) for a collocated nuclear power plant, the site of which has been evaluated under the criteria of 10CFR100, Appendix A (Reference 7).

Section 2.6 of the Prairie Island USAR discusses site seismology and the development of the SSE. An SSE of 0.12g horizontal and 0.08g vertical has been established as the design criteria.

A3.2.3.1 SEISMIC ACCELERATION LEVEL

The TN-40HT cask is a very stiff structure. The dominant structural frequency of vibration for a loaded cask in the lateral direction is determined as shown below:

$f = 3.89/\ (WL^3/8EI)^{1/2}$ (Reference 24, Page 369, Case #3)

Where:

W	= Weight of Cask = 240,000 lbs
L	= Height of Cask = 199.63 in.
E	= Modulus of Elasticity = 28.3×10^6 psi
D_o	= Cask Body O.D. = 89.5 in.
D_i	= Cask I.D. = 72.0 in.
I	$= (\pi/64)(D_o^4 - D_i^4) = (\pi/64)(89.5^4 - 72.0^4) = 1.83 \times 10^6\ in^4$

Substituting the values given above,

$f = 57$ Hz

The vertical structural frequency of cask will be still higher since the cask has higher axial stiffness than the lateral stiffness. Thus the cask standing vertically on its pad has dominant lateral and vertical frequencies higher than 33 Hz (corresponding to the maximum ground acceleration, NUREG 1.60 Reference 19).

Therefore, the cask can be treated as a rigid body and the maximum seismic load on the cask is the peak ground acceleration times the mass of the cask. The cask is, therefore, evaluated using an equivalent static seismic loading method, and there is no need to specify a design response spectrum or its associated time history. The equivalent static load used conservatively includes a factor of 1.5 times (per NUREG-0800, Reference 4) the basic g level specified earlier.

A3.2.3.2 SEISMIC-SYSTEM ANALYSIS

The only significant effects of seismic loading that might occur would be sliding and/or tipping (overturning) of the cask.

<u>Cask Sliding</u>

If the cask is to slide due to seismic loading, the horizontal component of the seismic load must overcome the friction force between the cask base and concrete pad. The friction force is equal to the normal force due to gravity acting at the cask/ground interface multiplied by the coefficient of friction.

The vertical seismic force is applied upward (0.08W * 1.5 = 0.12W) so as to decrease the normal force and hence the sliding resistance force. The downward load then becomes 0.88W and the friction force that must be overcome to slide the cask is 0.22W (0.25x 0.88W). The maximum side load is 0.12W x 1.5=0.18W; therefore, the cask will not slide.

Cask Tipping

The cask will not tip over due to a seismic event if the stabilizing moment due to cask weight is higher than the seismic tipping moment. For a cylindrical cask, the horizontal g value necessary to tip the cask is calculated below:

$$M_{tip} = g_h W L_v + (2/3) g_h W L_r$$

Where:

M_{tip} = Moment necessary to tip the cask, in-lbs
g_h = Horizontal acceleration value necessary to tip the cask
W = Weight of cask on pad
L_v = Vertical distance to C.G. = 91.58 in.
L_r = Radial distance to C.G. = 44.75 in.

$$M_{stab} = W L_r$$

Where:

M_{stab} = Stabilizing moment of the cask, in-lbs.
W = Weight of cask on pad
L_r = Radial distance to CG = 44.75 in

Therefore, the g value necessary to tip the cask is found by equating M_{tip} to M_{stab}:

$$g_h W L_v + (2/3) g_h W L_r = W L_r$$

$$g_h = 44.75/(91.58 + 0.667 \times 44.75) = 0.37$$

The two horizontal components of seismic load are combined as indicated in Section 2.1 of Reference 8. At 45° to either horizontal component, the response due to a N-S earthquake is sin 45° x N-S response and likewise for an E-W earthquake is cos 45° x E-W response. If both components are equal, the combined response is:

$(\sin^2 45° + \cos^2 45°)1/2$ x response = response in either axis.

Therefore, we only need to consider a single horizontal axis for the maximum seismic response.

For this evaluation the horizontal response is 0.12g x 1.5 = 0.18g which is less than the 0.37g required to tip the cask, the cask will not tip over.

A3.2.4 SNOW AND ICE LOADINGS

The decay heat of the contained fuel will continue to heat the cask throughout its service life thus provide a heat source to melt snow or ice. However, to bound the possibility of unmelted snow or ice, a loading corresponding to 50 psf (0.35 psi) is bounded by the analyses.

The temperature of the protective cover attached to the top of the cask above the lid under certain conditions could fall below 32 °F and a layer of snow or ice might build up. A 50 psf (0.35 psi) snow or ice load corresponds to approximately 6 ft of snow or 1 ft of ice. However, this load is insignificant on the TN-40HT since the cover is a 0.38 in. thick torispherical steel head which can withstand an external load over 20 psi. Therefore, the cover will maintain its intended protective function under snow or ice loading conditions.

A3.2.5 COMBINED LOAD CRITERIA

A3.2.5.1 INTRODUCTION

Sections A3.2.1 through A3.2.4, above, describe the most severe natural phenomena considered in the design of the TN-40HT. The forces and pressures applied to the cask due to these phenomena have been determined. These phenomena have been analyzed to show that the cask is stable. It will not tip over under any condition or slide on its pad more than approximately an inch.

All of the above phenomena are upper bound, low probability events. In most cases, however, there is a more regular or frequent similar phenomena of lower magnitude. For instance, some small wind loading occurs often, but tornado winds are unlikely. The forces and pressures determined for the severe phenomena can therefore be used as upper bound values for all similar events.

It has been assumed that these bounding forces and pressures, with a single exception, can occur at any time and their effects are combined with those due to normal operations. The sole exception is the loading(s) due to the tornado missiles as described in Section A3.2.1.3.

A3.2.5.2 TN-40HT CASK LOADING

A brief explanation of the cask loads due to events that will occur or can be expected to occur in the course of normal operation at the ISFSI follows. The cask loads due to the severe natural phenomena and accidents are compared with those for similar but less severe normal events. Then loads equal to or higher than the upper bound values selected for design and analysis of the TN-40HT, defined as Service Loads, are described. Finally, the Service Loads are separated into two levels and superposition of simultaneous loading (combined loads) is discussed.

A3.2.5.2.1 NORMAL OPERATION

During normal storage on the ISFSI pad, the cask is subjected to loading due to its own dead weight and that of its contents (fuel and basket), assembly stresses due to the bolt preload required to seat the double metal seals and react to the internal pressure, and internal pressure due to initial pressurization and any fuel clad failure resulting in fission gas release.

Additional normal loads include wind loading which produces a distributed lateral load on one side of the cask and can also result in slight external pressure drop on other portions of the cask.

Lifting loads due to cask dead weight, fuel and basket are applied to the cask through the trunnions.

An increased external pressure is applied to all surfaces of the cask during fuel loading when the cask is at the bottom of the spent fuel pool. Snow and ice loads apply local external pressure loading to the top of the protective cover. The cask will be subjected to the full range of thermal conditions produced by ambient variations (including insolation) and decay heat.

A3.2.5.2.2 LOADINGS DUE TO SEVERE NATURAL PHENOMENA AND ACCIDENTS

The tornado wind loading described in Section A3.2.1 could produce higher lateral loading than any normal wind loading or flood water drag force. The external pressure drop due to the tornado wind is also more severe than due to any normal condition.

External pressure loading of the cask could occur due to flooding (see Section A3.2.2), burial, or nearby explosion. The full range of thermal conditions due to ambient variations, decay heat and minor fires in the vicinity of the cask apply.

A3.2.5.2.3 THERMAL CONDITIONS

The TN-40HT component temperatures and thermal gradients are affected by the following thermal conditions:

- Fuel loading
- Decay heat
- Insolation
- Beginning of life unloading
- Ambient variations
- Lightning
- Minor fire
- Cask burial

The thermal conditions which are of concern structurally are the temperature distributions in the cask and the differential thermal expansions of interfacing cask components.

A3.2.5.2.4 FUEL LOADING

The cask is loaded in a spent fuel pool under water. The cask is cooled by pool water; therefore, the thermal gradients established during fuel loading are negligible.

A3.2.5.2.5 DECAY HEAT/SOLAR LOAD

After the cask is loaded and removed from the pool, the cask body will gradually reach steady state conditions. Since the mass of the cask is large, the time to reach equilibrium will be approximately 1 to 2 days. The temperature gradients in the cask body have an insignificant effect on the structural integrity of the body.

Thermal analyses have been performed to determine the temperatures within the cask for different normal and accident conditions. The methods used to obtain these results are discussed in Section A3.3.2.2. The cask temperature distribution for the off-normal condition was used for the structural analysis.

A3.2.5.2.6 BEGINNING OF LIFE UNLOADING

This condition would occur if it were necessary to place the cask back in the pool at the beginning of life after it had been loaded and reached thermal equilibrium. Prior to completely submerging the cask in the pool, the cask and fuel would have to be cooled by circulating water through the cask. Therefore, cold water would contact the hotter cask inside surfaces and fuel pins. Past experience/evaluations have shown that beginning of life unloading has little effect on the cask temperature and thus has an insignificant effect on the cask body and the fuel cladding loadings.

A3.2.5.2.7 AMBIENT VARIATIONS

Because the cask thermal inertia is large, the cask thermal response to changes in atmospheric conditions will be relatively slow. Ambient temperature variations due to changes in atmospheric conditions i.e., sun, ice, snow, rain and wind will not affect the performance of the cask. Snow or ice will melt as it contacts the cask because the outer surface will typically be above 32 °F. The cyclical variation of insolation during a day will also create insignificant thermal gradients.

A3.2.5.2.8 LIGHTNING

Lightning will not cause a significant thermal effect. If struck by lightning on the lid, the electrical charge will be conducted by paths provided by the lid bolts to the body. It is not anticipated that lightning could cause significant increase in seal temperatures.

A3.2.5.2.9 FIRE

The only real source of fuel for a fire in the vicinity of the cask is the fuel tank of the cask transport vehicle which transports the cask to the storage pad. An evaluation was made to determine the thermal response of the cask assuming this minor fire is an engulfing fire. The results of this analysis are provided in Section A3.3.2.2.2.4. The cask will maintain its containment integrity during and after this bounding hypothetical fire accident. 60400000330

A3.2.5.2.10 BURIED CASK

An evaluation is made to determine the increase in cask temperature with time assuming that the cask is completely buried by dirt and debris with very low thermal conductivity. The results of this analysis are given in Section A3.3.2.2.2.4. The analysis shows that the cask will maintain its containment integrity for a burial period of over 74 hours, assuming all fuel assemblies in the TN-40HT cask contain burnable poison rod assemblies (BPRAs), and for over 92 hours if the cask does not contain BPRAs. 60400000330

A3.2.5.3 BOUNDING LOADS FOR DESIGN AND SERVICE CONDITIONS

A3.2.5.3.1 DEAD (WEIGHT) LOADS

The only dead loads (hereafter referred to as weights) on the cask are the cask weight including the contents. The calculated weights of the individual components of the cask and the total weights are given in Table A3.2-1. The weight of the cask assembly is reacted as a contact force between cask and storage pad except when the cask is supported (lifted) by the pair of trunnions at the top of the cask during handling prior to fuel loading.

A3.2.5.3.2 LIFTING LOADS

The cask is provided with two trunnions at the top spaced 180 degrees apart for non-redundant lifting. The trunnions at the bottom of the cask are for rotation of the cask.

The upper trunnions are designed to meet the requirements of NUREG-0612 (Reference 3) for non-redundant lifting fixture. This is accomplished by evaluating the trunnions to the stress design factors required by ANSI N14.6 (Reference 9), i.e. capable of lifting 6 times and 10 times the cask weight without exceeding the yield and ultimate strengths of the material, respectively. The trunnion loads are shown in Figure A3.2-3 and listed in Table A3.2-3.

The local region of the cask body is conservatively evaluated for a vertical load of 3 g (i.e., 3 times the weight of the cask) which is reacted at the trunnions involved in the handling operation. The factor of 3 provides ample allowance for sudden load application during lifting.

A3.2.5.3.3 INTERNAL PRESSURE

The pressure inside the cavity of the storage cask results from several sources. Initially, the cavity is backfilled with helium to at least 19.5 psia . The basis for the initial pressure is to establish, and maintain, a cask environment with no more than 0.25% oxidizing gases by volume. Pressure variations due to daily and seasonal changes in ambient temperature conditions will be small due to the large thermal capacity of the cask. Fuel clad failure results in the release of fission gas which increases cavity pressure. Section A3.3.2.2.6.1 evaluates the increases in pressure due to off-normal and accident scenarios.

Another condition when internal pressure could increase is the cool down prior to unloading. This could occur at the beginning or end of life. Water will be gradually added to the cask during refilling to ensure that the cask pressure limits are not exceeded. See Section A3.3.2.2.5.2 for an evaluation of internal pressure during reflooding.

Table A3.2-2 presents a summary of internal pressures for the conditions identified. A pressure of 22 psig was chosen as the design internal pressure. This value bounds the normal and off-normal operating pressures.

A3.2.5.3.4 EXTERNAL PRESSURE

There are several conditions which can result in external pressure on the cask. The external pressure due to a flood is less than the designed external pressure as discussed in Section A3.2.2.

During fuel loading or unloading the cask is at the bottom of the spent fuel pool, nominally 40 ft. deep. This results in an external hydrostatic pressure of approximately 20 psi.

An explosion on a barge in the vicinity of the Prairie Island plant has been shown to produce an overpressure of less than 2.25 psi at the ISFSI location.

An earth pressure loading would occur if the cask were to be buried under dirt. This is similar to a hydrostatic pressure head of water. The density of loose dirt or earth is approximately 100 lb/ft^3 compared to 62.4 lb/ft^3 for that of water. Therefore 36 ft. of earth is equivalent to a 56 ft. head of water and an external pressure of 25 psi.

The various external pressures are also summarized in Table A3.2-2. The cask is designed and evaluated for an external pressure of 25 psi. This value was selected because it exceeds the maximum external pressure which would be anticipated for any of the loading conditions considered above including floodwater discussed in Section A3.2.2 and snow and ice in Section A3.2.4.

A3.2.5.3.5 CASK BODY LOADS

Globally distributed loads may be applied to the cask by wind (tornado is the upper bound case), flood water and seismic excitation. These loads are explained in detail and calculated in Sections A3.2.1 through A3.2.3. Table A3.2-4 lists the numerical values of these forces as calculated in the various sections. Note that bounding dynamic loads equal to the weight of the cask (1g load) in each direction (lateral and vertical) applied as inertial loads for stress analysis purposes envelope all of these distributed loads with a substantial margin.

A3.2.5.4 DESIGN AND SERVICE LOADS

The various cask loading conditions are listed in Table A3.2-5. These loading conditions include those described in 10CFR Part 72 (Reference 1), which are categorized as normal, man-made and natural phenomena. The applied loads acting on the different cask components due to these loading conditions have been determined and are discussed in the preceding sections and are listed in Table A3.2-2 through Table A3.2-4. This section describes the bases used to combine the loads for each cask component. The specific stress criteria against which each load combination will be evaluated are described in Section A4.2.3.

The bounding pressures and loads described above are used in the load combinations.

Certain combinations are evaluations of several events (e.g., one load combination represents stresses due to tornado wind, hurricane wind, normal wind, flood water, etc.).

Several loads are always present and are included in all evaluations. These are the assembly stresses due to bolt preload and metal seal compression. Lifting loads are always reacted by the cask weight (supported by trunnions - not the storage pad). Lifting loads are not combined with those due to extreme natural phenomena since cask operations would be halted during a flood, tornado, etc. Dead weight loads are reacted at the bottom of the cask by the storage pad for all cases except the lifting cases.

A3.2.5.4.1 CASK BODY

The loading conditions for the cask body including the containment vessel and gamma shielding are categorized based on the rules of the ASME Boiler and Pressure Vessel Code Section III, Subsection NB, for a Class 1 nuclear component (Reference 2). The ASME code categorizes component loadings into five service loading conditions. They include Design Conditions (same as the Primary Service) and Levels A, B, C and D Service Loadings. The code provides different stress limits for each of these service loadings.

For each of these service loading conditions, there are several applied loads acting on the cask. The Design Loads are listed in Table A3.2-6. They include internal and external pressure; lid bolt preload including the effect of the gasket reactions; distributed loads due to weight, wind, and handling, and attachment loads applied through the trunnion to the cask body.

The inertia g loads are quasistatically applied loads which are multiples of the weight of the cask and/or contents. The magnitude of the Design Loads envelope the maximum Level A Service Loads. Thermal effects are excluded, except for their influence on the preload of the lid bolts (if any) because the ASME Code does not consider them Design (i.e., primary) Loads.

The Level A Service loads are listed in Table A3.2-7 and are basically the same as the Design Loadings except that the thermal effects on the containment vessel are included. The thermal effects consist of secondary (thermal) stresses caused by differential thermal expansion due to temperature differences caused by decay heat, solar insolation, ambient temperature variations and ambient conditions.

There are no Level B or C Service Loading Conditions. Events which occur infrequently which could be considered Level B or Level C Service Loadings are conservatively considered Level A loadings.

The loads due to Level D Service Loading Conditions, which are extremely unlikely conditions, are listed in Table A3.2-8.

Loading combinations for Normal Conditions (Design Conditions and Levels A Service Loadings) are given in Table A3.2-9. Loading combinations for Accident Conditions (Level D) are provided in Table A3.2-10. The loads are listed across the top of the table and the Load Combinations are designated in the first column of the table.

There are eight normal (Design and Level A Service Loadings) load combinations listed, and five accident condition (Level D) combinations. The loads which are acting simultaneously for each of these combinations are denoted by an "X" under the load column heading. For example, for Normal Condition Load Combination N3, lid bolt preload, fabrication loads, distributed weight, internal pressure due to cavity pressurization and fission gas release, and heat due to maximum normal temperatures are acting simultaneously.

A3.2.5.4.2 BASKET

Cask body internal and external pressures have no effect on the basket. External loads applied to the TN-40HT cask do not result in basket loads unless the cask actually moves. Therefore, tornado wind and flooding produce no basket loads. Seismic loading, however, is an inertial loading as discussed in Section A3.2.3, and is applied to the basket. The seismic acceleration loading (much less than 1g acceleration) is combined with dead weight loading since the two effects occur simultaneously.

Temperature effects due to snow, minor fire and ambient temperature variations which can cause thermal transients on the outside of the cask body will not cause similar transients in the basket. The high heat capacity of the body slows the temperature response and effectively eliminates transients at the wall of the cask cavity. The steady state temperature and temperature differences throughout the basket are, however, affected by decay heat, solar insolation and ambient temperature variations.

The basket is important for control of criticality of the fuel assemblies stored in the cask. The bounding lateral and vertical inertial loadings on the basket are equal to 1g (in each direction) and have been shown to envelope the basket loadings. For the basket evaluation, an even more conservative 3g loading in the vertical direction is analyzed.

The stresses in the 304 stainless steel portions of the basket due to the primary loading, 1g in any lateral direction combined with 3g vertical (including dead weight), are determined by conservatively neglecting the tensile and bending strength of the plates (aluminum and/or poison) between fuel compartment boxes. The through thickness strength of the plates which separate the boxes is considered. Thus the aluminum and/or poison material is conservatively neglected in the primary load analysis where it can react some of the load. These primary stresses in the steel are evaluated at the maximum metal temperature occurring under extreme ambient conditions.

Clearance is provided between the aluminum/poison and stainless steel plates to provide for differential thermal expansion. The basket design criteria described in Section A4.2.3.3.3 is based on Section III Subsection NG and Appendix F of the ASME Code for stress limits.

The basket evaluation is provided in Appendix A4B.

A3.2.5.4.3 UPPER TRUNNIONS

The upper trunnions are designed to meet the requirements of NUREG-0612 (Reference 3) for non-redundant lifting fixture. This is accomplished by evaluating the trunnions to the stress design factors required by ANSI N14.6 (Reference 9). During lifting, the trunnions are evaluated for vertical lifting reactions applied at the lifting shoulders required to support 6 times or 10 times the maximum weight of a fully loaded cask. When the load is equal to 6 times the weight, the maximum tensile stresses shall not exceed the minimum yield strength of the trunnion material. For the load equal to 10 times the weight, the maximum tensile stresses shall not exceed the minimum ultimate tensile strength of the trunnion material.

The loads acting on the trunnions are shown in Table A3.2-3. The structural analysis of the trunnions is presented in Section A4.2.3.

In a response to questions from the NRC Staff, NSP provided justification in Reference 10 for the adequacy of the load testing performed on the TN-40 cask trunnions during fabrication. In a Safety Evaluation dated May 11, 1995 (Reference 11) the NRC concluded that NSP had demonstrated that the trunnion-to-cask attachment welds have an acceptable level of quality and that load testing of the trunnions as described in Reference 10 provides an acceptable demonstration of the adequacy of the TN-40 cask trunnions. Since the trunnions for the TN-40HT cask are designed to the same requirements as the trunnions for the TN-40 cask, and the attachment welds have the same level of quality, the conclusions of Reference 11 are applicable to the TN-40HT cask.

A3.2.5.4.4 OUTER SHELL

The outer shell is evaluated for the combined effects of inertia g loads due to lifting and internal pressure.

Out-gassing from the resin between the cask body and outer shell may cause a slight pressure on the inside of the outer shell. A pressure relief valve is provided in the outer shell to assure any pressure buildup is small. The outer shell is completely supported by the resin when subjected to an external pressure. An internal pressure of 3 psig will occur due to the reduced external pressure during a tornado. An internal pressure of 25 psig is conservatively used to evaluate the outer shell. The structural analysis of the outer shell is presented in Appendix A4A7. A summary of results and comparison with design criteria are given in Section A4.2.3.4.6.

A3.3 SAFETY PROTECTION SYSTEMS

A3.3.1 GENERAL

The TN-40HT cask is designed to provide storage of spent fuel. The cask cavity pressure is always above ambient during the storage period as a precaution against the in-leakage of air which might be harmful to the fuel. Since the containment vessel consists of a steel cylinder with an integrally-welded bottom closure, the cavity gas can escape only through the lid closure system. In order to ensure cask leak tightness, two systems are employed. A double barrier system for all potential lid leakage paths consisting of covers with multiple seals is utilized. Additionally, pressurization of monitored seal interspaces provides a continuous positive pressure gradient which guards against a release of the cavity gas to the environment and the admission of air to the cavity.

A3.3.2 PROTECTION BY MULTIPLE CONFINEMENT BARRIERS AND SYSTEMS

A3.3.2.1 CONFINEMENT BARRIERS AND SYSTEMS

A combined cover-seal pressure monitoring system (Figure A3.3-1) always meets or exceeds the requirement of a double barrier closure which guarantees tight, permanent confinement. There are two lid penetrations, one for a drain pipe and one for venting and pressurization. When the cask is placed in storage, a pressure greater than that of the cavity is set up in the gaps (interspaces) between the double metallic seals of the lid and the lid penetrations. A decrease in the pressure of the monitoring system would be signaled by a pressure transmitter mounted at the side of the cask (Figure A3.3-1). The system is pressurized through a fill valve mounted near the overpressure tank. Lead shielding will be provided to reduce radiation exposure to the transmitter to acceptable levels.

Connections to the overpressure tank are welded fittings. A quick connect coupling with a diaphragm valve is used to fill the tank.

The Helicoflex metal seals of the lid and lid penetrations possess long-term stability and have high corrosion resistance over the entire storage period. These high performance seals are comprised of two metal linings formed around a helically-wound spring. The sealing principle is based on plastically deforming the seal's outer lining. Permanent contact of the lining against the sealing surface is ensured by the outward force exerted by the helically-wound spring. Additionally, all metal seal seating areas are stainless steel overlay for improved surface control. The overlay technique has been previously used for the TN-40 casks.

For protection against the environment, a torispherical protective cover equipped with an elastomeric seal is provided above the lid. The lid and cover seals described above are contained in grooves. A high level of sealing over the storage period is assured by utilizing seals in a deformation-controlled design. The deformation of the seals is constant since bolt loads assure that the mating surfaces remain in contact. The seal deformation is set by its original diameter and the depth of the groove. 60400000330

Metal gasket face seal fittings, diaphragm valves, and Helicoflex metal seals are all capable of limiting leak rates to less than 1 x 10^{-7} atm cm^3/sec of helium.

The initial operating pressure of the monitoring system's overpressure tank is set at 5.5 atm abs minimum. Over the storage period, the pressure decreases as a result of leakage from the system and as a result of temperature reduction of the gas in the system. Since the level of permeation through the containment vessel is negligible and leakage past the higher pressure of the monitoring system is physically impossible, a decrease in cavity pressure during the storage period occurs only as a result of a reduction in the cavity gas temperature with time. As long as the pressure in the monitoring system is greater than that of the cavity and ambient pressure, no in-leakage of air or out-leakage of cavity gas is possible.

The analyses provided in Appendix A7A define the monitoring system helium test leakage rate which ensures that no cavity gas can be released to the environment nor air admitted to the casks for a 25 year period. If needed during or after the 25 year period, the monitoring system is capable of being repressurized. All seals are considered collectively in the analysis as the monitoring system pressure boundary. 60400000330

A3.3.2.2 HEAT TRANSFER DESIGN

The TN-40HT cask is designed to passively reject decay heat under normal conditions of storage and hypothetical accident conditions while maintaining appropriate packaging temperatures and pressures within specified limits. An evaluation of the TN-40HT cask thermal performance is presented in this section. Objectives of the thermal analyses performed for this evaluation include:

- Determination of maximum and minimum temperatures with respect to material limits
- Determination of temperature distributions for analysis of thermal stresses
- Determination of temperatures for containment pressurization

The TN-40HT basket consists of an assembly of 40 stainless steel fuel compartments with aluminum and neutron poison plates sandwiched between them. The compartments are joined by a fusion welding process to 1.75 in. wide stainless steel bars. Above and below the bars are slotted aluminum and neutron poison plates which form an egg-crate structure. Stainless steel basket rails including aluminum inserts are bolted to the basket periphery to provide a conduction path from the basket to the cask cavity wall. This thermal design feature of the basket allows the heat from the fuel assemblies to be conducted along the basket structure to the basket rails and dissipated to the cask cavity wall.

The neutron shielding is provided by a resin compound cast into long slender aluminum containers placed around the cask shell and enclosed within a smooth outer shell. By butting against the adjacent shell surfaces, the aluminum containers provide a conduction path and allow decay heat to be conducted across the neutron shield.

To establish the heat removal capability, several thermal design criteria are established for the TN-40HT cask. These are:

- Confinement of radioactive material and gases is another design consideration. Seal temperatures must be maintained below specified limits to satisfy the confinement function during normal and accident conditions. A maximum temperature of 536 °F (280 °C) is set for the double metallic seals in the containment vessel closure lid.
- To maintain the stability of the neutron shield resin during normal storage conditions, the neutron shield bulk average temperature cannot exceed 300 °F (149 °C).
- Maximum temperatures of the containment structural components must not adversely affect the confinement function.
- Maintaining fuel cladding integrity during storage is a major design requirement. Fuel cladding temperature limits have been established per ISG-11 (Reference 25). For normal conditions of storage and short term loading operations such as vacuum drying, fuel cladding temperature limit is 400 °C (752 °F). For off-normal storage, and accident conditions, the fuel cladding temperature is limited to 570 °C (1058 °F).

In general, all thermal criteria are associated with maximum temperature limits and not with minimum temperatures. All materials can be subjected to the minimum environment temperature of -40 °F (-40 °C) without adverse effects.

The TN-40HT cask is analyzed based on a maximum heat load of 32 kW from 40 fuel assemblies with a maximum decay heat of 0.80 kW per fuel assembly (including inserts).

A3.3.2.2.1 THERMAL MODEL

A3.3.2.2.1.1 THERMAL MODEL FOR NORMAL AND OFF-NORMAL STORAGE CONDITIONS

To determine the maximum component temperatures, two finite element models are developed using the ANSYS computer code (Reference 44).

- Full-length cask model
- Sub-model of cask top

ANSYS is a comprehensive thermal, structural, and fluid flow analysis package. It is a finite element analysis code capable of solving steady-state and transient thermal analysis problems in one, two, and three dimensions. Heat transfer via a combination of conduction, radiation, and convection can be modeled by ANSYS.

A3.3.2.2.1.1.1 FULL LENGTH CASK MODEL

The full length model is three dimensional and represents a 90° symmetric section of the TN-40HT cask. This model includes the geometry and the material properties of the basket, basket rails, cask shells, cask lid, protective cover, cask bottom plates, radial neutron shield, and top neutron shield, as well as concrete pad and supporting soil. The full-length model is used to determine the maximum temperatures for the fuel cladding and the other components (except the seals and the top neutron shield located within and above the cask lid).

The protective cover is modeled using SHELL57 elements (Reference 44). For conservatism, no heat transfer is considered between the protective cover and the upper surface of the cask lid in the full-length model to minimize the axial heat transfer.

Fuel assemblies are modeled as a homogenized material within the fuel compartments.

It is assumed that no convection heat transfer occurs within the cask cavity. The effective conductivity calculated for the homogenized fuel includes the radiation heat transfer. The conduction heat transfer through the basket and cask components is modeled using SOLID70 elements (Reference 44).

The aluminum basket rails are divided into four 40 in. sections. Axial gaps of 0.06” are considered between each two adjacent rail pieces. This model conservatively bounds the structural design of three-piece rails.

The following gaps are considered between components in the model at thermal equilibrium:

a) Air gaps:

- 0.01” radial gaps between the aluminum resin boxes and the adjacent shells
- 0.01” axial gap between the cask lid and the cask flange
- 0.01” axial gap between flange of the protective cover and the cask flange
- 0.01” axial gap between the cask lid and the shield plate
- 0.02” axial gap between the top neutron shield and the cask lid outer plate
- 0.125” axial gap between the bottom inner plate and the bottom shield plate
- 0.01” axial gap between the bottom shield plate and the shield shell

b) Helium gaps:

- 0.01” transverse gap between a poison plate or a stainless steel bar and the fuel compartment wall
- 0.02” transverse gap between an aluminum or a stainless steel bar and the fuel compartment wall
- This gap in combination with the above gap allows for using of multiple sheets and plates instead of using one pair of aluminum and poison plates.
- 0.06” axial gap between basket rail segments
- 0.125” axial gap between the basket and the inner bottom plate
- 0.13” radial gap between the rails and the cask inner shell
- 0.02” gap between the aluminum inserts and stainless steel plates of the basket rails at bolted joints
- 0.10” gap between the aluminum inserts and stainless steel plates of the basket rails at unbolted locations
- 0.01″ gap between the basket plates and the basket rails or shims
- 1.00″ gap at each end of the poison and aluminum plates.

The axial cold gap of 0.07” between the stainless steel structural bars and the poison/aluminum plates is conservatively modeled as a larger gap of a 0.01″ axial gap at the bottom and a 0.19” axial gap at the top of the stainless steel bars.

The width of the cutout in basket aluminum plates or poison plates is considered to be 1.11” which is larger than the nominal cold cutout width of 1.00”.

A gap of 0.01” is used between the cask inner shell and the shield shell to simulate the thermal resistance of the shrink fit gap between these shells. Identical to Section 3.3.2.2.1, a contact conductance of 350 Btu/hr-ft^2 equal to an effective conductivity of 0.0243 Btu/hr-in-°F is used to model the shrink fit gap.

The geometry of the full-length model for TN-40HT cask is shown in Figure A3.3-2 and Figure A3.3-3. The locations of the gaps are shown in Figure A3.3-4 and Figure A3.3-5.

A3.3.2.2.1.1.2 SUB-MODEL FOR CASK TOP

The second finite element model represents only the top portion of the TN-40HT cask. This model is a sub-model of the full cask model in which radiation between the top neutron shield and protective cover are added to determine the maximum temperatures of the seals and the top neutron shield resin.

The cask top sub-model includes the cask flange, cask top shield plate, cask lid, protective cover, and the overpressure tank. The dimensions and the material properties for the sub-model are identical to those for the full-length model.

The geometry of the sub-model for the cask top is shown in Figure A3.3-6.

A3.3.2.2.1.1.3 STEADY STATE BOUNDARY CONDITIONS

TH-40HT cask is designed for ambient temperatures between -40 °F and 120 °F. The maximum daily average temperature of 100°F is used for the maximum off-normal storage temperature.

Under the cold condition of -40 °F (-40 °C) ambient, the resulting packaging minimum component temperatures will approach -40 °F if no credit is taken for the decay heat load. Since the packaging materials, including containment structures and the seals, continue to function at this temperature, the minimum temperature condition has no adverse effect on the performance of the TN-40HT cask. Thermal analysis for minimum ambient temperature of -40 °F and no insolance is performed using the maximum decay heat load of 32 kW to determine the temperature distributions for structural evaluation.

Normal storage conditions (50 °F ambient) are bounded by the hot off-normal storage conditions (100 °F ambient). The temperature profiles for hot off-normal conditions are conservatively used for normal storage conditions.

The SOLID70 elements representing the homogenized fuel are given heat generation load throughout the 144” active fuel length. The active fuel length begins at about 4.0” above the bottom of the fuel assembly. The effective fuel properties are used for the entire basket length (160”) within the homogenized fuel regions.

A typical axial decay heat profile from Reference 26 with a peaking factor of 1.1 is used to apply the heat in the active fuel region. The decay heat profile is smoothed and converted to a local average for each of the axial fuel segments defined for the homogenized fuel assemblies in the finite element model. Section A3.3.2.2.1.3 describes the conversion method and lists the resulting peaking factors used in the model.

Convection and radiation to the ambient are combined together to form a total heat transfer coefficient, which is defined as a temperature dependent material property in the model. The total heat transfer coefficients are used to apply to the outer surface of the cask. Section A3.3.2.2.4 describes the correlations to calculate these total heat transfer coefficients.

Solar radiation is considered as a constant heat flux applied on the SURF152 elements overlaid on the outer surface of the cask. The outer surfaces of the cask are painted white. The insolance values from 10CFR71 (Reference 38) are considered as the maximum amount of solar radiation that is available for absorption on any surface. These values are multiplied by the absorptivity factor of each surface to calculate the amount of solar heat flux that each surface absorbs. The resultant value is applied as a constant heat flux to the corresponding surface. The heat flux values used in the model are listed below.

Surface	Insolance (Reference 38) (gcal/cm^2)	Total solar heat flux averaged over 24 hrs. (Btu/hr-in^2)	Absorptivity	Solar heat flux in the model (Btu/hr-in^2)
Cask Surface, Curved, Painted	400	0.427	0.3	0.128
Cask Surface, Flat Horizontal, Painted	800	0.853	0.3	0.256
Concrete, Flat, Horizontal	800	0.853	1.0	0.853

It is assumed that soil has a temperature of 70 °F at 10 feet below the cask bottom plate for hot conditions. The soil temperature for the cold condition (-40 °F) is assumed to be 45 °F. The concrete pad is 3 feet thick. Due to low conductivity of concrete and soil, the model is insensitive to the thickness of the pad / soil and the soil temperature.

Typical boundary conditions for the TN-40HT cask full-length model are shown in Figure A3.3-7.

The full-length model shows approximately 1.00 kW (3412.3 Btu/Hr) of heat dissipates from the top of the cask. To bound the analysis, a heat flow of 1.2 kW equal to 3.5% of the total heat load (decay heat plus insolance) is considered to be transferred to the cask top in the sub-model. This heat flow is applied as uniform heat flux at the bottom of the cask top sub-model.

$$q''_{top} = \frac{q_{top}}{\pi/4\ D^2} = \frac{1.2 \times 3412.3}{\pi/4 \times 89.5^2} = 0.6509 \text{ Btu/hr-in}^2$$

The boundary conditions for the cask top sub-model are shown in Figure A3.3-8.

A3.3.2.2.1.2 Thermal Models for Accident Conditions

The TN-40HT casks will be stored on a concrete pad away from combustible material. Therefore, no fires other than small electrical fires are considered credible at the ISFSI. However, a hypothetical fire accident is evaluated for the TN-40HT cask based on a diesel fuel fire, resulting from a ruptured fuel tank of the cask transport vehicle. The bounding capacity of the fuel tank is 200 gallons and the bounding hypothetical fire is an engulfing fire around the cask. 604000000330

Another evaluation performed on the cask is the thermal response of the cask in the postulated event of it being completely buried by dirt and debris with very low thermal conductivity. The temperature-time history of the cask components during these events are reported in this section.

The purpose of the accident thermal analyses is to calculate the maximum fuel cladding and the maximum seal temperatures in order to demonstrate the containment integrity of the TN-40HT cask.

Two models, a cask cross section model and a lid-seal region model, are used for the evaluation. The cask cross-section model is created by selecting the nodes and elements at the midsection of the full-length cask model described in Section A3.3.2.2.1.1.1. The selected segment contains all the nodes and elements of the full-length cask model from z = 37.57" to z = 67.57" in the axial direction, where the decay heat generation and the resultant temperatures are at their highest for the hot off-normal storage conditions. The height of this model is 30", which is twice the nominal height of one basket segment. The lid-seal region model is identical to the cask top sub-model described in Section A3.3.2.2.1.1.2.

The geometry and the material properties of these sub-models are the same as those for the normal and off-normal cask models described above. The models for accident condition analysis are shown in Figure A3.3-9.

The initial temperatures for both cases are retrieved from the result file of the off-normal storage conditions using the sub-modeling ANSYS commands "NWRITE" and "CBDOF" (Reference 44). The boundary conditions for the sub-models are discussed in the following sections.

A3.3.2.2.1.2.1 BOUNDARY CONDITIONS FOR THE HYPOTHETICAL FIRE ACCIDENT

An average flame temperature of 1475 ^{o}F and flame emissivity of 0.9 from Reference 38 and a forced convection heat transfer coefficient of 4.5 Btu/hr-ft^{2}-^{o}F from Reference 39 were used for the fire accident case.

The "pool" of fuel is assumed to extend 1 meter beyond the cask surface (Reference 40). Based on an outer shell diameter of 101 inches, this gives a "pool" diameter of approximately 180” (with the cask standing upright) and a pool surface of 25,400 in^2. A fuel consumption rate of 0.15 in/min. was selected from a Sandia Report (Reference 39) concerning gasoline/tractor kerosene experimental burning rates. This translates into a fuel consumption rate of approximately 16.5 gal/min. Therefore, the 200 gallons of fuel will sustain a fire for about 12 minutes and hence a 15 minute fire is evaluated.

The convection and radiation heat transfer from the fire are combined together as a total heat transfer coefficient. The calculation of the total heat transfer coefficient for fire is discussed in Section A3.3.2.2.4. The total heat transfer coefficients are defined as temperature dependent material properties and used to apply the boundary conditions on the outer surface of the cask. The free convection and radiation during the post fire cool down period are also added together as a total heat transfer coefficient. An ambient temperature of 100 °F equal to the maximum hot off-normal storage temperature is assumed for the cool down period.

The fire accident can occur only during the transfer operation where combustible fuel is available. During transfer operation, the transferred cask is not surrounded by other casks. Nevertheless, a view factor of 0.8 is considered for the cask during cool down period for conservatism.

During the cool down period, the solar radiation is applied as a constant heat flux on the SURF152 elements (Reference 44) overlaid on the outer surface of the cask. It is assumed that the outer surfaces of the cask are covered with soot after the fire accident. A solar absorptivity of 1.0 (maximum value) is considered for these surfaces to bound the condition. The solar heat flux values applied in the model are listed below.

Surface	Insolance (Reference 38) (gcal/cm^2)	Total solar heat flux averaged over 24 hrs (Btu/hr-in^2)	Absorptivity	Solar heat flux in the model (Btu/hr-in^2)
Cask surface, curved, painted	400	0.427	1.0	0.427
Cask surface, flat horizontal, painted	800	0.853	1.0	0.853

For the cross-section model, the heat generating boundary conditions are applied on the elements representing the homogenized fuel with a peaking factor of 1.1. No axial heat transfer is considered at the top and bottom ends of the cross-section model.

Heat generation rate = $\dot{q}'' = \dfrac{q}{a^2\ L_a} \times PF = 0.3218$ Btu/hr-in^3

where,

q = Decay heat load per assembly = 2,730 Btu/hr (0.80 kW)
a = Width of the modeled fuel assembly = 8.05”
L_a =Active fuel length = 144”
PF = maximum peaking factor =1.1

Although the solid neutron shield resin might degenerate in the first few minutes of the fire accident, it is assumed that its conductivity remains unchanged throughout the fire. After the fire, the conductivity of the neutron shield is replaced by air conductivity.

To maximize the heat input from fire into the transfer cask, the 0.01” air gaps between the neutron shield aluminum boxes and the adjacent shells are removed and replaced by properties of Al-6063. For the same reason, the shrink fit gap between the inner shell and the shield is also removed during the burning time and replaced by properties of SA 516, Gr. 70 (cask shield shell). These gaps are restored immediately after the fire to maximize the thermal resistance, which consequently maximizes the fuel cladding temperature.

The maximum poison plate conductivity would be lower than that of pure aluminum. Thus the conductivity of the poison plates was increased to the values for aluminum 1100 during the burning time and restored to the lower conductivity during the cool down period to bound the uncertainty about the conductivity of poison plates.

For the lid-seal region model, the heat flux from the cask calculated in Section A3.3.2.2.1.1.3 (0.6509 Btu/hr-in^2) is applied at the bottom of the model. Radiation heat transfer between the protective cover and the upper surfaces of the cask lid and the top neutron shield is considered in the lid-seal region model. This radiation heat transfer maximizes the heat input from the fire via the protective cover to the vent and port seals located in the cask lid.

Similar to the cask cross-section model, the 0.01” air gaps between the top neutron shield and the cask lid, the cask lid and the top shield plate, and the protective cover and cask flange in the cask top model are removed during the fire and replaced by properties of SA 516, Gr. 70 carbon steel. These gaps are restored in their original location during the cool down period.

The conductivity of neutron shield resin is considered for the elements within the top neutron shield case during the burning period. The conductivity of these elements is changed to air during the cool down period.

The resultant time-temperature histories of the fuel cladding, discussed in Section A3.3.2.2.2.4, show a continuous temperature increase without any extreme for the fire accident case. Therefore, the maximum fuel temperature for the post-fire accident case is calculated using a steady-state run of the cask cross-section model.

A3.3.2.2.1.2.2 BOUNDARY CONDITIONS FOR THE POSTULATED BURIED CASK

The heat generation boundary conditions of the fuel are identical to those described for the hypothetical fire accident case. The heat flux toward the cask top applied at the bottom of the cask top sub-model is also identical to those described for the hypothetical fire accident case. Adiabatic boundary conditions are considered on the outermost nodes of the cask cross-section and the lid-seal models for buried cask case.

A3.3.2.2.1.3 AXIAL DECAY HEAT PROFILE

The normalized axial burnup profile for typical PWR fuels with burnups higher than 30 GWd/MTU is given in Reference 26 and is listed in Table A3.3-1. The active fuel length is 144”.

Seventeen axial fuel regions are defined for the fuel assembly in the finite element model. Local peaking factors (PF_z) at the start and end of each region are calculated based on linear interpolation between data in Table A3.3-1. The average of the local peaking factors at the start and end of each region is assigned as PF_m. The average peaking factors (PF_m) are smoothed to give an axial decay heat profile identical to the profile from Reference 26.

The average peaking factors used in the model are listed in Table A3.3-2.
Figure A3.3-10 compares the decay heat profile used in the model with the profile from Reference 26.

The area underneath the smoothed peaking factor profile is calculated as follows.

$$A = \sum_{1}^{n} PF_{m,i} \left(z_i - z_{i-1}\right)$$

Where,

A = total area underneath the axial heat profile

$PF_{m,i}$ = average peaking factor in fuel region i

z_i= fuel region level at the end of region i

The total area under the axial decay heat profile divided by the active fuel length must be equal to 1. As seen in Table A3.3-2, the resultant value is 0.993. A correction factor of 1/0.993 is therefore multiplied by the heat generating rate to avoid any degradation of the applied decay heat in the finite element model.

A3.3.2.2.1.4 Thermal Models with Lower Poison Plate Conductivity

To provide more flexibility in the manufacturing of the baskets, models were created and analyses performed utilizing a lower conductivity for poison plates than the models described in the previous sections.

The lower conductivity models were created by combining the poison plate conductivity of 0.68 Btu/hr-in-°F (independent of temperature) and the conductivities of the aluminum 1100 plate taken from Table A3.3-8 together as one set of effective conductivities for both materials. The paired aluminum and poison plates build up parallel thermal resistances along the plate surface and serial thermal resistance across the plate thickness. The effective conductivities for the paired plates are calculated as follows.

$$k_{eff,along} = \frac{k_{Al} \times t_{Al} + k_p \times t_p}{t_{Al} + t_p}$$

$$k_{eff,across} = \frac{t_{Al} + t_P}{\frac{t_{Al}}{k_{Al}} + \frac{t_P}{k_P}}$$

Where

$k_{eff,\ along}$ = parallel thermal conductivity of the paired plates
$k_{eff,\ across}$ = serial thermal conductivity of the paired plates
k_{Al} = thermal conductivity of Al-1100, see Table A3.3-8
t_{Al} = aluminum plate thickness as modeled = 0.312 in.
k_P = thermal conductivity of poison plate = 0.68 Btu/hr-in-°F
t_P = poison plate thickness as modeled = 0.125 in.

As shown in Figure A3.3-5, Detail A and Detail D, the 0.02 inches and 0.01 inches gaps between the aluminum/poison plates and the stainless steel bars/fuel compartment are modeled discretely. Therefore, they are not included in the calculation of the effective conductivities for the paired plates.

The orientations of the paired plates in the thermal model are shown in Figure A3.3-42 and are designated as vertical and horizontal for ease of reference in this calculation. As seen in Figure A3.3-42, the horizontal paired plates provide parallel thermal resistances in the x and z directions and serial thermal resistances in the y direction. For these plates, $k_{eff,along}$ is applied in the x and z directions and $k_{eff,across}$ is applied in the y direction in the cask model. Similarly, the vertical paired plates provide parallel thermal resistances in the y and z directions and serial thermal resistances in the x directions. For the vertical paired plates shown in Figure A3.3-42, $k_{eff,along}$ is applied in the y and z directions and $k_{eff,across}$ is applied in the x direction in the cask model.

The calculated effective conductivities and their directional application in the model are presented in Table A3.3-35. Except for the calculated effective conductivities, $k_{eff,along}$ and $k_{eff,across}$, for the paired aluminum and poison plates, the other thermal properties of the aluminum and poison plates remain unchanged.

The full length model of the TN-40HT cask described in Section A3.3.2.2.1.1.1 and the ANSYS computer code (Reference 44) were used to evaluate the cask thermal performance with reduced conductivity of the poison plates. In addition to changing the poison plate conductivity to 0.68 Btu/hr-in-°F, the transverse effective fuel conductivities were changed to the values presented in Table A3.3-9 for evaluation of the off-normal storage, hypothetical fire accident, and postulated buried cask accident conditions. The other material properties used in these models are the same as those listed in Table A3.3-8. As discussed in Section A3.3.2.2.1.1.3, normal storage conditions are bounded by off-normal conditions and are not further evaluated.

The boundary conditions used in the reanalysis for the off-normal storage, hypothetical fire accident, and postulated buried cask accident conditions were the same as those described in Sections A3.3.2.2.1.1.3, A3.3.2.2.1.2.1, A3.3.2.2.1.2.2, respectively. Similar to the evaluation methodology described in Section A3.3.2.2.1.2.1, the transient evaluation of the full length cask model for the fire accident condition is followed by a steady-state evaluation to verify that the maximum fuel cladding temperature for the post-fire conditions has been identified.

The full length model of the TN-40HT cask was also used for the vacuum drying reanalysis. The boundary conditions used in the reanalysis for the vacuum drying condition are the same as those described in Sections A3.3.2.2.5.1. Similar to the approach described in Section A3.3.2.2.5.1, adiabatic boundary conditions were applied on the cask lid and cask bottom shield of the full length model and an average initial temperature of 215°F was assumed for the cask components at the start of water draining. The boundary conditions and times for the cask residing in the pool and in the fuel handling building were also the same as those described in Section A3.3.2.2.5.1.

Identical to the conditions described in Section A3.3.2.2.5.1, effective conductivity values in a vacuum were considered for elements representing homogenized fuel assemblies and air conductivity was given to the elements representing the gas within the cask cavity for the vacuum drying reanalysis. Except for the conductivity of poison plate, the other material properties used in this model were the same as those listed in Table A3.3-8.

The results of the reanalysis are compared to the results utilizing the design basis models in the previous sections in Table A3.3-36 through Table A3.3-39 for the off-normal storage, hypothetical fire accident, postulated buried cask accident conditions, and vacuum drying condition. The resulting maximum temperature histories of the cask components during fire accident are illustrated in Figure A3.3-43.

As seen in Table A3.3-36, the evaluations of the TN-40HT cask with a poison plate conductivity of 0.68 Btu/hr-in-°F for off-normal storage conditions result in a lower maximum fuel cladding temperature. The maximum basket and cask component temperatures remain either unaffected or bounded by the values calculated with the design basis model. The average cavity gas temperature is also bounded by the design basis model.

The amount of conduction heat flow rate from the cask top toward the protective cover is retrieved from the low conductivity model using the same approach used in Section A3.3.2.2.1.1.3. The amount of conduction heat from the cask to the protective cover is 1.00 kW, which is the same as that determined in Section A3.3.2.2.1.1.3 for the design basis model. As described in Section A3.3.2.2.1.1.3, the top cask model uses a uniform heat flux equivalent to a heat flow of 1.2 kW. Therefore, the maximum component temperatures at the top of the cask, such as cask lid, cask lid seal, etc., remain bounded by those determined using the top cask sub-model described in Section A3.3.2.2.1.1.2 and no reevaluation using the top cask sub-model is required.

The evaluation for the minimum ambient temperature of -40°F and no insolance described in Section A3.3.2.2.2.2 maximizes the temperature gradient across the cask body for structural evaluation. Since the maximum temperatures remain bounded by the design basis model and the cold ambient temperature is unchanged, the temperature gradient across the cask body remains bounded by the design basis model.

As seen in Table A3.3-37 and Figure A3.3-43, the evaluations of the TN-40HT cask with a poison plate conductivity of 0.68 Btu/hr-in-°F using the full length cask model for fire accident conditions result in a peak maximum fuel cladding temperature during the transient. As discussed in Section A3.3.2.2.2.4, the cask cross-section model used as the design basis model does not show a peak temperature until steady state conditions are reached after the fire. The reason for this behavior is that the full length model provides a heat dissipation area which is larger than the active fuel length. Given the long period of time during cool-down and available large heat dissipation area, the maximum fuel cladding temperature decreases slightly as shown in Figure A3.3-43 and as indicated in Table A3.3-37 for the full-length model. The peak maximum temperature and the steady state temperature reported in Table A3.3-37 for the low conductivity model remain bounded by the values resulting from the design basis model.

A comparison of Figure A3.3-14 (page 1 of 2) and Figure A3.3-43 indicates a higher peak maximum temperature for the outer shell when the full length model is used to evaluate the fire accident condition. This higher peak temperature is located at the joint between the outer shell and the top and bottom outer shell ring, which is included in the full length model but not in the cross section model. The outer shell joint region provides a larger area for fire heat intake and thus a higher peak temperature. The high temperature region is localized and concentrated in the joint as shown in Figure A3.3-44 and does not result in a higher volumetric average temperature as shown on Table A3.3-37.

As seen in Table A3.3-38, the evaluations of the TN-40HT cask with a poison plate conductivity of 0.68 Btu/hr-in-°F using the full length cask model for buried cask accident conditions result in a lower fuel cladding and cask component temperatures. Thus, the values calculated with the design basis model remain bounding.

This evaluation shows that using the lower conductivity of 0.68 Btu/hr-in-°F for the poison plates in the basket is compensated for by removing the conservatism in the transverse effective fuel assembly conductivity and utilizing the full length model. Therefore, the results and conclusion in Section A3.3.2.2.2 remain conservatively bounding or unaffected.

The reanalysis of the vacuum drying conditions for the TN-40HT cask with lower poison plate conductivity results in a maximum fuel cladding temperature of 718°F at the end of vacuum drying (34 hours). This is lower than the maximum design basis model fuel cladding temperature of 731°F listed in Table A3.3-14. The maximum component temperatures resulting from the vacuum drying reanalysis are compared to the results utilizing the design basis model in Table A3.3-39. The maximum temperatures for fuel cladding, radial neutron shielding material, and seals remain bounded by the values calculated with the design basis model for vacuum drying condition as shown in Table A3.3-39.

This evaluation shows that using a conductivity of 0.68 Btu/hr-in-°F for the poison plates does not affect the time limit for vacuum drying, and the time limit of 34 hours for vacuum drying as specified in Section A3.3.2.2.5.1 remains valid.

A3.3.2.2.2 RESULTS OF THE THERMAL ANALYSES

A3.3.2.2.2.1 MAXIMUM TEMPERATURES FOR NORMAL/OFF-NORMAL STORAGE CONDITIONS

Steady state thermal analyses are performed using a total decay heat load of 32 kW (0.80 kW/assembly), 100 °F daily average temperature, and the maximum insolance per 10CFR71 (Reference 38). Insolance is averaged over a 24 hour period.

The resultant temperature distributions for the cask models are shown in Figure A3.3-11, Figure A3.3-12 and Figure A3.3-13. Summaries of the maximum component temperatures are listed in Table A3.3-3. The temperatures for the normal storage conditions are bounded by those for hot off-normal conditions. Therefore, thermal stresses and cask maximum internal pressures are calculated based on the temperatures resulting from hot off-normal conditions.

The volumetric average temperatures for the basket, aluminum shim, cask inner shell, basket support bars, and basket aluminum plates at the hottest cross section are retrieved from the thermal models and are listed in Table A3.3-4.

A3.3.2.2.2.2 MINIMUM TEMPERATURES FOR NORMAL/OFF-NORMAL STORAGE CONDITIONS

Temperature distributions under the minimum ambient temperature of –40 °F with no insolance and the maximum design heat load of 32 kW are determined under steady state conditions to maximize the temperature gradients in the cask. Table A3.3-5 summarizes the results of this analysis.

A3.3.2.2.2.3 EVALUATION OF THERMAL PERFORMANCE FOR NORMAL/OFF-NORMAL STORAGE CONDITIONS

The thermal analysis for storage conditions demonstrates that the TN-40HT cask design meets all applicable requirements.

The maximum component temperatures calculated using conservative assumptions are lower than the allowable limits. The maximum cask lid seal and vent and port seal temperatures are below the long-term limit specified for continued seal function. The average resin temperature at the hottest cross section in the radial neutron shield and the top neutron shield are lower than the limit. Therefore, no degradation of the neutron shielding is expected. The calculated maximum fuel cladding temperature is well below the temperature limit considered for normal conditions of storage given in ISG-11 (Reference 25).

A3.3.2.2.2.4 MAXIMUM TEMPERATURES FOR ACCIDENT CONDITIONS

The time-temperature histories of the cask components are shown in Figure A3.3-14 for the hypothetical fire accident analysis performed on the cask cross-section and the lid-seal models. As Figure A3.3-14 shows, the fuel cladding temperature increases during and after the fire without reaching a peak. Therefore, a steady-state run using post fire conditions is used to determine maximum fire accident temperature. Final temperature distributions resulting from the steady state run of the cask cross-section model are shown in Figure A3.3-15. The temperature distribution for the lid-seal model is shown in Figure A3.3-16 for fire accident conditions. Table A3.3-6 summarizes the maximum temperatures resulting from the transient or the steady state runs for the fire accident case.

Due to adiabatic boundary conditions assumed at the outer surface of the buried cask, the cask component temperatures will continue to increase as a function of time. The times at which the component temperatures reach the allowable limits are listed in Table A3.3-7.

A3.3.2.2.2.5 EVALUATION OF THERMAL PERFORMANCE FOR ACCIDENT CONDITIONS

The thermal analysis for the accident conditions demonstrates that the TN-40HT cask meets all applicable requirements.

The maximum fuel cladding temperature for the fire accident case is well below the allowable limit of 1058 °F recommended in Reference 25. The lid-seal temperature reaches the peak value at the end of fire. The vent and port seals reach their peak temperatures at 1.2 hours after the end of the fire. The seal temperatures remain well below the allowable limit of 536 °F. It is assumed that the solid neutron shield degenerates during the fire. Therefore, the maximum temperature of the solid neutron shield is irrelevant. 60400000330

The analysis results of the buried cask accident show that if the cask is not uncovered within 1.23 hours, the neutron shield temperature exceeds the allowable limit of 300 °F. The fuel temperature exceeds the allowable limit of 1058 °F about 92 hours after the cask is buried completely.

Approximately 74 hours after the cask is buried, the average cavity gas temperature reaches 843 °F. The pressure based on this temperature is below a cavity internal pressure of 100 psig as concluded in Section A3.3.2.2.6. The seal temperature remains well below the allowable limit of 536 °F. 60400000330

A3.3.2.2.3 MATERIAL PROPERTIES

The temperature dependent thermal properties of material used in the thermal analyses are provided in Table A3.3-8. The tables are linearly interpolated to obtain values for temperature between table values.

A3.3.2.2.3.1 DETERMINATION OF NEUTRON ABSOBER (POISON) PLATES THERMAL PROPERTIES

Boral™, borated aluminum, and a metal matrix composite are possible poison materials to be used in the TN-40HT cask. Boral™ is the poison plate material conservatively analyzed below. The poison material consists of two cladding layers and one core. The core material conductivity is significantly lower than the cladding material conductivity. For conservatism, no credit is taken for the cladding conductivity.

Boral™	Thermal conductivity of Core		Thermal conductivity of Poison Plate
Temperature (°F)	(W/cm-K) (Reference 33)	(Btu/hr-in-°F)	(Btu/hr-in-°F)
100	0.859	4.14	4.14
500	0.768	3.70	3.70

Based on data from Reference 33, the average density for Boral™ plate is calculated as follows:

$D_a = 2.713\,(g/cm^3) \times t_a\,(cm)$; t_a = cladding thickness

$D_c = 2.481\,(g/cm^3) \times t_c\,(cm)$; t_c = core thickness

$D_t = (2 \times D_a + D_c)$

Poison plate density = D_t / t_t; t_t= Boral™ plate thickness

For a core thickness of 0.1" for a 0.125" thick Boral™ plate, the plate density is 0.091 lbm/in^3. A value of 0.0896 lbm/in^3 is conservatively used for poison plates in the analysis.

Specific heat for Boral™ plate can be calculated as follows:

$$Cp_t = \frac{2\,Cp_a \times D_a + Cp_c \times D_c}{D_t}$$ (Reference 33)

Boral™	Specific heat of Aluminum Cladding (Cp_a)		Specific heat of Core (Cp_c)		Specific heat of Poison Plate (Cp_t)
Temperature (°F)	(kJ/kg-K)	(Btu/lbm-°F)	(kJ/kg-K)	(Btu/lbm-°F)	(Btu/lbm-°F)
100	0.919	0.22	0.936	0.22	0.22
500	1.12	0.27	1.38	0.33	0.32*

*0.33 Btu/lbm-°F is used in the model. Due to small differences between these values the thermal evaluation remains unaffected.

A3.3.2.2.3.2 DETERMINATION OF HELIUM THERMAL PROPERTIES

The thermal properties for helium are calculated based on the following polynomial function from Reference 27.

$$k = \sum C_i\, T_i$$ for conductivity in (W/m-K) and T in (K)

For 300 < T < 500 K			for 500< T < 1050 K	
c0	-7.761491E-03		c0	-9.0656E-02
c1	8.66192033E-04		c1	9.37593087E-04
c2	-1.5559338E-06		c2	-9.13347535E-07
c3	1.40150565E-09		c3	5.55037072E-10
c4	0.0E+00		c4	-1.26457196E-13

A3.3.2.2.3.3 DETERMINATION OF AIR THERMAL PROPERTIES

The thermal properties for air are calculated based on the following polynomial function from Reference 27.

$k = \sum C_i \; T_i$ for conductivity in (W/m-K) and T in (K)

For 250 < T < 1050 K	
c0	-2.2765010E-03
c1	1.2598485E-04
c2	-1.4815235E-07
c3	1.7355064E-10
c4	-1.0666570E-13
c5	2.4766304E-17

A3.3.2.2.3.4 DETERMINATION OF CONCRETE AND SOIL THERMAL PROPERTIES

The thermal conductivity of normal, saturated concrete varies from 1.2 to 2.0 Btu/ft-hr-°F at temperatures ranging from 50 to 150 °F (Reference 30). The conductivity of concrete decreases rapidly with the rise in temperature and assumes, at 750 °C (1382 °F) a conductivity value equal approximately to 50 percent of that of normal temperature (Reference 30). For the thermal analyses a thermal conductivity of 1.15 Btu/hr-ft-°F (0.0958 Btu/hr-in-°F) is used for concrete at 70 °F. This conductivity is reduced by half to a value of 0.0479 Btu/hr-in-°F at 1382 °F. A thermal conductivity of 0.3 W/m-K (0.0144 Btu/hr-in-°F) is considered for soil (Reference 31).

Since the concrete pad is not included in the transient runs such as the fire accident and the vacuum drying cases, the density and specific heat of concrete and soil are not provided.

A3.3.2.2.3.5 EMISSIVITIES AND ABSORPTIVITIES

All outer surfaces of TN-40HT cask and all inner and outer surfaces of the protective cover are painted white. Reference 32 gives an emissivity between 0.92 and 0.96, and a solar absorptivity between 0.09 and 0.23 for white paints. To account for dust and dirt and to bound the problem, the thermal analysis uses an emissivity of 0.9 and a solar absorptivity of 0.3 for white painted surfaces.

Emissivity of concrete is between 0.9 and 0.94 (References 31 and 32). An emissivity of 0.90 is used for concrete surfaces. For conservatism a solar absorptivity of 1.0 is used for concrete surface to bound the effect of insolation.

The emissivity of the cask outer surface is set to 0.8 to be consistent with the requirements in Reference 38 during the accident fire. It is assumed that the cask surface is covered with soot after the fire. The solar absorptivity of soot is 0.95 (Reference 32). To bound the problem, the thermal analysis uses a solar absorptivity of 1.0 and an emissivity of 0.9 for cask surfaces after the fire.

A3.3.2.2.3.6 EFFECTIVE FUEL THERMAL PROPERTIES

A3.3.2.2.3.6.1 DISCUSSION

The finite element models of the TN-40HT cask simulate the effective thermal properties of the fuel with a homogenized material occupying the volume within the basket where the fuel assemblies are stored. Effective values for density, specific heat, and conductivity are determined for this homogenized material to use in the finite element models.

The characteristics of the fuel assemblies to be stored in the TN-40HT cask are listed in Section A7, Table A7.2-1. Among these assemblies, the smallest cladding thickness and the largest gap between the fuel pellet and clad are chosen to determine the bounding thermal conductivities for the homogenized fuel assemblies.

A3.3.2.2.3.6.2 SUMMARY OF FUEL MATERIAL PROPERTIES

The properties used for UO_2 and Zircaloy for calculation of the effective fuel properties are given below. The conductivities of helium and air as backfill gases are listed in Table A3.3-8.

The air conductivity is used for vacuum drying conditions. The vacuum drying process generally does not reduce the pressure sufficiently to reduce the thermal conductivity of the water vapor and air in the cask cavity. Therefore, air conductivity is assumed for the backfill gas for vacuum drying conditions. For other conditions, the conductivity of helium is used for backfill gas.

A3.3.2.2.3.6.2.1 FUEL PELLET, UO_2

The conductivity, specific heat, and density for UO_2 fuel pellets are taken from Reference 14 and listed below.

Temperature (°C)	k (cal/s-cm-°C)	Temperature (°F)	k (Btu/hr-in-°F)
25	0.025	77	0.503
100	0.021	212	0.423
200	0.018	392	0.362
300	0.015	572	0.302
500	0.0132	932	0.266
700	0.0123	1292	0.248
800	0.0124	1472	0.250

Temperature (°C)	c_p (cal/g-°C)	Temperature (°F)	c_p (Btu/lbm-°F)
0	0.056	32	0.056
100	0.063	212	0.063
200	0.0675	392	0.068
400	0.0722	752	0.072
1200	0.079	2192	0.079

The density of fuel pellets (UO_2) is 10.96 g/cc = 0.396 lbm/in^3.

The thermal conductivities shown above represent values for un-irradiated UO_2 pellets. A study performed by Transnuclear (TN) and provided to the NRC in Reference 37 shows that the transverse effective fuel conductivity with irradiated UO_2 conductivity is approximately 3% lower than the one with un-irradiated UO_2 conductivity at a temperature of 700°F.

The sensitivity runs in the TN study showed that the fuel cladding temperature changes by approximately 1°F when using irradiated UO_2 conductivity. Since a cladding temperature change of 1ºF is negligible, the results of the study show that the fuel cladding temperature is not sensitive to the conductivity of UO_2. Therefore, use of un-irradiated UO_2 fuel pellet conductivity from NUREG/CR-0200 (Reference 14) is reasonable for irradiated UO_2.

A3.3.2.2.3.6.2.2 FUEL CLADDING, ZIRCALOY-4 / ZIRLO

Table B-2.I of Reference 41 lists measured and calculated values of thermal conductivity for zircaloy at various temperatures. The measured values used in this calculation are listed below.

Temperature (K)	k (W/m-K)	Temperature (°F)	k (Btu/hr-in-°F)
373.2	13.6	212	0.655
473.2	14.3	392	0.689
573.2	15.2	572	0.732
673.2	16.4	752	0.790
773.2	18.0	932	0.867
873.2	20.1	1112	0.968

Table B-1.1 of Reference 41 lists specific heat values for zircaloy as a function of temperature.

Temperature (K)	c_p (J/kg-K)	Temperature (°F)	c_p (Btu/lbm-°F)
300	281	80	0.067
400	302	260	0.072
640	331	692	0.079
1090	375	1502	0.090

The density of zircaloy is 6.56 g/cm^3 = 0.237 lbm/in^3, as defined in Reference 41.

Table B-3.11 of Reference 41 lists the measured emissivity values for fuel cladding. For ease of calculation a temperature independent emissivity of 0.8 is set for Zircaloy-4 in this calculation.

Note that Reference 42 states that ZIRLO and Zircaloy-4 alloys are very similar in terms of their thermal characteristics. Therefore zircaloy properties above are adequate for modeling ZIRLO.

A3.3.2.2.3.6.2.3 EMISSIVITY OF FUEL COMPARTMENTS, STAINLESS STEEL PLATES

An emissivity of 0.3 for the stainless steel plates is used for the fuel compartments in calculating the transverse effective fuel conductivity. This value is conservative relative to the values provided in Reference 6.

A3.3.2.2.3.6.3 EFFECTIVE FUEL CONDUCTIVITY

A3.3.2.2.3.6.3.1 TRANSVERSE EFFECTIVE CONDUCTIVITY

The purpose of the effective conductivity in the transverse direction of a fuel assembly is to relate the temperature drop of a homogeneous heat generating square to the temperature drop across an actual assembly cross section for a given heat load. This relationship is established by the following equation obtained from Reference 43:

$$k_{eff} = \frac{q}{4L_a\,(T_c - T_o)}(0.29468) = \frac{q_{react}}{(T_c - T_o)}(0.29468)$$

Where:

k_{eff} = Effective thermal conductivity (Btu/hr-in-ºF)

q = Assembly heat generation (Btu/hr)

q_{react} = Reaction solution retrieved from the quarter-symmetric 2D model (Btu/hr)

$q = 4 \times q_{react} \times L_a$

L_a = Assembly active length (in)

T_c = Maximum temperature (ºF)

T_o = Compartment Wall temperature (ºF)

A two dimensional, quarter-symmetric finite element model of a 14x14 fuel assembly is developed using the ANSYS computer code (Reference 36). All components are modeled using 2D PLANE55 thermal solid elements. This two-dimensional model simulates the heat transfer by radiation and conduction. No convection is considered within the fuel assembly for conservatism. Radiation between the fuel rods and the compartment walls is simulated using the /AUX12 processor in ANSYS. For this purpose, LINK32 elements are placed on the exteriors of the fuel rods for creation of the radiation super-element. All LINK32 elements are unselected prior to solution of the thermal problem.

The geometry of this model is shown in Figure A3.3-17.

A fuel assembly decay heat load of 0.80 kW is used for heat generation. An active length of 144" is assumed for the model. Several computational runs were made for the model using isothermal boundary temperatures ranging from 100 to 1000 ºF. The isothermal boundary conditions are applied on the outermost nodes of the model, which represent the compartment walls. In determining the temperature dependent effective conductivities of the fuel assembly an average temperature, equal to $(T_o + T_c)/2$, is used for the fuel temperature. A typical temperature distribution for the fuel assembly model is shown in Figure A3.3-18.

The transverse effective conductivity is calculated with helium as backfill gas for all conditions except for vacuum drying. For vacuum drying conditions, the conductivity of helium is replaced by conductivity of air.

A3.3.2.2.3.6.3.2 AXIAL EFFECTIVE CONDUCTIVITY

The backfill gas, fuel pellets, and fuel cladding behave like resistors in parallel. However, due to the small conductivity of the fill gas and the axial gaps between fuel pellets, credit is only taken for the Zircaloy-4 in fuel cladding in the determination of the axial effective conductivities.

$$k_{eff,axl} = \frac{cladding\ area}{4a^2} \times k_{Zr} \qquad \text{(Btu/hr-in-°F)}$$

a = half of compartment width = 8.05”/2 = 4.025”

A3.3.2.2.3.6.4 EFFECTIVE FUEL DENSITY AND SPECIFIC HEAT

Volume average density and weight average specific heat are calculated to determine the effective density and specific heat for the fuel assembly. The equations to determine the effective density and specific heat are shown below.

$$\rho_{eff} = \frac{\sum \rho_i V_i}{V_{assembly}} = \frac{\rho_{UO_2}\ V_{UO_2} + \rho_{Zr}\ V_{Zr}}{4a^2 L_a}$$

$$C_{p,eff} = \frac{\sum m_i\ C_{Pi}}{\sum m_i} = \frac{M_{UO_2}\ C_{P,UO_2} + M_{Zr}\ C_{P,Zr}}{M_{UO_2} + M_{Zr}}$$

A3.3.2.2.3.6.5 CONCLUSION

The transverse effective conductivity values for fuel assemblies in helium are listed in Table A3.3-9. The effective transverse conductivity used for fuel assemblies in thermal analyses for normal/off-normal (when in helium) and accident conditions is lower than the value calculated in this section. The applied values for transverse fuel conductivity are shown in Table A3.3-8 and are compared to the calculated value in Figure A3.3-19. Note that the transverse effective conductivity values for fuel assemblies in air are also shown on Table A3.3-8 as are other calculated effective properties for a homogenized fuel assembly.

The transverse effective conductivities for fuel assemblies reported in Table A3.3-8 (Page 1 of 7) were calculated based on an incorrect Stefan-Boltzmann constant of 1.983E-13 Btu/hr-in^2-°R^4. This value is 60 times lower than the correct value of 1.190E-11 Btu/hr-in^2-°R^4. The transverse effective fuel conductivities calculated with correct parameters are reported in Table A3.3-9. As seen in Figure A3.3-19, the transverse effective fuel conductivities applied in the TN-40HT model are lower than those calculated with the correct parameters.

Since the transverse effective conductivities applied in the TN-40HT model are lower than the corrected values, the results for peak cladding temperatures under normal and off-normal storage conditions were not changed and are conservative.

As described in Section A3.3.2.2.2.4, the peak cladding temperature under fire accident conditions is determined using a steady-state run with the post fire conditions. Therefore, using the lower transverse effective fuel conductivities is also conservative for peak cladding temperature under fire accident conditions.

The peak cladding temperatures will decrease for all transient conditions analyzed in the SAR as the transverse effective fuel conductivities increase. This is primarily due to the lower initial temperatures caused by higher conductivities at the initial conditions of the transient runs.

A3.3.2.2.4 HEAT TRANSFER COEFFICIENTS

A3.3.2.2.4.1 TOTAL HEAT TRANSFER COEFFICIENT TO AMBIENT (NORMAL/OFF-NORMAL)

The outer surfaces of the cask dissipate heat to the ambient via free convection and radiation. Total heat transfer coefficient is defined as:

$$H_t = h_r + h_c$$

Where,

h_r = radiation heat transfer coefficient

h_c = free convection heat transfer coefficient

The radiation heat transfer coefficient, h_r, is given by the equation:

$$h_r = \varepsilon F_{12}\left[\frac{\sigma\left(T_1^{\,2} - T_2^{\,2}\right)}{T_1 - T_2}\right] \text{ (Btu/hr-ft}^2\text{-°F)}$$

Where,

ε = surface emissivity

F_{12} = view factor from cask surface to ambient

$\sigma = 0.1714 \times 10^{-8}$ Btu/hr-ft^2-°R^4

T_1 = cask surface temperature, °R

T_2 = ambient temperature, °R

Since the TN-40HT casks can be modeled as being stored in a $2 \times \infty$ array with a nominal pitch of 18 ft. as shown in Figure A3.3-20, the radiation view factor from the radial cask surfaces to the environment is less than 1.0. A view factor of 0.8138 is calculated for in Section 3.3.2.2.1 between the TN-40 cask and the ambient for this same configuration. This value is multiplied by surface emissivity to calculate radiation heat transfer from cask radial surfaces.

Cask gray body exchange factor = $F_{12} \times \varepsilon = 0.8138 \times 0.9 = 0.7324$

For conservatism, a value of 0.72 is used in the determination of the total heat transfer coefficient that is applied in the detailed TN-40HT cask model described in Section A3.3.2.2.1.1 for calculating of radiation heat transfer.

A3.3.2.2.4.1.1 STORAGE ARRAY RADIANT HEAT TRANSFER EVALUATION

The view factor between the cask surface and the concrete pad and service road surrounding the concrete pad were not considered explicitly in the calculation of the view factor for the TN-40 in Section 3.3.2.2.1.

The surface temperature of the concrete pad and service roads maybe higher than ambient temperature due to solar radiation and thermal radiation from the casks, but it is significantly lower than the cask surface temperature. Therefore, the radiation exchange between the casks and the concrete pad/service road is significant, but it maybe lower than the radiation exchange between the casks and the ambient.

A three dimensional model of TN-40HT casks in a storage array is developed using ANSYS (Reference 36) to investigate the effects of the cask view factor on the thermal performance. The model includes 18 casks and considers a cask pitch of 18 ft. The storage pad width is extended three times the cask pitch (72 ft.) to minimize any uncertainty regarding the radiation exchange between the casks and the surroundings. This model is shown in Figure A3.3-21.

Effective conductivities for cask shells and cask body in axial and radial directions are calculated using the detailed model of TN-40HT cask described in Section A3.3.2.2.1.1.1. The TN-40HT cask is divided into five sections as shown in Figure A3.3-22 to calculate the effective conductivities. The methodologies and results for effective conductivities of cask sections are described in below. These effective conductivities are used in the storage array model to reduce the number of elements and create manageable input and output files.

The dimensions of the TN-40HT cask in the storage array model are identical to those used in Section A3.3.2.2.1.1.1. The decay heat load is applied as a uniform heat flux on the cask inner surface over the length of basket (160 in.). This heat flux is calculated as follows.

Decay heat = 32 kW = 109,193.6 Btu/hr

ID_{cask} = 72”

$Height_{basket}$ = 160”

Decay heat flux = Decay heat /(π $ID_{cask} \times Height_{basket}$) = 3.017 Btu/hr-in^2

The solar heat flux on the cask outer surface and the fixed temperatures at 10 ft. below the cask bottom plate are identical to those described in Section A3.3.2.2.1.1.3. Free convection boundary conditions are considered at the cask outer surface using correlations described in Section A3.3.2.2.4.3. Radiation exchange between cask and surroundings is simulated using radiosity methodology in ANSYS (Reference 36). An ambient temperature of 100 °F is considered for this model.

The resultant temperature distributions are shown in Figure A3.3-23 for cask outer surfaces, in Figure A3.3-24 for the storage pad surface temperature, and in Figure A3.3-25 for the cask inner shell.

As seen in Figure A3.3-21, the storage array model considers complete casks without symmetry planes. The detail cask model described in Section A3.3.2.2.1.1.1 considers a 90 degree, quarter symmetric segment of the cask. In order to compare the temperature profiles of these two models, average temperatures at the hottest cross sections are retrieved form each model.

The average and maximum temperatures for storage array model and TN-40HT detailed cask model are compared in Table A3.3-10.

As seen in Table A3.3-10, the average temperatures for the cask inner shell in the array storage and the cask detail models are within 1 °F of each other. Therefore, the temperatures for the basket and its contents would not be affected significantly if the view factor from the cask to surrounding storage pads were included in the thermal model.

The average cask surface temperature in the detailed cask model is 242 °F while the average cask surface temperature in the storage array model is 260 °F. This shows a temperature increase of 18 °F due to the cask view factors.

The calculated average resin temperature at the hottest cross section of the detailed model is 267 °F. The addition of the storage pad to the cask view factor calculation increases the average resin temperature at the hottest cross section by at most 18 °F to 285 °F. This temperature remains below the allowable limit of 300 °F for the radial resin.

Since the basket temperatures calculated in the TN-40HT detailed model remain unaffected, these temperatures can be used for calculation of the thermal stress, thermal expansion, and cask cavity pressure for the structural evaluation.

The view factors from the emitting cask (shown in Figure A3.3-20) to other casks and to the storage pad are calculated from the storage array model. These view factors are compared in Table A3.3-11 to the values calculated in Section 3.3.2.2.1 for information purposes only.

<u>Impact of Southeast ISFSI Pad Expansion</u>

As discussed in Section A3.3.2.2.4.1, the view factor in the detailed TN-40HT cask model is based on a cask alignment of two rows of infinite length, which is conservative for the existing configuration. As shown in Figure A3.3-20 and documented in the existing analysis, the view factors from the emitting cask to the receiving casks beyond cask 5 are not considered in the calculation due to their negligible effect.

60400000330

Note that the distance from the emitting cask to cask 5 is approximately, $(18\text{ ft.}2 + (4 \times 18\text{ ft.})^2)^{0.5} \approx 74$ ft., and the distance between the closest cask on the existing northwest ISFSI pad and the southeast ISFSI pad is approximately, $((9\text{ ft.} + 40\text{ ft.} + 9\text{ ft.})^2 + (11\text{ ft.} + 38\text{ ft.} + 9\text{ ft.})^2)^{0.5} \approx 82$ ft., given a 38 ft. separation between the existing northeast ISFSI pad and the southeast ISFSI pad. As such, the southeast ISFSI pad installation does not affect the calculated view factors used in the detailed TN-40HT cask model.

However, similar to how to the storage array model was used to estimate the increase in the cask outer shell temperature due to the concrete pad and the service road, the effect on the average cask surface temperature due to the addition of a southeastern ISFSI pad should be evaluated for the existing northeastern pad. The impact of the southeast ISFSI pad, fully loaded with TN-40HT casks, on the existing northeast ISFSI pad, fully loaded with TN-40HT casks, on the radiant heat transfer between the casks, ground, and environment is evaluated with the use of a computational fluid dynamics (CFD) model. The CFD model is developed using STAR-CCM+ (Reference 49). STAR-CCM+ is a commercially available computer code developed by Siemens Product Lifecycle Management Software Inc.

This model evaluated the radiation heat transfer between the casks, ground, and environment but did not model air flow around the cask (i.e., convection is modeled as a boundary condition), similar to how the ANSYS model evaluates radiant heat transfer. Although heat conduction through the casks and ground is also included in the models, only the temperature distributions on the outer surfaces of the casks are to be regarded as valid results since the internal details of the casks and conduction heat transfer through solid casks were modeled in a simplified manner. For both casks and ground, the thermal conductivity is considered using three parametric runs with values ranging from 0.5 W/m-K to 5.0 W/m-K in order to envelop typical expected values. The model is discretized in approximately 300,000 cells. A benchmark was performed against the results of the existing storage array model using a CFD model case with one set of two rows of casks, and it was determined that the CFD model yields cask exterior temperature results that were essentially the same as the ANSYS storage array model. Another case with two sets of two rows of casks with pads spaced 38 ft. apart was used to determine the maximum and average cask exterior temperatures, as shown in Table A3.3-10A. This model is shown in Figure A3.3-21A. Additional conservatism to address the modeling uncertainty was then incorporated into the results of the CFD analysis so that the cask surface temperature is conservatively considered to increase by 5 °F. 60400000330

As previously discussed in this section, the storage array model results in Table A3.3-10 demonstrated an increase in the average cask surface temperature of 18 °F that corresponded to an increase in the average cask inner shell temperature of 1 °F or less, as compared to the detailed TN-40HT cask model. These results are scaled to estimate an increase in the internal cask temperatures, due to the addition of the southeast ISFSI pad, as shown below.

$$\Delta T_{\text{ave increase}} = \frac{(18°F + 5°F)}{18°F} = 1.28°F$$

This would indicate the effect of the southeast ISFSI pad on average cask interior temperature is also less than 1 °F (i.e., 0.28 °F). In order to conservatively evaluate the impact of the southeast ISFSI pad. The overall increase in cask inner average temperatures of 1.28 °F (i.e., 1 °F from the existing storage array model and an additional 0.28 °F for the effect of the southeast ISFSI pad) is conservatively rounded to 2 °F and used to confirm the remaining margin for design limits is sufficient.

604000000330

As before, since the basket temperatures calculated in the TN-40HT detailed model remain relatively unaffected, these temperatures can continue to be used for calculation of the thermal stress, thermal expansion, and cask cavity pressure for the structural evaluation.

Further thermal analysis and review of allowable limits associated with cask exterior and interior temperatures (including the effects on internal pressure and thermal expansion) was performed and demonstrated that there is sufficient margin to account for an increase in the cask exterior temperatures of 5°F and increase in the interior temperatures of 2 °F.

Effective Conductivity for Cask Sections

To calculate the axial and the radial effective conductivities of the cask sections shown in Figure A3.3-22, corresponding nodes and elements for each section are selected from the detailed finite element model of the TN-40HT cask.

To calculate the axial effective conductivity of each cask section, constant temperature boundary conditions are applied at the top and bottom of that section. The value of reaction solution for the colder surface is retrieved from the model using PRNDL command (Reference 36) after solution was completed. Since the model is quarter symmetric, the amount of heat leaving the colder surface is four times the reaction solution resulted from PRNLD command. The axial effective conductivity is calculated using the following equation:

$$k_{eff,axl} = \frac{Q \times L}{A \times \Delta T}$$

Q = Amount of heat leaving the colder face of the cask section = Qreaction $\times$ 4

L = Length of the cask section

A = Surface area of the colder face (upper face) of the cask section

= π ($r_2^2 - r_1^2$)

r_1 = Cask cavity radius = 36" for cask sections 1 through 4, 0 for cask section 5

r_2 = Outer radius of the cask section = 44.75" for cask sections 1, 2, and 4

= 50.5" for cask section 3

= 36" for cask section 5

ΔT = ($T_2 - T_1$) = Temperature difference between lower and upper faces of the section (°F)

T_1 = Constant temperature applied on the upper face of the model (°F)

T_2 = Constant temperature applied on the lower face of the model (°F)

To calculate the radial effective conductivity of the cask sections, constant temperature boundary conditions are applied on the outermost and innermost nodes of the sections. The value of reaction solution on the colder surface is then retrieved from the model using PRNDL command and multiplied by four to give the amount of heat leaving the colder surface. The radial effective conductivity is calculated using the following equation with the same terms defined for axial effective conductivity:

$$k_{eff,rad} = \frac{Q \times \ln\left(r_2/r_1\right)}{2\pi\ L\ \Delta T}$$

For Section 5, the lowest conductivity between the cask lid and cask top shield (SA203, Gr. E, Table 3.3-8) is used for radial conductivity.

In determining the temperature dependent effective conductivities an average temperature, equal to $(T_2 + T_1)/2$, is used. The resulting effective conductivities are listed in Table 3.3-12.

A3.3.2.2.4.2 TOTAL HEAT TRANSFER COEFFICIENT TO AMBIENT FOR FIRE

The radiation and forced convection from the fire toward the cask surface are combined together as a total heat transfer coefficient. Total heat transfer coefficient is defined as:

$$H_{t,fire} = h_{r,fire} + h_f$$

Where,

$h_{r,fire}$ = radiation heat transfer coefficient from fire

h_f = forced convection heat transfer coefficient

A forced convection value of 4.5 Btu/hr-ft^2-°F (0.03125 Btu/hr-in^2-°F) is considered during the burning time from Reference 39.

The radiation heat transfer coefficient during the burning period of the hypothetical fire accident, $h_{r,fire}$, is given by the following equation:

$$h_r = \varepsilon_s \; F_{sf} \left[\frac{\sigma(\varepsilon_f \; T_f{}^4 - T_s{}^4)}{(T_f - T_s)} \right] \quad \text{(Btu/hr-ft}^2\text{-°F)}$$

Where,

ε_s= surface emissivity = 0.8 (Reference 38)

ε_f = fire emissivity = 0.9 (Reference 38)

F_{sf} = view factor from surface to fire = 1

$\sigma = 0.1714 \times 10^{-8}$ Btu/hr-ft^2-°R^4

T_f = fire flame temperature, 1475°F = 1935°R (Reference 38)

T_s = cask surface temperature, °R

A3.3.2.2.4.3 FREE CONVECTION COEFFICIENTS

The free convection coefficients are calculated based on the shape and position of the convective surface using correlations from Reference 27. The convection correlations are described in the following sections.

A3.3.2.2.4.3.1 VERTICAL CYLINDER

The following equations from Reference 27 are used to calculate the free convection coefficients for vertical cylindrical surfaces.

$$h_c = \frac{Nu \; k}{L}$$

With L = height of the vertical cylinder

D= diameter of vertical cylinder

k = air conductivity

$$Ra = Gr \Pr \quad ; \quad Gr = \frac{g \, \beta \, (T_w - T_\infty) \, L^3}{\nu^2}$$

$$Nu^T_{Plate} = \overline{C}_l \; Ra^{1/4} \, , \qquad \overline{C}_l = 0.515 \text{ for gases (Reference 27)}$$

$$Nu_{l,Plate} = \frac{2.0}{\ln(1 + 2 / Nu^T_{Plate})}$$

$$\xi = \frac{1.8\, L/D}{Nu_{Plate}^{T}}$$

$$Nu_l = \frac{\xi}{\ln(1+\xi)} Nu_{Plate}^{T}$$ Nusselt number for fully laminar heat transfer

$$C_t^V = \frac{0.13\,\Pr^{0.22}}{(1+0.61\,\Pr^{0.81})^{0.42}}$$

$$f = 1 + 0.078\left(\frac{T_w}{T_\infty} - 1\right)$$

$$Nu_t = C_T^v\, f\, Ra^{1/3} \Big/ \left(1 + 1.4\times10^9\,\Pr/Ra\right)$$ Nusselt number for fully turbulent heat transfer

$$Nu = \left[(Nu_l)^m + (Nu_t)^m\right]^{1/3}$$ with m=6

The correlations to calculate the total heat transfer coefficient are incorporated in the ANSYS model via a macro. Air properties are taken from Reference 27 and listed in Table A3.3-8.

A3.3.2.2.4.3.2 HORIZONTAL FLAT SURFACES FACING DOWNWARDS

The following equations from Reference 27 are used to calculate the free convection coefficients for horizontal flat surfaces facing downwards.

$$h_c = \frac{Nu\, k}{L}$$

With L = A/P

A=surface area of heated surface

P= perimeter of the heated surface

k = air conductivity

$$Ra = Gr\,\Pr \quad ; \quad Gr = \frac{g\,\beta\,(T_w - T_\infty)\,L^3}{\nu^2}$$

$$Nu_l = \frac{0.527\,Ra^{1/5}}{[1+(1.9/\Pr)^{9/10})^{2/9}}$$

$$Nu = Nu_l$$

The above correlations are incorporated in ANSYS model via a macro. Air properties are taken from Reference 27 and listed in Table 3.3-8.

A3.3.2.2.4.3.3 HORIZONTAL FLAT PLATE FACING UPWARDS

The following equations from Reference 27 are used to calculate the free convection coefficients for horizontal flat surfaces facing upwards.

$$h_c = \frac{Nu\ k}{L}$$

With L = A/P

A=surface area of heated surface

P= perimeter of the heated surface

k = air conductivity

$$Ra = Gr\ \mathrm{Pr} \quad ; \quad Gr = \frac{g\,\beta\,(T_w - T_\infty)\,L^3}{\nu^2}$$

$$Nu^T = 0.835\ \overline{C}_l\ Ra^{1/4}$$

$\overline{C}_l = 0.515$ for gases (Reference 27)

$Nu_l = \dfrac{1.4}{\ln(1 + 1.4/Nu^T)}$ Nusselt number for fully laminar heat transfer

$C_t^H \approx 0.14$ for Pr < 100 (Reference 27)

$Nu_t = C_t^H\ Ra^{1/3}$ Nusselt number for fully turbulent heat transfer

$$Nu = \left[(Nu_l)^m + (Nu_t)^m\right]^{1/m} \qquad with \quad m = 10 \quad for \ \ Ra > 1$$

The above correlations are incorporated in ANSYS model via a macro. Air properties are taken from Reference 27 and listed in Table 3.3-8.

A3.3.2.2.5 THERMAL EVALUATION OF LOADING AND UNLOADING

Fuel loading and unloading operations occur in the fuel handling building. During loading operation fuel assemblies are submerged in pool water permitting heat dissipation. After fuel loading is complete, the cask is removed from the pool, drained, sealed, dried, and backfilled with helium.

A3.3.2.2.5.1 VACUUM DRYING

The vacuum drying operation evaluated is the heatup of the cask before helium is introduced into the cask cavity. The time for this operation ($t_{loading}$) is defined as the interval from the start of water being drained out of the cask cavity to the beginning of helium backfilling.

The duration of vacuum drying operation being evaluated is limited by the amount of time required to reach the maximum fuel cladding temperature of 752 ºF (400 °C) allowed by ISG-11 (Reference 25).

To determine the time-temperature histories of the cask components, a transient analysis is performed using the cross-section model of the cask described in Section A3.3.2.2.1.2. Although cask cavity is full of water at $t_{loading}$=0, the following changes are considered to occur immediately at the start of the transient run and remain unchanged.

- Effective conductivity values in a vacuum are considered for elements representing homogenized fuel assemblies.
- Air conductivity is given to the elements representing the gas within the cask cavity.

The conductivity of air or helium is independent of the pressure for the conditions considered during the loading and vacuum drying operations. All other material properties of the cask cross-section model remain unchanged. The effective fuel conductivity values used for vacuum conditions are listed in Table A3.3-8.

The decay heat is applied as heat generation load on the elements representing the homogenized fuel assemblies with a peaking factor of 1.1. The applied value for the heat generation is:

Heat generation rate = $\dot{q}'' = \dfrac{q}{a^2\ L_a} \times PF = 0.3218$ Btu/hr-in^3

where,

q = Decay heat load per assembly = 2,730 Btu/hr (0.80 kW)

a = Width of the modeled fuel assembly = 8.05 in.

L_a =Active fuel length = 144 in.

PF = maximum peaking factor = 1.1 (Reference 26)

Adiabatic boundary conditions are applied on the top and bottom faces of the cross-section model for conservatism.

An average, initial temperature of 215 °F is assumed for the cask at the start of water draining. This temperature is higher than boiling point of water.

It is assumed that the cask resides in the pool for 2 hours after the water draining starts. Maximum pool temperature is 150 °F. Conservatively, a constant temperature of 215 °F is applied on the cask surface during this period.

After leaving the pool, the cask dissipates heat to ambient inside of the fuel handling building. The free convection and radiation are combined together to calculate the total heat transfer coefficient from the cask outer surface to the ambient. An ambient temperature of 120 °F is considered conservatively for the fuel handing building.

The volumetric average temperatures of the basket, rails, inner shells, basket support bars and basket aluminum plates are retrieved from the thermal model to calculate the thermal expansion. A zero hot gap at thermal equilibrium is assumed between the rails and the cask inner shell in retrieving the average temperatures. These temperatures are listed in Table A3.3-13.

The time-temperature history of the maximum fuel cladding temperature is illustrated in Figure A3.3-26 for loading operations with 32 kW decay heat load. The time period for this operation was defined as the time from the beginning of cask draining to when helium backfilling begins. A time limit of 34 hours was chosen for this operation to ensure that the fuel cladding temperature limit of 752 ºF was not exceeded.

The temperature distribution for cask cross-section model at $t_{loading}$ = 34 hours is shown in Figure A3.3-27.

The temperature limits for fuel cladding, radial neutron shielding material, and seals are not exceeded at 34 hours as shown in Table A3.3-14.

Once helium is introduced, subsequent evacuation and backfilling with helium will not change the conductivity of the cavity gas, and therefore no repeated cycling of the fuel cladding temperature occurs.

A3.3.2.2.5.2 REFLOODING

For unloading operations, the cask will be slowly filled with borated water to gradually cool the fuel in the cask.

As pool water is added to the cask cavity containing hot fuel and basket components, some of the water will flash to steam causing the internal cavity pressure to rise. This steam pressure is released through the vent port. The reflooding procedures will require that the pressure be monitored and the reflood flow controlled such that the pressure does not exceed the analyzed internal pressure of 100 psig. To provide margin to the analyzed limit and to account for any pressure drop between the monitoring location and the cask internal pressure, the procedure shall limit the monitored pressure to less than 75 psig.

A3.3.2.2.5.3 HELIUM ENVIRONMENT

Prior to exceeding the time limit determined in Section A3.3.2.2.5.1, Vacuum Drying, a helium environment must be established within the cask cavity. The evaluation below is used to determine the minimum percentage (in terms of partial pressure) of cavity gas that must be helium to ensure that the maximum fuel cladding temperature limit of 752ºF (400ºC) allowed by ISG-11 (Reference 25) is not exceeded during Loading Operations.

To determine the minimum amount of helium required within the cask cavity during Loading Operations, a series of thermal evaluations were performed with varying quantities of helium, air and water vapor mixtures. These evaluations used the thermal model described in Section A3.3.2.2.1.1.1 except for the following changes:

- The thermal conductivity of the helium gas within the fuel compartments and cask cavity is replaced with the effective thermal conductivity of the helium/air/water vapor mixture.
- The effective thermal conductivity of the homogenized fuel assemblies is determined in the helium/air/water vapor mixture environment.
- The protective cover, top neutron shield, concrete pad and soil beneath the concrete pad are removed from the model.
- Adiabatic boundary conditions are considered for the top and bottom surfaces of the cask.
- The ambient temperature is set at 120ºF.
- No solar heating is included.
- The final evaluation used the lower poison/aluminum plate conductivity values described in Section A3.3.2.2.1.4.

In determining the effective conductivity of the helium, air and water vapor mixture, the properties for air are used for the air and water vapor mixture. This is conservative since air has a lower thermal conductivity than water vapor for temperatures greater than 400ºF which is the temperature range of interest within the cask cavity.

The effective thermal conductivity of the gas mixtures is determined using the following equation:

$$\mathrm{k_m} = \frac{\sum \mathrm{y_i} k_i (M_i)^{1/3}}{\sum y_i (M_i)^{1/3}}$$

Where:

k_m = thermal conductivity of the mixture
y_i = mole fraction of component i (for ideal gases, the mole fraction is equal to the volume percentage)
k_i = thermal conductivity of component i
M_i = molecular weight of component i.

To account for the uncertainties in the above equation, the thermal conductivity of the mixture is further reduced by 5%.

The effective conductivities for the homogenized fuel assemblies were determined using the same methodology described in Section A3.3.2.2.3.6, except:

- That the helium gas properties within the fuel compartment were replaced with the thermal properties for the gas mixtures calculated using the above equation, and
- The effective properties were reduced 3% to account for the effect of irradiation fuel properties vs un-irradiated fuel properties.

Table A3.3-33 lists the thermal conductivities with a 75% helium, 25% Air and Water Vapor mixture used in the evaluation.

The temperature limits for fuel cladding, radial neutron shielding material, and seals are not exceeded with a 75% helium, 25% Air and Water Vapor mixture as shown in Table A3.3-34.

Therefore, the maximum fuel cladding temperature limit of 752ºF (400ºC) is not exceeded during Loading Operations provided a 75% helium environment is established within the cask prior to exceeding the time limit determined in Section A3.3.2.2.5.1.

A3.3.2.2.6 INTERNAL CASK PRESSURE DETERMINATION

A3.3.2.2.6.1 MAXIMUM INTERNAL PRESSURE

The following methodology is used to determine the maximum pressures within the TN-40HT cask cavity for normal, off-normal, and accident conditions:

- Average cavity gas temperatures are derived from the TN-40HT cask thermal models.
- The amount of helium present within the cask cavity after the initial backfilling is determined via the ideal gas law.
- The total amount of free gas within the fuel assemblies, including both fill and fission gases, are calculated based on NUREG 1536 (Reference 35) guidelines.
- The amount of released gas from the fuel rods into the cask cavity is determined based on the maximum fraction of the ruptured fuel rods considered in NUREG 1536 (Reference 35).
- The amount of helium backfill gas is added to the amount of released gases to make the total amount of gases in the cask cavity.
- Finally, the maximum cask internal pressures are determined via the ideal gas law.

To bound the maximum internal pressure, the maximum daily average temperature of 100 °F is considered for both normal and off-normal conditions.

As it is assumed in NUREG 1536 (Reference 35), the maximum fractions of the fuel rods (f_B) that can rupture and release their free gases to the cask cavity for normal, off-normal, and accident conditions are 1, 10, and 100%, respectively.

A3.3.2.2.6.1.1 AVERAGE GAS TEMPERATURE

To determine the average cavity gas temperature, volume average temperatures of the elements representing the helium gaps ($T_{avg,void}$) and the homogenized fuel assemblies ($T_{avg,fuel}$) are retrieved from the thermal models using the ETABLE commands in ANSYS (Reference 44). Although the average temperature of the homogenized fuel elements includes the fuel rods and the helium gas between them, this average temperature is conservatively used as the average gas temperature within the fuel compartments.

The volume of helium gaps in the model is (V_{void}) is retrieved from the model using ETABLE commands (Reference 44) and is equal to 28,565 in^3.

The approximate volume of the gas in the fuel compartments ($V_{gas,comp}$) is determined as follows (note this is only an approximation and not intended to represent the physical configuration of the fuel, e.g. actual fuel pin length, open guide tubes, and fuel assembly hardware).

$V_{gas,comp} = N_c \times$ (Volume of one fuel compartment – Volume of fuel rods in one assembly)
N_c = Number of fuel compartment in finite element model (1/4 of cask is modeled) = 10
Volume of one fuel compartment = W x W x H
Volume of fuel rods in one assembly = N x π/4 OD^2 $\times$ H

W = compartment width = 8.05”
H = compartment height = 160”
N = number of fuel rods and tubes = 196
OD = the smallest outer diameter of fuel rods and tubes = 0.40 in.

Volume of one fuel compartment = 10,368 in^3
Volume of fuel rods in one assembly = 3,941 in^3
$V_{gas,comp}$ = 64270 in^3

The average gas temperature in the cask cavity is calculated as follows.

$$\overline{T}_{Cavity} = \frac{T_{avg,fuel} \times V_{gas,comp} + T_{avg,void} \times V_{void}}{(V_{gas,comp} + V_{void})}$$

The results are summarized below.

Operating Condition	$\overline{T}$ Cavity (°F)
Normal (Off-Normal) Storage Conditions*	466
Fire Accident*	605
Buried Cask Accident, 74.6 hrs after occurrence (with BPRAs)	843
Buried Cask Accident, 92.6 hrs after occurrence (without BPRAs)	925

* These values include an additional 2 °F to bound the effect of the southeast ISFSI pad on radiant heat transfer.

60400000330

A3.3.2.2.6.1.2 AMOUNT OF INITIAL HELIUM BACKFILL

A maximum cavity pressure of 1.43 atm abs (21 psia) is considered for the initial backfill pressure of helium. The amount of the helium backfill gas at this moment is calculated based on the ideal gas law.

The cavity gas temperature for the cask located in the fuel handling building is calculated considering an ambient temperature of 70 °F, a view factor of 1.0, and no insolance. The full-length cask model described in Section A3.3.2.2.1.1.1 (except for the 1″ gap at each end of the poison and aluminum plates) is used for this purpose with steady state conditions. The average cavity gas temperature is retrieved from the model using the methodology described in Section A3.3.2.2.6.1.1. The retrieved average cavity gas temperature when cask is in the handling building is 426 °F (886 °R).

For the maximum gas backfill, it is assumed that helium does not instantaneously reach 426 °F, but is conservatively assumed to be the average of the ambient (70 °F) and the steady state cavity temperature of 426 °F.

A displacement of 480 in^3 is used for each BPRA.

From the backfill pressure and the backfill gas temperature, the amount of helium backfill gas is calculated as follows.

n_{back} = (PV)/(RT) = 0.580 lb-moles without BPRAs

= 0.549 lb-moles with BPRAs

P = maximum initial backfill pressure = 1.43 atm = 21 psia

V = cask cavity free volume without BPRAs (loaded) = 362,440 in^3 = 209.7 ft^3

= cask cavity free volume with BPRAs = cavity volume – BPRA volume

= (362,440 – 40*480)/12^3 = 198.6 ft^3

T = initial backfill temperature = 0.5 (70+426) = 248 °F = 708 °R

R = universal gas constant = 10.730 psia-ft^3/lb-moles-°R (Reference 29)

A3.3.2.2.6.1.3 FREE GAS WITHIN FUEL ASSEMBLIES

As indicated in Section A7.2, Table A7.2-1, the maximum volume of free gas per assembly is 0.226 m^3 at standard temperature and pressure (0 °C and 760 mmHg). Total amount of free gases within the fuel assemblies is:

$$n_{fuel} = N \times \frac{P_{Std} \cdot V_{free}}{R \cdot T_{Std}} = 40 \times \frac{760 \times 0.226 \times 10^3}{62.361 \times 273.15} = 403.3 \text{ g-mole} = 0.889 \text{ lb-mole}$$

With

N = number of fuel assemblies in the cask = 40

P_{Std} = standard pressure = 760 mmHg

V_{free} = maximum volume of free gas per assembly = 0.226 m^3

T_{Std} = standard temperature = 0 °C = 273.15 K

R = universal gas constant = 62.361 (mmHg-lit/g-mole-K) (Reference 29)

A bounding amount of 2.0E-4 lb-mole is considered for free gas in each BPRA rod. The maximum amount of free gases from the BPRA rods is:

$$n_{BPRA} = N \times n_{Rod} \times (2.0E-4\ lb-mole/rod) = 40 \times 16 \times 2.0E-4 = 0.128 \text{ lb-mole}$$

With

N = number of fuel assemblies in the cask = 40
n_{Rod} = maximum number of BPRA rods in one assembly = 16

Total amount of free gases within fuel assemblies is:

$n_{free} = n_{fuel}$ = 0.889 lb-mole without BPRAs
$= n_{fuel} + n_{BPRA}$ = 1.017 lb-mole with BPRAs

A3.3.2.2.6.1.4 TOTAL AMOUNT OF GASES WITHIN CASK CAVITY

The total amount of gases within the cask cavity is equal to the amount of the initial helium backfill gas plus any free gases that are released to the cask cavity from ruptured fuel and BPRA rods.

Total amount of gases in the cask cavity is:

$$n_{total} = n_{back} + f_B\,(n_{free})$$

n_{back} = total amount of backfill gas
n_{free} = total amount of free gases
f_B = fraction of the ruptured fuel rods from NUREG-1536 (Reference 35)

A3.3.2.2.6.1.5 MAXIMUM CASK INTERNAL PRESSURE

The maximum cask internal pressure (P_{cavity}) is determined via the ideal gas law:

$$P_{cavity} = (n_{total}\, R\, \bar{T}_{cavity})/V$$

V = cask cavity free volume without BPRAs = 209.7 ft^3
= cask cavity free volume with BPRAs = 198.6 ft^3
R = universal gas constant = 10.73 (psia-ft^3/lb-mol-°R)

The results are summarized in Table A3.3-15 and Table A3.3-16.

The internal cask cavity pressures are at or below the design limit of 100 psig.

A3.3.2.2.6.2 OXIDIZING GASES WITHIN CASK CAVITY

To provide an inert environment within the cask cavity, the cask is evacuated and then pressurized with helium such that the residual oxidizing gases within the cavity are no more than 0.25% by volume.

As discussed in SAR Section 5.1, cask cavity vacuum is broken after completion of the vacuum dryness test. Thus, the cask cavity will be exposed to oxidizing gases such as air or water vapor prior to the final helium backfill. This calculation assumes that the entire cask cavity is filled with air after breaking the vacuum to maximize the amount of oxidizing gases within the cask cavity. According to PNL-6365 report (Reference 48), the gases of concern are those that can oxidize exposed UO_2 fuel: O_2, CO_2, and CO. Therefore, assuming dry air with an oxygen content of 21% (covering for both O_2 and CO_2 in air) maximizes the amount of oxidizing gases.

Ideal gas law is used to determine the volume percentage of the oxidizing gases within the cask cavity after completion of the final backfill. Per the ideal gas law, the volume percentage of the gases within a mixture is equal to the ratio of the moles. Thus, the volume percent of oxidizing gases may be determined by the following equation:

$$V_{O2}\% = 21 \times \frac{P_v}{P_b} \times \frac{T_b}{T_v}\ (\%)$$

Where,

$V_{O2}\%$ = the volume percent of oxidizing gases in the cask cavity,

P_v and P_b = evacuation vacuum and backfill pressure, respectively

T_v and T_b = average cavity gas temperature prior and after backfill, respectively

Since helium conductivity is much higher than air, the average cavity gas temperature decreases after the backfilling with helium. Hence, T_b is lower than T_v and their ratio is lower than 1. However, to conservatively increase the volume percentage of oxidizing gases, it is assumed that T_b is equal to T_v and their ratio is 1.0.

Assuming a conservative evacuation pressure (P_v) of 15 mbar prior to final backfill and a conservative pressure of 1320 mbar after final backfill (P_b), the volume percentage of oxidizing gases within the cask cavity is:

$$V_{O2}\% = 21 \times \frac{P_v}{P_b} = 21 \times \frac{15}{1320} = 0.239\%$$

The conservatively calculated volume percentage of the oxidizing gases within the cask is below the limit of 0.25%.

A3.3.2.2.7 RADIAL HOT GAP BETWEEN THE BASKET RAILS AND THE CASK INNER SHELL

A nominal diametrical cold gap of 0.30 in. is considered between the basket and the cask cavity wall for the TN-40HT cask.

A radial, hot gap of 0.13" at thermal equilibrium is assumed in the ANSYS model for normal storage conditions. To verify this assumption, the hot dimensions of the cask inner diameter and basket outer diameter are calculated at thermal equilibrium as follows.

The outer diameter of the hot basket is:

$OD_{B,hot} = OD_B + [L_{SS,B} \times \alpha_{SS} (T_{avg,B} – T_{ref}) + L_{Al} \times \alpha_{Al} (T_{avg,Al} – T_{ref})]$

Where:

$OD_{B,hot}$ = Hot outer diameter of the basket

OD_B = Cold outer diameter of the basket = 72" – 0.30" = 71.70"

$L_{SS,B}$ = Length of basket at 90-270 direction = O_{DB} – 2×0.46" = 70.78"

L_{Al} = Length of aluminum shim = 2×0.46 = 0.92"

α_{SS} = Stainless steel axial coefficient of thermal expansion

= 9.69E-6 in/in-°F @ 494 °F (Reference 28)

α_{Al} = Aluminum coefficient of thermal expansion

= 13.49E-6 in/in-°F @ 373 °F (Reference 28)

$T_{avg,B}$ = Average basket temperature at the hottest cross section = 494 °F (Table A3.3-4)

$T_{avg,Al}$ = Average shim temperature at the hottest cross section = 373°F (Table A3.3-4)

T_{ref} = reference temperature for stainless steel and aluminum alloys = 70°F (Reference 28)

The inner diameter of the hot cask is:

$ID_{c,hot} = ID_c [1 + \alpha_{LS} (T_{avg,C} – T_{ref})]$

Where:

$ID_{C,hot}$ = Hot inner diameter of cask cavity
ID_C = Cold inner diameter cask cavity = 72”
α_{LS} = Coefficient of thermal expansion for low alloy steel
= 6.90E-6 in/in-°F @ 302 °F (Reference 28)
$T_{avg,C}$ = Average cask inner shell and gamma shield temperature at hottest x- section = 302 °F (Table A3.3-4)
T_{ref} = reference temperature for low alloy steel = 70°F (Reference 28)

The hot gap between the basket outer diameter and cask inner diameter is:

$G_{hot} = ID_{C,hot} – OD_{B,hot}$ =0.120” (diametrical)

Radial hot gap = 0.060”

The assumed radial hot gap of 0.13” is larger than the above calculated hot gap. This assumption is therefore conservative.

A3.3.2.2.8 HEAT GENERATION RATE AS A FUNCTION OF SPENT FUEL PARAMETERS

A3.3.2.2.8.1 INTRODUCTION

The spent fuel loading into the TN-40HT Cask is based on a uniform loading of 800 watts per fuel assembly. The objective of this section is to describe a mathematical function that determines the heat generation rate for high burnup fuel as a function of initial enrichment, assembly burnup and cooling time. This attachment also provides a sample fuel qualification table for heat generation rate, based on the mathematical function. This function applies only to 14x14 high burnup fuel assemblies.

A3.3.2.2.8.2 CALCULATIONAL METHODOLOGY AND INPUT MODELS

The SAS2H and the ORIGEN-S modules of SCALE4.4 (Reference 14) computer code, with the 44 Group ENDF-V cross section library, are used to determine the thermal source terms.

**PROPRIETARY - TRADE SECRET INFORMATION
WITHHELD PURSUANT TO 10 CFR 2.390**

A3.3.2.2.8.3 MATHEMATICAL FUNCTION TO DETERMINE HEAT GENERATION

**PROPRIETARY - TRADE SECRET INFORMATION
WITHHELD PURSUANT TO 10 CFR 2.390**

The functional form is expressed below with decay heat (DH) in watts as:

$$DH = F1 * \mathrm{Exp}(\{G*[1-(12.0/X3)]\}*[(X3/X1)^{H}]*[(X2/X1)^{I}])$$

Where:

$$F1 = A + B*X1 + C*X2 + D*X1^2 + E*X1*X2 + F*X2^2$$

and,

F1	Intermediate Function, basically the Thermal source at 12 year cooling
X1	Assembly Burnup in GWd/MTU (45 to 60)
X2	Initial Enrichment in wt % U235 (3.4 – 5.0)
X3	Cooling Time in Years (12 min)
A	18.76
B	11.27
C	6.506

D	0.163
E	-1.826
F	6.617
G	-0.309
H	0.431
I	-0.374

PROPRIETARY - TRADE SECRET INFORMATION WITHHELD PURSUANT TO 10 CFR 2.390

A3.3.2.2.8.4 DECAY HEAT FOR LOW BURNUP ASSEMBLIES

For assemblies with burnups less than 44 Gwd/Mtu, the SASH2 analyses shows that decay heat load is less than 800 watts with a minimum cooling time of 12 years.

A3.3.2.2.8.5 HEAT GENERATION FOR INSERTS

The decay heat load for a thimble plug device with a minimum of 16 years cooling was determined to be 0.42 watts. This value was based on a maximum cumulative host assembly(s) burnup of 125,000 Mwd/Mtu.

The decay heat load for a burnable poison rod assembly with a minimum of 18 years cooling was determined to be 0.90 watts. This value was based on a maximum cumulative host assembly(s) burnup of 30,000 Mwd/Mtu.

If the fuel assembly to be stored contains an insert, these heat loads are added to the fuel assembly heat load to determine a combined heat load for comparison to the 800 watt criterion.

A3.3.3 PROTECTION BY EQUIPMENT AND INSTRUMENTATION SELECTION

A3.3.3.1 EQUIPMENT

The design criteria for the TN-40HT casks are described in Section A3.4 and summarized in Table A3.4-1.

A3.3.3.2 INSTRUMENTATION

Due to the totally passive and inherently safe nature of the storage system, important to safety instrumentation is not necessary. Instrumentation to monitor cask pressure is furnished. Appropriate capabilities to check and recalibrate these monitors are also provided. The pressure monitoring system is further described in Section A3.3.2.1.

A3.3.4 NUCLEAR CRITICALITY SAFETY

A3.3.4.1 CONTROL METHODS FOR PREVENTION OF CRITICALITY

The design criterion for criticality is that an upper subcritical limit (USL) of 0.95 minus benchmarking bias and modeling bias will be maintained for all postulated arrangements of fuel within the cask. The fuel assemblies are assumed to stay within their basket compartment based on the cask and basket geometry.

The control methods used to prevent criticality are:

1. Incorporation of neutron absorbing material (boron) in the basket material.

2. Loading of the irradiated fuel assemblies in the fuel pool containing at least 2450 ppm boron.

3. Prevention of fresh water entering the loaded cask.

The basket has been designed to assure an ample margin of safety against criticality under the conditions of fresh fuel in a cask flooded with borated pool water. The method of criticality control is in keeping with the requirements of 10 CFR72.124.

The TN-40HT cask system's criticality safety is ensured by fixed neutron absorbers in the basket, soluble boron in the pool. The cask basket uses a Borated-Aluminum alloy, Aluminum/B4C metal matrix composite or Boral® as the fixed neutron poison material. The collective term B-Al refers to the Borated-Aluminum alloy and Aluminum/B4C metal matrix composite materials where the analysis uses a 90% credit for the neutron poison. A credit of 75% is taken for the presence of neutron poison for Boral® plates.

A single fixed poison loading is utilized in the TN-40HT basket. Table A3.3-17 lists the minimum B10 poison loading required for the various poison materials and the corresponding poison content modeled in the analyses.

The minimum soluble boron concentration in the pool credited in the analysis is 2450 ppm.

A3.3.4.1.1 DISCUSSION AND RESULTS

Figure A3.3-28 shows the cross section of the TN-40HT cask. The TN-40HT cask stainless steel basket consists of an "egg-crate" plate design. The fuel assemblies are housed in 40 stainless steel fuel compartment tubes. The basket structure, including the fuel compartment tubes, is held together with stainless steel insert bars (note that the input files in Appendix A3A refer to these bars as plates) and the poison and aluminum plates that form the "egg-crate" structure. The fuel compartment tube structure is connected to the perimeter rail assemblies forming the cylindrical outer geometry required to be housed within the cask. The poison/aluminum plates are located between the fuel compartment tubes.

The analysis presented herein is performed for a TN-40HT Cask during normal, off-normal and accident loading conditions. This analysis also bounds all conditions of storage, including loading and transfer. The cask consists of an inner steel shell, a steel gamma shield shell and a hydrogenous neutron shield.

Table A3.3-18 lists the fuel assemblies considered as authorized contents of the TN-40HT cask system. The criticality analysis begins by determining the most reactive assembly type for the Westinghouse 14x14 fuel assembly (WE 14x14) class identified in Table A3.3-18. Then the most reactive configuration for the basket (including rail configuration) and fuel assembly position is determined. Next, criticality calculations are performed using the maximum allowable initial fuel enrichment for the TN-40HT cask shown in Table A3.3-17. These calculations determine k_{eff} with the CSAS25 control module of SCALE-4.4 (Reference 14) including all uncertainties to assure criticality safety under all credible conditions.

The Control Components (CCs) are also authorized for storage in the TN-40HT casks. The authorized CCs are Burnable Poison Rod Assemblies (BPRAs) and Thimble Plug Devices (TPDs).

The results of the evaluation demonstrate that the maximum expected k_{eff}, including all applicable biases and uncertainties, is less than the Upper Subcritical Limit (USL) determined from a statistical analysis of benchmark criticality experiments. The statistical analysis procedure includes a confidence band with an administrative safety margin of 0.05.

A3.3.4.1.2 PACKAGE FUEL LOADING

The TN-40HT Cask is capable of transferring and storing a maximum 40 intact WE 14x14 class PWR fuel assemblies. The reactivity of a cask loaded with less than 40 PWR fuel assemblies is lower than that calculated here since the more absorbing borated water replaces the fuel in the empty locations. Reconstituted fuel assemblies, where the fuel pins are replaced by lower enriched fuel pins or non-fuel pins that displace the same amount of borated water, would also lower the reactivity of the cask.

Table A3.3-19 lists the fuel parameters for the PWR fuel assemblies considered in this evaluation. Reload fuel from other manufacturers with the same parameters are also considered as authorized contents.

For the WE 14x14 class assemblies, CCs are also included as authorized contents. The only change to the package fuel loading to evaluate the addition of these CCs is replacing the borated water in the water holes conservatively with $^{11}B_4C$. Since these CCs displace borated moderator in the assembly guide tubes, an evaluation is performed to determine the potential impact of storage of CCs that extend into the active fuel region on the system reactivity. For CCs such as BPRAs no credit is taken for the cladding and absorbers; rather the CCs are modeled as $^{11}B_4C$ in the entire tube of the respective design. Thus, the highly borated moderator in the tube is conservatively modeled as $^{11}B_4C$. The inclusion of more Boron-11 and carbon enhances neutron scattering causing the neutron population in the fuel assembly to be slightly increased which increases reactivity. Therefore, these calculations bound any CC design that is compatible with the WE 14x14 class assemblies. CCs that do not extend into the active fuel region of the assembly (e.g., TPD) do not have any effect on the reactivity of the system as evaluated because only the active fuel region is modeled in this evaluation with periodic boundary conditions making the model infinite in the axial direction. The dimensions of the fuel assemblies reported in Table A3.3-19 remain unchanged for the CC cases. The models that include CCs only differ in that the region inside the guide tubes are modeled as $^{11}B_4C$ instead of moderator.

A3.3.4.1.3 MODEL SPECIFICATION

The following subsections describe the physical models and materials of the TN-40HT cask used for input to the CSAS25 module of SCALE-4.4 (Reference 14) to perform the criticality evaluation. The reactivity of cask under storage conditions is bounded by the analysis with zero (or near zero) internal moderator density case during loading and transfer.

A3.3.4.1.3.1 DESCRIPTION OF CALCULATIONAL MODEL

The TN-40HT cask is explicitly modeled using the appropriate geometry options in KENO V.a of the CSAS25 module in SCALE-4.4. Several models are developed to evaluate the fabrication tolerances of the basket/cask, fuel assembly locations, fuel assembly design and storage of fuel with CCs like BPRAs and TPDs.

The criticality evaluation is performed using an “egg-crate” section length of 14.49 inches in the basket. The actual “egg-crate” length is 15.0 inches in the active fuel region of the assembly. This represents more reactive design than the actual basket because of the shorter “egg-crate” section length. Utilizing a shorter section length in the calculational model ensures that the model is conservative since the amount of poison per unit length is minimized. The key basket dimensions utilized in the calculation are shown in Table A3.3-20.

The fixed poison modeled in the calculation is based on a poison plate thickness of 0.075 inches for initial sensitivity calculations and 0.125 inches for the final design basis calculations. The important parameter is the minimum B-10 areal density; therefore the modeled thickness of the poison plate does not affect the results of the calculation.

The basic calculational KENO model, as discussed above, is a 14.49-inch axial section and full-radial cross section of the basket within the cask with periodic boundary conditions at the axial boundaries (top and bottom) and reflective boundary conditions at the radial boundaries (sides). This axial section essentially models one building block of the egg crate basket structure. Periodic boundary conditions ensure that the resulting KENO model is essentially infinite in the axial direction. The model does not explicitly include the solid neutron shield (polyester resin); however the infinite array of casks without the neutron shield does contain unborated water between the casks. For the purpose of storage, the TN-40HT cask configuration is not expected to encounter any regions containing unborated water once the fuel assemblies are loaded. Therefore, this hypothetical configuration that models an infinite array of casks in close reflection is conservative.

The fuel assemblies within the basket are modeled as arrays of fuel pins and guide/instrument tubes. Spacer grids and sub-components like oversleeves (when present) are not modeled since their effect on reactivity is insignificant. The fuel compartment tubes surround each fuel assembly that is in-turn bounded by the basket plates consisting of 0.4375" aluminum/poison plates. These plates are arranged to represent an egg-crate design with the 0.3625"- Aluminum and a 0.075"-poison plate. The thermal expansion and egg-crate slot gaps are not modeled assuming plate continuity, thus replacing the more absorbing borated water (internal moderator) with basket material (aluminum/poison). KENO model plots in 2D for the various views of the basket compartment are shown in Figure A3.3-29 through Figure A3.3-35.

There are a total of 13 poison plates in the TN-40HT basket. They are located at all the faces where at least five fuel assemblies are lined up. Thus, all the interior 30 fuel assemblies are surrounded by poison plates on all four faces and the outer 10 fuel assemblies do not have poison plates on the radially outward face. The fuel assembly and poison plate positions (and the aluminum plate positions) in the KENO model of the basket is shown in Figure A3.3-36. Even though the poison and aluminum plates have been shown as discrete plates around the fuel compartment, they are all continuous running from one end of the basket to the other. A sensitivity study was performed with the poison plates being one inch shorter on each end of the plate. The results of the study showed that the change in K_{eff} was statistically insignificant.

The basket structure is connected to the cask shell by perimeter rail assemblies. The rail material is a combination of aluminum and SS304. The rails provide a structural function as well as provide a heat conduction path from the basket to the cask shell. Due to limitations in the geometry options available in KENO, it is not possible to exactly model the rails. However, bounding evaluations are performed to determine the effect of rail material / geometry modeling on the reactivity of the system.

A list of all the geometry units used in the basic KENO model is shown in Table A3.3-21. Figure A3.3-37 shows the various radial "cylinders" utilized in the KENO model surrounding the fuel assemblies. Basically, this shows the cask details.

The first model developed uses nominal dimensions for the fuel compartments, fuel compartment thickness, poison plate thickness and the fuel assemblies centered in the fuel compartment. The rails are modeled simply using horizontal and vertical aluminum plates around the periphery of the basket. The cavity between the fuel compartments and the cask inner shell is modeled with internal moderator.

This basic KENO model is used to determine the most reactive fuel assembly design, the most reactive assembly-to-assembly pitch, and to determine the most reactive cask configuration accounting for manufacturing tolerances. The second model is of the most reactive configuration identified above. This model is used to determine the maximum allowable initial enrichment for the TN-40HT cask. Plots of the various KENO models utilized in these calculations are shown in Figure A3.3-38 through Figure A3.3-41.

A3.3.4.1.3.2 PACKAGE REGIONAL DENSITIES

The Oak Ridge National Laboratory (ORNL) SCALE code package (Reference 14) contains a standard material data library for common elements, compounds, and mixtures. All the materials used for the TN-40HT cask analysis are available in this data library. Table A3.3-22 provides a complete list of all the relevant materials used for the criticality evaluation. The material density for the B10 in the poison plates includes a 10% reduction for B-Al poison and a 25% reduction for Boral® poison.

A3.3.4.1.4 CRITICALITY CALCULATIONS

This section describes the analysis methodology utilized for the criticality analysis. The analyses are performed with the CSAS25 module of the SCALE system. A series of calculations are performed to determine the relative reactivity of the various fuel assembly designs to determine the most reactive assembly type without CCs. The most reactive intact fuel design, as demonstrated by the analyses, is the WE 14x14 Standard assembly. The most reactive credible configuration is an infinite array of flooded casks, each containing 40 fuel assemblies, with minimum fuel compartment tube ID, maximum fuel compartment tube thickness, minimum stainless steel plate thickness, and minimum assembly-to-assembly pitch.

Finally, using the most reactive credible configuration determined above, k_{eff} is determined for the maximum initial enrichment for the WE 14x14 assembly class at a soluble boron concentration of 2450 ppm.

A3.3.4.1.4.1 CALCULATIONAL METHOD

A3.3.4.1.4.1.1 COMPUTER CODES

The CSAS25 control module of SCALE-4.4 (Reference 14) is used to calculate the effective multiplication factor (k_{eff}) of the fuel in the TN-40HT Cask. The CSAS25 control module allows simplified data input to the functional modules BONAMI-S, NITAWL-II, and KENO V.a. These modules process the required cross sections and calculate the k_{eff} of the system. BONAMI-S performs resonance self-shielding calculations for nuclides that have Bondarenko data associated with their cross sections. NITAWL-II applies a Nordheim resonance self-shielding correction to nuclides having resonance parameters. Finally, KENO V.a calculates the k_{eff} of a three-dimensional system. A sufficiently large number of neutron histories are run so that the standard deviation is below 0.0015 for all calculations.

A3.3.4.1.4.1.2 PHYSICAL AND NUCLEAR DATA

The physical and nuclear data required for the criticality analysis include the fuel assembly data and cross-section data as described below.

Table A3.3-19 provides the pertinent data for criticality analysis for each fuel assembly evaluated in the TN-40HT cask. The criticality analysis used the 44-group cross-section library built into the SCALE system. ORNL used ENDF/B-V data to develop this broad-group library specifically for criticality analysis of a wide variety of thermal systems.

A3.3.4.1.4.1.3 BASES AND ASSUMPTIONS

The analytical results reported in Section A4 demonstrate that the cask containment boundary, basket structure and fuel cladding do not experience any significant distortion under hypothetical accident conditions. Therefore, for both normal and hypothetical accident conditions the cask geometry is identical except for the neutron shield and neutron shield jacket (outer skin). As discussed above, the neutron shield and neutron shield jacket (outer skin) are removed and the interstitial space modeled as water.

The TN-40HT cask is modeled with KENO V.a using the available geometry input. This option allows a model to be constructed that uses regular geometric shapes to define the material boundaries. The following conservative assumptions are also incorporated into the criticality calculations for intact fuel:

1. No credit is taken for the presence of burnable poisons such as Gadolinia, Erbia or any other absorber in the fuel.

2. CCs that extend into the active fuel region, such as BPRAs are conservatively assumed to exhibit neutronic properties of $^{11}B_4C$.

3. Unirradiated fuel – no credit taken for fissile depletion due to burnup or fission product poisoning.

4. For intact fuel, the lattice average fuel enrichment is modeled as uniform everywhere throughout the assembly. Natural Uranium blankets and axial or radial enrichment zones are modeled as enriched uranium at the lattice average enrichment.

5. All fuel rods are filled with full density fresh water in the pellet/cladding gap.

6. Only a 14.49-inch section of the basket (actual is 15.0-inches) with fuel assemblies is explicitly modeled with periodic axial boundary conditions, therefore the model is effectively infinitely long and the actual poison height for each section is conservatively modeled about 0.5 inches shorter.

7. The neutron shield material is modeled using water and is not expected to result in any significant change in the system reactivity since it is located in a relatively unimportant region for criticality.

8. Only 90% credit is taken for the B10 in the B-Al poison plates and 75% credit for Boral® in the KENO models.

9. The fuel rods are modeled assuming a stack density of 96.5% theoretical density with no allowance for dishing or chamfer. This assumption conservatively increases the total fuel content in the model.

10. All calculations are carried out at a temperature of 20 °C (293 K).

11. All basket stainless steel materials are modeled as SS304. The cask steel materials are modeled as SS304 and carbon-steel. The small differences in the composition of the various stainless steels have no effect on results of the calculation.

12. All zirconium based materials in the fuel (including ZIRLO) are modeled as Zircalloy-4. The small differences in the composition of the various clad / guide tube materials have no effect on the results of the calculation.

13. The thermal expansion and egg-crate gaps are replaced with the basket material wherever present. This modeling assumption results in replacing the soluble boron moderator in the gap regions with basket material (aluminum/poison), thereby, decreasing the neutron absorption around the fuel.

14. The transition rails between the basket and the cask shell are modeled as solid aluminum with cuboid “holes” of borated water in the aluminum.

A3.3.4.1.4.1.4 DETERMINATION OF K_{EFF}

The Monte Carlo calculations performed with CSAS25 (KENO V.a) use a flat neutron starting distribution. The total number of histories traced for each calculation is approximately 800,000. This number of histories is sufficient to achieve source convergence and produce standard deviations of less than 0.0015 in Δk_{eff}. The maximum k_{eff} for the calculation is determined with the following formula:

$$k_{eff} = k_{KENO} + 2\sigma_{KENO}$$

A3.3.4.1.4.2 FUEL LOADING OPTIMIZATION

A. Determination of the Most Reactive Fuel Type

All fuel assemblies listed in Table A3.3-19 are evaluated to determine the most reactive fuel assembly type with initial enrichments of 4.50 wt. % U-235. The fuel types are analyzed with fresh water in the fuel pellet cladding annulus, a soluble boron concentration of 2400 ppm and a fixed borated aluminum poison loading of 18.7 mg B10/cm^2. The parameters utilized for these sensitivity evaluations are not critical since it is intended to determine the most reactive configuration that estimates a “relative” reactivity and not “absolute” reactivity of the system. Nominal basket dimensions are utilized in the KENO model.

These evaluations are carried out for two fuel assembly positions within the fuel compartment – “centered” and “inward.” The centered position is when the fuel assemblies are centered within the fuel compartment while the inward position is when the fuel assemblies are positions closest relative to the center of the basket. The inward position results in the fuel assemblies being clustered closer together, thereby resulting in an increase in the reactivity. The internal moderator density (IMD) is varied from 80% to 100% of full density to determine any sensitivity of the fuel assembly design reactivity to moderator density.

In all other respects, the model is the same as the basic model described above. A simple representation of the peripheral rails as shown in Figure A3.3-38 is utilized for this evaluation.

The Cask model for this evaluation differs from the actual design in the following ways:

- The neutron shield of the cask is conservatively replaced with water between the casks.
- The stainless steel and aluminum basket rails, which provide support to the fuel compartment tube grid, are modeled as aluminum plates located in the periphery.
- The “egg-crate” section length is modeled as 14.49″ high (12.67″ basket section + 1.75″ steel insert bar + 0.07″ gap). The actual design for the TN-40HT has an “egg-crate” section length of 15.0″ (13.18″ basket section + 1.75″ steel insert bar + 0.07″ gap).

The results of this evaluation are provided in Table A3.3-23. The most reactive design is the Westinghouse 14x14 Standard fuel assembly. The results also indicate that the inward position of the fuel assemblies results in a more reactive configuration and that the relative reactivity ranking of the fuel assemblies remains unchanged with IMD variations. The case corresponding to the highest k_{eff} in this evaluation is highlighted in Table A3.3-23.

B. Determination of the Most Reactive Configuration

The fuel loading configuration of the cask affects the reactivity of the package. Several series of analyses determined the most reactive configuration for the TN-40HT cask.

For this analysis, the most reactive fuel type is used to determine the most reactive configuration. The cask is modeled with the WESTD assembly, over a 14.49-inch axial section with periodic axial boundary conditions and reflective radial boundary conditions. This represents and infinite array in the x-y direction of the cask that is infinite in length, which is conservative for criticality analysis. The starting model is identical to the model used above.

The cask model for this evaluation differs from the actual design in the following ways:

- The neutron shield of the cask is conservatively replaced with water between the casks.
- The stainless steel and aluminum basket rails, which provide support to the fuel compartment tube grid, are modeled as aluminum plates located in the periphery. Further, an evaluation is performed to determine an acceptable and conservative representation of the rails in the basket periphery.
- The “egg-crate” section length is modeled as 14.49″ high (12.67″ basket section + 1.75″ steel insert bar + 0.07″ gap). The actual design for the TN-40HT has an “egg-crate” section length of 15.0″ (13.18″ basket section + 1.75″ steel insert bar + 0.07″ gap).

Each evaluation is performed with the fuel assemblies in the inward position at various IMD values to determine the optimum moderator density where the reactivity is maximized.

The first set of analyses evaluates the effect of fuel compartment tube internal width on the system reactivity. The model starts with the nominal poison plate thickness modeled as above. For this evaluation the fuel compartment tube internal width is varied from 8.00 to 8.10 inches square. The results of the evaluation are given in Table A3.3-24. The results show that the most reactive configuration is with the minimum fuel compartment tube size. The balance of this evaluation uses the minimum fuel compartment tube width because it represents the most reactive configuration. An example input file for the most reactive fuel evaluation is included in Appendix A3A.

The second set of analyses evaluates the effect of fuel compartment tube and the stainless steel tie bar thicknesses on reactivity. The model starts with the most reactive configuration basket model determined above. The compartment tube thickness is varied from 0.1775″ to 0.2325″. The stainless steel tie bar thickness is varied from 0.4275″ to 0.4925″. Varying the thickness of the tie bar also serves the purpose of varying the aluminum plate thickness as the thickness of the poison plate is maintained constant. The results in Table A3.3-25 show that the system reactivity is not very sensitive to the compartment and stainless steel bar thicknesses.

However, in order to obtain a design basis configuration for criticality analyses, a few of the more reactive combinations are evaluated for variations with other parameters. Therefore, the next sets of analyses are performed with bounding configurations that are highlighted in Table A3.3-25. Note that there are four bounding configurations and they are statistically similar.

The third set of analyses evaluates the effect of poison plate thickness and modeling on the system reactivity. Three of the bounding configurations identified above are utilized in this evaluation. For this evaluation Boral® is utilized as the poison material with a core thickness of 0.050″ and a total (core + clad) thickness of 0.075″. The effect of poison plate thickness (and hence the absorber thickness) variation on the system reactivity is shown to be statistically insignificant based on the results in Table A3.3-26. These results also indicate that poison plates of higher thicknesses can be used as long as the minimum absorber loading is maintained. These results also demonstrate that there is no effect on the reactivity due to the aluminum panels when Boral® poison is used. These results further indicate that effect of a change in the thickness of the egg-crate plates (poison and aluminum) is statistically insignificant provided the total thickness remains constant.

The fourth set of analyses evaluates the effect of rail structure modeling on the system reactivity. Due to the limitations in the geometry capabilities of the CSAS25 code, it is not possible to exactly model the rail structure. However, due to relatively low importance of the rail structure modeling to the criticality of the system, an exact model is not essential. In addition to the simplistic rail model utilized so far in these evaluations, three additional variations of the rails are also evaluated. The first variation is based on a modeling the rails as internal moderator (*rail1* option). The second variation is based on *rail1* option with cuboids of aluminum placed within the periphery using “hole” modeling (*rail2* option). The third variation is different from the *rail2* option where the periphery is modeled with solid aluminum with cuboids of internal moderator (*rail3* option where the aluminum and internal moderator from *rail2* are interchanged). The modeling of the cuboids as “holes” at the periphery (*rail2* and *rail3* options) is shown in Figure A3.3-40.

Note that the models – *rail1*, *rail2* and *rail3* represent a reduction in the volume fraction of internal moderator in the basket periphery. The results of the evaluation are given in Table A3.3-27. These results indicate that the *rail3* option results in a bounding configuration. The results also indicate that the reactivity of the basket increases with a reduction in the volume fraction of the internal moderator at the basket periphery. It is clear based on a comparison of the rail configurations from Figure A3.3-28 and Figure A3.3-40 that the *rail3* option conservatively models a lower volume fraction of internal moderator. Therefore, modeling the basket periphery with the *rail3* option is appropriate and conservative. All the four bounding configurations identified above are utilized in this evaluation. These calculations also result in the determination of the most reactive configuration for the four bounding configurations evaluated.

Based on these evaluations the most reactive cask configuration is for:

- Fuel assemblies pushed toward the center of the basket (inward arrangement),
- Minimum fuel compartment tube internal width,
- Maximum fuel compartment tube wall thickness,
- Nominal poison plate thickness,
- Minimum stainless steel bar thickness and
- Basket periphery modeled using the *rail3* option.

C. Maximum Initial Enrichment for the TN-40HT Cask

The analysis performed in this section is performed using the most reactive configuration as determined in Section B above. The internal moderator density is varied to determine the peak reactivity for the specific configuration. The maximum initial enrichment (5.00 wt. % U-235) is also shown in Table A3.3-17.

The cask model for this evaluation differs from the actual design in the following ways:

- The neutron shield of the cask is conservatively replaced with water between the casks.
- The stainless steel and aluminum basket rails, which provide support to the fuel compartment tube grid, are modeled conservatively using the *Rail3* option.
- The worst case material conditions, as determined in the previous Section above, are modeled,
- The “egg-crate” section length is modeled as 14.49″ high (12.67″ basket section + 1.75″ steel insert bar + 0.07″ gap). The actual design for the TN-40HT has an “egg-crate” section length of 15.0″ (13.18″ basket section + 1.75″ steel insert bar + 0.07″ gap).

A fixed poison loading of 33.7 mg B-10/cm^2 is utilized in the criticality calculations as described in Table A3.3-17. The soluble boron concentration utilized for these calculations is 2450 ppm. A maximum initial enrichment of 5.0 wt. % U-235 is utilized in these calculations. An example input file is included in Appendix A3A.

The most reactive WE 14x14 class assembly is the WE 14x14 Standard fuel assembly as demonstrated in Table A3.3-23. The results for the WE 14x14 class assembly calculations without CCs are listed in Table A3.3-28.

The results for the WE 14x14 class assembly calculations with CCs are listed in Table A3.3-29. The results demonstrate that the no reduction in the initial enrichment is required due to the presence of CCs.

The maximum calculated k_{eff} corresponds to the configuration with an initial enrichment of 5.0 wt. % U235 with 2450 ppm borated water with CCs. The maximum calculated k_{eff} is 0.9357 ± 0.0008 or 0.9373 which is below the USL (0.9419) calculated in Section A3.3.4.3.2. The maximum calculated dry k_{eff} (normal condition for storage) is 0.5787 ± 0.0004 or 0.5795.

A3.3.4.2 ERROR CONTINGENCY CRITERIA

Provision for error contingency is built into the criterion used in Section A3.3.4.1 above. The criterion, used in conjunction with the KENO-Va and NITAWL codes, is common practice for licensing submittals. Because conservative assumptions are made in modeling, it is not necessary to introduce additional contingency for error.

A3.3.4.3 VERIFICATION ANALYSIS – BENCHMARKING

The computer codes described in Section A3.3.4.1.4.1.1 were used to benchmark 121 experiments. The results of these benchmarks were used to determine the Upper Subcritical Limit (USL-1).

The benchmark problems used to perform this verification are representative of benchmark arrays of commercial light water reactor (LWR) fuels with the following characteristics:

(1) water moderation,

(2) boron neutron absorbers,

(3) unirradiated light water reactor type fuel (no fission products or “burnup credit”) near room temperature (vs. reactor operating temperature),

(4) close reflection, and

(5) uranium oxide.

The 121 uranium oxide experiments were chosen to model a wide range of uranium enrichments, fuel pin pitches, assembly separation, soluble boron concentration and control elements in order to test the codes ability to accurately calculate k_{eff}. These experiments are discussed in detail in NUREG/CR-6361 (Reference 18).

A3.3.4.3.1 BENCHMARK EXPERIMENTS AND APPLICABILITY

A summary of all of the pertinent parameters for each experiment is included in Table A3.3-30 along with the results of each run. The best correlation is observed for fuel assembly separation distance with a correlation of 0.66. All other parameters show much lower correlation ratios indicating no real correlation. All parameters were evaluated for trends and to determine the most conservative USL.

The USL is calculated in accordance to NUREG/CR-6361 (Reference 18). USL Method 1 (USL-1) applies a statistical calculation of the bias and its uncertainty plus an administrative margin (0.05) to the linear fit of results of the experimental benchmark data. The basis for the administrative margin is from NUREG/CR-5661 (Reference 20). Results from the USL evaluation are presented in Table A3.3-31.

The criticality evaluation used the same cross section set, fuel materials and similar material/geometry options that were used in the 121 benchmark calculations as shown in Table A3.3-30.

The modeling techniques and the applicable parameters listed in Table A3.3-32 for the actual criticality evaluations fall within the range of those addressed by the benchmarks in Table A3.3-30.

A3.3.4.3.2 RESULTS OF THE BENCHMARK CALCULATIONS

The results from the comparisons of physical parameters of each of the fuel assembly types to the applicable USL value are presented in Table A3.3-32. The minimum value of the USL is determined to be 0.9419 based on comparisons to the limiting assembly parameters as shown in Table A3.3-32.

A3.3.5 RADIOLOGICAL PROTECTION

Provisions for radiological protection by confinement barriers and systems are described in Section A3.3.2.1.

A3.3.5.1 ACCESS CONTROL

The ISFSI does not require the continuous presence of operators or maintenance personnel. In addition, it is located within a fenced-in area shared only with the Equipment Storage Building and Security Building which will be used for storage of cask handling and security related equipment and will not be continuously manned. Access to the fenced-in area is limited to personnel needed during operations at the ISFSI. Activities will include periodic inspections of these facilities, emplacement of storage casks, and security checks. These activities will be defined and controlled by the Radiation Protection and Security procedures manuals covering the ISFSI.

A3.3.5.2 SHIELDING

The storage casks provide sufficient radiation shielding to allow handling of the loaded casks with as low as reasonably achievable (ALARA) doses to the operators and to comply with the radiation limits in 10 CFR72. For specific dose estimates, see Section A7.

A3.3.5.3 RADIOLOGICAL ALARM SYSTEMS

There are no credible events which result in releases of radioactive products or unacceptable increases in direct radiation. In addition, the releases postulated as the result of the hypothetical accidents described in Section A8 are of a very small magnitude. Therefore, radiological alarm systems are not necessary. However, as described in Section A3.3.2.1, not important to safety pressure monitors are provided. Procedures to be followed when these alarms are activated will be specified in the ISFSI operating procedures.

A3.3.6 FIRE AND EXPLOSION PROTECTION

No hydrocarbon fuel of any sort will be stored in the ISFSI. The quantity of fuel carried in the cask transport vehicle will be limited so that only a small fire of short duration would be possible. There are no other significant combustible sources within the ISFSI security fence. Due to the large thermal mass of the casks any minor fires in the vicinity of the ISFSI would raise the cask temperature by only a few degrees and are not expected to affect cask integrity.

604000000330

As indicated in Section 2.2, overpressures of 2.25 psi can be conservatively postulated to occur at the ISFSI as a result of accidents involving explosive materials which are stored or transported near the site. This impact is less than that postulated to result from the tornado wind loading and missile impact analysis, as described in Section A3.2.1, and is well within the design basis of the cask.

A3.3.7 MATERIAL HANDLING AND STORAGE

A3.3.7.1 SPENT FUEL HANDLING AND STORAGE

The handling of spent fuel within the Prairie Island Nuclear Generating Plant will be conducted in accordance with existing fuel handling procedures. Only fuel that is not a DAMAGED FUEL ASSEMBLY will be considered for storage in the TN-40HT casks.

In the TN-40HT casks, a DAMAGED FUEL ASSEMBLY is a Spent Nuclear Fuel Assembly that:

a. has visible deformation of the rods in the spent nuclear fuel assembly. Note: This is not referring to the uniform bowing that occurs in the reactor. This refers to bowing that significantly opens up the lattice spacing;
b. has individual fuel rods missing from the assembly. Note: The assembly is not a DAMAGED FUEL ASSEMBLY if a dummy rod that displaces a volume equal to, or greater than, the original fuel rod, is placed in the empty rod location;
c. has missing, displaced, or damaged structural components such that radiological and/or criticality safety is adversely affected (e.g., significantly changed rod pitch);
d. has missing, displaced, or damaged structural components such that the assembly cannot be handled by normal means (i.e., crane and grapple);
e. has reactor operating records (or other records) indicating that the spent nuclear fuel assembly contains cladding breaches; or
f. is no longer in the form of an intact fuel bundle (e.g., consists of, or contains, debris such as loose fuel pellets or rod segments).

Handling of the sealed casks outside of the Auxiliary Building in the process of emplacing them at the ISFSI will be done according to procedures that ensure that their safety functions and the power station capability for safe shutdown are not impaired. These operations for the TN-40HT casks are the same as for a TN-40 cask and are described in Section 5.4.

A3.3.7.2 RADIOACTIVE WASTE TREATMENT

The ISFSI will not generate radioactive waste. However, cask loading and decontamination operations, while in the Auxiliary Building, may generate small amounts of waste. This waste is disposed of in accordance with the radioactive waste handling procedures described in Section A6, and is part of the 10 CFR50 licensed activities. Waste storage facilities are neither required nor provided for the ISFSI.

A3.4 SUMMARY OF STORAGE CASK DESIGN CRITERIA

A3.4.1 Cask Design Criteria

The principal design criteria for the TN-40HT cask are presented in Table A3.4-1. The TN-40HT cask is designed to store 40, 14 x 14 PWR spent fuel assemblies with or without fuel inserts. The maximum allowable initial enrichment is 5.0 wt% U-235. The maximum bundle average burnup, maximum decay heat, and minimum cooling time for the fuel assembly are 60 GWd/MTU, 0.80 kW/assembly, and 12 years respectively.

The maximum total heat generation rate of the stored fuel is limited to 32 kW in order to keep the maximum fuel cladding temperature below the limit necessary to ensure cladding integrity. The fuel cladding integrity is assured by the cask and basket design which limits fuel cladding temperature and maintains a non-oxidizing environment in the cask cavity.

The containment vessel (body and lid) is designed and fabricated to the maximum practicable extent as a Class I component in accordance with the rules of the ASME Boiler and Pressure Vessel Code, Section III, Subsection NB, Article NB-3200. The alternatives to ASME code requirements are documented in Section A3.5. The cask design, fabrication and testing are covered by a Quality Assurance Program which conforms to the criteria in Subpart G of 10 CFR72.

The cask is designed to maintain a subcritical configuration during loading, handling, storage and accident conditions. Poison materials in the fuel basket are employed to maintain the upper subcritical limit of 0.95 minus benchmarking bias and modeling bias. The TN-40HT basket is designed and fabricated to the maximum practicable extent in accordance with the rules of the ASME Boiler and Pressure Vessel Code, Section III, Subsection NG, Article NG-3200 (Reference 2). The alternatives to ASME code requirements are documented in Section A3.5.

The TN-40HT cask is designed to withstand the effects of severe environmental conditions and natural phenomena such as earthquakes, tornadoes, lightning and floods. Section A8 describes the cask behavior under these accident conditions.

A3.4.2 Design Basis Limits for Fission Product Barriers (DBLFPBs)

The NRC has defined the design basis limit for a fission product barrier as the controlling numerical value for a parameter established during the license review as presented in the Safety Analysis Report for any parameter(s) used to determine the integrity of the barrier. The list of DBLFPBs for the TN-40HT cask is listed in Table A3.4-2.

A3.5 ASME CODE ALTERNATIVES

The cask containment boundary is designed, fabricated and inspected in accordance with the ASME Code Subsection NB (Reference 2) to the maximum practical extent. The gamma shielding, which is primarily for shielding, but also provides structural support to the containment boundary, was designed in accordance with Subsection NF of the code. Inspections of the gamma shielding are performed in accordance with ASME code Subsection NF as detailed in the SAR. Other cask components, such as the protective cover, outer shell and neutron shielding are not governed by the ASME Code. The Code Alternatives are described below.

Component	Reference ASME Code/Section	Code Requirement	Alternatives, Justification & Compensatory Measures
TN-40HT Cask, Basket	NB/NF/ NG-1100 NB/NF/ NG-2130 NB/NF/ NG-4121	Stamping and preparation of reports by the Certificate Holder, Use of ASME Certificate Holders	The TN-40HT cask is not stamped, nor is there a code design specification or stress report generated. A design criteria document is generated in accordance with Transnuclear's (TN) QA Program and the design and analysis is performed under TN's QA Program. The cask may also be fabricated by other than N-stamp holders and materials may be supplied by other than ASME Certificate holders.
TN-40HT Cask, Basket	NCA	All	Not compliant with NCA. TN Quality Assurance requirements, which are based on 10 CFR72 Subpart G, are used in lieu of NCA-4000. Fabrication oversight is performed by TN personnel in lieu of an Authorized Nuclear Inspector.
Pressure Test of the Containment Boundary	NB-6000	Hydrostatic Testing	The containment vessel is hydrostatically tested in accordance with the requirements of the ASME B&PV Code, Section III, Articles NB-6200 with the exception that some of the containment vessel may be installed in the shield shell during testing. The containment vessel is supported by the shield shell during all design and accident events.

Component	Reference ASME Code/Section	Code Requirement	Alternatives, Justification & Compensatory Measures
Weld of bottom inner plate to the containment shell	NB-5231	Full penetration corner welded joints require the fusion zone and the parent metal beneath the attachment surface to be UT'd after welding.	The joint may be welded after the containment shell is shrink-fit into the shield shell. The geometry of the joint does not allow for UT inspection. In this case, the joint will be examined by RT and either PT or MT methods in accordance with ASME subsection NB requirements. If the containment shell is welded complete before shrink fitting, UT examination per NB-5231 will be performed.
Containment Shell Rolling Qualification	NB-4213	The rolling process used to form the inner vessel should be qualified to determine that the required impact properties of NB-2300 are met after straining by taking test specimens from three different heats.	If the plates are made from less than three heats, each heat will be tested to verify the impact properties.
Welds of the Bottom Shield to Shield Shell and Shield Shell to Shell Flange	NB-4243 and NB-5230	Category C weld joints in vessels and similar weld joints in other components shall be full penetration joints. These welds shall be examined by UT or RT and either PT or MT.	Certain welds are partial penetration welds. As an alternative to the NDE requirements of NB-5230, for Category C welds, all of these closure welds are multi-layer welds that are progressive PT examined.
Containment Vessel	NB-7000	Vessels are required to have overpressure protection	No overpressure protection is provided. Function of containment vessel is to contain radioactive contents under normal and accident conditions. The containment vessel is designed to withstand maximum internal pressure considering 100% fuel rod failure and maximum accident temperatures.
Containment Vessel, Basket	NB-8000 NG-8000	Requirements for nameplates, stamping and reports per NCA-8000	The TN-40HT cask is to be marked and identified in accordance with 10 CFR 72 requirements. Code stamping is not required. QA data package to be in accordance with TN approved QA program.

Component	Reference ASME Code/Section	Code Requirement	Alternatives, Justification & Compensatory Measures
Weld of Shield Plate to Lid Outer Plate	NB-4335 NB-4620	Impact testing of weld and heat affected zone of lid to shield plate Post weld heat treatment	The lid shield plate is not in the component support path, and has no pressure-retaining function; it is a non-structural attachment, and NB jurisdiction does not apply to the plate or weld. The weld must conform to NB-4430.
Gamma Shielding and Trunnion	NB-1132 NF-1132	Attachments in the component support load path and not performing a pressure retaining function shall conform to Subsection NF.	The gamma shield shell and trunnions are not fabricated completely in accordance with Subsection NF. The shield shell's primary function is not structural. The weld of the bottom shield plate to the shield shell is subject to multilevel PT or MT to prevent complete loss of the bottom shielding in an accident. Other shield shell weld (shield shell to the shell flange) failures would not lead to loss of shielding. The trunnions and trunnion welds are designed to load factors much higher than those of subsection NF, the trunnion weld is subject to root and final PT or MT, and the trunnions are tested to 1.5 times design load.
Basket neutron poison material	NG-2000	Use of ASME Materials	The basket neutron poison material is not considered in the structural analysis of the basket. The material provides criticality control and adds a heat transfer path. The poison material is not a code material.
Basket	NG-3352	Table NG 3352-1 lists the permissible welded joints.	The fusion welds between the stainless steel insert plates and the stainless fuel compartment tube are not included in Table NG-3352-1. The required minimum tested capacity of the welded connection (at each side of the tube) shall be 35 kips (at room temperature). The capacity shall be demonstrated by qualification and production testing. ASME Code Section IX does not provide tests for qualification of these types of welds. Therefore, these welds are qualified using Section IX to the degree applicable together with the testing described here. The welds will be visually inspected to confirm that they are located over the insert plates, in lieu of the visual acceptance criteria of NG-5260 which are not appropriate for this type of weld. A joint efficiency (quality) factor of 1.0 is utilized for the fuel compartment longitudinal seam welds. Table NG-3352-1 permits a joint efficiency (quality) factor of 0.5 to be used for full penetration weld examined by ASME Section V visual examination (VT). For the TN-40HT basket, the compartment seam weld is thin (0.188" thick) and the weld will be made in one pass. Both surfaces of weld (inside and outside) will be fully examined by VT and therefore a factor of 2 x 0.5=1.0 will be used in the analysis. This is justified as both surfaces of the single weld pass/layer will be fully examined, and the stainless steel material that comprises the fuel compartment tubes is very ductile.

A3.6 REFERENCES

1. 10CFR Part 72, “Licensing Requirements For The Independent Storage Of Spent Nuclear Fuel, High-Level Radioactive Waste, And Reactor-Related Greater Than Class C Waste”.

2. American Society of Mechanical Engineers, ASME Boiler And Pressure Vessel Code, Section III, Division 1 - Subsections NB, NF and NG, 2004 edition including 2006 addenda.

3. NUREG-0612 “Control of Heavy Loads at Nuclear Power Plants”, July 1980.

4. Standard Review Plan, NRC NUREG-0800, Rev. 2, July, 1981.

5. T. W. Singell, Wind Forces on Structures: Forces on Enclosed Structures, ASCE Structural Journal, July 1958.

6. Baumeister and Marks, Standard Handbook for Mechanical Engineers, Seventh Edition, McGraw-Hill Book Co.

7. 10CFR 100, Reactor Site Criteria.

8. U.S. Nuclear Regulatory Commission, Regulatory Guide 1.92, Combining Modal Responses and Spatial Components in Seismic Response Analysis, Revision 1, February, 1976.

9. American National Standards Institute, "American National Standard for Special Lifting Devices for Shipping Containers Weighing 10,000 Pounds (4500 kg) or More for Nuclear Materials," ANSI N14.6, New York, 1986.

10. Letter, R.O.Anderson (NSP) to U S Nuclear Regulatory Commission, dated March 27, 1995, "Response to Request for Additional Information Regarding NUREG-0612, 'Control of Heavy Loads'".

11. Letter, B.A.Wetzel (NRC) to R.O.Anderson (NSP), transmittal date June 12, 1995, "Safety Evaluation and Safety Assessment Related to Dry Cask Storage At Prairie Island".

12. Not Used.

13. Safety Evaluation 72-448, TN-40 Cask Weight/Storage Slab Design, May 14, 1996.

14. "SCALE: A Modular Code System for Performing Standardized Computer Analyses for Licensing Evaluation for Workstations and Personal Computers," NUREG/CR-0200, Rev. 6, September, 1998.

15. Prairie Island Nuclear Generating Plant Updated Safety Analysis Report, Units 1 and 2, License Number DPR-42 and DPR-60.

16. Not used.

17. Warren C. Young, Richard G. Budynas, "Roark Formulas for Stress and Strain," Seventh Edition, 2002, McGraw Hill.`

18. U.S. Nuclear Regulatory Commission, "Criticality Benchmark Guide for Light-Water-Reactor Fuel in Transportation and Storage Packages," NUREG/CR-6361 April, 1997, ORNL/TM-11936.

19. U.S. Nuclear Regulatory Commission, Regulatory Guide 1.60, Rev. 1, Design Response Spectra for Seismic Design of Nuclear Plants, December, 1973.

20. U.S. Nuclear Regulatory Commission, "Recommendations for Preparing the Criticality Safety Evaluation of Transportation Packages," NUREG/CR-5661, Published April 1997, ORNL/TM-11936.

21. Not used.

22. Not used.

23. Not used.

24. "Formulas for Stress and Strain," Roark, 4th Edition.

25. USNRC, SFPO, Interim Staff Guidance – 11, Rev. 3, "Cladding Considerations for the Transportation and Storage of Spent Fuel."

26. Department of Energy, Report No. DOE / RW0472, Rev. 2, "Topical Report on Actinide-Only Burnup Credit for PWR Spent Nuclear Fuel Packages," 1998.

27. Rohsenow, W. M., Hartnett, J. P., Cho, Y. I., "Handbook of Heat Transfer Fundamentals," 3rd Edition, 1998.

28. ASME Boiler and Pressure Vessel Code, Section II, Part D, "Material Properties," 2004.

29. Perry, R. H., Chilton, C. H., “Chemical Engineers’ Handbook,” 5th Edition, 1973.

30. Zoldners, N. G., “Thermal Properties of Concrete under Sustained Elevated Temperatures,” ACI Publications, Paper SP 25-1, American Concrete Institute, Detroit, MI, 1970.

31. Bentz, D. P., “A Computer Model to Predict the Surface Temperature and Time-of-Wetness of Concrete Pavements and Bridge Decks,” Report # NISTIR 6551, National Institute of Standards and Technology, 2000.

32. Siegel, Robert, Howell, R. H., “Thermal Radiation Heat Transfer,” 4th Edition, 2002.

33. AAR Brooks & Perkins, Advanced Structures Division, “Standard Specification for Boral™ Composite Sheets.”

34. Not used.

35. USNRC, SFPO, NUREG-1536, “Standard Review Plan for Dry Cask Storage Systems - Final Report,” 1997.

36. ANSYS Computer Code and User’s Manuals, Version 8.0.

37. TN Letter to NRC, “Revision 1 to Transnuclear, Inc. (TN) Application for Amendment 1 to the NUHOMS® HD System, Response to Request for Additional Information (Docket No. 72-1030; TAC No. L24153)”, Enclosure 2, Response to RAI 4.1, TN Document No. E-27377, December 15, 2008.

38. USNRC, Code of Federal Regulations, Part 71, “Packaging and Transportation of Radioactive Material,” 2004.

39. Gregory, J. J., Mata, R., Keltner, N. R., “Thermal Measurements in a Series of Long Pool Fires,” SANDIA Report, SAND 85-0196, TTC-0659, 1987.

40. IAEA Safety Standards, “Regulations for the Safe Transport of Radioactive Material,” 1985.

41. USNRC, SFPO, NUREG/CR-0497, “A Handbook of Materials Properties for Use in the Analysis of Light Water Reactor Fuel Rod Behavior,” MATPRO - Version II (Revison 2), EG&G Idaho, Inc., TREE-1280, 1981.

42 Letter, Ashok Thadani (NRC) to S. R. Tritch (Westinghouse), “Acceptance for Referencing of Topical Report WCAP-12610 ‘Vantage+ Fuel Assembly Reference Core Report’ (TAC No. 77258)” July 1, 1991.

43. SANDIA Report, SAND90-2406, “A Method for Determining the Spent Fuel Contribution to Transport Cask Containment Requirements,” 1992.

44. ANSYS Computer Code and User’s Manuals, Version 10.0.

45. USNRC, Regulatory Issue Summary 2013-11, Resolution of Licensing Process Expectations for Pressurized Water Reactor Fuel Assemblies Susceptible to Top Nozzle Stress Corrosion Cracking in Dry Cask Spent Fuel Storage and Transportation; September 4, 2013

46. NSP Design Change No 99FH02, Repair Regions D, E and F Spent Fuel Assemblies, Rev 0.

47. 10CFR72.48 Safety Evaluation 573, Rev 0

48. Knoll, R.W., et al., “Evaluation of Cover Gas Impurities and Their Effects on the Dry Storage of LWR Spent Fuel, “PNL-6365, DE88 003983, PNNL, November 1987.

49. Siemens Product Lifecycle Management Software Inc., STAR-CCM+, Version 12.02 (Sargent & Lundy, LLC (S&L) Program No. 03.7.863-12.02).

604000000330

TABLE A3.1-1
PRAIRIE ISLAND FUEL ASSEMBLY DESIGN CHARACTERISTICS

Fuel Designations	Exxon/ANF (ANP) (14x14) Standard	Exxon/ANF (ANP) High Burnup (14x14)	Exxon/ANF (ANP) TOPROD (14x14)	Westinghouse Standard (14x14)	Westinghouse OFA (Including Vantage+) (14x14)
Max Length (in)	161.3	161.3	161.3	161.3	161.3
Max Width (in)	7.763	7.763	7.763	7.763	7.763
Maximum No. of Fuel Rods	179	179	179	179	179
Nominal Fuel Rod OD (in)	0.4240	0.4260	0.4170	0.4220	0.4000
Clad Material	Zr-4	Zr-4	Zr-4	Zr-4	Zr-4/ZIRLO
Guide Tube #	16	16	16	16	16
Instrument Tube #	1	1	1	1	1
Maximum MTU/assembly(1)	0.370	0.370	0.370	0.410	0.360

Note:

(1) The maximum MTU/assembly is calculated based on the theoretical density. The calculated value is higher than the actual value.

TABLE A3.1-2
THERMAL, GAMMA AND NEUTRON SOURCES
FOR THE DESIGN BASIS 14X14 WESTINGHOUSE STANDARD FUEL ASSEMBLY

U^{235} Bundle Average Initial Enrichment (% wt)	3.4
Burnup (MWD/MTU)	60,000
Cooling Time (years)	18
Decay Heat (kW/assembly)	0.845[(2)]
Gamma Source (photon/sec/assembly)[(1)]	3.37E+15
Neutron Source (neutrons/sec/assembly)	7.59E+08

Note:

(1) Includes fuel insert (BPRA/TPA) activation gamma source

(2) 0.845 kW is used for source term calculation.

TABLE A3.1-3
FUEL QUALIFICATION CRITERIA

Low Range

$2.0 \le$ Enrichment < 3.4 wt% U-235
≤ 44 GWD/MTU
Minimum cooling time = 12 years (verify decay heat ≤ 800 watts with equation below)

High Range

$3.4 \le$ Enrichment ≤ 5.0 wt% U-235
≤ 60 GWD/MTU
Minimum cooling time = 12 years (verify decay heat ≤ 800 watts with equation below)

The Decay Heat (DH) in watts is expressed as:

$$F1 = A + B*X1 + C*X2 + D*X1^2 + E*X1*X2 + F*X2^2$$
$$DH = F1*Exp(\{G*[1-(12/X3)]\}*[(X3/X1)^H])*[(X2/X1)^I])$$

where,

F1	Intermediate Function, the thermal source at 12 year cooling
X1	Assembly Burn-up in GWD/MTU
X2	Initial Enrichment in wt. % U-235 (max 5% wt)
X3	Cooling Time in Years (min 12 yrs)

A=18.76 B=11.27 C= 6.506 D= 0.163 E= -1.826
F= 6.617 G= -0.309 H= 0.431 I= -0.374

TABLE A3.2-1
TN-40HT CASK COMPONENT WEIGHTS AND CENTER OF GRAVITY LOCATIONS

Component	Weight (lbs)	CG Location (in.)
Cask Shell	105,849	93
Lid	13,314	177.05
Bottom Assembly	15,579	4.375
Neutron Shield	22,062	89.25
Top Neutron Shield	1,638	184.0
Overpressure Tank	131	190.56
Protective cover	1,362	186.6
Upper Trunnion	667	155.25
Lower Trunnion	253	7.5
Basket	28,488	88.75
40 Fuel Assemblies	52,000	89.4
Misc(2)	1,000	91.58
Total(1)	**242,343**	**91.58**

(1) Actual weight(s) will vary. Fully loaded cask weight is 244,000 lbs max (Reference 13).
(2) Additional weight to account for small items not explicitly included in the weight calculation of the other components, e.g. head of bolts, drain tube, etc.

TABLE A3.2-2
SUMMARY OF INTERNAL AND EXTERNAL PRESSURES
ACTING ON THE TN-40HT CASK

Individual Load Conditions	Maximum Pressure, psig
Internal Pressure:	
(a) Initial Cavity Pressurization	13.2
(b) With 10% Fuel & BPRA Failure	17.8
(c) With 100% Fuel & BPRA Failure	See condition (d)
(d) In a Minor Fire (assumed 100% fuel & BPRA failure)	75.2
(e) Beginning of Life Unloading	57.3
(f) Cask Burial (assumes 100% fuel & BPRA failure)	95.5
(g) Tornado	3*
(h) Selected Bounding Pressure	100
External Pressure	
(a) Flood	25
(b) Snow and Ice Loading	0.35
I Explosion	2.25
(d) Selected bounding Pressure	25

*This is due to a reduced external pressure.

TABLE A3.2-3
SUMMARY OF LIFTING LOADS USED FOR UPPER TRUNNIONS

Handling Condition	**Load at Cask CG (1)** **Vertical**
Lifting - Cask Vertical	
Yield Evaluation	1.500×10^6 lbs.
Ultimate Evaluation	2.500×10^6 lbs.
	Load at each Trunnion (2)
Yield Evaluation	0.750×10^6 lbs.
Ultimate Evaluation	1.250×10^6 lbs.

Notes:

(1) Based on a cask weight of 250,000 lbs.

(2) Load evenly divided between one pair of upper trunnions.

TABLE A3.2-4
SUMMARY OF LOADS ACTING ON THE TN-40HT CASK DUE TO ENVIRONMENTAL AND NATURAL PHENOMENA

Distributed Loads

Lateral Loading:	
(a) Wind (external force on cask body)	46,480 lb
(b) Seismic (inertial force throughout system) 0.18W	45,000 lb.[(2)]
Selected Bounding Load W x 1G	250,000 lb.[(2)]
Vertical Loading[(1)]:	
(a) Seismic (inertial force throughout system) 0.12W	30,000 lb.[(2)]
Selected Bounding Load W x 1G	250,000 lb.[(2)]

Notes:

(1) Does not include dead weight or lifting loads

(2) A low weight is used for stability analysis. A high weight of the cask is used for stress analysis.

TABLE A3.2-5
TN-40HT CASK LOADING CONDITIONS

Normal

Assembly Loads (bolt preload and seal compression)
Pressure (internal and external)
Weight
Lifting Loads
Handling
Wind
Thermal variations (e.g., insolation, decay heat, ambient)

Man-Made (Accident)

Fuel cladding failure (due to loading or unloading error)
Minor Fire
Explosion

Natural Phenomena (Accident)

Earthquakes
Tornadoes
Cask Burial
Flood
Lightning

TABLE A3.2-6
TN-40HT CASK DESIGN LOADS
(NORMAL CONDITIONS)

Applied Load	Loading Condition
Internal Pressure	Note (1)
External Pressure	Note (2)
Distributed Loads	Weight (Cask Body, Contents)
Snow	
Ice	
Wind (Tornado)	
Lifting	
Attachment Loads	Lifting
Bolt Loads	Preload for 100 psig and metal seal compression

Notes:

(1) Cask design pressure is 22 psig but evaluated for 100 psig internal pressure which envelopes all internal pressure levels including fission gas release.

(2) Cask designed for 25 psig external pressure which envelopes all external pressure effects.

TABLE A3.2-7
LEVEL A SERVICE LOADS
(NORMAL CONDITIONS)

Applied Load	Loading Condition
Internal Pressure	Note (1)
External Pressure	Note (2)
Distributed Loads	Weight (Cask Body, Contents)
Snow	
Ice	
Wind (Tornado)	
Lifting	
Attachment Loads	Lifting
Bolt Loads	Preload for 100 psig and metal seal compression
Thermal Effects	Decay Heat
Insolation	

Notes:

(1) Cask design pressure is 22 psig but evaluated for 100 psig internal pressure which envelopes all internal pressure levels including fission gas release.

(2) Cask designed for 25 psig external pressure which envelopes all external pressure effects.

TABLE A3.2-8
LEVEL D SERVICE LOADS
(ACCIDENT CONDITIONS)

Load Cause	
Internal Pressure	Note (1)
External Pressure	Note (2)
Distributed Loads	Weight (Cask Body, Contents)
Tornado Wind	
Flood Water	
Seismic	
Bolt Loads metal seal compression and drop impact	Preload for 100 psig,
50 g Bottom Impact (Handling Accident)	18" Vertical Drop

Notes:

(1) Cask design pressure is 22 psig but evaluated for 100 psig internal pressure which envelopes all internal pressure levels including fission gas release.

(2) Cask designed for 25 psig external pressure which envelopes all external pressure effects including flood water level, cask burial and explosion.

TABLE A3.2-9
NORMAL CONDITION LOAD COMBINATIONS

Individual Load Combined Load	Bolt Preload	Fabrication	1g Down	Internal Pressure 100 psig	External Pressure 25 psig	Thermal (Hot)	Thermal (Cold)	3g Lifting	Trunnion Local Stress
N1	X	X	X	X					
N2	X	X	X		X				
N3	X	X	X	X		X			
N4	X	X	X		X		X		
N5	X	X		X		X		X(1)	
N6	X	X			X		X	X(1)	
N7				X		X			X(2)
N8					X		X		X(2)

Notes:

(1) Calculated cask global stresses due to 3g lifting load

(2) Calculated cask local stresses at trunnion/shield shell due to 3g lifting load

TABLE A3.2-10
ACCIDENT CONDITION LOAD COMBINATIONS

Individual Load Combined Load	Bolt Preload	Fabrication	18" Bottom End Drop 50 g	Internal Pressure 100 psig	External Pressure 25 psig	Seismic, Tornado, or Flood 1 g-Lateral + 2 g-Down
A1	X	X	X			
A2	X	X	X	X		
A3	X	X	X		X	
A4	X	X		X		X
A5	X	X			X	X

TABLE A3.3-1
AXIAL DECAY HEAT PROFILE

% of Core Height	Corresponding Length for Active Fuel of 144” (in)	Peaking Factor
0.00	0.00	0
2.78	4.00	0.652
8.33	12.00	0.967
13.89	20.00	1.074
19.44	27.99	1.103
25.00	36.00	1.108
30.56	44.01	1.106
36.11	52.00	1.102
41.67	60.00	1.097
47.22	68.00	1.094
52.78	76.00	1.094
58.33	84.00	1.095
63.89	92.00	1.096
69.44	99.99	1.095
75.00	108.00	1.086
80.56	116.01	1.059
86.11	124.00	0.971
91.67	132.00	0.738
97.22	140.00	0.462
100.00	144.00	0

TABLE A3.3-2
PEAKING FACTORS APPLIED IN THE FINITE ELEMENT MODEL

Fuel Region No.	z_i (in)	Local Peaking Factor $PF_{z,i}$	Average Height (in)	Average Peaking Factor $PF_{m,i}$	Area underneath Profile (A_i)
	0.000	0			
1	1.320	0.215	0.660	0.107	0.1419
2	7.070	0.773	4.195	0.617	3.5501
3	14.500	1.000	10.785	0.940	6.9833
4	22.070	1.082	18.285	1.072	8.1167
5	29.500	1.104	25.785	1.093	8.1189
6	37.070	1.108	33.285	1.106	8.3712
7	52.070	1.102	44.570	1.105	16.573
8	67.070	1.094	59.570	1.098	16.472
9	82.070	1.095	74.570	1.095	16.418
10	97.070	1.095	89.570	1.095	16.426
11	102.750	1.092	99.910	1.094	6.2118
12	111.940	1.073	107.345	1.082	9.9464
13	117.690	1.040	114.815	1.067	6.1361
14	126.940	0.885	122.315	1.001	9.2634
15	134.500	0.652	130.720	0.799	6.0431
16	141.940	0.238	138.220	0.534	3.971
17	144.000	0.000	142.970	0.119	0.2449
SUM					143.0
Average					0.993

TABLE A3.3-3
MAXIMUM TEMPERATURES FOR HOT NORMAL/OFF-NORMAL CONDITIONS

Normal/Off-Normal Storage, 100 °F Ambient		
Component	Maximum Temperature (°F)	Temperature Limit (°F)
Fuel Cladding**	696	752
Fuel Compartment**	647	---
Basket Rails**	471	---
Cask Inner Shell *,**	307	---
Shield Shell*,‡	303	---
Radial Resin †,‡	290	300
Cask Outer Shell †,‡	265	---
Top Shield Plate ‡	199	---
Cask Lid ‡	196	---
Top Resin ‡	196	300
Protective Cover ‡	194	---
Inner Bottom Plate ‡	374	---
Bottom Shield ‡	270	---
Lid Seal ‡	189	536
Vent & Port Seal ‡	190	536

60400000330

* This value is the average temperature at the hottest cross section.

† This value is the volumetric average temperature at the hottest cross section plus 18 °F to bound the effects of storage pad on the cask view factor. See Section A3.3.2.2.4 for discussion.

‡ An additional 5°F is added to account for the effect of the southeast ISFSI pad expansion on cask exterior temperatures. See Section A3.3.2.2.4.1.1 for discussion.

** An additional 2°F is added to account for the effect of the southeast ISFSI pad expansion on cask interior temperatures. See Section A3.3.2.2.4.1.1 for discussion.

60400000330

TABLE A3.3-4
AVERAGE TEMPERATURES AT THE HOTTEST CROSS SECTION
FOR 100 °F STORAGE CONDITIONS

Component	Average Temperature* (°F)
Basket	496
Aluminum Shims	375
Cask Inner Shell	307
Basket Support Bar 90-270	552
Basket Support Bar 0-180	577
Basket Aluminum Plate 90-270	553
Basket Aluminum Plate 0-180	589
Shield Shell	303

*An additional 2 °F is added to account for the effect of the southeast ISFSI pad expansion on cask interior temperatures, with the exception of the Shield Shell. An additional 5 °F is added to the Shield Shell average temperature to account for the effect of the southeast ISFSI pad expansion on cask exterior temperatures. See Section A3.3.2.2.4.1.1 for discussion.

604000000330

TABLE A3.3-5
MAXIMUM TEMPERATURES FOR COLD NORMAL/OFF-NORMAL CONDITIONS

Normal/Off-Normal Storage, -40 °F Ambient	
Component	Maximum Temperature (°F)
Fuel Cladding **	598
Fuel Compartment **	545
Basket Rails **	364
Cask Inner Shell *,**	190
Shield Shell*, ‡	186
Radial Resin †, ‡	172
Cask Outer Shell †, ‡	146
Top Shield Plate ‡	67
Cask Lid ‡	63
Top Resin ‡	63
Protective Cover ‡	26
Inner Bottom Plate ‡	257
Bottom Shield ‡	142
Lid Seal ‡	57
Vent & Port Seal ‡	57

604000000330

* This value is the average temperature at the hottest cross section.

† This value is the volumetric average temperature at the hottest cross section plus 18 °F to bound the effects of storage pad on the cask view factor. See Section A3.3.2.2.4 for discussion.

‡ An additional 5°F is added to account for the effect of the southeast ISFSI pad expansion on cask exterior temperatures. See Section A3.3.2.2.4.1.1 for discussion.

** An additional 2°F is added to account for the effect of the southeast ISFSI pad expansion on cask interior temperatures. See Section A3.3.2.2.4.1.1 for discussion.

604000000330

.

TABLE A3.3-6
MAXIMUM COMPONENT TEMPERATURE FOR FIRE ACCIDENT

Component	Temperature (°F)	Time (hr)	Limit (°F)
Fuel Cladding **	790	∞	1058
Fuel Compartment **	744	∞	---
Basket Rails **	555	∞	---
Cask Inner Shell *,**	372	∞	---
Shield Shell *,***	366	∞	---
Radial Resin	N/A ‡	---	---
Cask Outer Shell †, ***	918	End of fire	---
Top Shield Plate ***	258	1.2 hr after fire	---
Cask Lid ***	372	End of fire	---
Top Resin ***	N/A ‡	---	---
Protective Cover ***	1243	End of fire	---
Lid Seal ***	379	End of fire	536
Vent & Port Seal ***	270	1.2 hr after fire	536

60400000330

* This value is the average temperature at the hottest cross section.

† This value is the volumetric average temperature at the hottest cross section plus 18 °F to bound the view factor effects on the initial temperatures. See Section A3.3.2.2.4 for discussion.

‡ Neutron shield resin is assumed to be burnt and decomposed during the fire

** An additional 2°F is added to account for the effect of the southeast ISFSI pad expansion on cask interior temperatures. See Section A3.3.2.2.4.1.1 for discussion.

*** An additional 5°F is added to account for the effect of the southeast ISFSI pad expansion on cask exterior temperatures. See Section A3.3.2.2.4.1.1 for discussion.

60400000330

TABLE A3.3-7
MAXIMUM COMPONENT TEMPERATURES FOR BURIED CASK
(FUEL ASSEMBLY WITHOUT BPRAS)

Component	Temperature (°F)	Time (hr)	Limit (°F)
Fuel Cladding**	1058	92.49	1058
Fuel Compartment**	1024	92.51	---
Basket Rails **	889	92.56	---
Cask Inner Shell *,**	774	92.6	---
Shield Shell *, ‡	769	92.61	---
Radial Resin †, ‡	300	1.23	300
Cask Outer Shell †, ‡	779	92.1	---
Top Shield Plate ‡	319	91.92	---
Cask Lid ‡	316	91.92	---
Top Resin ‡	300	81.82	300
Protective Cover ‡	316	92.7	---
Lid Seal ‡	317	92.15	536
Vent & Port Seal ‡	316	92.1	536

604000000330

* This value is the volumetric average temperature at the hottest cross section.

† This value is the volumetric average temperature at the hottest cross section plus 18 °F to bound the view factor effects on the initial temperatures. See Section A3.3.2.2.4 for discussion.

‡ An additional 5°F is added to account for the effect of the southeast ISFSI pad expansion on cask exterior temperatures. See Section A3.3.2.2.4.1.1 for discussion.

** An additional 2°F is added to account for the effect of the southeast ISFSI pad expansion on cask interior temperatures. See Section A3.3.2.2.4.1.1 for discussion.

604000000330

TABLE A3.3-8
MATERIAL THERMAL PROPERTIES
(PAGE 1 OF 7)

Homogenized PWR Fuel

Temperature (°F)	k_{trans} in Helium (Btu/hr-in-°F)	Temperature (°F)	k_{trans} in Vacuum (Air) (Btu/hr-in-°F)
136	0.0161	195	0.007345
233	0.0177	276	0.009133
330	0.0193	361	0.01138
428	0.0210	449	0.01417
526	0.0228	540	0.01735
624	0.0246	633	0.02136
722	0.0263	727	0.02571
821	0.0281	823	0.03085
920	0.0298	919	0.03653
1019	0.0317	1016	0.04338

Temperature (°F)	k_{axial} (Btu/hr-in-°F)	Temperature (°F)	$c_{P,\,eff}$ (Btu/lbm-°F)
212	0.0558	80	0.059
392	0.0587	260	0.065
572	0.0623	692	0.073
752	0.0673	1502	0.078
932	0.0738		
1112	0.0824		

ρ_{eff} = 0.135 lb/in^3

TABLE A3.3-8
MATERIAL THERMAL PROPERTIES
(PAGE 2 OF 7)

Stainless Steel, Type 304
(Fuel Compartments, Basket Plate Support Bars, and Rail Plates)
(The Material group, conductivity, and diffusivity values are from Reference 28. The density value is from Reference 29.)

Mat. group J	Thermal conductivity		Thermal Diffusivity	Specific heat capacity*
Temperature (°F)	(Btu/hr-ft-°F)	(Btu/hr-in-°F)	(ft^2/hr)	(Btu/lbm-°F)
70	8.6	0.717	0.151	0.116
100	8.7	0.725	0.152	0.117
150	9.0	0.750	0.154	0.119
200	9.3	0.775	0.156	0.121
250	9.6	0.800	0.158	0.124
300	9.8	0.817	0.160	0.125
350	10.1	0.842	0.162	0.127
400	10.4	0.867	0.165	0.128
450	10.6	0.883	0.167	0.129
500	10.9	0.908	0.169	0.131
550	11.1	0.925	0.172	0.132
600	11.3	0.942	0.174	0.132
650	11.6	0.967	0.177	0.134
700	11.8	0.983	0.179	0.134
750	12.0	1.000	0.182	0.134
800	12.3	1.025	0.184	0.136
850	12.5	1.042	0.186	0.137
900	12.7	1.058	0.189	0.137
950	12.9	1.075	0.191	0.138
1000	13.1	1.092	0.194	0.138
1050	13.4	1.117	0.196	0.139
1100	13.6	1.133	0.198	0.140
1150	13.8	1.150	0.201	0.140
1200	14.0	1.167	0.203	0.141
ρ = 0.29 lbm/in^3				

* Thermal diffusivity, $\alpha = \frac{k}{\rho\, c_P}$, is used to calculate the specific heat with a density of 0.284 lbm/in^3 for steel alloys.

TABLE A3.3-8
MATERIAL THERMAL PROPERTIES
(PAGE 3 OF 7)

Low Alloy Steel, SA 203, Gr. E or SA350, LF3

(Cask Inner Shell, Cask Lid Outer Plate, Shell Flange, and Bottom Inner Plate)

(The Material group, conductivity, and diffusivity values are from Reference 28. The density value is from Reference 29.)

Mat. group C	Thermal conductivity		Thermal Diffusivity	Specific heat capacity *
Temperature (°F)	(Btu/hr-ft-°F)	(Btu/hr-in-°F)	(ft^2/hr)	(Btu/lbm-°F)
70	23.7	1.975	0.459	0.105
100	23.6	1.967	0.451	0.107
200	23.5	1.958	0.424	0.113
300	23.4	1.950	0.401	0.119
400	23.1	1.925	0.379	0.124
500	22.7	1.892	0.357	0.130
600	22.2	1.850	0.336	0.135
700	21.6	1.800	0.314	0.140
800	21.0	1.750	0.292	0.147
900	20.3	1.692	0.269	0.154
1000	19.7	1.642	0.247	0.163
1100	19.1	1.592	0.223	0.175
1200	18.3	1.525	0.200	0.186
1300	16.6	1.383	0.164	0.206
1400	15.3	1.275	0.077	0.405
ρ = 0.284 lbm/in^3				

* Thermal diffusivity, $\alpha = \dfrac{k}{\rho\, c_P}$, is used to calculate the specific heat with a density of 0.284 lbm/in^3 for steel alloys.

TABLE A3.3-8
MATERIAL THERMAL PROPERTIES
(PAGE 4 OF 7)

Carbon Steel, SA 266, CL. 2 or SA516, Gr. 70 or SA 105
(Gamma Shield, Cask Outer Shell, Shield Plate, Bottom Shield, & Protective Cover)
(The Material group, conductivity, and diffusivity values are from Reference 28. The density value is from Reference 29.)

Mat. group B	Thermal conductivity		Thermal Diffusivity	Specific heat capacity *
Temperature (°F)	(Btu/hr-ft-°F)	(Btu/hr-in-°F)	(ft^2/hr)	(Btu/lbm-°F)
70	27.3	2.275	0.530	0.105
100	27.6	2.300	0.520	0.108
200	27.8	2.317	0.487	0.116
300	27.3	2.275	0.455	0.122
400	26.5	2.208	0.426	0.127
500	25.7	2.142	0.399	0.131
600	24.9	2.075	0.373	0.136
700	24.1	2.008	0.346	0.142
800	23.2	1.933	0.319	0.148
900	22.3	1.858	0.291	0.156
1000	21.1	1.758	0.263	0.163
1100	19.8	1.650	0.234	0.172
1200	18.3	1.525	0.204	0.183
1300	16.9	1.408	0.157	0.219
1400	15.7	1.308	0.078	0.410
ρ = 0.280 lbm/in^3				

* Thermal diffusivity, $\alpha = \dfrac{k}{\rho\, c_P}$, is used to calculate the specific heat with a density of 0.284 lbm/in^3 for steel alloys.

TABLE A3.3-8
MATERIAL THERMAL PROPERTIES
(PAGE 5 OF 7)

Aluminum Alloy 1100 (Basket Aluminum Plates)

(The conductivity, diffusivity and density values are from Reference 28.)

Al91100	Thermal conductivity		Thermal Diffusivity	Specific heat capacity *
Temperature (°F)	(Btu/hr-ft-°F)	(Btu/hr-in-°F)	(ft^2/hr)	(Btu/lbm-°F)
70	133.1	11.092	3.671	0.214
100	131.8	10.983	3.606	0.216
150	130.0	10.833	3.505	0.219
200	128.5	10.708	3.418	0.222
250	127.3	10.608	3.347	0.225
300	126.2	10.517	3.285	0.227
350	125.3	10.442	3.227	0.229
400	124.5	10.375	3.170	0.232
ρ = 0.098 lbm/in^3				

Aluminum Alloy 6061 (Basket Rail Shims)

(The conductivity, diffusivity and density values are from Reference 28.)

Al96061	Thermal conductivity		Thermal Diffusivity	Specific heat capacity*
Temperature (°F)	(Btu/hr-ft-°F)	(Btu/hr-in-°F)	(ft^2/hr)	(Btu/lbm-°F)
70	96.1	8.008	2.661	0.213
100	96.9	8.075	2.660	0.215
150	98.0	8.167	2.650	0.218
200	99.0	8.250	2.649	0.221
250	99.8	8.317	2.641	0.223
300	100.6	8.383	2.629	0.226
350	101.3	8.442	2.620	0.228
400	101.9	8.492	2.620	0.230
ρ = 0.098 lbm/in^3				

* Thermal diffusivity, $\alpha = \dfrac{k}{\rho\, c_P}$, is used to calculate the specific heat with a density of 0.098 lbm/in^3 for aluminum alloys.

TABLE A3.3-8
MATERIAL THERMAL PROPERTIES
(PAGE 6 OF 7)

Aluminum Alloy 6063 (Radial Neutron Shield Boxes)

(The conductivity, diffusivity and density values are from Reference 28.)

Al96063	Thermal conductivity		Thermal Diffusivity	Specific heat capacity *
Temperature (°F)	(Btu/hr-ft-°F)	(Btu/hr-in-°F)	(ft^2/hr)	(Btu/lbm-°F)
70	120.8	10.067	3.340	0.214
100	120.3	10.025	3.299	0.215
150	119.7	9.975	3.232	0.219
200	119.0	9.917	3.177	0.221
250	118.5	9.875	3.133	0.223
300	118.1	9.842	3.088	0.226
350	118.0	9.833	3.040	0.229
400	117.6	9.800	3.000	0.231
ρ = 0.098 lbm/in^3				

Neutron Absorber (Poison) Plates

Boral™	Thermal conductivity of Poison Plate	Specific heat of Poison Plate (Cp_t)
Temperature (°F)	(Btu/hr-in-°F)	(Btu/lbm-°F)
100	4.14	0.22
500	3.70	0.33

Solid Neutron Shield Resin (Borated Polyester – also used for Polypropylene)

Thermal conductivity	Density	Specific heat capacity
(Btu/hr-in-°F)	(lbm/in^3)	(Btu/lbm-°F)
0.0083	0.057	0.311

* Thermal diffusivity, $\alpha = \dfrac{k}{\rho\, c_P}$, is used to calculate the specific heat with a density of 0.098 lbm/in^3 for aluminum alloys.

TABLE A3.3-8
MATERIAL THERMAL PROPERTIES
(PAGE 7 OF 7)

Helium

Temperature	Thermal conductivity	Temperature	Thermal conductivity
(K)	(W/m-K)	(°F)	(Btu/hr-in-°F)
300	0.1499	80	0.0072
400	0.1795	260	0.0086
500	0.2115	440	0.0102
600	0.2466	620	0.0119
800	0.3073	980	0.0148
1000	0.3622	1340	0.0174
1050	0.3757	1430	0.0181

Air

Temperature	Thermal conductivity	Temperature	Thermal conductivity
(K)	(W/m-K)	(°F)	(Btu/hr-in-°F)
250	0.02228	-10	0.0011
300	0.02607	80	0.0013
400	0.03304	260	0.0016
500	0.03948	440	0.0019
600	0.04557	620	0.0022
800	0.05698	980	0.0027
1000	0.06721	1340	0.0032

Concrete and Soil (Storage Pad)

(The conductivity values for concrete are from Reference 30 and the values for soil are from Reference 31.)

Concrete		**Soil**
Temperature	Conductivity	Conductivity
(°F)	(Btu/hr-in-°F)	(Btu/hr-in-°F)
70	0.0958	0.0144
1382	0.0479	

TABLE A3.3-9
TRANSVERSE EFFECTIVE FUEL CONDUCTIVITY IN HELIUM

T_O	T_C	T_{avg}	k_{eff}
(°F)	(°F)	(°F)	(Btu/hr-in-°F)
100	171	136	1.96E-02
200	262	231	2.24E-02
300	353	327	2.62E-02
400	446	423	3.02E-02
500	540	520	3.47E-02
600	635	618	3.97E-02
700	731	716	4.48E-02
800	827	814	5.14E-02
900	924	912	5.78E-02
1000	1021	1011	6.61E-02

TABLE A3.3-10
COMPARISON OF MAXIMUM AND AVERAGE TEMPERATURES

	Storage Array Model		TN-40HT Detailed Model	
	Maximum Temp (°F)	Average Temp (°F)	Maximum Temp (°F)	Average Temp (°F)
Cask Inner Shell	331	306	310	305
Cask Outer Shell	276	260	244	242
Radial Resin	---	---	283	267

TABLE A3.3-10A
COMPARISON OF MAXIMUM AND AVERAGE TEMPERATURES WITH A SOUTHEAST ISFSI PAD

	Thermal conductivity of cask / ground [W/m-K]	Cask Maximum Temperature [°F]	Casks Average Temperature [°F]	Temperature Difference [°F]	
				Cask Maximum	Cask Average
One set of two rows	0.5	271.8	257.2	Reference Value	Reference Value
Two sets of two rows - 38 ft apart	0.5	274.6	258.7	+2.8	+1.5
One set of two rows	2.5	270.7	257.0	Reference Value	Reference Value
Two sets of two rows - 38 ft apart	2.5	273.5	258.5	+2.8	+1.5
One set of two rows	5.0	269.7	257.0	Reference Value	Reference Value
Two sets of two rows - 38 ft apart	5.0	272.3	258.4	+2.6	+1.4

604000000330

TABLE A3.3-11
COMPARISON OF VIEW FACTORS

View Factors	Detailed TN-40HT Model	Storage Array Model
Cask to Casks	0.1862	0.156
Cask to Pad	0	0.305
Cask to Ambient	0.8138	0.538

TABLE A3.3-12
EFFECTIVE CONDUCTIVITIES FOR CASK SECTIONS

	Section 1, Mat # 1		Section 2, Mat # 2	
T_{avg}	$k_{eff,axl}$	$k_{eff,rad}$	$k_{eff,axl}$	$k_{eff,rad}$
(°F)	(Btu/hr-in-°F)	(Btu/hr-in-°F)	(Btu/hr-in-°F)	(Btu/hr-in-°F)
-50	0.98	2.21	2.23	1.99
50	1.02	2.21	2.23	1.99
150	1.07	2.24	2.25	2.01
250	1.10	2.23	2.24	2.00
350	1.11	2.18	2.19	1.96
450	1.12	2.12	2.13	1.92
550	1.13	2.06	2.07	1.87
650	1.12	1.99	2.01	1.82
750	1.12	1.92	1.94	1.76
	Section 3, Mat # 3		**Section 4, Mat # 4**	
T_{avg}	$k_{eff,axl}$	$k_{eff,rad}$	$k_{eff,axl}$	$k_{eff,rad}$
(°F)	(Btu/hr-in-°F)	(Btu/hr-in-°F)	(Btu/hr-in-°F)	(Btu/hr-in-°F)
-50	1.73	0.50	1.14	1.69
50	1.73	0.52	1.15	1.69
150	1.74	0.56	1.19	1.69
250	1.73	0.58	1.22	1.69
350	1.70	0.60	1.25	1.68
450	1.66	0.61	1.27	1.66
550	1.62	0.62	1.28	1.63
650	1.59	0.63	1.29	1.59
750	1.54	0.64	1.28	1.55
	Section 5, Mat # 5			
T_{avg}	$k_{eff,axl}$	T_{avg}	$k_{eff,rad}$	
(°F)	(Btu/hr-in-°F)	(°F)	(Btu/hr-in-°F)	
-50	0.83	70	1.975	
50	0.87	100	1.967	
150	0.93	200	1.958	
250	0.98	300	1.950	
350	1.01	400	1.925	
450	1.04	500	1.892	
550	1.05	600	1.850	
650	1.07	700	1.800	
750	1.07	800	1.750	

**TABLE A3.3-13
AVERAGE TEMPERATURES AT THE HOTTEST CROSS SECTION
FOR VACUUM DRYING CONDITIONS WITH ZERO GAP BETWEEN BASKET AND
CASK INNER SHELL**

Component	Average Temperature (°F)
Basket	580
Aluminum Shims	374
Cask Inner Shell	364
Basket Support Bar 90-270	608
Basket Support Bar 0-180	635
Basket Aluminum Plate 90-270	607
Basket Aluminum Plate 0-180	644
Shield Shell	356

TABLE A3.3-14
MAXIMUM COMPONENT TEMPERATURE AT THE END OF VACUUM DRYING OPERATIONS

Component	Time (hr)	Temperature (°F)	Limit (°F)
Fuel Cladding	34	731	752
Fuel Compartment	34	692	---
Basket Rails	34	541	---
Cask Inner Shell	34	235	---
Shield Shell	34	232	---
Radial Resin	34	219	300
Top Resin	34	<235 *	300
Lid Seal	34	<235 *	536
Vent and Port Seal	34	<235 *	536

* Temperature is bounded by maximum temperature of the cask inner shell.

TABLE A3.3-15
CASK INTERNAL PRESSURE (FUEL ASSEMBLY WITHOUT BPRAS)

Operating Condition	n_{back}	f_B	n_{free}	n_{total}	$\bar{T}_{cavity}$	P_{cavity}	
	(lb-mole)	(---)	(lb-mole)	(lb-mole)	(°F)	(psia)	(psig)
Normal *	0.580	0.01	0.889	0.589	466	27.9	13.2
Off-Normal *	0.580	0.10	0.889	0.669	466	31.7	17.0
Fire Accident *	0.580	1.00	0.889	1.469	605	80.1	65.4
Buried Cask Accident @ 92.6 hr	0.580	1.00	0.889	1.469	925	104.1	89.4

* An additional 2 °F is added to average T_{cavity} to account for the effect of the southeast ISFSI pad expansion on cask interior temperatures.
See Section A3.3.2.2.4.1.1 for discussion. P_{cavity} is recalculated based on the new temperature. There is no impact on the buried cask accident values because the maximum temperature reached is unchanged and only the time is adjusted.

604000000330

TABLE A3.3-16
CASK INTERNAL PRESSURE (FUEL ASSEMBLY WITH BPRAS)

Operating Condition	n_{back}	f_B	n_{free}	n_{total}	$\bar{T}_{cavity}$	P_{cavity}	
	(lb-mole)	(---)	(lb-mole)	(lb-mole)	(°F)	(psia)	(psig)
Normal *	0.549	0.01	1.017	0.559	466	28.0	13.3
Off-Normal *	0.549	0.10	1.017	0.651	466	32.6	17.9
Fire Accident *	0.549	1.00	1.017	1.566	605	80.1	75.4
Buried Cask Accident @ 74.6 hr	0.549	1.00	1.017	1.566	843	110.2	95.5

* An additional 2 °F is added to average Tcavity to account for the effect of the southeast ISFSI pad expansion on cask interior temperatures.
See Section A3.3.2.2.4.1.1 for discussion. Pcavity is recalculated based on the new temperature. There is no impact on the buried cask accident values because the maximum temperature reached is unchanged and only the time is adjusted.

604000000330

TABLE A3.3-17
MAXIMUM ENRICHMENT AND MINIMUM B10 CONTENT

Maximum Assembly Average Initial Enrichment (wt. % U-235)	Minimum B10 Content for Boral® (mg/cm^2)	Minimum B10 Content for B-Al[(1)] (mg/cm^2)	B10 Content Used in Criticality Evaluation (mg/cm^2)
5.00	45.0	37.5	33.7

Notes:

(1) B-Al = Metal Matrix Composites and Borated Aluminum Alloys.

TABLE A3.3-18
AUTHORIZED CONTENTS FOR TN-40HT SYSTEM

Assembly Type	Array	Assembly Class	Assembly ID(1)
Exxon/ANF (ANP) 14x14 WE	14x14	WE 14x14	EXSTD
Exxon/ANF (ANP) 14x14 High Burnup	14x14	WE 14x14	EXHBU
Exxon/ANF (ANP) 14x14 Toprod	14x14	WE 14x14	EXTOP
Westinghouse 14x14 Standard	14x14	WE 14x14	WESTD
Westinghouse 14x14 OFA	14x14	WE 14x14	WEOFA

Notes:

(1) Assembly ID is a simplification for the purpose of this evaluation to identify these fuel assembly Types.

TABLE A3.3-19
PARAMETERS FOR WE 14X14 CLASS FUEL ASSEMBLIES

Parameters[1][2]	Assembly ID				
	EXSTD	EXHBU	EXTOP	WESTD	WOFA
Active fuel length (in)	144	144	144	144	144
Number of fuel rods per assembly	179	179	179	179	179
Pitch (in)	0.556	0.556	0.556	0.556	0.556
Fuel pellet OD (in)	0.3565	0.3565	0.3505	0.3659	0.3444
Clad thickness (in)	0.0300	0.0310	0.0295	0.0243	0.0243
Clad OD (in)	0.424	0.426	0.417	0.422	0.400
Guide/instrument tube OD (in)	16@0.541 1@0.424	16@0.541 1@0.424	16@0.541 1@0.424	16@0.539 1@0.422	16@0.528 1@0.4015
Guide/Instrument tube ID (in)	16@0.507 1@0.374	16@0.507 1@0.374	16@0.507 1@0.374	16@0.505 1@0.3734	16@0.490 1@0.3499

Notes:

(1) Reload fuel from other manufacturers with these parameters are also acceptable.

(2) All dimensions shown are nominal

TABLE A3.3-20
TN-40HT BASKET DIMENSIONS

Basket Component Description	Actual Dimension inches	Dimension Used in Model inches (cm)
Compartment inside (maximum) Compartment inside (nominal) Compartment inside (minimum)	8.10 8.05 8.00	8.10 (20.574) 8.05 (20.447) 8.00 (20.320)
Compartment wall (maximum) Compartment wall (nominal) Compartment wall (minimum)	0.2325 0.1875 0.1775	0.2325 (0.59055) 0.1870 (0.47490) 0.1775 (0.45085)
Stainless steel insert bar height	1.75	1.75 (4.445)
SS insert bar thickness (maximum) SS insert bar thickness (nominal) SS insert bar thickness (minimum)	0.4925 0.4375 0.4275	0.4925 (1.2509) 0.4375 (1.1111) 0.4275 (1.0858)
Poison/Al plate height	13.18	12.67 (32.1772)
Poison plate thickness(1)	0.075	0.075 (0.19049)
Al plate thickness(1)	0.3625	0.3625 (0.92075)
Horizontal gap	0.07	Modeled as aluminum 0.07 (0.1778)
Vertical slot width/height	1.00 / 5.75	No slot (Replaced with basket)
Section height	15.00	14.49 (36.80)
Cask inside radius	36.00	36.00 (91.44)
Thickness of the inner shell	1.50	1.50 (3.81)
Thickness of the gamma shield shell	7.25	7.65 (19.42)
Thickness of the neutron shield shell	5.25	5.00 (12.70)
Thickness of the skin shell	0.50	Not modeled (included in gamma shield shell)

Notes:

(1) Dimensions given are based on 0.075 inch thick poison plate. Since the SS insert bar thickness is varied from 0.4925 inches to 0.4275 inches, the aluminum plate thickness is also varied from 0.4175 to 0.3525 inches and the poison plate thickness is kept constant at 0.075 inches.

TABLE A3.3-21
DESCRIPTION OF THE BASIC KENO MODEL UNITS

Geometry Units	Description
1	Fuel Pin Cell
2	Guide Tube
3	Instrument Tube
21 - 23	Basket Cells with Poison along the West Face of F/A
31 - 33	Basket Cells without Poison along North Face of F/A
41 - 43	Basket Cells without Poison along the East Face of F/A
51 - 53	Basket Cells with Poison along the South Face of F/A
25, 35, 45, 55	Arrays that define the West, North, East and South Faces of the Basket Cell without fuel
61 - 63	Basket Cells without Poison along the West Face of F/A
71 - 73	Basket Cells without Poison along North Face of F/A
81 - 83	Basket Cells without Poison along the East Face of F/A
91 - 93	Basket Cells without Poison along the South Face of F/A
65, 75, 85, 95	Arrays that define the West, North, East and South Faces of the Basket Cell without fuel and poison
201	Basket Cell with Fuel Assembly Positions 201, 202, 205, 206 representing the South West Interior Positions
101, 102, 103	Units that model the vertical and horizontal rail plates.
206	Unit describing fuel assembly positions 201, 202, 205 and 206
207	Unit describing fuel assembly positions 203, 204, 207 and 208
210	Unit describing fuel assembly positions 209, 210 and 223
211	Unit describing fuel assembly positions 211, 212 and 228
214	Unit describing fuel assembly positions 213, 214, 217 and 218
215	Unit describing fuel assembly positions 215, 216, 219 and 220
221	Unit describing fuel assembly positions 221 and 222
225	Unit describing fuel assembly positions 224 and 225
226	Unit describing fuel assembly positions 226 and 227
230	Unit describing fuel assembly positions 229 and 230
231 - 240	Units describing fuel assembly positions 231 - 240
241 - 245	6x5 Array of Basket Cells defining the inner 30 locations
10	Global Unit includes the fuel compartments, rails and the cask radial shells

TABLE A3.3-22
MATERIAL PROPERTY DATA

Material	ID	Density g/cm^3	Element	Weight %	Atom Density (atoms/b-cm)
UO_2 (Enrichment - 5.0 wt. %)	1	10.576	U-235	4.407	1.19435E-03
			U-238	83.743	2.24060E-02
			O	11.850	4.72006E-02
Zircaloy-4	2	6.56	Zr	98.23	4.2541E-02
			Sn	1.45	4.8254E-04
			Fe	0.21	1.4856E-04
			Cr	0.10	7.5978E-05
			Hf	0.01	2.2133E-06
Water (Pellet Clad Gap)	3	0.998	H	11.1	6.6769E-02
			O	88.9	3.3385E-02
Stainless Steel (SS304)	4	7.94	C	0.080	3.1877E-04
			Si	1.000	1.7025E-03
			P	0.045	6.9468E-05
			Cr	19.000	1.7473E-02
			Mn	2.000	1.7407E-03
			Fe	68.375	5.8545E-02
			Ni	9.500	7.7402E-03
Borated Water (2450 ppm Boron)	5	1.00	H	11.165	6.67692E-02
			O	88.590	3.33846E-02
			B10	0.045	2.71583E-05
			B11	0.200	1.09316E-04
$^{11}B_4C$ in CC	7	2.556	B11	78.586	1.0988E-01
			C	21.414	2.7470E-02
Aluminum	8	2.702	Al	100.0	6.0307E-02
BORAL Poison 0.05″ core thickness (18.7 mg B-10/cm^2)	9	2.450	B10	5.973	8.8013E-03
			B11	26.434	3.5426E-02
			C	8.993	1.1057E-02
			Al	58.600	3.2044E-02
Aluminum - Boron Poison 0.075″ thickness (18.7 mg B-10/cm^2)	9	2.693	B10	3.636	5.88913E-03
			B11	0.404	5.95126E-04
			Al	95.960	5.76775E-02
Aluminum - Boron Poison 0.125″ thickness (33.7 mg B-10/cm^2)	9	2.693	B10	3.93	6.37017E-03
			B11	0.44	6.43737E-04
			Al	95.63	5.74791E-02
Water	10	0.998	H	11.1	6.6769E-02
			O	88.9	3.3385E-02
Carbonsteel	11	7.821	C	1.00	3.92503E-03
			Fe	99.0	8.34982E-02

TABLE A3.3-23
MOST REACTIVE FUEL TYPE EVALUATION RESULTS
(PAGE 1 OF 2)

Description	k_{KENO}	1σ	k_{eff}
Exxon 14x14 High Burnup			
Centered, 80% IMD	0.9052	0.0009	0.9070
Centered, 90% IMD	0.9043	0.0007	0.9057
Centered, 100% IMD	0.9014	0.0008	0.9030
Inward, 80% IMD	0.9079	0.0007	0.9093
Inward, 90% IMD	0.9097	0.0007	0.9111
Inward, 100% IMD	0.9052	0.0007	0.9066
Exxon 14x14 Standard			
Centered, 80% IMD	0.9054	0.0007	0.9068
Centered, 90% IMD	0.9059	0.0007	0.9073
Centered, 100% IMD	0.9023	0.0008	0.9039
Inward, 80% IMD	0.9099	0.0007	0.9113
Inward, 90% IMD	0.9083	0.0008	0.9099
Inward, 100% IMD	0.9064	0.0008	0.9080
Exxon 14x14 Top Rod			
Centered, 80% IMD	0.8995	0.0008	0.9011
Centered, 90% IMD	0.8987	0.0008	0.9003
Centered, 100% IMD	0.8930	0.0007	0.8944
Inward, 80% IMD	0.9022	0.0007	0.9036
Inward, 90% IMD	0.9016	0.0008	0.9032
Inward, 100% IMD	0.8974	0.0008	0.8990

TABLE A3.3-23
MOST REACTIVE FUEL TYPE EVALUATION RESULTS

(PAGE 2 OF 2)

Description	k_{KENO}	1σ	k_{eff}
WE 14x14 OFA			
Centered, 80% IMD	0.8921	0.0007	0.8935
Centered, 90% IMD	0.8884	0.0007	0.8898
Centered, 100% IMD	0.8840	0.0007	0.8854
Inward, 80% IMD	0.8954	0.0007	0.8968
Inward, 90% IMD	0.8928	0.0008	0.8944
Inward, 100% IMD	0.8867	0.0008	0.8883
WE 14x14 Standard			
Centered, 80% IMD	0.9175	0.0008	0.9191
Centered, 90% IMD	0.9189	0.0007	0.9203
Centered, 100% IMD	0.9147	0.0007	0.9161
Inward, 80% IMD	**0.9218**	**0.0009**	**0.9236**
Inward, 90% IMD	0.9215	0.0008	0.9231
Inward, 100% IMD	0.9182	0.0007	0.9196

TABLE A3.3-24
FUEL COMPARTMENT TUBE INTERNAL DIMENSION EVALUATION RESULTS

Description	k_{KENO}	1σ	k_{eff}
Nominal ID = 8.05″ from previous evaluation			
80% IMD	0.9218	0.0009	0.9236
90% IMD	0.9215	0.0008	0.9231
100% IMD	0.9182	0.0007	0.9196
Maximum ID = 8.10″			
80% IMD	0.9187	0.0008	0.9203
90% IMD	0.9201	0.0008	0.9217
100% IMD	0.9163	0.0007	0.9177
Minimum ID = 8.00″			
80% IMD	**0.9251**	**0.0007**	**0.9265**
90% IMD	0.9238	0.0006	0.9250
100% IMD	0.9210	0.0007	0.9224

TABLE A3.3-25
COMPARTMENT TUBE AND STEEL BAR THICKNESS EVALUATION RESULTS

Description	k_{KENO}	1σ	k_{eff}
Nominal Tube Thickness = 0.1875″, Nominal Steel Bar Thickness = 0.4375″ (from previous evaluation)			
80% IMD	**0.9251**	**0.0007**	**0.9265**
90% IMD	0.9238	0.0006	0.9250
100% IMD	0.9210	0.0007	0.9224
Maximum Tube Thickness = 0.2325″, Maximum Steel Bar Thickness = 0.4925″			
80% IMD	0.9241	0.0008	0.9257
90% IMD	0.9229	0.0007	0.9243
100% IMD	0.9212	0.0007	0.9226
Maximum Tube Thickness = 0.2325″, Minimum Steel Bar Thickness = 0.4275″			
80% IMD	0.9226	0.0007	0.9240
90% IMD	**0.9252**	**0.0007**	**0.9266**
100% IMD	0.9213	0.0007	0.9227
Maximum Tube Thickness = 0.2325″, Nominal Steel Bar Thickness = 0.4375″			
80% IMD	0.9237	0.0008	0.9253
90% IMD	0.9237	0.0007	0.9251
100% IMD	0.9204	0.0007	0.9218
Minimum Tube Thickness = 0.1775″, Maximum Steel Bar Thickness = 0.4925″			
80% IMD	0.9227	0.0009	0.9245
90% IMD	0.9237	0.0007	0.9251
100% IMD	0.9215	0.0007	0.9229
Minimum Tube Thickness = 0.1775″, Minimum Steel Bar Thickness = 0.4275″			
80% IMD	0.9226	0.0008	0.9242
90% IMD	**0.9248**	**0.0008**	**0.9264**
100% IMD	0.9229	0.0008	0.9245
Minimum Tube Thickness = 0.1775″, Nominal Steel Bar Thickness = 0.4375″			
80% IMD	0.9234	0.0007	0.9248
90% IMD	**0.9249**	**0.0008**	**0.9265**
100% IMD	0.9219	0.0007	0.9233

TABLE A3.3-26
POISON BAR THICKNESS AND MATERIAL EVALUATION RESULTS

Description	k_{KENO}	1σ	k_{eff}
Nominal Tube Thickness = 0.1875″, Nominal Steel Bar Thickness = 0.4375″, BORAL			
80% IMD	0.9244	0.0008	0.9260
90% IMD	0.9238	0.0008	0.9254
100% IMD	0.9206	0.0008	0.9222
Maximum Tube Thickness = 0.2325″, Minimum Steel Bar Thickness = 0.4275″, BORAL			
80% IMD	0.9241	0.0007	0.9255
90% IMD	0.9241	0.0008	0.9257
100% IMD	0.9208	0.0008	0.9224
Minimum Tube Thickness = 0.1775″, Minimum Steel Bar Thickness = 0.4275″, BORAL			
80% IMD	0.9237	0.0007	0.9251
90% IMD	0.9242	0.0007	0.9256
100% IMD	0.9216	0.0008	0.9232

TABLE A3.3-27
RAIL MODELING EVALUATION RESULTS

Description	k_{KENO}	1σ	k_{eff}
Nominal Tube Thickness = 0.1875″, Nominal Steel Bar Thickness = 0.4375″, *Rail1*			
80% IMD	0.9235	0.0008	0.9251
90% IMD	0.9240	0.0007	0.9254
100% IMD	0.9204	0.0007	0.9218
Nominal Tube Thickness = 0.1875″, Nominal Steel Bar Thickness = 0.4375″, *Rail2*			
80% IMD	0.9242	0.0008	0.9258
90% IMD	0.9233	0.0008	0.9249
100% IMD	0.9213	0.0008	0.9229
Nominal Tube Thickness = 0.1875″, Nominal Steel Bar Thickness = 0.4375″, *Rail3*			
80% IMD	0.9271	0.0008	0.9287
90% IMD	0.9280	0.0007	0.9294
100% IMD	0.9245	0.0009	0.9263
Maximum Tube Thickness = 0.2325″, Minimum Steel Bar Thickness = 0.4275″, *Rail3*			
80% IMD	0.9273	0.0008	0.9289
90% IMD	**0.9297**	**0.0008**	**0.9313**
100% IMD	0.9212	0.0007	0.9226
Minimum Tube Thickness = 0.1775″, Minimum Steel Bar Thickness = 0.4275″, *Rail3*			
80% IMD	0.9264	0.0007	0.9278
90% IMD	0.9267	0.0007	0.9281
100% IMD	0.9250	0.0007	0.9264
Minimum Tube Thickness = 0.1775″, Nominal Steel Bar Thickness = 0.4375″, *Rail3*			
80% IMD	0.9260	0.0007	0.9274
90% IMD	0.9270	0.0007	0.9284
100% IMD	0.9228	0.0006	0.9240

TABLE A3.3-28
WE 14X14 CLASS ASSEMBLY WITHOUT CCS FINAL RESULTS

Model Description	k_{KENO}	1σ	k_{eff}
Enrichment = 5.00 wt. % U-235, Soluble Boron = 2450 ppm, 33.7 mg B-10/cm^2			
Internal Moderator Density = 01%	0.5705	0.0004	0.5713
Internal Moderator Density = 10%	0.6496	0.0005	0.6506
Internal Moderator Density = 20%	0.7286	0.0007	0.7300
Internal Moderator Density = 30%	0.7926	0.0007	0.7940
Internal Moderator Density = 40%	0.8444	0.0007	0.8458
Internal Moderator Density = 50%	0.8805	0.0008	0.8821
Internal Moderator Density = 60%	0.9037	0.0008	0.9053
Internal Moderator Density = 70%	0.9200	0.0007	0.9214
Internal Moderator Density = 80%	0.9293	0.0008	0.9309
Internal Moderator Density = 90%	0.9313	0.0008	0.9329
Internal Moderator Density = 100%	0.9310	0.0007	0.9324

TABLE A3.3-29
WE 14X14 CLASS ASSEMBLY WITH CCS FINAL RESULTS

Model Description	k_{KENO}	1σ	k_{eff}
Enrichment = 5.00 wt. % U-235, Soluble Boron = 2450 ppm, 33.7 mg B-10/cm^2			
Internal Moderator Density = 01%	**0.5787**	**0.0004**	**0.5795**
Internal Moderator Density = 10%	0.6480	0.0005	0.6490
Internal Moderator Density = 20%	0.7206	0.0006	0.7218
Internal Moderator Density = 30%	0.7808	0.0007	0.7822
Internal Moderator Density = 40%	0.8305	0.0007	0.8319
Internal Moderator Density = 50%	0.8673	0.0007	0.8687
Internal Moderator Density = 60%	0.8944	0.0008	0.8960
Internal Moderator Density = 70%	0.9132	0.0007	0.9146
Internal Moderator Density = 80%	0.9266	0.0007	0.9280
Internal Moderator Density = 90%	0.9333	0.0007	0.9347
Internal Moderator Density = 100%	**0.9357**	**0.0008**	**0.9373**

TABLE A3.3-30
BENCHMARKING RESULTS
(PAGE 1 OF 4)

Run ID	U Enrich. Wt%	Pitch (cm)	H_2O/fuel volume	Separation of assemblies (cm)	AEG	k_{eff}	1σ
B1645SO1	2.46	1.41	1.015	1.78	32.8118	0.9965	0.0008
B1645SO2	2.46	1.41	1.015	1.78	32.7528	1.0006	0.0008
BW1231B1	4.02	1.511	1.139		31.1429	0.9966	0.0009
BW1231B2	4.02	1.511	1.139		29.8872	0.9990	0.0007
BW1273M	2.46	1.511	1.376		32.2213	0.9961	0.0007
BW1484A1	2.46	1.636	1.841	1.636	34.5373	0.9975	0.0008
BW1484A2	2.46	1.636	1.841	4.908	35.1630	0.9934	0.0008
BW1484B1	2.46	1.636	1.841		33.9415	0.9984	0.0008
BW1484B2	2.46	1.636	1.841	1.636	34.5780	0.9961	0.0009
BW1484B3	2.46	1.636	1.841	4.908	35.2638	0.9978	0.0008
BW1484C1	2.46	1.636	1.841	1.636	34.6547	0.9936	0.0009
BW1484C2	2.46	1.636	1.841	1.636	35.2469	0.9944	0.0010
BW1484S1	2.46	1.636	1.841	1.636	34.5159	1.0002	0.0008
BW1484S2	2.46	1.636	1.841	1.636	34.5530	0.9990	0.0008
BW1484SL	2.46	1.636	1.841	6.544	35.4203	0.9944	0.0009
BW1645S1	2.46	1.209	0.383	1.778	30.1060	0.9987	0.0008
BW1645S2	2.46	1.209	0.383	1.778	29.9920	1.0049	0.0008
BW1810A	2.46	1.636	1.841		33.9524	0.9987	0.0006
BW1810B	2.46	1.636	1.841		33.9711	0.9995	0.0006
BW1810CR	2.46	1.636	1.841		33.1556	0.9995	0.0008
BW1810D	2.46	1.636	1.841		33.0876	0.9981	0.0010
BW1810E	2.46	1.636	1.841		33.1520	0.9991	0.0007
BW1810F	2.46	1.636	1.841		33.9581	1.0029	0.0007
BW1810GR	2.46	1.636	1.841		32.9478	0.9986	0.0007
BW1810H	2.46	1.636	1.841		32.9370	0.9981	0.0008
BW1810I	2.46	1.636	1.841		33.9613	1.0028	0.0007
BW1810J	2.46	1.636	1.841		33.1379	0.9995	0.0008
EPRU65	2.35	1.562	1.196		33.9138	0.9959	0.0008
EPRU65B	2.35	1.562	1.196		33.4073	1.0000	0.0009
EPRU75	2.35	1.905	2.408		35.8676	0.9968	0.0009
EPRU75B	2.35	1.905	2.408		35.3074	1.0002	0.0008
EPRU87	2.35	2.21	3.687		36.6120	1.0011	0.0009
EPRU87B	2.35	2.21	3.687		36.3460	1.0003	0.0008
NSE71SQ	4.74	1.26	1.823		33.7627	0.9978	0.0009
NSE71W1	4.74	1.26	1.823		34.0088	0.9981	0.0010
NSE71W2	4.74	1.26	1.823		34.3856	0.9995	0.0010

TABLE A3.3-30
BENCHMARKING RESULTS
(PAGE 2 OF 4)

Run ID	U Enrich. Wt%	Pitch (cm)	H_2O/fuel volume	Separation of assemblies (cm)	AEG	k_{eff}	1σ
P2438BA	2.35	2.032	2.918	5.05	36.2244	0.9973	0.0009
P2438SLG	2.35	2.032	2.918	8.39	36.2906	0.9985	0.0009
P2438SS	2.35	2.032	2.918	6.88	36.2690	0.9979	0.0009
P2438ZR	2.35	2.032	2.918	8.79	36.2891	0.9976	0.0009
P2615BA	4.31	2.54	3.883	6.72	35.7276	1.0005	0.0011
P2615SS	4.31	2.54	3.883	8.58	35.7456	0.9959	0.0011
P2615ZR	4.31	2.54	3.883	10.92	35.7709	0.9980	0.0010
P2827L1	2.35	2.032	2.918	13.72	36.2491	1.0051	0.0008
P2827L2	2.35	2.032	2.918	11.25	36.2939	1.0005	0.0010
P2827L3	4.31	2.54	3.883	20.78	35.6740	1.0095	0.0009
P2827L4	4.31	2.54	3.883	19.04	35.7173	1.0066	0.0010
P2827SLG	2.35	2.032	2.918	8.31	36.3010	0.9957	0.0008
P3314BA	4.31	1.892	1.6	2.83	33.1874	1.0000	0.0009
P3314BC	4.31	1.892	1.6	2.83	33.2334	0.9992	0.0009
P3314BF1	4.31	1.892	1.6	2.83	33.2422	1.0024	0.0009
P3314BF2	4.31	1.892	1.6	2.83	33.2121	1.0001	0.0010
P3314BS1	2.35	1.684	1.6	3.86	34.8545	0.9957	0.0010
P3314BS2	2.35	1.684	1.6	3.46	34.8324	0.9940	0.0008
P3314BS3	4.31	1.892	1.6	7.23	33.4328	0.9996	0.0009
P3314BS4	4.31	1.892	1.6	6.63	33.4152	1.0000	0.0008
P3314SLG	4.31	1.892	1.6	2.83	34.0109	0.9971	0.0010
P3314SS1	4.31	1.892	1.6	2.83	33.9613	0.9984	0.0010
P3314SS2	4.31	1.892	1.6	2.83	33.7719	1.0014	0.0009
P3314SS3	4.31	1.892	1.6	2.83	33.8956	0.9995	0.0010
P3314SS4	4.31	1.892	1.6	2.83	33.7604	0.9962	0.0009
P3314SS5	2.35	1.684	1.6	7.8	34.9476	0.9947	0.0010
P3314SS6	4.31	1.892	1.6	10.52	33.5406	1.0010	0.0008
P3314W1	4.31	1.892	1.6		34.3962	1.0009	0.0010
P3314W2	2.35	1.684	1.6		35.2153	0.9972	0.0008
P3314ZR	4.31	1.892	1.6	2.83	33.9897	0.9977	0.0010
P3602BB	4.31	1.892	1.6	8.3	33.3198	1.0031	0.0010
P3602BS1	2.35	1.684	1.6	4.8	34.7746	1.0034	0.0009
P3602BS2	4.31	1.892	1.6	9.83	33.3649	1.0047	0.0010
P3602N11	2.35	1.684	1.6	8.98	34.7410	1.0025	0.0008
P3602N12	2.35	1.684	1.6	9.58	34.8378	1.0048	0.0009

TABLE A3.3-30
BENCHMARKING RESULTS
(PAGE 3 OF 4)

Run ID	U Enrich. Wt%	Pitch (cm)	H_2O/fuel volume	Separation of assemblies (cm)	AEG	k_{eff}	1σ
P3602N13	2.35	1.684	1.6	9.66	34.9334	1.0006	0.0009
P3602N14	2.35	1.684	1.6	8.54	35.0287	0.9969	0.0010
P3602N21	2.35	2.032	2.918	10.36	36.2787	0.9999	0.0009
P3602N22	2.35	2.032	2.918	11.2	36.1963	1.0014	0.0008
P3602N31	4.31	1.892	1.6	14.87	33.2015	1.0063	0.0010
P3602N32	4.31	1.892	1.6	15.74	33.3085	1.0072	0.0010
P3602N33	4.31	1.892	1.6	15.87	33.4168	1.0084	0.0010
P3602N34	4.31	1.892	1.6	15.84	33.4653	1.0028	0.0010
P3602N35	4.31	1.892	1.6	15.45	33.5169	1.0030	0.0009
P3602N36	4.31	1.892	1.6	13.82	33.5832	1.0003	0.0010
P3602N41	4.31	2.54	3.883	12.89	35.5269	1.0127	0.0010
P3602N42	4.31	2.54	3.883	14.12	35.6711	1.0068	0.0009
P3602N43	4.31	2.54	3.883	12.44	35.7505	1.0049	0.0009
P3602SS1	2.35	1.684	1.6	8.28	34.8708	1.0007	0.0009
P3602SS2	4.31	1.892	1.6	13.75	33.4133	1.0026	0.0010
P3926L1	2.35	1.684	1.6	10.06	34.8569	1.0003	0.0009
P3926L2	2.35	1.684	1.6	10.11	34.9374	1.0020	0.0008
P3926L3	2.35	1.684	1.6	8.5	35.0657	0.9967	0.0010
P3926L4	4.31	1.892	1.6	17.74	33.3262	1.0066	0.0009
P3926L5	4.31	1.892	1.6	18.18	33.4035	1.0054	0.0010
P3926L6	4.31	1.892	1.6	17.43	33.5141	1.0038	0.0009
P3926SL1	2.35	1.684	1.6	6.59	35.0674	0.9950	0.0009
P3926SL2	4.31	1.892	1.6	12.79	33.5810	0.9998	0.0009
P4267B1	4.31	1.89	1.59		31.7989	0.9992	0.0008
P4267B2	4.31	1.89	1.59		31.5288	1.0027	0.0007
P4267B3	4.31	1.715	1.09		30.9907	1.0057	0.0009
P4267B4	4.31	1.715	1.09		30.5098	0.9993	0.0008
P4267B5	4.31	1.715	1.09		30.1008	1.0009	0.0008
P4267SL1	4.31	1.89	1.59		33.4692	0.9987	0.0011
P4267SL2	4.31	1.715	1.09		31.9346	0.9995	0.0011
P62FT231	4.31	1.891	1.6	5.67	32.9228	1.0020	0.0009
P71F14F3	4.31	1.891	1.6	5.19	32.8227	1.0009	0.0010
P71F14V3	4.31	1.891	1.6	5.19	32.8587	0.9977	0.0010
P71F14V5	4.31	1.891	1.6	5.19	32.8662	0.9980	0.0010
P71F214R	4.31	1.891	1.6	5.19	32.8669	0.9976	0.0009

TABLE A3.3-30
BENCHMARKING RESULTS
(PAGE 4 OF 4)

Run ID	U Enrich. Wt%	Pitch (cm)	H_2O/fuel volume	Separation of assemblies (cm)	AEG	k_{eff}	1σ
PAT80L1	4.74	1.6	3.807	2	35.0276	1.0014	0.0009
PAT80L2	4.74	1.6	3.807	2	35.1079	0.9986	0.0011
PAT80SS1	4.74	1.6	3.807	2	35.0125	0.9998	0.0009
PAT80SS2	4.74	1.6	3.807	2	35.1128	0.9967	0.0010
W3269A	5.7	1.422	1.93		33.1383	0.9976	0.0009
W3269B1	3.7	1.105	1.432		32.4010	0.9962	0.0008
W3269B2	3.7	1.105	1.432		32.3940	0.9965	0.0008
W3269B3	3.7	1.105	1.432		32.2464	0.9945	0.0008
W3269C	2.72	1.524	1.494		33.7731	0.9979	0.0009
W3269SL1	2.72	1.524	1.494		33.3854	0.9973	0.0010
W3269SL2	5.7	1.422	1.93		33.1006	1.0024	0.0010
W3269W1	2.72	1.524	1.494		33.5160	0.9972	0.0012
W3269W2	5.7	1.422	1.93		33.1786	1.0015	0.0010
W3385SL1	5.74	1.422	1.932		33.2320	1.0004	0.0009
W3385SL2	5.74	2.012	5.067		35.8876	1.0014	0.0010
Correlation	0.32	0.41	0.19	0.66	-0.04	N/A	N/A

TABLE A3.3-31
USL-1 RESULTS

Parameter	Range of applicability	Formula for USL-1 (0.05 Δk_{eff} Margin)
U Enrichment (wt% U-235)	2.35 – 5.74	0.9404 + (1.0545E-03)*X (X < 3.5906) 0.9442 (X >= 3.5906)
Fuel Rod Pitch (cm)	1.105 – 2.540	0.9357 + (4.7885E-03)*X (X < 1.7997) 0.9443 (X >= 1.7997)
Water/Fuel Volume Ratio	0.383 – 5.067	0.9421 + (7.5929E-04)*X (X < 2.1362) 0.9438 (X >= 2.1362)
Assembly Separation (cm)	1.636 – 20.78	0.9409 + (5.0511E-04)*X (X < 7.1170) 0.9442 (X >= 7.1170)
Average Energy Group Causing Fission (AEG)	29.9 – 36.6	0.9438 (X < 32.694) 0.9467 + (-8.8965E-05)*X (X >= 32.694)

TABLE A3.3-32
USL DETERMINATION FOR CRITICALITY ANALYSIS

Parameter	Value from Limiting Analysis	Bounding USL-1
U Enrichment (wt. % U-235)	3.6(1)	0.9442
Fuel Rod Pitch (cm)	1.412	0.9425
Water/Fuel Ratio	1.610(2)	0.9433
Assembly Separation (cm)	2.063(3)	0.9419
Average Energy Group Causing Fission (AEG)	30(4)	0.9438

(1) A bounding lower enrichment value is utilized and is conservative, since the minimum enrichment credited herein is 5.00 wt. % U-235.
(2) The water to fuel volume ratio is calculated using 179 rods.
(3) Separation Distance = 2*0.1875" + 0.4375" = 0.8125" = 2.06375 cm, calculated with nominal dimensions for the stainless steel in the fuel compartment, nominal stainless steel tie bar width and inward fuel assembly positioning.
(4) Examination of the results shows that the value is between 30 and 34 and hence a conservative value that produces the minimum USL was chosen.

TABLE A3.3-33
THERMAL CONDUCTIVITY WITH A 75% HELIUM, 25% AIR AND WATER VAPOR MIXTURE

Temperature	75% Helium, 25% air and water vapor	Transverse Effective Fuel conductivity
(ºF)	(BTU/hr-in-ºF)	(BTU/hr-in-ºF)
430	---	0.0226
440	0.0066	---
525	---	0.0265
620	0.0077	---
622	---	0.0311
719	---	0.0361
816	---	0.0417
914	---	0.0480
980	0.0096	---
1012	---	0.0548

TABLE A3.3-34
MAXIMUM COMPONENT TEMPERATURES WITH A 75% HELIUM, 25% AIR AND WATER VAPOR MIXTURE

Component	Temperature (ºF)	Limit (ºF)
Fuel Cladding	739	752
Fuel Compartment	706	---
Basket Rails	519	---
Cask Inner Shell	322	---
Gamma Shield	317	---
Bulk Radial Resin [1]	279	300
Lid Seal	250	536

[1] The bulk radial resin temperature is the volumetric average temperature at the hottest cross section

TABLE A3.3-35
EFFECTIVE CONDUCTIVITIES IN THE MODEL

	Al-1100	Poison (Neutron Absorber) Plate	$k_{eff,along}$	$k_{eff,across}$
Temperature (°F)	Thermal conductivity (Btu/hr-in-°F)	Thermal conductivity (Btu/hr-in-°F)	(Btu/hr-in-°F)	(Btu/hr-in-°F)
70	11.092	0.68	8.11	2.06
100	10.983	0.68	8.04	2.06
150	10.833	0.68	7.93	2.06
200	10.708	0.68	7.84	2.05
250	10.608	0.68	7.77	2.05
300	10.517	0.68	7.70	2.05
350	10.442	0.68	7.65	2.04
400	10.375	0.68	7.60	2.04
			Direction in Model	Direction in Model
Horizontal Paired Plates			x and z	y
Vertical Paired Plates			y and z	x

TABLE A3.3-36
TEMPERATURES FOR OFF-NORMAL STORAGE CONDITIONS WITH LOWER POISON PLATE CONDUCTIVITY

	Design Basis Model Off-Normal Storage 100°F ambient (Table A3.3-3)	Lower Conductivity Model Off-Normal Storage 100°F ambient	
Component	Maximum Temperature (°F)	Maximum Temperature (°F)	Temperature Limit (°F)
Fuel Cladding ***	696	674	752
Fuel Compartment ***	647	646	---
Basket Rails ***	471	471	---
Inner Bottom Plate ‡	374	373	---
Bottom Shield ‡	270	270	---
Cask Inner Shell *, ***	307	307	---
Shield Shell *, ‡	303	303	---
Radial Resin †, ‡	290	290	300
Cask Outer Shell †, ‡	265	265	---
Average Cavity Gas ($\overline{T}_{cavity}$) ***	466 **	460	---

60400000330

* This value is the volumetric average temperature at the hottest cross section.

† This value is the volumetric average temperature at the hottest cross section plus 18 °F to bound the effects of storage pad on the cask view factor. See Section A3.3.2.2.4 for discussion.

** This value is taken from Table A3.3-15.

‡ An additional 5°F is added to account for the effect of the southeast ISFSI pad expansion on cask exterior temperatures. See Section A3.3.2.2.4.1.1 for discussion.

*** An additional 2°F is added to account for the effect of the southeast ISFSI pad expansion on cask interior temperatures. See Section A3.3.2.2.4.1.1 for discussion.

60400000330

TABLE A3.3-37
TEMPERATURES FOR FIRE ACCIDENT CONDITIONS WITH LOWER POISON PLATE CONDUCTIVITY

	Design Basis Model Fire Accident (Table A3.3-6)		Lower Conductivity Model Fire Accident				
	Transient / Steady State		Transient		Steady State		
Component	Maximum Temperature (°F)	Time (hr)	Maximum Temperature (°F)	Time (hr)	Maximum Temperature (°F)	Time (hr)	Temperature Limit (°F)
Fuel Cladding ***	790	∞	694	36.7	689	∞	1058
Fuel Compartment ***	744	∞	668	36.7	663	∞	---
Basket Rails ***	555	∞	495	12.7	488	∞	---
Cask Inner Shell *, ***	372	∞	353	2.0	325	∞	---
Shield Shell *, §	366	∞	327	0.25 (end of fire)	321	∞	---
Radial Resin	N/A ‡	---	N/A ‡	---	N/A ‡	---	---
Cask Outer Shell †, §	918	0.25 (end of fire)	916	0.25 (end of fire)	282	∞	---
Average Cavity Gas ($\overline{T}$ cavity) ***	605 **	∞	483	36.7	477	∞	---

* This value is the volumetric average temperature at the hottest cross section.

† This value is the volumetric average temperature at the hottest cross section plus 18 °F to bound the effects of storage pad on the cask view factor. See Section A3.3.2.2.4 for discussion.

‡ Neutron shield resin is assumed to be burnt and decomposed during the fire

** This value is taken from Table A3.3-15.

*** An additional 2°F is added to account for the effect of the southeast ISFSI pad expansion on cask interior temperatures. See Section A3.3.2.2.4.1.1 for discussion.

§ An additional 5°F is added to account for the effect of the southeast ISFSI pad expansion on cask exterior temperatures. See Section A3.3.2.2.4.1.1 for discussion.

6040000000330

6040000000330

TABLE A3.3-38
TEMPERATURES FOR BURIED CASK ACCIDENT CONDITIONS WITH LOWER POISON PLATE CONDUCTIVITY (FUEL ASSEMBLY WITHOUT BPRAS)

	Design Basis Model Buried Cask Accident (Table A3.3-7)		Lower Conductivity Model Buried Cask Accident		
Component	Maximum Temperature (°F)	Time (hr)	Maximum Temperature (°F)	Time (hr)	Temperature Limit (°F)
Fuel Cladding ***	1058	92.49	909	93	1058
Fuel Compartment ***	1024	92.51	892	93	---
Basket Rails ***	889	92.56	761	93	---
Cask Inner Shell *, ***	774	92.6	652	93	---
Shield Shell *, ‡	769	92.61	651	93	---
Radial Resin †, ‡	300	1.23	299	1.19	300
Cask Outer Shell †, ‡	779	92.1	642	93	---
Average Cavity Gas ($\overline{T}_{cavity}$) ***	925 **	92.6	737	93	---

* This value is the volumetric average temperature at the hottest cross section.

† This value is the volumetric average temperature at the hottest cross section plus 18 °F to bound the effects of storage pad on the cask view factor. See Section A3.3.2.2.4 for discussion.

** This value is taken from Table A3.3-15.

‡ An additional 5°F is added to account for the effect of the southeast ISFSI pad expansion on cask exterior temperatures. See Section A3.3.2.2.4.1.1 for discussion.

*** An additional 2°F is added to account for the effect of the southeast ISFSI pad expansion on cask interior temperatures. See Section A3.3.2.2.4.1.1 for discussion.

604000000330

604000000330

TABLE A3.3-39
TEMPERATURES FOR VACUUM DRYING OPERATIONS WITH LOWER POISON PLATE CONDUCTIVITY

		Design Basis Model Vacuum Dry (Table A3.3-14)	Lower Conductivity Model Vacuum Drying	
Component	Time (hr)	Maximum Temperature (°F)	Maximum Temperature (°F)	Temperature Limit (°F)
Fuel Cladding	34	731	713	752
Fuel Compartment	34	692	671	---
Basket Rails	34	541	517	---
Cask Inner Shell	34	235	227	---
Shield Shell	34	232	224	---
Radial Resin	34	219	212	300
Top Resin	34	<235 **	<227 **	300
Lid Seal	34	<235 **	<227 **	536
Vent and Port Seal	34	<235 **	<227 **	536

** This temperature is bounded by maximum temperature of the cask inner shell.

TABLE A3.4-1
DESIGN CRITERIA FOR TN-40HT CASKS

Maximum Gross Weight on Crane (with lift beams, without water)	 125 tons
Maximum Cask Height with Lid Removed	16 ft. 1 in.
Upper Subcritical Limit	< 0.95- minus biases
Payload Capacity	≤40 intact 14x14 PWR assemblies (Including inserts)
Spent Fuel Characteristics	
a) Design Basis Initial Enrichment(max)	5.0 wt % U-235
b) Burnup (max)	60 GWD/MTU,
c) Cooling time (min)	12 years
d) Decay Heat	32 kW (total)
Max Clad Temperature	400 °C (752 °F) - Normal 570 °C (1058 °F) -Accident
Cask Cavity Atmosphere	helium gas
Maximum Internal Pressure for Stress Evaluation	100 psig
Minimum/Maximum Ambient Temperature	-40 to 120ºF
Daily Averaged Ambient Temperature Over 24 hr. period (min-max)	-40 to 100 °F
Maximum Solar Heat Load (Averaged over 24 hour)	61.488 Btu/Hr-ft^2 (curved surfaces) 122.83 Btu/Hr-ft^2 (horizontal surfaces)
Tornado Wind	360 mph (rotational plus translational)
Tornado Missiles	4000 lb. auto at 50 mph 4" x 12" x 12' wood plank at 300 mph
Cask Drop	18" Drop onto concrete pad or equivalent end drop resulting in 50 g
Seismic Design Earthquake	0.12 g horizontal 0.08 g vertical
Snow and Ice	50 psf load

TABLE A3.4-2
DESIGN BASIS LIMITS FOR FISSION PRODUCT BARRIERS FOR 72.48 REVIEWS

Fission Product Barrier	Design Basis Parameter	Transnuclear TN-40HT Design Basis Limit
Fuel Cladding	Clad Temperature	Less than 752°F (Normal) 1058°F (Accident)
Fuel Cladding	Decay Heat Per Assembly	0.800 kW/FA (32 kW total for cask)
Fuel Cladding	Sub-criticality	K_{eff} less than 0.95
Confinement Boundary	MSB/DSC Pressure	100 psig
Confinement Boundary	MSB/DSC Vessel Stresses	Code allowable stresses for ASME Boiler and Pressure Vessel Code, Section III, Division 1, Subsection NB, Article NB-3200
Confinement Boundary	MSB/DSC Leak Rate	1 x 10^{-5} atm cm^3/sec

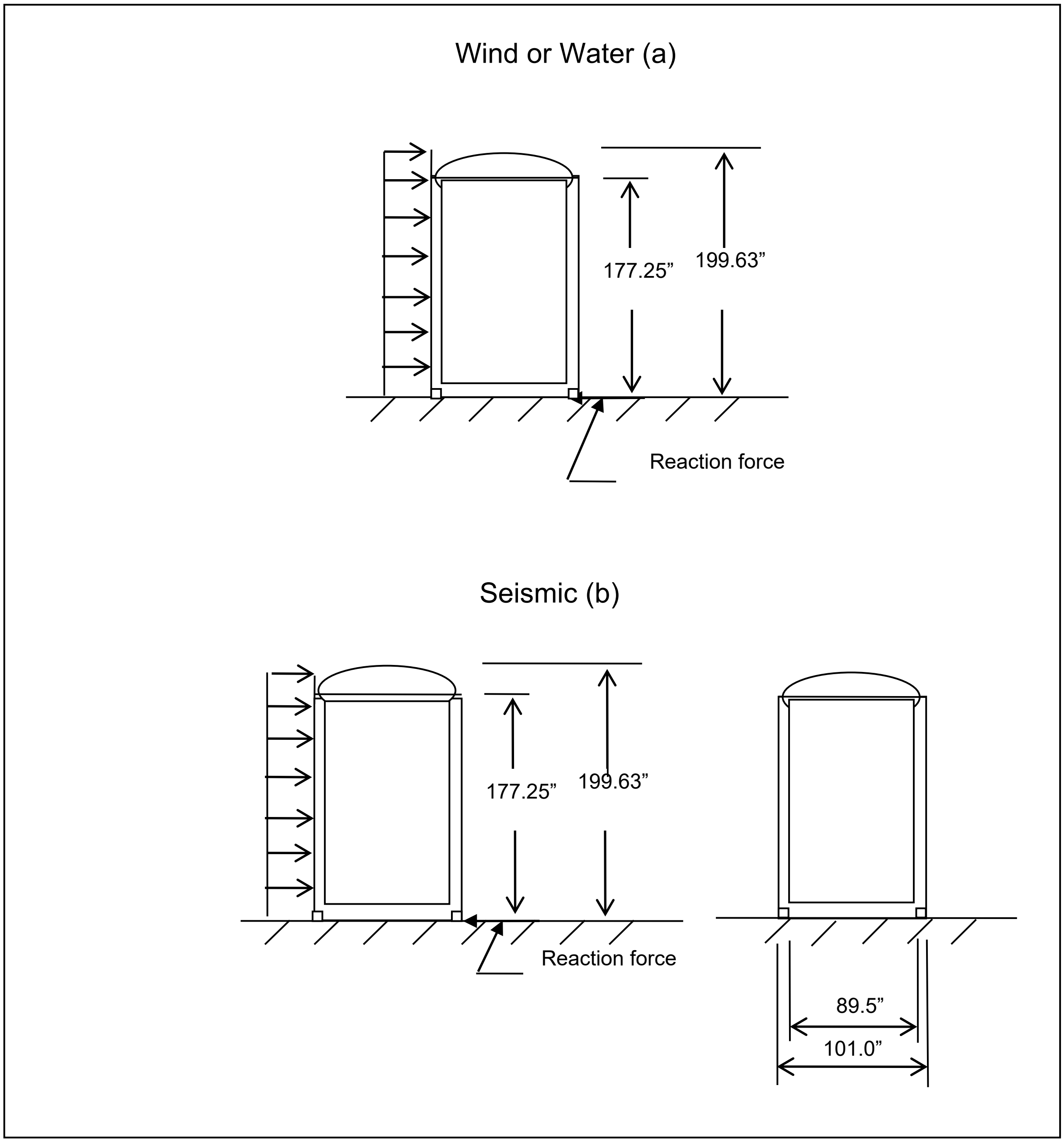

FIGURE A3.2-1
EARTHQUAKE, WIND, AND WATER LOADS

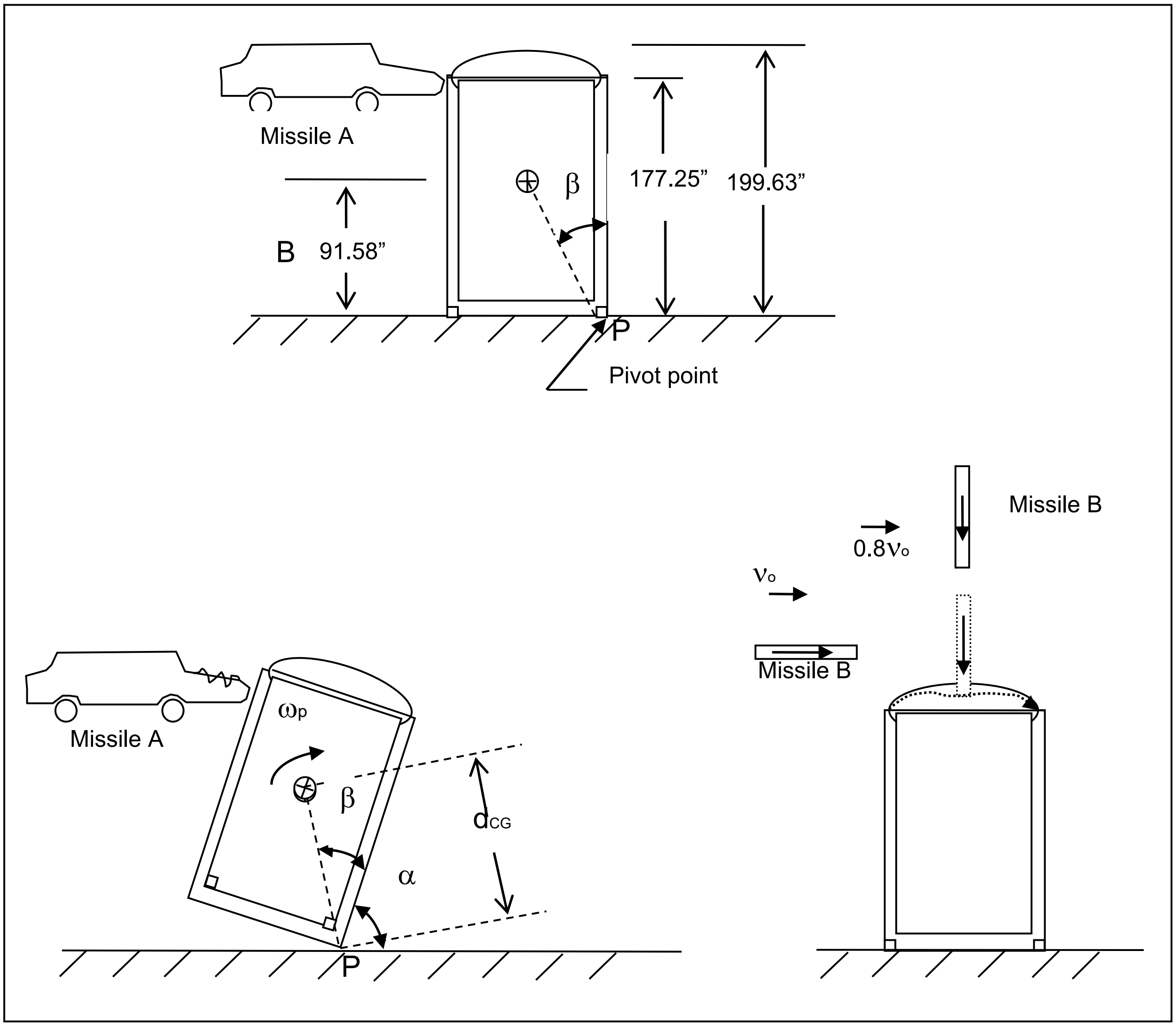

FIGURE A3.2-2
TORNADO MISSILE IMPACT LOADS

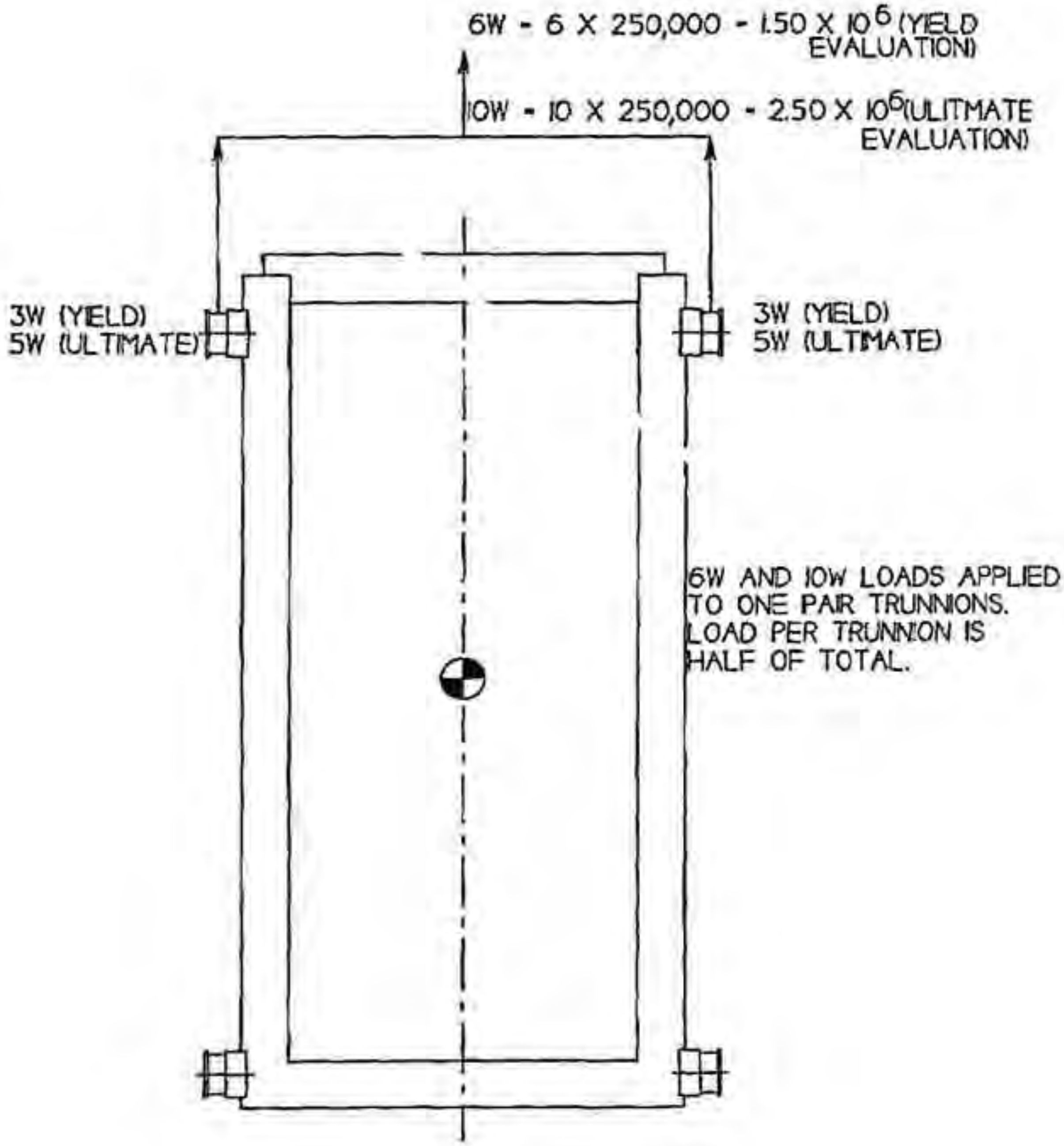

FIGURE A3.2-3
LIFTING LOADS

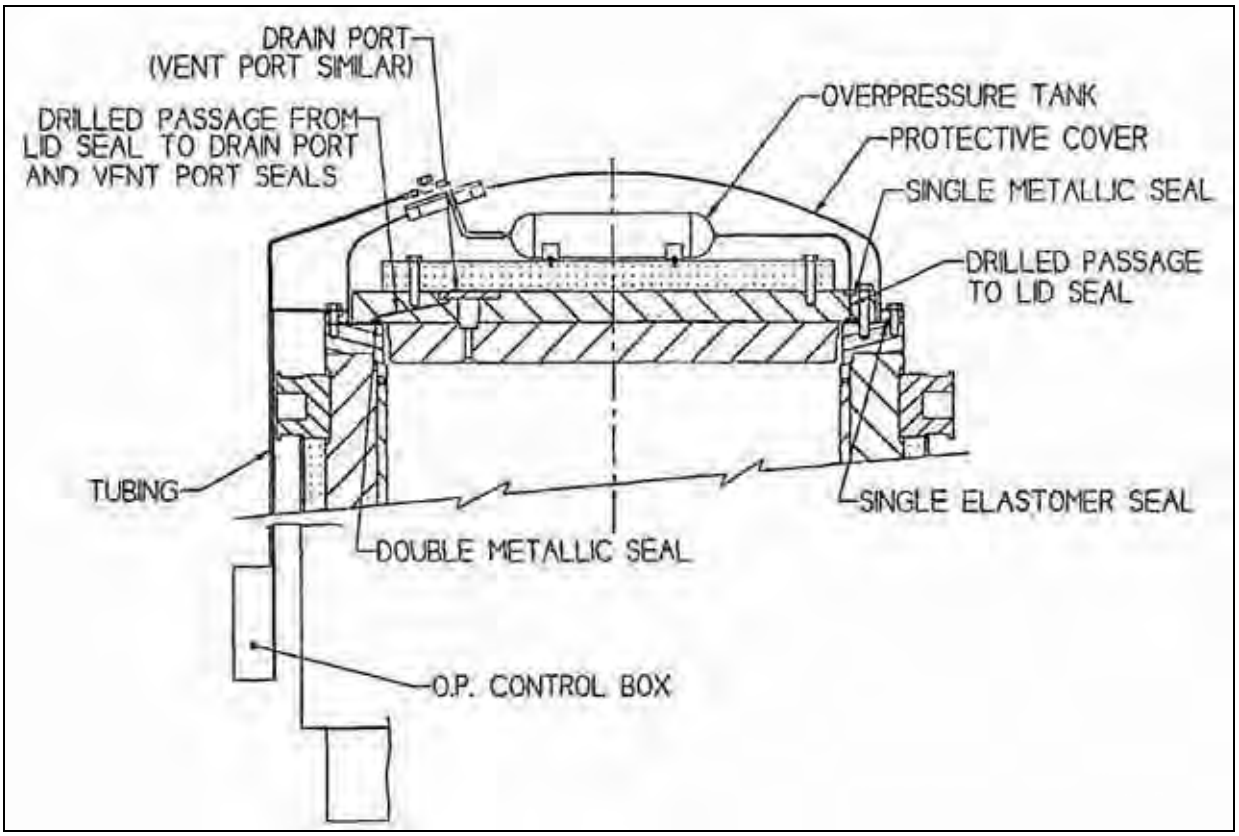

FIGURE A3.3-1
TN-40HT CASK SEAL PRESSURE MONITORING SYSTEM

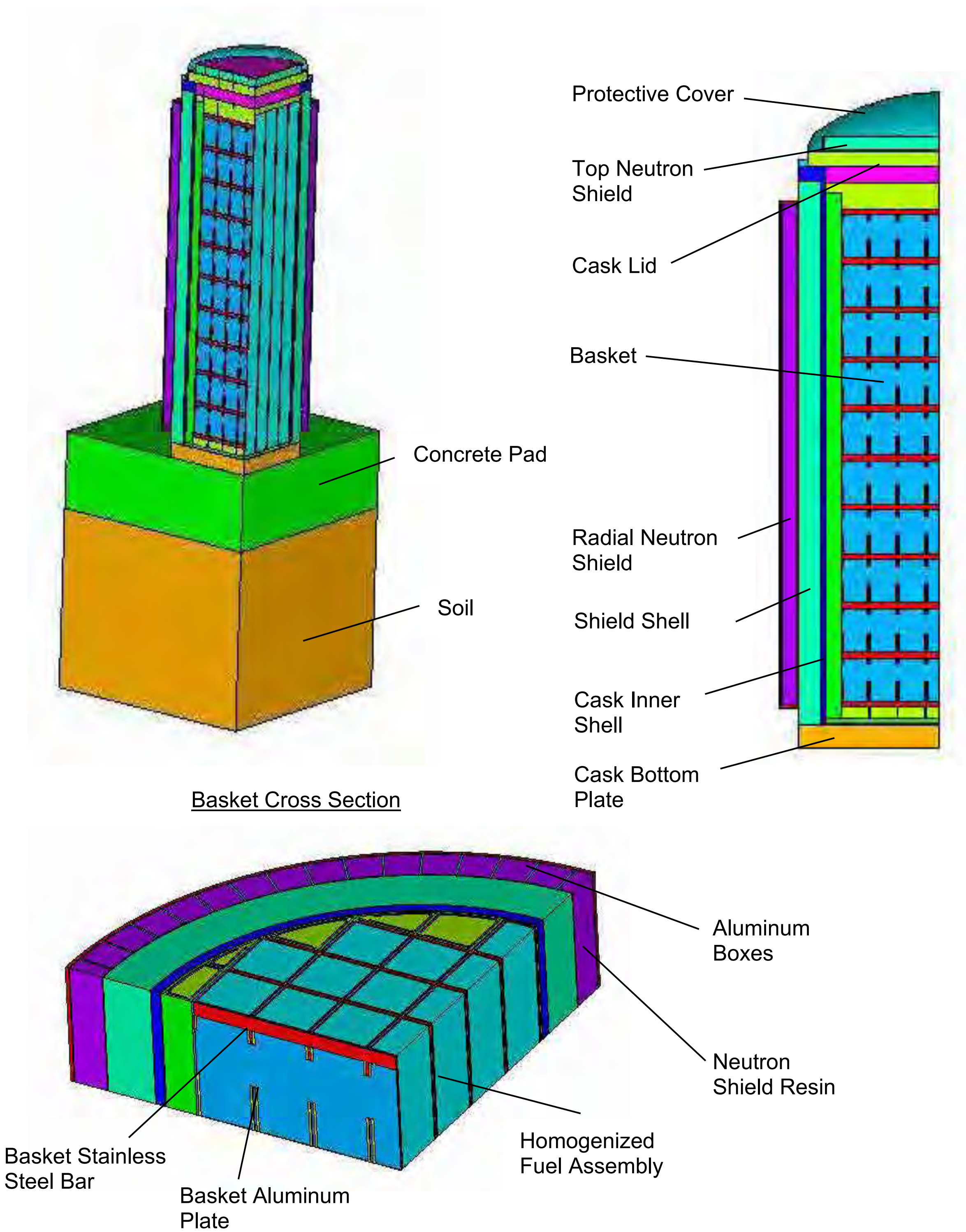

FIGURE A3.3-2
FULL-LENGTH CASK MODEL

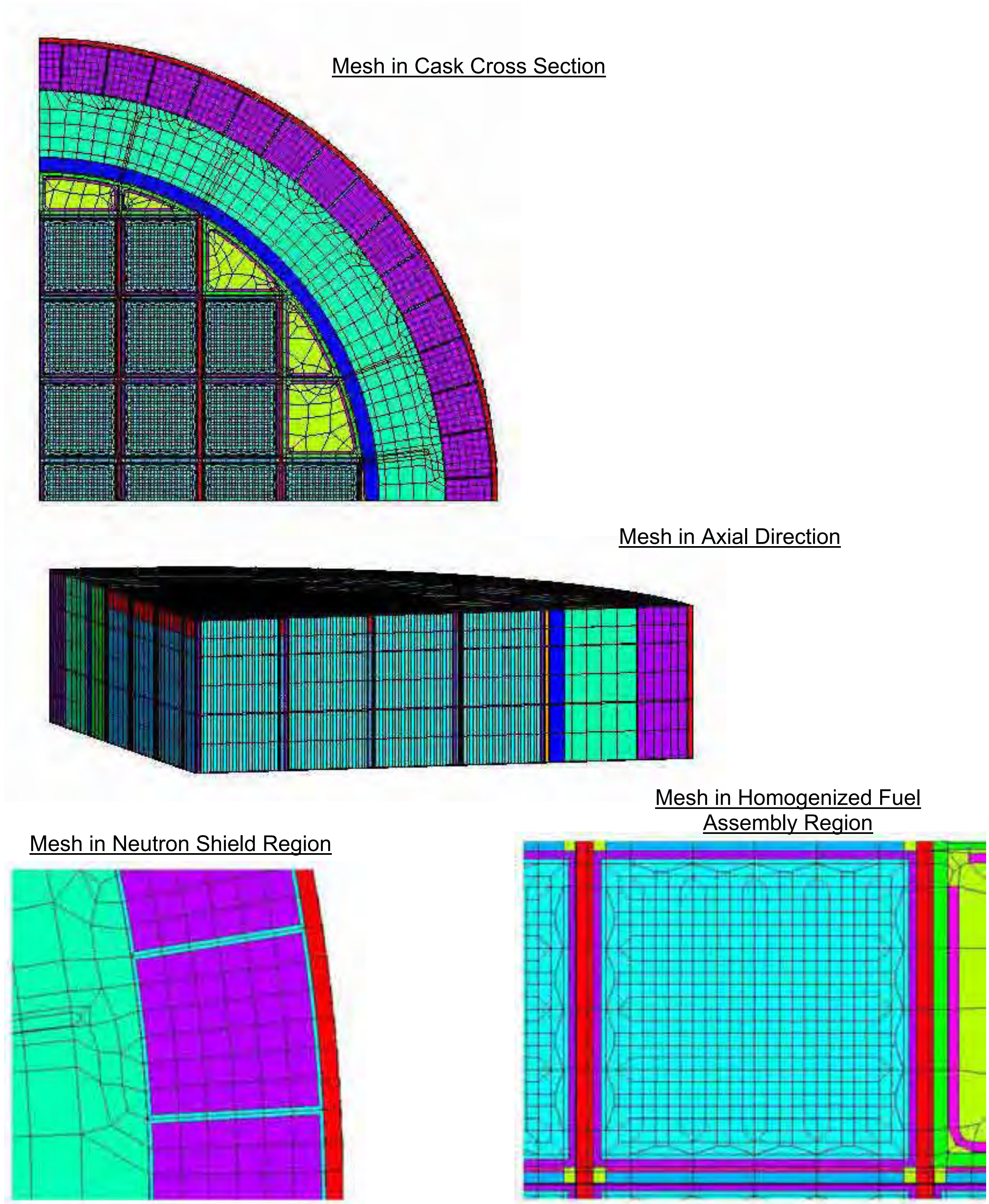

FIGURE A3.3-3
MESH DENSITY OF FINITE ELEMENT MODEL

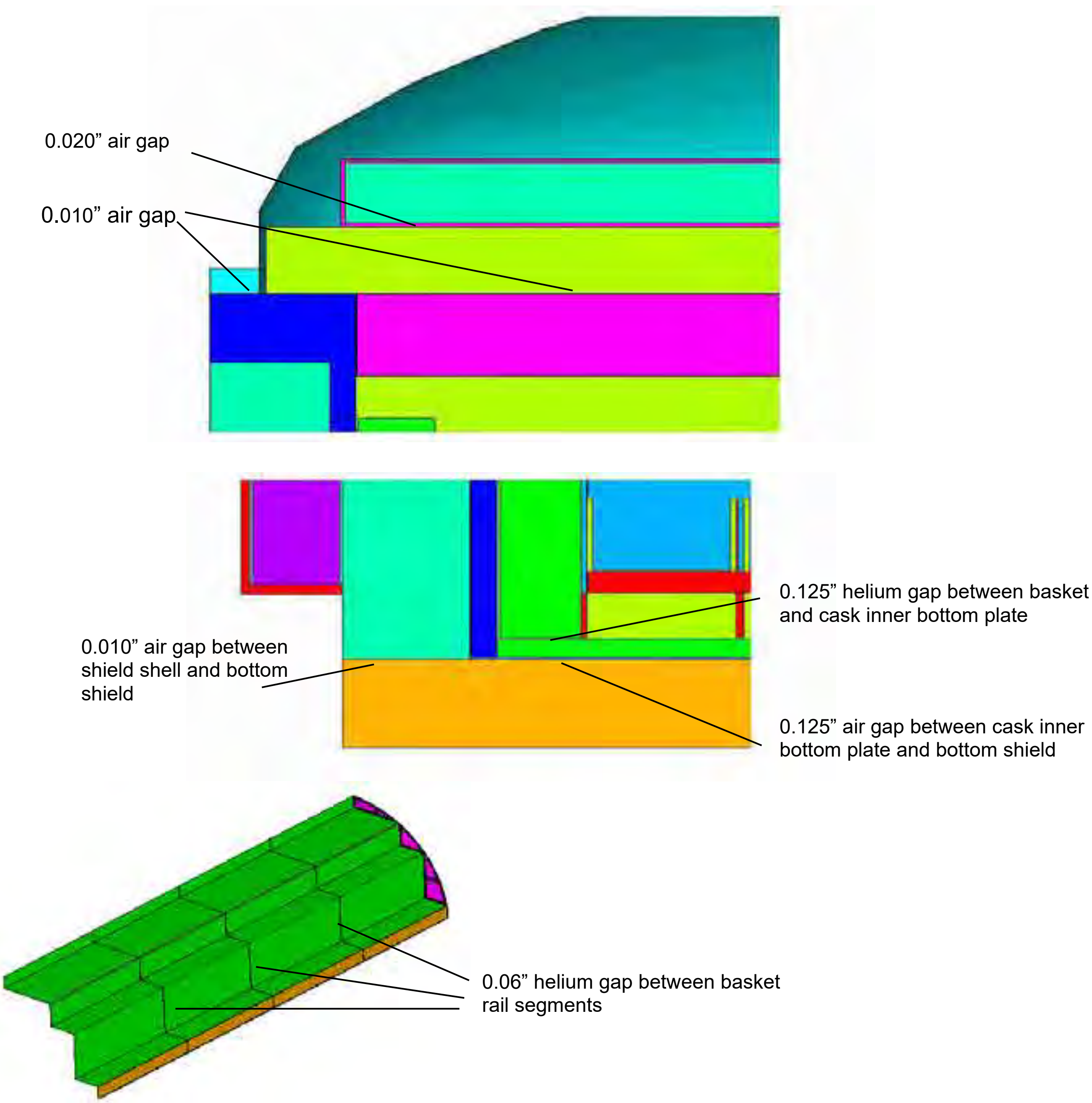

FIGURE A3.3-4
GAPS IN AXIAL DIRECTION

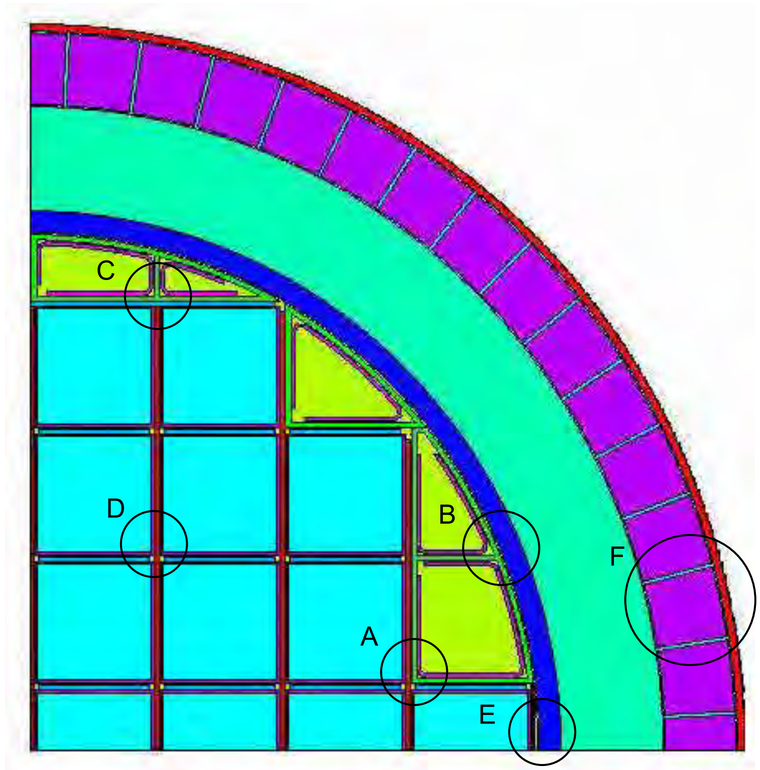

Detail A

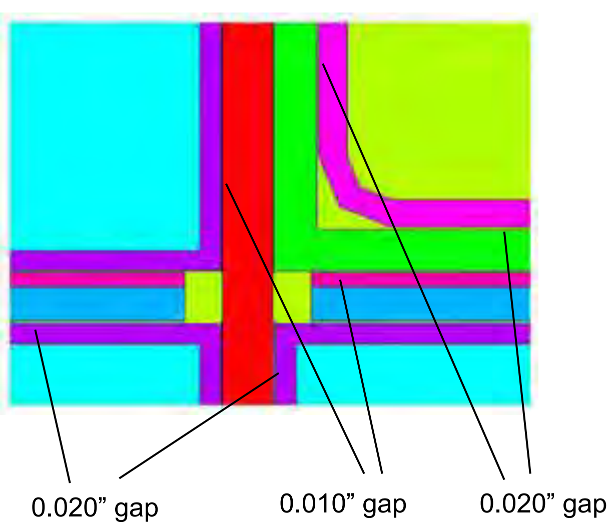

Detail B

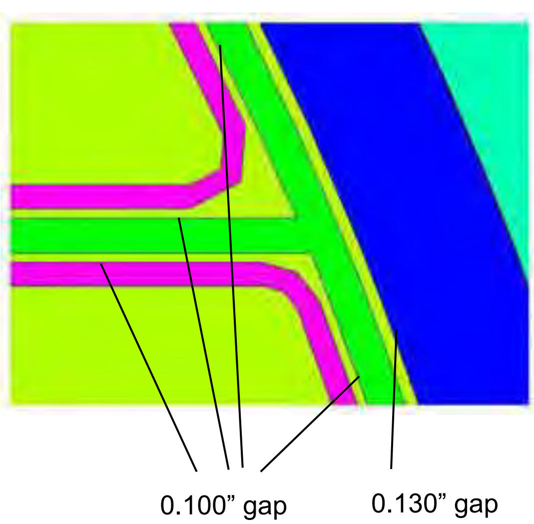

FIGURE A3.3-5
GAPS IN RADIAL DIRECTION
(PAGE 1 OF 2)

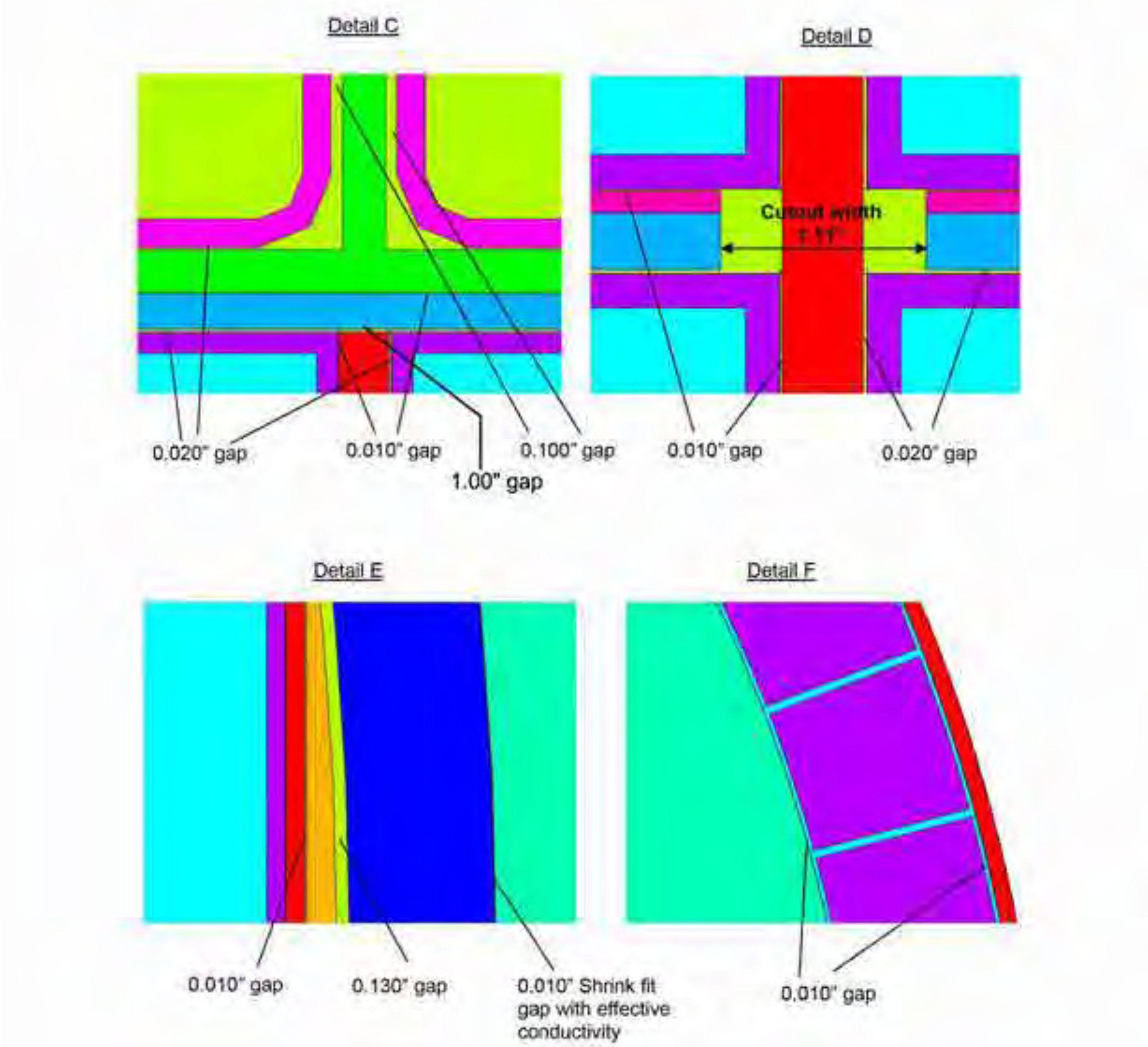

FIGURE A3.3-5
GAPS IN RADIAL DIRECTION
(PAGE 2 OF 2)

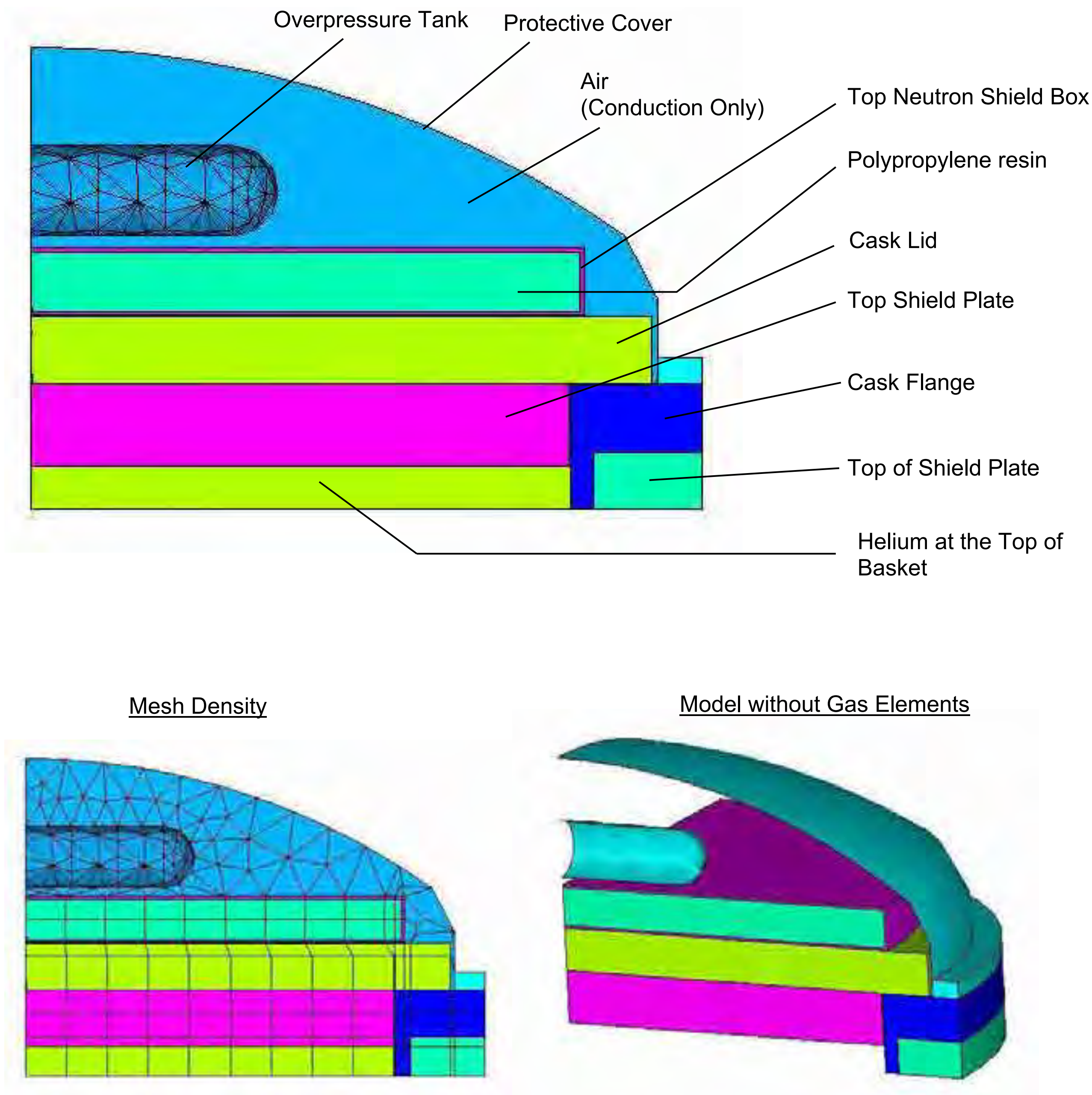

FIGURE A3.3-6
TOP CASK SUB-MODEL

Convection & Radiation to Ambient and Fixed Temperatures at Soil

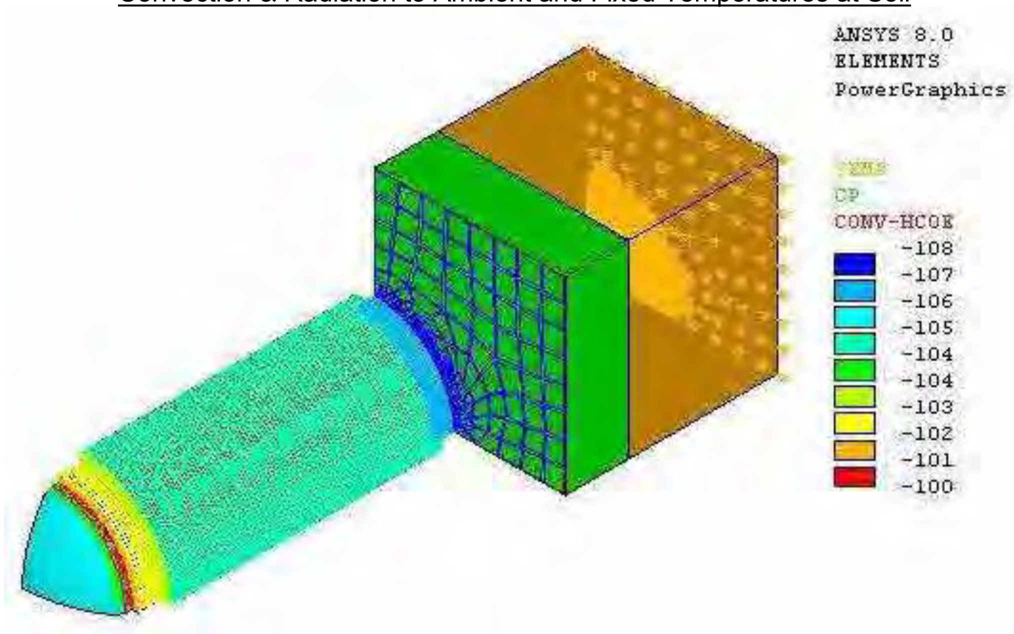

Solar Heat Flux

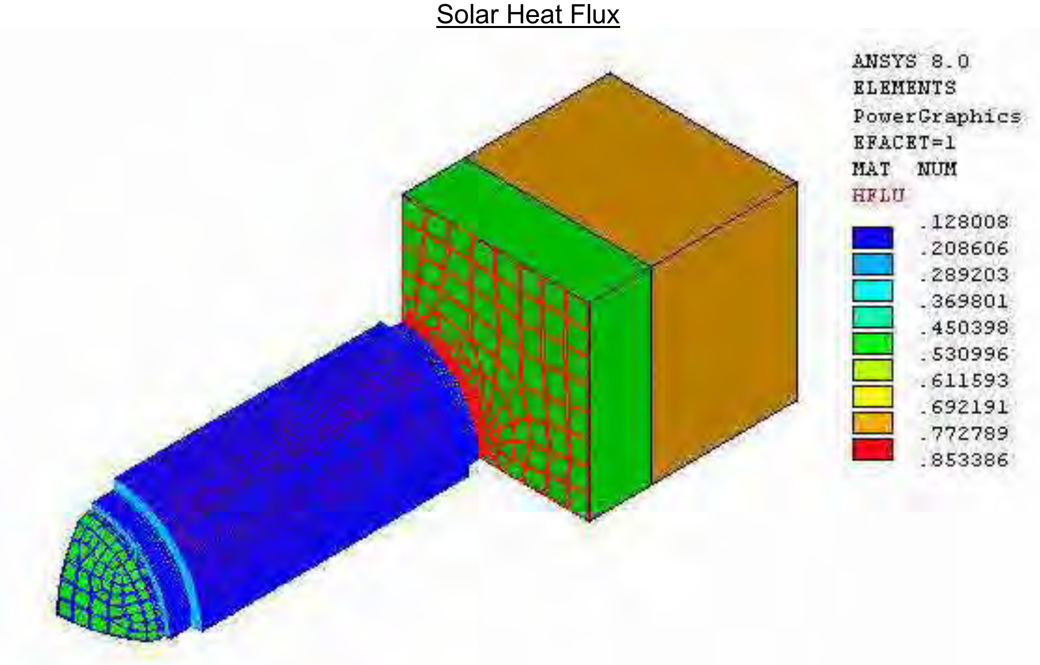

FIGURE A3.3-7
BOUNDARY CONDITIONS FOR FULL-LENGTH CASK MODEL
(PAGE 1 OF 2)

Heat Generating Rates in Fuel Assemblies

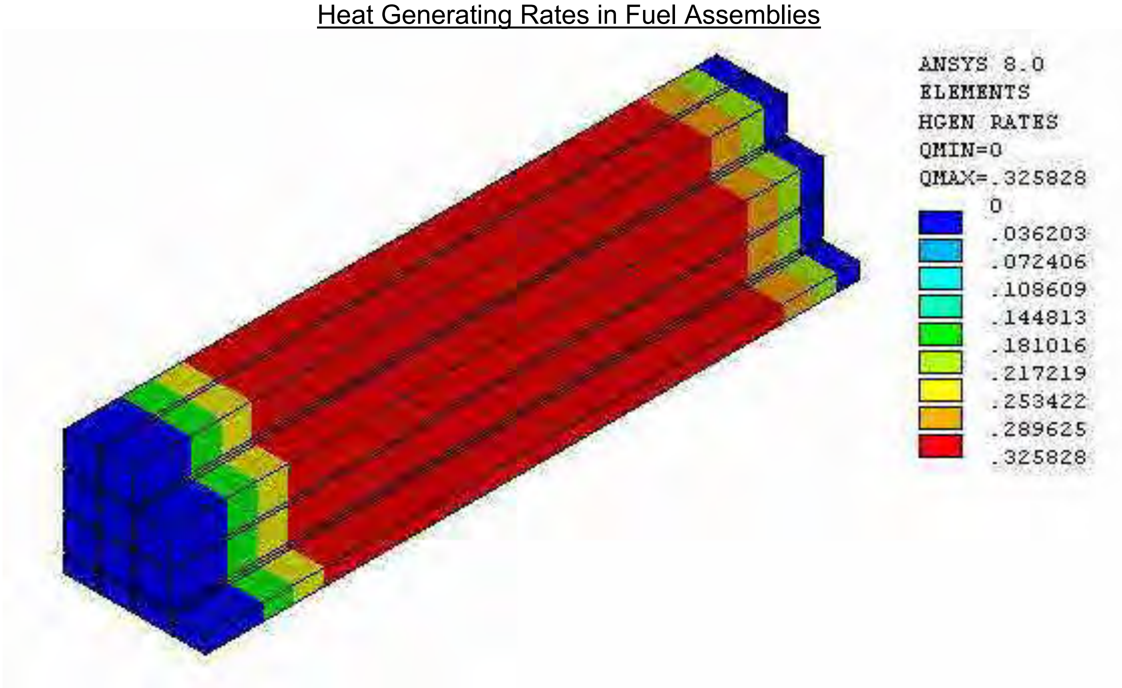

FIGURE A3.3-7
BOUNDARY CONDITIONS FOR FULL-LENGTH CASK MODEL
(PAGE 2 OF 2)

Heat Flux to Cask Top

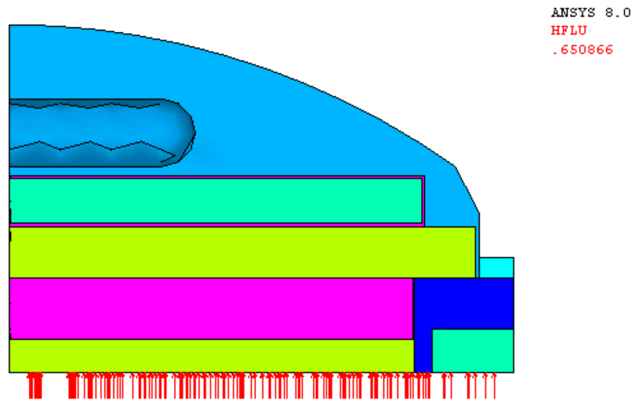

Convection + Radiation to Ambient

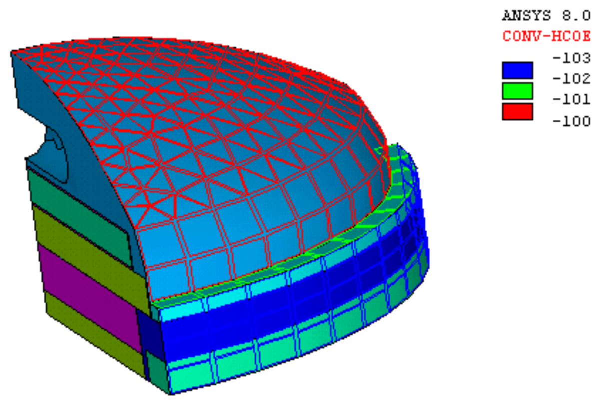

Solar Heat Flux

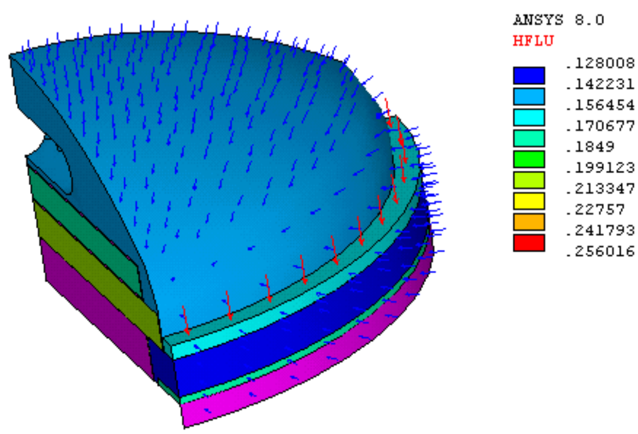

FIGURE A3.3-8
BOUNDARY CONDITIONS FOR CASK TOP SUB-MODEL

Cross-Section Sub-Model

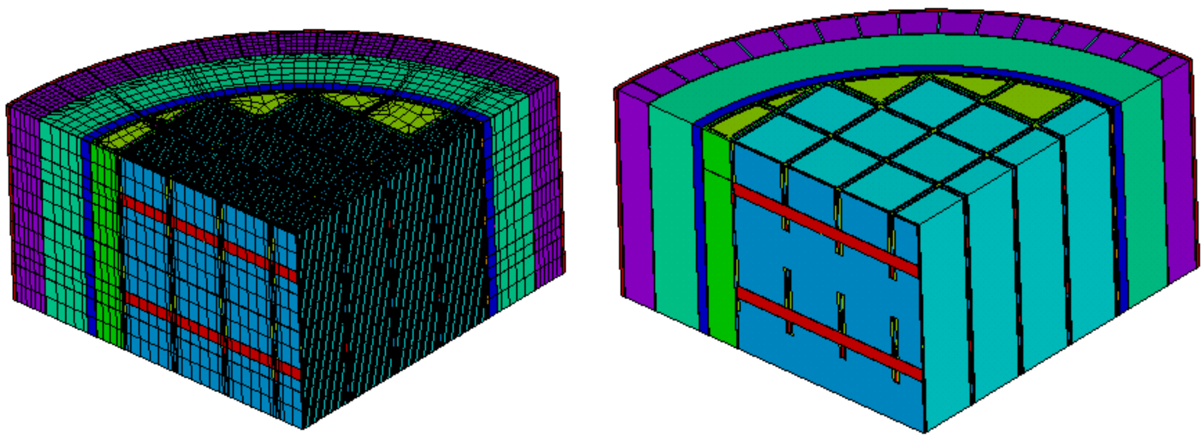

Lid-Seal Region Model

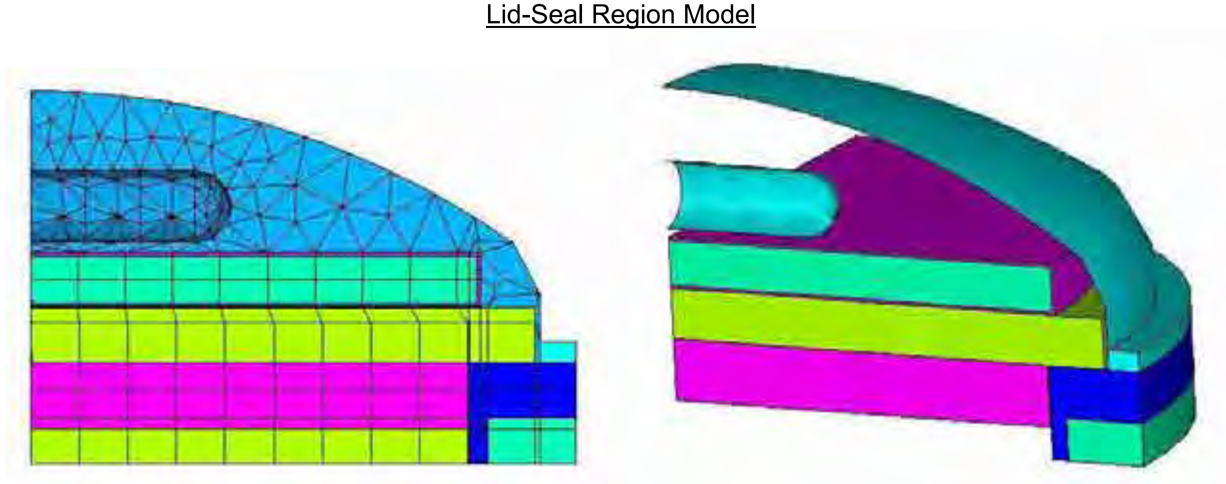

FIGURE A3.3-9
FINITE ELEMENT MODELS FOR ACCIDENT CONDITIONS

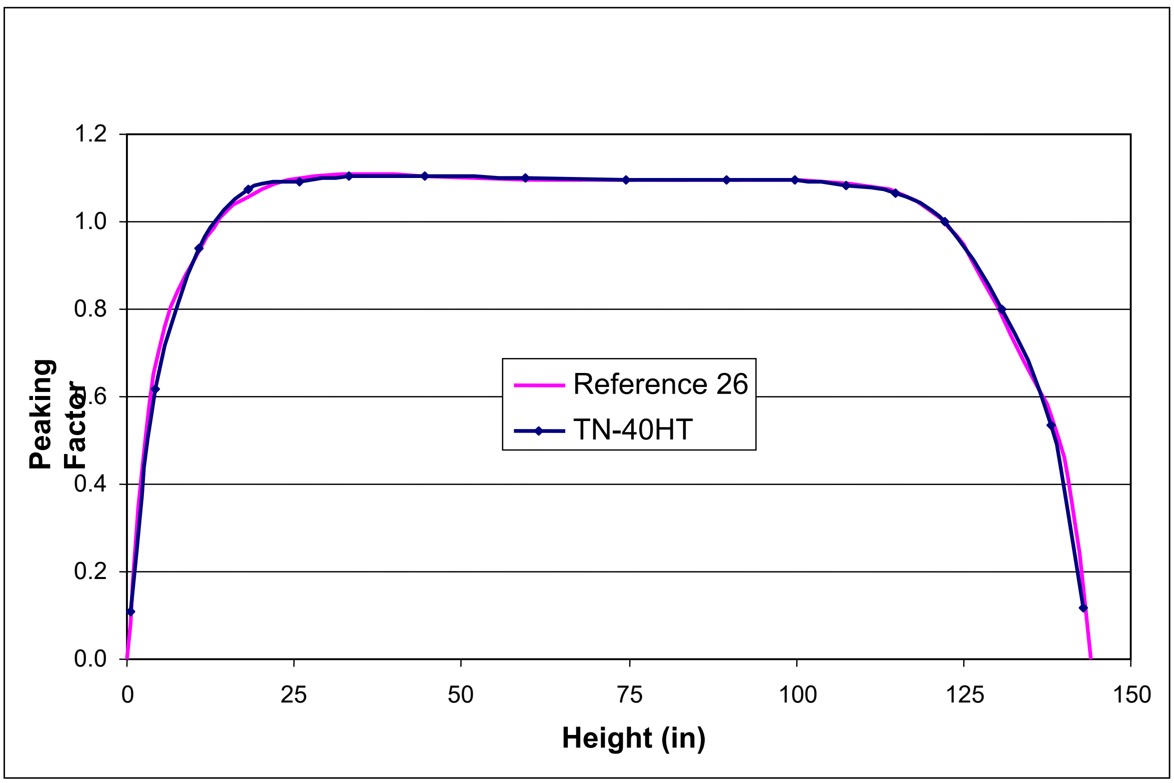

FIGURE A3.3-10
COMPARISON OF THE AXIAL HEAT PROFILES IN THE MODEL

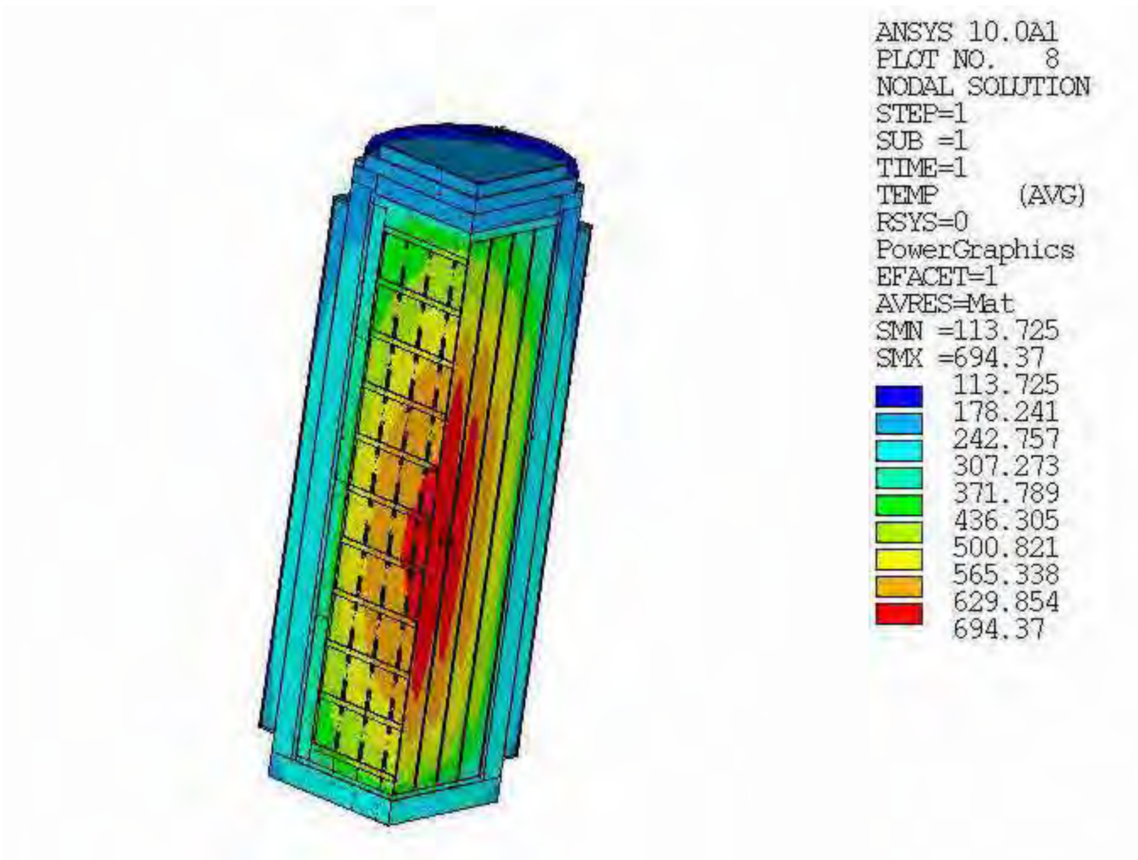

FIGURE A3.3-11
TEMPERATURE DISTRIBUTIONS FOR FULL-LENGTH MODEL
NORMAL/OFF-NORMAL STORAGE CONDITIONS

Fuel Compartments

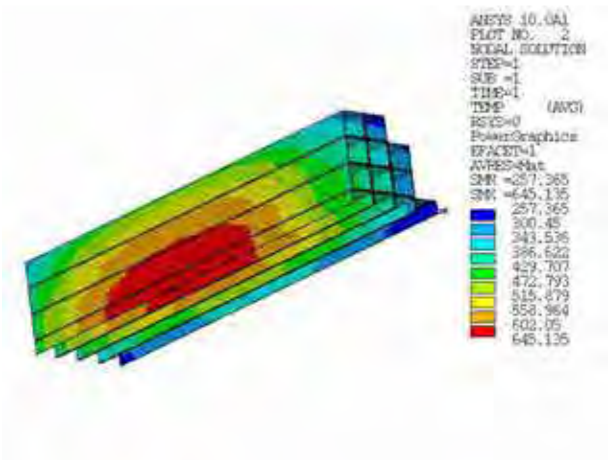

Homogenized Fuel Assemblies

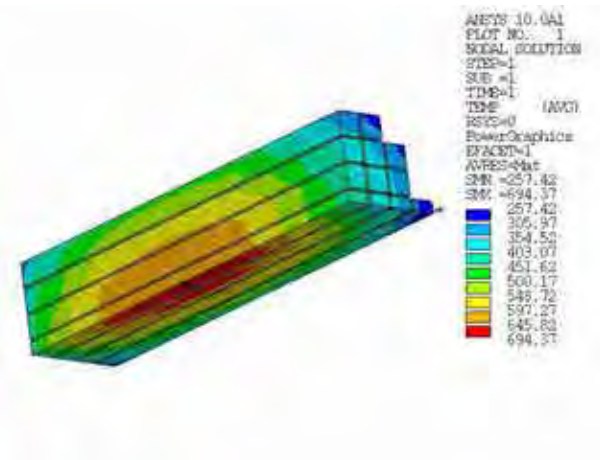

Basket Rails

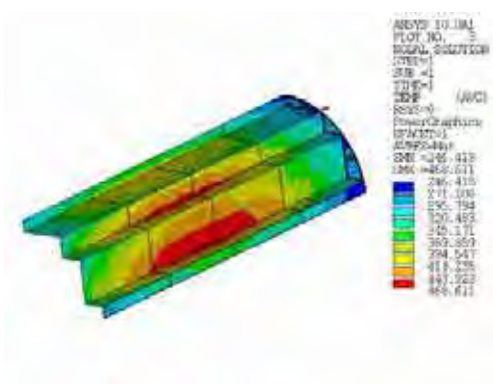

Radial Resin

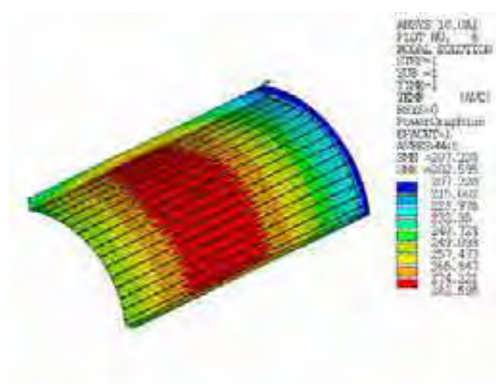

FIGURE A3.3-12
NORMAL / OFF-NORMAL TEMPERATURE DISTRIBUTION
FOR COMPONENTS OF FULL-LENGTH MODEL

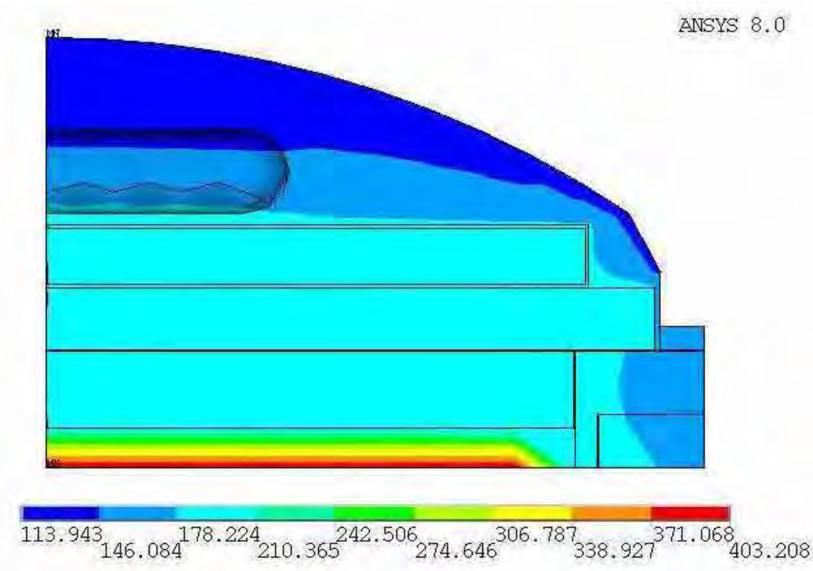

Cask lid and Top Shield Plate

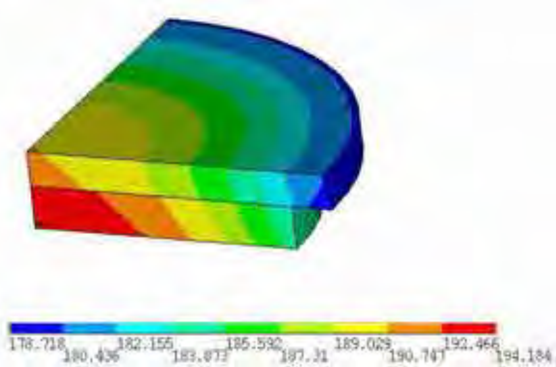

Top Resin

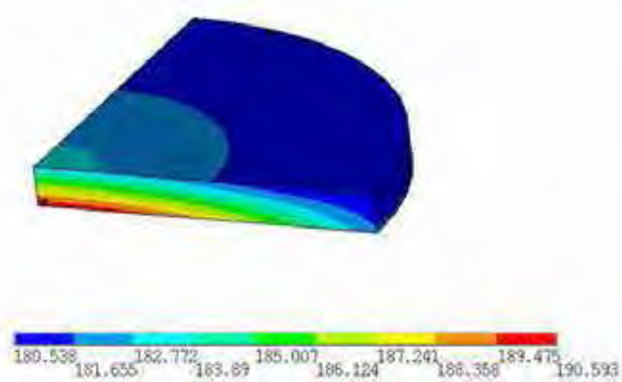

Protective Cover

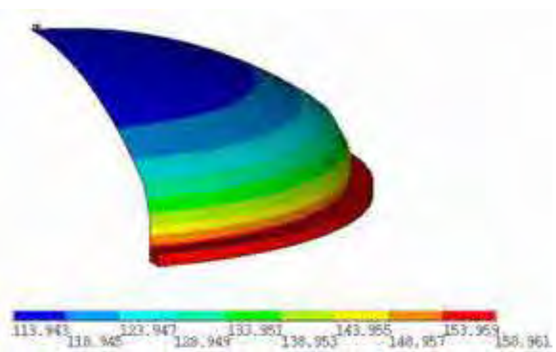

FIGURE A3.3-13
NORMAL / OFF-NORMAL TEMPERATURE DISTRIBUTION FOR CASK TOP SUB-MODEL

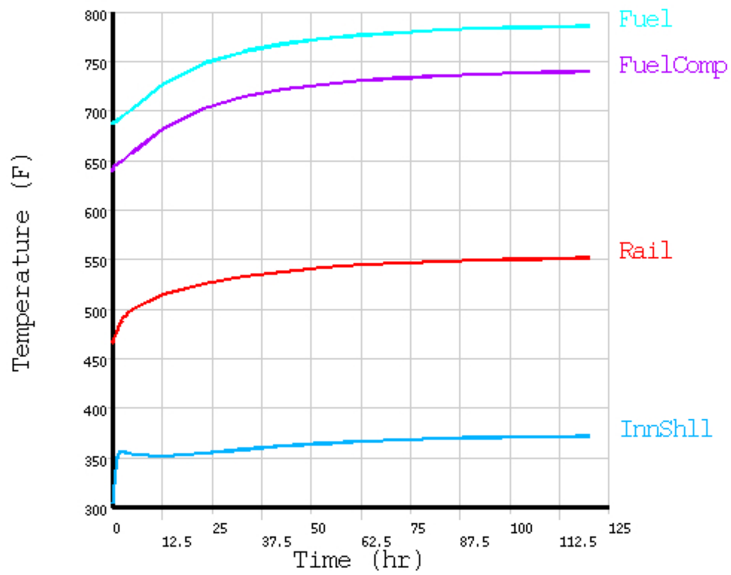

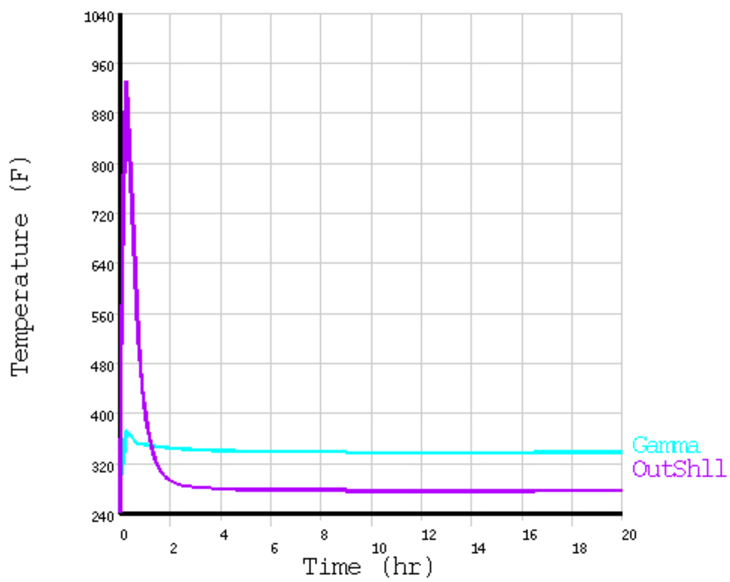

FIGURE A3.3-14
COMPONENT TIME-TEMPERATURE HISTORY FOR FIRE ACCIDENT
(PAGE 1 OF 2)

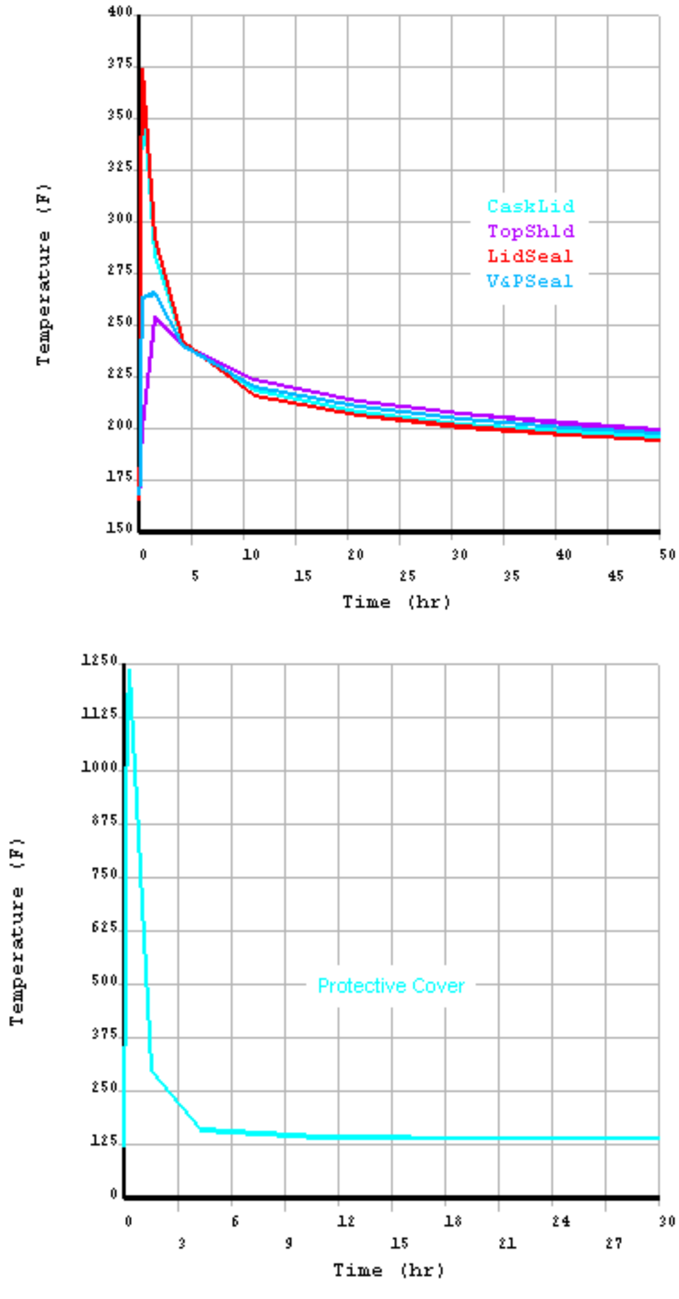

FIGURE A3.3-14
COMPONENT TIME-TEMPERATURE HISTORY FOR FIRE ACCIDENT
(PAGE 2 OF 2)

Entire Model

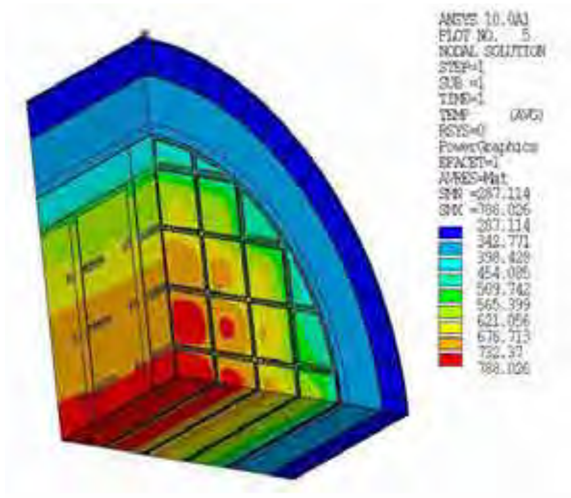

Fuel Assemblies

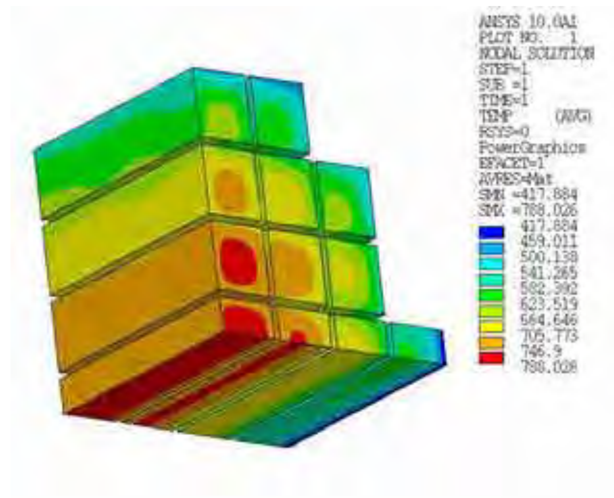

Fuel Compartments

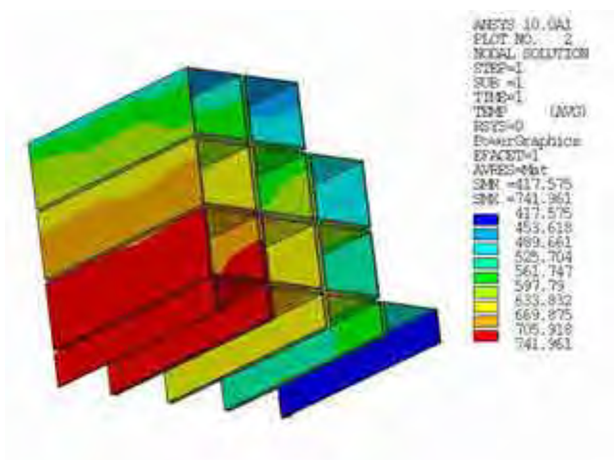

Basket Rails

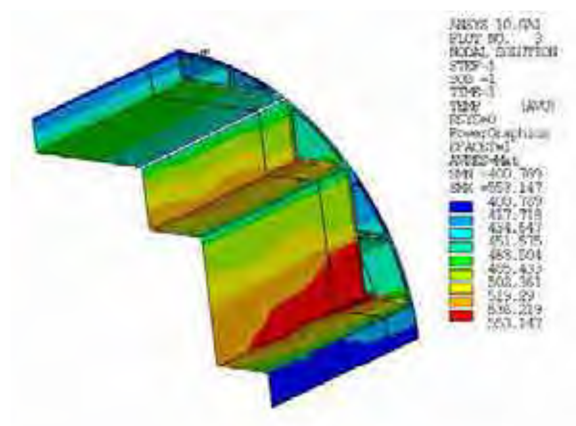

FIGURE A3.3-15
TEMPERATURE DISTRIBUTION FOR FIRE ACCIDENT
STEADY STATE, CROSS-SECTION MODEL

Initial Temperatures

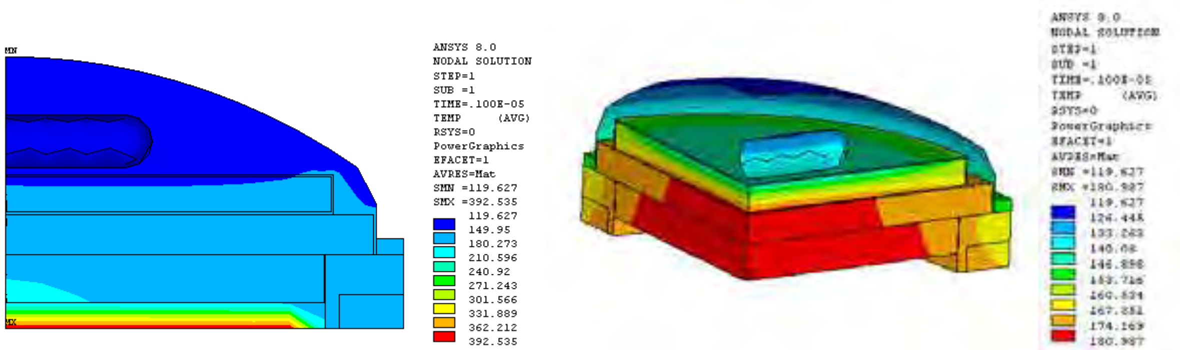

Temperatures at the End of Fire

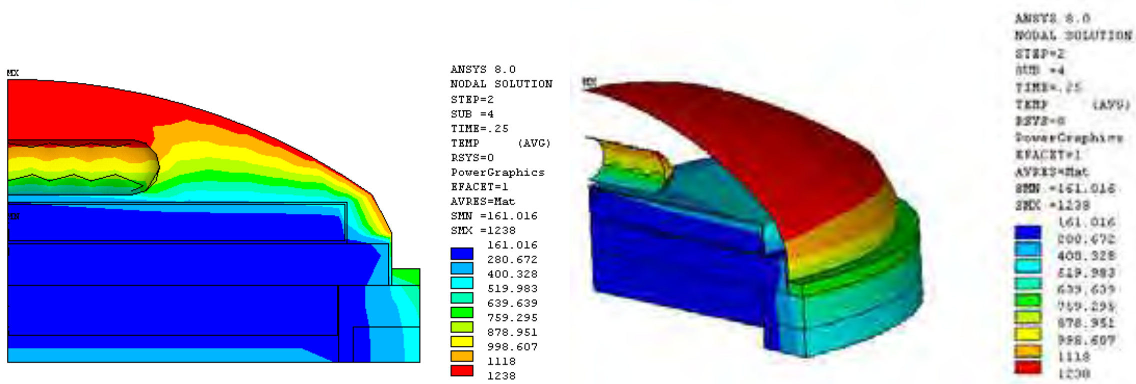

Temperatures at 119.75 hrs after End of Fire

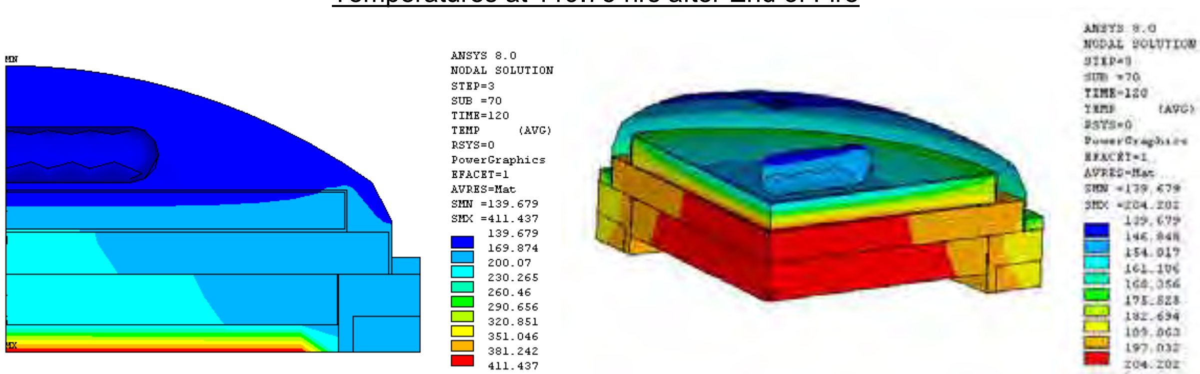

FIGURE A3.3-16
TEMPERATURE DISTRIBUTION FOR FIRE ACCIDENT TRANSIENT RUN FOR LID-SEAL REGION MODEL

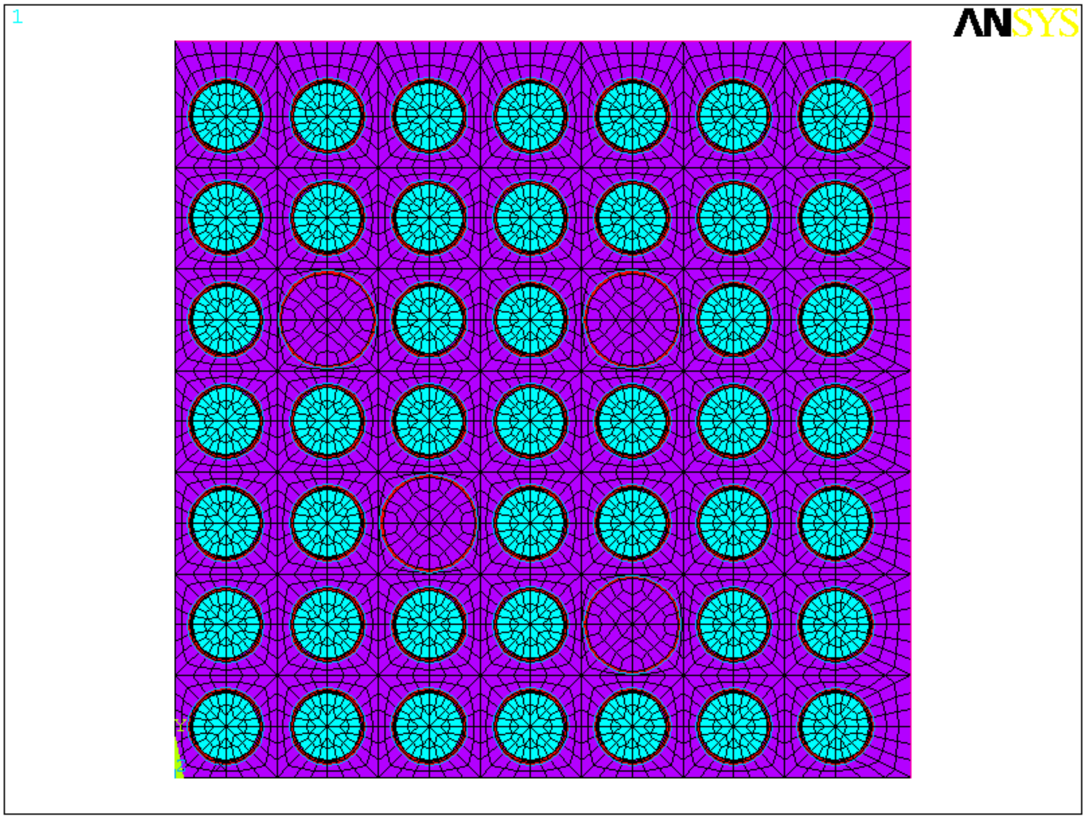

FIGURE A3.3-17
FINITE ELEMENT MODEL OF WE14X14 FUEL ASSEMBLY

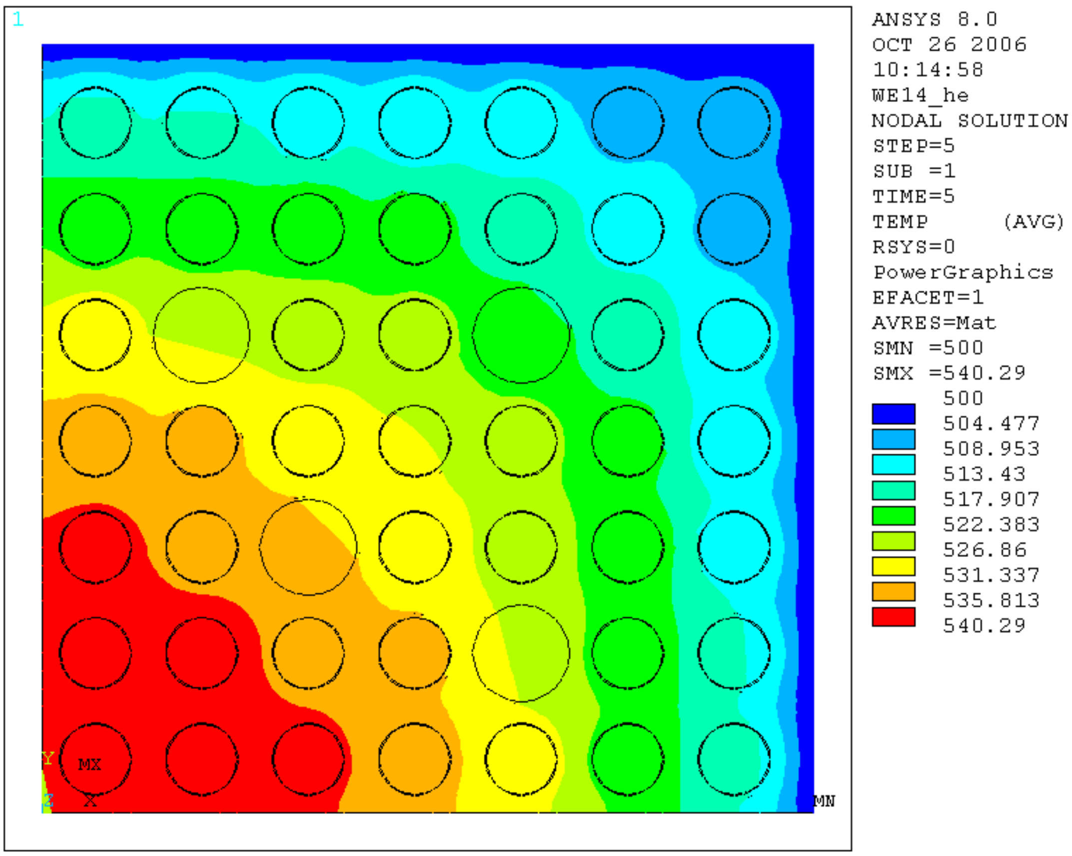

FIGURE A3.3-18
TEMPERATURE PLOT FOR WE14X14 FA IN HELIUM

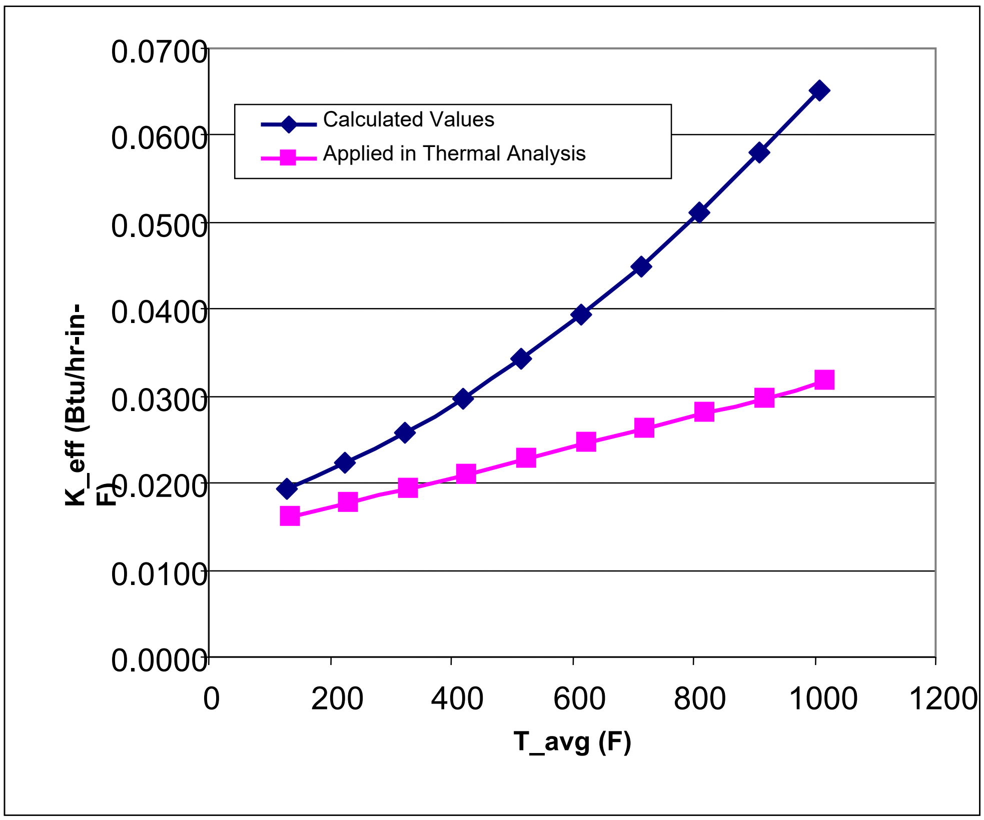

FIGURE A3.3-19
COMPARISON OF TRANSVERSE EFFECTIVE CONDUCTIVITIES

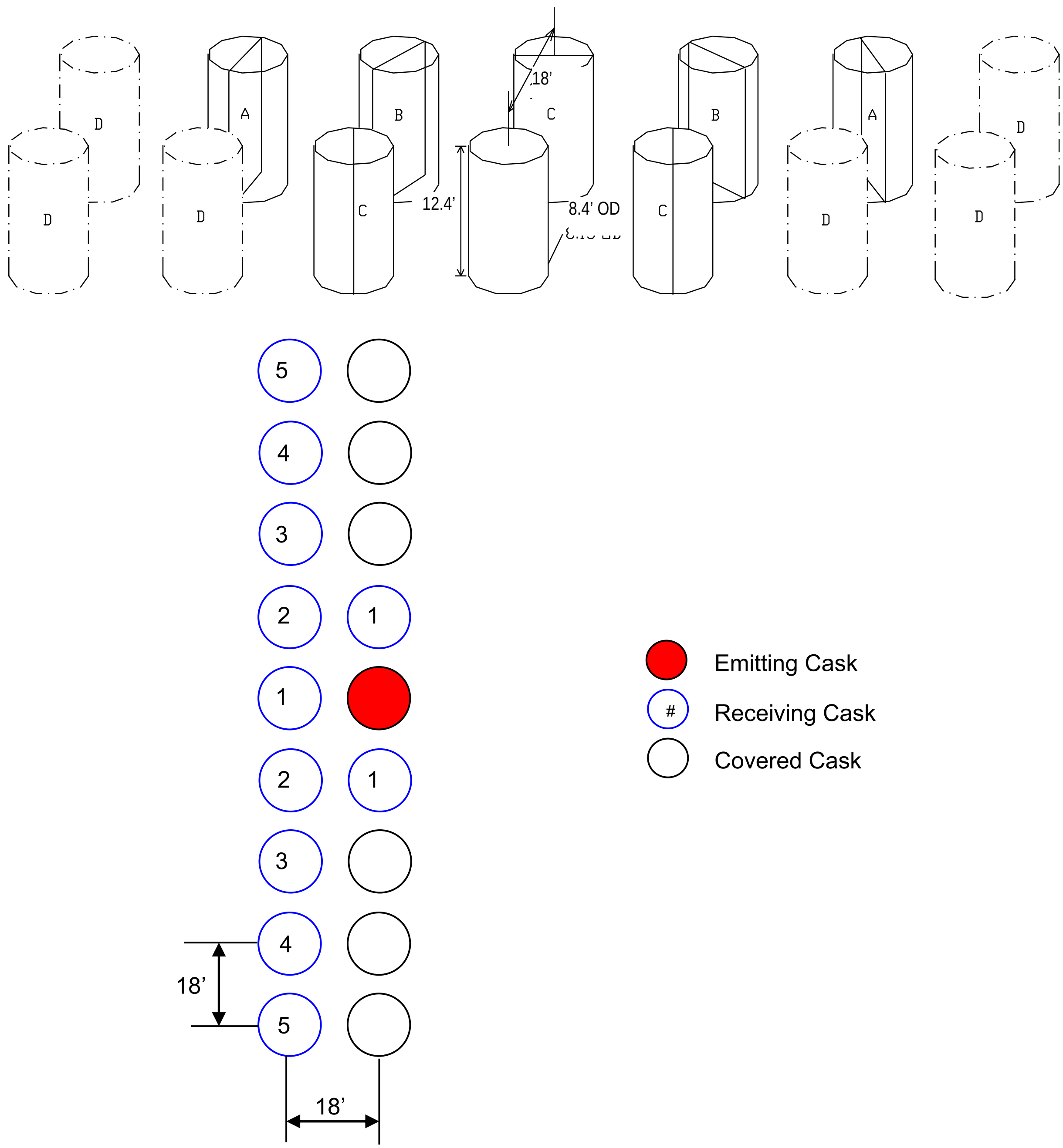

FIGURE A3.3-20
STORAGE CONFIGURATION FOR TN-40HT CASKS

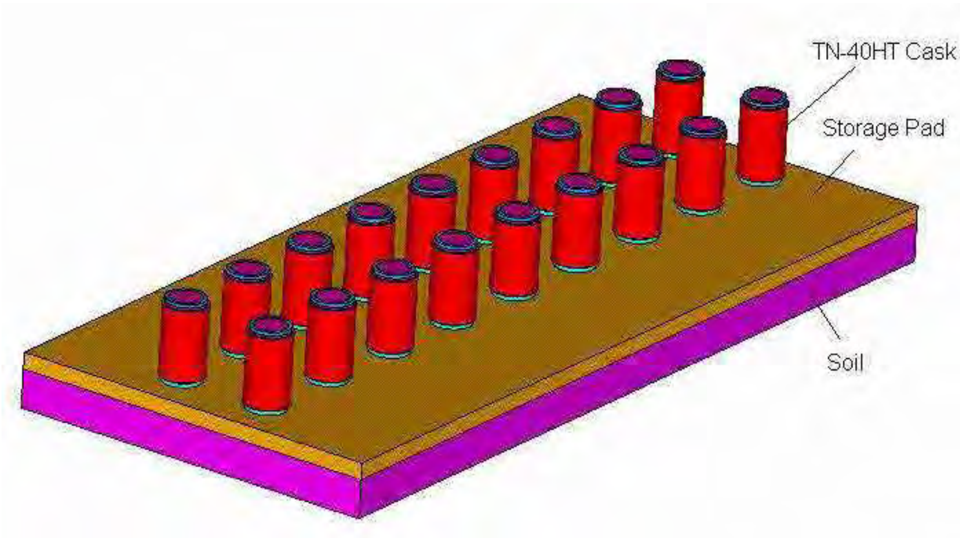

3D View

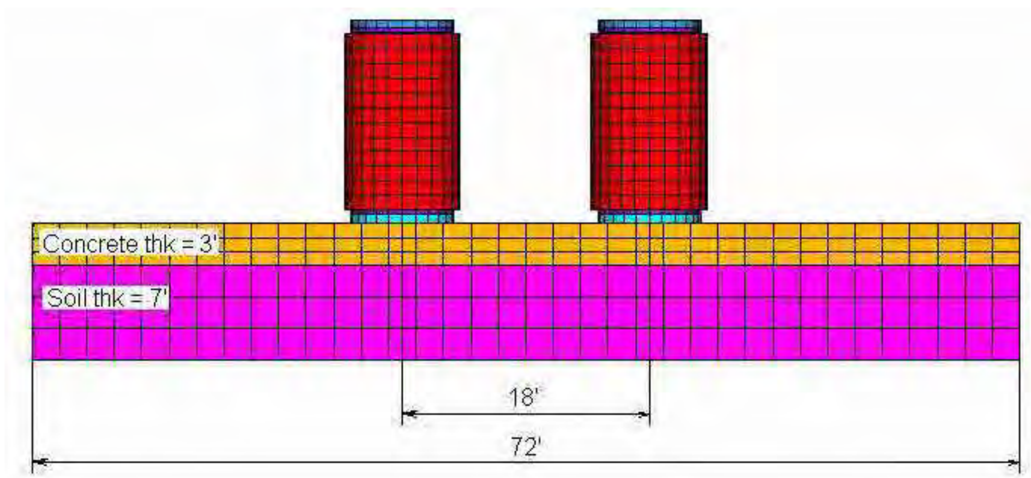

Front View

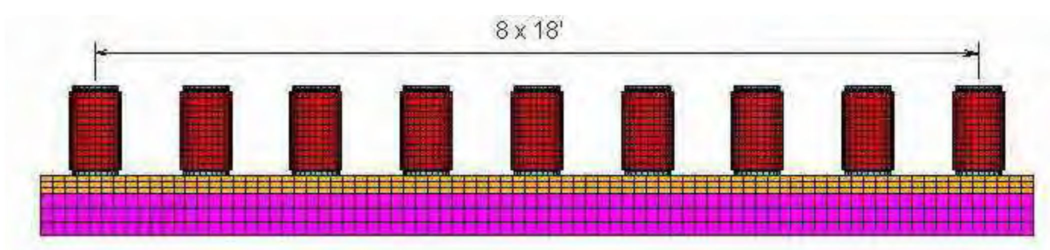

Side View

FIGURE A3.3-21
STORAGE ARRAY MODEL FOR TN-40HT CASKS

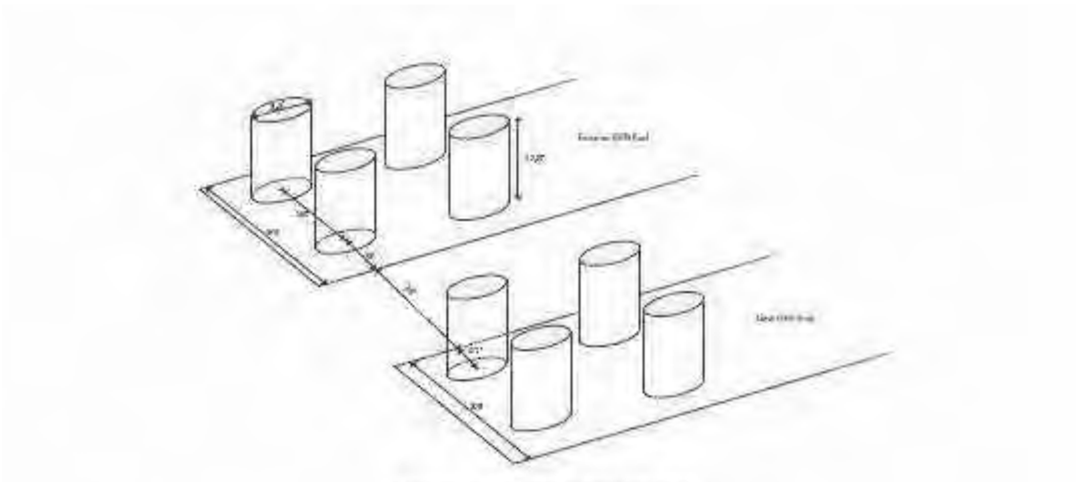

Dimensions for CFD Model

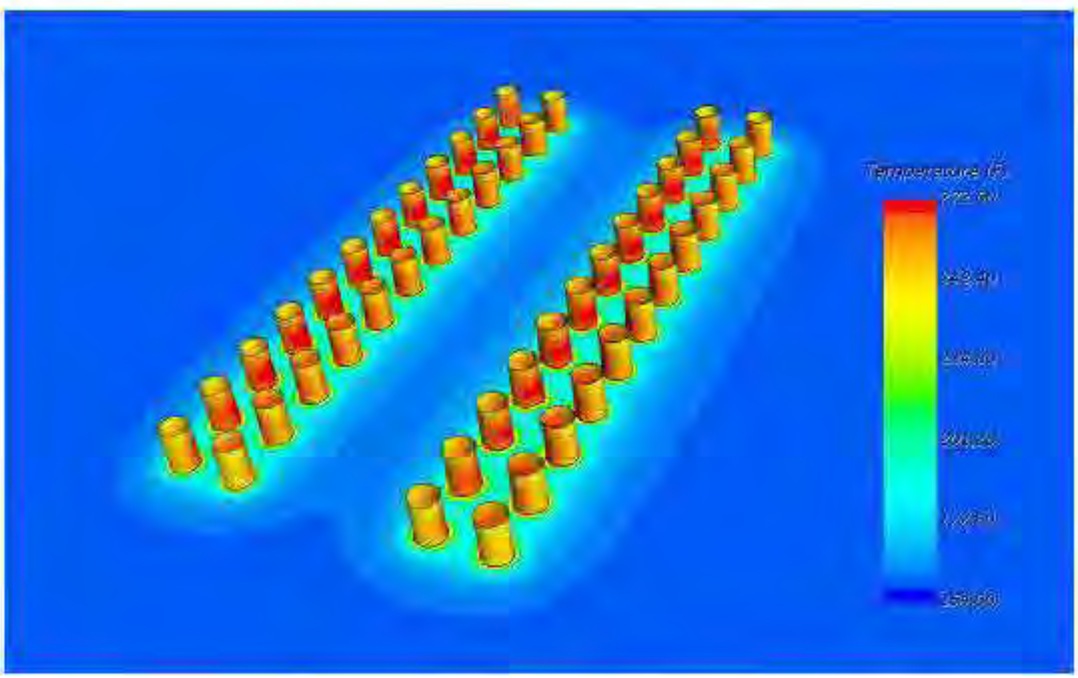

604000000330

FIGURE A3.3-21A
CFD MODEL FOR THE SOUTHEAST ISFSI PAD EXPANSION

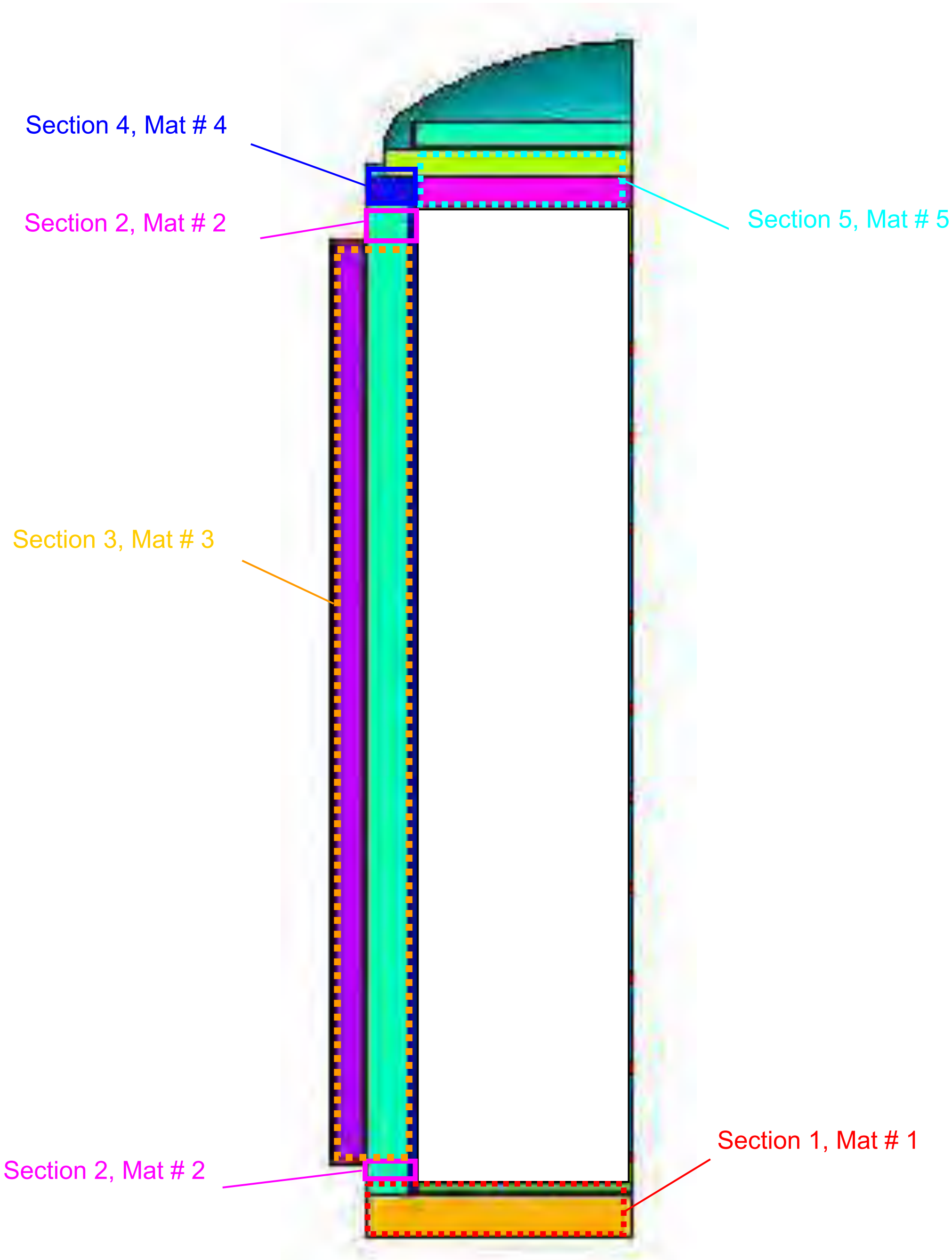

FIGURE A3.3-22
CASK SECTION FOR EFFECTIVE CONDUCTIVITIES

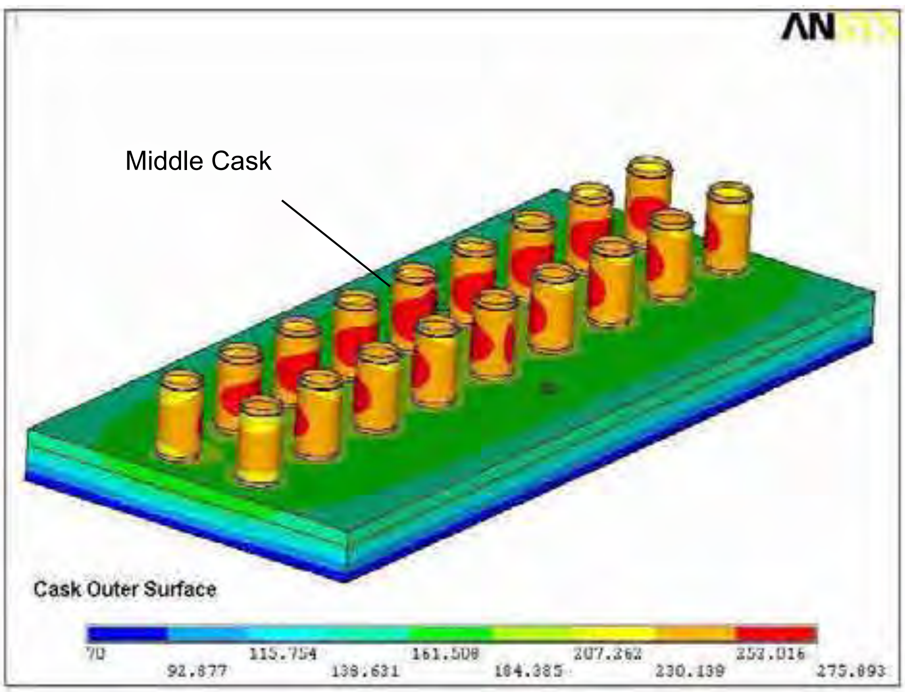

FIGURE A3.3-23
TEMPERATURE DISTRIBUTION ON CASK OUTER SURFACES ON STORAGE PADS

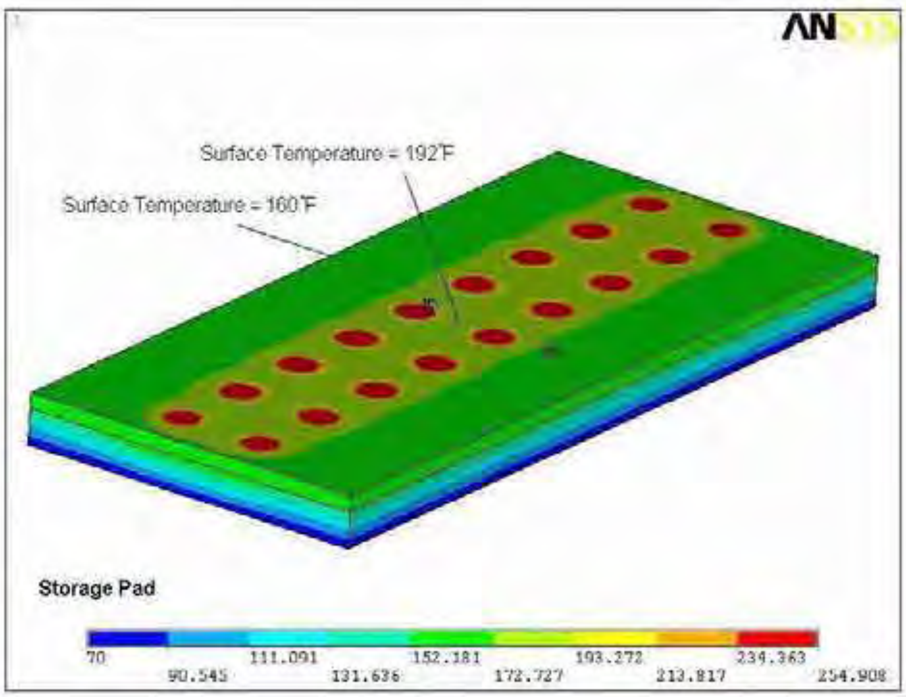

FIGURE A3.3-24
TEMPERATURE DISTRIBUTION ON STORAGE PAD SURFACE

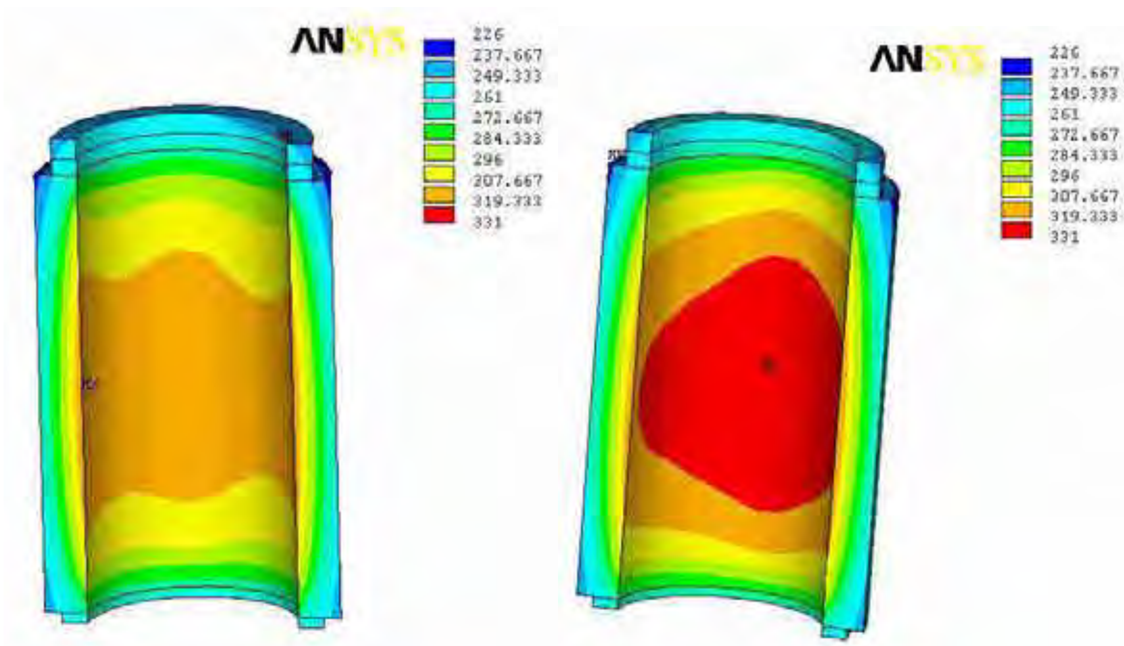

FIGURE A3.3-25
TEMPERATURE DISTRIBUTION ON HALVES OF CASK INNER SHELL
(MIDDLE CASK)

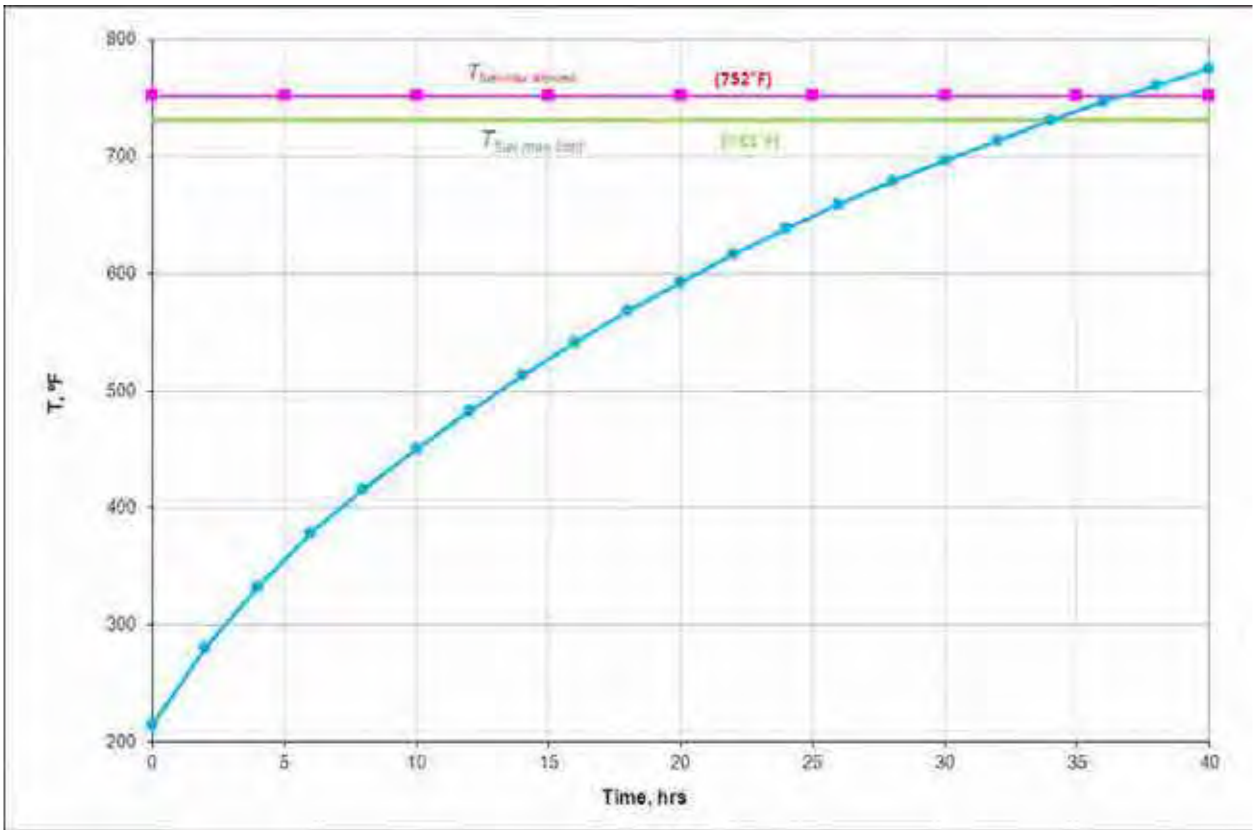

FIGURE A3.3-26
MAXIMUM FUEL CLADDING TEMPERATURE DURING VACUUM DRYING OPERATIONS

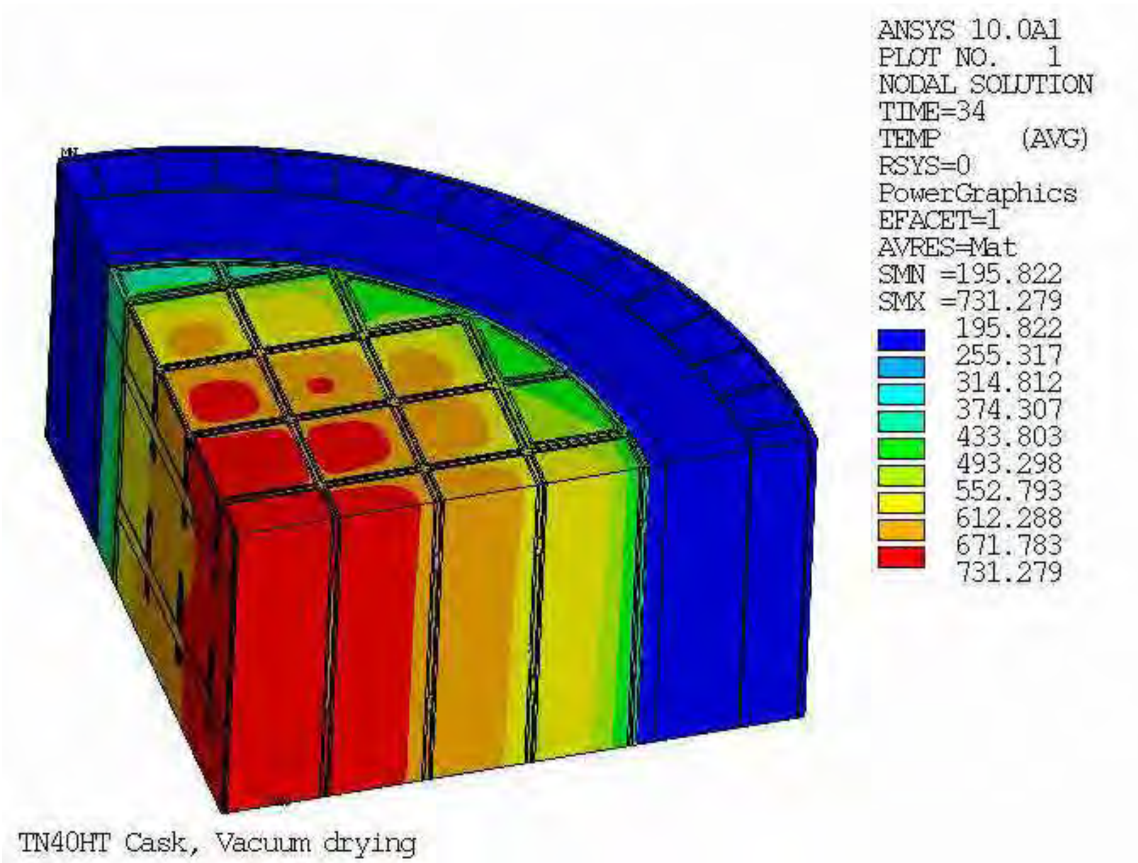

FIGURE A3.3-27
TEMPERATURE DISTRIBUTION AT THE END OF VACUUM DRYING OPERATION

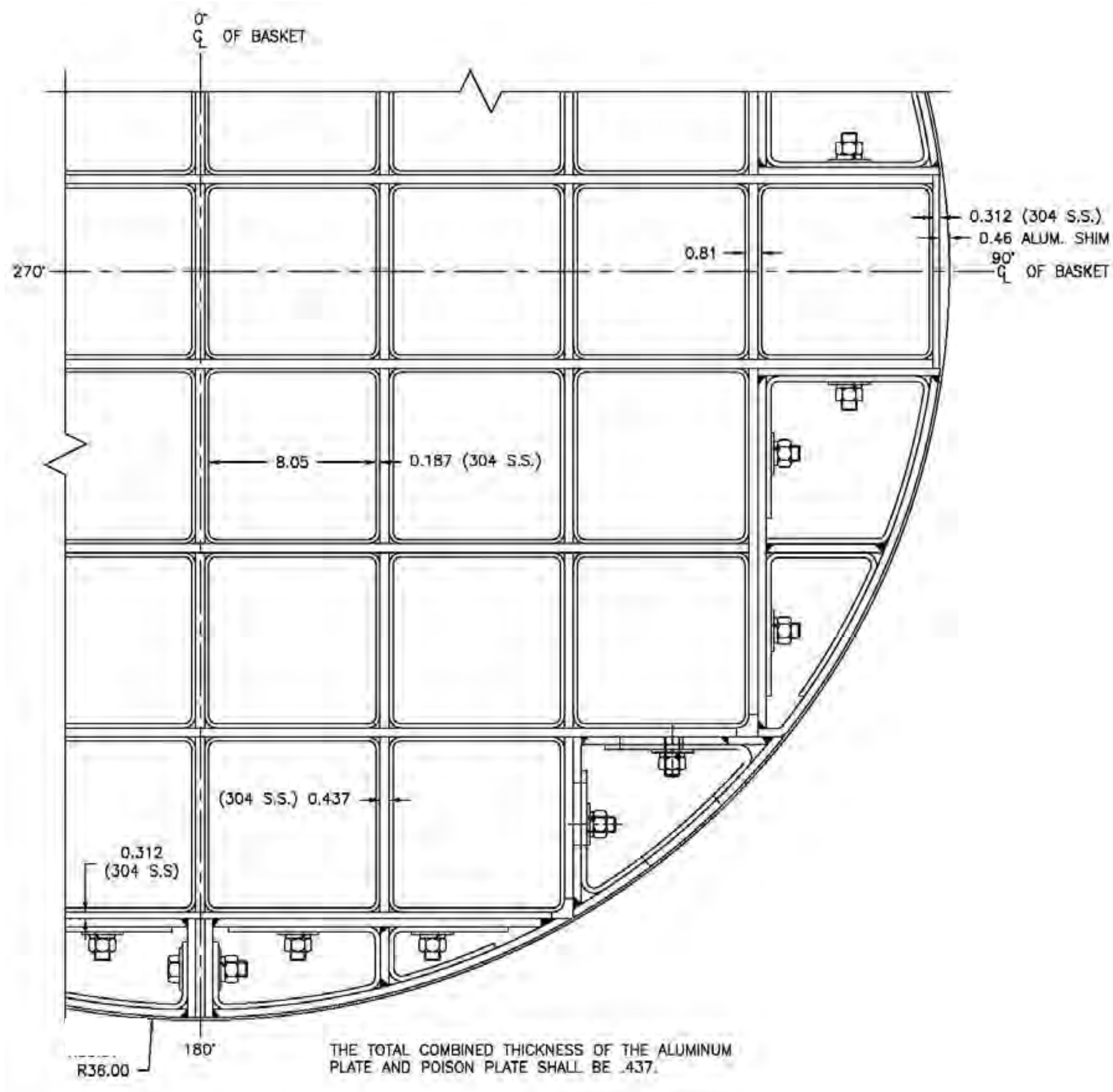

FIGURE A3.3-28
TN-40HT BASKET CROSS SECTION

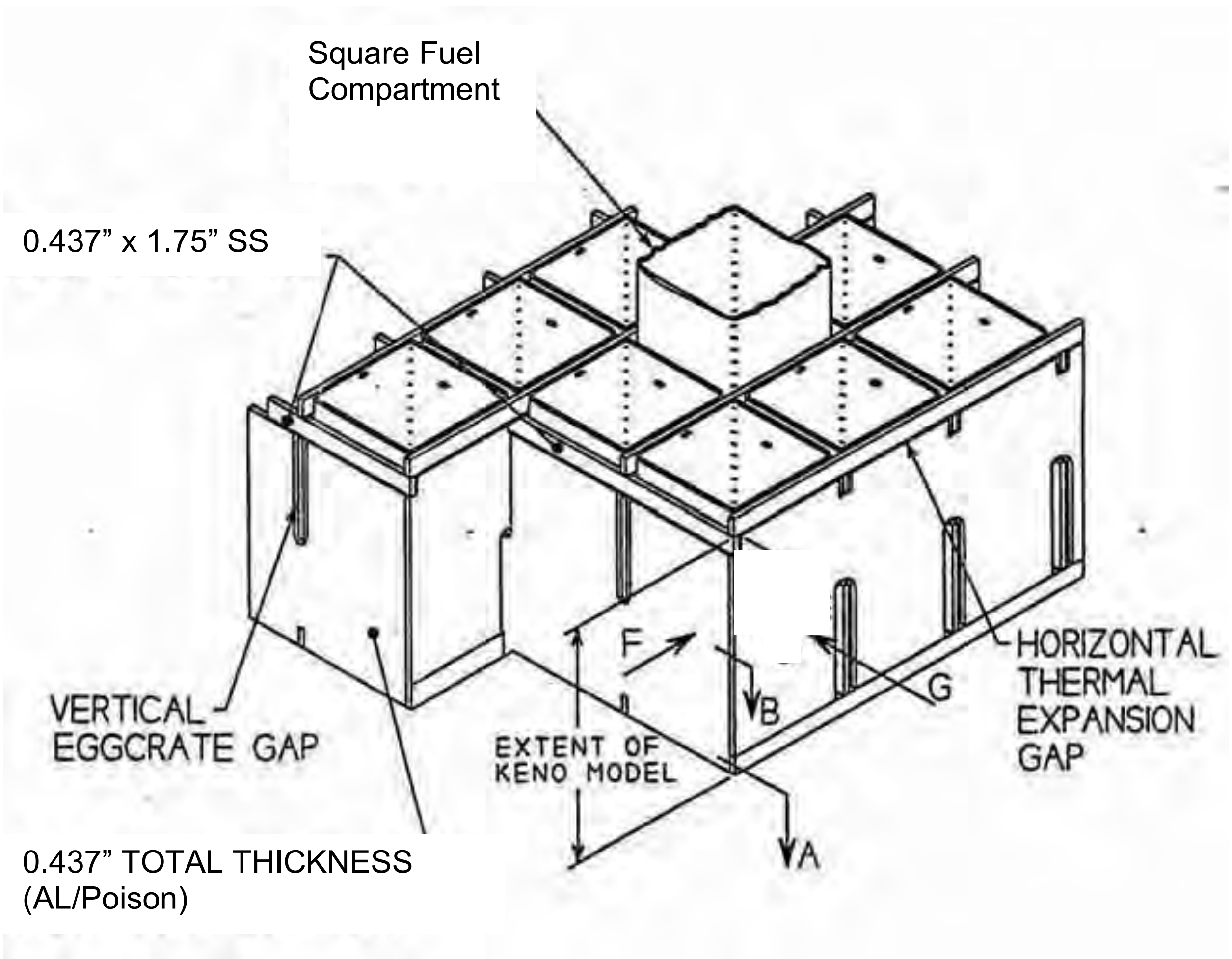

FIGURE A3.3-29
BASKET VIEWS AND DIMENSIONS

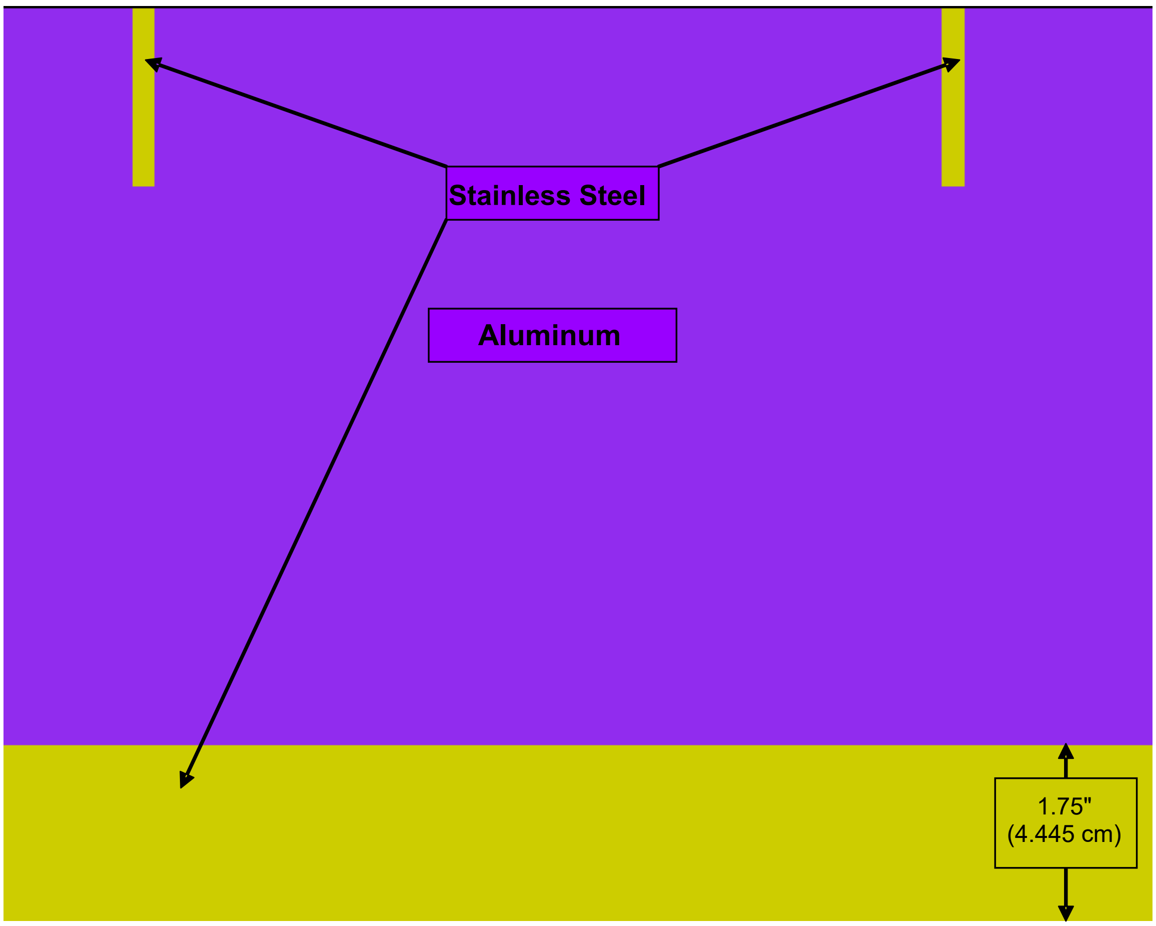

Periodic Boundary at the Bottom of Model

FIGURE A3.3-30
BASKET MODEL COMPARTMENT WALL (VIEW G)
(NOT TO SCALE)

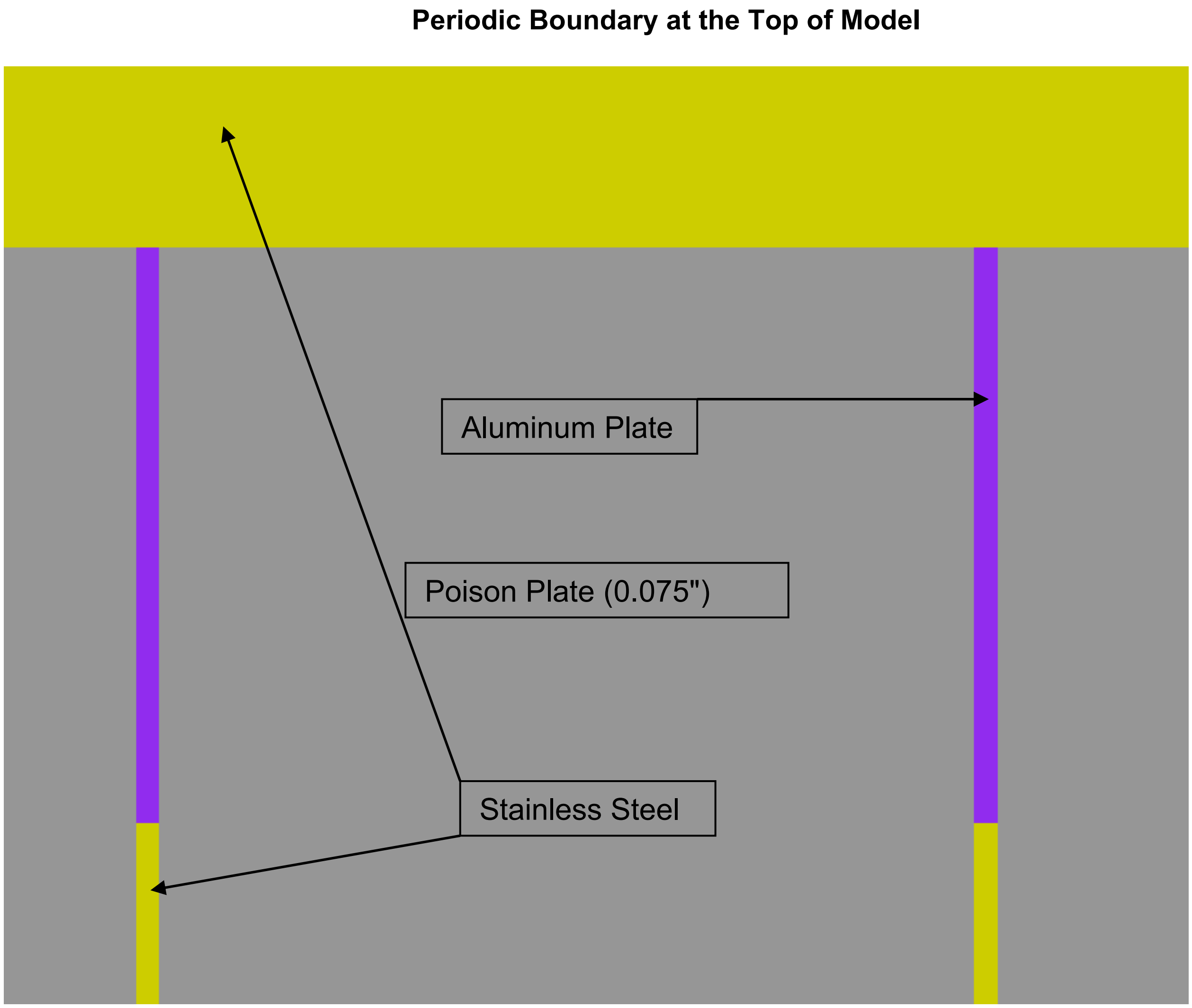

FIGURE A3.3-31
BASKET MODEL COMPARTMENT WALL (VIEW F)
(NOT TO SCALE)

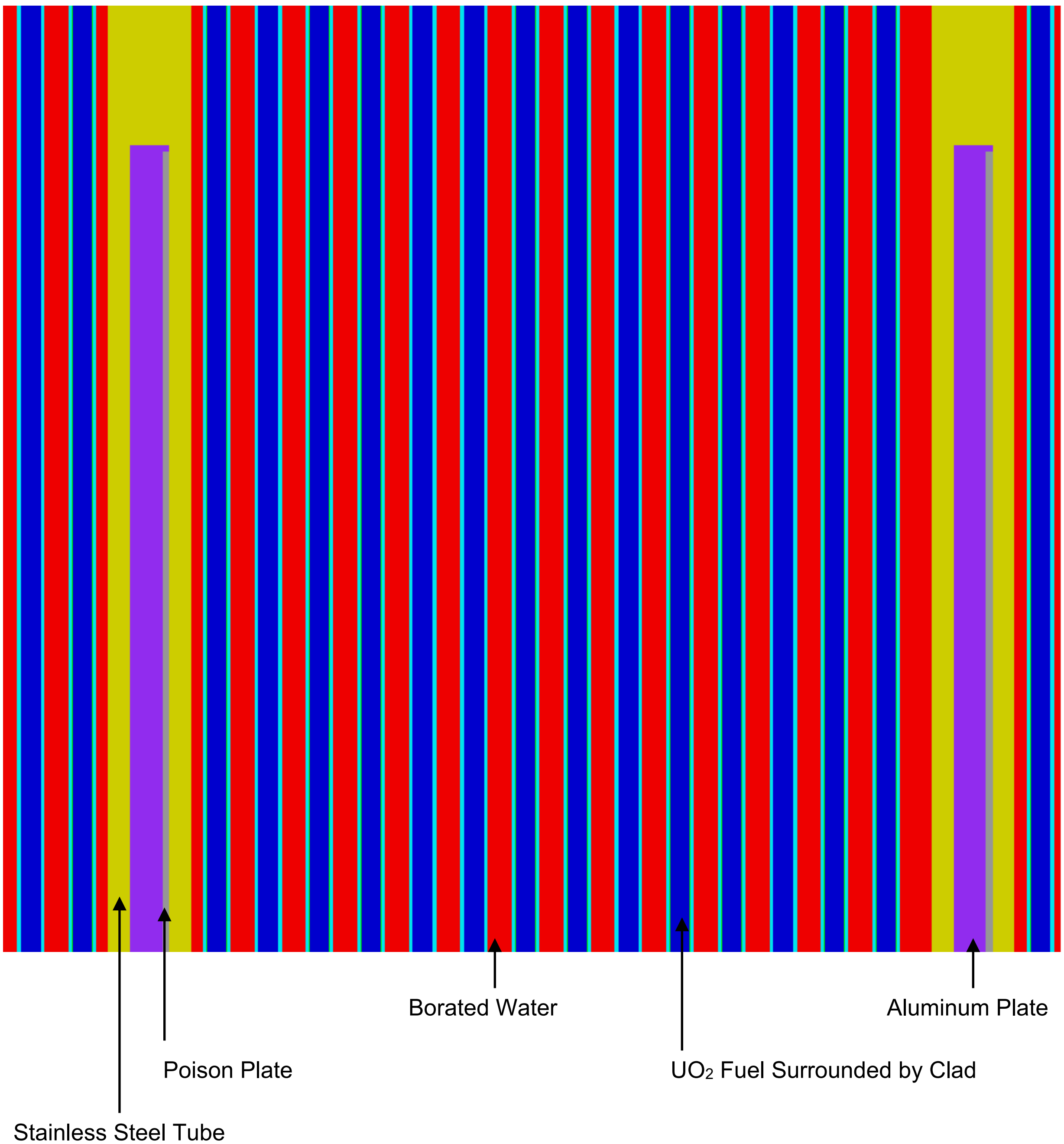

FIGURE A3.3-32
BASKET MODEL COMPARTMENT WALL WITH FUEL ASSEMBLY (VIEW G)
(NOT TO SCALE)

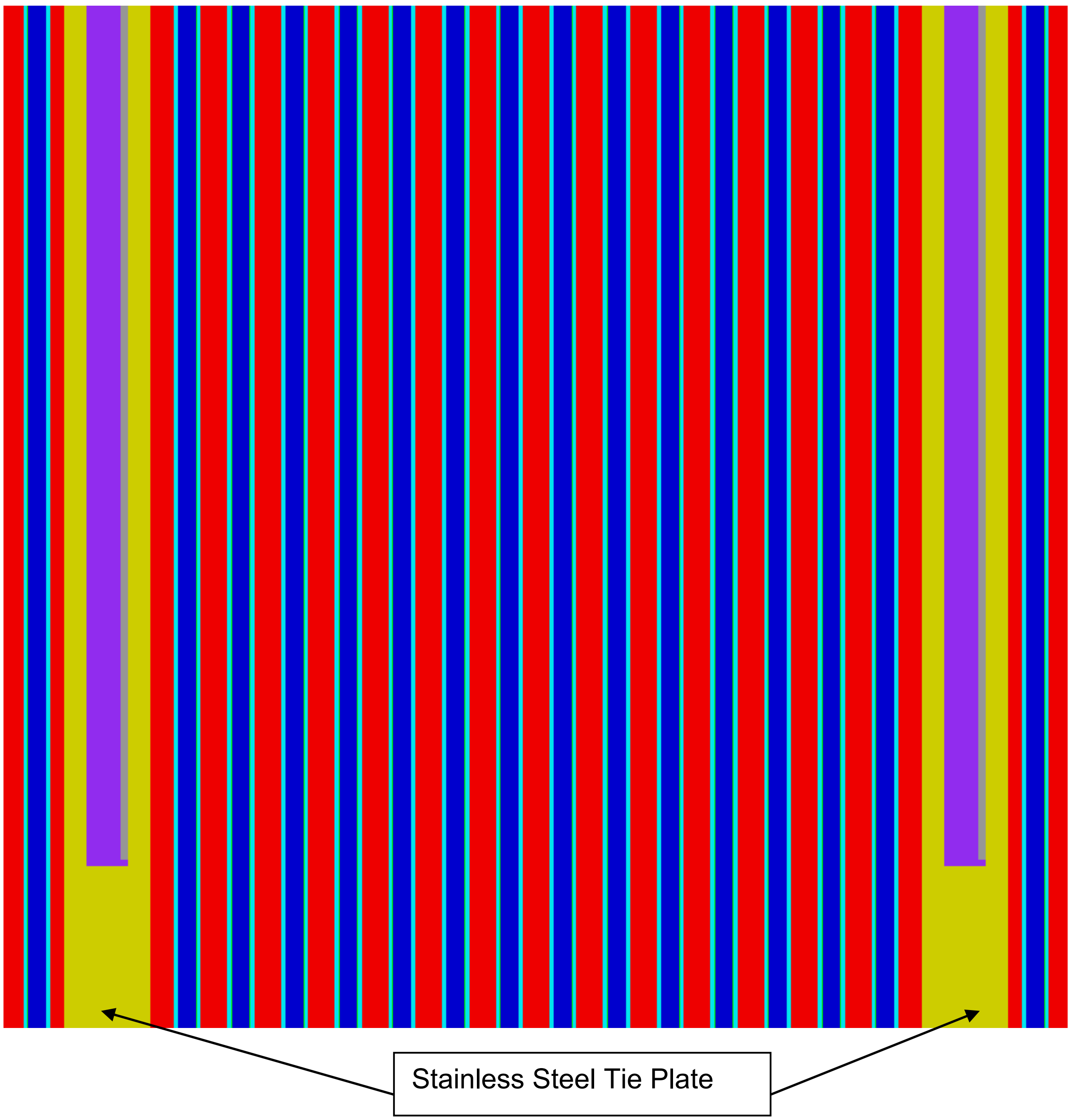

FIGURE A3.3-33
BASKET MODEL COMPARTMENT WALL WITH FUEL ASSEMBLY (VIEW F)
(NOT TO SCALE)

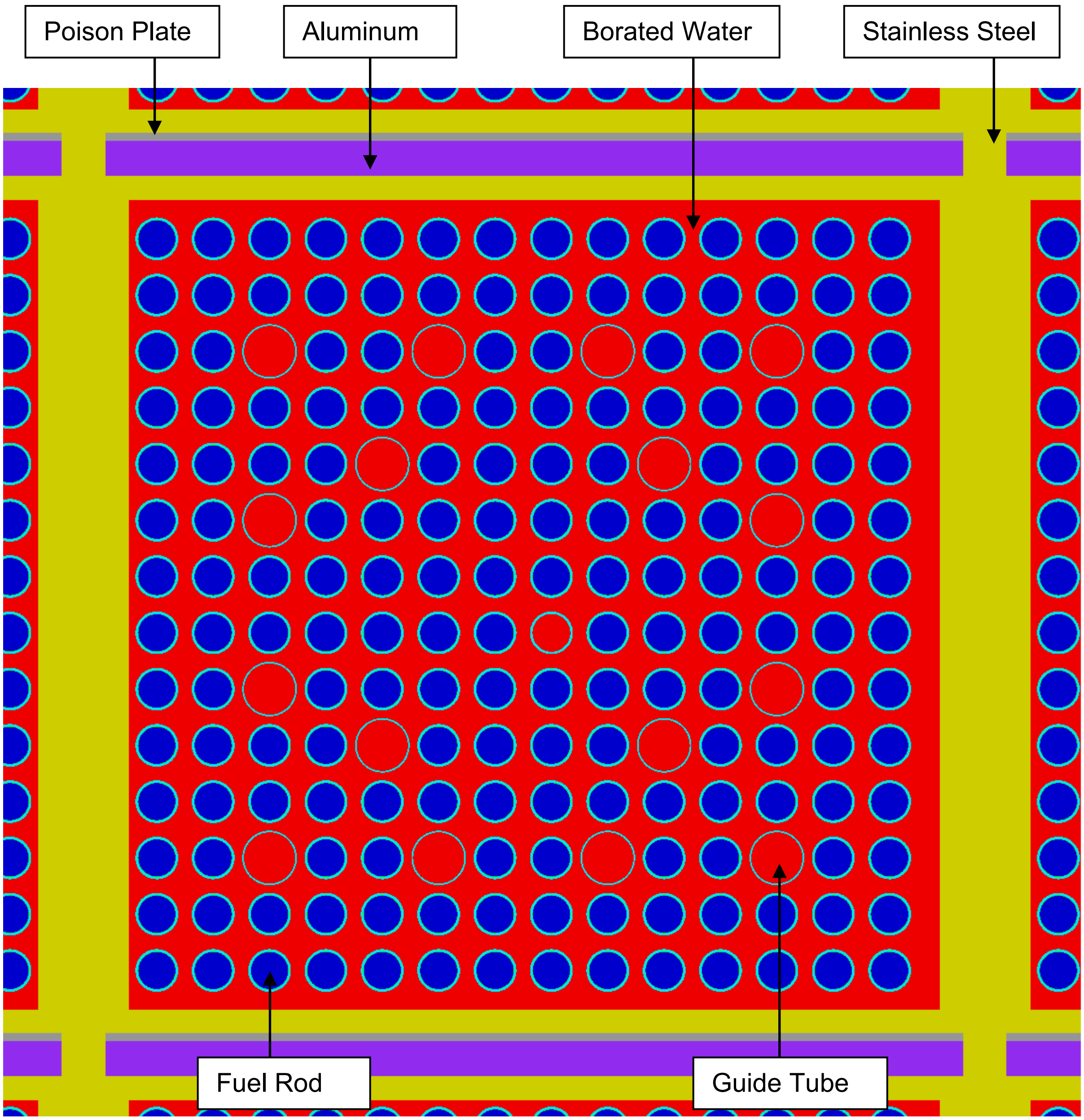

FIGURE A3.3-34
BASKET COMPARTMENT WITH WE 14X14 FUEL ASSEMBLY (SECTION A)
(NOT TO SCALE)

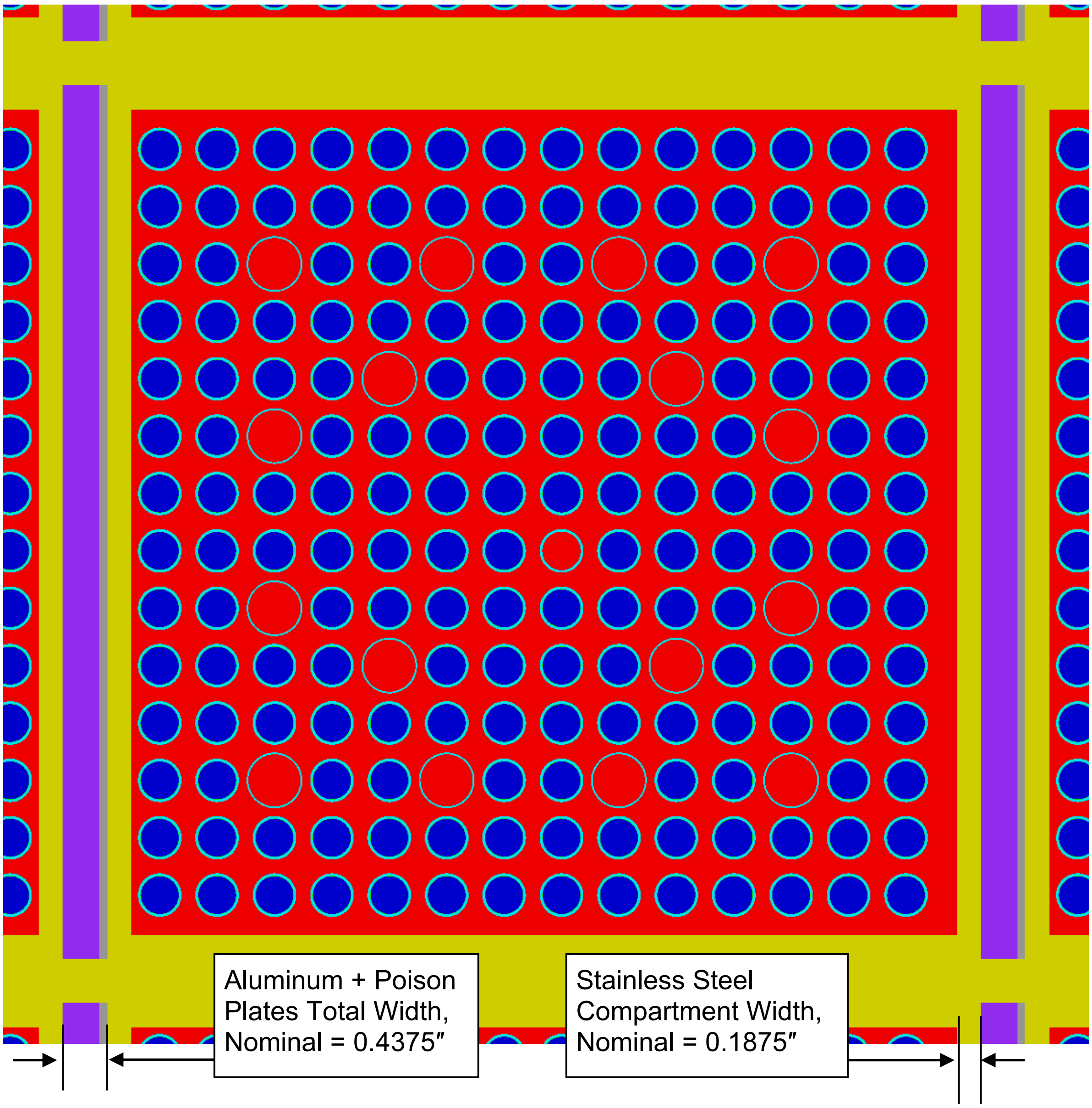

FIGURE A3.3-35
BASKET COMPARTMENT WITH WE 14X14 FUEL ASSEMBLY (SECTION B)
(NOT TO SCALE)

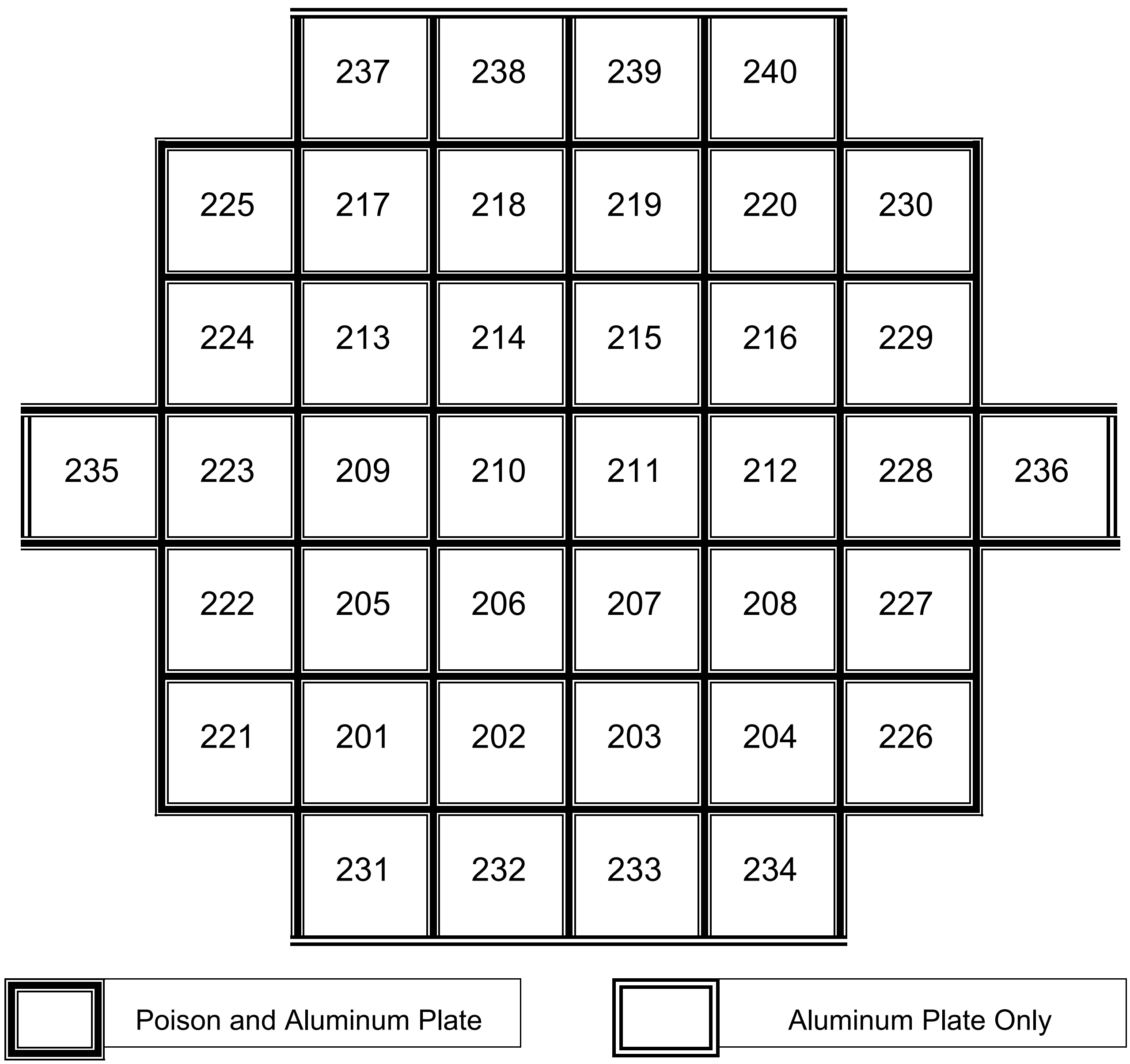

FIGURE A3.3-36
FUEL POSITION AND POISON PLATE LOCATION IN THE TN-40HT BASKET
(NOT TO SCALE)

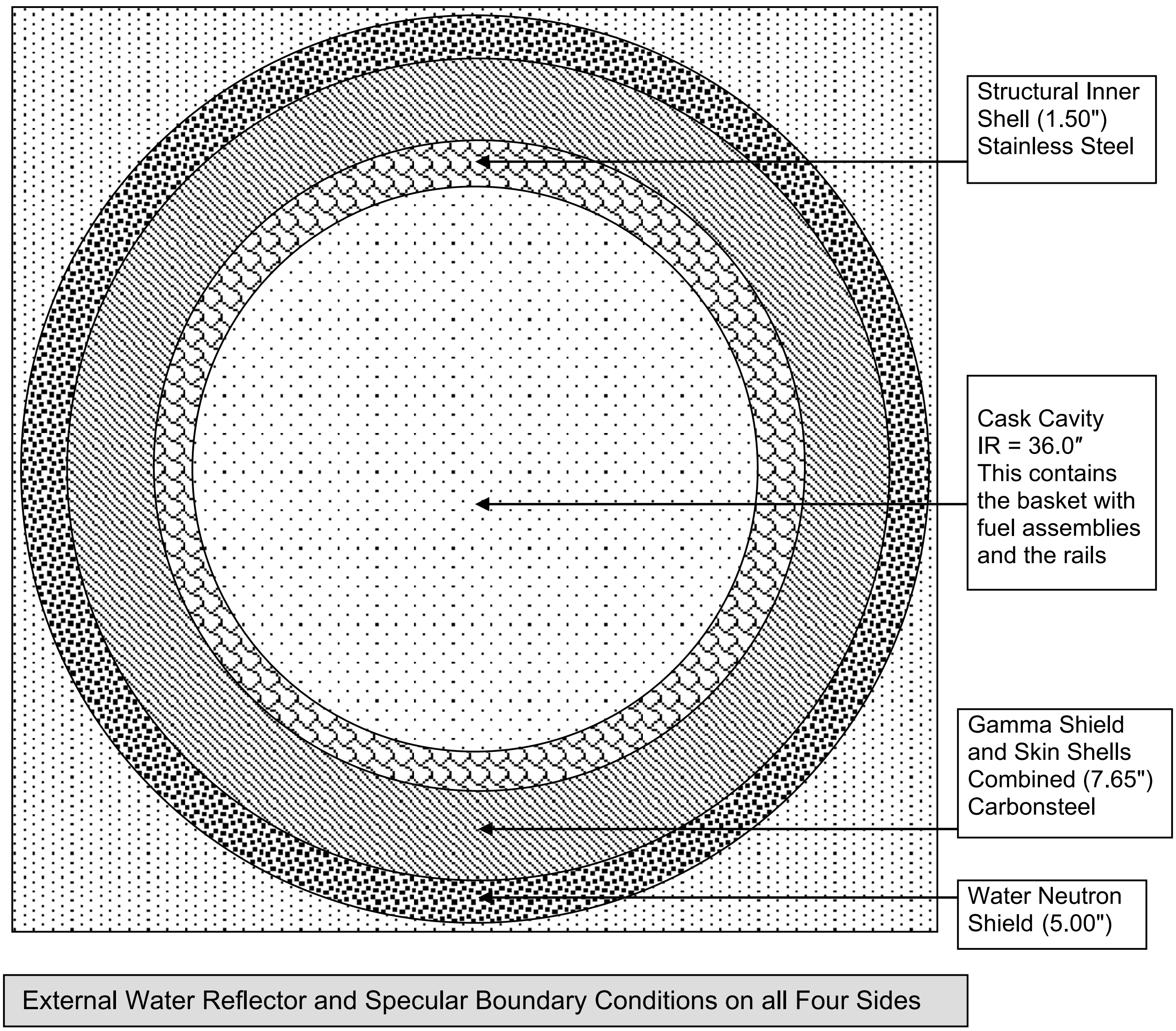

FIGURE A3.3-37
TN-40HT CASK DESCRIPTION IN THE KENO MODEL
(NOT TO SCALE)

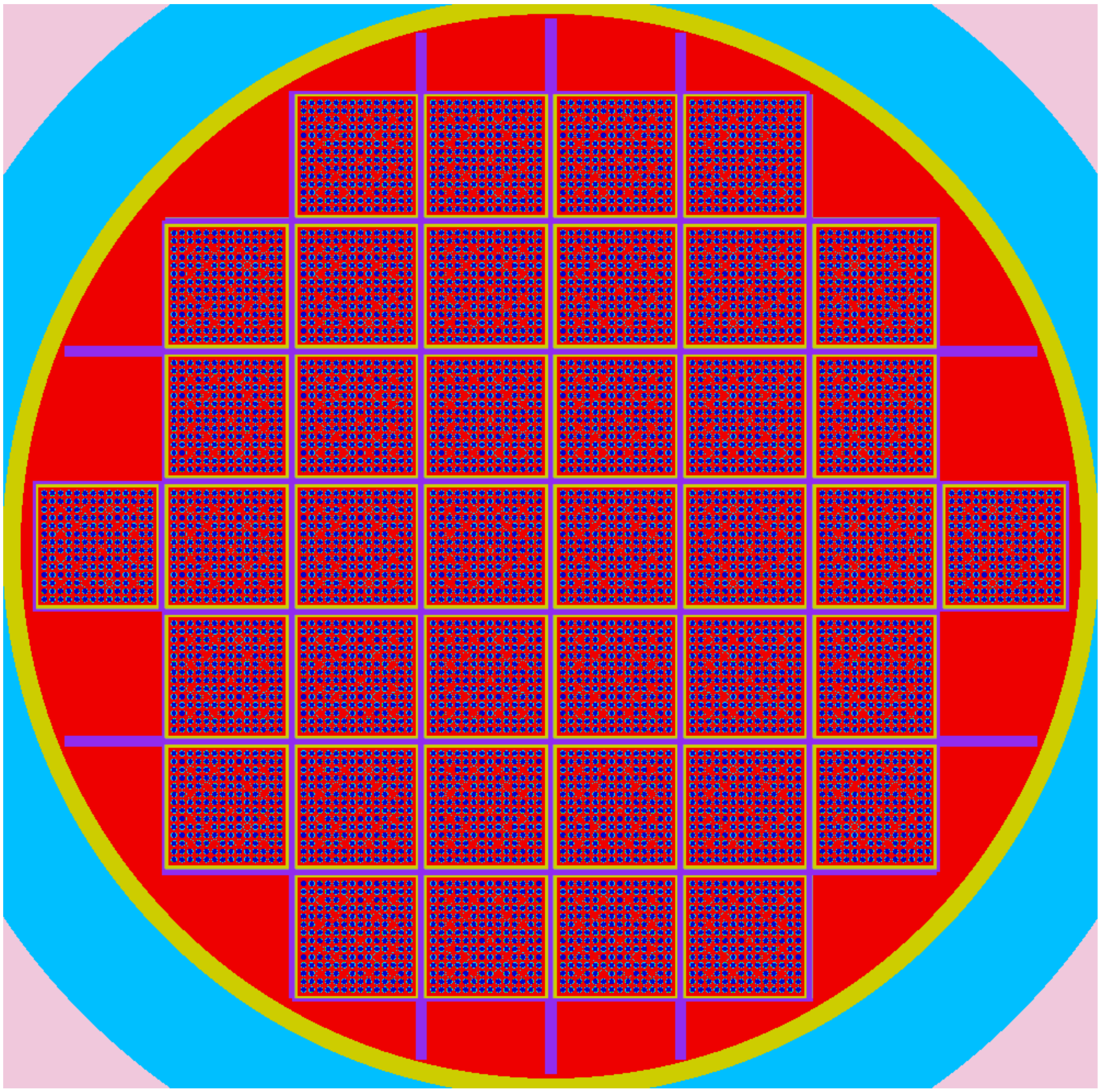

FIGURE A3.3-38
EXXON 14X14 TOP ROD FUEL ASSEMBLY (CENTERED) KENO MODEL

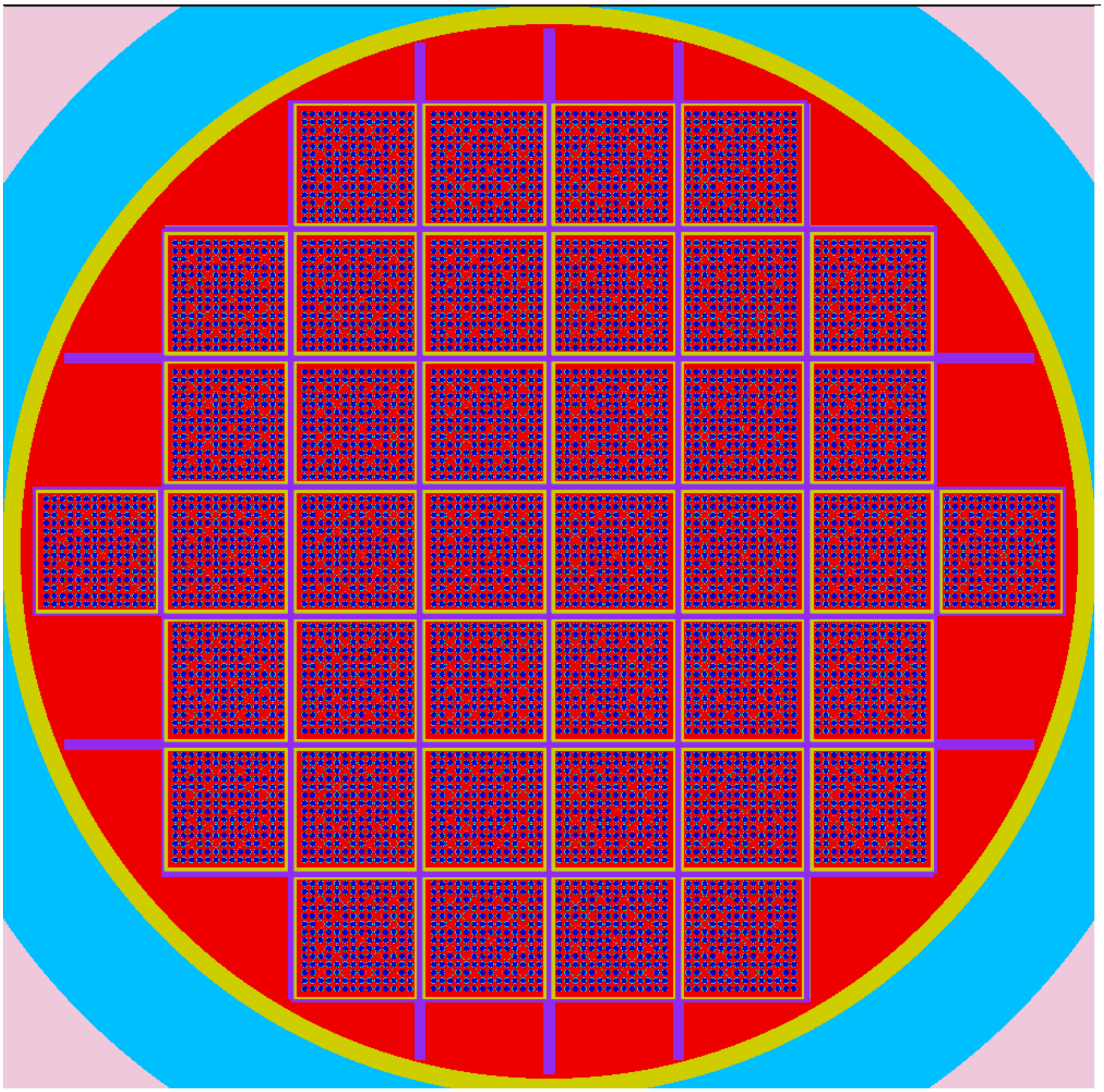

FIGURE A3.3-39
WE 14X14 STANDARD FUEL ASSEMBLY (INWARD) KENO MODEL

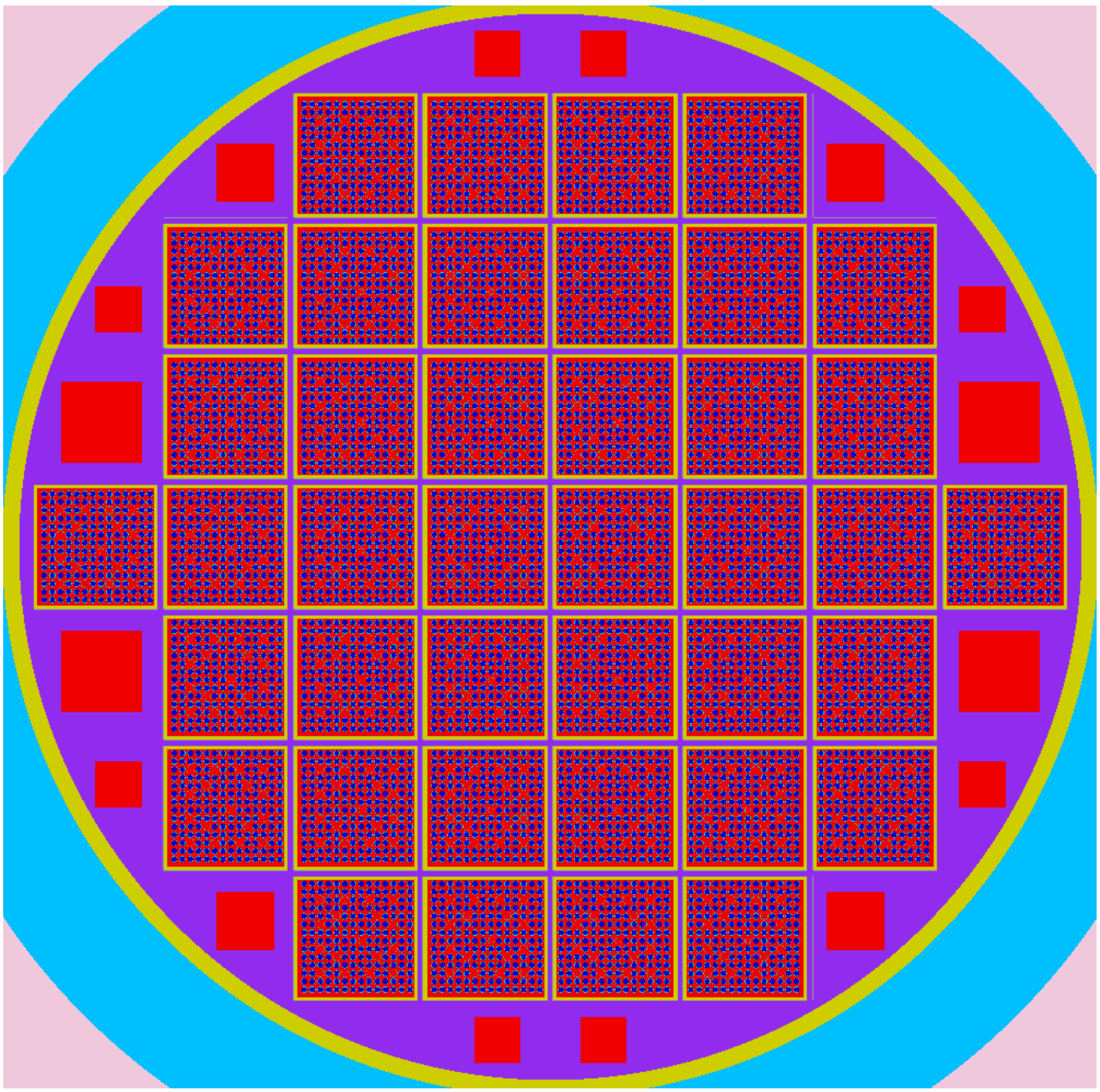

FIGURE A3.3-40
TN-40HT DESIGN BASIS KENO MODEL WITHOUT CCS

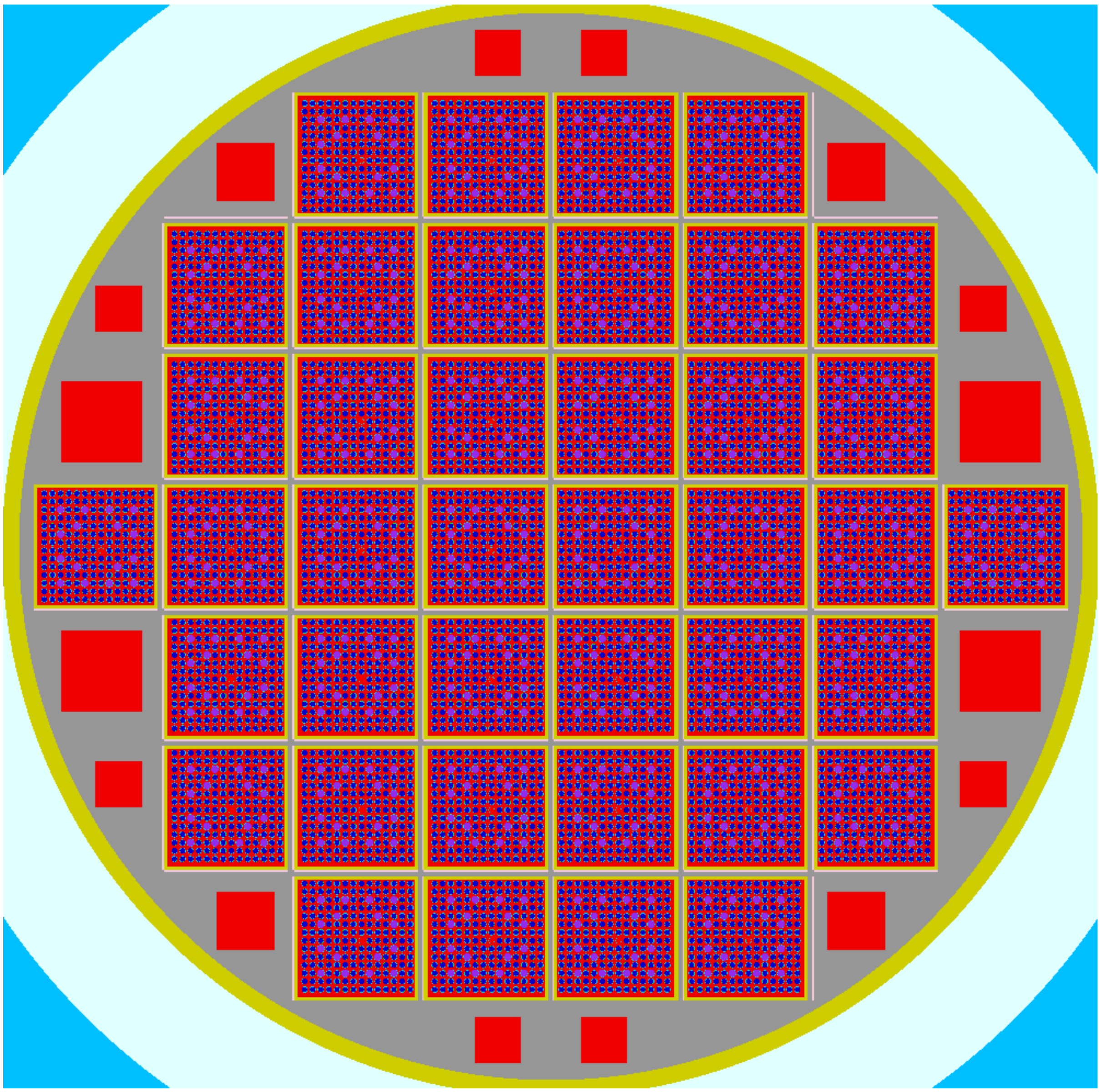

FIGURE A3.3-41
TN-40HT DESIGN BASIS KENO MODEL WITH CCS

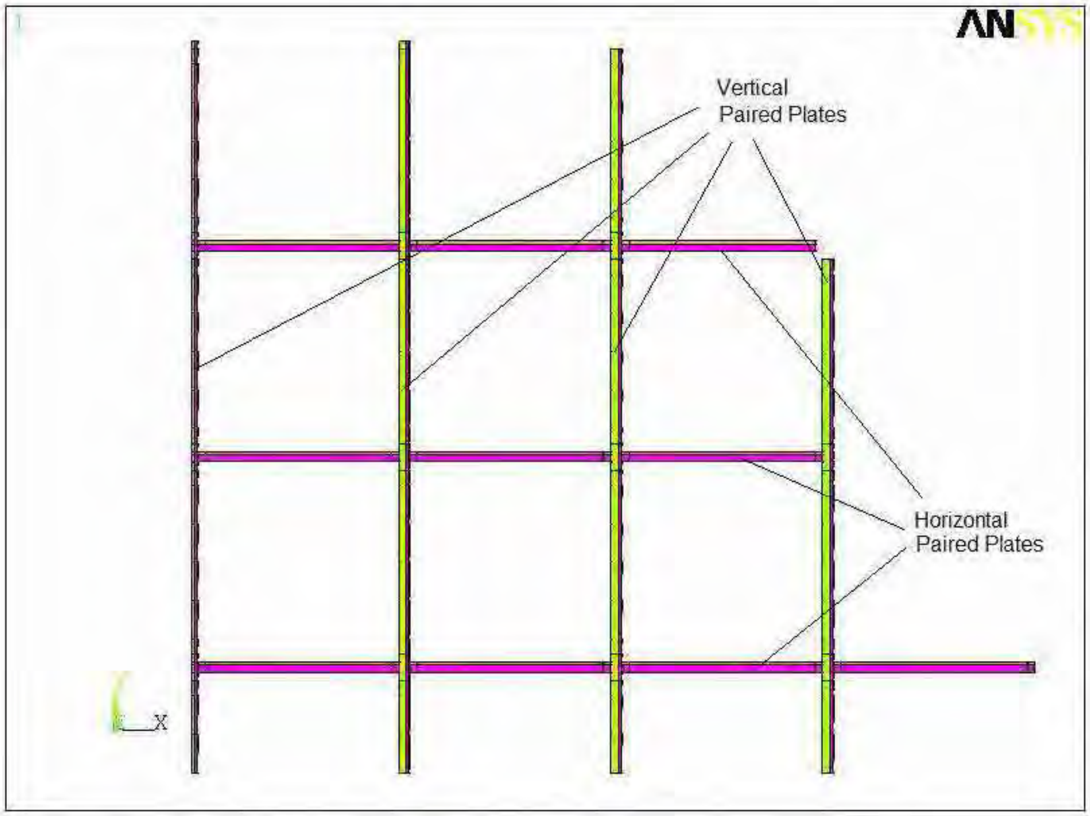

FIGURE A3.3-42
Orientation of Paired Aluminum and Poison Plates in TN-40HT Cask Model

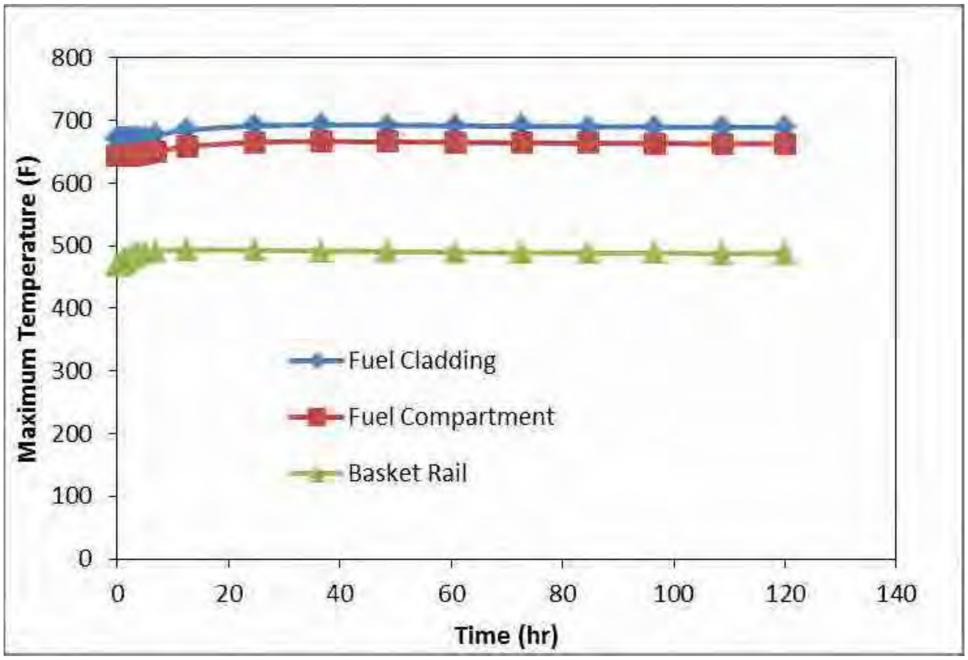

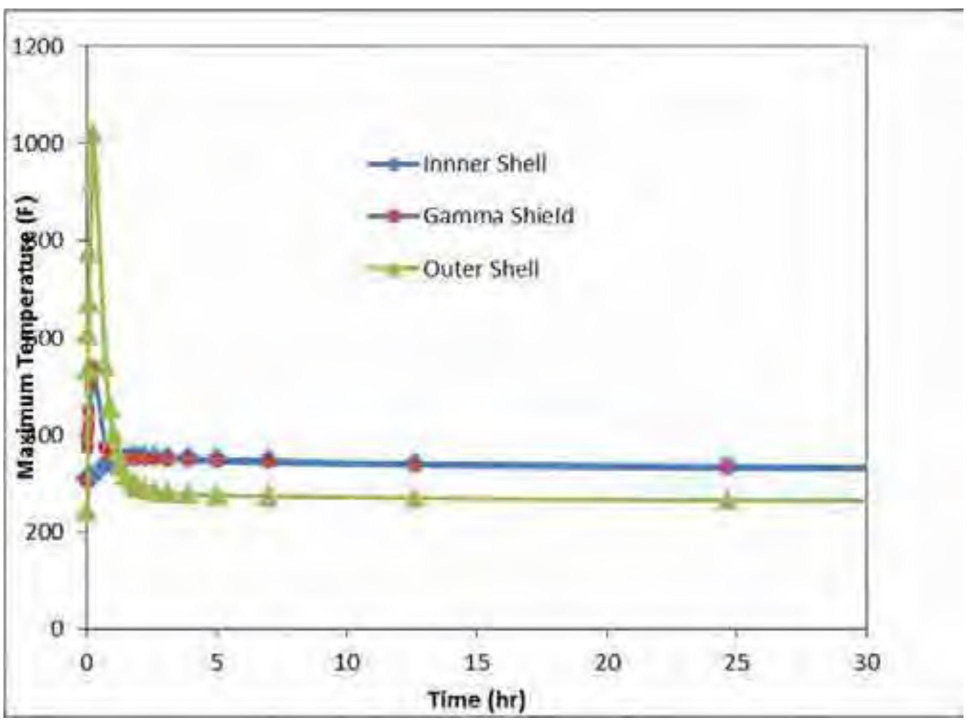

FIGURE A3.3-43
COMPONENT TIME-TEMPERATURE HISTORY FOR FIRE ACCIDENT WITH LOWER POISON PLATE CONDUCTIVITY

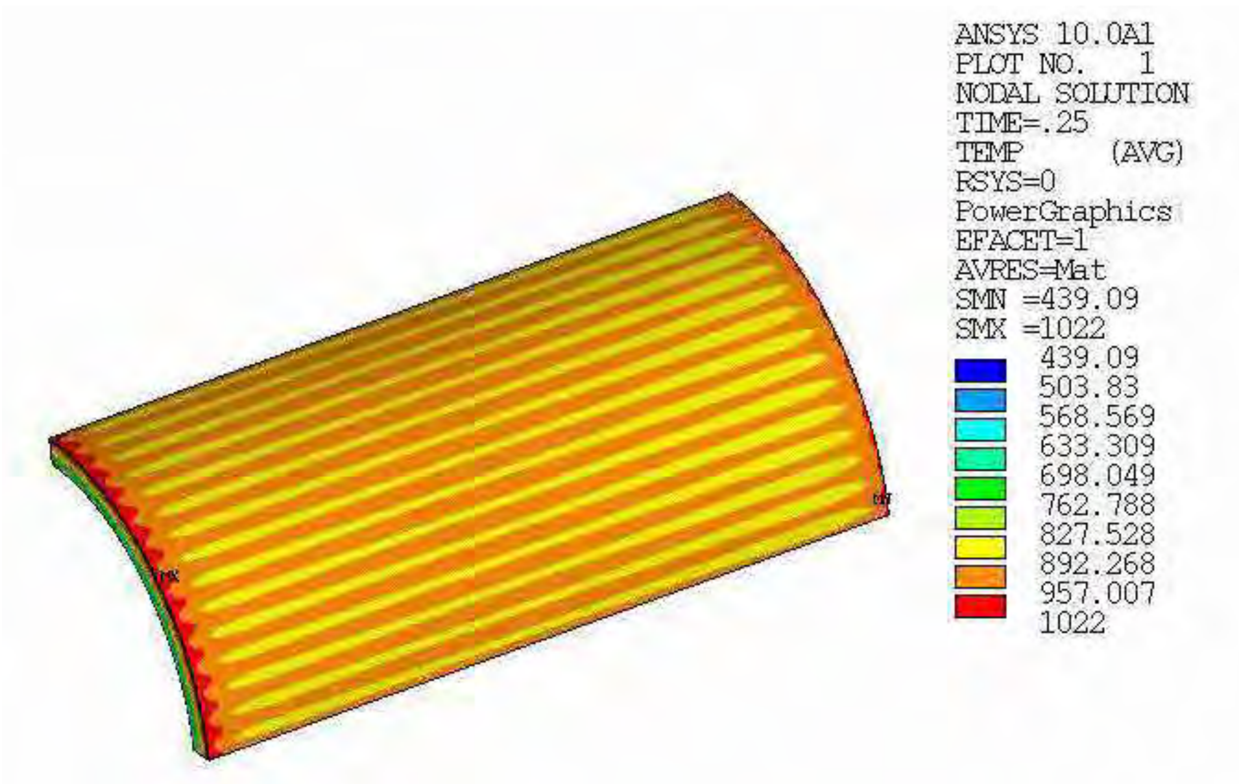

FIGURE A3.3-44
OUTER SHELL TEMPERATURE DISTRIBUTION AT THE END OF FIRE WITH LOWER POISON PLATE CONDUCTIVITY

604000000330

PROPRIETARY - TRADE SECRET INFORMATION WITHHELD PURSUANT TO 10 CFR 2.390

Appendix A3A

TN-40HT CRITICALITY EVALUATION COMPUTER INPUT

A3A.1 Most Reactive Fuel Type Example Input File

Input file: tn40hb-box-min-090.inp.

PROPRIETARY - TRADE SECRET INFORMATION
WITHHELD PURSUANT TO 10 CFR 2.390

**PROPRIETARY - TRADE SECRET INFORMATION
WITHHELD PURSUANT TO 10 CFR 2.390**

PROPRIETARY - TRADE SECRET INFORMATION
WITHHELD PURSUANT TO 10 CFR 2.390

**PROPRIETARY - TRADE SECRET INFORMATION
WITHHELD PURSUANT TO 10 CFR 2.390**

PROPRIETARY - TRADE SECRET INFORMATION
WITHHELD PURSUANT TO 10 CFR 2.390

**PROPRIETARY - TRADE SECRET INFORMATION
WITHHELD PURSUANT TO 10 CFR 2.390**

PROPRIETARY - TRADE SECRET INFORMATION
WITHHELD PURSUANT TO 10 CFR 2.390

PROPRIETARY - TRADE SECRET INFORMATION
WITHHELD PURSUANT TO 10 CFR 2.390

**PROPRIETARY - TRADE SECRET INFORMATION
WITHHELD PURSUANT TO 10 CFR 2.390**

**PROPRIETARY - TRADE SECRET INFORMATION
WITHHELD PURSUANT TO 10 CFR 2.390**

A3A.2 Input Listing for Case with Maximum Calculated k_{eff}

Case with: Enrichment = 5.00 wt. % U-235, Soluble Boron = 2450 ppm, With CCs.

Input File: tn40hb-e500bp-100.inp

**PROPRIETARY - TRADE SECRET INFORMATION
WITHHELD PURSUANT TO 10 CFR 2.390**

**PROPRIETARY - TRADE SECRET INFORMATION
WITHHELD PURSUANT TO 10 CFR 2.390**

PROPRIETARY - TRADE SECRET INFORMATION
WITHHELD PURSUANT TO 10 CFR 2.390

**PROPRIETARY - TRADE SECRET INFORMATION
WITHHELD PURSUANT TO 10 CFR 2.390**

PROPRIETARY - TRADE SECRET INFORMATION
WITHHELD PURSUANT TO 10 CFR 2.390

PROPRIETARY - TRADE SECRET INFORMATION
WITHHELD PURSUANT TO 10 CFR 2.390

**PROPRIETARY - TRADE SECRET INFORMATION
WITHHELD PURSUANT TO 10 CFR 2.390**

PROPRIETARY - TRADE SECRET INFORMATION
WITHHELD PURSUANT TO 10 CFR 2.390

PROPRIETARY - TRADE SECRET INFORMATION
WITHHELD PURSUANT TO 10 CFR 2.390

PROPRIETARY - TRADE SECRET INFORMATION
WITHHELD PURSUANT TO 10 CFR 2.390

SECTION A4

STORAGE SYSTEM

A4.1 LOCATION AND LAYOUT-

The TN-40HT casks will be stored on the same site and use the same transport route as the TN-40 casks. Therefore the location and layout information provided in Section 4.1 is also applicable to the use of the TN-40HT casks.

A4.2 STORAGE SITE

The TN-40HT casks are designed in accordance with the General Design Criteria set forth in 10CFR72(F) as discussed in Section 4.2. Additional details are provided below. 60400000330

A4.2.1 STRUCTURES

The discussion of the two original ISFSI pads in Section 4.2.1 is independent of cask design. Likewise, the discussion of the ISFSI expansion pad in this section is independent of cask design. The location of the cask drop accident analyses of the TN-40HT cask applicable to all three pads is in Section A8.2.8.

ISFSI Expansion.

The primary function of the ISFSI expansion concrete pad is to provide a uniform level surface for storing the casks. The "minimum" pad elevation criterion has been set at 693 ft.-0 in. msl to preclude immersion of the cask seals during the probable maximum flood. The actual pad minimum elevation is 694 ft.-1 in. The southeast pad is slightly wider (4 ft. total) than the original pads. The gravel areas around the pads are compacted to allow for movement and positioning of the transport vehicle and tow vehicle. The subgrade preparation regimen (e.g., design of the mudmat foundation, use of compacted structural fill) for the southeast pad is the same as for the original pads. 60400000330

The design of the southeast ISFSI pad used the guidance in NUREG-1536, Revision 1, "Standard Review Plan for Spent Fuel Dry Storage Systems at a General License Facility" (Reference 24), for the design load requirements of the concrete pad. Note that an additional load combination is also considered to check overturning and sliding for the flooding condition so that the design load combinations for the new ISFSI pad are also consistent with the design requirements for the original ISFSI pads, discussed in Section 4.2.1. In addition, the computer program SAFE (Reference 25), was used to perform the finite element analysis for the static analysis used to evaluate the design of the southeast ISFSI pad. The analysis was performed to verify that the strength of the pad was adequate to prevent unacceptable cracking or differential settlement and that the casks would not tip under design loads.

The original ISFSI pads were designed for a minimum concrete compressive strength of 3,000 psi at 28 days in accordance with ACI 349-85, and the 1990 supplement. The cask drop analysis for the TN-40HT cask design is based on a maximum compressive strength of 4,000 psi. The southeast ISFSI expansion pad design is based on the requirements in ACI 349-13, consistent with the guidance in NRC NUREG-1536, Revision 1. Note that later editions of ACI 349 (beyond ACI 349-85) required a higher minimum compressive strength (> 4,000 psi) to meet freeze-thaw and durability requirements. Therefore, for the design of the southeast ISFSI pad, an exception is taken to the code provision requiring 4,500 psi minimum compressive strength to meet durability requirements so that the specified compression strength of the southeast ISFSI pad is 3,000 to 4,000 psi. Thus, the pad will represent a target of similar or lesser stiffness than the original ISFSI pads so that the existing cask drop analysis remains valid for the southeast ISFSI pad. 604000000330

Sliding and overturning of casks is not reevaluated for the southeast pad, except for seismic loads, because hydrological loads (i.e., design basis flooding) and accident loads (i.e., the design basis munitions barge explosion) are enveloped by the tornado wind load. The tornado wind load and missile impact analysis in this addendum remains applicable (i.e., the coefficient of friction for the southeast pad is the same as for the original pads). The effect of seismic loads associated with the design basis safe shutdown earthquake (SSE) was evaluated because the dynamic analysis is performed using a different method which results in the development of new seismic loads (see Section A4.2.1.2).

A4.2.1.1 STATIC ANALYSIS

Original ISFSI Design 604000000330

The ISFSI reinforced concrete cask pad analysis described in Section 4.2.1.1 was reviewed for the incorporation of the TN-40HT cask parameters and for increasing the allowed cask weight to a maximum of 250,000 lbs. The increase in cask weight input was reviewed in combination with a 1.5 inch decrease in the cask base diameter for the TN-40HT cask. The existing analysis utilizing the TN-40 input parameters contains considerable design margin. For example, as described in Section 4.2.1.1, the cask pad flexure strength margin indicates a safety factor of 2.14.

The review concluded that the increase to the maximum cask weight of 3.9% ((250 kip – 240.7 kip) / 240.7 kip) greater than used in the analysis and the 1.6% ((91” – 89.5”) / 91”) decrease in the cask base diameter will have a negligible effect on the adequacy determination of the cask pad analysis and design, and a more rigorous reanalysis is not warranted given the large margins that exist.

ISFSI Expansion

As discussed in Section A4.2.1, the southeast ISFSI pad expansion pad design is based on the requirements in ACI 349-13, consistent with the guidance in NRC NUREG-1536, Revision 1, “Standard Review Plan for Spent Fuel Dry Storage Systems at a General License Facility” (Reference 24). The static analysis of the ISFSI expansion pad was performed using the SAFE computer program (Reference 25). The SAFE program was specifically developed for performing finite element analysis of slabs and beams. The TN-40HT cask parameters were used in the analysis for the southeast pad. The design model consists of slab elements supported by subgrade springs. The slab elements are modeled as four-node, isotropic, rectangular thick-plate elements that combine membrane and plate-bending behavior. The finite element mesh is defined to have maximum dimensions of 2ft. x 2ft. and is automatically generated by SAFE. The storage casks are not explicitly modeled in the SAFE design model. Vertical forces and overturning moments induced by the casks are calculated and applied directly as vertical pressures to the concrete pad. Several cask loading conditions were evaluated.

604000000330

The analysis concluded that the southeast pad is acceptable for its design loading. Additionally, the cask drop criterion (i.e., specified compression strength of 3,000 to 4,000 psi) is met, the pad has no net uplift, and the pad stability is maintained for the maximum differential settlement.

A4.2.1.2 DYNAMIC ANALYSIS

Original ISFSI Design

604000000330

The ISFSI concrete cask pad dynamic analysis described in Section 4.2.1.2 was reviewed for the incorporation of the TN-40HT cask parameters and for increasing the allowed cask weight to a maximum of 250,000 lbs. The increase in cask weight input was reviewed in combination with a 1.5 in decrease in the cask base diameter for the TN-40HT cask.

As noted in Section 4.2.1.2, ultimate static stresses govern the design, and dynamic seismic load combinations need not be further considered for the reinforced concrete and acceptable bearing stress design.

The review of the TN-40HT cask input section properties affecting dynamic analysis relative to the TN-40 properties indicated that the seismic accelerations at the center of gravity of the casks would not change significantly, and given the conservatism in the dynamic analysis, a reanalysis is not warranted. Therefore, the dynamic stability of the TN-40HT cask was determined from the governing seismic accelerations established by the existing dynamic analysis utilizing five modes for the controlling single cask configuration.

The cask overturning moment resulting from the governing accelerations was compared to the restoring moment resulting from the TN-40HT parameters. The factor of safety is the ratio of the restoring moment to the overturning moment. The minimum factor of safety for overturning was calculated to be 1.35. The minimum factor of safety for sliding was calculated to be 1.14.

ISFSI Expansion

The effect of seismic loads associated with the design basis safe shutdown earthquake (SSE) was evaluated for the southeast ISFSI pad using input parameters for the TN 40HT casks. The dynamic analysis is performed using a different method than that used for the original pads, which resulted in the development of new seismic loads.

New SSE response spectra consistent acceleration input motions were generated in accordance with the guidance in NUREG-0800, “Standard Review Plan for the Review of Safety Analysis Reports for Nuclear Power Plants: LWR [Light Water Reactor] Edition,” (SRP) Section 3.7.1, “Seismic Design Parameters,” to be used in the soil structure interaction (SSI) analysis for the pad. Also, new SSE-induced strain-compatible shear modulus (shear wave velocity) and damping values at various soil depths are determined, using SHAKE2000 (Reference 26), in accordance with the guidance in SRP Section 3.7.2, “Seismic System Analysis”, for use in the SSI analysis. To provide for the dynamic analysis of the pad, a calculation was developed to evaluate the seismic stability of free-standing casks placed on the pad for the SSE. The calculation also evaluates the structure-soil-structure interaction (SSSI) effects of the southeast pad on the original eastern pad. Linear SSI analyses are performed using the SASSI2010 program (Reference 27) and the SSSI is performed using results from the Response Spectrum Generator (RSG) program (Reference 28). 60400000330

The dynamic analysis determined that the design of the southeast pad is acceptable and concluded that:

(1) The casks do NOT slide or overturn during an SSE;

(2) The pad does NOT slide relative to the soil during SSE; and,

(3) The SSSI effects between the southeast pad and original pads are insignificant.

A4.2.2 STORAGE SITE LAYOUT

The storage site layout described in Section 4.2.2 remains applicable with the use of the TN-40HT casks.

A4.2.3 STORAGE CASK DESCRIPTION

This section summarizes the structural analysis of the TN-40HT cask. For purposes of structural analysis, the cask has been divided into four components: the cask body (consisting of containment vessel and gamma shield shell), the basket, the trunnions and the neutron shield outer shell.

A4.2.3.1 DESIGN BASIS

A4.2.3.1.1 CASK BODY

The cask body is described in Section A1. Drawings are included in Section A1.5. The containment boundary inner shell and bottom inner plate material is SA-203 Gr. E, and shell flange and lid outer plate is SA-350 Gr. LF3 or SA-203 Gr. E. The shield shell and bottom shield material is SA-266 CL 2 or SA-516 Gr. 70. The lid shield plate material is SA-105 or SA-516 Gr. 70.

The TN-40HT containment vessel is designed, fabricated, examined and tested in accordance with the requirements of Section III, Subsection NB of the ASME Code (Reference 1) to the maximum practical extent. Alternatives taken to the ASME code are specified in Section A3.5. The containment boundary consists of the inner shell and bottom inner plate, shell flange, lid outer plate, lid bolts, vent and drain cover plates and bolts, bolts and the inner portions of the lid seal and the two lid penetrations (vent and drain).

The containment boundary welds are full penetration welds examined volumetrically by radiograph. These welds are also magnetic particle or liquid penetrant examined. Acceptance standards are in accordance with Section III, Article NB-5000.

Other structural and structural attachment welds are examined by the liquid penetrant or the magnetic particle method in accordance with Section V of the ASME Code (Reference 1). The magnetic particle and liquid penetrant examination acceptance standards are in accordance with Section III, Subsection NF, Acticle NF-5000 (Reference 1).

Seal welds are examined visually or by liquid penetrant or magnetic particle methods in accordance with Section V of the ASME Code (Reference 1). Electrodes, wire, and fluxes used for fabrication comply with the applicable requirements of the ASME Code, Section II, Part C (Reference 1).

The welding procedures, welders and weld operators are qualified in accordance with Section IX (and NB-4300 where required) of the ASME Code (Reference 1).

A4.2.3.1.2 BASKET

The basket is a welded assembly of stainless steel boxes and is designed to accommodate 40, 14x14 PWR fuel assemblies. The stainless steel fuel compartments are fusion welded to Type 304 stainless steel structural plates, sandwiched between the box sections. The fusion welds are spaced intermittently along the box sections. Neutron poison plates and aluminum plates are sandwiched between the sections of the stainless steel walls of the adjacent box and the adjacent stainless steel plates. The Type 304 stainless steel members are the primary structural components. The neutron poison plates provide criticality control and the aluminum plates provide a heat conduction path from the fuel assemblies to the cask shell.

Stainless steel transition rails and aluminum shim are oriented parallel to the axis of the basket and attached to the periphery of the basket to establish and maintain basket orientation and to support the basket.

Tangential alignment between the basket and cask cavity is maintained by a key at the perimeter of the basket. This key is designed to prevent the basket from rotating in the cask cavity wall under normal lateral inertial loadings.

A4.2.3.1.3 TRUNNIONS

The TN-40HT cask has two top and two bottom trunnions each of which are one piece forgings composed of SA-105 or SA-266 CL 2 or CL 4 carbon steel.

The two upper trunnions are designed to lift the loaded TN-40HT cask vertically, while the lower trunnions provide capability to rotate the cask prior to loading of spent fuel. The upper trunnions are designed to meet the requirements of NUREG-0612 (Reference 21) for non-redundant lifting fixture. This is accomplished by evaluating the trunnions to the stress design factors required by ANSI N14.6 (Reference 2), i.e. capable of lifting 6 times and 10 times the cask weight without exceeding the yield and ultimate strengths of the material, respectively.

The trunnions are shown in Section A1.5 drawings.

A4.2.3.1.4 OUTER SHELL

The outer shell of the neutron shield consists of a cylindrical shell section with segmented closure plates at each end. Each segmented closure plate is welded together. The top and bottom closure plates are welded to the outer surface of the cask body shield shell. The outer shell provides an enclosure for the resin-filled aluminum containers and maintains the resin in the proper location with respect to the active length of the fuel assemblies in the cask cavity. The outer shell has no other structural function. The shell is painted carbon steel.

A4.2.3.1.5 TOP NEUTRON SHIELD

The top neutron shield consists of a disk of commercial grade polypropylene enclosed in stainless steel. The top neutron shield is attached to and rests on the cask lid. It is protected from the environment by the protective cover.

A4.2.3.2 INDIVIDUAL LOAD CASES

This section describes the analyses performed for the TN-40HT cask under the various loading conditions identified in Section A3.2. These loadings include all of the normal events that are expected to occur regularly. In addition, they include severe natural phenomena and man-induced low probability events postulated because of their potential impact on the immediate environs.

The TN-40HT cask loadings are summarized in Table A3.2-5 and described in Section A3. The loads selected for analysis of the cask are discussed in Section A3.2.5.3. Numerical values of these loads are listed in Tables A3.2-2 through A3.2-4.

The TN-40HT cask components have been evaluated using numerical analyses. Finite element models of the cask body and basket have been developed, and detailed computer analyses have been performed using the ANSYS computer program (Reference 3). The stress analysis of the lid bolts is performed based on the methodology of NUREG/CR-6007 (Reference 4). Other components such as trunnions are analyzed using conventional textbook methods. Table A4.2-1 lists the specific individual load cases analyzed for each major TN-40HT cask component. The sections describing the analyses and the tables listing the stress results, where applicable, are also indicated. TN-40HT cask components are not subjected to any significant cyclic loads such as pressure or temperature fluctuations resulting in an appreciable fatigue usage factor. Also, in the operating temperature range, the materials selected are not subject to significant creep.

A4.2.3.3 STRUCTURAL DESIGN CRITERIA

This section describes the structural design criteria for the major components of the TN-40HT storage cask. The cask consists of four major types of components:

- Containment Boundary
- Non-containment Structure
- Basket
- Trunnions

The structural design criteria for these components are described below:

A4.2.3.3.1 CONTAINMENT BOUNDARY

The containment boundary consists of the inner shell (both cylinder and bottom inner plate) and closure flange out to the seal seating surface and the lid assembly outer plate. The lid bolts and seals and vent and drain plate bolts and seals are also part of the containment boundary. The containment boundary is designed to the maximum practical extent as an ASME Class I component in accordance with the rules of the ASME Code, Section III, Subsection NB. Alternatives to the ASME Code are discussed in Section A3.5

The stresses due to each load are categorized as to the type of stress induced, e.g., membrane, bending, etc., and the classification of stress, e.g., primary, secondary, etc. Stress limits for containment vessel components, other than bolts, for Normal (Design and Level A) and Hypothetical Accident (Level D) Loading Conditions are given in Table A4.2-2. The stress limits used for Level D conditions, determined on an elastic basis, are based on the entire structure (containment shell and shield shell material) resisting the accident load. Local yielding is permitted at the point of contact where the load is applied. If the elastic stress limits cannot be met, the plastic system analysis approach and acceptance criteria of Appendix F of Section III may be used.

The allowable stress limits for all bolts are based on NUREG/CR-6007 (Reference 4) and are listed in Table A4A4-3, Table A4A.4-4, Table A4A.5-1, and Table A4A.5-2.

The allowable stress intensity value, S_m, as defined by the Code, is taken at the maximum temperature calculated for each service load condition.

A4.2.3.3.2 NON-CONTAINMENT STRUCTURES

Certain components such as the shield shell, the neutron shield outer shell and the trunnions are not part of the cask containment boundary but do have structural functions. These components, referred to as non-containment structures, are required to react to the containment or environmental loads and in some cases share loadings with the containment structure. The stress limits for the non-containment structures (excluding the basket and trunnions) are given in Table A4.2-3.

The top neutron shield and the radial neutron shielding including the carbon steel enclosure have not been designed to withstand all of the hypothetical accident loads. The shielding may degrade during the fire or due to cask burial. Also there may be local damage due to tornado impacts. Therefore a bounding analysis assuming that the exterior neutron shielding is completely removed has been performed. This analysis shows that the site boundary accident dose rates are not exceeded. These accidents are described in Section A8.

A4.2.3.3.3 BASKET

The basket is designed, fabricated and inspected in accordance with the ASME Code Subsection NG (Reference 1) to the maximum practical extent. Alternatives to the ASME Code are discussed in Section A3.5.

The stress limits for the basket are summarized in Table A4.2-4. The basket fuel compartment wall thickness is established to meet heat transfer, nuclear criticality, and structural requirements. The basket structure must provide sufficient rigidity to maintain a subcritical configuration under the applied loads. The 304 stainless steel members in the TN-40HT basket are the primary structural components. The aluminum plates are the primary heat conductors and neutron poison plates provide the necessary criticality control.

The fusion welds between the stainless steel support bars and the stainless steel fuel compartments shall be qualified by testing. The required minimum tested capacity of the weld connection shall be based on a margin of safety (test to design) of 1.43 (see Appendix F, Section F-1342 (c) of Reference 1), corrected for temperature difference between testing and basket operating conditions and the maximum weld load at any weld location in the basket.

A4.2.3.4 EVALUATION

The stress calculations performed on the cask and basket are presented in Appendices A4A and A4B respectively. The off-normal loads are bound by normal loads and compared with normal load allowables. Finite element models of the cask body and basket have been developed, and detailed computer analyses have been performed using the ANSYS computer program (Reference 3). The stress analysis of the lid bolts is based on the methodology of NUREG/CR-6007 (Reference 4). Other components such as trunnions are analyzed using conventional textbook methods. Table A4.2-1 lists the specific individual load cases analyzed for each major cask component. The SAR sections where these analyses are described and the tables listing the stress results, where applicable, are also indicated.

Section A3.2 categorizes the loads for the cask body as indicated in Tables A3.2-5 through A3.2-8 into Normal (Level A) and Hypothetical Accident (Level D) Service Loadings. Table A3.2-9 and Table A3.2-10 lists the load combinations to be evaluated. Table A4.2-5 and Table A4.2-6 summarize the combination of the cask body individuals loads evaluated for normal conditions and hypothetical accident conditions respectively. Table A4.2-7 summarizes the basket load combinations. Each combination is a set of loads that are assumed to occur simultaneously.

Key dimensions for the TN-40HT cask body are shown in Figure A4.2-1.

A4.2.3.4.1 CONTAINMENT VESSEL

The evaluation of the containment vessel stresses are summarized along with the evaluation of the gamma shield stress discussed in Section A4.2.3.4.2 below.

A4.2.3.4.2 GAMMA SHIELDING

The maximum nodal stress intensities in cask body components are given in Table A4.2-8 and Table A4.2-9 for normal and accident condition load combinations, respectively. Since trunnions were not modeled, pressure and thermal load nodal stress intensities are reported in outer shield cylinder at nodes close to the trunnion locations.

The following process is used for the evaluation of the load combination stress results presented in Table A4.2-8 and Table A4.2-9.

1. Compare the maximum nodal primary stress intensities (due to mechanical loads) with the membrane stress allowable and compute factors of safety. If no factor of safety is less than 1.5 (a conservatively selected number), then both the P_m & $P_L + P_b$ criteria are met, and the structure is deemed adequate for that loading condition.

2. Compare the maximum nodal primary plus secondary stress intensity (due to mechanical + thermal loads) with $3S_m$ allowable and compute factors of safety. If no factor of safety is less than 1.5 (a conservatively selected number), then $P_L + P_b + Q$ criteria is met, and the structure is deemed adequate for that loading condition.

3. However, if a nodal stress intensity results in factor of safety less than 1.5, then the nodal stresses are linearized for comparison with the allowable stresses.

Using the above conservative process, normal and accident condition nodal stresses are as presented in Table A4.2-8 and Table A4.2-9, respectively. Only the nodal stresses, where factor of safety is less than 1.5, are linearized and evaluated in Table A4.2-10 for normal conditions. For accident condition, margins of safety in Table A4.2-9 are all higher than 1.5 for all load combinations.

Weld stresses for all normal and accident condition load combinations are evaluated in Table 4.2-11. Individual load nodal global forces FX, FY and FZ at weld location nodes are summed up by ANSYS Postprocessor. Weld stresses are calculated for the summed tensile force (FY) and shear force $[FX^2 + FZ^2]^{1/2}$. Weld 1, 2 and 3 locations are defined in Figure A4.2-2, Figure A4.2-3, and Figure A4.2-4 respectively.

- Weld-1 (Between Bottom Plate and Gamma Cylinder), 1.5 inch groove weld
- Weld-2 (Between Flange and Gamma Cylinder), 1 inch groove weld
- Weld-3 (Between Lid and Outer Shield Cylinder), ¾ inch groove and ¼ inch fillet weld

The results of the analysis show that stresses in TN-40HT cask for normal and accident condition loads are below allowable limits with adequate factors of safety. This ensures the structural integrity of TN-40HT cask under normal and accident storage loads.

A4.2.3.4.3 LID BOLTS

The stress intensities in the lid bolts as calculated in Appendix A4A are summarized in Table A4.2-12. The stresses are well below the allowables.

A4.2.3.4.4 BASKET

Analyses for individual basket loads for both normal and accident conditions are provided in Appendix A4B. These individual loads are combined as shown in Table A4.2-7. A summary of the basket stresses for the bounding normal and accident conditions is given in Table A4.2-13 and Table A4.2-14, respectively.

During a hypothetical accident end drop, the fuel assemblies and fuel compartments are forced against the bottom of the cask. It is important to note that, for any vertical loading, the fuel assemblies react directly against the bottom or top end of the cask and not through the basket structure as in lateral loading. It is the dead weight of the basket only that causes axial compressive stress during an end drop. Axial compressive stresses were conservatively computed in Appendix A4B by assuming that all load acts on the compartment tubes during an end drop. During the end drop, the rail supports its own weight by contact with the bottom or top of the cask. Therefore there will not be any stress in rail studs during an end drop.

A4.2.3.4.5 TRUNNIONS

The two upper trunnions are used for lifting the cask and are designed to meet the requirements of NUREG-0612 (Reference 21) for non-redundant lifting fixture. This is accomplished by evaluating the trunnions to the stress design factors required by ANSI N14.6 (Reference 2), i.e. capable of lifting 6 times and 10 times the cask weight without exceeding the yield and ultimate strengths of the material, respectively. The upper trunnion stresses are summarized in Tables A4.2-15 and Table A4.2-16.

The local stresses in the cask body at the trunnion locations due to the loadings applied through the trunnions are not included in the result tables reported in Section A4.2.3.4.2. These local stresses are superimposed on the ANSYS stress results for the cases where the inertial lifting loads are reacted at the trunnions. The local stresses are calculated in accordance with the methodology of WRC Bulletin 107 (Reference 5) which is based on the Bijlaard analysis for local stresses in cylindrical shells due to external loadings. The stress intensity due to the local trunnion loading are combined with the finite element results at the trunnion attachment locations and presented in Table A4A.6-3.

The lower trunnions are not relied upon to support the cask when loaded with fuel, thus their structural analysis is not presented.

A4.2.3.4.6 OUTER SHELL

The neutron shield outer shell stress analyses are summarized in Table A4.2-17. The shell stresses are the highest when the cask is vertical and subjected to 3g inertia load and 25 psig internal pressure. Stresses in the shell will be much lower during normal storage of the TN-40HT cask on the ISFSI pad. The outer shell is not analyzed under tornado missile loading, but it could be damaged by either Missile A or Missile B, as defined in Section A3.2.1.2. The effect of any damage to the outer shell is bounded by the cask body structural evaluation where the outer shell is assumed to be completely removed.

A4.2.3.5 MATERIAL DURABILITY

Materials must maintain the ability to perform their safety functions over the cask's 60-year licensed period under the cask's thermal, radiological, corrosion, and stress environment.

Metallic components

Gamma radiation has no significant effect on metals. The effect of fast neutron irradiation of metals is a function of the integrated fast neutron flux, which is on the order of 10^{14} n/cm^2 inside the TN-40HT cask after 25 years. The integrated fast neutron flux at the end of a 60-year period is projected by conservatively assuming that the average fast neutron flux over the period is the same as that during the first 25 years of storage. Thus, the integrated fast neutron flux for the entire 60-year period is on the order of 2.4E14 n/cm^2. Studies on fast neutron damage in aluminum, stainless steel, and low alloy steels rarely evaluate damage below 10^{17} n/cm^2 because it is not significant (Reference 14). Extrapolation of the data available down to the 10^{14} range confirms that there will be virtually no neutron damage to any of the TN-40HT cask metallic components.

The effect of the TN-40HT cask temperature environment on the required structural properties is accounted for in the structural evaluation. There is no long term degradation of metals in the TN-40HT cask temperature environment. The effect of creep at temperature is the basis for establishing the seal temperature limits.

The cask exterior carbon steel components are protected from corrosion by the paint (epoxy, acrylic urethane, or equivalent enamel coating). A thermal spray coating may be applied before painting. The interior is protected by a thermal spray coating during loading, and by the helium environment inside the cask during storage. The aluminum, carbon steel, neutron absorber, and stainless steel components are not subject to significant corrosion as discussed in Section A4.2.3.6.

The neutron absorbers (Boral®, borated aluminum, or metal matrix composites) consist of aluminum with boron added in the inert form of boron carbide, aluminum diboride, or titanium diboride. The durability of these materials in the dry storage thermal and radiation environment is similar to that of aluminum.

<u>Non-metallic components:</u>

The radial neutron shield resin is inert with respect to water, and the fire retardant mineral fill makes it self-extinguishing. Furthermore, the resin is contained in aluminum tubes inside a steel shell, so that the material is retained in place, and isolated from both water and from sources of ignition.

Elastomer o-rings or gaskets in the weather cover, quick disconnects, drain tube, and pressure relief valve are not important to safety. The quick disconnects are not part of the containment boundary.

Radiation levels and temperature on the cask exterior are not high enough to damage the paint. This is confirmed by dry cask experience. Paint is subject to routine maintenance and touch-up.

The polypropylene in the top neutron shield is slow burning to non-burning according to Table 24, Section 1 of the Handbook of Plastics and Elastomers (Reference 11). Polypropylene is inert with respect to water. Furthermore, the weather protective cover and stainless steel enclosure isolates the top neutron shield material from sources of ignition and from water.

A4.2.3.6 CHEMICAL AND GALVANIC REACTIONS

This section discusses the chemical, galvanic or other reactions of the TN-40HT cask materials that might occur during any phase of loading, unloading, handling or storage.

The TN-40HT cask components are exposed to the following environments:

- During loading and unloading, the casks are submerged in borated pool water. This affects the interior and exterior surfaces of the cask body, lid and the basket. The protective cover, the top neutron shield, and the overpressure system are not submerged in the spent fuel pool. The casks are only kept in the spent fuel pool for a short period of time. Upon removal, the casks are drained, dried, and then backfilled with helium.
- During handling and storage, the exterior of the cask is exposed to normal environmental conditions of temperature, rain, snow, etc. The exterior surfaces with the exception of stainless steel components and trunnion bearing surfaces are protected from environmental exposure by an epoxy, acrylic urethane, or equivalent paint. Thermal spray of the exterior cask surface prior to painting is optional.
- During storage, the interior of the cask is exposed to an inert helium environment. The helium environment does not support the occurrence of chemical or galvanic reactions because moisture or oxygen must be present for corrosion to occur. The cask is thoroughly dried before storage by a vacuum drying process. It is then sealed and backfilled with helium.

- The radial neutron shielding materials and the aluminum resin boxes are sealed during all normal operations. The free volume in the sealed region is very small. The resin material is inert after it has cured and does not affect the aluminum boxes or the carbon steel housing.

A4.2.3.6.1 CASK INTERIOR

The TN-40HT cask materials are shown in the Parts List on the Drawings included in Section A1.5. The containment vessel is made from SA-203 Grade E and SA-350 LF3. This low-alloy carbon steel is grit blasted and coated with a Zn/Al metallic spray for corrosion protection.

The aluminum metallic spray coating is subject to the following service environments:

- After fabrication, closed, and shipped under air.
- At fuel loading, borated spent fuel pool water for a short duration.
- Vacuum-dried and helium backfilled for storage.
- At fuel removal, it may again be exposed to borated spent fuel pool water for a short duration.

The coating is not subject to abrasion except for the one time insertion of the basket.

All sealing surfaces are stainless steel clad by weld overlay. The metallic seals have a stainless steel liner and an aluminum jacket.

The basket is assembled from SA-240 Type 304 stainless steel fuel compartments which are joined to SA-240 Type 304 stainless steel strips by a fusion welding process. Aluminum and neutron absorber plates fit between the fuel compartments. They are not welded or bolted to the stainless steel, but are held in place by the geometry of the compartments and strips. Transition rails made from SA-240 Type 304 stainless steel and aluminum are bolted to the basket.

A4.2.3.6.2 CASK EXTERIOR

The exterior of the cask is carbon steel. The exterior of the cask, with the exception of the trunnion bearing surfaces, is painted using an epoxy, acrylic urethane, or equivalent enamel coating. The paint is selected to be compatible with the pool water and easy to decontaminate. Thermal spray coating prior to painting is optional.

A4.2.3.6.3 LUBRICANTS AND CLEANING AGENTS

Neolube, Loctite N-5000, or equivalent may be used to coat the threads and bolt shoulders of the TN-40HT cask closure bolts. Loctite N-5000 or equivalent may be used to coat the contact areas of the top and bottom trunnions prior to lifting operations. The lubricant shall be removed prior to immersing the cask into the spent fuel pool unless the lubricant has been approved for compatibility with the spent fuel pool water.

The cask and basket are cleaned at the fabricator in accordance with approved procedures. The cleaning agents and lubricants have no significant effect on the cask materials and their important to safety functions.

A4.2.3.6.4 HYDROGEN GENERATION

Prairie Island's report to the NRC (Reference 7) in response to NRC Bulletin 96-04 demonstrates that galvanic reactions in hydrogen generation are insignificant for the TN-40 cask. This report is also applicable for the TN-40HT cask.

A4.2.3.6.5 EFFECT OF GALVANIC REACTIONS ON THE PERFORMANCE OF THE CASK

There are no significant reactions that could reduce the overall integrity of the cask or its contents during storage. The period of immersion in pool water is too short, and any oxidizing gases remaining after vacuum drying and helium backfill is too small to cause corrosion that could have significant effect on the fuel cladding, neutron absorber integrity, or the basket and cask structural performance.

There are no reactions that would cause binding of the mechanical surfaces or the fuel to basket compartment boxes due to galvanic or chemical reactions.

The stainless steel, aluminum, neutron absorber and thermal spray are negligibly affected by the short term exposure to borated water during loading. The three acceptable neutron absorber materials, Boral®, borated aluminum, and metal matrix composites, are all aluminum-based, with the addition of boron in the inert form of boron carbide, aluminum diboride, or titanium diboride. The corrosion behavior of these materials is bounded by Boral® because of its porous core.

While formation of blisters in Boral® during vacuum drying and heating has been reported, this has not been associated with displacement of the Boral® core material containing the boron carbide and therefore has no effect on the Boral® criticality safety design function (Reference 8). Furthermore, in the TN-40HT cask, the Boral® is captured between the structural basket components, including 3/16 inch thick walls of the fuel compartments, to provide it with added mechanical support and durability.

The outer aluminum lid seals may experience some combination of crevice and galvanic corrosion if they are exposed to water for an extended period. However, this would affect only the outer (non-containment) seal, and the overpressure monitoring system would detect any significant leakage.

There is no significant degradation of any important to safety components caused directly by the effects of the reactions or by the effects of the reactions combined with the effects of long term exposure of the materials to neutron or gamma radiation, high temperatures, or other possible ambient or operating conditions.

A4.2.3.7 DIFFERENTIAL THERMAL EXPANSION

This section determines the thermal growths among components of fuel cladding, basket, and cask inner shell in TN-40HT cask. This thermal expansion evaluation covers events of vacuum drying, normal/off-normal and accident storage conditions.

A thermal evaluation of the cask was performed in Section A3.3.2.2 to determine the maximum temperature of the cask components under normal conditions. The analysis considers maximum decay heat and maximum solar heat loading.

The temperature dependent thermal expansion coefficients for structural materials used in this calculation are taken from Table A4.2-18 for the cask and Table A4.2-19 for the basket. The reference temperature for these materials is 70 °F. The thermal expansion coefficient of zircaloy (including ZIRLO) is 6.72×10^{-6} (m/m-K) (3.73×10^{-6} in/in-°F) for temperatures between 300 and 1,073 K (80 to 1,472 °F) as shown in (Reference 9), Figure B-4.3. The reference temperature for zircaloy is 300 K (80 °F) (Reference 9).

<u>Thermal Expansion between the Length of Fuel Assembly and Cask Cavity</u>

The bounding temperatures for the fuel cladding and cask shell under different cases were obtained from Section A3.3.2.2 and are listed in Table A4.2-20.

The hot lengths of fuel assembly and cask cavity are calculated as follows.

The length of the spent fuel assembly when hot is:

$$L_{F,hot} = L_F + [L_Z \times \alpha_Z (T_{max,F} - T_{ref,Z}) + L_{SS} \times \alpha_{SS} (T_{max,F} - T_{ref,SS})] + L_{irr}$$

Where:

$L_{F,hot}$ = Hot length of PWR fuel assembly

L_F = Total length of fuel assembly at room temperature = 161.3 in.

L_Z = Length of Zircaloy guide tube =144 in. (conservatively use active fuel length).

α_Z = Zircaloy axial coefficient of thermal expansion = 3.73E-6 in/in-°F (Reference 9)

L_{SS} = Length of stainless steel per fuel assembly = $L_F - L_z$ = 17.3 in.

α_{SS} = Stainless steel coefficient of thermal expansion (in/in-°F; interpolated using data in Table A4.2-19)

$T_{max,F}$ = Maximum fuel cladding temperature (°F)

$T_{ref,z}$ = Reference temperature for Zircaloy = 80 °F (Reference 9)

$T_{ref,SS}$ = Reference temperature for stainless steel = 70 °F

L_{irr} = Irradiation growth of the spent fuel assembly = 1.25 in.

The hot length of the cask cavity is:

$$L_{C,hot} = L_C\, [1 + \alpha_{LS}\, (T_{avg,C} - T_{ref,C})]$$

Where:

$L_{C,hot}$ = Hot length of cask cavity
L_C = Cold length of cask cavity = 163 in.
α_{LS} = Coefficient of thermal expansion for low alloy steel (in/in-°F; interpolated using data in Table A4.2-18)
$T_{avg.,C}$ = Average temperature of cask inner shell and gamma shield (°F)
$T_{ref,C}$ = Reference temperature for low alloy steel = 70 °F

The hot gap between the fuel assembly and cask cavity is:

$$G_{hot} = L_{C,hot} - L_{F,hot}$$

The calculated hot lengths and gaps for differential length growth between the fuel cladding and the cask cavity are listed in Table A4.2-20.

As seen in Table A4.2-20, the hot gaps are larger than zero. Therefore, adequate clearance has been provided between the spent fuel assemblies and the cask cavity length to permit free thermal expansion.

<u>Thermal Expansion between the OD of Basket and ID of Cask</u>

The average temperatures for the basket, aluminum shim, and cask inner shell at the hottest cross section are retrieved from the result files of thermal analysis performed in Section A3.3.2.2 for storage conditions. Only the stainless steel components of the basket and rails are considered to calculate the average temperature of the basket. These temperatures are used to calculate the differential diametrical growth between the basket and the cask inner shell for storage conditions. These temperatures are listed in Table A4.2-21.

The nominal diametrical cold gap between the basket rails and the cask inner shell is 0.30 in. The size of this gap decreases at elevated temperatures during vacuum drying. Additionally, the maximum temperature of the basket decreases as the gap shrinks. In the worst case of expansion, the gap between the basket and cask inner shell shrinks to zero. Expansion stresses result if the temperature causes additional basket growth. To investigate this worst case condition, the thermal model for vacuum drying described in Section A3.3.2.2 is re-run assuming a zero gap between the basket and the cask inner shell. Reduction of the gap size to zero is implemented in the model by giving a very high conductivity (1000 Btu/hr-in-°F) to the elements in the gap region. To bound the problem and determine the maximum achievable temperatures for basket growth, steady state conditions are considered for the vacuum drying model. An ANSYS macro is used to retrieve the average temperatures for the steady state, vacuum drying model with a zero gap. These temperatures are listed in Table A4.2-21.

The hot diameters of the basket and cask inner shell are calculated as follows.

The largest outer diameter of the hot basket is:

$$OD_{B,hot} = OD_B + [L_{SS,B} \times \alpha_{SS} (T_{avg,B} - T_{ref}) + L_{Sh} \times \alpha_{Al} (T_{avg,Sh} - T_{ref})]$$

Where:

$OD_{B,hot}$ = Hot outer diameter of the basket

OD_B = Maximum cold outer diameter of the basket = 72” – 0.30” = 71.7 in.

$L_{SS,B}$ = Length of basket at 0-180 direction = OD_B – 2×0.46” = 70.83 in.

L_{Sh} = Length of aluminum shim = 2×0.46 = 0.92 in.

α_{SS} = Stainless steel axial coefficient of thermal expansion (in/in-°F; interpolated using data in Table A4.2-19)

α_{Al} = Aluminum coefficient of thermal expansion (in/in-°F; interpolated using data in Table A4.2-19)

$T_{avg,B}$ = Average basket temperature at the hottest cross section (°F)

$T_{avg,Sh}$ = Average shim temperature at the hottest cross section (°F)

T_{ref} = Reference temperature for stainless steel and aluminum alloys = 70 °F

The inner diameter of the hot cask is:

$$ID_{c,hot} = ID_c [1 + \alpha_{LS} (T_{avg,C} - T_{ref})]$$

Where:

$ID_{C,hot}$ = Hot inner diameter of cask cavity

ID_C = Cold inner diameter cask cavity = 72 in.

α_{LS} = Coefficient of thermal expansion for low alloy steel (in/in-°F; interpolated using data in Table A4.2-18)

$T_{avg,C}$ = Average cask inner shell and Gamma Shield temperature at hottest cross section (°F)

T_{ref} = Reference temperature for low alloy steel = 70 °F

The hot gap between the basket outer diameter and cask inner diameter is:

$$G_{hot} = ID_{C,hot} - OD_{B,hot}$$

The calculated hot diameters and gaps for differential diametrical growth between the basket outer diameter and cask inner diameter are listed in Table A4.2-21.

As seen in Table A4.2-21, the hot gaps are larger than zero. Therefore, adequate clearance has been provided between the basket and the cask inner shell to permit free thermal expansion of basket diameter.

Thermal Expansion between Basket Stainless Steel Support Bars and Aluminum Plates along Plate Height

A cold gap of 0.07 in. is considered between the stainless steel support plates and aluminum plates in the basket along the plate height. The average temperatures for the fuel compartments and aluminum plates at the hottest cross section are retrieved from the result files of thermal analyses performed in Section A3.3.2.2 for storage and vacuum drying conditions. The average temperatures for vacuum drying conditions are retrieved at 34 hours after the start of drainage. These temperatures are used to calculate the differential growth between the aluminum plates and the space between two stainless steel support bars. These temperatures are listed in Table A4.2-22.

The space between two stainless steel support bars when hot is:

$$H_{C,hot} = H_C\,[1 + \alpha_{SS}\,(T_{avg,C} - T_{ref})]$$

Where:

$H_{C,hot}$ = Hot space between two stainless steel support bars

H_C = Cold space between two SS support bars = 13.25 in.

α_{SS} = Coefficient of thermal expansion for stainless steel (in/in-°F; interpolated using data in Table A4.2-19.

$T_{avg,C}$ = Average fuel compartment temperature at hottest cross section (°F)

T_{ref} = Reference temperature for stainless steel = 70 °F

The hot height of aluminum plate is:

$$H_{Al,hot} = H_{Al}\,[1 + \alpha_{Al}\,(T_{avg,Al} - T_{ref})]$$

Where:

$H_{Al,hot}$ = Hot height of aluminum plate

H_{Al} = Cold height of aluminum plate = 13.18 in.

α_{Al} = Coefficient of thermal expansion for aluminum alloys (in/in-°F; interpolated using data in Table A4.2-19)

$T_{avg,Al}$ = Average aluminum plate temperature at hottest cross section (°F)

T_{ref} = Reference temperature for stainless steel = 70 °F

The hot gap between the basket aluminum plate and two stainless steel bars is:

$$G_{hot} = H_{C,hot} - H_{Al,hot}$$

The calculated hot dimensions and gaps for differential growth between the aluminum plates and the space between two stainless steel support bars are listed in Table A4.2-22 for both 0-180 and 90-270 directions.

As seen in Table A4.2-22, the hot gaps are larger than zero. Therefore, adequate clearance has been provided between the aluminum plates and stainless steel support bars to permit free thermal expansion along the height of aluminum plates.

Thermal Expansion between Basket Stainless Steel Support Bars and Aluminum Plates along Plate Length

In order to maintain free thermal expansion for basket plates, the edge of an aluminum plate notch should not hit the stainless steel bar located in that notch. Since the aluminum expansion coefficient is larger than stainless steel expansion coefficient, the smallest gap between the notch edge and the stainless steel bar after thermal expansion is located at the furthest notch from the centerline of the aluminum plate.

The average temperatures for the basket aluminum plates and stainless steel support bars at the hottest cross section are retrieved from the result files of thermal analyses performed in Section A3.3.2.2 for storage and vacuum drying conditions. The average temperatures for vacuum drying conditions are retrieved at 34 hours after the start of drainage. These temperatures are used to calculate the differential growth between the aluminum plates and the stainless steel support bars along the plate length. An ANSYS macro is used to retrieve the average temperatures. These temperatures are listed in Table A4.2-23.

The cold distance between the centerline of the aluminum plate and the edge of the furthest notch is:

$$L_{Al,270} = 3 \times 8.86 - 0.75/2 = 26.205 \text{ in.} \quad \text{for 90-270 direction}$$

$$L_{Al,180} = 2.5 \times 8.86 - 0.75/2 = 21.775 \text{ in.} \quad \text{for 0-180 direction}$$

The cold distance between the centerline of the aluminum plate and the edge of the stainless steel plate in the furthest notch is:

$$L_{SS,270} = L_{Al,270} + (0.75\text{-}7/16)/2 = 26.361 \text{ in.} \quad \text{for 90-270 direction}$$

$$L_{SS,180} = L_{Al,180} + (0.75\text{-}7/16)/2 = 21.931 \text{ in.} \quad \text{for 0-180 direction}$$

The hot dimensions for the above distances are:

$$L_{Al,180,hot} = L_{Al,180}\ (1 + \alpha_{Al}\ (T_{avg,Al,180} - T_{ref})]$$

$$L_{Al,270,hot} = L_{Al,270}\ (1 + \alpha_{Al}\ (T_{avg,Al,270} - T_{ref})]$$

$$L_{SS,180,hot} = L_{SS,180}\ (1 + \alpha_{SS}\ (T_{avg,SS,180} - T_{ref})]$$

$$L_{SS,270,hot} = L_{SS,270}\ (1 + \alpha_{SS}\ (T_{avg,SS,270} - T_{ref})]$$

Where:

α_{Al} = Coefficient of thermal expansion for aluminum alloys (in/in-°F; interpolated using data in Table A4.2-19)

α_{SS} = Coefficient of thermal expansion for stainless steel (in/in-°F; interpolated using data in Table A4.2-19)

$T_{avg,xx,yyy}$ = Average temperature of xx plate in yyy direction at hottest cross section (°F)

T_{ref} = Reference temperature for stainless steel = 70 °F

The hot gap between the edge of the notch and the stainless steel plate is:

$G_{hot} = L_{Al,180,hot} - L_{SS,180,hot}$ or $G_{hot} = L_{Al,270,hot} - L_{SS,270,hot}$

The calculated hot distances and gaps between the notch edges of the aluminum plates and the stainless steel bars are listed in Table A4.2-23 for both 0-180 and 90-270 directions.

As seen in Table A4.2-23, the hot gaps are larger than zero. Therefore, adequate clearance has been provided between the aluminum plate notch and the stainless steel support bars to permit free thermal expansion along the plates.

<u>Summary of Differential Thermal Expansion Analysis</u>

The hot gaps calculated between the TN-40HT cask components after thermal expansion are summarized in Table A4.2-24.

As seen in Table A4.2-24, the hot gaps are larger than zero. Therefore, adequate clearance has been provided between the TN-40HT cask components to permit free thermal expansion.

PROPRIETARY - TRADE SECRET INFORMATION WITHHELD PURSUANT TO 10 CFR 2.390

**PROPRIETARY - TRADE SECRET INFORMATION
WITHHELD PURSUANT TO 10 CFR 2.390**

PROPRIETARY - TRADE SECRET INFORMATION
WITHHELD PURSUANT TO 10 CFR 2.390

A4.2.3.8.3 MATERIAL PROPERTIES OF FUEL CLADDING

The fuel cladding is evaluated based on the mechanical properties obtained from Reference 17 which provides expressions to calculate the modulus of elasticity and yield strength for both Zircaloy-2 (BWR cladding) and Zircaloy-4 (PWR cladding). These expressions were derived from correlations of experimental results of several different investigations. Assumptions used include the following:

PROPRIETARY - TRADE SECRET INFORMATION WITHHELD PURSUANT TO 10 CFR 2.390

Temperature is a significant factor in derivation of Zircaloy properties. These properties are calculated over a range of temperatures for Zircaloy-4. An example calculation is carried out below for Zircaloy-4 (PWR cladding) at 750°F.

Modulus of Elasticity (Page 4 of Reference 17)

$$E = \frac{1.088 \times 10^{11} - 5.475 \times 10^{7} \cdot T + K_1 + K_2}{K_3}$$

Where:

E = elastic modulus, Pa

T = temperature, K
= 672.052K (750°F)

$$K_1 = \left(6.61 \times 10^{11} + 5.912 \times 10^{8} \cdot T\right)\Delta$$
= 1.270×10^9

PROPRIETARY - TRADE SECRET INFORMATION
WITHHELD PURSUANT TO 10 CFR 2.390

Where:

CW = cold work, unitless ratio of areas (valid between 0 and 0.75)

PROPRIETARY - TRADE SECRET INFORMATION
WITHHELD PURSUANT TO 10 CFR 2.390

$$K_3 = 0.88 + 0.12 \exp\left(-\Phi / 10^{25}\right)$$

PROPRIETARY - TRADE SECRET INFORMATION
WITHHELD PURSUANT TO 10 CFR 2.390

Φ = fast neutron fluence, n/m^2

PROPRIETARY - TRADE SECRET INFORMATION
WITHHELD PURSUANT TO 10 CFR 2.390

Substituting these values into the expression for E above:

PROPRIETARY - TRADE SECRET INFORMATION
WITHHELD PURSUANT TO 10 CFR 2.390

Yield Stress (Equation 3, Page 3 of Reference 17)

$$\sigma_y = \left[\frac{K}{E^n}\left(\frac{\varepsilon}{10^{-3}}\right)^m\right]^{\frac{1}{1-n}}$$

Strength coefficient

$$K = K(T)\cdot(1+K(CW)+K(\Phi))/K(Zry)$$

Where:

$$K(T) = 1.17628\times10^{9} + 4.54859\times10^{5}T - 3.28185\times10^{3}T^{2} + 1.72752\cdot T^{3}$$
$$= 5.24\times10^{8}$$

PROPRIETARY - TRADE SECRET INFORMATION WITHHELD PURSUANT TO 10 CFR 2.390

$K(\Phi) = 0.731995$ for $\Phi > 7.5 \text{ X } 10^{25}$ n/m^2

$K(Zry) = 1.0$ for Zircaloy-4

Substituting these values into the expression for K above:

PROPRIETARY - TRADE SECRET INFORMATION WITHHELD PURSUANT TO 10 CFR 2.390

Strain Hardening Exponent

$$n = n(T)\cdot n(\Phi)/n(Zry)$$

Where:

n = strain hardening exponent

$$n(T) = -9.490\times10^{-2} + 1.165\times10^{-3}T - 1.992\times10^{-6}T^{2} + 9.588\times10^{-10}T^{3}$$
$$419.4 < T < 1099.0772K$$

$n(\Phi) = 1.608953$ $\Phi > 7.5\times10^{25}\, n/m^{2}$

$n(Zry) = 1.0$ for Zircaloy-4

Substituting these values into the expression for K above:

$$n = 0.07938\cdot1.608953/1.0 = 0.1277$$

Strain Rate

PROPRIETARY - TRADE SECRET INFORMATION WITHHELD PURSUANT TO 10 CFR 2.390

Strain Rate Exponent

$$m = 0.015 \qquad T < 750K$$

$m =$ strain rate exponent

The values calculated above can then be inserted into the following expression for yield stress, σ_y:

$$\sigma_y = \left[\frac{K}{E^n} \left(\frac{\varepsilon}{10^{-3}} \right)^m \right]^{\frac{1}{1-n}}$$

PROPRIETARY - TRADE SECRET INFORMATION
WITHHELD PURSUANT TO 10 CFR 2.390

<u>Calculated values for Modulus of Elasticity and Yield Stress</u>

The expressions above are used to calculate the modulus of elasticity E and the yield stress σ_y over a range of temperatures. The result for Zircaloy-4 (PWR) is presented in Table A4.2-25, Figure A4.2-6 and Figure A4.2-7. Note that the figures included calculated data points not summarized in the Table.

<u>ZIRLO vs Zircaloy-4</u>

Reference 22 states that ZIRLO and Zircaloy-4 alloys are very similar in terms stress/strain characteristics. Therefore Zircaloy-4 properties above are adequate for modeling ZIRLO cladding.

**PROPRIETARY - TRADE SECRET INFORMATION
WITHHELD PURSUANT TO 10 CFR 2.390**

PROPRIETARY - TRADE SECRET INFORMATION
WITHHELD PURSUANT TO 10 CFR 2.390

PROPRIETARY - TRADE SECRET INFORMATION WITHHELD PURSUANT TO 10 CFR 2.390

A4.2.3.8.6 CONCLUSION

From the above results, for an accident condition bottom end drop of a fuel assembly inside a TN-40HT cask, the maximum total strain remains in the elastic range. Since plastic deformation does not occur in this case, it can be concluded that the fuel assembly cladding will not fail in the event of an 18 inch bottom end drop accident.

A4.2.3.9 THERMAL STRESS OF FUEL CLADDING DUE TO UNLOADING OPERATIONS

To evaluate the effects of the thermal loads on the fuel cladding during unloading operations, the following assumptions are made:

- A conservative high maximum fuel cladding temperature of 700 °F and quench water temperature of 50 °F are used.
- The Fuel rod is assumed to be simply supported at both ends.
- The outer surface temperatures of the fuel cladding are conservatively assumed as shown in Figure A4.2-13. 50 °F (water), 212 °F (steam), and 700 °F (cladding) temperature occurs at three equal heights.
- The fuel cladding thickness and cladding outside diameter are reduced by 0.00270 inch to account for oxidation.

A4.2.3.9.1 FINITE ELEMENT MODEL

The finite element model is shown in Figure A4.2-14. ANSYS (Reference 3) finite element Plane 55 and Plane 42 (Axisymmetric) are used for thermal and structural analysis respectively. The fuel rod with the thinnest cladding (WE14 x 14 STD) is modeled, as this will result in the largest temperature gradient across the cladding (temperatures are kept constant at the inner and outer surfaces). The cladding thickness is 0.0216 inches and the rod outer diameter is 0.4166 inches. A tube length of 2 inches is considered for the analysis such that maximum stresses are not affected by the boundary conditions.

A4.2.3.9.2 MATERIAL PROPERTIES

The following material properties are used for the thermal and structural analysis:

Material Properties for Thermal Analysis

Temp °F	Conductivity Btu/hr-in- °F
212	0.655
392	0.689
572	0.732
752	0.790

Material Properties for Structural Analysis

Temp °F	E (psi)	α in/in- °F	γ	S_y (psi) at 750 °F
300	12.2×10^{6}	3.73×10^{-6}	0.404	126,102
400	11.7×10^{6}			116,272
500	11.2×10^{6}			108,921
600	10.7×10^{6}			102,512
700	10.2×10^{6}			95,793
750	9.93×10^{6}			92,000

A4.2.3.9.3 THERMAL ANALYSIS

Steady state thermal analysis was conducted using the surface nodal temperatures as shown in Figure A4.2-13. The inside surface nodal temperatures are all assumed to be 700 °F , and the outside surface temperatures to conservatively represent the quench water temperature. The temperature distribution resulting from this analysis is shown in Figure A4.2-15.

A4.2.3.9.4 THERMAL STRESS ANALYSIS AND RESULTS

A thermal stress analysis using the same model was conducted using the nodal temperatures obtained from the thermal analysis. The resulting nodal stress intensity distribution is shown in Figure A4.2-16. The maximum nodal stress intensity in the fuel cladding is 24.0 ksi. This stress is less than the yield strength of Zircaloy, which is 92 ksi at 750 °F.

A4.2.4 INSTRUMENTATION SYSTEM DESCRIPTION

No important to safety instrumentation is required for the TN-40HT casks due to the passive nature of the ISFSI design.

A4.3 TRANSPORT SYSTEM

A4.3.1 FUNCTION

The information in Section 4.3.1 is independent of cask design.

A4.3.2 COMPONENTS

The information in Section 4.3.2 is independent of cask design.

A4.3.3 DESIGN BASIS AND SAFETY ASSURANCE

The information in Section 4.3.3 is independent of cask design.

A4.3.4 DETERMINATION OF NATURAL FORCES ON A LOADED TRANSPORT VEHICLE

The information in Section 4.3.4 is independent of cask design.

A4.3.4.1 STABILITY OF A LOADED TRANSPORT VEHICLE UNDER TORNADO LOADING

The information in Section 4.3.4.1 is independent of cask design.

A4.3.4.1.1 WIND LOADING

Comparing the dimensions and weight of a TN-40HT cask to a TN-40 cask shows that 1) the overall out side dimension is the same, 2) the TN-40HT cask is slightly shorter, and 3) the nominal weight of a TN-40HT cask is larger. Thus; 1) the clearance between the side of a TN-40HT cask and the cask transport vehicle side members is the same, 2) the center of gravity of the loaded cask transport vehicle is slightly lower, and 3) the weight of the loaded cask transport vehicle would be slightly more. Therefore, the wind speed required to tip the cask transport vehicle with a loaded TN-40HT cask is more than that determined in Section 4.3.4.1.1 and the conclusion that a loaded cask transport vehicle will not tip as a result of the design tornado wind loads is applicable to the TN-40HT casks.

60400000330

60400000330

A4.3.4.1.2 TORNADO MISSILE IMPACT

Comparing the dimensions and weight of a TN-40HT cask to a TN-40 cask shows that 1) the TN-40HT cask is slightly shorter, and 2) the nominal weight of a TN-40HT cask is higher. Thus; 1) the center of gravity of the loaded cask transport vehicle is slightly lower and 2) the weight of the loaded cask transport vehicle would be slightly more. Therefore, the distance the center of gravity would raise due to a tornado missile impact is less than that determined in Section 4.3.4.1.2 and the conclusion that a loaded cask transport vehicle will not tip as a result of the design tornado missile impact is applicable to the TN-40HT casks. 604000000330

A4.3.4.2 FLOOD LEVEL

The information in Section 4.3.4.2 is independent of cask design. 604000000330

A4.3.4.3 EARTHQUAKE

Comparing the dimensions and weight of a TN-40HT cask to a TN-40 cask shows that 1) the TN-40HT cask is slightly shorter, and 2) the nominal weight of a TN-40HT cask is larger. Thus; 1) the center of gravity of the loaded cask transport vehicle is slightly lower and 2) the weight of the loaded cask transport vehicle would be slightly more. Therefore, the g value necessary to tip the loaded cask transport vehicle is higher than that determined in Section 4.3.4.3 and the conclusion that a loaded cask transport vehicle will not tip as a result of the design seismic event is applicable to the TN-40HT casks. 604000000330

A4.4 OPERATING SYSTEMS

A4.4.1 LOADING AND UNLOADING SYSTEMS

A4.4.1.1 FUNCTION

The information in Section 4.4.1.1 is independent of cask design.

A4.4.1.2 MAJOR COMPONENTS AND OPERATING CHARACTERISTICS

The information in Section 4.4.1.2 is independent of cask design.

A4.4.1.3 SAFETY CONSIDERATION AND CONTROLS

The information in Section 4.4.1.3 is independent of cask design.

A4.4.2 DECONTAMINATION SYSTEM

The information in Section 4.4.2 is independent of cask design.

A4.4.3 STORAGE CASK REPAIR AND MAINTENANCE

Maintenance on the TN-40HT casks can be performed as described in Section A5.1.3.3.

A4.4.4 UTILITY SUPPLIES AND SYSTEMS

The TN-40HT storage casks are passive devices. No utility services are needed for operation of the casks.

A4.4.5 OTHER SYSTEMS

A4.4.5.1 ELECTRICAL SYSTEMS

The information in Section 4.4.5.1 is independent of cask design.

A4.4.5.2 ALARM SYSTEM

The information in Section 4.4.5.2 remains applicable with the use of the TN-40HT casks.

A4.4.5.3 FIRE PROTECTION SYSTEM

The information in Section 4.4.5.3 is independent of cask design.

A4.4.5.4 VACUUM SYSTEMS

The information in Section 4.4.5 remains applicable with the use of the TN-40HT casks.

A4.5 CLASSIFICATION OF STRUCTURES, SYSTEMS AND COMPONENTS

The structures, components, and systems of the TN-40HT Dry Storage Casks are classified as “important to safety” or “not important to safety” in accordance with the criteria of 10 CFR 72.3. A tabulation of the major systems and components for a TN-40HT cask is shown in Table A4.5-1. Structures, components, and systems are classified as “important to safety” whose function is:

- to maintain the conditions required to store spent fuel safely,
- to prevent damage to the spent fuel cask during handling and storage, or
- to provide reasonable assurance that spent fuel can be received, handled, packaged, stored, and retrieved without undue risk to the health and safety of the public.

Items that are “important to safety” are further categorized using a graded quality approach based on the following definitions:

Category A Item

Category A items are critical to safe operations. These items include systems and components whose failure could directly result in a condition adversely affecting public health and safety. The failure of a single item could cause loss of primary containment leading to release of radioactive material, loss of shielding, or an unsafe geometry compromising criticality control.

Category B Item

Category B items have a major impact on safety. These items include systems and components whose failure or malfunction could indirectly result in a condition adversely affecting public health and safety. The failure of a Category B item, in conjunction with the failure of an additional item, could result in an unsafe condition.

Category C Item

Category C items have a minor impact on safety. These items include systems and components whose failure or malfunction would not significantly reduce the packaging effectiveness and would not be likely to create a situation adversely affecting public health and safety.

The drawings contained in Section A1.5 show the category classification for each part of a TN-40HT cask.

A4.5.1 CONTAINMENT VESSEL

The containment vessel components are classified as important to safety Category A since they serve as the primary confinement structure for the fuel assemblies. Failure of any of these components could lead to a release of radioactive material.

A4.5.2 PENETRATION GASKETS

The metallic seals on the lid, vent port cover, and drain port cover are classified as important to safety Category A since the inner seal is part of the confinement boundary and a failure of a seal could lead to a release of radioactive material.

A4.5.3 SHIELDING

The gamma and neutron shielding are classified as important to safety Category B. During normal operations there is no credible failure mode for the gamma shield that would prevent it from fulfilling its design shielding function. Under accident conditions the analyses show that the gamma shield remains in place and thus still performs its shielding function. While the neutron shielding may be lost during a fire accident, the analyses show that the resultant dose rates still meet the applicable accident dose limits. The failure of an additional item is necessary for there to be an unsafe condition. Therefore, these components are classified as Category B.

A4.5.4 PROTECTIVE COVER AND OVERPRESSURE SYSTEM

The weather cover and overpressure system serve no safety function and are thus classified as not important to safety.

A4.5.5 CONCRETE STORAGE PADS

The information in Section 4.5.5 remains applicable with the use of the TN-40HT casks except that the accidents are described and analyzed in Section A8.

A4.6 DECOMMISSIONING PLAN

The TN-40HT cask design features inherent ease and simplicity of decommissioning. At the end of its service life, cask decommissioning will be preceded by one of the following options:

> Option 1, the TN-40HT cask, including spent fuel in storage, could be shipped to either a monitored retrievable storage system (MRS) or a geological repository for final disposal, or
>
> Option 2, the spent fuel could be removed from the TN-40HT cask (either at the utility or at another off site location) and shipped in a DOE approved cask.

The first option does not require any decommissioning of the TN-40HT cask at Prairie Island Nuclear Generating Plant. No residual contamination is expected to be left behind on the concrete base pad. The base pad, fence, and periphery utility structures will require no decontamination or special handling after the last cask is removed. The ISFSI pad could be demolished with normal construction techniques.

The second option would require decontamination of the TN-40HT cask. The sources of contamination in the interior of the cask would primarily be crud left from the spent fuel pool water or crud from the spent fuel pins. These are expected to be low levels of contamination which could simply be removed with high pressure water spray. After decontamination, the TN-40HT cask could either be cut up for scrap or partially scrapped. For surface decontamination of the TN-40HT cask, electropolishing or chemical etching can be used to remove the contaminated surface of the cask if necessary.

Section 4.6 contains the cask activation analyses for the TN-40 cask to quantify the specific activities of the cask materials after 20 and 60 years of storage. The results of that analysis are shown in Tables 4.6-1, 4.6-2 and 4.6-3.

Since the TN-40 cask and the TN-40HT cask are very similar in design, the TN-40 activation evaluation can be used to estimate the activity of the TN-40HT cask. Factors are determined that can be applied to results of the TN-40 activation analysis.

The cask bodies are very similar; the TN-40HT has a slightly thinner body and a slightly thicker neutron shield. The TN-40HT basket is heaver than the TN-40 basket with more stainless steel in the basket and the basket rails. The mass factors are shown in the table below:

Zone	TN-40 Mass (kg)	TN-40HT Mass (kg)	TN-40HT Factor
Basket			
SS304	2,770	6,250	2.256
Body, Lid, Rails			
C Steel (SA-105)	56,070	48,563	0.8661
C Steel (SA-203)	12,260	12,555	1.024
SS304	681	3,926	5.765
Neutron Shield			
Resin	4,858	5,573	1.147
Shell, Prot Cover			
C Steel (SA-516)	4,131	4,039	0.9778

The neutron source term for the high burnup fuel assembly in the TN-40HT cask is 7.59E+08 n/s, (Table A7.2-8). From Table 3.1-2, the neutron source for the TN-40 cask is 2.19E+08 n/s. Therefore, the activation flux in each of the zones (cask centerline, cavity wall, etc.) of the TN-40HT is predicted to be 3.466 times larger (7.59E+08/2.19E+08) than the fluxes determined for the TN-40 (Table 4.6-1). To determine the activities after 40 years of storage, an additional factor of 2 is applied, (TN-40 is 20 years).

Utilizing the nuclide activities reported for the TN-40 in Table 4.6-2 and the mass and activation flux factor shown above, the activities can be estimated for the TN-40HT cask. These values are listed in Table A4.6-1. Note the majority of the activated nuclides come from stainless steel. The actual material volumes of the cask components are used to determine the specific activity values for 40 years of storage. The specific activity after 60 years of storage was obtained by increasing the specific activities calculated for 40 years of storage by a factor of 1.5.

To evaluate the TN-40HT cask and basket for disposal, the specific activity of the isotopes listed in Tables 1 and 2 of 10 CFR 61.55 is determined and compared with the limits for Class A waste in those tables.

It is expected that after the application of a surface decontamination method, the radiation levels will be below the acceptable limits of Regulatory Guide 1.86 (Reference 6). The results of the calculation, shown in Table A4.6-2, show that activation of TN-40HT will be far below the specific activity limits for both long and short lived nuclides for Class A waste. A detailed evaluation will be performed at the time of decommissioning to determine the appropriate mode of disposal.

The volume of waste material produced incidental to ISFSI decommissioning is expected to be limited to that resulting from the surface decontamination of the casks if the spent fuel assemblies must be removed.

Furthermore, it is estimated that the cask materials will be only slightly activated as a result of their long term exposure to the relatively small neutron flux emanating from the spent fuel, and that the resultant activation level will be well below the allowable limits for general release of the casks as noncontrolled material. Therefore, it is anticipated that the casks, may be decommissioned from nuclear service by surface decontamination alone, which could be performed at the cask decontamination area in the Auxiliary Building.

The costs of decommissioning the ISFSI are expected to represent a small and negligible fraction of the cost of decommissioning the Prairie Island Nuclear Generating Plant.

A4.7 REFERENCES

1. American Society of Mechanical Engineers, ASME Boiler and Pressure Vessel Code, Sections II, III, V and IX, and appendices 2004 through 2006 addenda.

2. American National Standards Institute, ANSI N14.6, “American National Standard for Special Lifting Devices for Shipping Containers Weighing 10,000 Pounds or More for Nuclear Materials”, 1986.

3. ANSYS Engineering Analysis System, Users Manual for ANSYS Release. 8.0 and 8.1, Swanson Analysis Systems, Inc., Houston, PA.

4. NUREG/CR-6007 "Stress Analysis of Closure Bolts for Shipping Casks," By Mok, Fischer, and Hsu, Lawrence Livermore National Laboratory, 1992.

5. WRC Bulletin 107, March 1979 Revision “Local Stresses in Spherical and Cylindrical Shells Due to External Loadings.”

6. Regulatory Guide 1.86, "Termination of Operating Licenses for Nuclear Reactors."

7. Northern State Power Company, Prairie Island Nuclear Generating Plant, Response to NRC Bulletin 96-04, Docket No. 72-10, Materials License No. SNM-2506.

8. USNRC, Resolution of Generic Safety Issue 196, ADAMS Accession No. MC063520459.

9. US NRC, NUREG/CR-0497 – TREE-1280, Rev. 2, “MATPRO-Version 11 (Rev. 2) A Handbook of material Properties for Use in the Analysis of Light Water Reactor Fuel Rod Behavior.”

10. Aluminum Association Catalog, Aluminum Standards and Data, 1990.

11. Harper, Charles A., ed., “Handbook of Plastics and Elastomers”, McGraw-Hill, 1975.

12. H. E. Adkins, Jr., B. J. Koeppel, and D. T. Tang, “Spent Nuclear Fuel Structural Response when Subject to an End Impact Accident”, PVP-Vol. 483, San Diego, CA, July 25-29 2004.

13. NUREG 1864 “A Pilot Probabilistic Risk Assessment of a Dry Cask Storage System at a Nuclear Power Plant”.

14. U.S. NRC, Regulatory Guide 1.99, Rev. 2, “Radiation Embrittlement of Reactor Vessel Materials”, 1988.

15. T Sanders et al., “A Method for Determining the Spent-Fuel Contribution to Transport Cask Containment Requirements”, Sandia Report SAND90-2406, Sandia National Laboratories, Albuquerque, NM, 1992.

16. UCID - 21246, “Dynamic Impact Effects on Spent Fuel Assemblies”, Lawrence Livermore National Laboratory, October 20, 1987.

17. K. J. Geelhood and C. E. Beyer, “PNNL Stress/Strain Correlation for Zircaloy”, March 2005 (summarized in “Mechanical Properties of Irradiated Zircaloy,” Transactions of the American Nuclear Society, pp 707-708, November 2005).

18. LS-DYNA Keyword User’s Manual, Volumes 1 & 2, Version 9.71s, Rev. 7600.398 August 17, 2006, Livermore Software Technology Corporation.

19. L. F. Van Swam, A. A. Strasser, J. D. Cook, and J. M. Burger, “Behavior of Zircaloy-4 and Zirconium Linear Zircaloy-4 Cladding at High Burnup”, Proceedings of the1997 International Topical Meeting on LWR Fuel Performance, Portland, Oregon March 2-6, 1997.

20. SCALE: “A Modular Code System for Performing Standardized Computer Analyses for Licensing Evaluation”, Vols. I-III, NUREG/CR-0200, Rev. 5 (ORNL/NUREG/CSD-2/R5), March 1997 (Standard Composition Library, Table M8.2.4).

21. NUREG-612 “Control of Heavy Loads at Nuclear Power Plants”, July 1980

22. Letter, Ashok Thadani (NRC) to S. R. Tritch (Westinghouse), “Acceptance for Referencing of Topical Report WCAP-12610 ‘Vantage+ Fuel Assembly Reference Core Report’ (TAC No. 77258)” July 1, 1991.

23. Siegmann, Eric R., J. Kevin McCoy, Robert Howard, “Cladding Evaluation in the Yucca Mountain Repository Performance Assessment,” Material Research Society Symp. Proc. Vol. 608, 2000.

24. NUREG-1536, Revision 1, “Standard Review Plan for Spent Fuel Dry Storage Systems at a General License Facility”, July 2010.

25. SAFE, Version 12.3.1, Computers & Structures, Inc. (Sargent & Lundy, LLC (S&L) Program No. 03.7.241-12.3.1).

604000000330

26. SHAKE2000, Version 9.95 (S&L Program No. 03.7.402-9.95)

27. SASSI2010, Version 1.0 (S&L Program No. 03.7.316-1.0-250USER-M01)

28. Response Spectrum Generator (RSG), Version 2.0 (S&L Program No. 03.7.414-2.0)

604000000330

TABLE A4.2-1
INDIVIDUAL LOAD CASES ANALYZED

Individual Load Description	SAR Section	Individual Stress Result Tables
Cask Body		
Bolt Preload and Lid Seating Pressure	A4A.3 (IL-1)	A4A.3-2
Fabrication Stress	A4A.3 (IL-2)	A4A.3-2
1g Down (Cask vertical, supported at bottom)	A4A.3 (IL-3)	A4A.3-2
Internal Pressure (100 psig)	A4A.3 (IL-4)	A4A.3-2
External Pressure (25 psig)	A4A.3 (IL-5)	A4A.3-2
Thermal Stress Due to Hot Environment (100 ^{o}F ambient)	A4A.3 (IL-6)	A4A.3-2
Thermal Stress Due to Cold Environment (-40 ^{o}F ambient)	A4A.3 (IL-7)	A4A.3-2
3g on Top Trunnion Lifting Load (Calculating cask global stresses, Cask Vertical, 3g Up)	A4A.3 (IL-8)	A4A.3-2
Bounding Loads for Seismic, Tornado and Flood (1g Lateral (resultant) + 2g Down)	A4A.3 (IL-9)	A4A.3-2
Trunnion Local Stress due to 3g Lifting (calculating cask local stress at trunnion / cask shell interface)	A4A.6	A4A.6-3
Lid Bolts		
Bolt Preload	A4A.4	A4A.4-5 A4A.4-6 A4A.4-7
Gasket Seating Load (1399 lb/in.)		
Pressure Load (100 psig)		
Temperature Load (300 °F)		
Basket		
Normal Condition Bounding Loads (3g vertical + 3g lateral)	A4B.1.5	A4B.1-5 A4B.1-6
Accident Condition End Drop (50g)	A4B.1.5	A4.2-14
Trunnions		
6g / 10g Vertical Lifting Load	A4A.6	A4A.6-1 A4A.6-2

TABLE A4.2-2
CONTAINMENT VESSEL STRESS LIMITS

Classification	Stress Intensity Limit
Normal (Level A) Conditions[1]	
P_m	S_m
P_l	$1.5\ S_m$
(P_m or P_l) + P_b	$1.5\ S_m$
Shear Stress	$0.6\ S_m$
Bearing Stress	S_y
(P_m or P_l) + P_b + Q	$3\ S_m$
(P_m or P_l) + P_b + Q + F	S_a
Containment Bolt Normal (Level A) Conditions[3]	
Tensile Stress, F_{tb}	$2/3\ S_y$
Shear Stress, F_{vb}	$0.4\ S_y$
Combined Stress Intensity, S.I.	$0.9\ S_y$
Interaction limit	$\frac{\sigma_{tb}^2}{F_{tb}^2}+\frac{\tau_{yb}^2}{F_{yb}^2}\le 1.0$
Hypothetical Accident (Level D)[2]	
P_m	Smaller of $2.4\ S_m$ or $0.7\ S_u$
P_l	Smaller of $3.6\ S_m$ or S_u
(P_m or P_l) + P_b	Smaller of $3.6\ S_m$ or S_u
Shear Stress	$0.42\ S_u$
Containment Bolt Hypothetical Accident (Level D)[3]	
Tensile Stress, F_{tb}	Minimum ($0.7\ S_u$, S_y)
Shear Stress, F_{vb}	Minimum ($0.42\ S_u$, $0.6\ S_y$)
Combined Stress Intensity, S.I.	Not Required
Interaction Limit	$\frac{\sigma_{tb}^2}{F_{tb}^2}+\frac{\tau_{yb}^2}{F_{yb}^2}\le 1.0$

Notes:
1. Classifications and Stress Intensity Limits are as defined in ASME B&PV Code, Section III, Subsection NB.
2. Stress intensity limits are in accordance with ASME B&PV Code, Section III, Appendix F.
3. Bolt allowables are from Reference 4

TABLE A4.2-3
NON-CONTAINMENT STRUCTURES STRESS LIMITS

Classification	Stress Intensity Limit
Normal (Level A) Conditions[1]	
P_m	S_m
P_l	1.5 S_m
$(P_m + P_l) + P_b$	1.5 S_m
$(P_m + P_l) + P_b + Q$	3 S_m
Shear Stress	0.60 S_m
Bearing Stress	S_y
Hypothetical Accident (Level D)[2]	
P_m	Smaller of 2.4 S_m or 0.7 S_u
P_l	Smaller of 3.6 S_m or S_u
$(P_m + P_l) + P_b$	Smaller of 3.6 S_m or S_u
Shear Stress	0.42 S_u

Notes:

1. Classifications and stress intensity limits are as defined in ASME B&PV Code, Section III, Subsection NB (Reference 1).
2. Stress intensity limits are in accordance with ASME B&PV Code, Section III, Appendix F (Reference 1).

TABLE A4.2-4
BASKET STRESS LIMITS

Classification	Stress Intensity Limit
Normal (Level A) Conditions[1]	
P_m	S_m
P_l	1.5 S_m
$(P_m + P_l) + P_b$	1.5 S_m
$(P_m + P_l) + P_b + Q$	3 S_m
$(P_m + P_l) + P_b + Q + F$	S_a
Shear Stress	0.6 S_m
Hypothetical Accident (Level D)[2]	
P_m	Smaller of 2.4 S_m or 0.7 S_u
P_l	Smaller of 3.6 S_m or S_u
$(P_m + P_l) + P_b$	Smaller of 3.6 S_m or S_u
Shear Stress	Smaller of 0.42 S_u or 2(0.6S_m)

Notes:

1. Classifications and stress intensity limits are as defined in ASME B&PV Code, Section III, Subsection NG (Reference 1).
2. Limits are in accordance with ASME B&PV Code, Section III, Appendix F (Reference 1).

TABLE A4.2-5
SUMMARY OF LOAD COMBINATIONS FOR NORMAL CONDITIONS

Load Comb.	IL-1 Pre-load	IL-2 Fabric-ation	IL-3 Gravity (1g)	IL-4 Internal Pressure	IL-5 External Pressure	IL-6 Thermal (Hot)	IL-7 Thermal (Cold)	IL-8 3g Lift.	IL-10 3g Lifting Trunn. Local Stress
N1	x	x	x	x					
N2	x	x	x		x				
N3	x	x	x	x		x			
N4	x	x	x		x		x		
N5	x	x		x		x		X(1)	
N6	x	x			x		x	X(1)	
N7				x		x			X(2)
N8					x		x		X(2)

Notes:

(1) Calculated cask global stresses due to 3g lifting load.

(2) Calculated cask local stresses at Trunnion/Shield shell due to 3g lifting load.

TABLE A4.2-6
SUMMARY OF LOAD COMBINATIONS FOR ACCIDENT CONDITIONS

Load Comb.	IL-1 Preload	IL-2 Fabrication	IL-3 End Drop (50g)	IL-4 Internal Pressure	IL-5 External Pressure	IL-9 Seismic, Tornado or Flood
A1	x	x	x			
A2	x	x	x	x		
A3	x	x	x		x	
A4	x	x		x		x
A5	x	x			x	x

Note (1): The stress components for the end drop are generated by multiplying the stresses from the 1g load determined in IL-3 by 50.

TABLE A4.2-7
BASKET NORMAL AND ACCIDENT CONDITION LOAD COMBINATIONS

Normal Condition Load Combination	IL-2 3g Lifting	IL-3 3g Vertical, 3g Lateral(1)	IL-4 Thermal (Hot)	IL-5 Thermal (Cold)
N1	x			
N2	x		x	
N3	x			x
N4		x		
N5		x	x	
N6		x		x

Note:
1. This load case not only bounds the normal and off-normal loads but also bounds the loads due to seismic, tornado, or flood and conservatively compares with normal condition load allowables.

Accident Loading Condition	IL-1 50g Vertical Bottom End Drop
A1	x

TABLE A4.2-8
SUMMARY OF LOAD COMBINATION STRESSES FOR NORMAL CONDITIONS

Load Cmb.	Stress Type(3)	Cask Component Nodal Stress Intensity (ksi)								Allow. (ksi)	Min. FOS(2)
		Inner Shell & Bottom Inner Plate	Shell Flange	Lid Outer Plate	Lid Shield plate	Gamma Shield Shell	Bottom Shield Plate	Top Trunn. Region	Bottom Trunn. Region		
N1	Primary	14.07(1)	11.63	8.68	2.17	8.79	7.96	5.48	8.79	20.5	1.46
	Primary+ Secondary	14.07	11.63	8.68	2.17	8.79	7.96	5.48	8.79	61.5	4.37
N2	Primary	15.47(1)	12.29	8.22	0.88	6.61	4.37	4.99	6.61	20.5	1.33
	Primary+ Secondary	15.47	12.29	8.22	0.88	6.61	4.37	4.99	6.61	61.5	3.98
N3	Primary	14.07(1)	11.63	8.68	2.17	8.79	7.96	5.48	8.79	20.5	1.46
	Primary+ Secondary	20.58	12.67	8.55	2.47	10.12	20.81	7.54	10.10	61.5	2.99
N4	Primary	15.47(1)	12.29	8.22	0.88	6.61	4.37	4.99	6.61	20.5	1.33
	Primary+ Secondary	19.44	13.35	7.95	1.05	10.79	15.24	6.74	10.65	61.5	3.16
N5	Primary	12.98	11.43	8.69	2.09	9.23	14.52(1)	5.77	9.23	20.5	1.41
	Primary+ Secondary	24.51	12.44	8.45	2.31	10.63	27.61	7.28	10.59	61.5	2.23
N6	Primary	13.88(1)	12.09	8.22	0.93	7.06	7.89	5.34	7.06	20.5	1.48
	Primary+ Secondary	23.09	13.12	7.95	1.07	10.67	21.94	6.47	10.53	61.5	2.66

Notes:
(1) These stresses result in factor of safety less than 1.5 and are linearized in Table A4.2-10 for revised factors of safety.
(2) Factor of safety for primary loads is calculated by dividing the membrane allowable by nodal stress intensity, hence very conservative.
(3) Primary stress is the nodal stress intensity due to mechanical loads. Primary + Secondary stress is the nodal stress intensity due to mechanical loads + thermal loads.

TABLE A4.2-9
SUMMARY OF LOAD COMBINATION STRESSES FOR ACCIDENT CONDITIONS

Load Cmb.	Cask Component Nodal Stress Intensity (ksi)								Allow. (ksi)	Min.* FOS
	Inner Shell & Btm. Inner Plate	Shell Flange	Lid Outer Plate	Lid Shield Plate	Gamma Shield Shell	Btm. Shield Plate	Top Trunn. Region	Btm. Trunn. Region		
A1	19.31	13.33	8.31	3.62	5.62	5.25	4.44	5.41	49.0	2.54
A2	18.21	12.76	8.43	1.75	5.93	8.97	4.74	5.79	49.0	2.69
A3	19.59	13.47	8.28	4.17	5.56	5.05	4.38	5.43	49.0	2.50
A4	14.68	11.69	8.73	2.10	8.96	9.81	5.47	8.76	49.0	3.33
A5	16.07	12.35	8.24	0.99	6.81	4.72	4.98	6.59	49.0	3.05

* Factor of safety is calculated by dividing the membrane allowable by nodal stress intensity, hence very conservative. All factors of safety are higher than 1.5.

TABLE A4.2-10
LINEARIZED STRESS EVALUATION FOR NORMAL CONDITION LOAD COMBINATIONS

Load Comb.	Component	Nodal Stress Intensity (ksi)	Linearized Stress Intensity			Allow. (ksi)	Factor of Safety
			Node Nos.	Type	Magnitude (ksi)		
N1	Inner Shell & Bottom Inner Plate	14.07	223-253	P_m	12.83	22.9	1.78
				$P_l + P_b$	12.91	34.35	2.66
N2	Inner Shell & Bottom Inner Plate	15.47	224-254	P_m	13.17	22.9	1.74
				$P_l + P_b$	13.60	34.35	2.53
N3	Inner Shell & Bottom Inner Plate	14.07	224-254	P_m	12.64	22.9	1.81
				$P_l + P_b$	13.06	34.35	2.63
N4	Inner Shell & Bottom Inner Plate	15.47	224-254	P_m	13.17	22.9	1.74
				$P_l + P_b$	13.60	34.35	2.53
N5	Bottom Shield	14.52	938-1218	P_m	1.98	20.5	10.35
				$P_l + P_b$	5.67	30.75	5.42
N6	Inner Shell & Bottom Inner Plate	13.53	224-254	P_m	13.12	22.9	1.75
				$P_l + P_b$	13.52	34.35	2.54

TABLE A4.2-11
WELD STRESSES
(PAGE 1 OF 3)

Condition	Load Comb.	Weld No.	Maximum Nodal Forces (kips)		Weld Area (in^2)	Stress (ksi)	Allow-able (ksi)	Factor of Safety
Normal	N1	W-1	Tensile	364	207.35	1.76	21.00	> 10
			Shear	54	207.35	0.26	12.32	> 10
		W-2	Tensile	88	139.02	0.63	21.00	> 10
			Shear	48	139.02	0.35	12.32	> 10
		W-3	Tensile	80	104.95	0.76	21.00	> 10
			Shear	96	104.95	0.91	12.32	> 10
Normal	N2	W-1	Tensile	193	207.35	0.93	21.00	> 10
			Shear	21	207.35	0.10	12.32	> 10
		W-2	Tensile	66	139.02	0.47	21.00	> 10
			Shear	56	139.02	0.40	12.32	> 10
		W-3	Tensile	31	104.95	0.30	21.00	> 10
			Shear	70	104.95	0.67	12.32	> 10
Normal	N3	W-1	Tensile	65	207.35	0.31	21.00	> 10
			Shear	411	207.35	1.98	12.32	6.22
		W-2	Tensile	149	139.02	1.07	21.00	> 10
			Shear	65	139.02	0.47	12.32	> 10
		W-3	Tensile	85	104.95	0.81	21.00	> 10
			Shear	128	104.95	1.23	12.32	> 10
Normal	N4	W-1	Tensile	259	207.35	1.25	21.00	> 10
			Shear	515	207.35	2.48	12.32	4.96
		W-2	Tensile	126	139.02	0.91	21.00	> 10
			Shear	72	139.02	0.52	12.32	> 10
		W-3	Tensile	26	104.95	0.25	21.00	> 10
			Shear	47	104.95	0.45	12.32	> 10

TABLE A4.2-11
WELD STRESSES
(PAGE 2 OF 3)

Condition	Load Comb.	Weld No.	Maximum Nodal Forces (kips)		Weld Area (in^2)	Stress (ksi)	Allow-able (ksi)	Factor of Safety
Normal	N5	W-1	Tensile	164	207.35	0.79	21.00	> 10
			Shear	417	207.35	2.01	12.32	6.13
		W-2	Tensile	157	139.02	1.13	21.00	> 10
			Shear	103	139.02	0.74	12.32	> 10
		W-3	Tensile	82	104.95	0.78	21.00	> 10
			Shear	127	104.95	1.21	12.32	> 10
Normal	N6	W-1	Tensile	358	207.35	1.73	21.00	> 10
			Shear	521	207.35	2.51	12.32	4.91
		W-2	Tensile	133	139.02	0.96	21.00	> 10
			Shear	109	139.02	0.78	12.32	> 10
		W-3	Tensile	29	104.95	0.28	21.00	> 10
			Shear	46	104.95	0.44	12.32	> 10
Accident	A1	W-1	Tensile	1124	207.35	5.42	42.00	7.75
			Shear	1	207.35	0.01	24.64	> 10
		W-2	Tensile	24	139.02	0.17	42.00	> 10
			Shear	53	139.02	0.38	24.64	> 10
		W-3	Tensile	159	104.95	1.52	42.00	> 10
			Shear	281	104.95	2.68	24.64	9.23
Accident	A2	W-1	Tensile	1266	207.35	6.11	42.00	6.89
			Shear	26	207.35	0.13	24.64	> 10
		W-2	Tensile	45	139.02	0.32	42.00	> 10
			Shear	46	139.02	0.33	24.64	> 10
		W-3	Tensile	66	104.95	0.63	42.00	> 10
			Shear	156	104.95	1.49	24.64	> 10

TABLE A4.2-11
WELD STRESSES
(PAGE 3 OF 3)

Condition	Load Comb.	Weld No.	Maximum Nodal Forces (kips)		Weld Area (in^2)	Stress (ksi)	Allow-able (ksi)	Factor of Safety
Accident	A3	W-1	Tensile	1095	207.35	5.28	42.00	7.95
			Shear	8	207.35	0.04	24.64	> 10
		W-2	Tensile	23	139.02	0.17	42.00	> 10
			Shear	54	139.02	0.39	24.64	> 10
		W-3	Tensile	173	104.95	1.65	42.00	> 10
			Shear	314	104.95	2.99	24.64	8.24
Accident	A4	W-1	Tensile	384	207.35	1.85	42.00	> 10
			Shear	100	207.35	0.48	24.64	> 10
		W-2	Tensile	87	139.02	0.63	42.00	> 10
			Shear	51	139.02	0.37	24.64	> 10
		W-3	Tensile	77	104.95	0.73	42.00	> 10
			Shear	93	104.95	0.89	24.64	> 10
Accident	A5	W-1	Tensile	213	207.35	1.03	42.00	> 10
			Shear	85	207.35	0.41	24.64	> 10
		W-2	Tensile	65	139.02	0.47	42.00	> 10
			Shear	59	139.02	0.42	24.64	> 10
		W-3	Tensile	32	104.95	0.30	42.00	> 10
			Shear	73	104.95	0.70	24.64	> 10

TABLE A4.2-12
SUMMARY OF LID BOLT STRESSES

Stress Type	Normal Condition		Accident Condition	
	Stress	Allowable	Stress	Allowable
Average Tensile (ksi)	50.1	93.5	50.1	115.5
Shear (ksi)	13.5	56.1	13.5	69.3
Combined stress intensity (ksi)	57.6	126.3	Not Required (Reference 4)	
Interaction E.Q. $R_t^2 + R_s^2 < 1$	0.345	1	0.226	1
Bearing (ksi)	32.2	33.2	Not Required (Reference 4)	

TABLE A4.2-13
NORMAL CONDITION LOADS AND BASKET STRESS ANALYSIS RESULTS

Loading	Component	Load Comb.	Stress Classification	Loads	Stress (ksi)	Allow. Stress (ksi)
3g Vertical, 3g Lateral + Thermal	Fuel Compartment[1]	N5	$P_m + P_b + Q$	Primary plus Secondary	18.40	48.6
	Rails		$P_m + P_b + Q$		25.84	34.13[2]

Notes:
(1) The component includes fuel compartments and support plates (bars).
(2) The allowable stress in the rail is based on welds with surface PT examination (0.65 factor, per Subsection NG, Table NG-3352-1 (Reference 1).

TABLE A4.2-14
ACCIDENT CONDITION BASKET STRESS ANALYSIS RESULTS

Drop Orientation	Component	Stress Category	Maximum Stress (ksi)	Allowable Stress (ksi)	Factor of Safety
End Drop	Fuel Compartments	P_m	6.56	38.88	5.92

TABLE A4.2-15
SUMMARY OF UPPER TRUNNION STRESSES (YIELD STRENGTH CASE)

6/3g Load	Upper Trunnion (3g/Trunnion)	
Trunnion Location(1)	AA	BB
Stress Area (in sq)	113.9	79.8
Area Moment of Inertia (in^4)	3,082.0	755.6
Shear Force (lb)	750,000	750,000
Applied Moment (in lb)	5,062,500	1,590,000
Shear Stress (psi)	6,586	9,402
Bending Stress (psi)	13,962	11,837
Stress Intensity (psi)	19,195	22,220
Allowable Stress (psi)	31,800	31,800

(1) The cross section locations AA and BB are as shown on Figure A4A.6-1.

TABLE A4.2-16
SUMMARY OF UPPER TRUNNION STRESSES (ULTIMATE STRENGTH CASE)

10g Load	Upper Trunnion (5g/Trunnion)	
Trunnion Location[1]	AA	BB
Stress Area (in sq)	113.9	79.8
Area Moment of Inertia (in^4)	3,082.0	755.6
Shear Force (lb)	1,250,000	1,250,000
Applied Moment (in lb)	8,437,500	2,650,000
Shear Stress (psi)	10,976	15,671
Bending Stress (psi)	23,271	19,728
Stress Intensity (psi)	31,991	37,033
Allowable Stress (psi)	70,000	70,000

(1) The cross section locations AA and BB are as shown on Figure A4A.6-1.

TABLE A4.2-17
SUMMARY OF NEUTRON SHIELD OUTER SHELL STRESSES

Loading	Stress Intensities (ksi)	Allowable Stress[1] (ksi)
25 psig Internal Pressure	4.92	33.6
25 psig + 3g Inertia (Cask in Vertical Orientation)	7.04	33.6

Note:
(1) Allowable stress the outer shell material, SA-516 GR.70, at 300 °F is 1.5 S_m = 33.6 ksi.

TABLE A4.2-18
TEMPERATURE DEPENDENT CASK BODY PROPERTIES OF MATERIALS
(PAGE 1 OF 2)

Cask Component	Material(1)	Temp. (°F)	Ultimate Strength S_u (ksi)	Yield Strength S_y (ksi)	Allowable S_m (ksi)	Young's Modulus E (psi)	Thermal Expansion α (in/in/°F)
Inner Shell and Bottom Inner Plate	SA-203 Gr. E	70	70	40	23.3	27.8×10^6	6.4×10^{-6}
		200	70	36.6	23.3	27.1×10^6	6.7×10^{-6}
		300	70	35.4	23.3	26.7×10^6	6.9×10^{-6}
		400	70	34.2	22.9	26.2×10^6	7.1×10^{-6}
Shell Flange	SA-350 LF3, or SA-203 Gr. E	70	70	37.5	23.3	27.8×10^6	6.4×10^{-6}
		200	70	34.3	22.9	27.1×10^6	6.7×10^{-6}
		300	70	33.2	22.1	26.7×10^6	6.9×10^{-6}
		400	70	32.0	21.4	26.2×10^6	7.1×10^{-6}
Lid Outer Plate	SA-350 LF3 or SA-203 Gr. E	70	70	37.5	23.3	27.8×10^6	6.4×10^{-6}
		200	70	34.3	22.0	27.1×10^6	6.7×10^{-6}
		300	70	33.2	21.2	26.7×10^6	6.9×10^{-6}
		400	70	32.0	20.5	26.2×10^6	7.1×10^{-6}
Lid Shield Plate	SA-105 or SA-516, Gr.70	70	70	36	23.3	29.0×10^6	6.4×10^{-6}
		200	70	33	22.0	28.5×10^6	6.7×10^{-6}
		300	70	31.8	21.2	28.0×10^6	6.9×10^{-6}
		400	70	30.8	20.5	27.6×10^6	7.1×10^{-6}
Gamma Shield Shell and Bottom Shield	SA-266 CL 2 or SA-516, Gr.70	70	70	36	23.3	29.0×10^6	6.4×10^{-6}
		200	70	33	22.0	28.5×10^6	6.7×10^{-6}
		300	70	31.8	21.2	28.0×10^6	6.9×10^{-6}
		400	70	30.8	20.5	27.6×10^6	7.1×10^{-6}

TABLE A4.2-18
TEMPERATURE DEPENDENT CASK BODY PROPERTIES OF MATERIALS
(PAGE 2 OF 2)

Cask Component	Material(1)	Temp. (oF)	Ultimate Strength Su (ksi)	Yield Strength Sy (ksi)	Allowable Sm (ksi)	Young's Modulus E (psi)	Thermal Expansion α (in/in/oF)
Lid Bolt	SA-540 Gr. B24 or B23, Cl.1	70	165	150	50.0	$27.8x10^{6}$	$6.4x10^{-6}$
		200	165	144	47.8	$27.1x10^{6}$	$6.7x10^{-6}$
		300	165	140.3	46.2	$26.7x10^{6}$	$6.9x10^{-6}$
		400	165	137.9	44.8	$26.2x10^{6}$	$7.1 x10^{-6}$
Outer Shell	SA-516, Gr.70	70	70	38	23.3	$29.0x10^{6}$	$6.4x10^{-6}$
		200	70	34.8	23.2	$28.5x10^{6}$	$6.7x10^{-6}$
		300	70	33.6	22.4	$28.0x10^{6}$	$6.9x10^{-6}$
		400	70	32.5	21.6	$27.6x10^{6}$	$7.1 x10^{-6}$
Upper and Lower Trunnions	SA-105 or SA-266 CL 2 or CL 4	70	70	36	23.3	$29.0x10^{6}$	$6.4x10^{-6}$
		200	70	33	22.0	$28.5x10^{6}$	$6.7x10^{-6}$
		300	70	31.8	21.2	$28.0x10^{6}$	$6.9x10^{-6}$
		400	70	30.8	20.5	$27.6x10^{6}$	$7.1 x10^{-6}$
Protective Cover And Flange	SA-516, Gr.70 or SA-105	70	70	36	23.3	$29.0x10^{6}$	$6.4x10^{-6}$
		200	70	33	22.0	$28.5x10^{6}$	$6.7x10^{-6}$
		300	70	31.8	21.2	$28.0x10^{6}$	$6.9x10^{-6}$
		400	70	30.8	20.5	$27.6x10^{6}$	$7.1 x10^{-6}$
Vent /Drain Port Cover and Top Neutron Shield Bolts	SA-193 Gr. B7	70	125	105	35.0	$29.0x10^{6}$	$6.4x10^{-6}$
		200	125	98	32.6	$28.5x10^{6}$	$6.7x10^{-6}$
		300	125	94.1	31.4	$28.0x10^{6}$	$6.9x10^{-6}$
		400	125	91.5	30.5	$27.6x10^{6}$	$7.1 x10^{-6}$

Note:
(1) Lower strength of the different materials is listed in the table.

TABLE A4.2-19
TEMPERATURE DEPENDENT BASKET MATERIAL PROPERTIES

Part	Material	Temp. (˚F)	Ultimate Strength S_u (ksi)	Yield Strength S_y (ksi)	Allowable S_m (ksi)	Young's Modulus E (psi)	Thermal Expansion α (in/in/°F)
Stainless Steel Plates	SA-240, Type 304	70	75.0	30.0	20.0	28.3×10^6	8.5×10^{-6}
		300	66.2	22.4	20.0	27.0×10^6	9.2×10^{-6}
		400	64.0	20.7	18.6	26.4×10^6	9.5×10^{-6}
		500	63.4	19.4	17.5	25.9×10^6	9.7×10^{-6}
		600	63.4	18.4	16.6	25.3×10^6	9.8×10^{-6}
		700	63.4	17.6	15.8	24.8×10^6	10.0×10^{-6}
Aluminum Plates	SB-209 Type 6061	70	—	—	—	—	12.1×10^{-6}
		300	—	—	—	—	13.3×10^{-6}
		400	—	—	—	—	13.6×10^{-6}
		500	—	—	—	—	13.9×10^{-6}
		600	—	—	—	—	14.2×10^{-6}
		700	—	—	—	—	—
Aluminum Plates	SB-209 Type 1100	70	—	—	—	—	12.1×10^{-6}
		300	—	—	—	—	13.3×10^{-6}
		400	—	—	—	—	13.6×10^{-6}
		500	—	—	—	—	13.9×10^{-6}
		600	—	—	—	—	14.2×10^{-6}
		700	—	—	—	—	—

Note: Material properties are taken from ASME Section II, Part D, 2004 including 2006 Addenda (Reference 1) and Aluminum Standards and Data (Reference 10).

TABLE A4.2-20
LENGTH GROWTH BETWEEN FUEL AND CASK

Condition	$T_{max,F}$ (°F)	α_Z (in/in-°F)	α_{SS} (in/in-°F)	$L_{F,hot}$ (in)	$T_{max,C}$ (°F)	α_{LS} (in/in-°F)	$L_{C,hot}$ (in)	Hot Gap (in)
Storage	694	3.73E-6	9.96E-6	162.988	302$^{(1)}$	6.90E-6	163.261	0.273
Vacuum Drying	731	3.73E-6	10.0E-6	163.014	232$^{(1)}$	6.76E-6	163.179	0.165

Note:
(1) Conservatively use the average temperature of inner shell and gamma shield shell.

TABLE A4.2-21
DIAMETRICAL GROWTH BETWEEN THE BASKET AND THE CASK

Conditions	$T_{avg,B}$ (°F)	$T_{avg,Sh}$ (°F)	α_{SS} (in/in-°F)	α_{Al} (in/in-°F)	$OD_{B,hot}$ (in)	$T_{avg,C}$ (°F)	α_{LS} (in/in-°F)	$ID_{C,hot}$ (in)	Hot Gap (in)
Storage	494	373	9.69E-6	13.49E-6	71.995	302(1)	6.90E-6	72.115	0.120
Vacuum Drying	580	374	9.80E-6	13.50E-6	72.058	360(2)	7.02E-6	72.147	0.089

Notes:
(1) Based on the average temperature of both the inner shell and gamma shield.
(2) Based on the average temperature of both the inner shell and gamma shield calculated from zero gap between the basket and cask inner shell.

TABLE A4.2-22
AXIAL GROWTH BETWEEN BASKET AND ALUMINUM PLATES AND SS SUPPORT BARS

For 0-180 Direction									
Conditions	H_C (in)	$T_{avg,c,180}$ (°F)	α_{SS} (in/in-°F)	$H_{C,hot}$ (in)	H_{Al} (in)	$T_{avg,Al,180}$ (°F)	α_{Al} (in/in-°F)	$H_{Al,hot}$ (in)	Hot Gap (in)
Storage	13.25	575	9.80E-06	13.316	13.18	587	1.417E-05	13.277	0.039
Vacuum Drying	13.25	635	9.87E-06	13.324	13.18	644	1.429E-05	13.288	0.036
For 90-270 Direction									
Conditions	H_C (in)	$T_{avg,c,270}$ (°F)	α_{SS} (in/in-°F)	$H_{C,hot}$ (in)	H_{Al} (in)	$T_{avg,Al,270}$ (°F)	α_{Al} (in/in-°F)	$H_{Al,hot}$ (in)	Hot Gap (in)
Storage	13.25	550	9.80E-06	13.312	13.18	551	1.410E-05	13.269	0.043
Vacuum Drying	13.25	608	9.82E-06	13.320	13.18	607	1.421E-05	13.281	0.039

TABLE A4.2-23
LENGTH GROWTH BETWEEN ALUMINUM PLATES AND SS SUPPORT BARS

0-180 Direction									
Conditions	$L_{Al,180}$ (in)	$T_{avg,Al,180}$ (°F)	α_{Al} (in/in-°F)	$L_{Al,180,hot}$ (in)	$L_{SS,180}$ (in)	$T_{avg,SS,180}$ (°F)	α_{SS} (in/in-°F)	$L_{SS,180,hot}$ (in)	**Gap (in)**
Storage	21.775	587	14.17E-06	21.935	21.931	575	9.80E-06	22.040	0.105
Vacuum Drying	21.775	644	14.29E-06	21.954	21.931	635	9.87E-06	22.053	0.099
90-270 Direction									
Conditions	$L_{Al,270}$ (in)	$T_{avg,Al,270}$ (°F)	α_{Al} (in/in-°F)	$L_{Al,270,hot}$ (in)	$L_{SS,270}$ (in)	$T_{avg,SS,270}$ (°F)	α_{SS} (in/in-°F)	$L_{SS,270,hot}$ (in)	**Gap (in)**
Storage	26.205	551	14.10E-06	26.383	26.361	550	9.80E-06	26.485	0.102
Vacuum Drying	26.205	607	14.21E-06	26.405	26.361	608	9.82E-06	26.500	0.095

TABLE A4.2-24
SUMMARY OF HOT GAPS FOR THE TN-40HT CASK

Hot Gap (in)						
Conditions	Fuel Assembly / Cask Cavity	Basket OD / Cask ID	Al Plate / SS Bar Height		Al Plate / SS Bar Length	
			0-180	90-270	0-180	90-270
Storage	0.273	0.120	0.039	0.043	0.105	0.102
Vacuum Drying	0.165	0.089	0.036	0.039	0.099	0.095

PROPRIETARY - TRADE SECRET INFORMATION
WITHHELD PURSUANT TO 10 CFR 2.390

PROPRIETARY - TRADE SECRET INFORMATION WITHHELD PURSUANT TO 10 CFR 2.390

TABLE A4.5-1
CLASSIFICATION OF TN-40HT MAJOR COMPONENTS

IMPORTANT TO SAFETY	NOT IMPORTANT TO SAFETY
Containment vessel including lid, flange, inner containment shell & bottom containment plate Lid bolts Lid vent and drain covers, & bolts Basket assembly including fuel compartments, poison plates, & structural plates Trunnions Basket rails Lid, vent & drain seals Radial neutron shield Cask body shield shell Cask body bottom Lid shield plate Top neutron shield including bolts Outer shell	Pressure monitoring system, & overpressure cover Protective cover, bolts, & seal Paint on exterior of cask

TABLE A4.6-1
RESULTS OF 40 YR ACTIVATION ANALYSIS

Curies per TN-40HTCask

Nuclide	Basket	Body, Lid and Rails	Resin and Al Boxes	Outer Shell & Protective Cover	Total
Cr^{51}	5.959E-02	2.015E-02	-----	-----	7.973E-02
Mn^{54}	7.210E-03	5.379E-02	-----	-----	6.100E-02
Fe^{55}	7.914E-02	5.845E-01	-----	1.064E-04	6.637E-01
Fe^{59}	1.464E-03	1.088E-02	-----	-----	1.234E-02
Co^{58}	9.196E-03	6.222E-03	-----	-----	1.542E-02
Co^{60}	1.301E-04	8.692E-05		-----	2.170E-04
Ni^{63}	5.693E-03	3.855E-03		-----	9.548E-03
Zn^{65}	-----	-----	9.541E-05	-----	9.541E-05
Ni^{59}	7.007E-05	3.915E-05	-----	-----	1.092E-04
H^{3}	-----	-----	1.686E-09	-----	1.686E-09
C^{14}	-----	1.252E-09	4.071E-09	2.365E-13	5.324E-09
TOTAL					8.422E-01

Note: Only the nuclides with activity greater than 10^{-5} curies and those listed in 10 CFR 61.55 are reported here.

TABLE A4.6-2
COMPARISON OF TN-40HT ACTIVITY WITH CLASS A WASTE LIMITS

Specific Activity of Long-Lived Isotopes (10CFR61.55 Table 1)

Nuclide	After 40 yrs of storage Ci/m^3	After 60 yrs of storage Ci/m^3	Limit (Ci/m^3)	Volume (m^3)	Component
C^{14}	-----	-----	80	1.539	Basket
Ni^{59}	4.551E-5	6.83E-5	220		
C^{14}	1.461E-10	2.19E-10	80	8.571	Body
Ni^{59}	4.567E-6	6.85E-6	220		
C^{14}	1.153E-9	1.73E-9	80	3.532	Resin
C^{14}	4.587E-13	6.88E-13	80	0.516	Shell

Specific Activity of Short-Lived Isotopes (10CFR61.55 Table 2)

Nuclide	After 40 yrs of storage Ci/m^3 "A"	After 60 yrs of storage Ci/m^3	Limit (Ci/m^3) "B"	Volume (m^3)	Component
Co^{60}	8.453E-5	1.27E-4	700	1.539	Basket
Ni^{63}	3.698E-3	5.55E-3	35		
$T_{1/2}<5$	1.017E-1*	1.53E-1*	700		
Co^{60}	1.014E-5	1.52E-5	700	8.571	Body
Ni^{63}	4.497E-4	6.75E-4	35		
$T_{1/2}<5$	7.881E-2.*	1.18E-1.*	700		
$T_{1/2}<5$	2.064E-4*	3.10E-4*	700	0.516	Shell
H^3	4.773E-10	7.16E-10	40	3.532	Resin
$T_{1/2}<5$	2.701E-5*	4.05E-5*	700		

* - Sum of isotopes with half-life less than 5 years (Cr^{51},Mn^{54},Fe^{55},Fe^{59},Co^{58},Zn^{65})

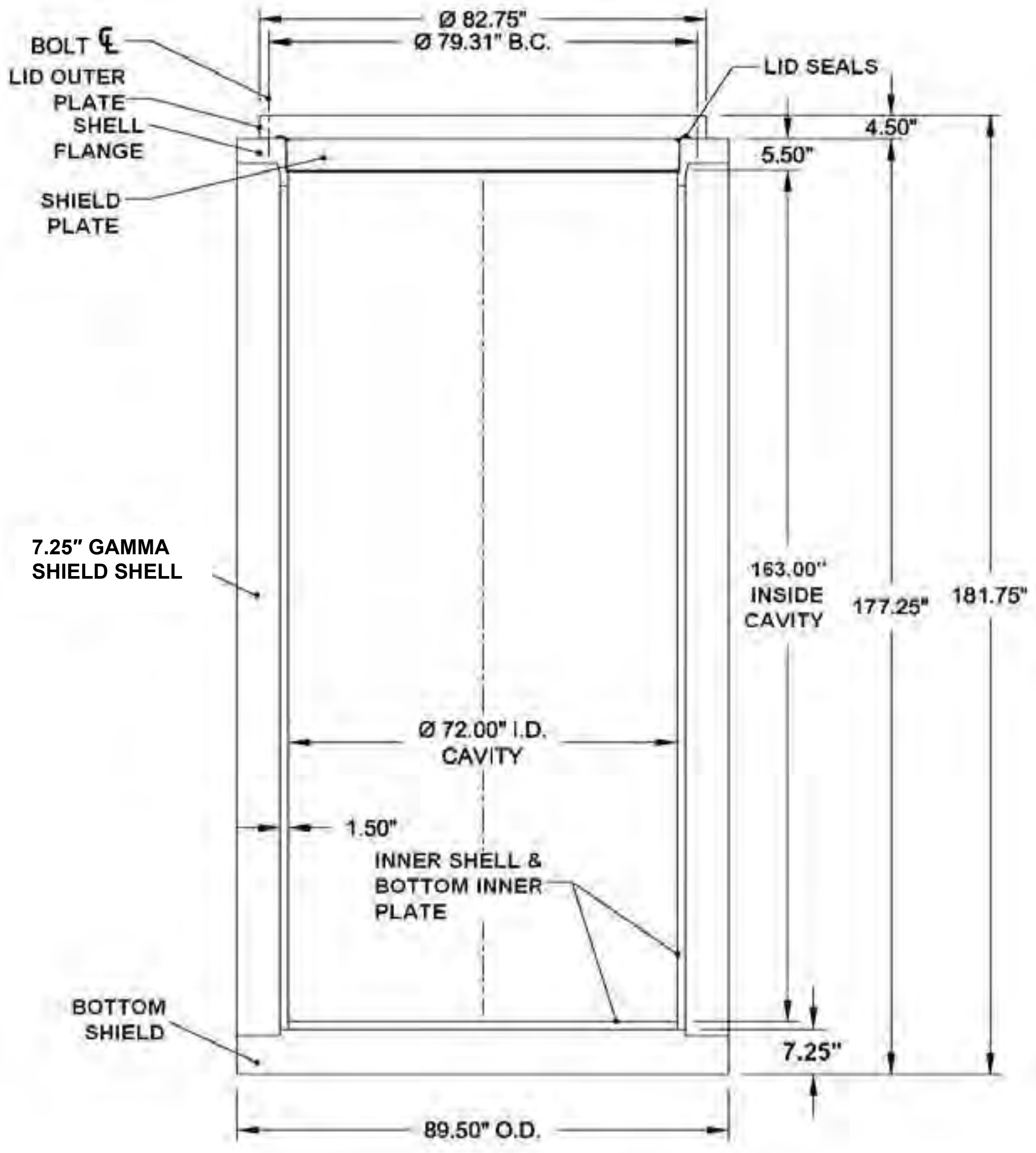

Figure A4.2-1
TN-40HT CASK BODY KEY DIMENSIONS

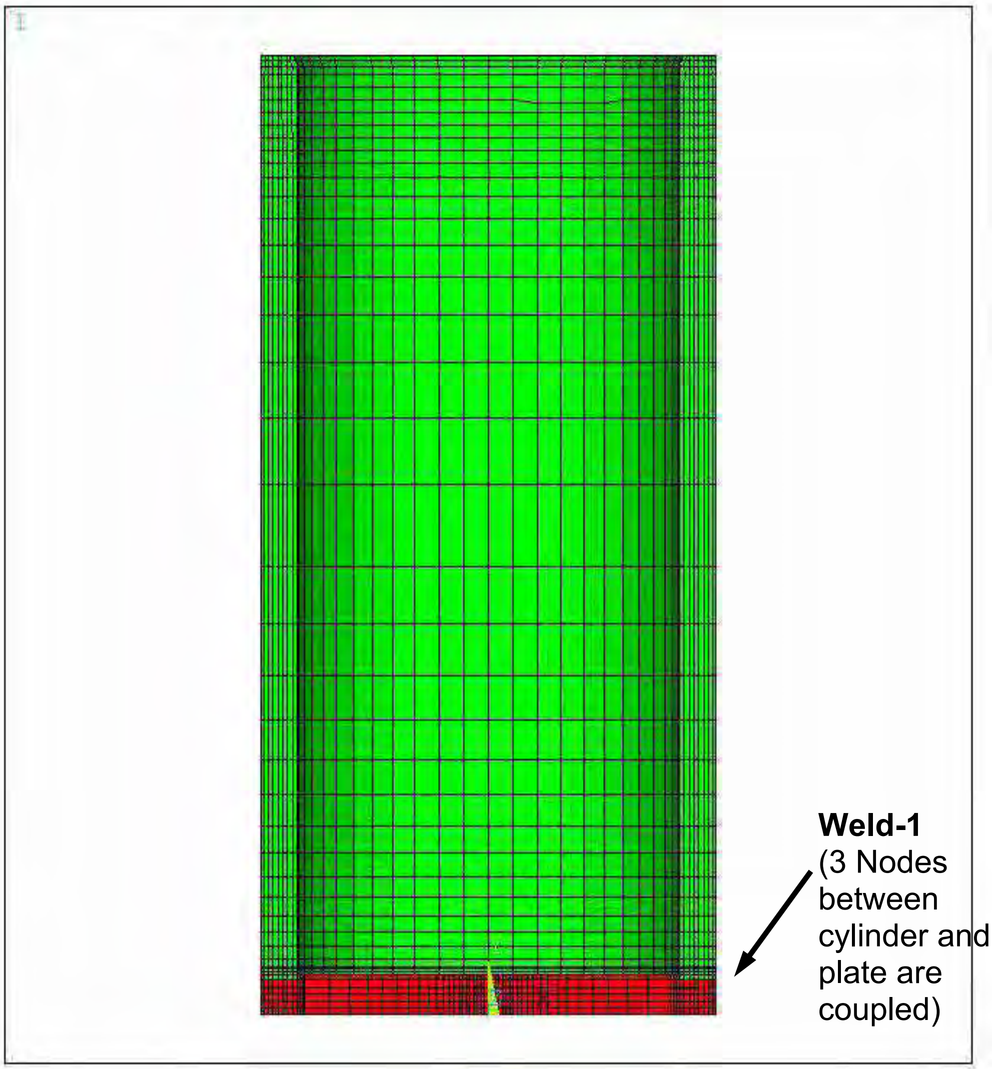

FIGURE A4.2-2
SHIELD SHELL TO BOTTOM SHIELD PLATE WELD

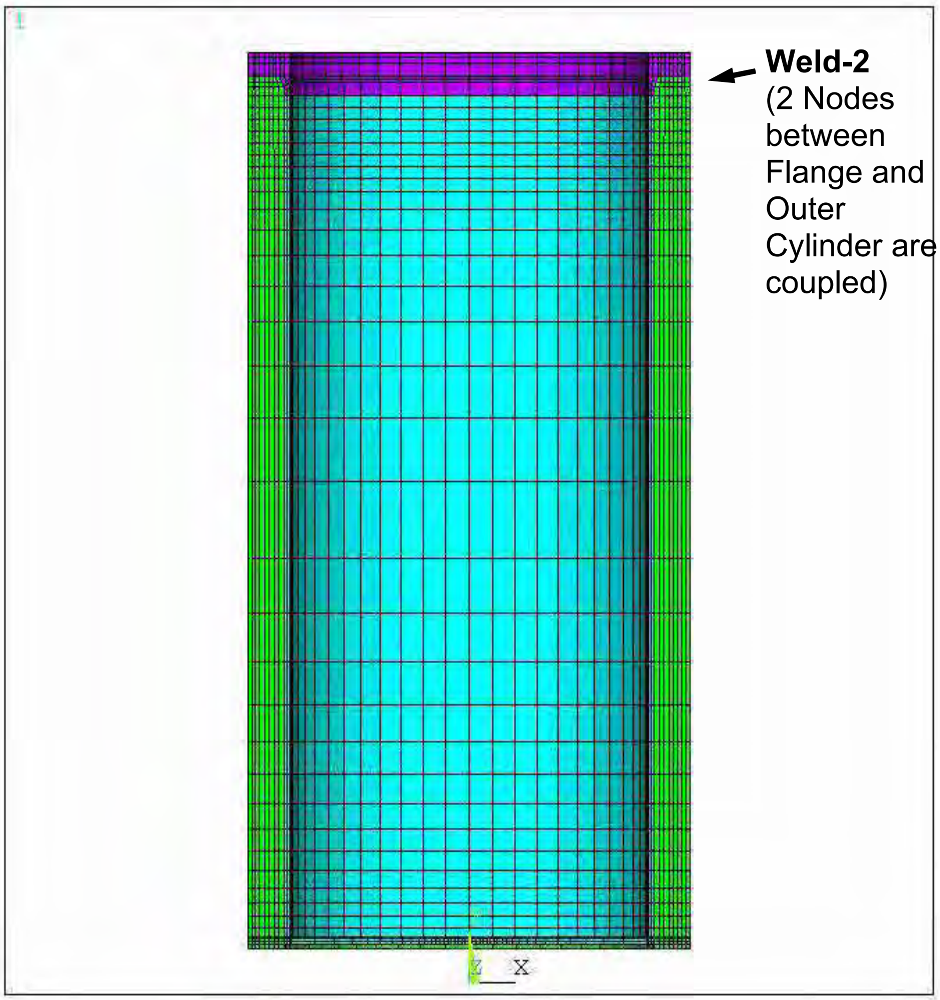

FIGURE A4.2-3
SHIELD SHELL TO SHELL FLANGE WELD

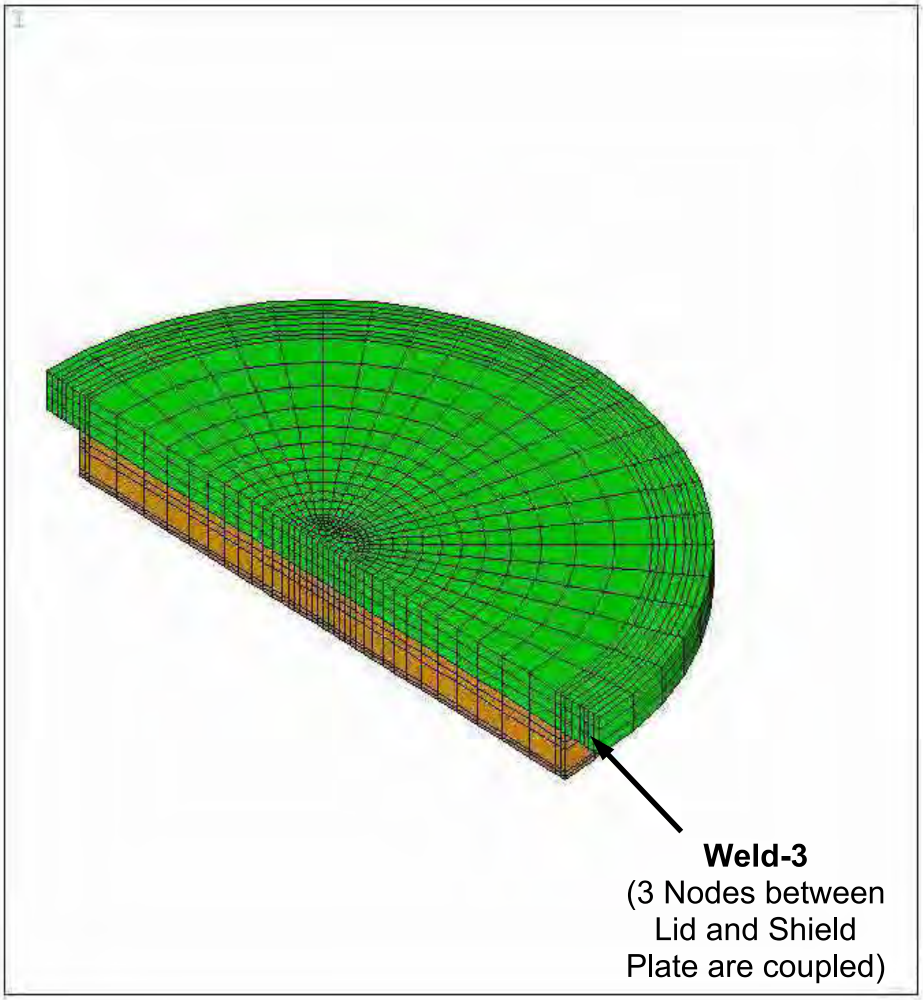

FIGURE A4.2-4
LID OUTER PLATE TO LID SHIELD PLATE WELD

PROPRIETARY - TRADE SECRET INFORMATION
WITHHELD PURSUANT TO 10 CFR 2.390

PROPRIETARY - TRADE SECRET INFORMATION WITHHELD PURSUANT TO 10 CFR 2.390

PROPRIETARY - TRADE SECRET INFORMATION
WITHHELD PURSUANT TO 10 CFR 2.390

PROPRIETARY - TRADE SECRET INFORMATION
WITHHELD PURSUANT TO 10 CFR 2.390

PROPRIETARY - TRADE SECRET INFORMATION
WITHHELD PURSUANT TO 10 CFR 2.390

**PROPRIETARY - TRADE SECRET INFORMATION
WITHHELD PURSUANT TO 10 CFR 2.390**

**PROPRIETARY - TRADE SECRET INFORMATION
WITHHELD PURSUANT TO 10 CFR 2.390**

PROPRIETARY - TRADE SECRET INFORMATION
WITHHELD PURSUANT TO 10 CFR 2.390

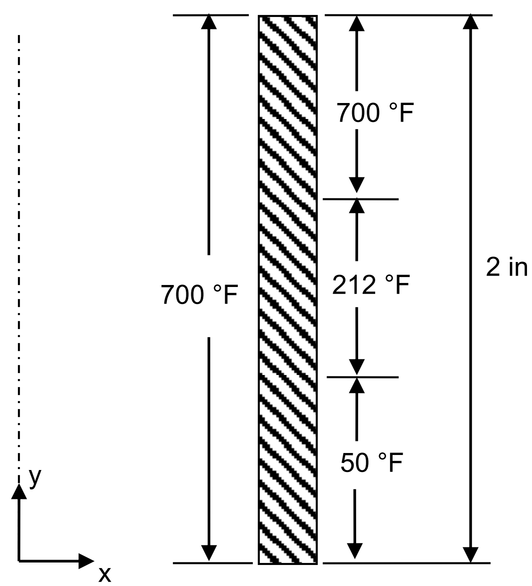

FIGURE A4.2-13
TN40HT FUEL CLADDING OUTER SURFACE TEMPERATURES

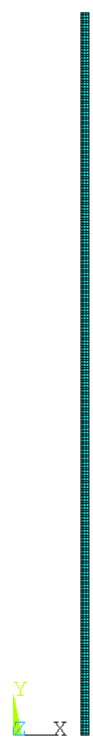

FIGURE A4.2-14
TN40HT FUEL CLADDING FINITE ELEMENT MODEL

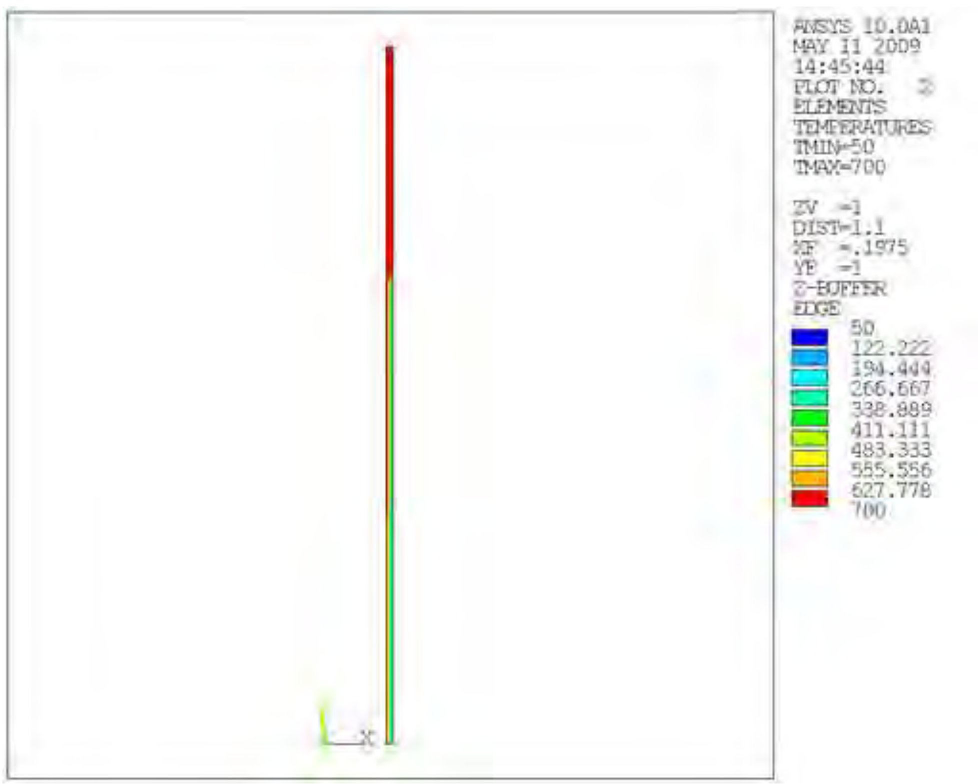

FIGURE A4.2-15
TN40HT FUEL CLADDING TEMPERATURE DISTRIBUTION

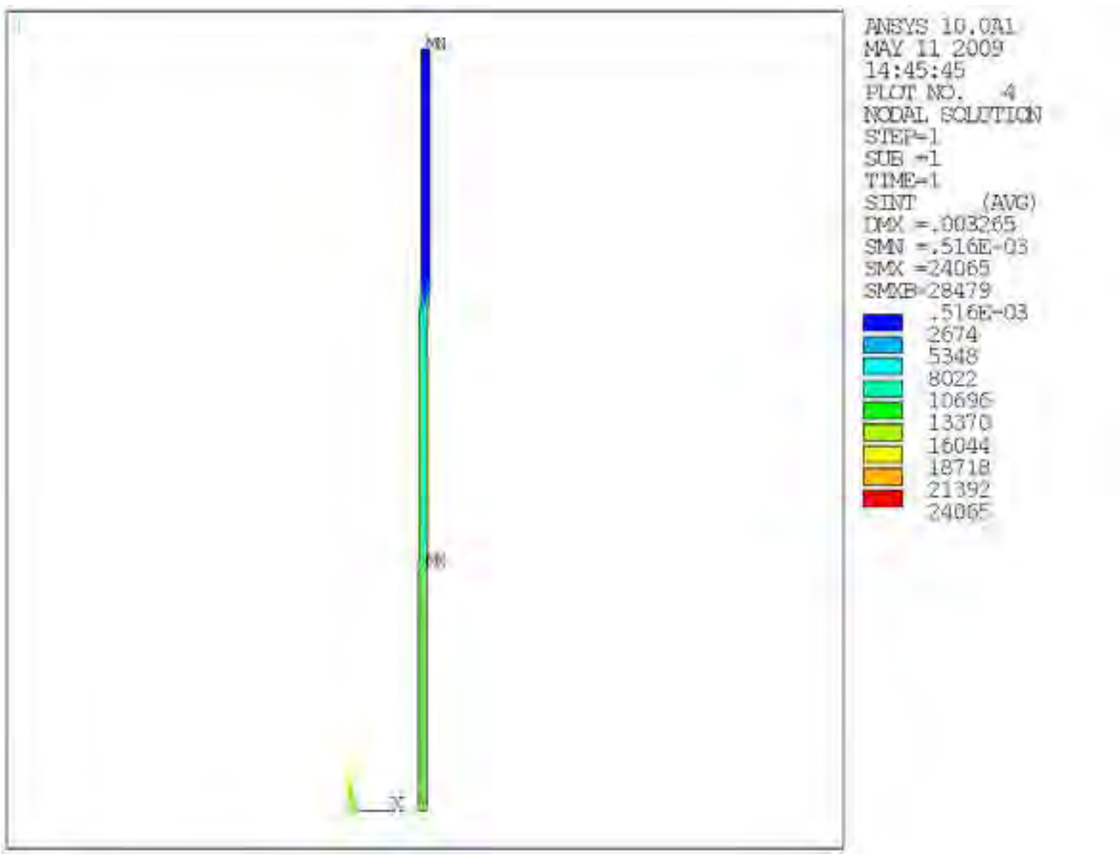

FIGURE A4.2-16
TN40HT FUEL CLADDING STRESS INTENSITY

APPENDIX A4A

STRUCTURAL ANALYSIS OF THE TN-40HT CASK BODY

A4A.1 INTRODUCTION

This appendix presents the structural analysis of the TN-40HT storage cask body which consists of the cask body, the trunnions and the outer shell. Analyses are performed to evaluate the various cask components under the loadings described in Section A3.2. Additional analyses are provided in Section A8 to evaluate the cask body under hypothetical accident loadings.

The detailed calculations for the cask body are presented in Section A4A.3 and the lid bolt analysis is reported in a separate Section A4A.4. The calculations for the trunnions and outer shell are reported in Sections A4A.6 and A4A.7, respectively. Section A4A.8 contains the calculations for the top neutron shield bolts and Section A4A.9 the facture toughness evaluation of the TN-40HT cask.

The design criteria used in the analyses of the cask components are discussed in Section A4.2.3. Key dimension of the storage cask are shown in Figure A4.2-1.

A4A.2 MATERIALS PROPERTIES DATA

This section provides the mechanical properties of materials used in the structural evaluation of the TN-40HT storage cask. Table A4A.2-1 lists the materials selected, the applicable components, and the minimum yield, ultimate, and design stress values specified by the ASME Code. All values reported in Table A4A.2-1 are for metal temperature up to 100°F. For higher temperatures, the temperature dependency of the material properties is reported in Table A4.2-18.

A4A.3 CASK BODY STRUCTURAL ANALYSIS

A4A.3.1 DESCRIPTION

The cask body consists of an inner shell and an outer shield shell (and a bottom shield). The inner shell (and bottom inner plate and shell flange) is the primary confinement barrier of the cask. Key dimensions of the cask body are shown in Figure A4.2-1. The inner shell is 1.5 in. thick cylinder welded to the shell flange and bottom inner plate. The inner shell is shrunk fit into the shield shell. The lid outer plate is bolted to the shell flange by 48, 1.375 in. diameter, high strength bolts and sealed with two metallic seals. The lid outer plate, inner shell, bottom inner plate, shell flange, shield shell and bottom shield components are made of low alloy steel forgings and plates. Two sets of trunnions are welded to the side of the shield shell upper and lower ends for handling and supporting the cask during lifting and handling operations. A basket assembly inside the cask cavity is used to position and support the fuel assemblies. A detailed physical description of the containment components is provided in Section A1. Section A1.5 contains reference drawings of the TN-40HT cask on which the analysis models are based.

A4A.3.2 ANSYS CASK MODEL

The outer shield shell, bottom shield plate, inner shell, bottom inner plate, shell flange, lid outer plate and lid shield plate are modeled utilizing ANSYS eight-node brick elements (SOLID45) as shown in Figure A4A.3-1. The individual cask components used for reporting stresses are shown in Figure A4A.3-2 through Figure A4A.3-6. Due to the cyclic symmetry of the TN-40HT cask body, some nodes in the FEM are rotated into a local cylindrical coordinate system (csys, 11) for easy application of node couplings and boundary conditions. This local coordinate system is located at the model axis of rotation (i.e. global Cartesian X =Y = Z = 0.0). The lid bolts are modeled using BEAM4 elements. The bolt preload is simulated using pre-strain in beam element real constant. The nodes at common surfaces between flange and lid are coupled in the axial direction. The contact surface nodes between outer shield shell inner surface and containment cylinder external surface are radially coupled. Also, the common nodes of the bottom shield plate and bottom inner plate are axially coupled. A total of 20,112 elements and 25,920 nodes comprise the TN-40HT cask finite element model. At the cask cut surface, symmetry boundary conditions are applied. Node couplings between the inner shell and outer shield shell are shown in Figure A4A.3-7. The loadings and displacement boundary conditions for individual load runs are shown in Figure A4A.3-8 through Figure A4A.3-15. To avoid congestion, symmetry boundary conditions (UZ) are not shown in these figures.

For all loading conditions, fuel and basket loads are applied as pressures based on specific component weights, accelerations and applied area. For the seismic loading, a radial cosine pressure distribution, derived in Section A4A.3.6, accounting for the fuel and basket inertial load is used. The radial pressures are applied using ANSYS macros. However, one radial pressure is hand-calculated for load case IL-9 (see below) to check that macro-computed pressures are in "order of magnitude."

Since outer shell, radial neutron shield, aluminum boxes, trunnions, protective cover and top neutron shield are not modeled, their weights are accounted for by increasing the shield shell and lid plate density as follows.

i) Shield Shell Density

Weight Shield Cylinder = π ($44.75^2 - 37.5^2$)(172.65-6.25) x 0.283 = 88,219 lb.

Weights of components not in model:

Radial neutron shield = 12,285 lb
Outer shell = 7,543 lb
Trunnions = 920 lb (955 lb is used)
Aluminum Boxes = 2,233 lb
Protective Cover = 1,362 lb (1,357 lb is used)

Total weight not in the model = 24,343 lb (24,373 lb is used)

Total Weight associated with shield Cylinder = 88,219 + 24,373 = 112,592 lb

Equivalent Density of Shield Cylinder
= (112,592/88,219) x 0.283 = 0.361 lb/in^3
(0.363 is conservatively used in the ANSYS runs)

ii) Lid Density

Weight of lid outer plate and Shield plate = 13,314 lb.

Weight of Top Neutron shield = 1,638 lb. (1,635 lb is used)

Total Weight = 13,314 + 1,635 = 14,949 lb

Equivalent Density of Lid & Shield
= (14,949/13,314) x 0.283 = 0.318 lb/in^3

A4A.3.3 INDIVIDUAL LOAD CASES

The loading conditions analyzed simulate or represent various effects due to the normal and hypothetical accident conditions of storage as specified in 10CFR72. A total of 10 individual loading conditions listed in Table A4A.3-1 are executed for normal and accident load combinations for storage. Load case numbers IL-1 to IL-9 are analyzed elastically in this attachment, using an ANSYS (Reference 1) 3-D Finite Element Model (FEM) and are described in detail in Section A4A3.2 above. Load case IL-10 requires calculation of local stresses at the top and bottom trunnions / shield shell interface and are executed by hand calculations. Load case IL-10 is described in Section A4A.6.

The following describes the individual load cases analyzed using the ANSYS model described above:

1. Bolt Preload and Lid Seating Pressure (IL-1)

    A bolt axial pre-stress of 50 ksi (see Section A4A.4) at the bolt shank (1.375 inch diameter) is simulated by specifying an initial strain in BEAM4 elements representing the bolts. The required initial strain value of 0.002128 in/in (in the bolts) was determined by first calculating the initial strain required to produce an axial stress of 50 ksi (i.e., $\varepsilon = \sigma / E = 50\times10^3 / 26.45\times10^6 = 0.00189$ in/in). Then, an initial analysis with the calculated strain (0.00189 in/in) was conducted and the resulting bolt pre-stress was backed out. Since, a portion of this strain becomes elastic preload strain in the bolts, and a portion becomes strain in the clamped parts, the backed out pre-stress from the initial analysis will not produce the desired 50 ksi. The FEM was then updated by multiplying the 0.00189 in/in strain by the ratio of (desired pre-stress 50 ksi / initial analysis pre-stress), and a second preload analysis was conducted, which resulted in a 50 ksi bolt pre-stress.

    Lid seating pressure due to seating of metallic seals is computed due to 660,129 lb seal reaction (see Section A4A.4). Based on the closest nodes in model to the seal location, the Lid Seating Pressure, $p = 660{,}129 / \pi(38.4^2 - 37.35^2) = 2{,}642$ psi.

    This pressure is applied to the lid and flange seal areas. For the bolt preload and lid seating pressure ANSYS run, the cask is supported as shown in Figure A4A.3-8.

2. Fabrication Stress (IL-2)

The fabrication stresses in the cask are computed due to a 0.040 inch nominal diametric interference between inner shell and shield shell. The shrink fit stresses are based on radial interference of 0.020 inches.

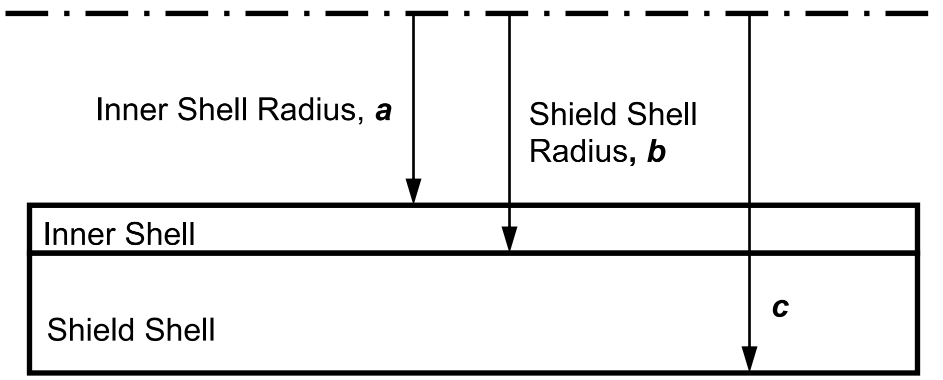

Interface pressure, $p = (E\delta / b) [(b^2 - a^2)(c^2 - b^2) / (2b^2(c^2 - a^2))]$ (Reference 2)

Where,

$\delta = 0.02$ in.
$E = 29.0\text{x}10^6$ psi
$a = 36.0$ in.
$b = 37.5$ in.
$c = 44.75$ in.

Note that using the higher value of *E* for the two materials at room temperature, is conservative, because it results in a higher interface pressure.

$p = (29.0\text{x}10^6 \text{ x } 0.02 / 37.5)$
$\times [(37.5^2 - 36.0^2)(44.75^2 - 37.5^2) / (2 \text{ x } 37.5^2 (44.75^2 - 36.0^2))]$
$= 511.7$ psi ... (515 psi is used)

The radial couplings between the inner shell and shield shell are deleted and the interface 515 psi pressure is applied to the two cylinders. During the run, the cask is supported as shown in Figure A4A.3-9.

3. 1g Down – Cask Support at Bottom (IL-3)

The following inertial load (pressure) magnitudes are applied to the FEM due to 1g vertical acceleration.

An axial pressure due to internals (P_i) is applied on the inside bottom surface of the cask cavity.

Weight of Fuel and Basket $\approx$ 80,100 lb.

$$P_i = 1.0 \times 80{,}100 / ((\pi) \times 36.0^2) = 19.673 \text{ psi}$$

The bottom nodes of cask are supported in the vertical direction. Loading and displacement boundary conditions are shown in Figure A4A.3-10.

4. Internal Pressure Loading (IL-4)

An internal pressure of 100 psig is applied to the cavity surface as shown in Figure A4A.3-11. The pressure is applied up to the metallic seal inner radius. The lid bolt preload and seal seating loads are removed in this run. During the run, the cask is supported as shown in Figure A4A.3-11.

5. External Pressure Loading (IL-5)

An external pressure of 25 psig is applied to the outer surface of the cask body. The pressure is applied up to the seal outer radius. During the run, the cask is supported as shown in Figure A4A.3-11.

6. Thermal Stress for 100 °F Hot Environment Ambient Temperature (IL-6)

The thermal analysis of the cask body is described in Section A3. The thermal model is used to obtain the steady state metal temperatures in the cask body for the normal condition which includes 100° F daily averaged ambient air temperature, maximum decay heat and maximum solar heat loading. The cask nodal temperatures from thermal results file are used to interpolate nodal temperatures in structural model. An ANSYS macro is used to get the nodal temperatures in the structural model. The resulting temperature distribution in cask is shown in Figure A4A.3-12. These temperatures are then used as ANSYS input for the thermal stress analysis. Temperature dependent material properties are used in this run. During the run, the cask is supported as shown in Figure A4A.3-12. It is noted that the maximum temperature in a small region of bottom inner plate exceeds assumed temperature of 350 °F. All other load cases (except thermal stress) are analyzed using the material properties at 350 °F. The effect of this temperature change on material modulus of elasticity will be negligible. The thermal stresses, however, are calculated using exact temperatures and material properties.

7. Thermal Stresses for -40 °F Cold Environment Ambient Temperature (IL-7)

The thermal analysis of the cask body is described in Section A3. The thermal model is used to obtain the steady state metal temperatures in the cask body for the normal condition which includes -40 °F ambient air temperature, minimum decay heat and minimum solar heat loading. The cask nodal temperatures from thermal results file are used to interpolate nodal temperatures in structural model. An ANSYS macro is used to get the nodal temperatures in the structural model. The resulting temperature distribution in cask is shown in Figure A4A.3-13. These temperatures are then used as ANSYS input for the thermal stress analysis. Temperature dependent material properties are used in this run. During the run, the cask is supported as shown in Figure A4A.3-13.

8. 3g Lifting on Front Trunnion (IL-8)

The cask is oriented vertically in space and held by the 2 top trunnions. The inertial loading is simulated by applying a 3g vertical acceleration to the finite element model.
Since the internals are not included in the model, their loading effects are simulated by distributed pressure (P_i) acting on the inside bottom surface of the cask cavity.

Weight of Fuel and Basket $\approx$ 80,100 lb.

$P_i = 3.0 \times 80{,}100 / (\pi \times 36.0^2) = 59.02$ psi.

Loading and displacement boundary conditions are shown in Figure A4A.3-14.

9. Bounding Loads for Seismic, Tornado and Flood (IL-9)

A bounding load of 1g lateral and 2g down for seismic, tornado and flood is applied to the cask in vertical orientation. The cask is assumed to be restrained at the bottom nodes. For the inertial loading, a vertical acceleration of 2g is applied in the global Y direction and 1g lateral acceleration in X direction. Since the internals are not included in the model, their effects are calculated as follows:

i) Vertical loading effect of internals is simulated by a distributed pressure (P_i) acting on the inside bottom surface of the cask cavity.

$P_i = 2.0 \times 80{,}100 / (\pi \times 36.0^2) = 39.347$ psi

ii) The lateral loading effect of internals is simulated by applying a radial cosine varying pressure (internal contact angle 0° to 150° range) to inner shell cavity. The formula below produces the cosine distribution of internal pressure and is derived in Section A4A.3.6.

$$P_r = g\frac{W}{LR}\left[\frac{1}{\dfrac{\sin\left(\dfrac{\pi}{2}+\theta\right)}{\dfrac{\pi}{2\theta}+1}+\dfrac{\sin\left(\dfrac{\pi}{2}-\theta\right)}{\dfrac{\pi}{2\theta}-1}}\right]\cos\left(\frac{\pi\theta i}{2\theta}\right)$$

Where:
θ = ½ Angle of contact = 75°
θ_i = Circumferential angle pressure is applied
W = Weight of internals ~ 80,100 lb
L = Length pressure is applied =163 in
R = Radius pressure is applied = 36 in
g = Acceleration = g's

For example, a pressure applied at an angle of 7.5° would be calculated as follows.

$$\mathrm{P_r} = 1.0\frac{80{,}100}{163.0\times 36}\left[\frac{1}{\dfrac{\sin(90+75)}{\dfrac{180}{2\times 75}+1}+\dfrac{\sin(90-75)}{\dfrac{180}{2\times 75}-1}}\right]\cos\left(\frac{180\times 7.5}{2\times 75}\right)$$

P_r = 13.65(0.7083) (0.9877) = 9.55 psi

Loading and displacement boundary conditions are shown in Figure A4A.3-15. The radial pressures are applied using an ANSYS macro.

A4A.3.4 TRUNNION LOCAL STRESSES

The analyses of the local stresses in the TN-40HT cask body due to the trunnion reactions (while lifting the cask) are evaluated in Section A4A.6 below.

A4A.3.5 EVALUATION (LOAD COMBINATIONS VS. ALLOWABLES)

ANSYS linear elastic analyses are performed for the above individual load cases. A summary of maximum nodal stress intensities in each major cask component under each individual load is presented in Table A4A.3-2. These individual loads are to be combined and evaluated for normal operating and accident conditions in Section A4.2.3.4.

A4A.3.6 PRESSURE DISTRIBUTION OVER CONTACT AREA OF CASK FOR IMPACT IN TRANSVERSE DIRECTION

Inertial loading from the internal basket acting in the transverse direction is applied as a load over the contact area on the inside surface of the cask. The pressure distribution is assumed to vary with a cosine distribution around the circumference of the cask. The circumferential cosine pressure distribution over a half angle θ is calculated as follows.

$$P_i = P_{\max} \cos(\pi\theta_i / 2\theta)$$

Where,

P_i = Pressure load at angle θ_i.
$P_{\max}$ = Peak pressure load, at point of impact, and
θ_i = Angle corresponding to point of interest.

The circumferential pressure distribution is illustrated in the following sketch.

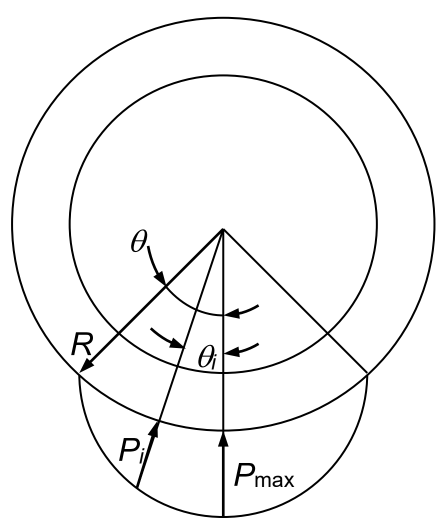

Circumferential Pressure Load Distribution

The peak pressure load $P_{\max}$ is determined by setting the integral of the vertical pressure components Q_i equal to the total transverse impact load F_t as follows.

$$F_t = \int_{-\theta}^{\theta} Q_i LR d\theta_i = \int_{-\theta}^{\theta} P_i \cos(\theta_i) LR d\theta_i = \int_{-\theta}^{\theta} P_{\max} \cos\left(\frac{\pi\theta_i}{2\theta}\right)\cos(\theta_i) LR d\theta_i$$

$$= \frac{P_{\max} LR}{2}\int_{-\theta}^{\theta}\left[\cos\left(\frac{\pi\theta_i}{2\theta}+\theta_i\right)+\cos\left(\frac{\pi\theta_i}{2\theta}-\theta_i\right)\right]d\theta_i$$

$$= \mathrm{P}_{max}\,\mathrm{LR}\left[\frac{sin\left(\frac{\pi}{2}+\theta\right)}{\left(\frac{\pi}{2\theta}\right)+1}+\frac{sin\left(\frac{\pi}{2}-\theta\right)}{\left(\frac{\pi}{2\theta}\right)-1}\right]$$

Rearranging terms gives the peak pressure $P_{\max}$.

$$\mathrm{P}_{max} = \frac{\mathrm{F_t}}{\mathrm{LR}}\left[\frac{sin\left(\frac{\pi}{2}+\theta\right)}{\left(\frac{\pi}{2\theta}\right)+1}+\frac{sin\left(\frac{\pi}{2}-\theta\right)}{\left(\frac{\pi}{2\theta}\right)-1}\right]^{-1}$$

Therefore, the pressure at any circumferential location is given by,

$$Pi = \frac{F_t}{LR}\left[\frac{\sin\left(\frac{\pi}{2}+\theta\right)}{\left(\frac{\pi}{2\theta}\right)+1}+\frac{\sin\left(\frac{\pi}{2}-\theta\right)}{\left(\frac{\pi}{2\theta}\right)-1}\right]^{-1}\cos\left(\frac{\pi\theta_i}{2\theta}\right)$$

where,

$F_t = g \times W$
W = Weight of internals or impact limiter
g = Acceleration in the transverse direction

Therefore,

$$Pi = g\frac{W}{LR}\left[\frac{\sin\left(\frac{\pi}{2}+\theta\right)}{\left(\frac{\pi}{2\theta}\right)+1}+\frac{\sin\left(\frac{\pi}{2}-\theta\right)}{\left(\frac{\pi}{2\theta}\right)-1}\right]^{-1}\cos\left(\frac{\pi\theta_i}{2\theta}\right)$$

A4A.4 LID BOLT ANALYSES

A4A.4.1 INTRODUCTION

This section evaluates the ability of the cask lid bolts to maintain the seal under all applicable loads. Also evaluated in this section are the lid bolt thread and internal thread stresses. The stress analysis is performed in accordance with NUREG/CR-6007 (Reference 3).

The 4.5 inch thick lid outer plate with a 5.5 inch shield plate is bolted directly to the shell flange by 48 high strength alloy steel 1.375 in. diameter bolts (with 1 ½ -8UN threaded portion). Close fitting alignment pins ensure that the lid is centered in the cask. The bolt material is SA-540 Gr. B24 or B23 CL 1 which has a minimum yield strength of 150 ksi at room temperature.

The bolt size, material and design loads for all TN-40HT closures including the lid bolts are provided in Table A4A.4-1.

The following ways to minimize bolt forces and bolt failures for cask are taken directly from Reference 3, page xiii. All of the following design methods are employed in the TN-40HT lid closure system.

- Use materials with similar thermal properties for the closure bolts, the lid, shell flange, and the cask wall to minimize the bolt forces generated by fire accident

- Apply sufficiently large bolt preload to minimize fatigue and loosening of the bolts by vibration.

- Lubricate bolt threads to reduce required preload torque and to increase the predictability of the achieved preload.

- Use closure lid design which minimizes the prying actions of applied loads.

- When choosing a bolt preload, pay special attention to the interactions between the preload and thermal load and between the preload and the prying action.

The following evaluations are presented in this section for the bolts where applicable:

- Bolt preload
- Gasket seating load
- Internal pressure load
- Temperature load
- Thread engagement length evaluation
- Bearing stress
- Load combinations for normal and accident conditions
- Bolt stresses and allowables

In this analysis the applicable load combinations from Reference 3 are analyzed using a bounding approach. The loads that are applicable to the lid bolts are preload, gasket seating load, internal pressure, and thermal. Furthermore, load combinations are split into two subsections for loads that are due to preload and loads that act against preload (internal pressure and gasket sealing forces). The specific design loads corresponding to the loading conditions mentioned above are presented in Table A4A.4-1.

It should be noted that tip over is not a credible event for the TN-40HT cask. The only accident load is 18” bottom end drop. The cask bottom end drop does not induce additional stress in the bolt. Since there are no credible accident loads, all normal condition loads are compared to both normal and accident condition allowable stresses. The design parameters for the lid closure are summarized in Table A4A.4-2. The lid bolt data and material allowables are presented in Table A4A.4-3 and Table A4A.4-4.

The maximum temperature at the lid seal region is less than 200 °F (Table A3.3-3). Thus, 300 °F is conservatively used for bolt stress evaluations.

A4A.4.2 LID BOLT LOAD CALCULATIONS

Symbols and terminology for this analysis are taken from Reference 3 and are reproduced in Table A4A.4-2.

Lid Bolt Preload:

The desired maximum preload stress in lid bolts is 50,000 psi.

For a 1.375 inch bolt shank diameter, the Tensile Stress Area is $(\pi/4)\times1.375^2 = 1.485$ in^2. Therefore,

$$F_a = 50{,}000 \text{ x Stress Area} = 50{,}000 \text{ x } 1.485 = 74{,}250 \text{ lb.}$$

The torque required to achieve this preload is (Reference 3, Section 4.0)

$$Q = K\,D_b\,F_a = 0.135\ (1.375)\ (74{,}250) = 13{,}783 \text{ in. lb.} = 1{,}149 \text{ ft. lb.}$$

A bolt torque range of 1,100 to 1,150 ft. lb. has been selected. Bolt preload for the maximum torque is,

$$F_a = Q/KD_b = 1{,}150 \times 12 / (0.135 \times 1.375) = 74{,}343 \text{ lbs, and}$$

$$\text{Preload stress} = 74{,}343 / 1.485 = 50{,}063 \text{ psi.}$$

Bolt Preload for the minimum torque is,

$$F_a = Q/KD_b = 1{,}100 \times 12 / (0.135 \times 1.375) = 71{,}111 \text{ lb.}$$

Residual torsional moment for maximum torque of 1,150 ft. lb. is,

$$M_{tr} = 0.5\text{Q} = 0.5(1{,}150 \times 12) = 6{,}900 \text{ in. lb.}$$

Residual torsional moment for minimum torque of 1,100 ft. lb. is,

$$M_{tr} = 0.5Q = 0.5(1{,}100 \times 12) = 6{,}600 \text{ in. lb.}$$

Residual tensile bolt force,

$$F_{ar} = F_a = 74{,}343 \text{ lbs}$$

Lid Closure Gasket Seating Load (Seal – Helicoflex HND 229 seals (Reference 6)):

The diameter of the inner seal, D_{is}, is 74.315 in., and the diameter of the outer seal, D_{lg}, is 75.882 in. The force to seat the seals is 1399 lbs./in (245 N/mm) (Reference 6, Helium sealing, Aluminum Jacket, 0.260 inch cross section) times the circumference of the seal. Therefore the force required to seat the seals is:

$$\text{Inner: } \pi\ (74.315)\ (1399) = 326{,}621 \text{ lb.}$$
$$\text{Outer: } \pi\ (75.882)\ (1399) = 333{,}508 \text{ lb.}$$

$$\text{Total, } F_a = 660{,}129 \text{ lb.}$$

Therefore, the gasket seating load is,

$$F_a/48 = 660{,}129 / 48 = 13{,}753 \text{ lb./bolt.}$$

Lid Bolt Internal Pressure Loads (Reference 3, Table 4.3)
Axial force per bolt due to internal pressure is,

$$F_a = \frac{\pi D_{lg}^2 \left(P_{li} - P_{lo}\right)}{4N_b}$$

D_{lg} diameter of the outer seal = 75.882 in. Then,

$$F_a = \frac{\pi(75.882^2)(100-0)}{4(48)} = 9{,}422 \text{ lb./bolt}$$

The fixed edge closure lid force is,

$$F_f = \frac{D_{lb}(P_{li} - P_{lo})}{4} = \frac{79.31(100)}{4} = 1{,}983 \text{ lb. in.}^{-1}$$

The fixed edge closure lid moment is,

$$M_f = \frac{(P_{li} - P_{lo})D_{lb}^2}{32} = \frac{100(79.31^2)}{32} = 19{,}656 \text{ in. lb. in.}^{-1}$$

The shear bolt force per bolt is,

$$F_s = \frac{\pi E_l t_l \left(P_{li} - P_{lo}\right) D_{lb}^{\ 2}}{2N_b E_c t_c \left(1 - N_{ul}\right)} = \frac{\pi\left(26.7\times10^6\right)\left(4.5\right)\left(100\right)\left(79.31\right)^2}{2\left(48\right)\left(26.7\times10^6\right)\left(8.8\right)\left(0.7\right)} = 15{,}037 \text{ lb./bolt}$$

The gap between the bolt shank and the lid (1.625 in. – 1.375 in. = 0.25 in.) is bigger than the gap between the lid and cask (72.87 - 72.67 = 0.20 in.) which ensures that the lid will contact the cask before the bolts get loaded in shear, therefore F_s = 0.

A4A.4.3 LID BOLT TEMPERATURE LOADS

The lid bolt material is SA 540 Gr B24 or B23 CL 1. The lid and flange are both made of SA-350 Gr. LF3 or SA-203 GR. E. The bolts, lid and flange have the same coefficient of thermal expansion (6.9×10^{-6} in/in-°F at 300°F). Therefore, heating to the maximum isothermal temperature will generate no bolt loads.

A4A.4.4 LID BOLT LOAD COMBINATIONS (REFERENCE 3, TABLE 4.9)

A summary of lid bolt individual load and load combinations are presented in the Table A4A.4-5 and Table A4A.4-6 respectively.

A4A.4.5 LID BOLT ADDITIONAL PRYING BOLT FORCE (REFERENCE 3, TABLE 2.1)

Since all applied loads are outward acting, and the additional prying bolt force specified in Reference 3 can only be generated by inward acting loads, no additional prying bolt forces act on the closure lid bolts.

A4A.4.6 LID BOLT BENDING MOMENT BOLT (REFERENCE 3, TABLE 2.2)

The maximum bending bolt moment, M_{bb}, generated by the applied load is evaluated as follows:

$$M_{bb} = \left(\frac{\pi D_{lb}}{N_b}\right)\left[\frac{K_b}{K_b + K_l}\right] M_f$$

The K_b and K_l are based on geometry and material properties and are defined in Reference 3, Table 2.2. By substituting the values given above,

$$K_b = \left(\frac{N_b}{L_b}\right)\left(\frac{E_b}{D_{lb}}\right)\left(\frac{D_b^4}{64}\right) = \left(\frac{48}{4.5}\right)\left(\frac{26.7\times10^6}{79.31}\right)\left(\frac{1.375^4}{64}\right) = 2.006 \times 10^5, \text{ and}$$

$$K_l \frac{E_l t_l^3}{3\left[\left(1-N_{ul}^2\right)+\left(1-N_{ul}\right)^2\left(\frac{D_{lb}}{D_{lo}}\right)^2\right]D_{lb}} = \frac{26.7\times10^6(10.0^3)}{3\left[\left(1-0.3^2\right)+\left(1-0.3\right)^2\left(\frac{79.31}{82.75}\right)^2\right]79.31}$$

$$= 8.2507 \times 10^7$$

Therefore,

$$M_{bb} = \left(\frac{\pi 79.31}{48}\right)\left[\frac{2.006\times10^5}{2.006\times10^5 + 8.2507\times10^7}\right]M_f \quad = 0.01259\ M_f.$$

For load case 2, M_f = 19,656 in. lb. Substituting this value into the equation above gives,

M_{bb} = 247.5 in. lb. / bolt.

A4A.4.7 LID BOLT STRESS CALCULATIONS (REFERENCE 3, TABLE 5.1)

Average Tensile Stress:

The bolt preload is calculated to withstand the worst case load combination and to maintain a clamping (compressive) force on the closure joint, under both normal and accident conditions. Based upon the load combination results (see Table A4A.4-6), it is shown that a positive (compressive) load is maintained on the clamped joint for all loads. Since there are no credible accident loads applicable for the lid bolts, all normal condition loads are compared to both normal and accident condition allowable stresses. The maximum non-prying tensile force for normal conditions is 74,343 lb, from load case 1.A. This load is used to compute bolt stresses below.

Normal Condition:

$$S_{ba} = 1.2732 \frac{F_a}{D_{ba}^2} = 1.2732 \frac{74{,}343}{1.375^2} = 50{,}065 \text{ psi.} = 50.1 \text{ ksi.}$$

Bending Stress:

Normal Condition:

$$S_{bb} = 10.186 \frac{M_{bb}}{D_{ba}^3} = 10.186 \frac{247.5}{1.375^3} = 970 \text{ psi.} = 0.97 \text{ ksi.}$$

Shear Stress:

The average shear stress caused by shear bolt force F_s is,

$$S_{bs} = 0.$$

For normal conditions the maximum shear stress caused by the torsional moment M_t is,

$$S_{bt} = 5.093 \frac{M_t}{D_{ba}^3} = 5.093 \frac{6{,}900}{1.375^3} = 13{,}518 \text{ psi.} = 13.5 \text{ ksi.}$$

Maximum Combined Stress Intensity:

The maximum combined stress intensity is calculated in the following way (Reference 3, Table 5.1).

$$S_{bi} = [(S_{ba} + S_{bb})^2 + 4(S_{bs} + S_{bt})^2]^{0.5}$$

For normal conditions combine tension, shear, bending, and residual torsion.

$$Sbi = [(50{,}065 + 970)^2 + 4\ (0 + 13{,}518)^2]^{0.5} = 57{,}754 \text{ psi.} = 57.8 \text{ ksi.}$$

Stress Ratios:

In order to meet the stress ratio requirement, the following relationship must hold for both normal and accident conditions.

$$R_t^2 + R_s^2 < 1$$

Where R_t is the ratio of average tensile stress to allowable average tensile stress, and R_s is the ratio of average shear stress to allowable average shear stress.

For normal conditions:

$$R_t = 50{,}065/93{,}500 = 0.5355,$$

$$R_s = 13{,}518/56{,}100 = 0.241,$$

$$R_t^2 + R_s^2 = (0.5355)^2 + (0.241)^2 = 0.345 < 1.$$

For accident conditions (using maximum normal condition loads):

$$R_t = 50{,}065/115{,}500 = 0.433,$$

$$R_s = 13{,}518/69{,}300 = 0.195,$$

$$R_t^2 + R_s^2 = (0.433)^2 + (0.195)^2 = 0.226 < 1.$$

A4A.4.8 LID BOLT BEARING STRESS (UNDER BOLT HEAD)

The maximum axial force is 74,343 lb for normal conditions. A bolt hole of 1.625 inch diameter is used for the shank.

H = 2.25/2 in.
B = 1.125 tan(30°) = 0.650 in.

Total Area of one triangle
= (1.125)(0.650) = .731 in^2.

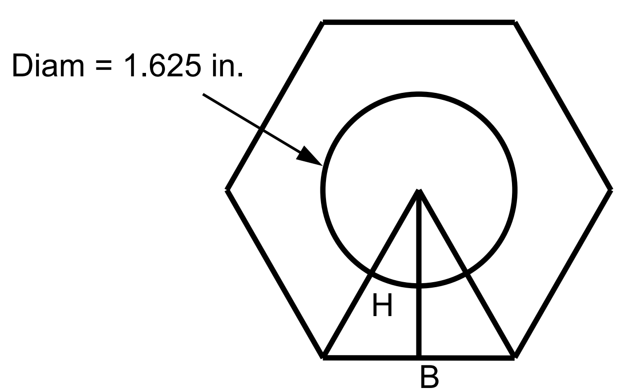

Total area under Bolt head - Bolt Hole area
$= 6(0.731) - (\pi/4)(1.625^2) = 2.31\ in^2$.

The total bearing area is 2.31 in.^{2} The bearing stress for normal conditions is,

Bearing Stress = 74,343/2.31 = 32,179 psi. = 32.2 ksi.

The allowable normal condition bearing stress on the lid is taken to be the yield stress of the lid material at 300 °F. The lid is manufactured out of SA-350 GR. LF3 or SA-203 GR. E, which has a yield strength of 33.2 ksi at 300 °F.

A4A.4.9 SUMMARY OF LID BOLT STRESSES

A summary of the stresses calculated above is listed in the Table A4A.4-7.

A4A.4.10 MINIMUM ENGAGEMENT LENGTH FOR LID BOLT AND FLANGE

For a 1½ – 8UN – 2A bolt, the material is SA – 540 Gr. B24 or B23 CL 1, with

S_u = 165 ksi., and
S_y = 150 ksi (at room temperature)

The flange material is SA – 350 Gr LF3 or SA-203 Gr. E, with

S_u = 70 ksi., and

S_y = 37.5 ksi (at room temperature)

The minimum engagement length L_e for the bolt and flange is (Reference 7, page 1490),

$$L_e = \frac{2A_t}{3.1416 K_{n\max}\left[\frac{1}{2} + .57735 n\left(E_{s\min} - K_{n\max}\right)\right]}$$

Where,

A_t = tensile stress area = 1.4718 in.^{2} (Reference 7, page 1490), for S_u>100,000 psi
n = number of threads per inch = 8,
$K_{n\,max}$ = maximum minor diameter of internal threads = 1.390 in., (Reference 7, page 1728)
$E_{s\,min}$ = minimum pitch diameter of external threads = 1.4093 in., (Reference 7, page 1728)

$D_{s\,min}$ = minimum major diameter of external threads = 1.4828 in. (Reference 7, page 1728)

Substituting the values given above,

$$L_e = \frac{2(1.4718)}{(3.1416)1.390\left[\frac{1}{2} + .57735(8)(1.4093 - 1.390)\right]} = 1.1442 \text{ in.}$$

$$J = \frac{A_s \times S_{ue}}{A_n \times S_{ui}} \quad \text{(Reference 7)}$$

Where, S_{ue} is the tensile strength of external thread material, and S_{ui} is the tensile strength of internal thread material.

A_s = shear area of external threads
= 3.1416 $n\, L_e\, K_{n\,max}$ [1/(2n) + 0.57735 ($E_{s\,min}$ – $K_{n\,max}$)]

A_n = shear area of internal threads
= 3.1416 $n\, L_e\, D_{s\,min}$ [1/(2n) + 0.57735($D_{s\,min}$ – $E_{n\,max}$)]

For the bolt / flange insert connection:

$E_{n\,max}$ = maximum pitch diameter of internal threads = 1.4283 in. (Reference 7 , page 1728).

Therefore,

A_s = 3.1416 (8) (1.1442) (1.390) [1 / (2 x 8) + 0.57735 (1.4093 – 1.390)]
= 2.944 in.^{2}

A_n = 3.1416 (8) (1.1442) (1.4828) [1 / (2 x 8) + 0.57735 (1.4828 – 1.4283)]
= 4.007 in.^{2}

So,

$$J = \frac{2.944(165.0)}{4.007(70.0)} = 1.73$$

Therefore, the minimum required engagement length, $Q = J\, L_e$ = 1.73 x 1.1442 = 1.98 in. The actual minimum engagement length = (7.00 bolt length – 4.50 lid thickness) = 2.50 in. > 1.98 in.

The above calculation bounds the minimum required engagement length if inserts are used because S_u of inserts (Reference 8) is higher than the S_u for the lid thus lowering the J value.

A4A.5 VENT AND DRAIN COVER BOLT ANALYSES

A4A.5.1 INTRODUCTION

This section evaluates the ability of the cask vent/drain cover bolts to maintain the seal under all applicable loads. The stress analysis is performed in accordance with NUREG/CR-6007 (Reference 3).

The bolt size, material and design loads for all TN-40HT vent/drain cover bolts are provided in Table A4A.4-1.

The following ways to minimize bolt forces and bolt failures for cask are taken directly from Reference 3, page xiii. All of the following design methods are employed in the TN-40HT lid closure system.

- Use materials with similar thermal properties for the closure bolts and the lid.
- Apply sufficiently large bolt preload to minimize fatigue and loosening of the bolts by vibration.
- Lubricate bolt threads to reduce required preload torque and to increase the predictability of the achieved preload.
- Use closure lid design which minimizes the prying actions of applied loads.
- When choosing a bolt preload, pay special attention to the interactions between the preload and thermal load and between the preload and the prying action.

The following evaluations are presented in this section for the bolts where applicable:

- Bolt preload
- Gasket seating load
- Internal pressure load
- Temperature load
- Bearing stress
- Load combinations for normal and accident conditions
- Bolt stresses and allowables

In this analysis the applicable load combinations from Reference 3 are analyzed using a bounding approach. The loads that are applicable to the vent/drain cover bolts are preload, gasket seating load, internal pressure, and thermal. Furthermore, load combinations are split into two subsections for loads that are due to preload and loads that act against preload (internal pressure and gasket sealing forces). The specific design loads corresponding to the loading conditions mentioned above are presented in Table A4A.4-1.

It should be noted that tip over is not a credible event for the TN-40HT cask. The only accident load is 18” bottom end drop. The cask bottom end drop does not induce additional stress in the bolt. Since there are no credible accident loads, all normal condition loads are compared to both normal and accident condition allowable stresses. The vent/drain cover bolt data and material allowables are presented in Table A4A.5-1 and Table A4A.5-2.

The maximum temperature at the lid seal region is less than 200 °F (Table A3.3-3). Thus, 300 °F is conservatively used for bolt stress evaluations.

A4A.5.2 VENT AND DRAIN BOLT LOAD CALCULATIONS

Vent and Drain Bolt Torque:

A bolt torque range of 67 to 82 ft. lb. has been selected for the vent and drain cover bolts. The calculations below used a range of Nut Factors (K) of 0.097 to 0.210 to permit a range of lubricants.

Bolt preload for the maximum torque is,

$$F_a = Q/KD_b = 82 \text{ x } 12 / (0.097\text{x } 0.75) = 13{,}526 \text{ lbs, and}$$

$$\text{Preload stress} = 13{,}526 / 0.334 = 40{,}497 \text{ psi.}$$

Bolt Preload for the minimum torque is,

$$F_a = Q/KD_b = 67 \text{ x } 12 / (0.210 \text{ x } 0.75) = 5{,}105 \text{ lb.}$$

Residual torsional moment for maximum torque of 82 ft. lb. is,

$$M_{tr} = 0.5Q = 0.5(82 \text{ x } 12) = 492 \text{ in. lb.}$$

Residual torsional moment for minimum torque of 67 ft. lb. is,

$$M_{tr} = 0.5Q = 0.5(67 \text{ x } 12) = 402 \text{ in. lb.}$$

Residual tensile bolt force,

$$F_{ar} = F_a = 13{,}526 \text{ lbs}$$

Vent and Drain Cover Gasket Seating Load (Seal – Helicoflex HND 229 seals (Reference 6)):

The diameter of the inner seal, D_{Is}, is 4.881 in., and the diameter of the outer seal, D_{os}, is 5.689 in. The force to seat the seals is 1,142 lbs./in (245 N/mm) (Reference 6, Helium sealing, Aluminum Jacket, 0.161 inch cross section) times the circumference of the seal. Therefore the force required to seat the seals is:

Inner: π (4.881) (1,142) = 17,512 lb.
Outer: π (5.689) (1,142) = 20,410 lb.

Total, F_a = 37,922 lb.

Therefore, the gasket seating load is,

$F_a/8$ = 37,922 / 8 = 4,740 lb./bolt.

A4A.5.3 VENT AND DRAIN BOLT INTERNAL PRESSURE LOADS (REFERENCE 3, TABLE 4.3):

Axial force per bolt due to internal pressure is,

$$F_a = \frac{\pi D_{lg}^2 (P_{li} - P_{lo})}{4N_b}$$

D_{lg} diameter of outer seal = 5.689 in. Then,

$$F_a = \frac{\pi(5.689^2)(100-0)}{4(8)} = 318 \text{ lb./bolt}$$

The fixed edge cover lid force is,

$$F_f = \frac{D_{lb}(P_{li} - P_{lo})}{4} = \frac{7.38(100)}{4} = 185 \text{ lb. in.}^{-1}$$

The fixed edge cover lid moment is,

$$M_f = \frac{(P_{li} - P_{lo})D_{lb}^2}{32} = \frac{100(7.38^2)}{32} = 170 \text{ in. lb. in.}^{-1}$$

The shear bolt force per bolt is,

$$F_s = \frac{\pi E_l t_l (P_{li} - P_{lo}) D_{lb}{}^2}{2 N_b E_c t_c (1 - N_{ul})} = \frac{\pi (27.0 \times 10^6)(0.25)(100)(7.38)^2}{2(8)(26.7 \times 10^6)(2.8)(0.7)} = 138 \text{ lb./bolt}$$

A4A.5.4 VENT AND DRAIN BOLT TEMPERATURE LOADS:

From Reference 5, the vent and drain bolt material is SA-193 Gr B7, with $\alpha = 6.9 \times 10^{-6}$ in/in °F. The vent and drain covers are made from SA-240, type 304 with $\alpha = 9.2 \times 10^{-6}$ in/in °F, and the cask lid outer plate is made from SA-350 Gr. LF3 or SA-203 Gr. E, with $\alpha = 6.9 \times 10^{-6}$ in/in °F. Assuming a maximum temperature difference of 230 °F (300° F – 70° F), then from Reference 3, the thermal loads are computed as follows.

$$F_a = 0.25\ \pi\ D_b^2\ E_b\ (a_l\ T_l - a_b\ T_b)$$

$$F_a = 0.25(\pi)(0.75^2)(28.0 \times 10^6)[(9.2 \times 10^{-6})(230) - (6.9 \times 10^{-6})(230)] = 6{,}544 \text{ lb.}$$

Even though the vent and drain covers and the cask lid outer plate are constructed from different materials, the shear force per bolt, F_s, due to a temperature change of 230 °F is, 0 psi, since the clearance holes in the lid are oversized (0.781 inch diameter) allowing the covers to grow in the radial direction.

$$F_s = 0.$$

The temperature difference between the inside and outside of the covers will always be less than one degree because the vent and drain cover is only 1 inch thick. Consequently, the resulting bending moment is negligible.

$$M_f = 0.$$

A4A.5.5 VENT AND DRAIN COVER BOLT LOAD COMBINATIONS (REFERENCE 3, TABLE 4.9)

A summary of individual load and load combinations are presented in Table A4A.5-3 and Table A4A.5-4, respectively.

A4A.5.6 VENT AND DRAIN COVER BOLT ADDITIONAL PRYING BOLT FORCE (REFERENCE 3, TABLE 2.1)

Since all applied loads are outward acting, and the additional prying bolt force specified in Reference 3 can only be generated by inward acting loads, no additional prying bolt forces act on the cover lid bolts.

A4A.5.7 VENT AND DRAIN COVER BOLT BENDING MOMENT BOLT (REFERENCE 3, TABLE 2.2)

The maximum bending bolt moment, M_{bb}, generated by the applied load is evaluated as follows:

$$M_{bb} = \left(\frac{\pi D_{lb}}{N_b}\right)\left[\frac{K_b}{K_b + K_l}\right] M_f$$

The K_b and K_l are based on geometry and material properties and are defined in Reference 3, Table 2.2. By substituting the values given above,

$$K_b = \left(\frac{N_b}{L_b}\right)\left(\frac{E_b}{D_{lb}}\right)\left(\frac{D_b^4}{64}\right) = \left(\frac{8}{0.25}\right)\left(\frac{28.0\times10^6}{7.38}\right)\left(\frac{0.75^4}{64}\right) = 6.002 \times 10^5, \text{ and}$$

$$K_l \frac{E_l t_l^3}{3\left[\left(1-N_{ul}^2\right)+\left(1-N_{ul}\right)^2\left(\frac{D_{lb}}{D_{lo}}\right)^2\right]D_{lb}} = \frac{27.0\times10^6(1.00^3)}{3\left[\left(1-0.3^2\right)+\left(1-0.3\right)^2\left(\frac{7.38}{9.00}\right)^2\right]7.38}$$

$$= 9.839 \times 10^5$$

Therefore,

$$M_{bb} = \left(\frac{\pi 7.38}{8}\right)\left[\frac{6.002\times10^5}{6.002\times10^5 + 9.839\times10^5}\right] M_f \quad = 1.098\ M_f.$$

For load case 2, M_f = 170 in. lb. Substituting this value into the equation above gives,

M_{bb} = 187.0 in. lb. / bolt.

A4A.5.8 VENT AND DRAIN BOLT STRESS CALCULATIONS (REFERENCE 3, TABLE 5.1)

Average Tensile Stress:

The bolt preload is calculated to withstand the worst case load combination and to maintain a clamping (compressive) force on the closure joint, under both normal and accident conditions. Based upon the load combination results (see Table A4A.5-4), it is shown that a positive (compressive) load is maintained on the clamped joint for all loads. Since there are no credible accident loads applicable for the vent and drain cover bolts, all normal condition loads are compared to both normal and accident condition allowable stresses. The maximum non-prying tensile force for normal conditions is 20,070 lb, from load case 1.A. This load is used to compute bolt stresses below.

The bolt diameter used for stress calculation is computed from the bolt stress area provided in Table A4A.4-1:

$$\text{Stress Area} = 0.334 = \pi/4\ D_{ba}^2 \Rightarrow D_{ba} = [\ 0.334 \times 4/\pi\ ]^{1/2} = 0.652 \text{ in.}$$

Normal Condition:

$$S_{ba} = 1.2732 \frac{F_a}{D_{ba}^2} = 1.2732 \frac{20{,}070}{0.652^2} = 60{,}110 \text{ psi.} = 60.1 \text{ ksi.}$$

Bending Stress:

Normal Condition:

$$S_{bb} = 10.186 \frac{M_{bb}}{D_{ba}^3} = 10.186 \frac{187}{0.652^3} = 6{,}872 \text{ psi.} = 6.9 \text{ ksi.}$$

Shear Stress:

The average shear stress caused by shear bolt force F_s is,

$$S_{bs} = 1.2732 \frac{F_s}{D_{ba}^2} = 1.2732 \frac{138}{0.652^2} = 413 \text{ psi.} = 0.4 \text{ ksi.}$$

For normal conditions the maximum shear stress caused by the torsional moment M_t is,

$$S_{bt} = 5.093 \frac{M_t}{D_{ba}^3} = 5.093 \frac{492}{0.652^3} = 9{,}041 \text{ psi.} = 9.0 \text{ ksi.}$$

Maximum Combined Stress Intensity:

The maximum combined stress intensity is calculated in the following way (Reference 3, Table 5.1).

$$S_{bi} = [(S_{ba} + S_{bb})^2 + 4(S_{bs} + S_{bt})^2]^{0.5}$$

For normal conditions combine tension, shear, bending, and residual torsion.

$$S_{bi} = [(60{,}110 + 6{,}872)^2 + 4\ (413 + 9{,}041)^2]^{0.5} = 69{,}600 \text{ psi.} = 69.6 \text{ ksi.}$$

Stress Ratios:

In order to meet the stress ratio requirement, the following relationship must hold for both normal and accident conditions.

$$R_t^2 + R_s^2 < 1$$

Where R_t is the ratio of average tensile stress to allowable average tensile stress, and R_s is the ratio of average shear stress to allowable average shear stress.

For normal conditions:

$$R_t = 60{,}110/62{,}700 = 0.96$$

$$R_s = 9{,}454/37{,}600 = 0.25$$

$$R_t^2 + R_s^2 = (0.96)^2 + (0.25)^2 = 0.98 < 1.$$

For accident conditions (using maximum normal condition loads):

$$R_t = 60{,}110/87{,}500 = 0.69$$

$$R_s = 9{,}454/52{,}500 = 0.18$$

$$R_t^2 + R_s^2 = (0.69)^2 + (0.18)^2 = 0.51 < 1.$$

A4A.5.9 SUMMARY OF VENT AND DRAIN BOLT STRESSES

A summary of the stresses calculated above is listed in the Table A4A.5-5.

A4A.6 TRUNNION ANALYSIS

A4A.6.1 INTRODUCTION

This section presents the evaluation of the TN-40HT cask trunnion stresses due to all applied loads as well as resulting local stresses generated in the cask shield shell.

The TN-40HT cask has two upper and two lower trunnions each of which are one piece forgings composed of SA-105 or SA-266 CL 2 or CL 4 carbon steel.

The upper trunnions are designed to meet the requirements of NUREG-0612 (Reference 17) for non-redundant lifting fixture. This is accomplished by evaluating the trunnions to the stress design factors required by ANSI N14.6 (Reference 9), i.e. capable of lifting 6 times and 10 times the cask weight without exceeding the yield and ultimate strengths of the material, respectively. The upper trunnions are also used to support the loaded cask in the vertical position during transfer to the ISFSI by a transport vehicle.

The lower trunnions are used to support the cask when the cask is in the horizontal position prior to fuel loading and also during rotation of the cask from a horizontal orientation to the vertical orientation. Since the lower trunnions are not relied upon to support the cask when loaded with fuel, their structural analysis is not presented.

The trunnion stress analysis is performed using standard bending and shear stress equations based on the trunnion loading configuration. Nominal dimensions of the trunnions and cask shell are used in the analysis.

Weight of TN-40HT cask used in this analysis is conservatively taken to be 250,000 lb when loaded with fuel.

For the trunnion stress analysis, the following load cases are evaluated:

- Lifting Loads (cask lifted from the pool to the decontamination area and then to the ISFSI). The upper trunnions are analyzed for 6g and 10g vertical loads.

The local shield shell stress calculation is based on the method described in Reference 10:

- 3g longitudinal lifting load applied to the upper trunnions (cask in the vertical orientation)

A spreadsheet was created to aid in the computation. Table A4A.6-4 is a hardcopy of this spreadsheet. The coefficients used in Table A4A.6-4 through are taken from Tables 1A through 4C of Reference 10.

A4A.6.2 MATERIAL PROPERTIES

The trunnions are one piece forgings composed of SA-105 or SA-266 CL 2 or CL 4 carbon steel with material properties shown in Table A4.2-18. These material properties are taken from ASME Code (Reference 5).

The shield shell material properties (SA-266 CL 2 or SA-516-70) used for the local stress analysis are also listed in Table A4.2-18.

The material properties used for the trunnion and shield shell stress analyses are taken at 300 ^{o}F, which is conservative based on the thermal evaluation described in Section A3.

A4A.6.3 STRESS CRITERIA

Stress in the Trunnion

The upper trunnions are designed to meet the requirements of NUREG-0612 (Reference 17) for non-redundant lifting fixture. This is accomplished by evaluating the trunnions to the stress design factors required by ANSI N14.6 (Reference 9), i.e. capable of lifting 6 times and 10 times the cask weight without exceeding the yield and ultimate strengths of the material, respectively.

Stress in the Shield Shell

The local stresses in the shield shell due to the trunnion loads are compared with the allowable stresses following requirements of the ASME Code, Section III, Subsection NB (Reference 11).

A4A.6.4 TRUNNION STRESS ANALYSIS

Analysis for the upper trunnions is based on a cask weight of 250 kips and corresponding 6/10g lifting loads. The trunnion cross sections are shown in Figure A4A.6-1.

Upper Trunnions:

Based on the nominal dimensions given in Figure A4A.6-1 the stress areas and moments of inertia (MOI) for the two different trunnion cross sections are calculated. For cross sections AA and BB the stress areas, MOI, and moment arms are computed as:

Stress Area AA = $\frac{\pi(17^2 - 12^2)}{4}$ = 113.9 in^2

MOI AA = $\frac{\pi(17^4 - 12^4)}{64}$ = 3082.0 in^4

Moment Arm AA = 8.94 – 0.63 – 0.31- (3-0.5)/2 = 6.75 in

Stress Area BB = $\frac{\pi(11.25^2 - 5^2)}{4}$ = 79.8 in^2

MOI BB = $\frac{\pi(11.25^4 - 5^4)}{64}$ = 755.6 in^4

Moment Arm BB = 4 – 0.63 – (3-0.5)/2 = 2.12 in

Table A4A.6-1 and Table A4A.6-2 summarize the stress evaluations. The applied shear load per trunnion is computed by multiplying the cask weight by the appropriate g-load per trunnion. The moment per trunnion is computed by multiplying the shear load by the moment arm length computed in this section.

A4A.6.5 TRUNNION LOCAL STRESS ANALYSIS

<u>Case 1: 3g Longitudinal Lifting Load (Upper Trunnions)</u>

For the 3g lifting load case, the cask is lifted vertically and supported by the upper trunnions. The g-load applied to the cask is 3g in the longitudinal direction.

At the upper trunnion the g load per trunnion is,

3g (longitudinal) / 2 sides / 1 trunnion = 1.5g longitudinal per trunnion

The following analytical method is taken from Reference 10. Figure A4A.6-2 illustrates the loads and moments as defined in this analysis as well as their orientation to the cask/trunnion system as a whole. Note that the all of the “u” locations are on the shield shell outer surface whereas “l” locations are on the inside shield shell surface.

Geometry:

Shield shell thickness at trunnion locations, T = 5.81 in.
Upper Trunnion radius, r_0 = 8.5 in.
Mean radius, R_M = (86.62 + 75.00)/4 = 40.405 in.
Upper trunnion moment arm = 9.66 in.

Shell Parameter (Reference 10) $\gamma = R_M/T$ = 40.405/5.81 = 6.954
Attachment Parameter (Reference 10) $\beta = 0.875 \times r_0/R_M$ = 0.875 × 8.5/40.405 = 0.184

Trunnion loads according to Reference 10 sign convention:

P = 0 lb.
M_L = 1.5 x (-250,000) x 9.66= -3,622,500 in. lb.
M_C = 0 in. lb.
M_T = 0 in. lb.
V_L = 1.5 x (-250,000) = -375,000 lb.
V_C = 0 lb.

Stress intensity calculation

Stress intensities are calculated in the following way.

$$S.I. = \max \begin{cases} \frac{1}{2}\left[(\sigma_X + \sigma_\phi) \pm \sqrt{(\sigma_X - \sigma_\phi)^2 + 4\tau^2}\right] \\ \sqrt{(\sigma_X - \sigma_\phi)^2 + 4\tau^2} \end{cases}$$

From Table A4A.6-4, the maximum stress intensity for case 1 is 8,072 psi, on the outside of the shield shell at the front and back of the trunnion (Bu/Au, compression/tension). Where,

σ_ϕ = 6,059 psi,
σ_x = 8,072 psi, and
τ = 0 psi

Membrane Stress Calculation

In order to calculate the membrane and bending stresses, only those components associated with membrane or bending stress respectively are summed to calculate σ_ϕ, σ_x and τ. For example, to calculate the maximum membrane stress on the outside of the vessel for the 3g lifting load (Table A4A.6-4, locations Du, Cu):

$\sigma_{\phi m}$ = 0 psi.
σ_{xm} = 0 psi.
τ_m = -2,417 psi.

Using the above formula for stress intensity, the corresponding membrane stress intensity is

$$S.I. = \max\begin{cases} \frac{1}{2}\left[(-0-0)-\sqrt{(0-0)^2+4(-2{,}417)^2}\right] = 4{,}834 \text{ psi.} \\ \sqrt{(0-0)^2+4(-2{,}417)^2} = 4{,}834 \text{ psi.} \end{cases}$$

$$= 4{,}834 \text{ psi}$$

A4A.6.6 CONCLUSIONS

From Table A4A.6-1 and Table A4A.6-2, it is shown that the trunnions are qualified for lifting/handling based on stress intensity according to the loading requirements set forth in Reference 9.

The results for the local shield shell stress analysis are presented in Table A4A.6-3. To evaluate load combinations N7 and N8 (see Table A4.2-5) the local stresses calculated are combined with stresses due to internal pressure and thermal load taken from Table A4A.3-2. A bounding approach was taken using the internal pressure load and the cold thermal load of the shield shell in order to envelope both load combinations N7 and N8. The combined results presented in these tables demonstrate that the cask shield shell is adequate to handle the required lifting and handling loads.

A4A.7 OUTER SHELL

A4A.7.1 INTRODUCTION

This attachment presents the structural analysis of the outer shell of the TN-40HT storage cask. The outer shell consists of a cylindrical shell section and outer shell rings (top and bottom closure plates) at each end which connect the shell to the cask body. The normal loads acting on the outer shell are due to internal pressure and normal handling loads.

A4A.7.2 DESCRIPTION

The outer shell is constructed from low-alloy carbon steel and is welded to the outer surface of the shield shell. The cylindrical shell section is 0.5 in. thick and the outer shell rings (top and bottom closure plates) are 0.75 inches thick. Pertinent dimensions are shown in Figure A4A.7-1. Section A1.5 contains reference drawings of TN-40HT storage cask on which the analysis are based.

A4A.7.3 MATERIALS INPUT DATA

The outer shell cylindrical section and outer shell rings are SA-516 Gr 70. The material properties are taken from the ASME Code (Reference 5) and are shown on Table A4.2-18.

A4A.7.4 APPLIED LOADS

While the cask is transported to the site in the horizontal position, it is always in the vertical position when loaded with fuel. Thus the structural analysis present here assumes the cask is in the vertical position with the following loading conditions:

- Cask in the Vertical Orientation
  - Stress due to 25 psig internal pressure
  - Stress due to 25 psig internal pressure and 3g inertia load (lifting)

A4A.7.5 METHOD OF ANALYSIS

ANSYS Model

A finite element model is built for the structural analysis of the outer shell and outer shell rings (top and bottom closure plates). The outer shell and outer shell rings (top and bottom closure plates) are modeled with ANSYS Solid 45 elements (Reference 1). The basic geometries of the outer shell, outer shell rings, and weld sizes used for analysis are shown in Figure A4A.7-1. The bounding weld sizes between the outer shell ring and shield shell, the outer shell ring and outer shell, weld between the outer shell ring pieces (ring may be fabricated from multiple pieces, groove weld size shall not be less than 0.55 in.) are used for the analysis. The finite element model is shown in Figure A4A.7-2.

Cask in the Vertical Orientation

- Stress due to 25 psig internal pressure

An internal pressure of 25 psig is used as the maximum pressure acting on the inner surface of the outer shell. The maximum shell stress intensity for this load case was determined to be 4,919 psi.

- Stress due to 25 psig internal pressure and 3g inertia load (lifting the cask in the vertical orientation)

The weight of the radial neutron shield and aluminum containers is modeled as an additional pressure on the inner surface of the bottom outer shell ring (closure plate). The added pressure load is 9.29 psi per g. The effect of the outer shell dead weight is accounted for by using a 3g gravitational load in the longitudinal direction. The maximum stress intensity for this load case was determined to be 7,044 psi.

A4A.7.6 ANALYSIS RESULTS

A. Maximum Stress Intensities for Each Loading Condition

A summary of the results obtained for maximum stress intensities for each loading condition is listed in Table A4A.7-1. These stresses are within the allowable stress of 1.5 S_m (at 300 ^oF, S_m= 22,400 psi, 1.5 S_m = 33,600 psi). The outer shell can be fabricated from two half cylindrical shell with 0.38" partial penetration weld. The maximum stress intensity and factors of safety at the weld location is also computed as follows:

Allowable stress at the weld = $0.3S_u$ = 0.3 x 70,000 = 21,000 psi (Reference 12)

In the vertical orientation loading condition, the outer shell is mainly in membrane tension/compression loads, the membrane stress is inverse proportion to the element thickness. The maximum weld stress is computed as follows:

25 psig internal pressure:
Max. stress intensity = 4,919 x 0.5 / 0.38 = 6,472 psi
Factor of Safety = 21,000 / 6,472 = 3.24

25 psig internal pressure + 3g inertia load:
Max. stress intensity = 7,044 x 0.5 / 0.38 = 9,268 psi
Factor of Safety = 21,000 / 9,268 = 2.27

B.   Maximum Stress at Weld Locations (see Figure A4A.7-1)

Weld stress intensities are also calculated at the locations noted in Figure A4A.7-1. These values are listed in Table A4A.7-2.

The weld stress intensities are less than the allowable stress of 21.0 ksi (Reference 12, $0.3S_u$, SA-516 GR.70, at 300 °F).

A4A.8 TOP NEUTRON SHIELD BOLTS

A4A.8.1 INTRODUCTION

This section evaluates the top neutron shield bolts. The stress analysis is performed in accordance with NUREG/CR-6007 (Reference 3).

The bolt size, material and design loads for all TN-40HT top neutron shield bolts are provided in Table A4A.4-1.

The following evaluations are presented in this section for the bolts where applicable:

- Bolt preload
- Temperature load
- Bearing stress
- Load combinations for normal and accident conditions
- Bolt stresses and allowables

In this analysis the applicable load combinations from Reference 3 are analyzed using a bounding approach. The loads that are applicable to the top neutron shield bolts, are only preload and temperature loads. In addition, a hypothetical 3g load is applied for the purpose of conservatively bounding any unforeseen loads in these areas. The specific design loads corresponding to the loading conditions mentioned above are presented in Table A4A.4-1.

It should be noted that tip over is not a credible event for the TN-40HT cask. The only accident load is 18" bottom end drop. The cask bottom end drop does not induce additional stress in the bolt. Since there are no credible accident loads, all normal condition loads are compared to both normal and accident condition allowable stresses. The top neutron shield lid bolt data and material allowables are presented in Table A4A.5-1 and Table A4A.5-2.

The maximum temperature at the lid seal region is less than 200 °F (Table A3.3-3). Thus, 300 °F is conservatively used for bolt stress evaluations.

A4A.8.2 TOP NEUTRON SHIELD COVER BOLT LOAD CALCULATIONS

Top neutron shield Cover Bolt Torque:

A bolt torque range of 90 to 100 ft. lb. has been selected for the top neutron shield cover bolts.

Bolt preload for the maximum torque is,

$$F_a = Q/KD_b = 100 \text{ x } 12 \text{ / } (0.135 \text{ x } 1.25) = 7{,}111 \text{ lbs, and}$$

$$\text{Preload stress} = 6{,}400 \text{ / } 0.969 = 7{,}339 \text{ psi.}$$

Bolt Preload for the minimum torque is,

$$F_a = Q/KD_b = 90 \text{ x } 12 \text{ / } (0.135 \text{ x } 1.25) = 6{,}400 \text{ lb.}$$

Residual torsional moment for maximum torque of 100 ft. lb. is,

$$M_{tr} = 0.5Q = 0.5(100 \text{ x } 12) = 600 \text{ in. lb.}$$

Residual torsional moment for minimum torque of 90 ft. lb. is,

$$M_{tr} = 0.5Q = 0.5(90 \text{ x } 12) = 540 \text{ in. lb.}$$

Residual tensile bolt force,

$$F_{ar} = F_a = 7{,}339 \text{ lbs}$$

A4A.8.3 TOP NEUTRON SHIELD COVER BOLT TEMPERATURE LOADS

The top neutron shield cover bolt material is SA-193 Gr B7, with $\alpha = 6.9 \text{x} 10^{-6}$ in/in °F. The top neutron shield cover is made from SA-516, Gr. 70 with $\alpha = 6.9 \text{x} 10^{-6}$ in/in °F. Since the coefficient of thermal expansion for all materials is the same, heating to the maximum isothermal temperature will generate no bolt loads.

A4A.8.4 TOP NEUTRON SHIELD COVER BOLT 3G ACCELERATION LOAD (REFERENCE 3, TABLE 4.6)

The loads generated in the top neutron shield cover bolts by the 3g vertical load are computed below. The weight of the top neutron shield cover is 1,638 lb. However, 1,800 lb. is used in this analysis for conservatism. Also, a dynamic load factor of 1.1 is conservatively applied to the analysis.

The neutron shield bolts have 1.25”-7 UNC threads with tensile area of 0.969 in^2. Under design conditions the assembled and loaded (with fuel) TN-40HT never experiences a net upward acceleration or a side load exceeding the 1.0g bounding load. Nevertheless, a 3.0g upward or lateral load (not simultaneous) is assumed to conservatively evaluate these shield attachment bolts. The load per bolt is then 1800(1.1)(3)/4 = 1485 lb/bolt. The bolt stress under the 3.0g loading is equal to 3.0g x attached weight divided by the total bolt area. The stress is 3 x 1,800 lbs/(4 x 0.969 in^2)(1.1) = 1,533 psi. This is a tensile stress in the upward load case and a shear stress in the side load case.

A4A.8.5 TOP NEUTRON SHIELD COVER BOLT LOAD COMBINATIONS (REFERENCE 3, TABLE 4.9)

A summary of top neutron shield bolt individual load and load combinations are presented in and Table A4A.8-1 and Table A4A.8-2, respectively.

A4A.8.6 TOP NEUTRON SHIELD COVER BOLT STRESS CALCULATIONS (REFERENCE 3, TABLE 5.1)

Average Tensile Stress:

The bolt diameter used for stress calculation is computed from the bolt stress area provided in Table A4A.4-1.

$$\text{Stress Area} = 0.969 = \pi/4\ D_{ba}^2 \Rightarrow D_{ba} = [\ 0.969 \times 4/\pi\ ]^{1/2} = 1.111 \text{ in.}$$

Normal Condition:

$$S_{ba} = 1.2732 \frac{F_a}{D_{ba}^2} = 1.2732 \frac{7{,}111}{1{,}111^2} = 7{,}335 \text{ psi.} = 7.3 \text{ ksi.}$$

For normal conditions the maximum shear stress caused by the torsional moment M_t is,

$$S_{bt} = 5.093 \frac{M_t}{D_{ba}^3} = 5.093 \frac{600}{1.111^3} = 2{,}228 \text{ psi.} = 2.2 \text{ ksi.}$$

Maximum Combined Stress Intensity:

The maximum combined stress intensity is calculated in the following way (Reference 3, Table 5.1).

$$S_{bi} = [(S_{ba} + S_{bb})^2 + 4(S_{bs} + S_{bt})^2]^{0.5}$$

For normal conditions combine tension, shear, bending, and residual torsion.

$$S_{bi} = [(7{,}335 + 0)^2 + 4\ (0 + 2{,}228)^2]^{0.5} = 8{,}582 \text{ psi.} = 8.6 \text{ ksi.}$$

Stress Ratios:

In order to meet the stress ratio requirement, the following relationship must hold for both normal and accident conditions.

$$R_t^2 + R_s^2 < 1$$

Where R_t is the ratio of average tensile stress to allowable average tensile stress, and R_s is the ratio of average shear stress to allowable average shear stress.

For normal conditions:

$$R_t = 7{,}335/62{,}700 = 0.117$$

$$R_s = 2{,}228/37{,}600 = 0.059$$

$$R_t^2 + R_s^2 = (0.117)^2 + (0.059)^2 = 0.017 < 1.$$

For accident conditions (using maximum normal condition loads):

$$R_t = 7{,}335/87{,}500 = 0.084$$

$$R_s = 2{,}228/52{,}500 = 0.042$$

$$R_t^2 + R_s^2 = (0.084)^2 + (0.042)^2 = 0.009 < 1.$$

A4A.8.7 SUMMARY OF TOP NEUTRON SHIELD COVER BOLT STRESSES

A summary of the stresses calculated above is listed in Table A4A.8-3.

A4A.9 FRACTURE TOUGHNESS

A4A.9.1 FRACTURE TOUGHNESS REQUIREMENTS OF THE CASK CONTAINMENT BOUNDARY

The TN-40HT cask material is a ferritic steel (penetration covers are stainless steel) and is therefore subject to fracture toughness requirements in order to assure ductile behavior at the lowest service temperature (LST) of –20 °F.

The design temperature of the TN-40HT cask is specified as -40°F. However, the brittle fracture evaluations were done for a -20°F operating temperature. The cask is shown to be able to withstand a -40°F environment but during operation, that is, any movement of the cask, the combination of loaded cask heat generation and actual ambient temperature is expected to maintain a temperature greater than -20°F for all cask containment material. This corresponds to the 10CFR71 practice of a -20°F minimum transportation temperature combined with a -40°F minimum material temperature.

The inner shell and bottom inner plate are fabricated from SA-203 Gr. E plate material, 1.5 inches thick. The shell flange is 4.6 inches thick, fabricated from SA-350 Gr. LF3 or SA-203 Gr. E material and the lid outer plate is 4.5 inches thick, fabricated from either SA-350 Gr. LF3 or SA-203 Gr. E material.

By interpolating between values provided in NUREG/CR-3826 (Reference 13) and NUREG/CR-1815 (Reference 14), the nil ductility transition temperatures (T_{NDT}) of the containment boundary materials are:

- Inner shell and bottom inner plates (1.5 in.): -80 °F
- Shell flange (4.6 in.): -137 °F
- Lid outer plate (4.5 in.): -125 °F

The 1.5 inch lid closure bolts are fabricated from SA-540 Grade B24 or B23, Class 1 material. All the lid closure bolt materials meet the ASME Code, Section III, Subarticle NB-2300 criteria.

All the material which forms the containment boundary meets the meets the fracture arrest criteria of Reference 13 or 14.

A4A.9.2 FRACTURE TOUGHNESS EVALUATION OF CASK COMPONENTS AND WELDS

The following sections document the fracture toughness evaluations of the non-containment boundary components as well as the containment boundary components.

A4A.9.3 METHODOLOGY

The allowable flaw sizes were determined using linear elastic fracture mechanics (LEFM) methodology from Section XI of the ASME Code (Reference 15). Flaws in the welds, if they occur, are welding defects, rather than initiated cracks. There is no active mechanism for crack initiation and growth at any of the weld locations since all the containment welds are volumetrically examined by RT and/or UT examination to assure no weld defects are present.

A4A.9.4 LOADINGS

Figure A4A.9-1 shows the selected locations on the cask numbered 1 through 10 for fracture toughness analysis. Stresses are linearized at these critical locations to determine maximum tensile membrane and bending stresses.

Table A4A.9-1 and Table A4A.9-2 list the maximum membrane and bending stresses at these selected locations under Normal and Accident Conditions of Storage.

A4A.9.5 MATERIAL FRACTURE TOUGHNESS

The shell flange is basically a forged cylinder, nominally 4.6 inches thick by 9 inches long, made from SA-350 Gr. LF-3 or SA-203 Gr. E material. The welding of the flange to the shell is performed using processes that meet ASME requirements so that fracture toughness properties are preserved. The lid outer plate is either a forged disc or a plate, nominally 4.5 inches thick with an 82.75 inch diameter, made from either SA-350 Gr. LF3 or SA-203 Gr. E material.

The electrodes used in the shell flange and lid outer plate weldments have high nickel content. The high alloy content of the electrodes and their typical usage in applications where good toughness is required indicate that the expected fracture toughness values for the weld filler material is as good as or better than that of the base material.

The shield shell is a plate or forged cylinder, nominally 7.25 inches thick by 166.4 inches long. The bottom shield is nominally 7.25 inches thick and 89.5 inches in diameter. These components are made from SA-266 Class 2 or SA-516 Gr. 70 material. Similarly, the 5.5 in. thick lid shield plate is made from SA-516 Gr. 70 or SA-105 material. The welding at the top flange and bottom plate is performed using processes that meet ASME requirements so that fracture toughness properties are preserved.

The fracture toughness values of these materials are enveloped by the low fracture toughness of the SA-266 forging material. Therefore, it is conservative to use fracture toughness of the SA-266 forging for the fracture toughness evaluations of the TN40-HT components.

Reference 16 is a very thorough review of the correlation between a range of ferritic steel material strength levels and Charpy impact energies.

Figure A4A.9-2 (reproduced from Figure 4-5 of Reference 16) corresponds to Charpy V-notch impact test results for a normalized SA-266 forging. The actual data points are shown along with a smoothed line that connects the average value at each test temperature. This data demonstrates that a lower bound Charpy impact value of 18 ft-lbs is appropriate for an exposure temperature of -20 ^{o}F. The various correlations between K_{ic} and K_{id} given in Table 4-2 of Reference 16 are compared at the 18 ft-lb level. Using the equation for yield strength of 36 to 50 ksi in transition in Table 4-2 of Reference 16, the Charpy impact measurement may be transformed into a fracture toughness value:

$K_{id} = [5E(C_v)]^{1/2} = 50{,}289$ psi-(in)$^{1/2}$ = 50 ksi-(in.)$^{1/2}$

Where

K_{id} = Dynamic Fracture Toughness (based on crack arrest), ksi -(in)$^{1/2}$
E = Modulus of Elasticity, 28.1×10^6 psi (conservatively use 300 ^{o}F)
C_v = Charpy Impact Measurement, 18 ft-lbs

For conservatism, the above calculated K_{id} was reduced to 47 ksi-(in)$^{1/2}$ for fracture toughness evaluations of the TN-40HT cask components (containment and non-containment boundary) and welds.

A4A.9.6 FRACTURE TOUGHNESS CRITERIA

Using the rule of Section XI, IWB-3613 (Reference 15), the limiting fracture toughness values are reduced by a factor of $\sqrt{10}$ for the normal and $\sqrt{2}$ for the accident conditions, to define the limiting allowable $K_{allowable}$. That is,

$K_{allowable} \leq K_{ia}/(\sqrt{10}) = 47/(\sqrt{10}) = 14.86$ ksi-$\sqrt{in}$ for normal conditions

$K_{allowable} \leq K_{ic}/(\sqrt{2}) = 47/(\sqrt{2}) = 33.23$ ksi-$\sqrt{in}$ for accident conditions

Where:

K_{ia} = the available fracture toughness based on crack arrest for the corresponding crack tip temperature

K_{ic} = the available fracture toughness based on crack initiation for the corresponding crack tip temperature

However, because of the dynamic nature of loadings, it is appropriate to use K_{id} in place of K_{ia} and K_{ic}.

A4A.9.7 STRESS INTENSITY FACTOR CALCULATIONS

The total applied stress intensity K_I (applied) is determined from the membrane and bending stresses. For purposes of analysis, the postulated surface flaws are oriented in both the axial and circumferential directions. The surface crack depth is assumed as 15% of component thickness. However, the maximum crack depth is limited to ½ inch. The crack length is assumed to be 10 times the crack depth. The assumed crack sizes are such that they can be readily spotted by visual examination. Compared to surface cracks, the same size subsurface cracks are less critical. The results of the applied stress intensity K_I calculations for normal and accident conditions are shown in Table A4A.9-3 and Table A4A.9-4, respectively.

A4A.9.8 CONCLUSIONS

Based on the results of fracture analysis of TN-40HT cask components and welds with the postulated surface crack sizes, it is concluded that there is no potential of fracture failure due to normal or accident storage loadings. The postulated surface flaw sizes are such that they can be readily detected by a visual inspection.

Note that the shield shell is not part of the containment boundary. Cracks postulated in the shield shell will not propagate into the containment boundary due to the geometry of the cask. If the shield shell were to fracture along the length or around the circumference or along the weld between the shield shell and shell flange, there is no credible mechanism that would result in the shield shell separating from the inner shell. The lid shield plate is welded to the underside of the lid outer plate and is captured by the inner shell. If the weld were to completely fail, the shield plate would still remain inside the containment boundary and would not lose its shielding capability. Therefore, even if a fracture were to occur in the shield shell or the weld between the shield shell and shell flange or weld between lid shield plate and lid outer plate, there would be no safety significance, since confinement would be maintained, and shielding would remain in place. The one exception is in the region of the weld joining the shield shell to the bottom shield. In this region, if the weld were to completely fail, the bottom shield could become detached and reduce the shielding capability of the cask. However, the bottom trunnions are independently welded to the shield shell and the bottom shield and these additional attachment points (welds) would resist detachment of the bottom shield from the shield shell.

A4A.10 TN-40HT STORAGE CASK END DROP ANALYSIS

The purpose of this section is to determine the rigid body accelerations for the TN-40HT Cask during a vertical drop height of 18 inches on concrete.

The rigid body transfer cask accelerations were predicted numerically by the LS-DYNA 3D explicit nonlinear dynamic analysis finite element solver, Version 9.71s (Reference 18). The methodology used in performing this analysis is based on work conducted at the Lawrence Livermore National Laboratory (LLNL), where an analysis methodology was developed and validated through comparisons with test data (Reference 19 and Reference 20). The analysis methodology was benchmarked in Reference 25.

The results of these analyses are used as input to the detailed analyses for the cask body, internal basket and fuel assemblies.

A4A.10.1 FINITE ELEMENT MODEL DESCRIPTION

The ANSYS finite element model of the TN-40HT Cask developed for the cask stress analysis (Appendix A4A.3) was simplified for use in the dynamic impact analysis. The TN-40HT Cask model consists of the cask body, simplified basket structure, concrete pad and soil. Each of these components was modeled using 3D 8-node brick elements. Fully integrated selectively-reduced solid elements were used for all elements to reduce the risk of hourglassing problems.

The finite element model was developed with ANSYS and transferred to LS-DYNA. Modifications were made to the LS-DYNA input file to add the material definitions, non-reflecting boundaries and equation of state into LS-DYNA. Features of the cask, such as the trunnions and neutron shield were neglected in terms of stiffness but their weight was lumped into the density of the cask.

The fuel and basket were modeled as a solid cylinder inside the cask walls with elastic material properties approximately equivalent to that of the structure as a whole.

The geometry of the cask finite element model including the cask internals, concrete and base soil is shown in Figure A4A.10-1 and Figure A4A.10-2.

Only ½ of the cask, internals, concrete and soil were modeled, because the entire arrangement is symmetric about the *x*-*y* plane. The concrete modeled was 16’-8” long, 6’-8” wide, and 3’ thick, and the soil modeled was 66’-8” long, 18’-9” wide, and 39’-2” deep.

A4A.10.2 MATERIAL PROPERTIES

The material properties required to perform the analysis include modulus of elasticity, E, Poison's Ratio, v, and material density (ρ) for the cask body, basket, concrete, and soil. The concrete pad requires a more detailed material model since all of the significant nonlinear deformations occur in the concrete. Material properties used for the concrete and soil were based on those developed at Lawrence Livermore National Labs (Reference 19 and Reference 20).

All material properties were taken at room temperature. This is considered conservative because the cask loaded with spent fuel will typically reach temperatures higher than room temperature, and the lower modulus of elasticity at higher temperatures tends to soften the impact and consequently lower the computed g-loads.

TN-40HT Cask Material

The cask material properties were the same at those used in Appendix A4A.3. All cask materials were modeled as elastic.

Cask Component	Elastic Modulus (psi)	Density (lb-sec²/in⁴)	Poisson's Ratio
Lid Outer Plate	$27.8X10^6$	$8.230x10^{-4}$	0.3
Shield Plate	$29.0X10^6$	$8.230x10^{-4}$	0.3
Shell Flange	$27.8X10^6$	$7.324x10^{-4}$	0.3
Shell	$29.0X10^6$	$9.394x10^{-4}$	0.3
Bottom Plate	$29.0X10^6$	$7.324x10^{-4}$	0.3
Inner Liner	$27.8X10^6$	$7.324X10^{-4}$	0.3

Fuel and Basket Material

The basket structure material properties were the same as those used in Reference 20 except for density. The density of the basket was adjusted to calibrate the overall weight of the cask and basket assembly. The basket was modeled as elastic.

$E = 2.8X10^6$ psi
$v = 0.3$
$\rho = 3.215X10^{-4}$ lb sec²/in⁴

Total modeled weight of the cask and basket is 121,174 lbs since it is a half model. Therefore the total modeled weight is 242,348 lbs. Total actual weight of the cask and basket is 242,400 lbs.

Concrete Material

The concrete was modeled using material law 16 in LS-DYNA, which was developed specifically for granular type materials. The concrete data used in the analysis was originally designed by LLNL for the Shippingport Station Decommissioning Project in 1988. This model was also used in the LLNL (Reference 19) cask drop analysis. Material constants were implemented into Material Model 16, Mode II.B in LS-DYNA. The material represents 4,200 psi compressive strength concrete. A summary of the input used in the analysis is as follows.

$\rho = 2.09675\times10^{-4}$ lb sec^2 / in^4
$v = 0.22$
$a_0 = 1606$
$a_1 = 0.418$
$a_2 = 8.35\times10^{-5}$ psi^{-1}
$b_1 = 0$
$a_{0f} = 0.0$ psi
$a_{1f} = 0.385$

Effective Plastic Strain versus Scale Factor for Concrete Material

Effective Plastic Strain	Scale Factor, *v*
0	0
0.00094	0.289
0.00296	0.465
0.00837	0.629
0.01317	0.774
0.0234	0.893
0.04034	1.0
1.0	1.0

The maximum principal stress tensile failure cutoff was set at 870 psi. Strain rate effects were neglected in the analysis. Dilger (Reference 21) suggests that the major impact of strain rate effects is in the softening part of the stress-strain curve. Since the purpose of these analyses is primarily to predict the peak accelerations, the strain rate effects on the material behavior may be neglected.

The pressure-volume behavior of the concrete was modeled with the following tabulated pressure versus volumetric strain rate relationship using the equation of state feature in LS-DYNA.

Tabulated Pressure versus Volumetric Strain Rate for the Concrete Material

Volumetric Strain, ε	**Pressure (psi)**
0	0
-0.006	4,600
-0.075	5,400
-0.01	6,200
-0.012	6,600
-0.02	7,800
-0.038	10,000
-0.06	12,600
-0.0755	15,000
-0.097	18,700

An unloading bulk modulus of 700,000 psi was assumed to be constant at any volumetric strain, as was assumed in Reference 19.

One percent deformation was assumed in the concrete pad to account for the pad reinforcement.

The material properties used for the reinforcing bar are as follows.

E = 30×10^6 psi
v = 0.3
S_y = 30,000 psi
Tangent Modulus, E_T = 30×10^4 psi

Soil Material

The Lawrence Livermore National Labs report (Reference 20) and Brookhaven National Laboratory report (Reference 23) indicates that the stiffness of the soil has little impact on the peak accelerations predicted in the cask. Thus the same soil model was assumed as that used in the Livermore report. The soil material properties assumed for the analysis are:

E = 6,000 psi

v = 0.45
ρ = 2.0368 x 10^{-4} lb-sec^2 / in^4

A4A.10.3 BOUNDARY CONDITIONS

Only ½ of the cask was modeled with symmetry boundary conditions used to simulate the full structure. Non-reflecting boundaries were applied to the bottom and sides of the modeled soil not aligned with the plane of symmetry (bottom, left side, right side, and back) to prevent artificial stress waves from reflecting back into the model. Both dilatation and shear waves were damped as described in the LS-DYNA *BOUNDARY command.

An automatic surface to surface (contact_automatic_single_surface) contact definition was applied between all parts except the soil. The contact definition has a 0.5 penalty stiffness scale factor to prevent excessive contact stiffness leading to unrealistic part accelerations. A surface to surface (contact_surface_to_surface) contact definition was applied between the concrete and the soil with soft contact option 2. Soft contact option 2 was necessary between the soil and concrete as the materials have very different material stiffness. A conservatively low coefficient of friction (static and kinetic) of 0.25 was applied between all contact surfaces. It is conservative to use a low value for the coefficient of friction because less energy is absorbed due to friction resulting in greater impact acceleration forces.

A4A.10.4 INITIAL CONDITIONS AND LOADING

The analysis begins with a 1" gap between the cask and concrete to allow for at least 5 ms of zero acceleration other than gravity. An initial velocity was applied to all parts of the cask model. The initial velocity was computed by equating potential and kinetic energies. Due to the initial 1" gap and gravitational acceleration, initial velocities were computed 1" shorter than the drop heights.

V = potential energy = mgh
T = kinetic energy = $\frac{1}{2}mv^2$

For an 18" Drop:
$mgh = \frac{1}{2}mv^2$
$\Rightarrow v = \sqrt{2gh} = \sqrt{2(386.4)(18-1)} =$ 114.62 in./sec.

A gravitational acceleration of 386.4 in/sec^2 was applied to the cask and basket model.

A4A.10.5 RESULTS OF LS-DYNA ANALYSES

The resulting rigid body acceleration time histories were computed by LS-DYNA. The rigid body accelerations were computed for the bottom plate, circumferential shell, and basket representation. The parts can be seen in Figure A4A.10-3.

The peak filtered accelerations and corresponding time history plot for different parts of the TN-40HT cask 18” end drop are listed below. All results were filtered with a 4th order low pass butterworth filter with a 350Hz cutoff frequency.

Results Summary

Part	Peak Acceleration (g)	Time History Figure Number
Shell	41.5	A4A.10-4
Bottom Plate	44.1	A4A.10-5
Basket Representation	28.8	A4A.10-6

Based on the Results shown in the above table, the maximum acceleration in the TN-40HT cask during the 18 inch accident condition end drop event is 44.1g and occurs in the bottom plate. Also from this table, the highest acceleration in the basket and fuel is 28.8g. However, since the basket and fuel were not modeled explicitly, the maximum acceleration (28.8g) must be multiplied by the appropriate dynamic load factor (DLF). The maximum DLF for a triangular load is 1.52 (Reference 24). This results in a maximum loading of 43.8g.

4A.11 REFERENCES

1. ANSYS Engineering Analysis System, Users Manual for ANSYS Release 8.0.

2. John Harvey, "Theory and Design of Modern Pressure Vessel," Second Edition.

3. Stress Analysis of Closure Bolts for Shipping Casks, NUREG/CR-6007, April 1992.

4. Baumeister, T. Marks, L.S., Standard Handbook for Mechanical Engineers, 7th edition, McGraw Hill, 1967.

5. ASME Boiler and Pressure Vessel Code, Section II, Materials Specifications, Part D, 2004, through 2006 addenda.

6. Garlock Helicoflex Catalog, "High Performance Seals and Sealing Systems", Catalog Reference HEL 1.

7. Machinery Handbook, 26th Edition, Industrial Press, 2000.

8. Helicoil Catalog, Heli-Coil 8-Pitch Inserts.

9. ANSI N14.6-1986 "Special Lifting Devices for Shipping Containers Weighing 10,000 lb or more."

10. WRC Bulletin 107, March 1979, "Local Stresses in Spherical and Cylindrical Shells Due to External Loadings".

11. ASME Boiler and Pressure Vessel Code, Section III, Division 1, Subsections NB and NCA, 2004, through 2006 addenda.

12. ASME Boiler and Pressure Vessel Code, Section III, Division 1, Subsection NF, 2004 through 2006 Addenda.

13. NUREG/CR-3826, "Recommendations for Protecting against Failure by Brittle Fracture in Ferritic Steel Shipping Containers Greater than Four Inches Thick", April 1984.

14. NUREG/CR-1815, Recommendations for Protecting Against Failure by Brittle Fracture in Ferritic Steel Shipping Containers up to Four Inches Thick, August 1991.

15. American Society of Mechanical Engineers, ASME Boiler and Pressure Vessel Code Section V and Section XI, 2004, through 2006 addenda.

16. SIR-98-110, Rev. 0, “Allowable Flaw Evaluation of the Transnuclear TN-32 Cask”, Structural Integrity Associates, Inc. 1998.

17. NUREG-612 “Control of Heavy Loads at Nuclear Power Plants”, July 1980.

18. LS-DYNA Keyword User’s Manual, Volumes 1 & 2, Version 9.71s, Rev. 7600.398 August 17, 2006, Livermore Software Technology Corporation.

19. Witte, M. et. Al. Evaluation of Low-Velocity Impact Testing of Solid Steel Billet onto Concrete Pads and Application to Generic ISFSI Storage Cask for Tipover and Side Drop. Lawrence Livermore National Laboratory. UCRL-ID-126295, Livermore, California. March 1997.

20. NUREG/CR-6608, UCRL-1D-12911," Summary and Evaluation of Low-Velocity Impact Tests of Solid Steel/Billet onto Concrete Pad," LLNL, February, 1998

21. Dilger, etc., Ductility of Plain and Confined Concrete under Different Stain Rates, ACI Journal, January-February, 1984.

22. Not Used.

23. BNL-NUREG-71196-2003-CP, “Impact Analysis of Spent Fuel Dry Casks Under Accidental Drop Scenarios,” BNL, 2003.

24. Methods for Impact Analysis of Shipping Containers, NUREG/CR-3966, UCID-20639, LLNL, 1987.

25 HUHOMS® HD Updated Final Safety Analysis Report, Revision 1

TABLE A4A.2-1
MECHANICAL PROPERTIES OF CASK BODY MATERIALS(1)(3)

Material Specification (Nominal Composition)	Application	Minimum Yield Strength S_y, psi	Minimum Ultimate Strength S_u, psi	Design Stress Value, psi(2)
ASME SA-350, Grade LF3 (3-½ Ni)	Shell flange, Lid outer plate	37,500	70,000	S_m = 23,300
ASME SA-203, Grade E (3-1/2 Ni)	Lid outer plate, Inner shell, Bottom inner plate	40,000	70,000	S_m = 23,300
ASME SA-266, Class 2 or SA-516 Gr. 70 (C-Si)	Shield shell, Bottom shield	36,000	70,000	S_m = 23,300
ASME SA-516, Gr. 70 or SA-105 (C-Mn-Si)	Outer shell Lid shield plate, Protective cover	36,000	70,000	S_m = 23,300
ASME SA-105 or SA-266 CL 2 or CL 4, (C-Si)	Lower and Upper Trunnions	36,000	70,000	S_m = 23,300
ASME SA-540 Gr. B24 or B23 CL 1 (2Ni-3/4 Cr-1/3 Mo)	Lid Bolts	150,000	165,000	S_m = 50,000
SA-193, Gr. B7	Vent / Drain port cover & Top neutron shield bolts	105,000	125,000	S_m = 35,000

Notes:

1. Mechanical properties listed are for metal temperatures up to 100 °F to provide a baseline comparison of all structural materials. Temperature dependent properties required for structural analysis are provided in Table A4.2-18.
2. Values listed are the stress parameters which form the basis for structural analysis acceptance criteria.
3. Data are taken from tables in ASME Section II, Part D, 2004 including 2006 Addenda, unless otherwise noted.

TABLE A4A.3-1
NORMAL AND HYPOTHETICAL ACCIDENT CONDITION INDIVIDUAL LOADS

Load Case No.	Individual Load Description
IL - 1	Bolt Preload and Lid Seating Pressure
IL - 2	Fabrication Stress
IL - 3	1g Down (Cask vertical, supported at bottom)
IL - 4	Internal Pressure (100 psi)
IL - 5	External Pressure (25 psi)
IL - 6	Thermal Stress Due to Hot Environment (100 °F ambient)
IL - 7	Thermal Stress Due to Cold Environment (–40 °F ambient)
IL - 8	3g on Top Trunnion Lifting Load (Calculating cask global stresses, Cask Vertical, 3g Up)
IL - 9	Bounding Loads for Seismic, Tornado and Flood (1g Lateral (resultant) + 2g Down)
IL-10	Trunnion Local Stress due to 3g Lifting

TABLE A4A.3-2
SUMMARY MAXIMUM NODAL STRESS INTENSITIES IN CASK COMPONENTS

(See Figure A4A.3-2 through Figure A4A.3-6 for component definition)

Load Number	Maximum Nodal Stress Intensity (ksi)							
	Inner Shell & Bottom Inner Plate	Shell Flange	Lid Outer Plate	Lid Shield Plate	Shield Shell	Bottom Shield	Top Trunnion Region	Bottom Trunnion Region
IL – 1 Bolt Pre-load	0.07	4.47	8.03	0.25	0.24	0.01	0.24	0.0
IL – 2 Fab.	15.11	12.11	1.43	0.73	7.11	4.20	5.01	7.11
IL – 3 Gravity 1g	0.08	0.11	0.07	0.07	0.08	0.08	0.03	0.08
IL – 4 Internal Pressure	2.40	3.69	2.12	2.24	1.97	5.62	0.69	1.97
IL – 5 External Pressure	0.60	0.92	0.53	0.56	0.49	1.41	0.17	0.49
IL – 6 Thermal 100ºF	23.55	3.33	1.79	1.13	11.22	13.19	2.30	10.73
IL – 7 Thermal -40°F	25.08	3.33	1.77	1.03	12.59	14.45	2.29	12.11
IL – 8 Lifting 3G	3.92	1.39	1.32	0.50	4.39	6.98	1.85	2.23
IL – 9 Seismic	0.71	0.26	0.22	0.16	1.21	2.04	0.19	1.23
IL-10 Trunnion Local Stress	Trunnion local stresses due to 3g are provided in Section A4A.6							

TABLE A4A.4-1
BOLT SPECIFICATIONS AND DESIGN LOADS

Bolt	Bolt Size	Material	Design Loads
Lid Bolt	1.375 inch shank 1.5-8UN threads (tensile area = 1.492 in^2 (Reference 4))	SA540, Gr. B24 or B23, Cl. 1	1. Bolt Preload (1100-1150 ft-lbs) 2. Gasket seating load (1399 lb./in, Reference 6) 3. Pressure load (100 psig) 4. Temperature load (300 °F) 5. Bearing stress
Vent/Drain Cover Bolt	0.75 inch 10UNC (tensile area = 0.334 in^2 (Reference 4))	SA-193 B7	Bolt Preload (67-82 ft-lbs) 1. Gasket seating load (1142 lb./in, Reference 6) 2. Pressure load (100 psig) 3. Temperature load (300 °F)
Top Neutron Shield Bolt	1.25 inch 7UNC (tensile area = 0.969 in^2 (Reference 4))	A-193 B7	1. Bolt Preload (90-100 ft-lbs) 2. 3g vertical up 3. Temperature load (300 °F)

TABLE A4A.4-2
DESIGN PARAMETERS FOR LID CLOSURE BOLTS

D_b	Nominal diameter of closure bolt; 1.375 in.
K	Nut factor for empirical relation between the applied torque and achieved preload is 0.135 for neolube
Q	Applied torque for the preload (in.-lb.)
D_{lb}	Closure lid diameter at bolt circle, 79.31 in.
D_{is}	Closure lid diameter at the seal (inner) = 74.315 in
D_{lg}	Closure lid diameter at the seal (outer) = 75.882 in.
E_c	Young's modulus of cask wall material (SA-350, LF3, 300 °F), 26.7×10^6 psi. (Reference 5)
E_l	Young's modulus of lid material (SA-350, LF3, 300 °F), 26.7 x 10^6 psi. (Reference 5)
N_b	Total number of closure bolts, 48
N_{ul}	Poisson's ratio of closure lid, 0.3, (Reference 4, p. 5-6 use nominal value).
P_{ei}	Inside pressure of cask, 100 psig.
D_{lo}	Closure lid diameter at outer edge, 82.75 in.
P_{li}	Pressure inside the closure lid, 100 psig.
t_c	Thickness of cask wall, 8.8 in.
t_l	Thickness of lid, 10.0, 4.5 in.
l_b	Thermal coefficient of expansion, bolt (SA-540, Gr B24), 6.4 x 10^{-6} at R.T., 6.9 x 10^{-6} in. in.$^{-1}$ °F^{-1} at 300 °F (Reference 5)
l_c	Thermal coefficient of expansion, cask (SA-350, LF3) 6.4 x 10^{-6} at R.T., 6.9 x 10^{-6} in. in.$^{-1}$ °F^{-1} at 300 °F (Reference 5)
l_l	Thermal coefficient of expansion, lid (SA-350, LF3) 6.4 x 10^{-6} R.T., 6.9 x 10^{-6} in. in.$^{-1}$ °F^{-1} at 300 °F (Reference 5)
E_b	Young's modulus of bolt material (SA-540, B24, 300 °F), 26.7 x 10^6 psi. (Reference 5)
LF	A factor to account for any difference between the rigid body acceleration and the acceleration of the contents and closure lid = 1.1
S_{yl}	Yield strength of closure lid material (SA-350, LF3, 300 °F), 33,200 psi. (Reference 5)
S_{ul}	Ultimate strength of closure lid (SA-350, LF3, 300 °F), 70,000 psi. (Reference 5)
S_{yb}	Yield strength of lid bolt material (see Table A4A.4-3)
S_{ub}	Ultimate strength of lid bolt material (see Table A4A.4-4)
P_{lo}	Pressure outside the lid
L_b	Bolt length between the top and bottom surfaces of closure, 4.5 in.

TABLE A4A.4-3
ALLOWABLE STRESSES IN LID CLOSURE BOLTS FOR NORMAL CONDITIONS

Temperature (°F)	Yield Stress[(1)] (ksi)	Normal Condition Allowables		
		F_{tb} [(2, 4)] (ksi)	F_{vb} [(3, 4)] (ksi)	*S.I.* [(5)] (ksi)
70	150.0	100.0	60.0	135.0
200	144.0	96.0	57.6	129.6
300	140.3	93.5	56.1	126.3
400	137.9	91.9	55.2	124.1

Notes:
1. Yield stress values are from Reference 5
2. Allowable Tensile stress, F_{tb} = 2/3 S_y (Reference 3, Table 6.1)
3. Allowable shear stress, F_{vb} = 0.4 S_y (Reference 3, Table 6.1)
4. Tension and shear stresses must be combined using the following interaction equation:

$$\frac{\sigma_{tb}^2}{F_{tb}^2} + \frac{\tau_{yb}^2}{F_{yb}^2} \le 1.0 \text{ (Reference 3)}$$

5. Stress intensity from combined tensile, shear and residual torsion loads, $S.I. \le 0.9\ S_y$ (Reference 3, Table 6.1)

TABLE A4A.4-4
ALLOWABLE STRESSES IN LID CLOSURE BOLTS FOR ACCIDENT CONDITIONS

Temperature (°F)	Yield Stress(1) (ksi)	Accident Condition Allowables		
		$0.6\ S_y$ (3) (ksi)	F_{tb} (2, 4) (ksi)	F_{vb} (3, 4) (ksi)
100	150.0	90.0	115.5	69.3
200	144.0	86.4	115.5	69.3
300	140.3	84.2	115.5	69.3
400	137.9	82.7	115.5	69.3

Notes:
1. Yield and tensile stress values are from Reference 5, Note that S_u is 165 ksi at all temperatures of interest
2. Allowable Tensile stress, F_{tb} = MINIMUM (0.7 S_u, S_y), where 0.7 S_u = 0.7 (165.0) = 115.5 ksi. (Reference 3, Table 6.3)
3. Allowable shear stress, F_{vb} = MINIMUM (0.42 S_u, 0.6 S_y), where 0.42 S_u = 0.42 (165.0) = 69.3 ksi. (Reference 3, Table 6.3)
4. Tension and shear stresses must be combined using the following interaction equation:

$$\frac{\sigma_{tb}^2}{F_{tb}^2} + \frac{\tau_{yb}^2}{F_{yb}^2} \le 1.0 \text{ (Reference 3)}$$

TABLE A4A.4-5
LID BOLT INDIVIDUAL LOAD SUMMARY

Load Case	Applied Load		Non-Prying Tensile Force, F_a (lb.)	Torsional Moment, M_t (in. lb.)	Prying Force, F_f (lb.in.$^{-1}$)	Prying Moment, M_f (in. lb. in.$^{-1}$)
Preload	Residual	Maximum Torque	74,343	6,900	0	0
		Minimum Torque	71,111	6,600	0	0
Gasket	Seating Load		13,753	0	0	0
Internal Pressure	100 psig Internal		9,422	0	1,983	19,656
Thermal	300° F		0	0	0	0

TABLE A4A.4-6
LID BOLT LOAD COMBINATIONS

Load Case	Combination Description		Non-Prying Tensile Force, F_a (lb.)	Torsional Moment, M_t (in. lb.)	Prying Force, F_f (lb.in.$^{-1}$)	Prying Moment, M_f (in. lb. in.$^{-1}$)
1.	Preload + Temperature (Normal Condition)	A. Maximum Torque	74,343	6,900	0	0
		B. Minimum Torque	71,111	6,600	0	0
2.	Gasket Seating Load + Internal Pressure		23,175	0	1,983	19,656

TABLE A4A.4-7
LID BOLT STRESS SUMMARY

Stress Type	Normal Condition		Accident Condition	
	Stress	Allowable	Stress	Allowable
Average Tensile (ksi)	50.1	93.5	50.1	115.5
Shear (ksi)	13.5	56.1	13.5	69.3
Combined stress intensity (ksi)	57.8	126.3	Not Required (Reference 3)	
Interaction Eq. $R_t^2 + R_s^2 < 1$	0.345	1	0.226	1
Bearing (ksi)	32.2	33.2	Not Required (Reference 3)	

TABLE A4A.5-1
ALLOWABLE STRESSES IN VENT/DRAIN, AND TOP NEUTRON SHIELDBOLTS FOR NORMAL CONDITIONS

Temperature (°F)	Yield Stress[1] (ksi)	Normal Condition Allowables		
		F_{tb} [2, 4] (ksi)	F_{vb} [3, 4] (ksi)	*S.I.* [5] (ksi)
70	105.0	70.0	42.0	94.5
200	98.0	65.3	39.2	88.2
300	94.1	62.7	37.6	84.7
400	91.5	61.0	36.6	82.4

Notes:

1. Yield stress values are from Reference 5
2. Allowable Tensile stress, $F_{tb} = 2/3\ S_y$ (Reference 3, Table 6.1)
3. Allowable shear stress, $F_{vb} = 0.4\ S_y$ (Reference 3, Table 6.1)
4. Tension and shear stresses must be combined using the following interaction equation:

$$\frac{\sigma_{tb}^2}{F_{tb}^2} + \frac{\tau_{yb}^2}{F_{yb}^2} \leq 1.0 \quad \text{(Reference 3)}$$

5. Stress intensity from combined tensile, shear and residual torsion loads, $S.I. \leq 0.9\ S_y$ (Reference 3, Table 6.1)

TABLE A4A.5-2
ALLOWABLE STRESSES IN VENT/DRAIN, AND TOP NEUTRON SHIELDBOLTS FOR ACCIDENT CONDITIONS

Temperature (°F)	Yield Stress[1] (ksi)	Accident Condition Allowables		
		0.6 S_y [3] (ksi)	F_{tb}[2, 4] (ksi)	F_{vb} [3, 4] (ksi)
100	105.0	63.0	87.5	52.5
200	98.0	58.8	87.5	52.5
300	94.1	56.5	87.5	52.5
400	91.5	54.9	87.5	52.5

Notes:

1. Yield and tensile stress values are from Reference 5, Note that S_u is 125 ksi at all temperatures of interest
2. Allowable Tensile stress, F_{tb} = MINIMUM (0.7 S_u, S_y), where 0.7 S_u = 0.7 (125.0) = 87.5 ksi. (Reference 3, Table 6.3)
3. Allowable shear stress, F_{vb} = MINIMUM (0.42 S_u, 0.6 S_y), where 0.42 S_u = 0.42 (125.0) = 52.5 ksi. (Reference 3, Table 6.3)
4. Tension and shear stresses must be combined using the following interaction equation:

$$\frac{\sigma_{tb}^2}{F_{tb}^2} + \frac{\tau_{yb}^2}{F_{yb}^2} \le 1.0 \text{ (Reference 3)}$$

Table A4A.5-3
Vent and Drain Cover Bolt Individual Load Summary

Load Case	Applied Load		Non-Prying Tensile Force, F_a (lb.)	Torsional Moment, M_t (in. lb.)	Prying Force, F_f (lb.in.$^{-1}$)	Prying Moment, M_f (in.lb.in.$^{-1}$)
Preload	Residual	Maximum Torque	13,526	492	0	0
		Minimum Torque	5,105	402	0	0
Gasket	Seating Load		4,740	0	0	0
Internal Pressure	100 psig Internal		318	0	185	170
Thermal	300° F		6,544	0	0	0

604000000330

TABLE A4A.5-4
VENT AND DRAIN COVER BOLT LOAD COMBINATIONS

Load Case	Combination Description		Non Prying Tensile Force, F_a (lb.)	Torsional Moment, M_t (in. lb.)	Prying Force, F_f (lb.in.$^{-1}$)	Prying Moment, M_f (in.lb.in.$^{-1}$)
1.	Preload + Temperature (Normal Condition)	A. Maximum Torque	20,070	492	0	0
		B. Minimum Torque	11,649	402	0	0
2.	Gasket Seating Load + Internal Pressure		5,058	0	185	170

TABLE A4A.5-5
VENT AND DRAIN COVER BOLT STRESS SUMMARY

Stress Type	Normal Condition		Accident Condition	
	Stress	Allowable	Stress	Allowable
Average Tensile (ksi)	60.1	62.7	60.1	87.5
Shear (ksi)	9.5	37.6	9.5	52.5
Combined Stress Intensity (ksi)	69.6	84.7	Not Required (Reference 3)	
Interaction Eq. $R_t^2 + R_s^2 < 1$	0.98	1	0.51	1

TABLE A4A.6-1
SUMMARY OF UPPER TRUNNION STRESSES (YIELD STRENGTH CASE)

6/3g Load	Upper Trunnion (3g/Trunnion)	
Trunnion Location	AA	BB
Stress Area (in^2)	113.9	79.8
Area Moment of Inertia (in^4)	3,082.0	755.6
Shear Force (lb)	750,000	750,000
Applied Moment (in lb)	5,062,500	1,590,000
Shear Stress (psi)	6,586	9,402
Bending Stress (psi)	13,962	11,837
Stress Intensity (psi)	19,195	22,220
Allowable Stress (psi)	31,800	31,800

TABLE A4A.6-2
SUMMARY OF UPPER TRUNNION STRESSES (ULTIMATE STRENGTH CASE)

10g Load	Upper Trunnion (5g/Trunnion)	
Trunnion Location	AA	BB
Stress Area (in^2)	113.9	79.8
Area Moment of Inertia (in^4)	3082.0	755.6
Shear Force (lb)	1,250,000	1,250,000
Applied Moment (in lb)	8,437,500	2,650,000
Shear Stress (psi)	10,976	15,671
Bending Stress (psi)	23,271	19,728
Stress Intensity (psi)	31,991	37,033
Allowable Stress(psi)	70,000	70,000

TABLE A4A.6-3
UPPER TRUNNION SHIELD SHELL LOCAL STRESS SUMMARY FOR 3G LIFTING LOAD

Location	Upper Trunnions, 3g Longitudinal Load (T = 300°F)			
	Stress Intensity (ksi) P_L	Allowable 1.5 *Sm* (ksi) (Reference 11)	Stress Intensity (ksi) $P_L + P_b + Q$	Allowable 3.0 *Sm* (ksi) (Reference 11)
Outside edge of shield shell.	4.834 + 1.97(1) = 6.804	31.8	8.072 + 1.97(1) + 12.59(1) = 22.632	63.6
Inside edge of shield shell.	4.834+ 1.97(1) = 6.804	31.8	7.511 + 1.97(1) + 12.59(1) = 22.071	63.6

1. Note that bounding internal pressure and thermal stress values are taken from Table A4A.3-2.

TABLE A4A.6-4
UPPER TRUNNION LOCAL STRESS DUE TO 3G LONGITUDINAL LIFTING LOAD

		3g Lifting Load										
Trunnion Loading		**Geometry**		**Cask Loading**								
Cask Weight lb	250000	Gamma Shield Thickness (in)	5.810	Longitudinal g	3							
		Mean Radius (in)	40.405	Vertical g	0							
Moment Arm (in)	9.66	Trunnion Outer Radius (in)	8.500	Lateral g	0							
Circumfrential Trunnion Moment Mc (in lb)	0	Geometry Factor Gamma	6.954									
Longitudinal Trunnion Moment ML (in lb)	-3622500	Geometry Factor Beta	0.184									
Torsional Trunnion Moment Mt (in lb)	0											
P (lb)	0											
Circumfrential Loading Vc (lb)	0											
Longitudinal Loading VL (lb)	-375000											
Reference Figure	**Reference Curve from Fig**	**Multiplier**	**Absolute Stress (psi)**	**Au**	**Al**	**Bu**	**Bl**	**Cu**	**Cl**	**Du**	**Dl**
3c or 4c	0	0.000	0.0	0.0	0.0	0.0	0.0	0.0	0.0	0.0	0.0
1c or 2c-1	0	0.000	0.0	0.0	0.0	0.0	0.0	0.0	0.0	0.0	0.0
3a	0	0.000	0.0					0.0	0.0	0.0	0.0
1a	0	0.000	0.0					0.0	0.0	0.0	0.0
3b	0.5	-2074.771	-1037.4	1037.4	1037.4	-1037.4	-1037.4				
1b or 1b-1	0.058	-86572.588	-5021.2	5021.2	-5021.2	-5021.2	5021.2				
Summation of Phi Stress				6058.6	-3983.8	-6058.6	3983.8	0.0	0.0	0.0	0.0
3c or 4c	0	0.000	0.0	0.0	0.0	0.0	0.0	0.0	0.0	0.0	0.0
1c-1 or 2c	0	0.000	0.0	0.0	0.0	0.0	0.0	0.0	0.0	0.0	0.0
4a	0	0.000	0.0					0.0	0.0	0.0	0.0
2a	0	0.000	0.0					0.0	0.0	0.0	0.0
4b	0.135	-2074.771	-280.1	280.1	280.1	-280.1	-280.1				
2b or 2b-1	0.09	-86572.588	-7791.5	7791.5	-7791.5	-7791.5	7791.5				
Summation of Chi Stress				8071.6	-7511.4	-8071.6	7511.4	0.0	0.0	0.0	0.0
	Torsional Shear Stress	0.0		0.0	0.0	0.0	0.0	0.0	0.0	0.0	0.0
	Circumferential Shear Stress	0.0		0.0	0.0	0.0	0.0				
	Longitudinal Shear Stress	-2417.1						2417.1	2417.1	-2417.1	-2417.1
Summation of Tau Stress				0.0	0.0	0.0	0.0	2417.1	2417.1	-2417.1	-2417.1
Stress Intensity Root 1				8071.6	3983.8	6058.6	7511.4	2417.1	2417.1	2417.1	2417.1
Stress Intensity Root 2				6058.6	7511.4	8071.6	3983.8	2417.1	2417.1	2417.1	2417.1
Stress Intensity Root 3				2013.0	3527.6	2013.0	3527.6	4834.1	4834.1	4834.1	4834.1
Max Stress Intensity	8071.6										
Membrane Stress Intensity Root 1				1037.4	1037.4	280.1	280.1	2417.1	2417.1	2417.1	2417.1
Membrane Stress Intensity Root 2				280.1	280.1	1037.4	1037.4	2417.1	2417.1	2417.1	2417.1
Membrane Stress Intensity Root 3				757.3	757.3	757.3	757.3	4834.1	4834.1	4834.1	4834.1
Max Membrane Stress Intensity	4834.1										

Table A4A.7-1
MAXIMUM STRESS INTENSITIES FOR EACH LOADING CONDITION

LOADING CONDITION	Max. Stress Intensity (ksi)	Allowable (ksi)	Factor of Safety
25 psig internal pressure	4.92	33.6	6.83
25 psig internal pressure + 3g inertia load (Cask in Vertical Orientation)	7.04	33.6	4.77

Table A4A.7-2
STRESS AT WELD LOCATIONS

Weld Location (Figure 3.10.3-1)	Max. Stress Intensity (ksi)
25 psig Internal Pressure	
Location 1	1.70
Location 2	4.92
Location 3	4.69
Location 4	1.65
25 psig Internal Pressure + 3g inertia load	
Location 1	5.27
Location 2	7.04
Location 3	2.67
Location 4	3.37
25 psig Internal Pressure + 3g Downward Load	
Location 1	2.86
Location 2	5.78
Location 3	5.50
Location 4	2.79

Note: All the stresses are less than the allowable stress of 21.00 ksi.

TABLE A4A.8-1
TOP NEUTRON SHIELD COVER BOLT INDIVIDUAL LOAD SUMMARY

Load Case	Applied Load		Non-Prying Tensile Force, F_a (lb.)	Torsional Moment, M_t (in. lb.)	Prying Force, F_f (lb.in.$^{-1}$)	Prying Moment, M_f (in.lb.in.$^{-1}$)
Preload	Residual	Maximum Torque	7,111	600	0	0
		Minimum Torque	6,400	540	0	0
Thermal	300 °F		0	0	0	0
Acceleration	3g Vertical		1,485	0	0	0

TABLE A4A.8-2
TOP NEUTRON SHIELD COVER BOLT LOAD COMBINATIONS

Load Case	Combination Description		Non-Prying Tensile Force, F_a (lb.)	Torsional Moment, M_t (in. lb.)	Prying Force, F_f (lb.in.$^{-1}$)	Prying Moment, M_f (in.lb.in.$^{-1}$)
1.	Preload + Temperature (Normal Condition)	A. Maximum Torque	7,111	600	0	0
		B. Minimum Torque	6,400	540	0	0
2.	Acceleration Loads		1,485	0	0	0

TABLE A4A.8-3
TOP NEUTRON SHIELD COVER BOLT STRESS SUMMARY

Stress Type	Normal Condition		Accident Condition	
	Stress	Allowable	Stress	Allowable
Average Tensile (ksi)	7.3	62.7	7.3	87.5
Shear (ksi)	2.2	37.6	2.2	52.5
Combined Stress Intensity (ksi)	8.6	84.7	Not Required (Reference 3)	
Interaction E.Q. $R_t^2 + R_s^2 < 1$	0.017	1	0.009	1

TABLE A4A.9-1
SUMMARY LINEARIZED STRESS COMPONENTS - NORMAL CONDITION

Cask Location from FIGURE A4A.9-1	**Max. Stress Type[(1)]**	**Membrane Stress (ksi)**			**Bending Stress (ksi)**		
		S_X (Rad.)	**S_Y (Tang.)**	**S_Z (Axial)**	**S_X (Rad.)**	**S_Y (Tang.)**	**S_Z (Axial)**
1. Weld	S_Y (N6)	1.74	3.61	0.38	2.65	1.73	2.40
	S_Z (N6)	1.76	3.26	0.38	2.65	1.75	2.59
2. Weld	S_Y (N5)	-0.30	1.46	-0.70	0.23	0.14	0.01
	S_Z (N5)	-0.20	1.53	-0.54	0.22	0.11	0.04
3. Weld	$S_{Y,Z}$ (N3)	1.0	1.06	0.19	0.04	0.09	0.22
4. Bottom Shield	$S_{X,}$ (N5)	1.89	3.38	-0.22	4.52	1.15	0.84
	S_Y (N5)	2.05	3.55	0.27	4.41	1.54	0.57
	S_Z (N5)	0.37	3.45	0.62	1.51	0.48	1.21
5. Shield Shell-Mid	$S_{Y,}$(N4)	-0.30	2.82	0.61	0.27	1.34	2.00
	S_Z (N4)	-0.30	2.88	1.35	0.29	0.82	1.66
6. Shield Shell-End	S_Y(N4)	2.18	4.57	0.87	6.99	2.41	0.03
	S_Z (N4)	2.07	4.06	0.91	7.01	2.35	0.06
7. Shell Flange	S_X (N4)	1.66	0.38	-3.18	3.73	3.24	7.80
	S_Y (N4)	-0.44	1.85	2.52	0.59	0.85	2.31
	S_Z (N4)	-0.44	1.69	2.55	0.61	0.79	2.29
8. Shield Plate	S_X (N3)	-0.07	0.65	0.17	0.12	0.37	0.12
	S_Y (N3)	-0.06	0.58	0.13	0.10	0.48	0.12
	S_Z (N3)	-0.06	0.65	0.17	0.12	0.38	0.12
9. Lid Outer Plate	S_X (N5)	0.17	0.91	-0.17	1.33	0.41	0.06
	$S_{Y,Z}$ (N5)	0.13	1.01	0.37	1.09	0.41	0.43
10. Inner Shell & Bottom Inner Plate	S_X (N5)	-0.04	-3.02	-4.72	1.05	2.40	7.69
	S_Y (N5)	-9.82	-3.42	-0.26	2.95	3.46	7.23
	S_Z (N5)	-13.04	-4.30	-0.10	2.21	1.51	5.64

1. S_X – Radial Stress S_Y – Tangential Stress S_Z – Axial Stress

TABLE A4A.9-2
SUMMARY LINEARIZED STRESS COMPONENTS – ACCIDENT CONDITION

Cask Location From Figure A4A.9-1	Max. Stress Type(1)	Membrane Stress (ksi)			Bending Stress (ksi)		
		S_X (Rad.)	S_Y (Tang.)	S_Z (Axial)	S_X (Rad.)	S_Y (Tang.)	S_Z (Axial)
1. Weld	S_Y(A2)	0.09	-0.63	-4.92	0.01	0.16	0.60
	S_Z (A2)	0.09	-0.63	-4.92	0.01	0.16	0.60
2. Weld	S_Y(A4)	-0.10	0.43	-0.32	0.13	0.03	0.03
	S_Z(A4)	-0.10	-0.36	-0.31	0.13	0.0	0.03
3. Weld	S_Y(A3)	0.51	0.41	1.06	0.24	0.43	1.19
	S_Z(A3)	0.52	0.42	1.09	0.25	0.46	1.29
4. Bottom Shield	S_X(A4)	0.45	0.64	0.49	2.80	0.78	0.63
	S_Y(A4)	0.44	0.53	-0.04	1.82	2.01	0.16
	S_Z(A4)	-0.14	0.76	1.37	1.49	0.72	1.66
5. Shield Shell-Mid	S_Y(A4)	-0.25	3.08	0.74	0.28	0.38	0.06
	S_Z(A4)	-0.26	3.04	0.90	0.28	0.25	0.0
6. Shield Shell-End	S_Y(A4)	1.64	1.12	1.23	2.54	1.76	3.37
	S_Z(A4)	1.18	0.56	0.36	1.24	1.51	4.26
7. Shell Flange	S_X(A3)	1.48	0.09	-2.95	3.67	3.42	8.34
	S_Y(A3)	1.47	0.90	-2.96	3.67	3.42	8.34
	S_Z(A3)	-0.22	0.85	2.18	1.11	0.85	2.55
8. Shield Plate	S_X,S_Y(A3)	0.79	0.79	-0.02	3.36	3.36	0.10
	S_Z(A3)	0.16	0.60	0.13	0.34	0.28	0.91
9. Lid Outer Plate	S_X(A4)	0.47	0.54	-0.19	1.78	0.35	0.0
	S_Y(A4)	0.72	0.72	-0.02	1.48	1.48	0.10
	S_Z(A4)	0.42	0.71	0.38	1.42	0.32	0.43
10. Inner Shell & Bottom Inner Plate	S_X(A3)	8.40	2.36	-2.17	4.10	2.48	3.65
	S_Y(A3)	8.40	2.36	-2.17	4.10	2.48	3.65
	S_Z (A3)	-2.43	-1.99	-4.46	0.67	2.55	7.91

1. S_X – Radial Stress S_Y – Tangential Stress S_Z – Axial Stress

TABLE A4A.9-3
SUMMARY STRESS INTENSITY FACTORS FOR NORMAL CONDITION

Component	Thick. t (in)	Crack depth, a (in)	Crack length, l (in)	Max. Stress Type(1)	Critical Crack Direction(1)	Stress Intens. Factor (ksi-√in)	Allow. Stress Intens. Factor (ksi-√in)	Factors of Safety
1. Weld	1.50	0.225	2.25	S_Y	Axial	4.64	14.86	3.20
2. Weld	1.00	0.150	1.50	S_Y	Axial	1.30	14.86	>10
3. Weld	0.75	0.1125	1.125	S_Y	Axial	0.80	14.86	>10
4. Bottom Shield	7.25	0.500	5.00	S_X	Tangential	8.61	14.86	1.73
5. Shield Shell-Mid	7.25	0.500	5.00	S_Y	Axial	5.64	14.86	2.64
6. Shield Shell End	7.25	0.500	5.00	S_Y	Axial	9.31	14.86	1.60
7. Shell Flange	4.6	0.500	5.00	S_Z	Hoop	9.32	14.86	1.59
8. Shield Plate	5.5	0.500	5.00	S_Y	Axial	1.69	14.86	9.27
9. Lid Outer Plate	4.5	0.500	5.00	S_Y	Axial	2.0	14.86	7.45
10. Inner Shell & Bottom Inner Plate	1.5	0.225	2.25	S_Z	Hoop	5.88	14.86	2.53

1. S_Y – Hoop Stress – Results in Axial crack S_Z – Axial Stress – Results in Hoop crack

   S_X – Radial Stress – Results in Tangential crack

TABLE A4A.9-4
SUMMARY STRESS INTENSITY FACTORS FOR ACCIDENT CONDITION

Component	Thick. t (in)	Crack depth, a (in)	Crack length, l (in)	Max. Stress Type[(1)]	Critical Crack Direction[(1)]	Stress Intens. Factor (ksi-√in)	Allow. Stress Intens. Factor (ksi-√in)	Factors of Safety
1. Weld	1.50	0.225	2.25	S_Z	Hoop	0.54	33.23	>10
2. Weld	1.00	0.150	1.50	S_Y	Axial	0.41	33.23	>10
3. Weld	0.75	0.1125	1.125	S_Z	Hoop	1.40	33.23	>10
4. Bottom Shield	7.25	0.500	5.00	S_X	Tangential	4.25	33.23	7.82
5. Shield Shell-Mid	7.25	0.500	5.00	S_Y	Axial	4.68	33.23	7.10
6. Shield Shell-End	7.25	0.500	5.00	S_Z	Hoop	7.15	33.23	4.65
7. Shell Flange	4.6	0.500	5.00	S_Z	Hoop	13.00	33.23	2.56
8. Shield Plate	5.5	0.500	5.00	S_X	Tangential	5.20	33.23	6.40
9. Lid Outer Plate	4.5	0.500	5.00	S_X	Tangential	3.22	33.23	>10
10. Inner Shell & Bottom Inner Plate	1.5	0.225	2.25	S_X	Tangential	10.89	33.23	3.05

1 S_Y – Hoop Stress – Results in Axial crack S_Z – Axial Stress – Results in Hoop crack

S_X – Radial Stress – Results in Tangential crack

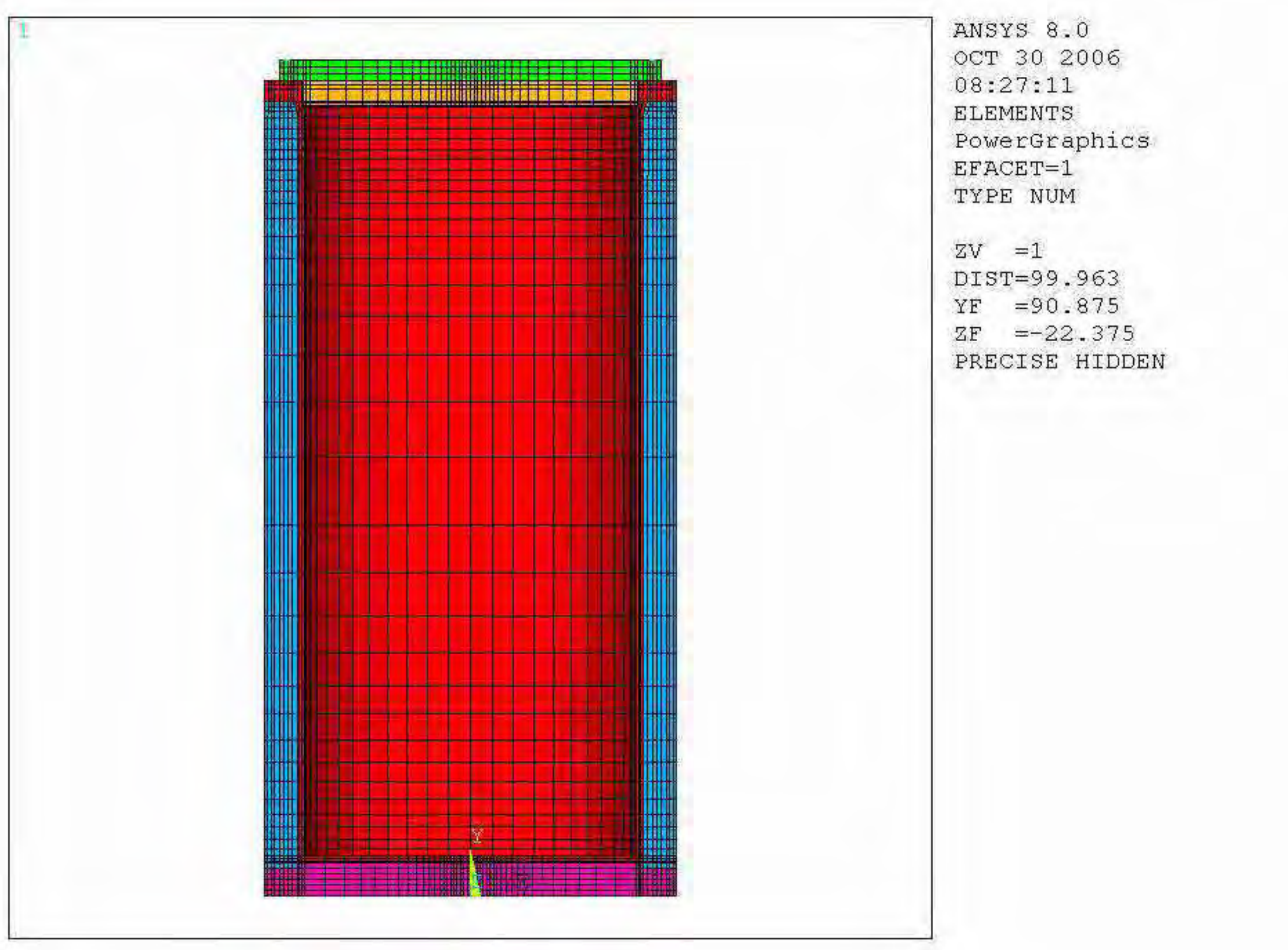

FIGURE A4A.3-1
TN-40HT STORAGE CASK FEM REPRESENTATION

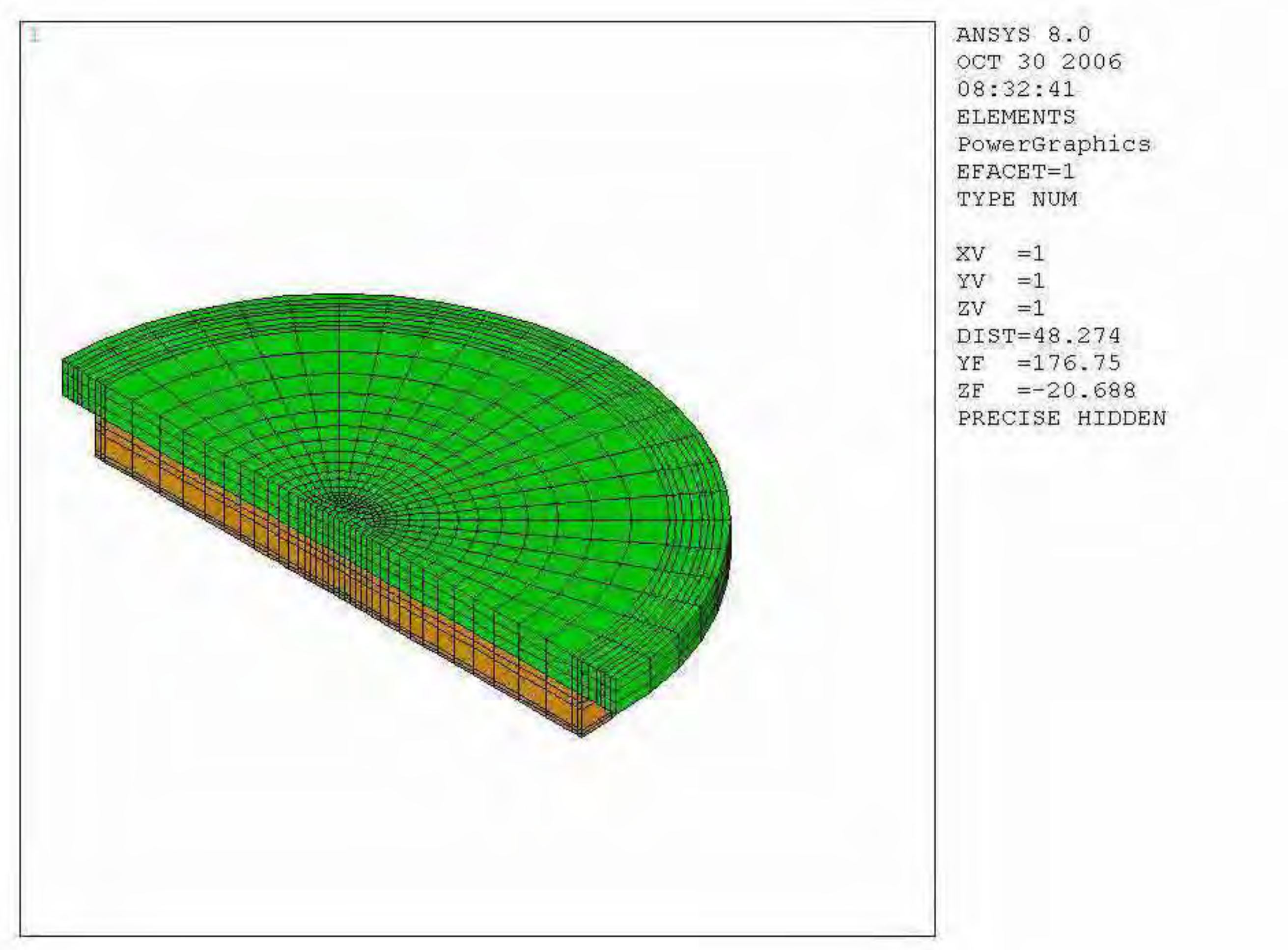

FIGURE A4A.3-2
FINITE ELEMENT MODEL—LID OUTER PLATE AND SHIELD PLATE

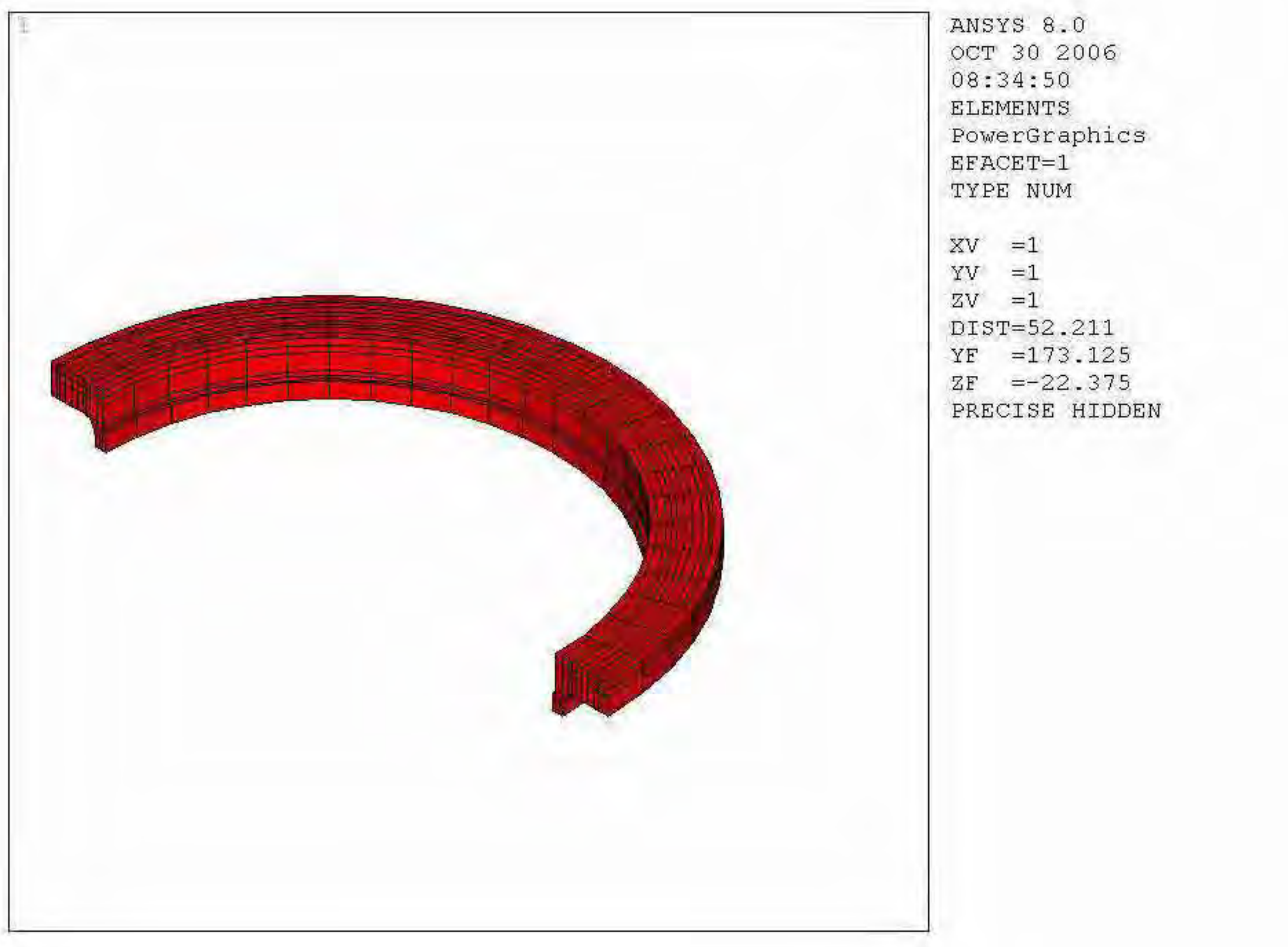

FIGURE A4A.3-3
FINITE ELEMENT MODEL – SHELL FLANGE

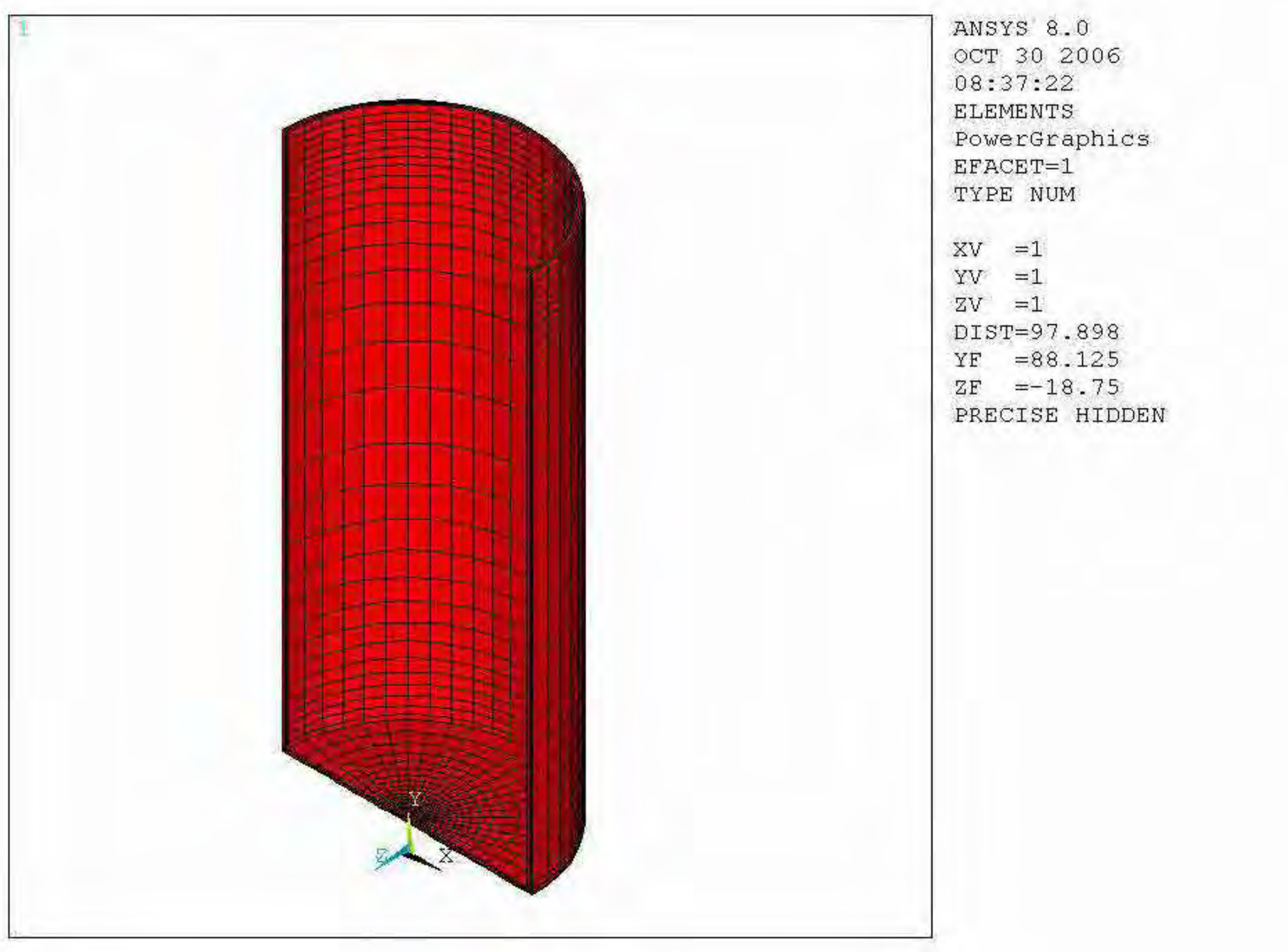

FIGURE A4A.3-4
FINITE ELEMENT MODEL – INNER SHELL AND BOTTOM INNER PLATE

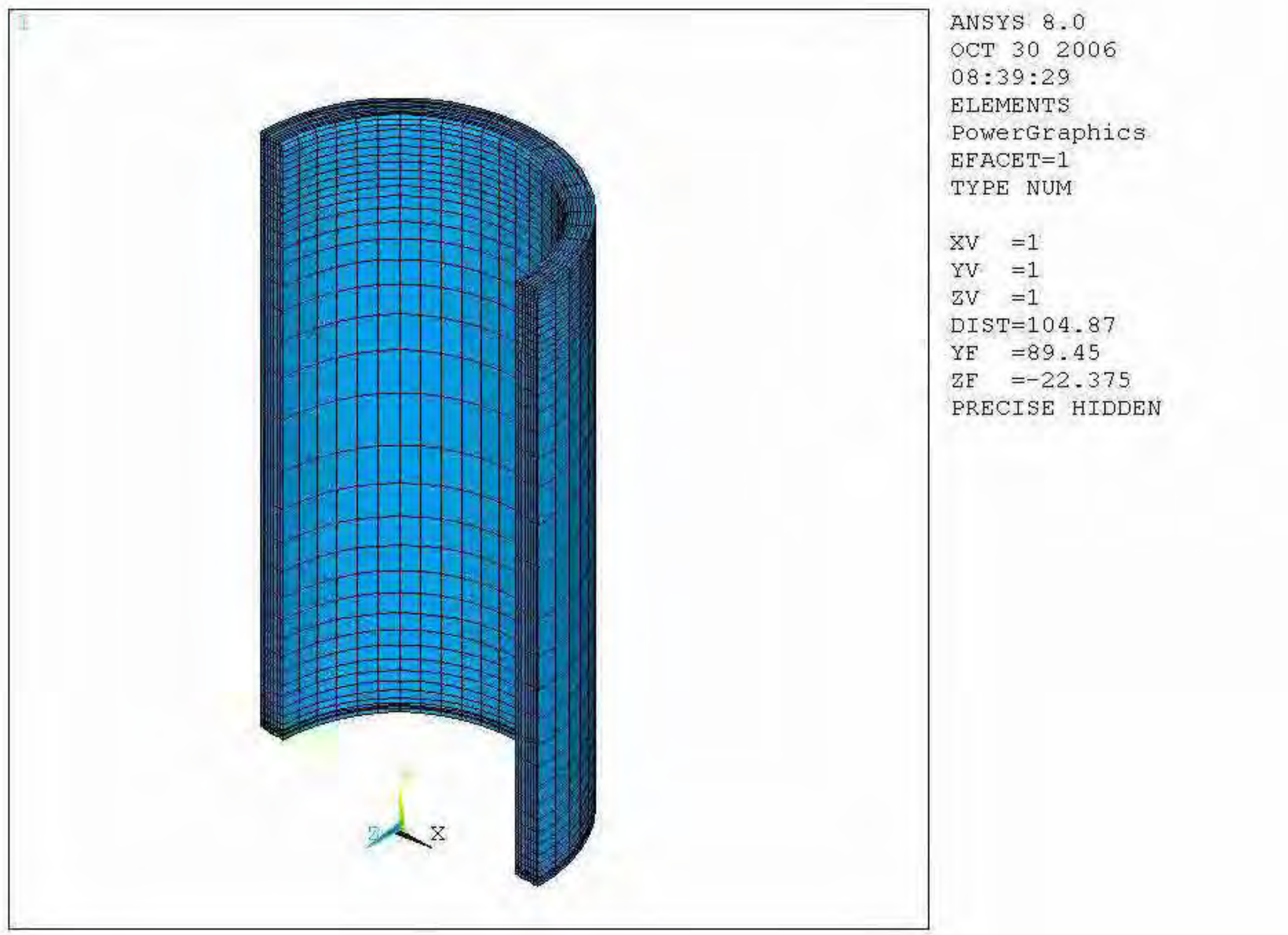

FIGURE A4A.3-5
FINITE ELEMENT MODEL – SHIELD SHELL

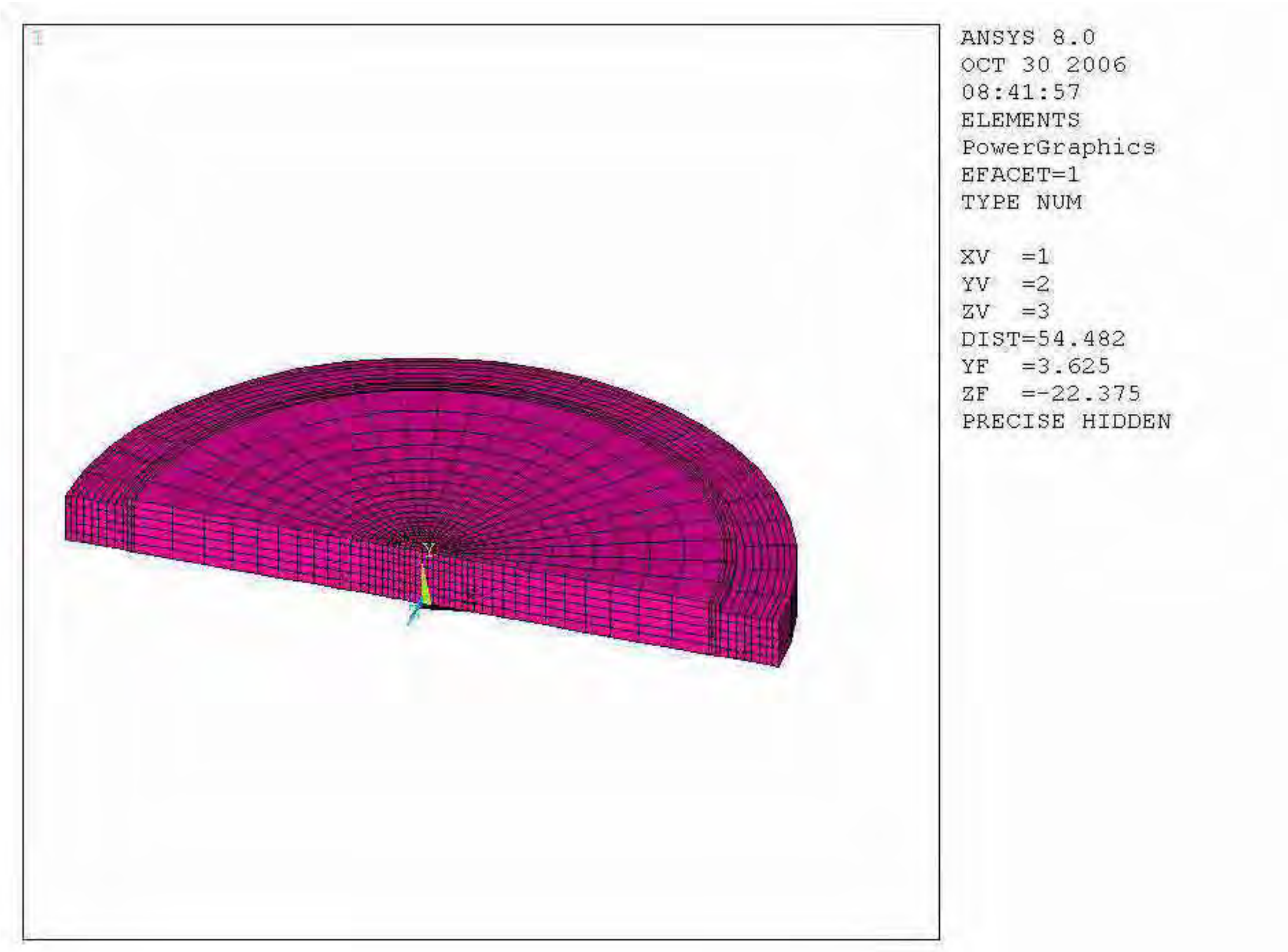

FIGURE A4A.3-6
FINITE ELEMENT MODEL – BOTTOM SHIELD

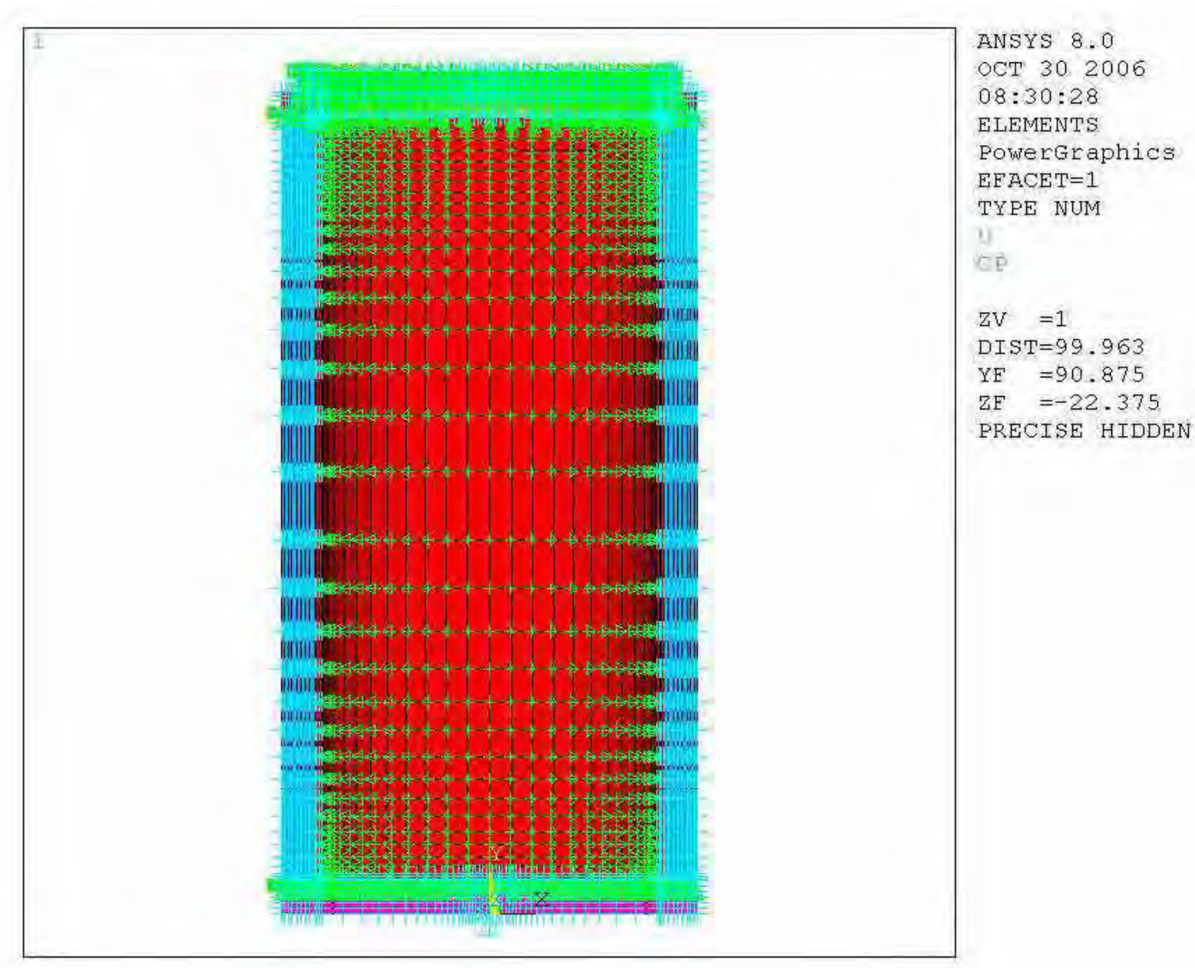

FIGURE A4A.3-7
COUPLING AND BOUNDARY CONDITIONS

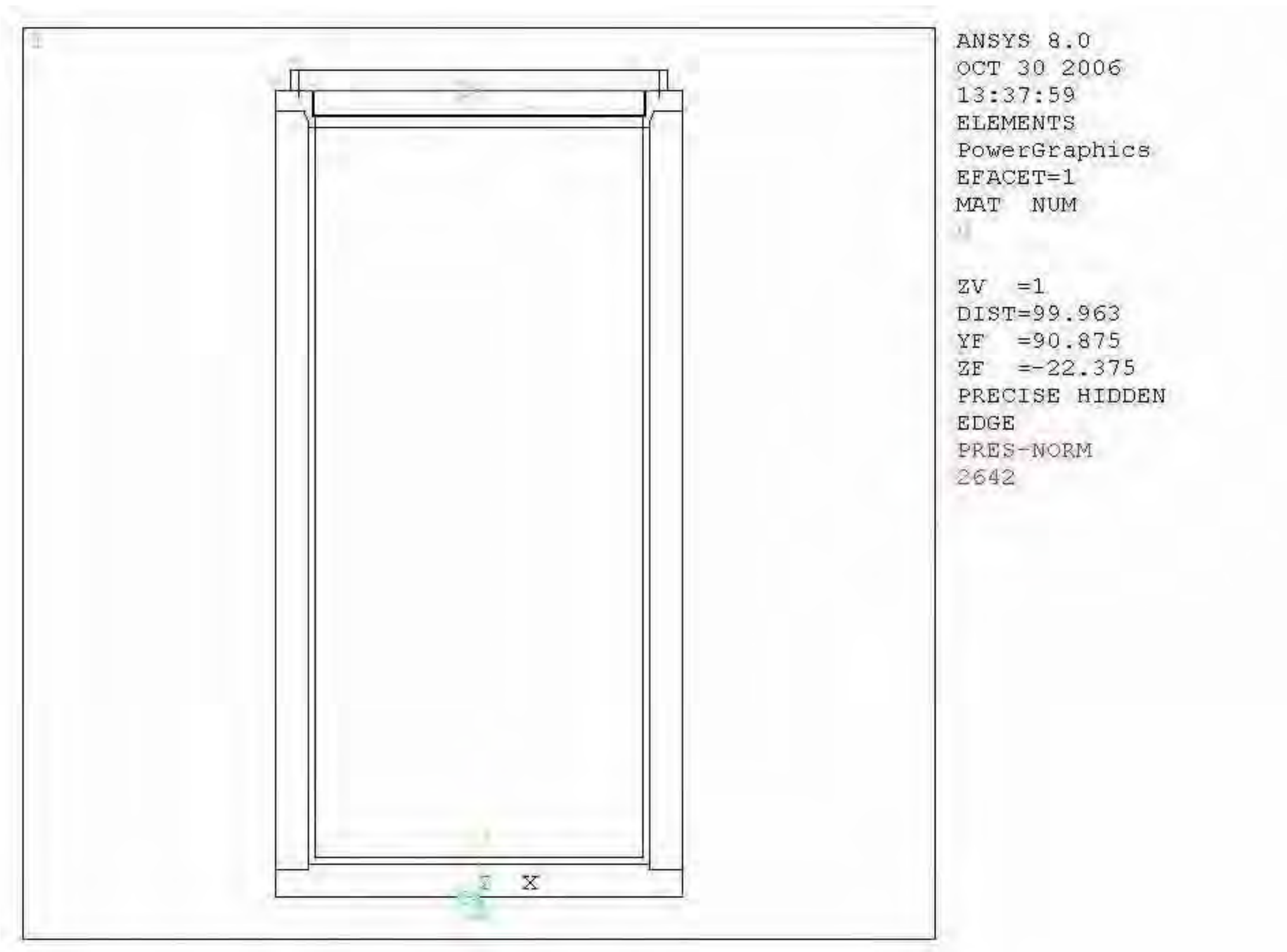

FIGURE A4A.3-8
BOLT PRELOAD AND LID SEATING PRESSURE – LOADING AND DISPLACEMENT BOUNDARY CONDITIONS

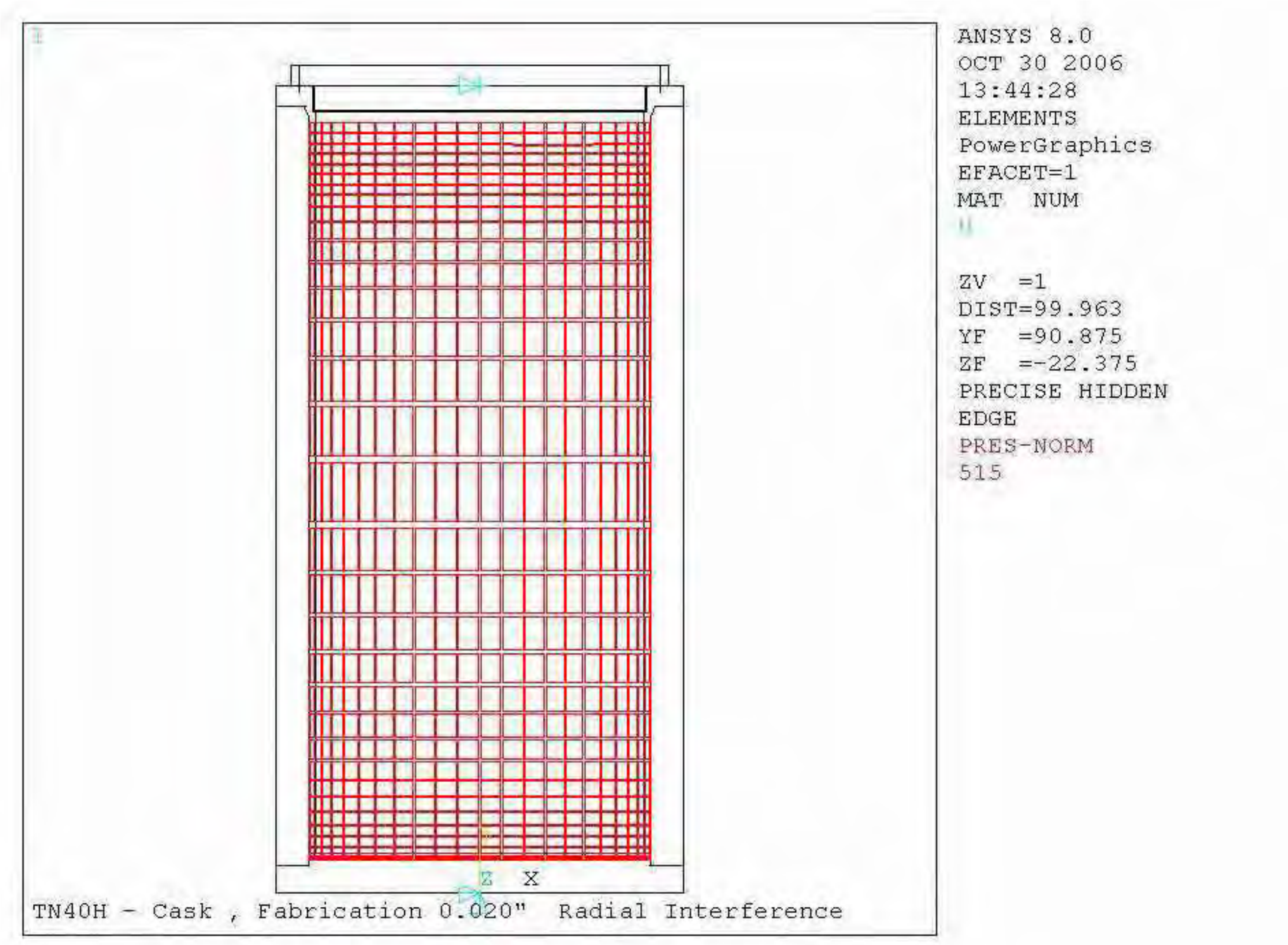

FIGURE A4A.3-9
FABRICATION STRESS – LOADING AND DISPLACEMENT BOUNDARY CONDITIONS

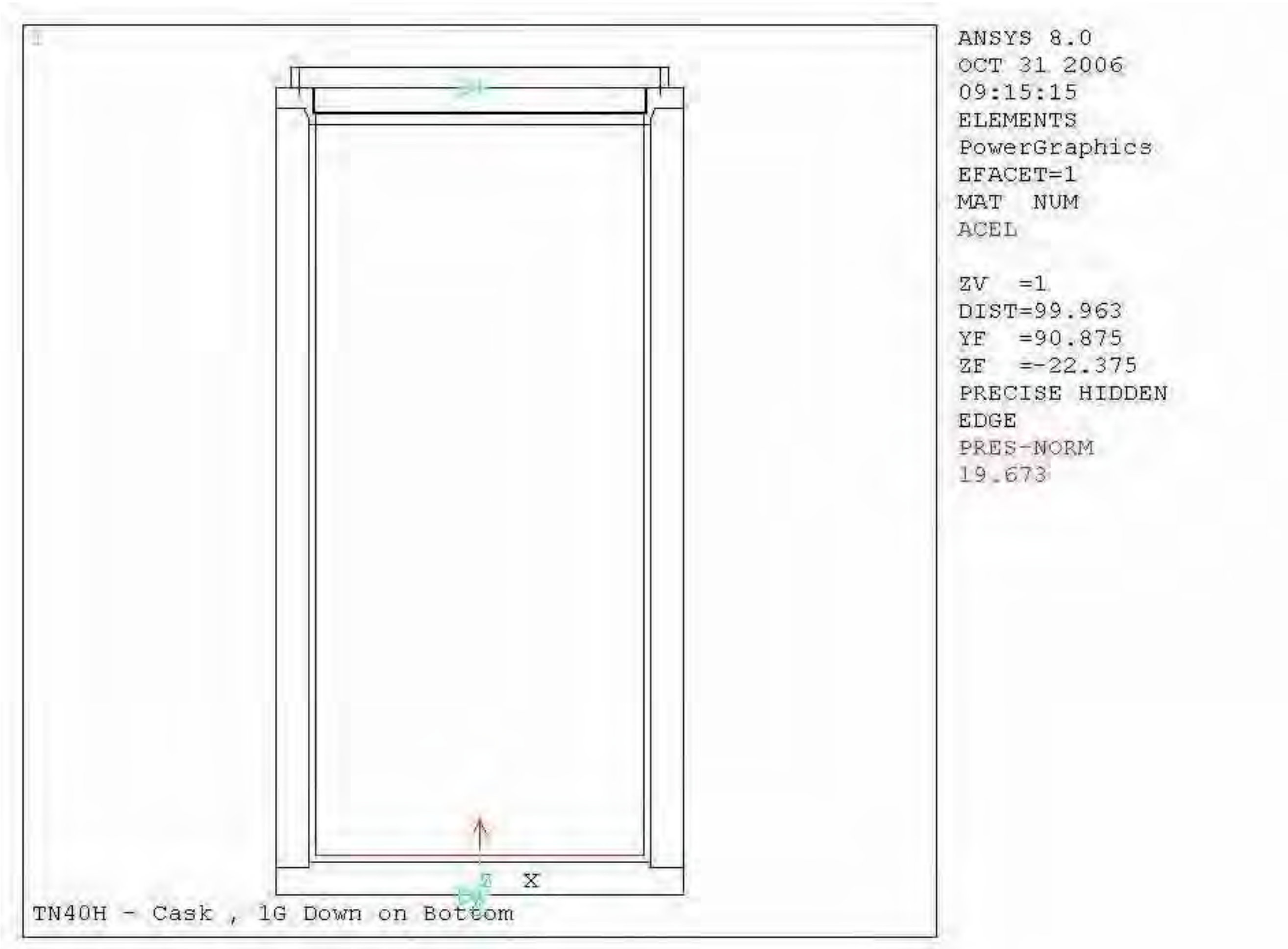

FIGURE A4A.3-10
1G DOWN – LOADING AND DISPLACEMENT BOUNDARY CONDITIONS

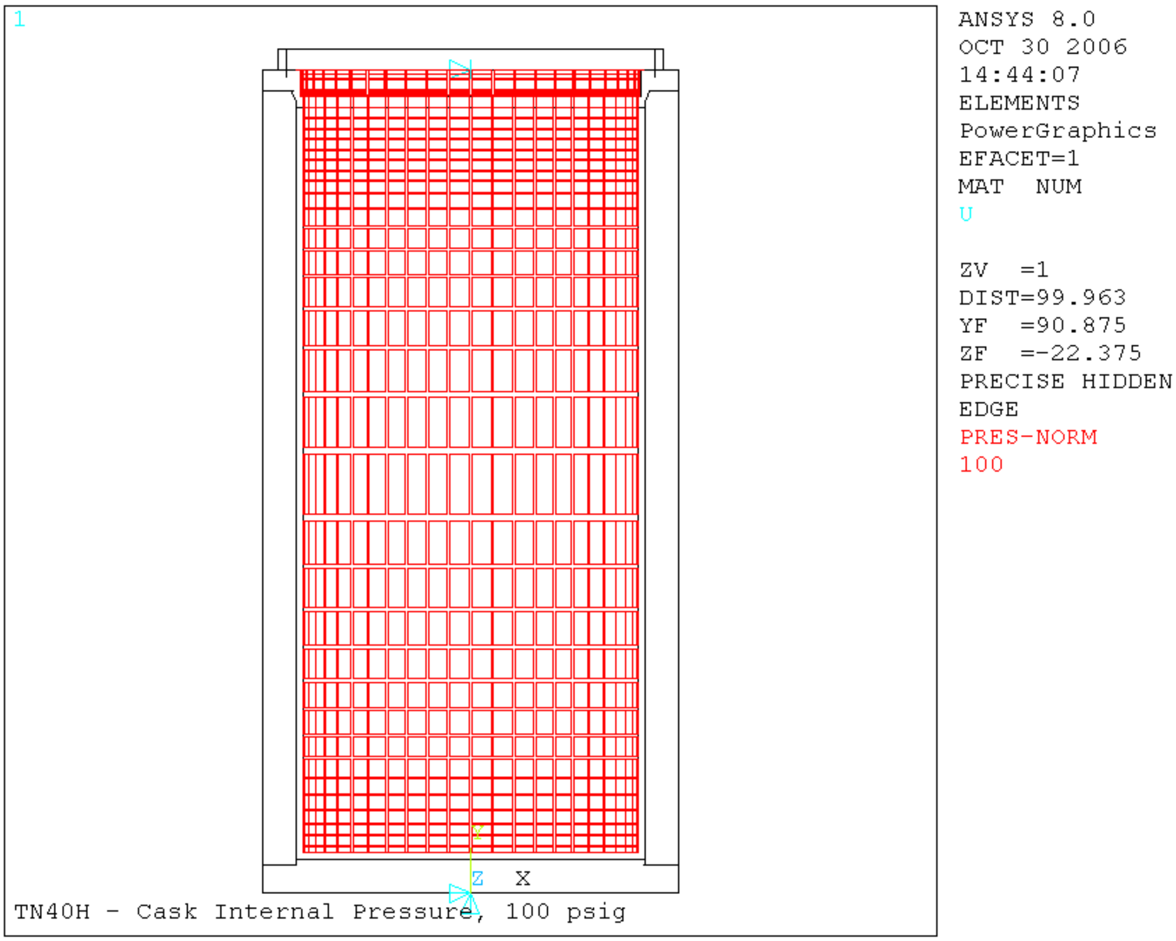

FIGURE A4A.3-11
INTERNAL PRESSURE – LOADING AND DISPLACEMENT BOUNDARY CONDITIONS

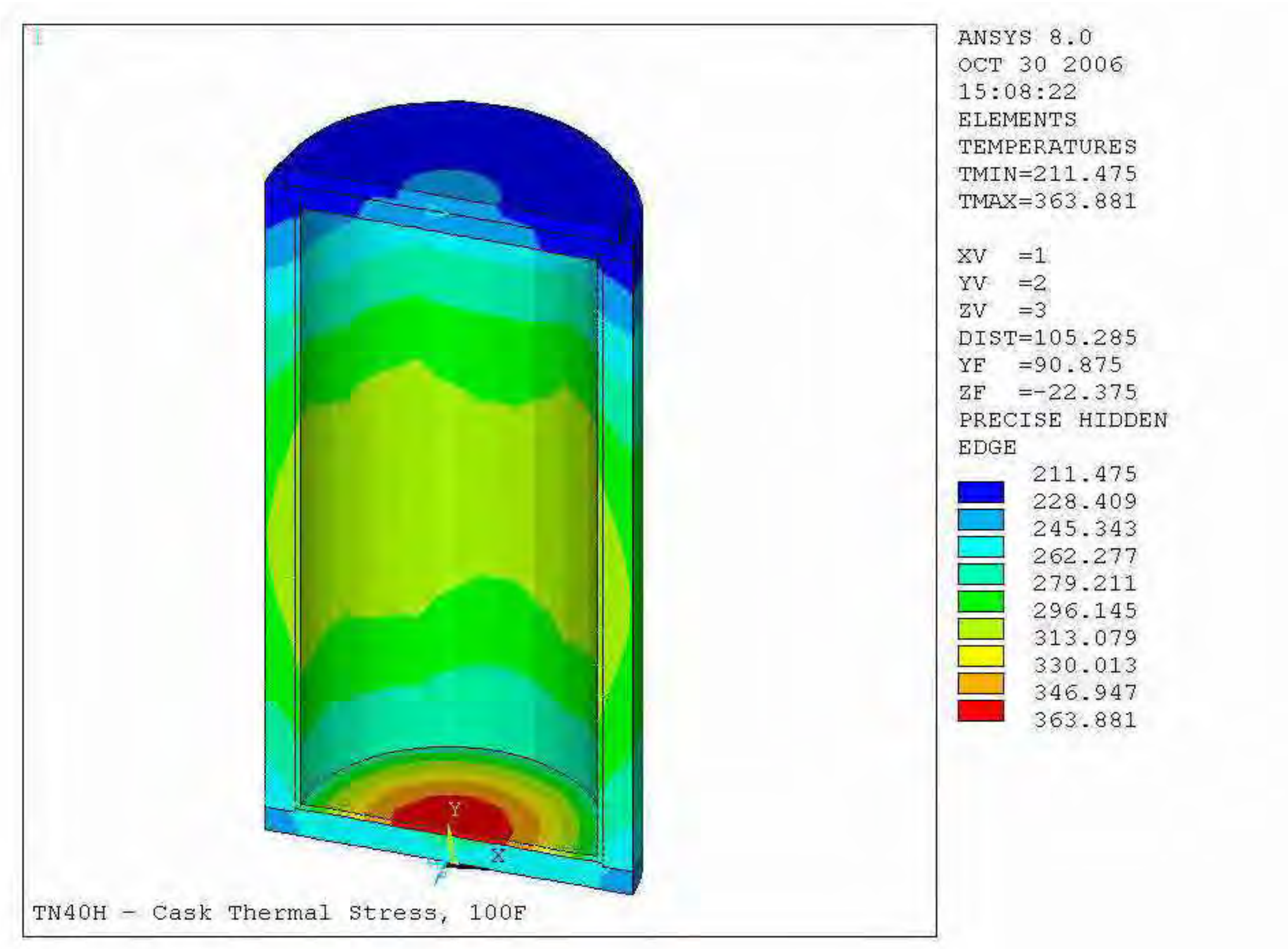

FIGURE A4A.3-12
THERMAL STRESS 100° F ENVIRONMENT – LOADING AND DISPLACEMENT BOUNDARY CONDITIONS

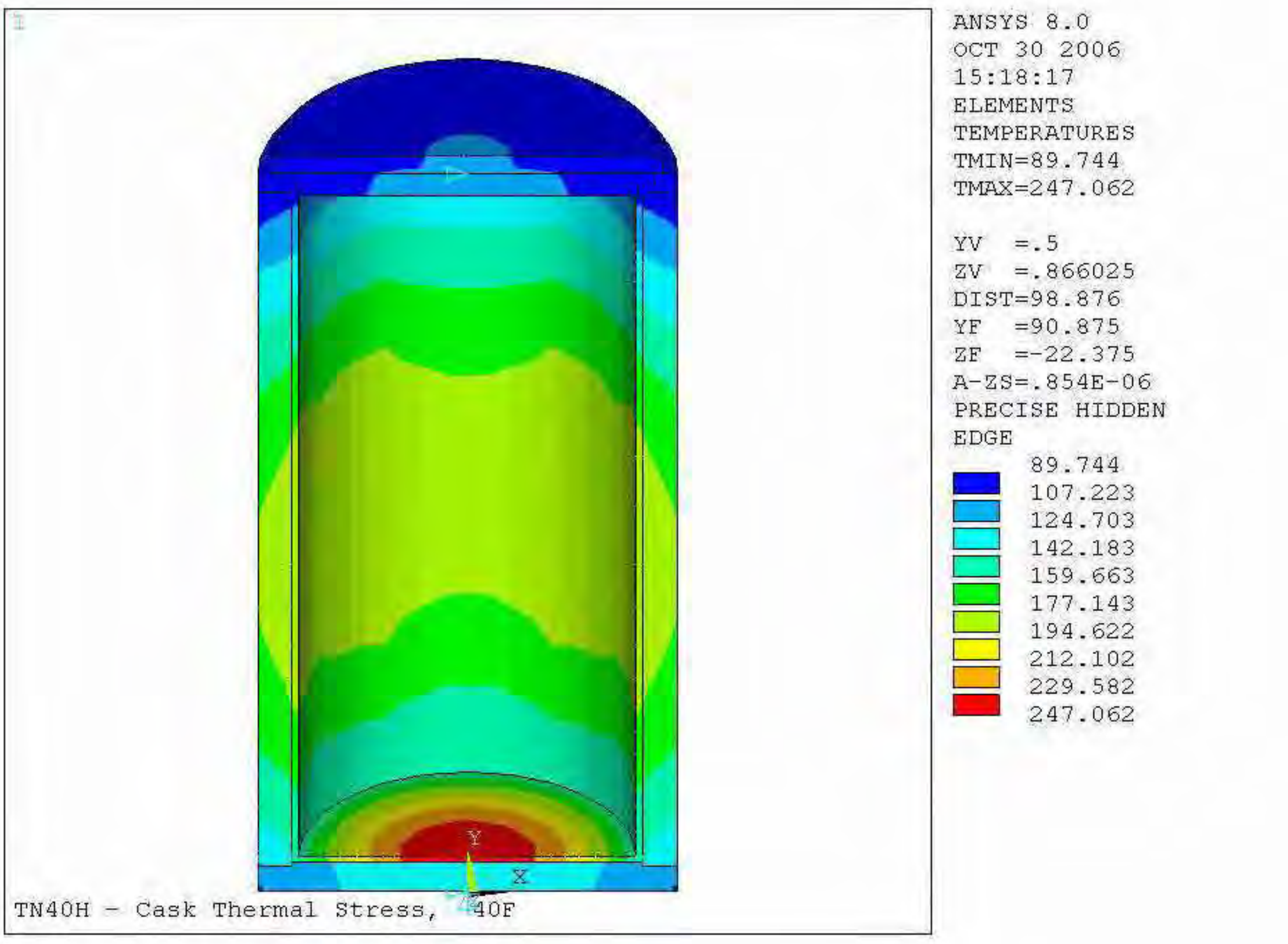

FIGURE A4A.3-13
THERMAL STRESS -40° F ENVIRONMENT – LOADING AND DISPLACEMENT BOUNDARY CONDITIONS

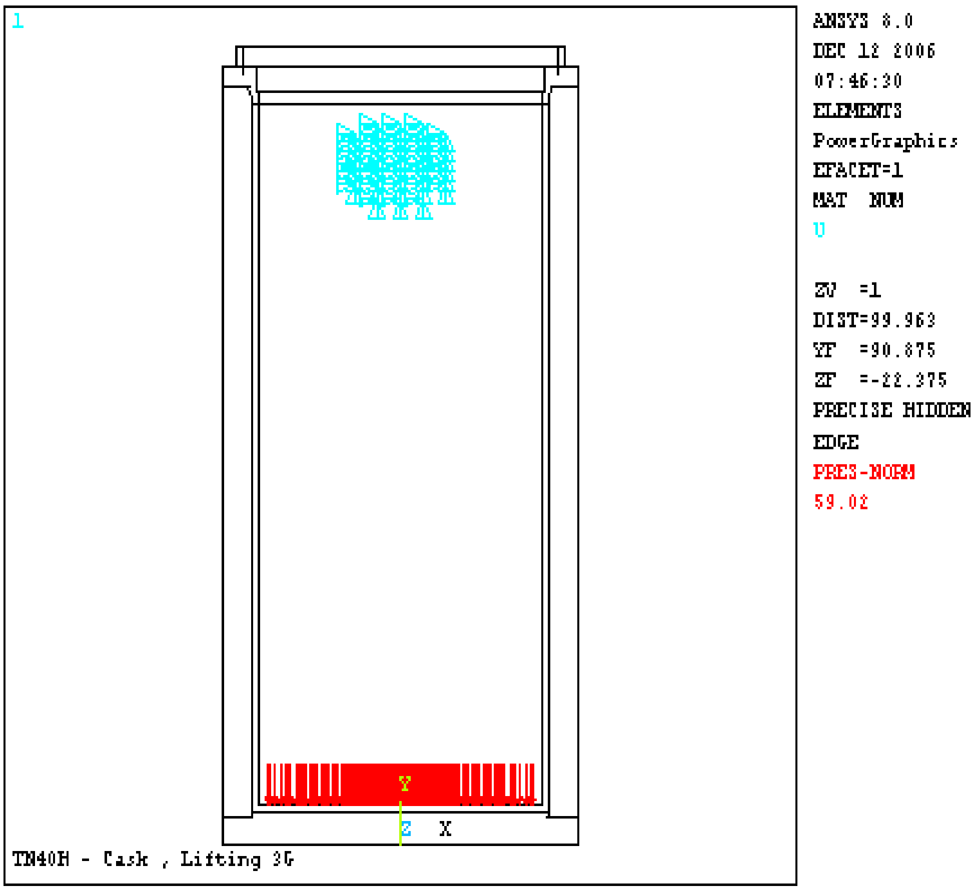

FIGURE A4A.3-14
3G VERTICAL LIFTING – LOADING AND DISPLACEMENT BOUNDARY CONDITIONS

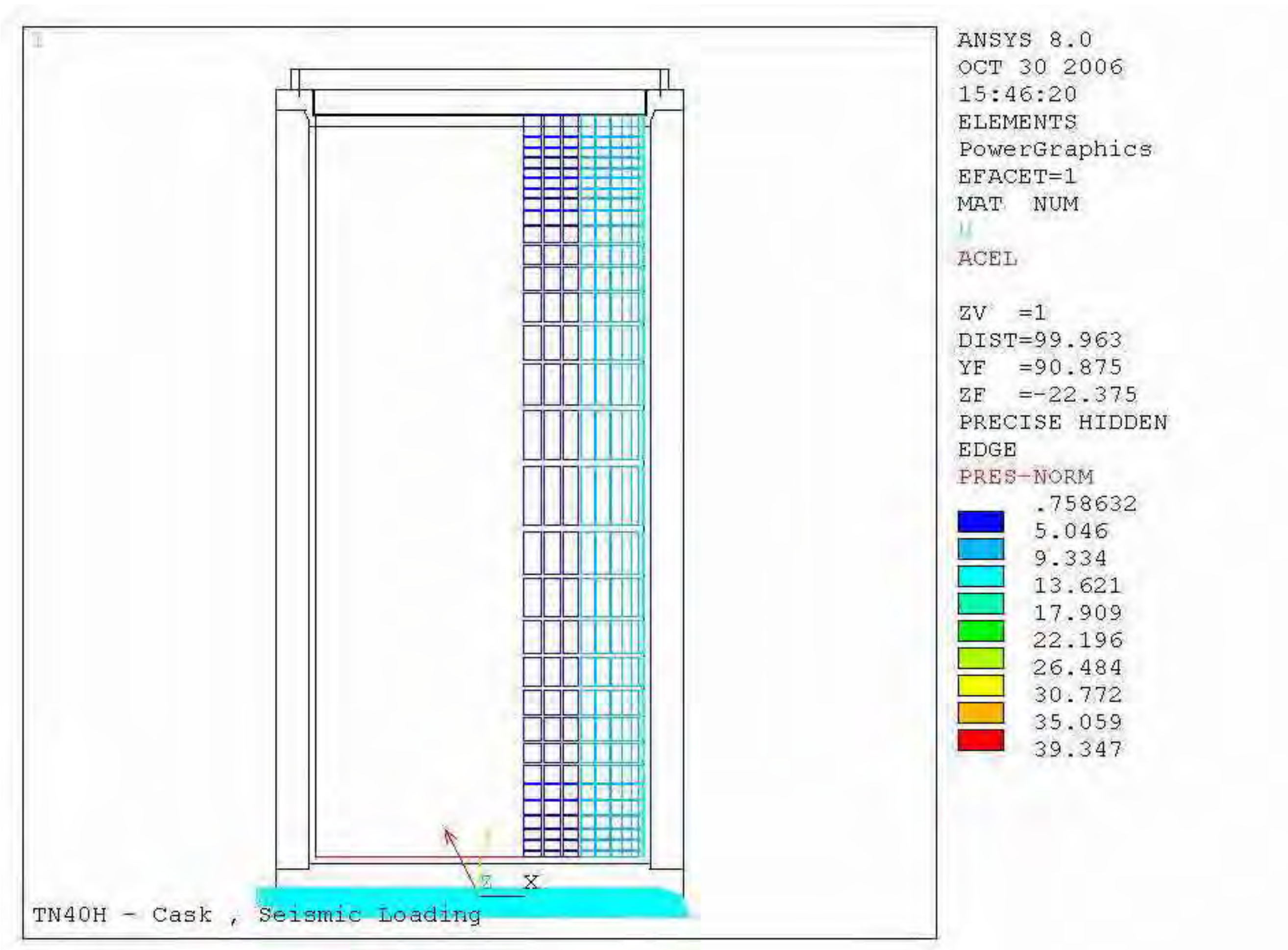

FIGURE A4A.3-15
SEISMIC – LOADING AND DISPLACEMENT BOUNDARY CONDITIONS

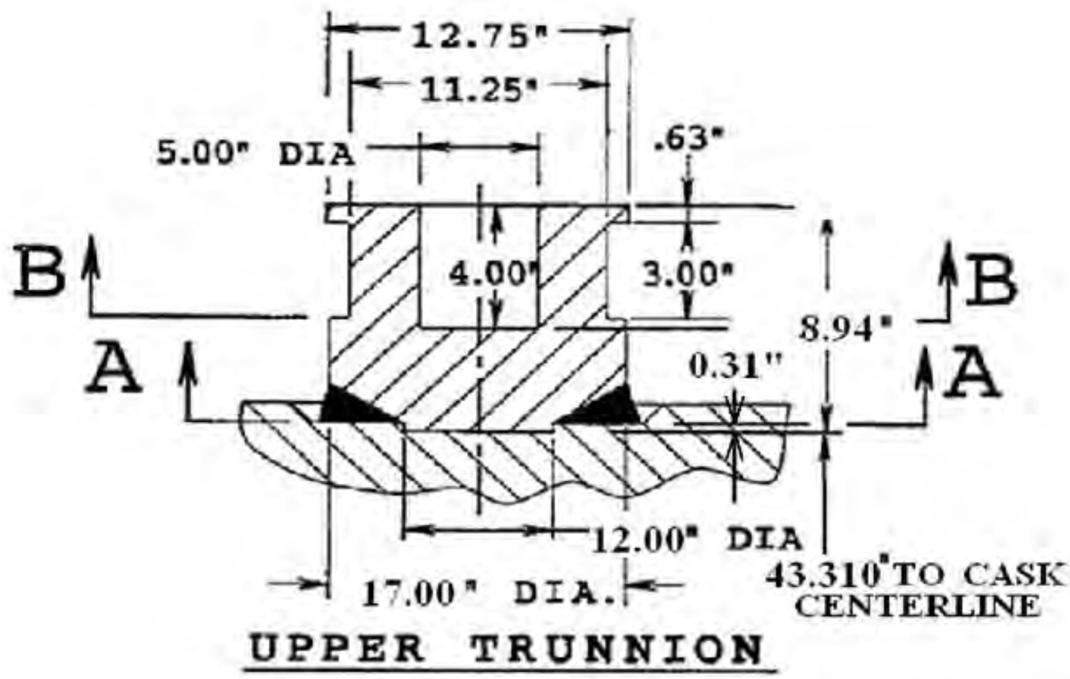

FIGURE A4A.6-1
TN-40HT TRUNNION DIMENSIONS

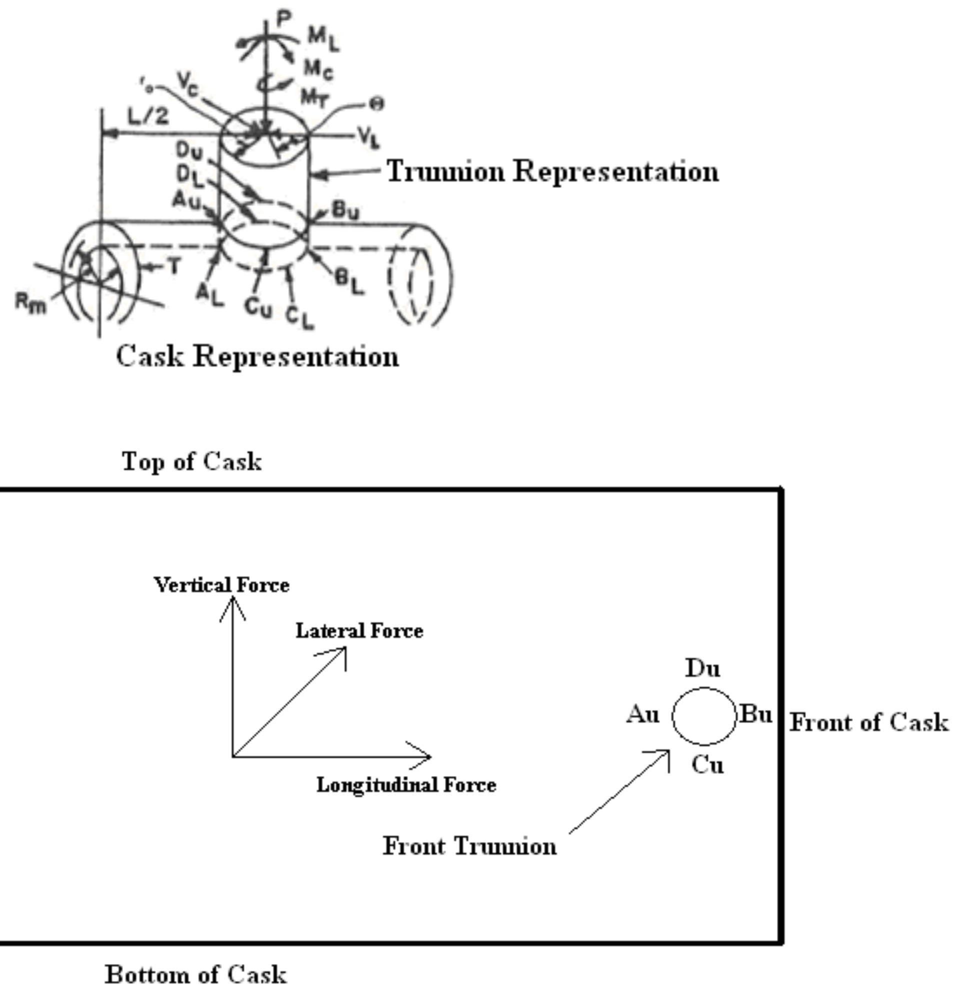

FIGURE A4A.6-2
ILLUSTRATION OF DEFINING FORCES, MOMENTS, AND STRESS LOCATIONS

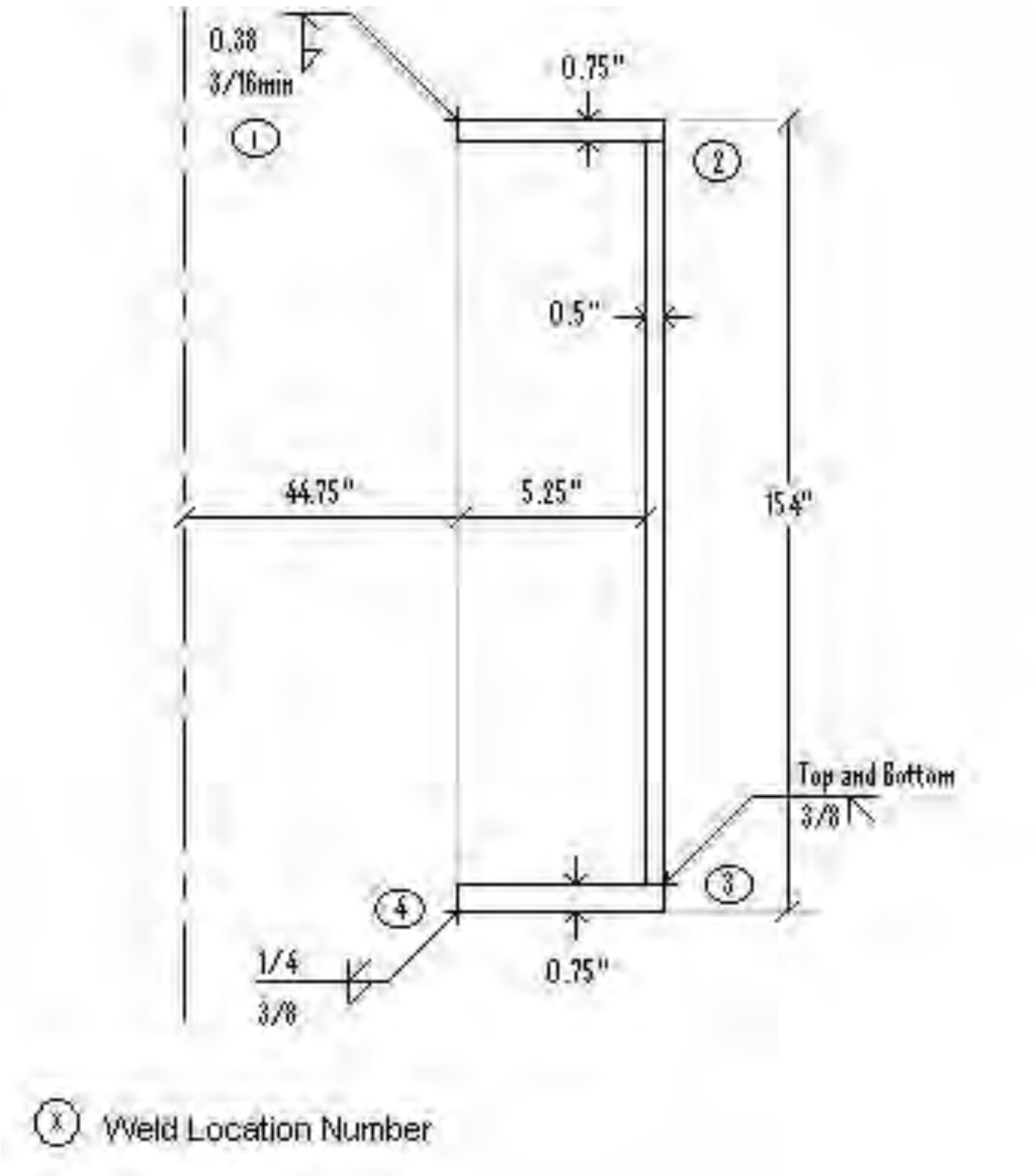

Figure A4A.7-1
CASK OUTER SHELL AND CONNECTION TO CASK BODY

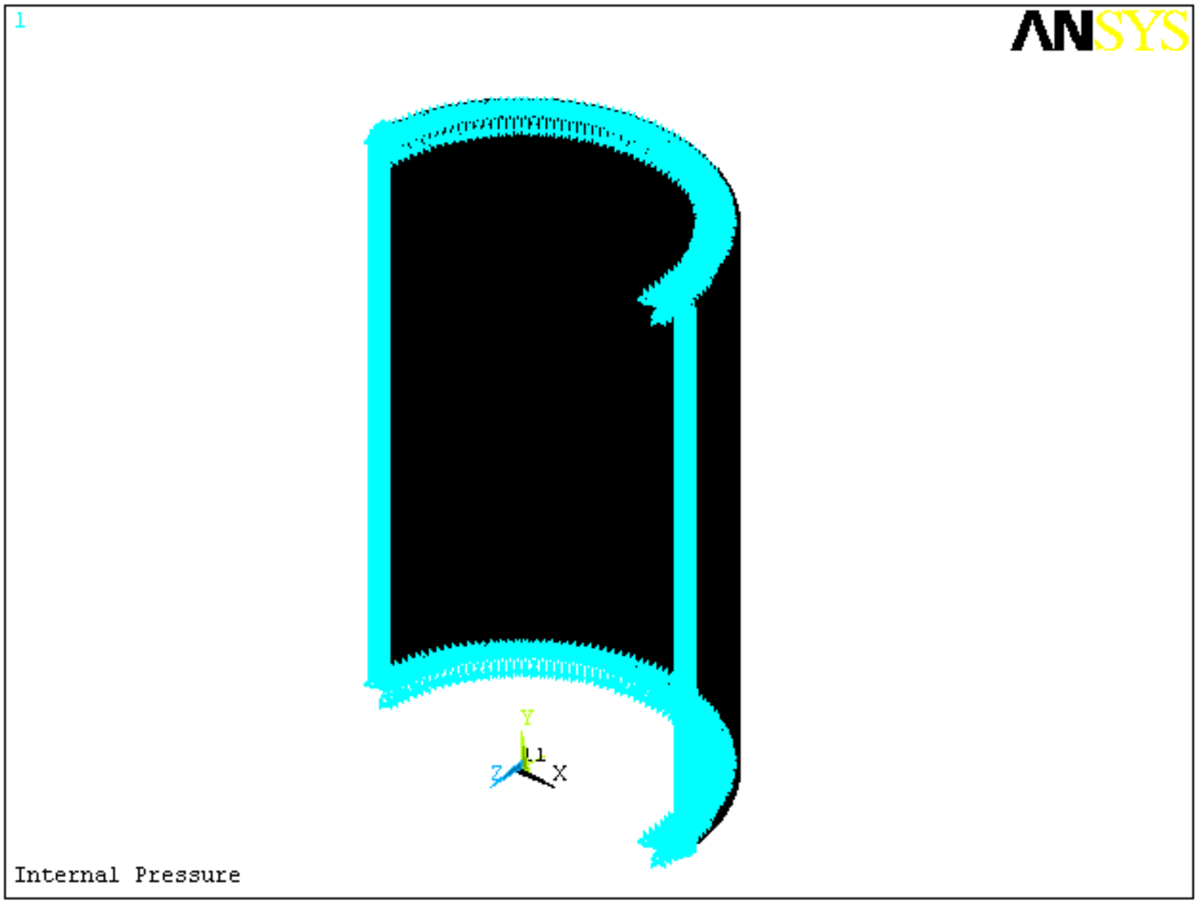

Figure A4A.7-2
FINITE ELEMENT MODEL - BOUNDARY CONDITIONS

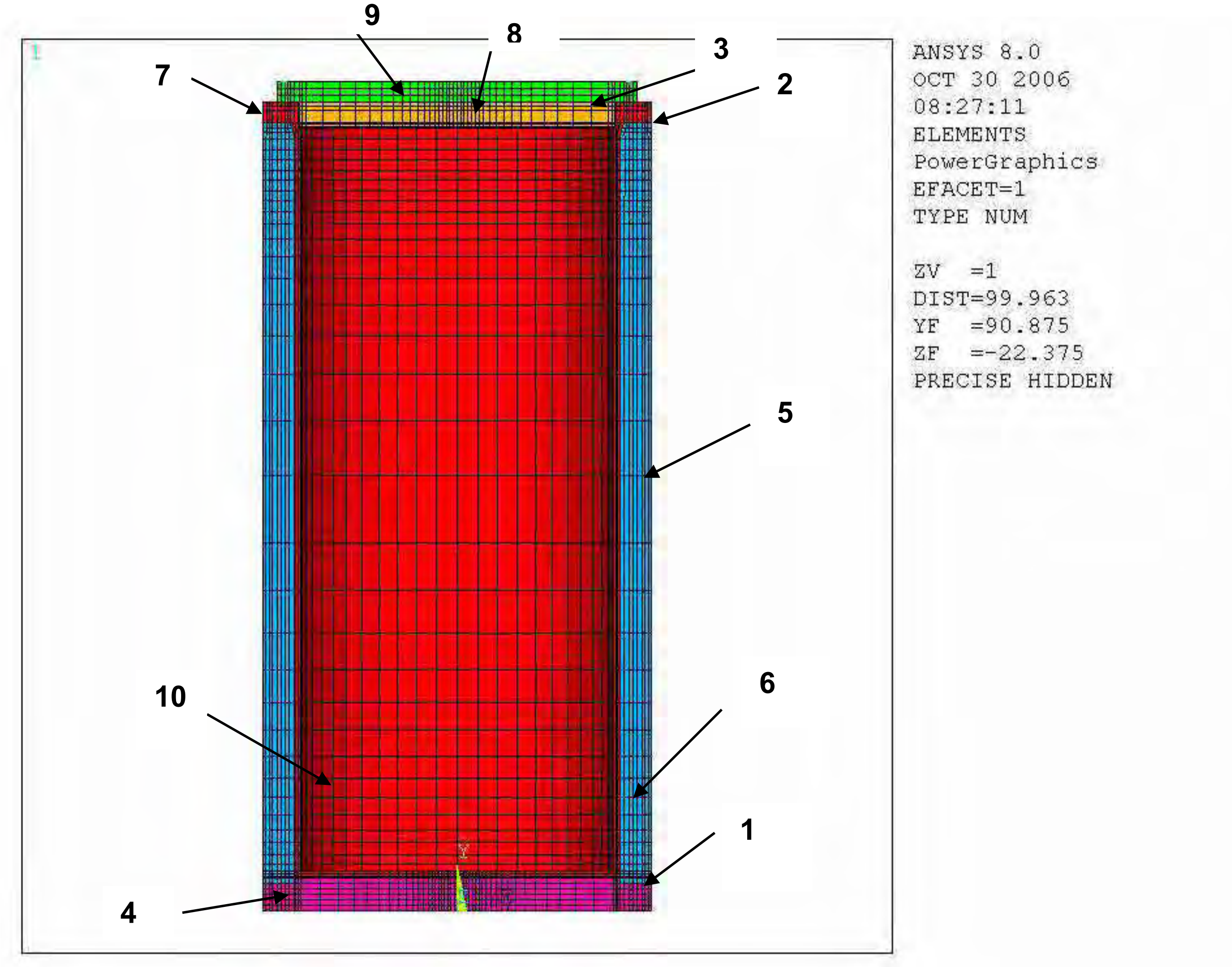

Note: Numbers indicate selected locations for fracture toughness evaluation.

FIGURE A4A.9-1
CASK BODY CRITICAL LOCATIONS FOR STRESS AND FRACTURE EVALUATION

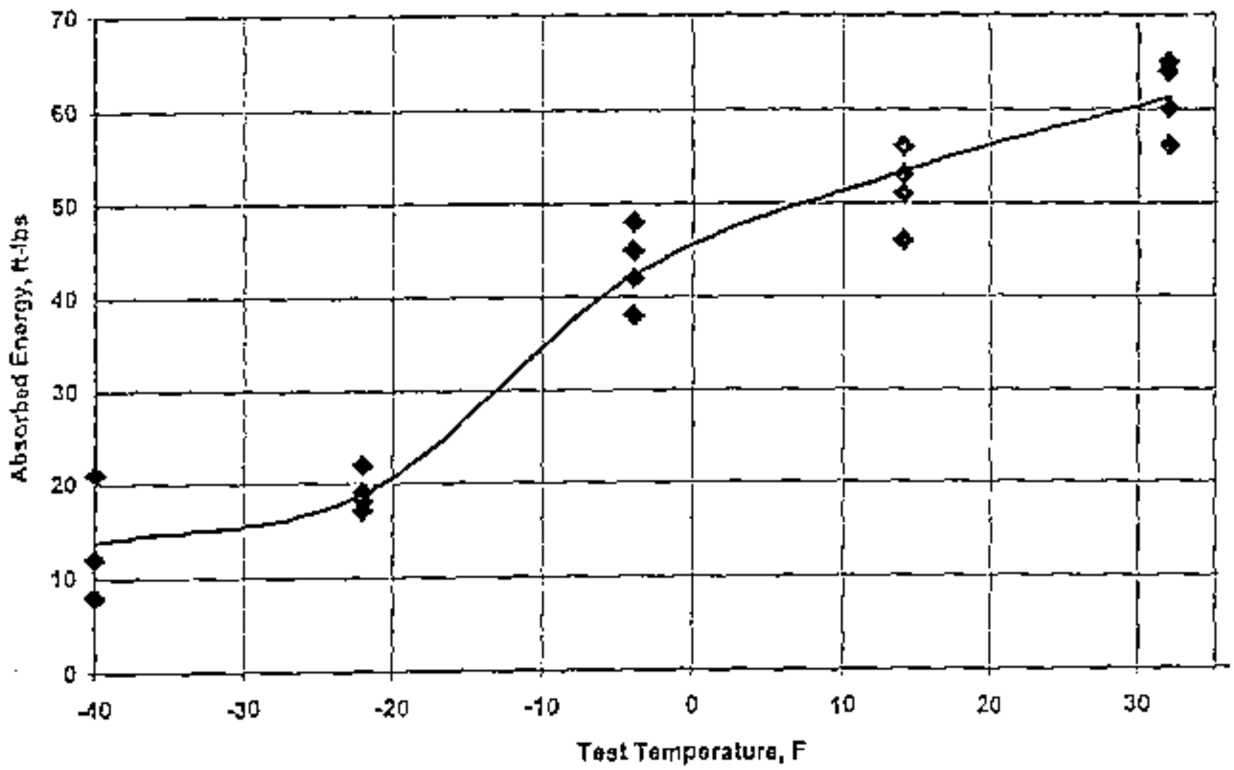

FIGURE A4A.9-2
CHARPY V-NOTCH TEST RESULTS FOR SA-266 FORGING

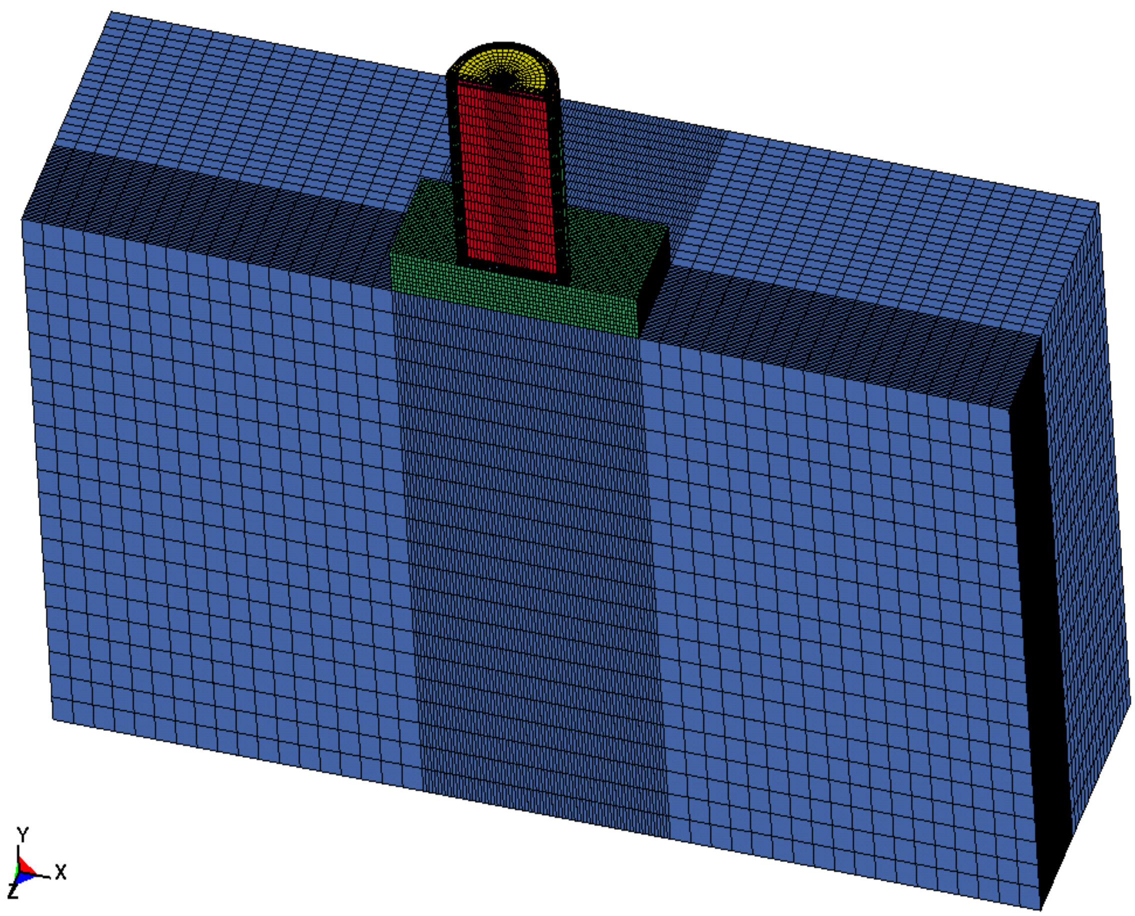

FIGURE A4A.10-1
OVERVIEW OF FINITE ELEMENT MODEL

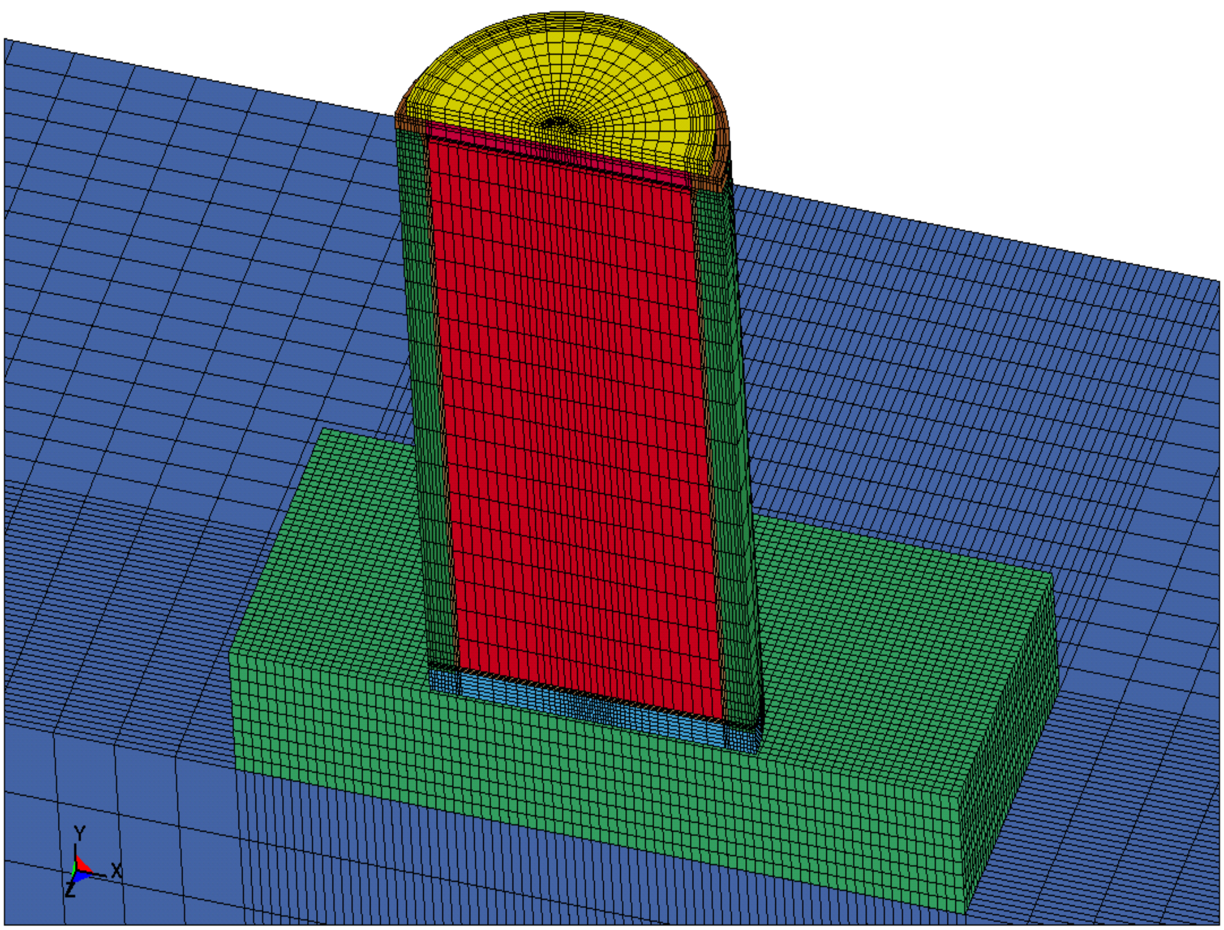

FIGURE A4A.10-2
OVERVIEW OF TN-40HT CASK FINITE ELEMENT MODEL

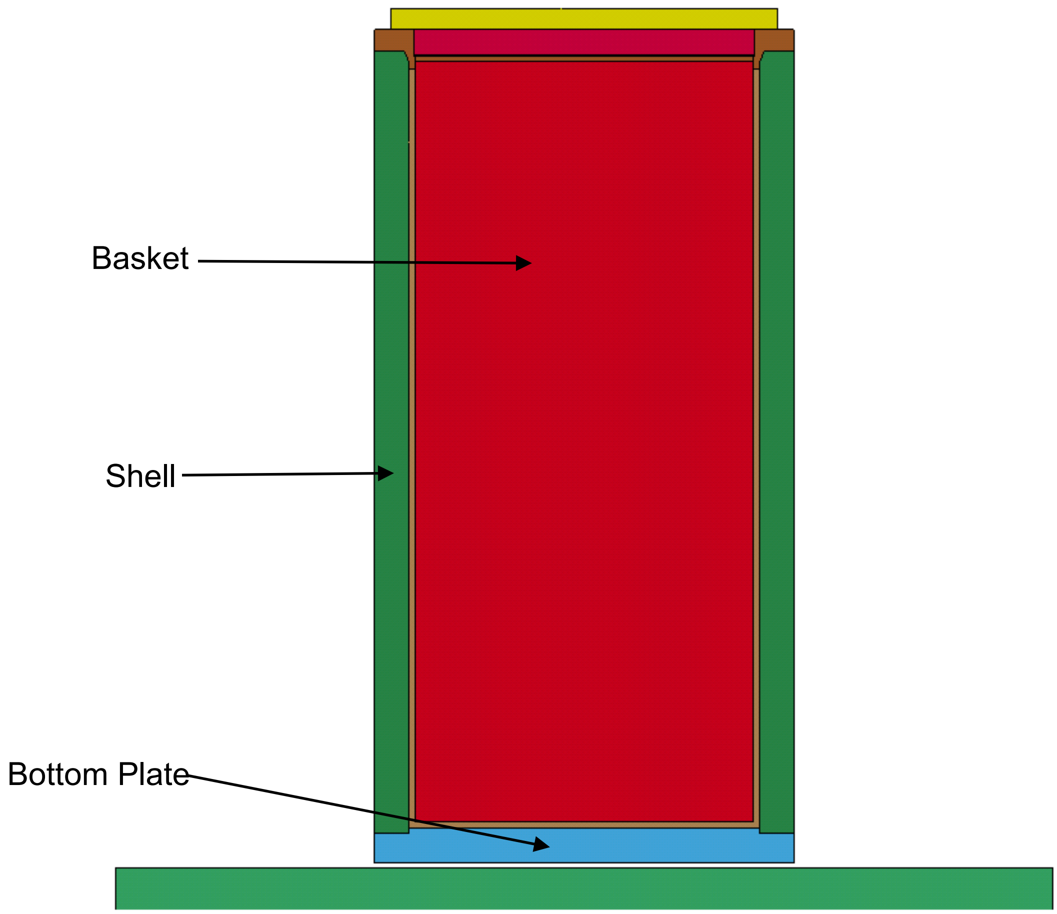

FIGURE A4A.10-3
PARTS ANALYZED FOR ACCELERATION TIME HISTORY

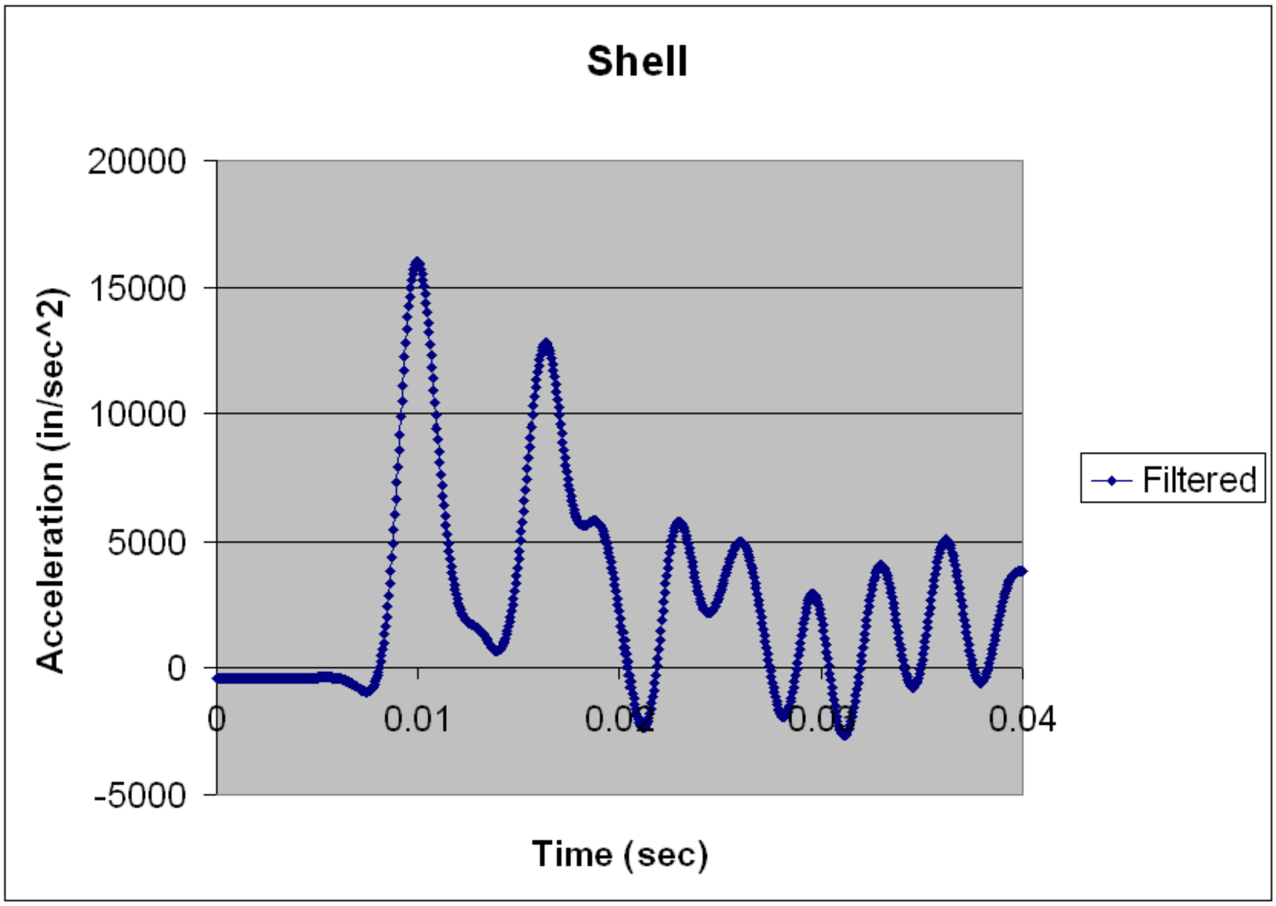

FIGURE A4A.10-4
CASK SHELL ACCELERATION TIME HISTORY (350HZ FILTER)

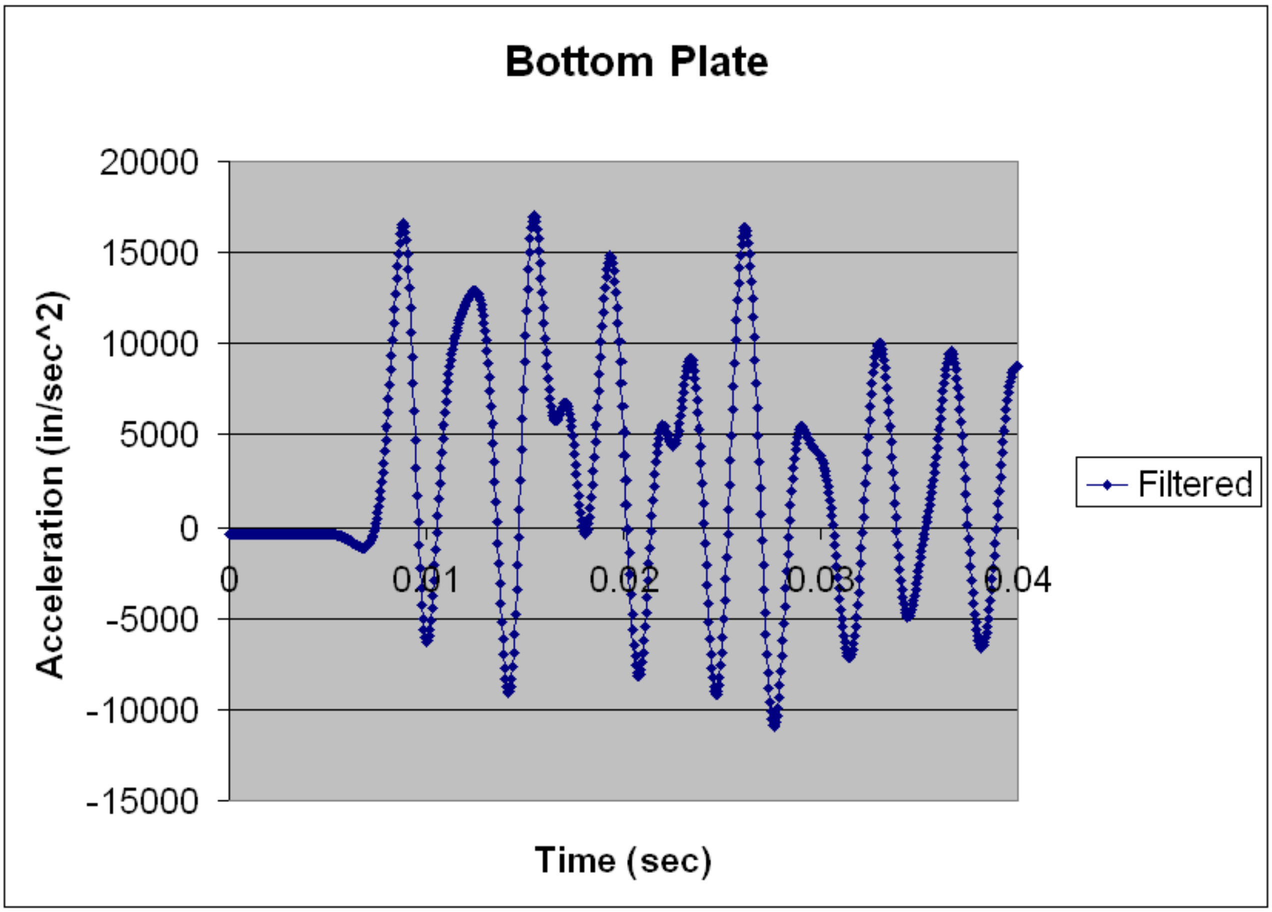

FIGURE A4A.10-5
CASK BOTTOM PLATE ACCELERATION TIME HISTORY (350HZ FILTER)

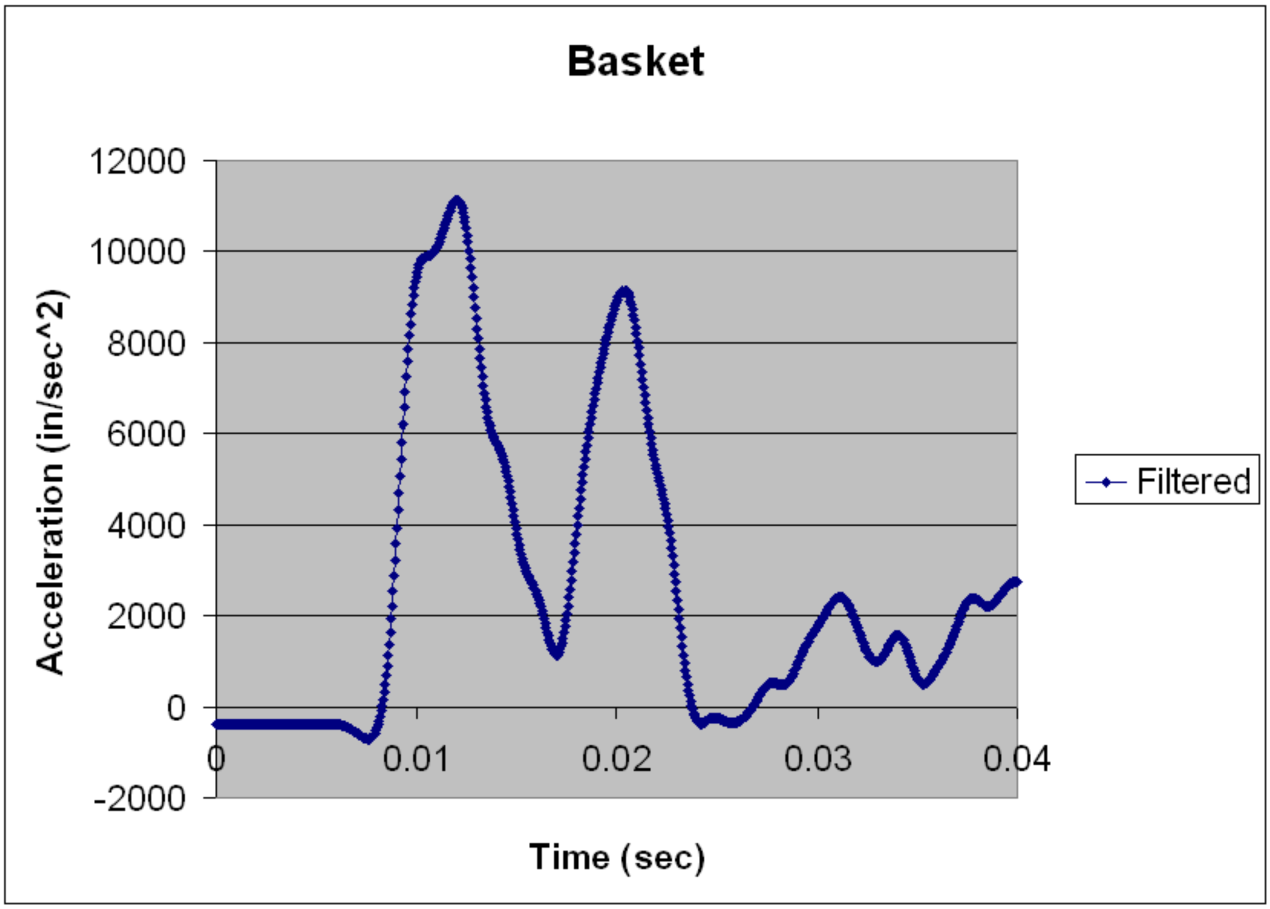

FIGURE A4A.10-6
CASK BASKET ACCELERATION TIME HISTORY (350HZ FILTER)

APPENDIX A4B

STRUCTURAL ANALYSIS OF THE TN-40HT BASKET

A4B.1 INTRODUCTION

This appendix presents the structural analysis of the TN-40HT basket. The basket is a welded assembly of stainless steel boxes designed to accommodate 40 PWR fuel assemblies. The stainless steel fuel compartments are fusion welded to Type 304 stainless steel structural plates, sandwiched between components. The fusion welds are spaced intermittently along the box sections. Neutron poison plates and aluminum plates are sandwiched between the sections of the stainless steel walls of the adjacent boxes and the adjacent stainless steel plates. The Type 304 stainless steel members are the primary structural components. The neutron poison plates provide criticality control and the aluminum plates provide a heat conduction path from the fuel assemblies to the inner shell.

Stainless steel rails are oriented parallel to the longitudinal axis of the cask and are attached to the periphery of the basket to establish and maintain basket orientation and to support the basket.

The basket structure is open at each end and therefore, longitudinal fuel assembly loads are applied directly to the cask body and not to the fuel basket structure. The fuel assemblies are laterally supported by the stainless steel fuel compartments, and the basket is laterally supported by the cask inner shell.

The deformations and stresses induced in the basket structure due to the applied vertical, lateral, and thermal loads are determined using the ANSYS computer program (Reference 1). The individual loads applicable for the TN-40HT basket are summarized in Table A4B.1-1. These include normal condition handling loads, thermal loads and 50g accident condition bottom end drop load. The inertial loads of the fuel assemblies are applied as equivalent pressures on the stainless steel box interior surfaces. Quasi-static stress analyses are performed with applied loads in equilibrium with the reactions at the periphery of the basket. The calculated stresses in the basket structure are compared in Section A4.2.3.4.4 to the allowable stress limits to demonstrate that the established design criteria are met.

A4B.1.1 TN-40HT FUEL BASKET GEOMETRY

The details of the TN-40HT basket are shown on TN Drawings in Section A1.5. A representative cross section of support bars between fuel compartments is shown in Figure A4B.1-1. The support bars are fusion welded to the fuel compartments. This method of construction forms a very strong honeycomb-like structure. The nominal open dimension of each fuel compartment box is 8.05 in. × 8.05 in. which provides a minimum of 1/8 in. clearance around the fuel assemblies. The pitch of the fuel compartments is approximately 8.86 in. The overall basket length (160 in.) is less than the cask cavity length to allow for loading the fuel assemblies and thermal expansion.

Structural transition rails oriented parallel to the longitudinal axis of the cask are attached to the periphery of the basket to establish and maintain basket orientation, to prevent twisting of the basket assembly, and to support the basket due to lateral initial loads.

A4B.1.2 FUEL BASKET ANALYSIS OVERVIEW

The fuel basket is evaluated for normal and accident condition loads specified in Table A4B.1-1. The basket stress analysis is performed using a finite element method for the normal condition handling and thermal load cases. The end drop load case is calculated by hand.

A4B.1.3 WEIGHT

The total weight of the TN-40HT basket is approximately 28,500 lbs., and the total weight of 40 fuel assemblies plus inserts is less than 52,000 lb. A uniform fuel weight of 1,300 lb is assumed to be distributed over the active fuel length of 144 inches. This methodology is conservative considering a maximum combined fuel and insert weight of 1,330 would be distributed over the entire fuel assembly length. The inertia of the basket structure (weight of the basket × g-load) is also included in the analysis.

A4B.1.4 TEMPERATURE

Thermal analyses are performed to obtain the temperature distributions in the basket for various conditions. These analyses are presented in Section A3.

A4B.1.5 TN-40HT FUEL BASKET STRESS ANALYSIS

A4B.1.5.1 APPROACH

Bounding inertial loads of 3g vertical plus 3g lateral for the normal conditions and 50g vertical bottom end drop for accident conditions are applied to the basket. These inertial loads bound all applicable basket loads described in Section A3. 0°, 30°, 45°, 60° and 90° azimuth orientations are analyzed in order to bound all possible lateral loads (Figure A4B.1-2). Nonlinear (gap element) elastic analyses of the basket structure were performed using ANSYS (Reference 1).

A4B.1.5.2 BASKET ANALYSIS FOR VERTICAL AND LATERAL INERTIAL LOADS

A4B.1.5.2.1 FINITE ELEMENT MODEL DESCRIPTION

A three-dimensional finite element model of the basket is constructed using shell elements. The overall finite element model of the fuel basket is shown in Figure A4B.1-3. The fuel compartments and transition rails are included in the model. For conservatism, the strengths of aluminum plates and poison plates in the basket are neglected by excluding them from the finite element model. However, their weights are accounted for by increasing the structural steel plate material densities to 0.39 lbs/in^3.

Because of the large number of plates in the basket and large size of the basket, certain modeling approximations were necessary. In view of continuous support of fuel compartment tubes by the transition rails along the entire basket length during storage condition lateral loads, only a 15.0 inch long axial section of the basket and transition rail is modeled. At the two cut faces of the model, symmetry boundary conditions are applied.

The fusion welds, connecting the fuel compartments and plates, are modeled with pipe elements connected at each end to adjacent fuel compartment boxes. All other interfaces (i.e., between fuel compartments, between fuel compartments and support plates, between fuel compartments and transition rails, and between transition rails and the cask) are modeled by gap elements. For all interfaces through aluminum and poison plates, the plates are assumed to be in contact to simulate support provided by the aluminum and poison plates. For the transition rails and cask interface the gap is varied in the circumferential direction such that it is zero at the point of contact, which depends on the orientation analyzed, and maximum 180 degrees from the point of contact.

The boundary conditions and interfaces for a typical fuel compartment are shown in Figure A4B.1-21 and Figure A4B.1-22.

A4B.1.5.2.2 MATERIAL PROPERTIES AND ALLOWABLE STRESSES

The stainless steel fuel compartment and transition rails are constructed from SA-240, Type 304 stainless steel. Table A4B.1-2 lists the material properties used in all analyses of the TN-40HT basket. Table A4B.1-3 and Table A4B.1-4 summarize the allowable stress for normal and accident conditions, respectively. Note that the transition rail allowable stresses are based on the allowable stress for surface PT weld (0.65 x S).

A4B.1.5.2.3 VERTICAL AND LATERAL INERTIAL LOADS

The basket structure is analyzed for 0°, 30°, 45°, 60° and 90° azimuth lateral loads. Due to the basket structure symmetry, these orientations are assumed to envelop all other possible loading orientations.

A uniform fuel weight distribution is assumed over 144 inches, which is the active fuel length. A 15.0 inch section of the basket assembly is modeled. The weight of the aluminum plates and poison plates are accounted for by increasing the density of the steel plates. The aluminum plate stiffness and poison plate stiffness are conservatively neglected in the analysis.

The basket temperature is taken as 650 °F, uniform. The rail temperature is taken as 500 °F, uniform. These temperatures are conservatively taken from the normal condition (100 ˚F) thermal analysis presented in Section A3.

The load resulting from the fuel assembly weight is applied as pressure on the fuel compartment plates. For the 0° orientation, the pressure acts only on the horizontal plates, and for the 90° orientation, the pressure acts only on the vertical plates. For the 30°, 45° and 60° orientation, the pressure was divided into components that act on both horizontal and vertical plates of the fuel compartments. The pressures for all orientations are calculated below for vertical and horizontal plates due to 1g and 3g lateral acceleration.

0° and 90° Drop Orientations

Pressure for 1g p = Fuel assembly weight / (Panel span × Panel length)
= 1300 lb./ (8.2375" x 144") = 1.096 psi
Pressure for 3g = 3 x 1.096 = 3.288 psi

30° Orientation

P_h on vertical plates for 1g = p sin 30° = 1.096 x 0.5 = 0.548 psi
P_v on horizontal plates for 1g = p cos 30° = 1.096 x 0.86603 = 0.949 psi
P_h on vertical plates for 3g = 3 x 0.548 = 1.644 psi
P_v on horizontal plates for 3g = 3 x 0.949 = 2.847 psi

45° Orientation

P_h on vertical plates for 1g = p sin 45° = 1.096 x 0.7071 = 0.775 psi
P_v on horizontal plates for 1g = p cos 45° = 1.096 x 0.7071 = 0.775 psi
P_h on vertical plates for 3g = 3 x 0.775 = 2.325 psi
P_v on horizontal plates for 3g = 3 x 0.775 = 2.325 psi

60° Orientation

P_h on vertical plates for 1g = p sin 60° = 1.096 x 0.86603 = 0.949 psi
P_v on horizontal plates for 1g = p cos 60° = 1.096 x 0.5 = 0.548 psi
P_h on vertical plates for 3g = 3 x 0.949 = 2.847 psi
P_v on horizontal plates for 3g = 3 x 0.548 = 1.644 psi

An increased axial acceleration is applied to the 15 inch section to simulate the compressive load due to the weight of the complete basket. The acceleration is (including the 3gs),

3.0 x (160/15) = 32 g

Note: This simplified approach yields the correct vertical reaction force, but yields a compressive stress in the plates varying from zero at the top-most elements to the full 0.39 ksi at the bottom-most elements. (See the end drop analysis in Section A4B.1.5.5. Multiplying the 1g stress of 0.13216 ksi by 3 gives a 3g stress of 0.39 ksi). In reality, at the lower extremities of the basket, the entire 15” modeled portion of the basket would have 0.39 ksi direct compressive stress.

The load distributions for the 0°, 30°, 45°, 60° and 90° analyses for the normal condition loads are shown in Figure A4B.1-8 through Figure A4B.1-12, respectively.

The accelerations applied in each run are as follows.

Orientation	Inertial Load (g)	a_x (g)	a_y (g)	a_z (g) (simulate 3g axial load)
0°	3g vert. & 3g lat.	0	3	32
30°	3g vert. & 3g lat.	-1.5	2.598	32
45°	3g vert. & 3g lat.	-2.121	2.121	32
60°	3g vert. & 3g lat.	-2.598	1.5	32
90°	3g vert. & 3g lat.	-3	0	32

A4B.1.5.2.4 ANSYS 3G VERTICAL & 3G LATERAL ANALYSES AND RESULTS

Nonlinear (gap element) elastic analyses of the basket structure were performed using ANSYS for the 0°, 30°, 45°, 60° and 90° vertical and lateral load orientations.

The nodal stress intensity distribution in the stainless steel fuel compartments and transition rails are computed by ANSYS. The membrane plus bending stress intensity distributions for the 45° loading condition are shown in Figure A4B.1-13 and Figure A4B.1-14 as representative sample of the resulting stresses. The shell middle surface nodal stress intensity is the membrane stress intensity and the top or bottom surface stress intensity is the membrane plus bending stress intensity. The maximum membrane and membrane plus bending stresses for each load orientation are summarized in Table A4B.1-5.

A4B.1.5.3 BASKET ANALYSIS FOR THERMAL LOADS

A4B.1.5.3.1 FINITE ELEMENT MODEL DESCRIPTION

<u>Thermal Stress Model for Basket Fuel Compartments</u>

A three-dimensional finite element model of the basket Fuel Compartments is constructed using shell elements. Due to symmetry, only ¼ of the model (see Figure A4B.1-15) is used in this analysis.

<u>Thermal Stresses for Transition Rails</u>

A three-dimensional finite element model of the transition rails is constructed using shell elements. Due to symmetry, only ¼ of the model (see Figure A4B.1-16) is used in this analysis.

A4B.1.5.3.2 THERMAL LOADS

The transition rails are attached to the basket with bolts in slotted holes, thus permitting free thermal growth of basket boxes. However, some thermal stresses in basket and rails can develop due to radial gradients (hot at center and cooler at periphery) for normal thermal conditions. Basket and Rail thermal stresses are calculated for the 100 °F (hot normal) and -40 °F (cold normal) ambient.

Elastic material properties described in Section A4B.1.5.2 are used, and conservative temperature gradients are applied (see paragraphs below).

Nodal Temperature for Basket Fuel Compartments

Analyses documented in Section A3 were used to obtain temperatures along a radial line from the basket center to the basket perimeter that give the largest radial thermal gradient. These temperatures were used to develop bounding polynomial curve-fit equations that give temperatures as a function of radial location. The temperature gradients were conservatively modified by increasing the temperature in the middle of the basket by 50 ºF and decreasing the temperature at the perimeter of the basket by 50 ºF for normal and off-normal thermal storage conditions. Temperatures between the middle of the basket and the perimeter of the basket were modified proportionally to maintain the same basic shape of the temperature distribution. For a given bounding curve, the conservative temperature gradient is mapped onto the basket models in all radial directions to give the largest gradient across the entire diameter of the basket. The temperature distribution in the fuel compartments for 100 °F and -40 °F are shown in Figure A4B.1-4 and Figure A4B.1-5, respectively.

Nodal Temperature for Transition Rails

The same conservative temperature gradient for fuel compartments is mapped onto the rail models in all radial directions to give the largest gradient across the entire diameter of the basket. The temperature distribution in the transition rails for 100 °F and -40 °F ambient conditions are shown in Figure A4B.1-6 and Figure A4B.1-7, respectively.

A4B.1.5.3.3 ANSYS THERMAL ANALYSIS AND RESULTS

Basket Compartment

Nodal stress intensity distributions in basket fuel compartments and the support plates are plotted at top or bottom surfaces in Figure A4B.1-17 and Figure A4B.1-18 for 100 °F and -40 °F ambient conditions, respectively.

The maximum stress intensities in the fuel compartments are 8.61 ksi and 8.74 ksi for 100 °F and -40 °F ambient conditions, respectively, and are shown in Table A4B.1-6.

Transition Rail

Nodal stress intensity distributions in transition rails are plotted at top or bottom surfaces in Figure A4B.1-19 and Figure A4B.1-20 for 100 °F and -40 °F ambient conditions, respectively.

The maximum stress intensities in the transition rails are 21.73 ksi and 21.60 ksi for 100 °F and -40 °F ambient conditions, respectively, and are shown in Table A4B.1-6.

A4B.1.5.4 SHEAR LOAD IN THE FUSION WELD

The results of the static load analyses were post-processed for Axial (FX) and Shear (FY and FZ) forces in the pipe elements representing the Fusion Welds. The maximum forces are listed as follow:

Maximum Force, FX = 314.92 lb. (at Element No. 32728, 60° lateral load orientation)

Maximum Force, FY = 950.88 lb. (at Element No. 32723, 90° lateral load orientation)

Maximum Force, FZ = 99.27 lb. (at Element No. 32553, 60° lateral load orientation)

The results of the thermal load analyses were also post-processed for Axial (FX) and Shear (FY and FZ) forces in the pipe elements representing the Fusion Welds. The maximum forces are listed as follow:

Maximum Force, FX = 310.69 lb. (at Element No. 32559, 100 °F ambient)
Maximum Force, FY = 608.83 lb. (at Element No. 32548, -40 °F ambient)
Maximum Force, FZ = 99.01 lb. (at Element No. 32717, -40 °F ambient)

The maximum combined shear load in a fusion weld is computed by vectorially adding the maximum FX, FY, and FZ (irrespective of their location).

Maximum Combined Shear Force = $[(314.92 + 310.69)^2 + (950.88 + 608.83)^2 + (99.27 + 99.01)^2]^{1/2}$ = 1,683 lb = 1.68 kips (per fusion weld)

For the fusion weld load capacity test at room temperature, a factor of safety of 1.43 is applied and the material strength is corrected for room temperature testing. Therefore the, the required minimum fusion weld test load per weld is:

= 1,683 * (Factor of Safety) * (S_u at room temperature / S_u at 650ºF)

=1,683 lb * 1.43 * (75 ksi/63.4 ksi) = 2,847 lb.
≈ 2.9 kips

A4B.1.5.5 FUEL BASKET VERTICAL END DROP ANALYSIS

During vertical end drop load case, the fuel assemblies and fuel compartments are forced against the bottom of the TN-40HT cask. It is important to note that, for any vertical or near vertical loading, the fuel assemblies react directly against the bottom of the cask and not through the basket structure as in lateral loading. It is the weight of the basket that causes axial compressive stress during an end drop. Axial compressive stresses are conservatively computed by assuming that all of the basket weight is reacted by the compartment tubes during an end drop. A basket weight of 28.5 kips is used in the end drop stress calculations.

Stainless Steel Basket Components

Total weight of basket assembly = 28.5 kips

Compressive stress in fuel compartments:

Section area of compartment tubes = $40 \times [(w + 2t)^2 - w^2] = 40 \times [8.425^2 - 8.05^2]$
$= 247.125 \text{ in}^2$

Area of drain slots = 40 x 4 slots/compartment x [1” x .1875”] = 30 in^2

Stress due to 1g = $P / A = -28.5 / [247.125 - 30] = -0.13126$ ksi

Stress due to 50g end drop is 50 x 0.13126 = 6.56 ksi

This stress is much lower than the accident membrane allowable of 38.88 ksi (2.4 S_m at 650 ^oF)

A4B.1.5.6 EVALUATION OF BASKET ALUMINUM COMPONENTS FOR LONG TERM STORAGE DEADWEIGHT

The long term storage load (deadweight) compressive stresses in the limiting aluminum components were compared to allowable stress values that have been reduced to limit the effects due to material creep.

In the TN-40HT basket, the steel support bars are welded between the fuel compartments and form a cavity for the aluminum plates. Thus, there is no additional compressive stress in the aluminum plates, except the dead weight. The maximum height of the basket aluminum plates is 13.14”. Since the dead weight compressive stresses in these plates is so small, these are not the limiting aluminum components.

The aluminum rail inserts are bolted at intervals to the R45 and R90 rails. The maximum compressive stress in the aluminum inserts is conservatively calculated as the entire length of the basket supported by itself at the bottom without taking credit for the bolts. The results are compared to allowable stress values that are reduced to limit the effect due to creep.

The compressive stress in the inserts is conservatively calculated as the entire length of the basket insert.

1g vertical bearing stress = Load / Area =

$$\frac{Volume\ X\ Density}{Area} = Length\ X\ Density = 160\ x\, 0.098 \quad = 15.68 \text{ psi}$$

Where,
Length = 160”
Density = 0.098 lb/in3,

PROPRIETARY - TRADE SECRET INFORMATION
WITHHELD PURSUANT TO 10 CFR 2.390

Based on the above evaluation, the basket aluminum components for the TN40HT Basket design are structurally adequate for long-term storage loads and creep strain is acceptable.

A4B.1.5.7 BASKET STRESS ANALYSIS CONCLUSIONS

Basket Compartment

As shown in Table A4B.1-5 and A4B.1-6, the maximum stress intensity ($P_m + P_b$) in the fuel compartments and support plates (bars) is 9.66 ksi (at 60° load orientation), this stress is less than the membrane allowable (P_m) of 16.2 ksi (S_m at 650 °F).

The maximum primary plus secondary stress intensity ($P_m + P_b + Q$) is 18.40 ksi (maximum primary stress 9.66 ksi + 8.74 ksi from the above thermal analysis shown on Table A4B.1-6). This stress intensity is lower than the allowable stress of 48.6 ksi (3 S_m at 650 °F).

Transition Rail

As shown in Table A4B.1-5 and A4B.1-6, the maximum stress intensity ($P_m + P_b$) in the transition rail is 4.11 ksi (at 90° load orientation), this stress is less than the membrane allowable (P_m) of 11.38 ksi (S_m at 500 °F, 17.5 ksi x 0.65 = 11.38 ksi). This allowable is based on rail welds with surface PT requirements (Reference 2).

The maximum primary plus secondary stress intensity ($P_m + P_b + Q$) is 25.84 ksi (maximum primary stress 4.11 ksi + 21.73 ksi from the above thermal analysis as shown on Table A4B.1-6). This stress intensity is lower than the allowable stress of 34.13 ksi (3 S_m at 500 °F, 3 x 17.5 ksi x 0.65 = 34.13 ksi). This allowable is based on rail welds with surface PT requirements (Reference 2).

A4B.2 REFERENCES

1. ANSYS Engineering Analysis System Computer Code and User's Manual, Section II – Part D, release. 8.0.

2. ASME Boiler and Pressure Vessel Code, Section III, Subsection NG & Appendices, 2004 through 2006 addenda.

3. TN Technical Report No. E-25768, Rev. 0, "Evaluation of Creep of NUHOMS® Basket Aluminum Components Under Long Term Storage Conditions", November, 2007.

TABLE A4B.1-1
SUMMARY OF INDIVIDUAL LOADS FOR STORAGE CONDITIONS-BASKET

Individual Load	Loads
IL-1	50g Vertical (Bottom End Drop)
IL-2	3g Vertical (Lifting)
IL-3	3g Vertical + 3g Lateral (bounds all normal and off normal loads)
IL-4	Thermal Stress due to Hot Environment (100°F ambient)
IL-5	Thermal Stress due to Cold Environment (-40°F ambient)

TABLE A4B.1-2
MATERIAL PROPERTIES FOR TN-40HT FUEL BASKET

Part	Material	Temp. (˚F)	S_y (ksi)	S_u (ksi)	S_m (ksi)	E (psi×10^6)	α_m (10^{-6} in/in/°F)
Steel Boxes and Rails	SA-240, Type 304	70	30.0	75.0	20.0	28.3	8.5
		300	22.4	66.2	20.0	27.0	9.2
		400	20.7	64.0	18.6	26.4	9.5
		500	19.4	63.4	17.5	25.9	9.7
		600	18.4	63.4	16.6	25.3	9.8
		700	17.6	63.4	15.8	24.8	10.0

Notes:

- Material Properties are obtained from ASME code Section II, Part D (Reference 2).

TABLE A4B.1-3
BASKET STRUCTURAL ALLOWABLE STRESSES, NORMAL CONDITIONS

Basket Compartment

Material	Temperature (˚F)	P_m (S_m) (ksi)	$P_m + P_b$ (1.5 S_m) (ksi)	$P_m + P_b + Q$ (3 S_m) (ksi)
SA-240, Type 304	650	16.2	24.3	48.6

Transition Rail

Material	Temperature (˚F)	P_m (S_m x 0.65) (ksi)	$P_m + P_b$ (1.5 S_m x 0.65) (ksi)	$P_m + P_b + Q$ (3 S_m x 0.65) (ksi)
SA-240, Type 304	500	11.38 (17.5 x 0.65)	17.06 (1.5 x 17.5 x 0.65)	34.13 (3 x 17.5 x 0.65)

Note: Allowable for transition rail is based on welds with surface PT examination [Reference 2 ASME Section III, Subsection NG, Table NG-3352-1].

TABLE A4B.1-4
BASKET STRUCTURAL ALLOWABLE STRESSES, ACCIDENT CONDITIONS

Material	Temperature (˚F)	P_m (lesser of 2.4 S_m or 0.7 S_u) (ksi)	$P_m + P_b$ (lesser of 3.6 S_m or S_u) (ksi)
SA-240, Type 304	500	42.0	63.0
	650	38.88	58.32

TABLE A4B.1-5
SUMMARY OF BASKET STRESS ANALYSIS RESULTS

Lateral Load Orientation	Component	Stress Category	Maximum Stress (ksi)
0°	Fuel Compartments(1)	P_m	3.98
		$P_m + P_b$	5.89
	Rails	P_m	1.35
		$P_m + P_b$	3.11
30°	Fuel Compartments(1)	P_m	4.89
		$P_m + P_b$	8.70
	Rails	P_m	1.71
		$P_m + P_b$	3.49
45°	Fuel Compartments	P_m	3.92
		$P_m + P_b$	8.90
	Rails	P_m	1.68
		$P_m + P_b$	3.51
60°	Fuel Compartments(1)	P_m	3.88
		$P_m + P_b$	9.66
	Rails	P_m	1.14
		$P_m + P_b$	3.50
90°	Fuel Compartments(1)	P_m	2.63
		$P_m + P_b$	6.46
	Rails	P_m	1.55
		$P_m + P_b$	4.11

Note:
1. The component includes fuel compartments and support plates (bars).

TABLE A4B.1-6
SUMMARY OF STRESSES IN FUEL COMPARTMENTS AND RAILS

Loading	Component	Load Condition	Stress Classification	Loads	Stress(3) (ksi)	Allow. Stress (ksi)
3g Lifting	Fuel Compartment(2)	IL-2	P_m	3g Axial	0.39	16.2
			$P_m + P_b$		0.39	24.3
	Rail		P_m		0.39(1)	11.38
			$P_m + P_b$		0.39(1)	17.06
3g Vertical, 3g Lateral	Fuel Compartment(2)	IL-3	P_m	3g Axial + 3g Lateral	4.89	16.2
			$P_m + P_b$		9.66	24.3
	Rail		P_m		1.71	11.38
			$P_m + P_b$		4.11	17.06
Thermal	Fuel Compartment(2)	IL-4	Q	100° F Amb.	8.61	48.6
	Rail		Q		21.73	34.13
	Fuel Compartment(2)	IL-5	Q	-40° F Amb.	8.74	48.6
	Rail		Q		21.60	34.13

(1) Assumed same stresses as for fuel compartment. Thinner walls (3/16) of the fuel compartment carry the weight of the entire basket (fuel compartments, rails, poison plates, aluminum plates, and support bars) while the thicker walls (3/8) of the rails carry only the rail self weigh and the thin aluminum inserts.

(2) The component includes fuel compartments and support bars. A quality factor of 1.0 is applied based on single pass weld and 100% VT inspection on both sides.

(3) The smallest margin between the calculated stress and the allowable is 9.67 ksi (11.38- 171). This margin is sufficient to address the additional 0.39 ksi compressive stress in the lower extremities of the basket discussed in Section A4B.1.5.2.3.

PROPRIETARY - TRADE SECRET INFORMATION
WITHHELD PURSUANT TO 10 CFR 2.390

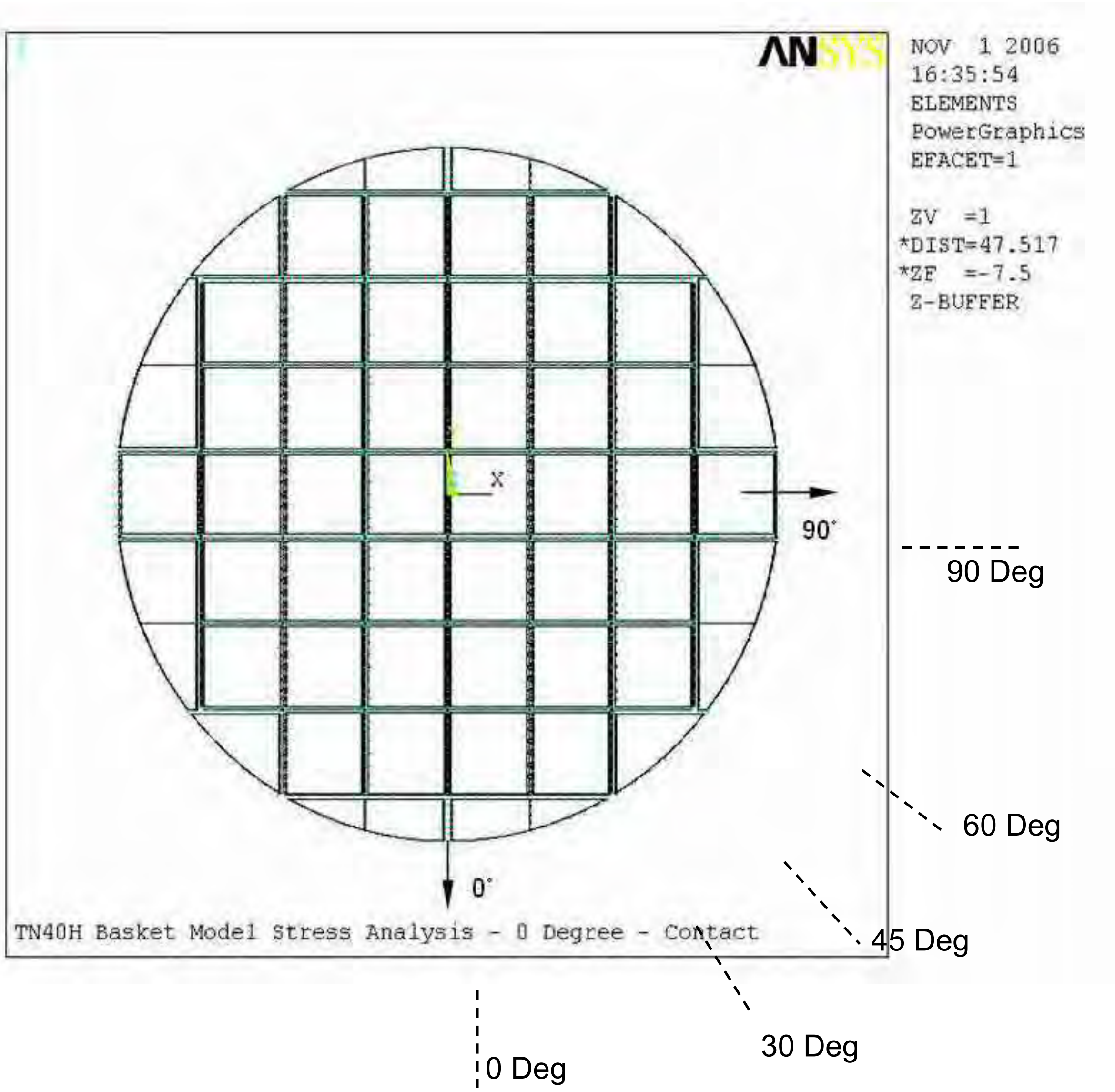

FIGURE A4B.1-2
TN-40HT BASKET LOADING ORIENTATION DEFINITIONS

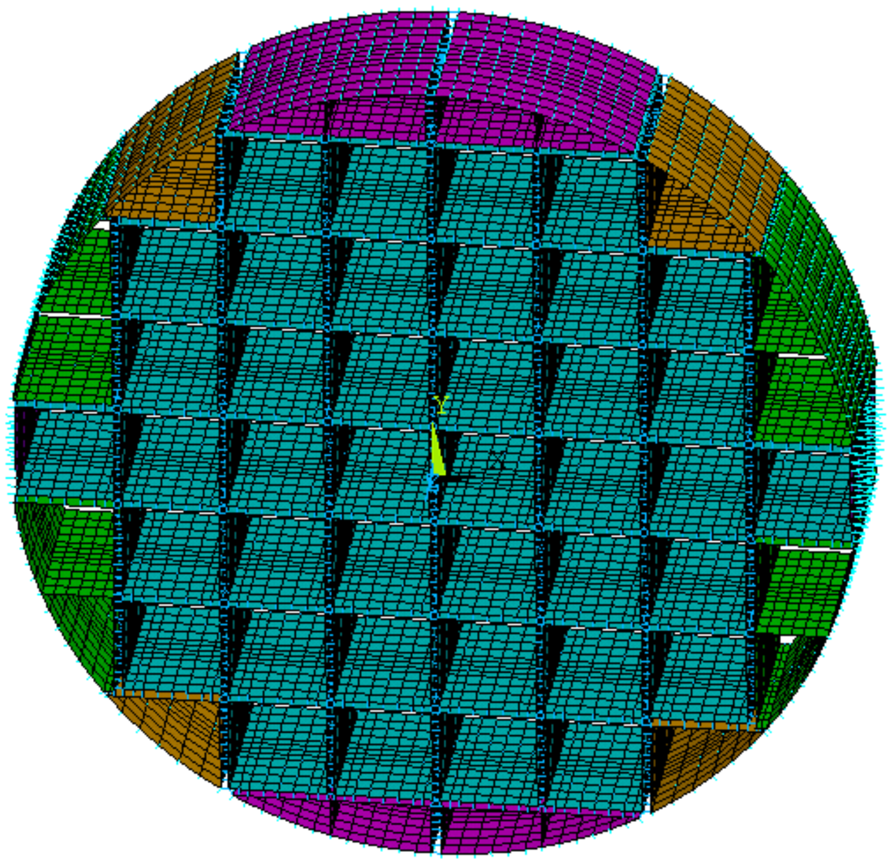

FIGURE A4B.1-3
BASKET FINITE ELEMENT MODEL

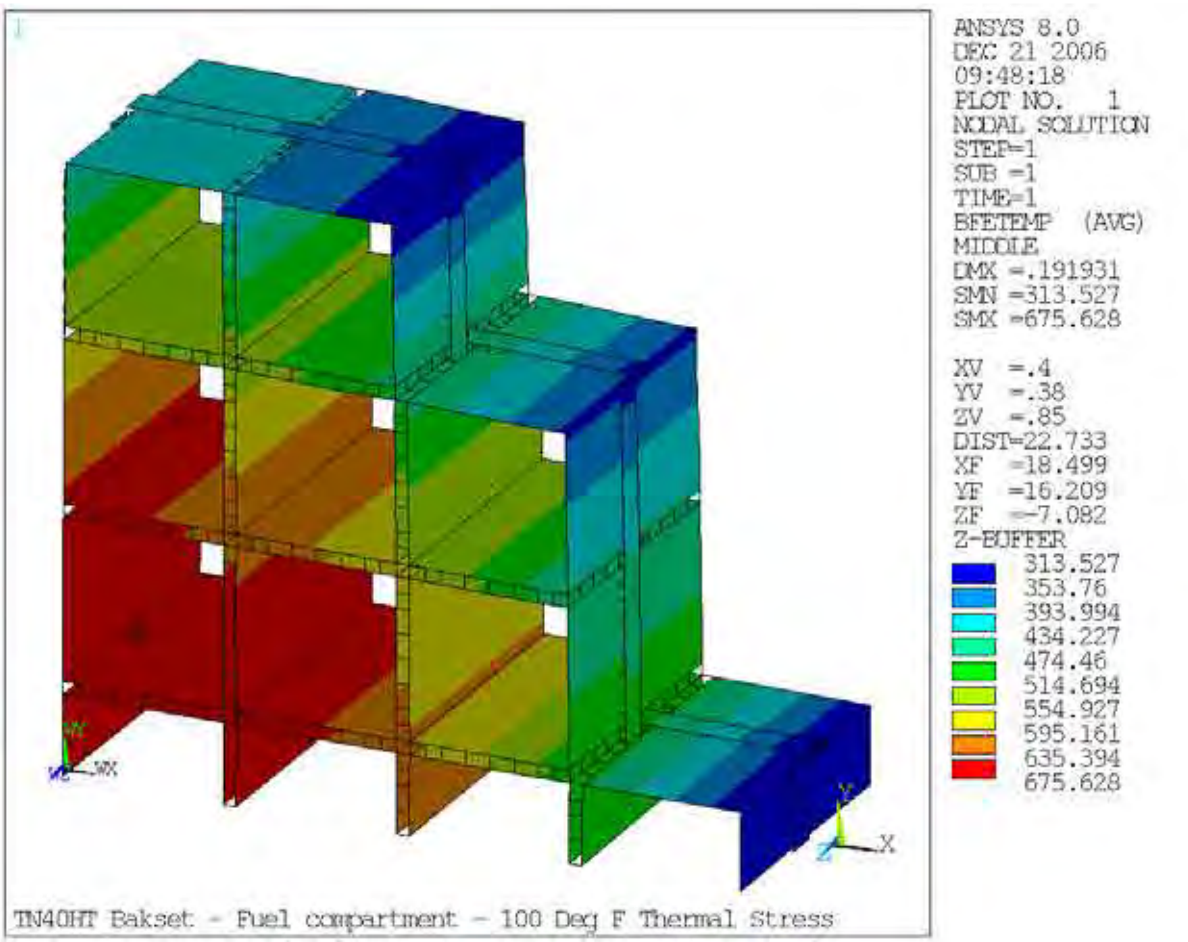

FIGURE A4B.1-4
FUEL COMPARTMENT FINITE ELEMENT MODEL TEMPERATURE DISTRIBUTION
100 °F AMBIENT

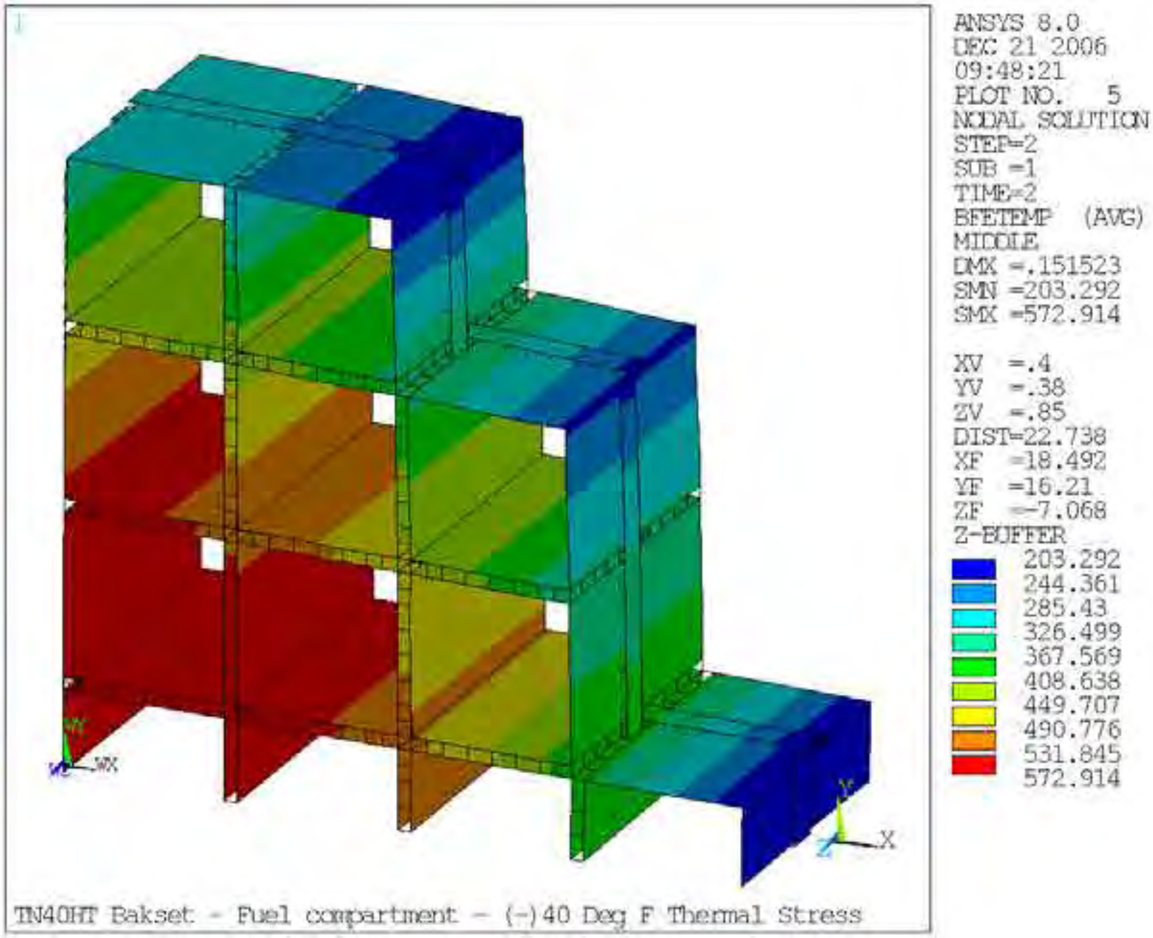

FIGURE A4B.1-5
FUEL COMPARTMENT FINITE ELEMENT MODEL TEMPERATURE DISTRIBUTION
-40 °F AMBIENT

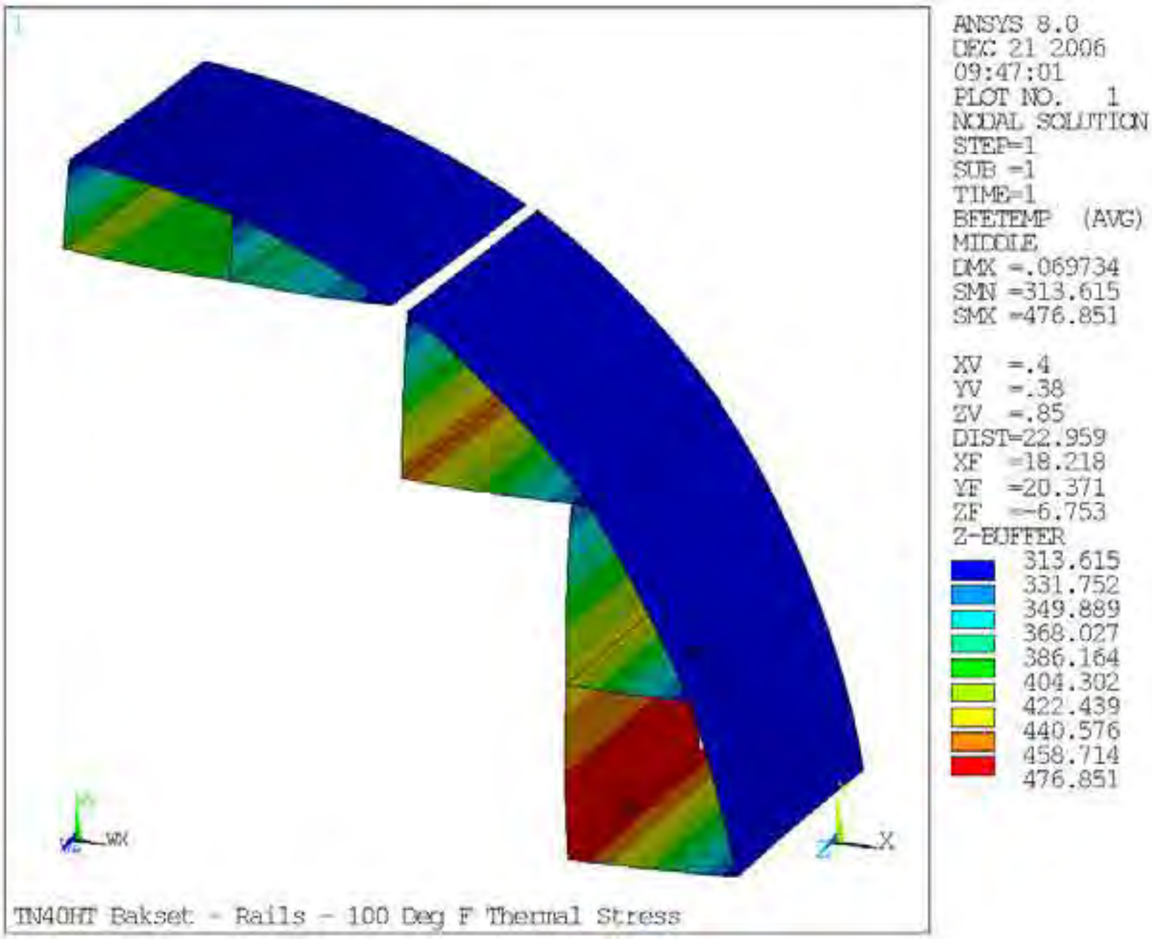

FIGURE A4B.1- 6
TRANSITION RAILS FINITE ELEMENT MODEL TEMPERATURE DISTRIBUTION
100 °F AMBIENT

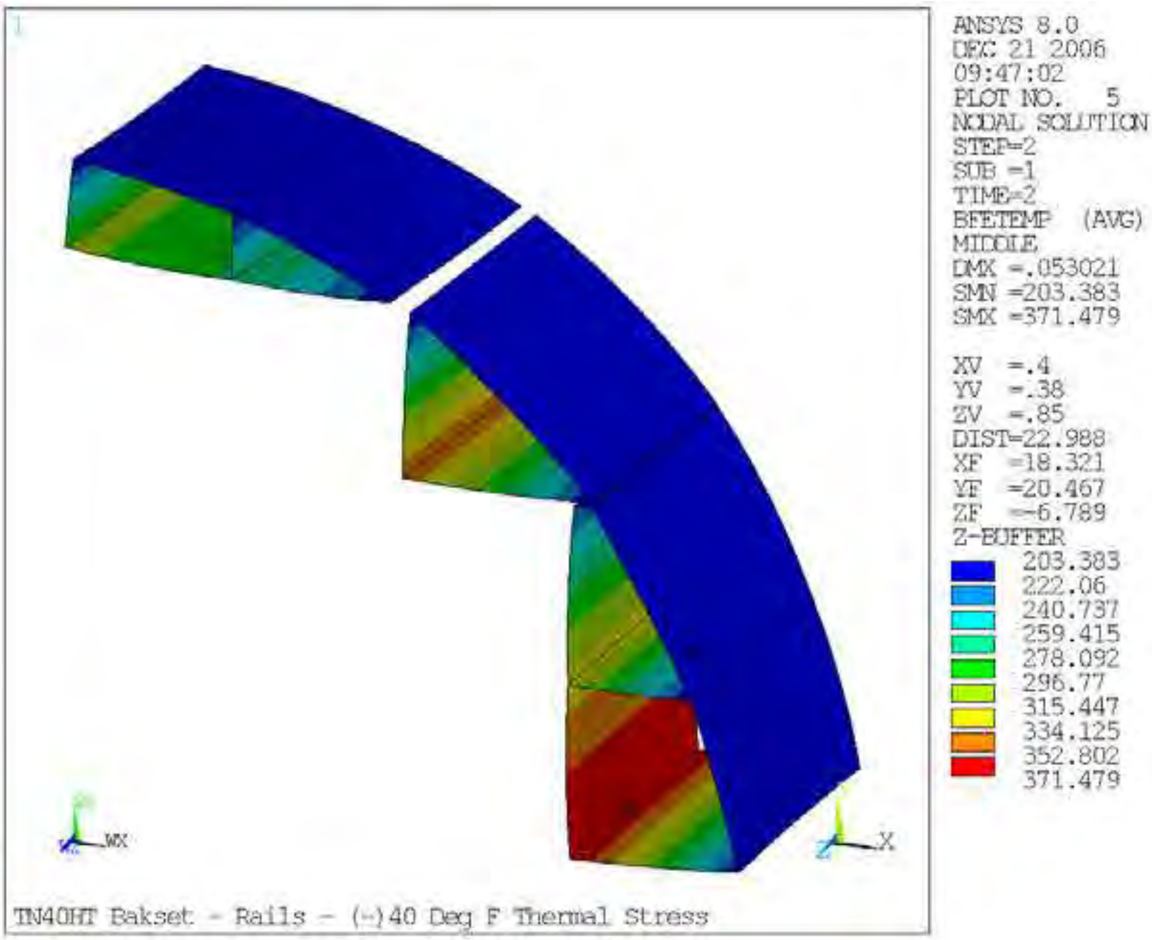

FIGURE A4B.1-7
TRANSITION RAILS FINITE ELEMENT MODEL TEMPERATURE DISTRIBUTION
-40 °F AMBIENT

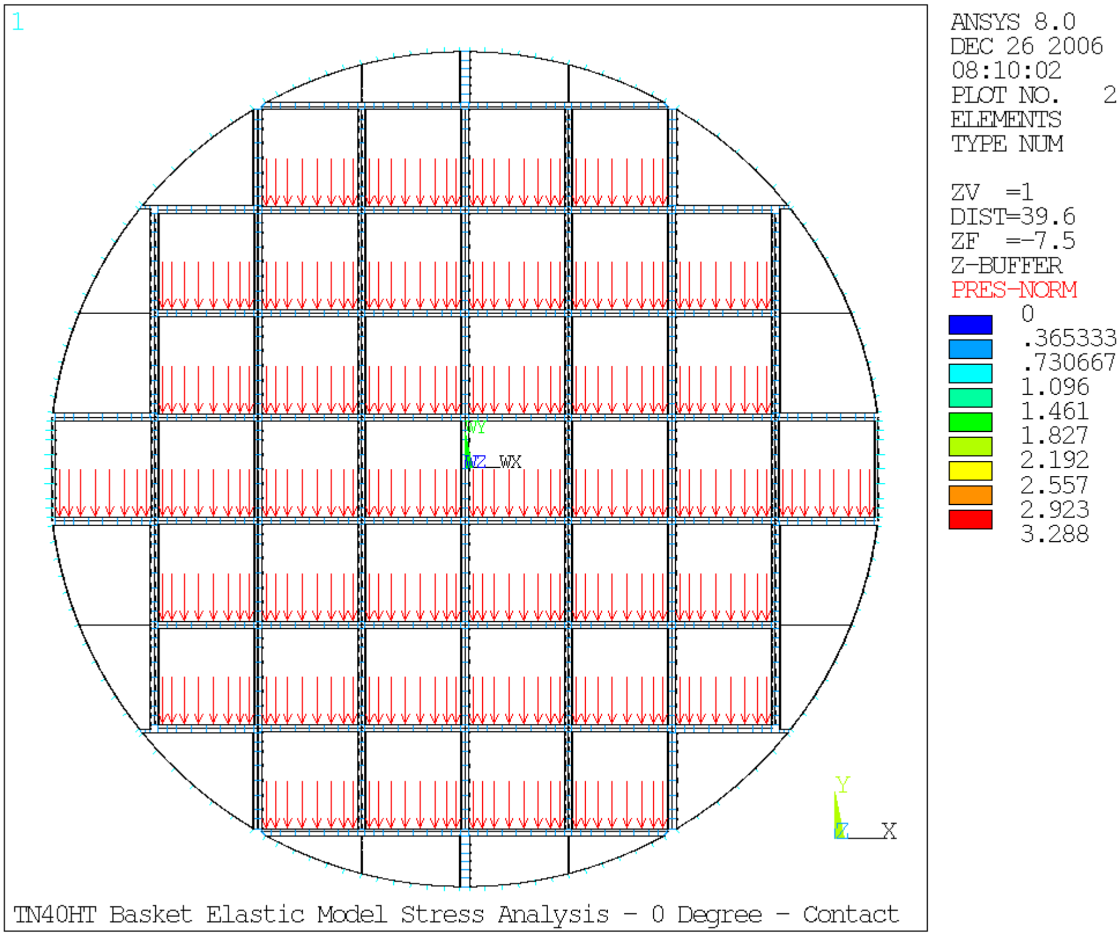

FIGURE A4B.1-8
BASKET FINITE ELEMENT MODEL APPLIED PRESSURES – 0° AZIMUTH

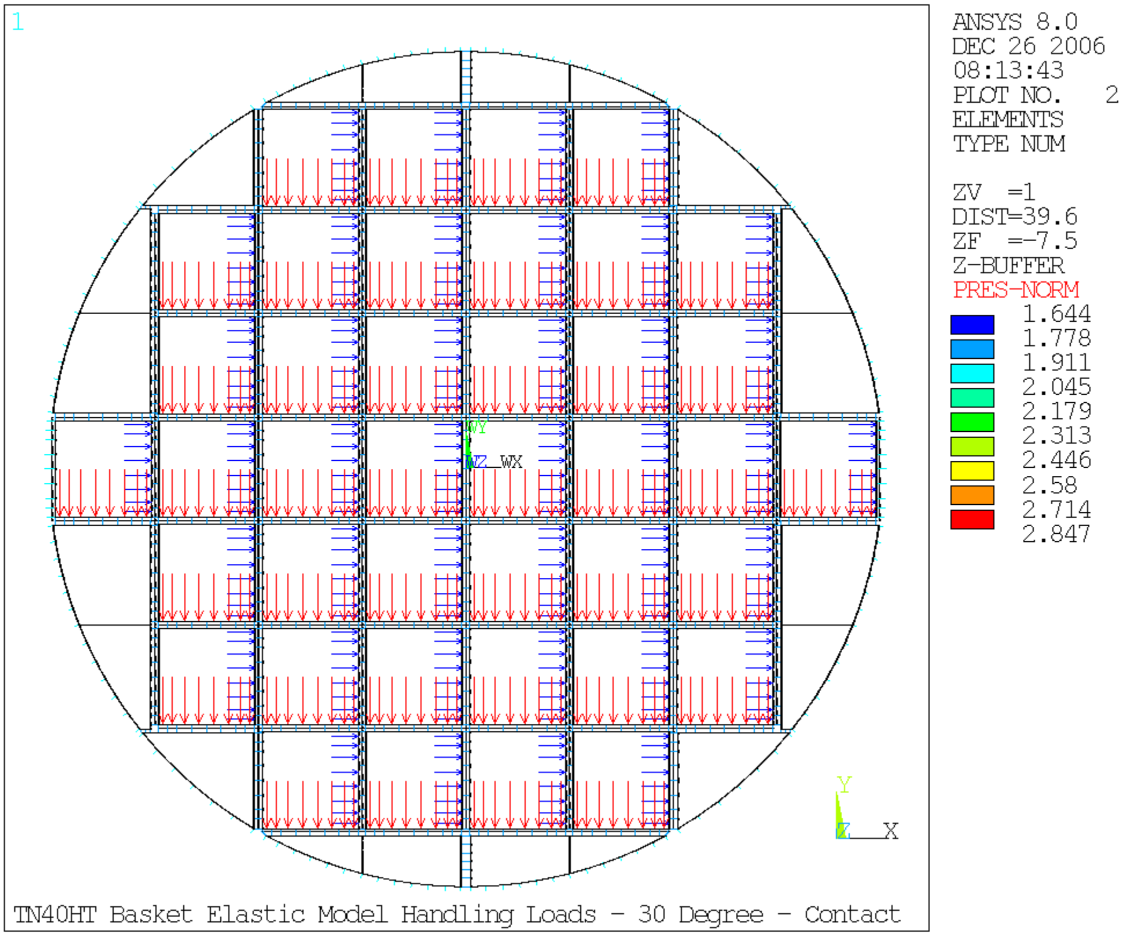

FIGURE A4B.1-9
BASKET FINITE ELEMENT MODEL APPLIED PRESSURES – 30° AZIMUTH

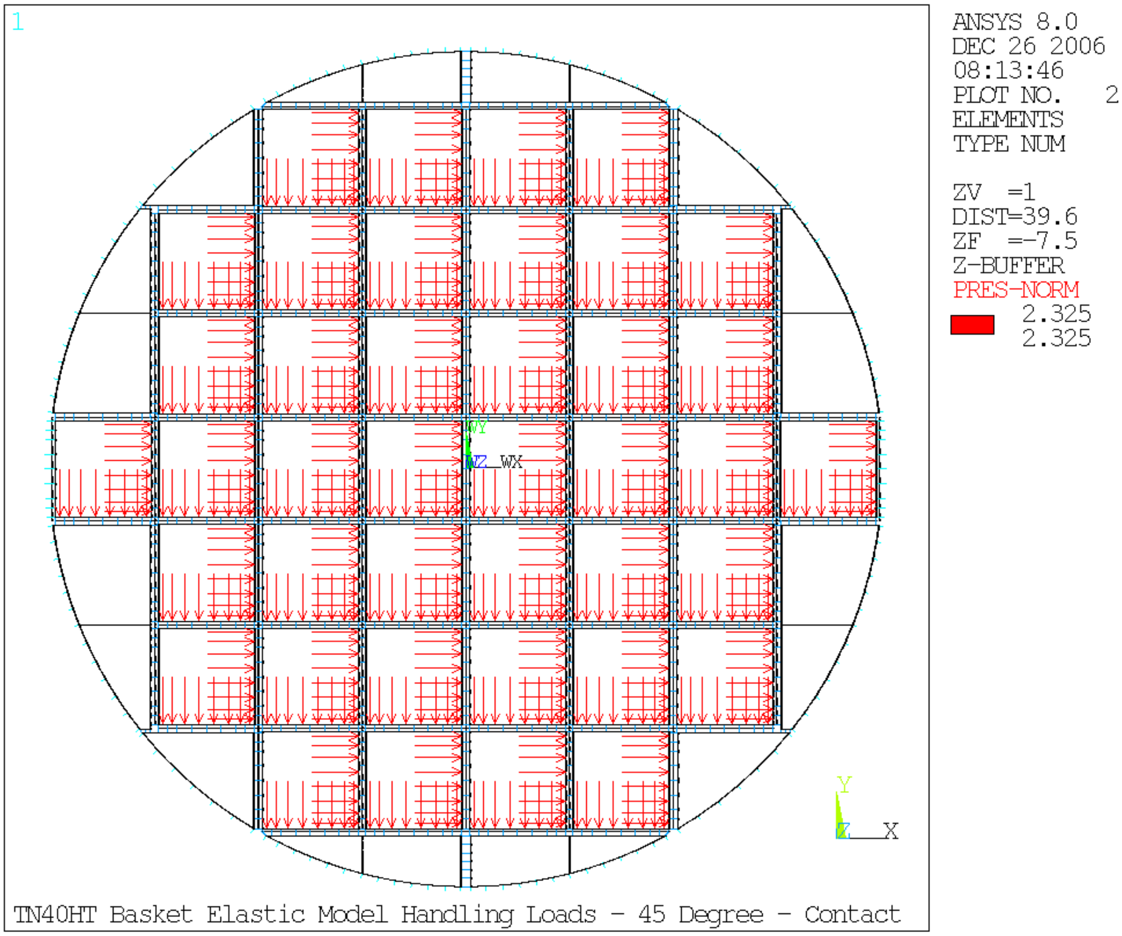

FIGURE A4B.1-10
BASKET FINITE ELEMENT MODEL APPLIED PRESSURES – 45° AZIMUTH

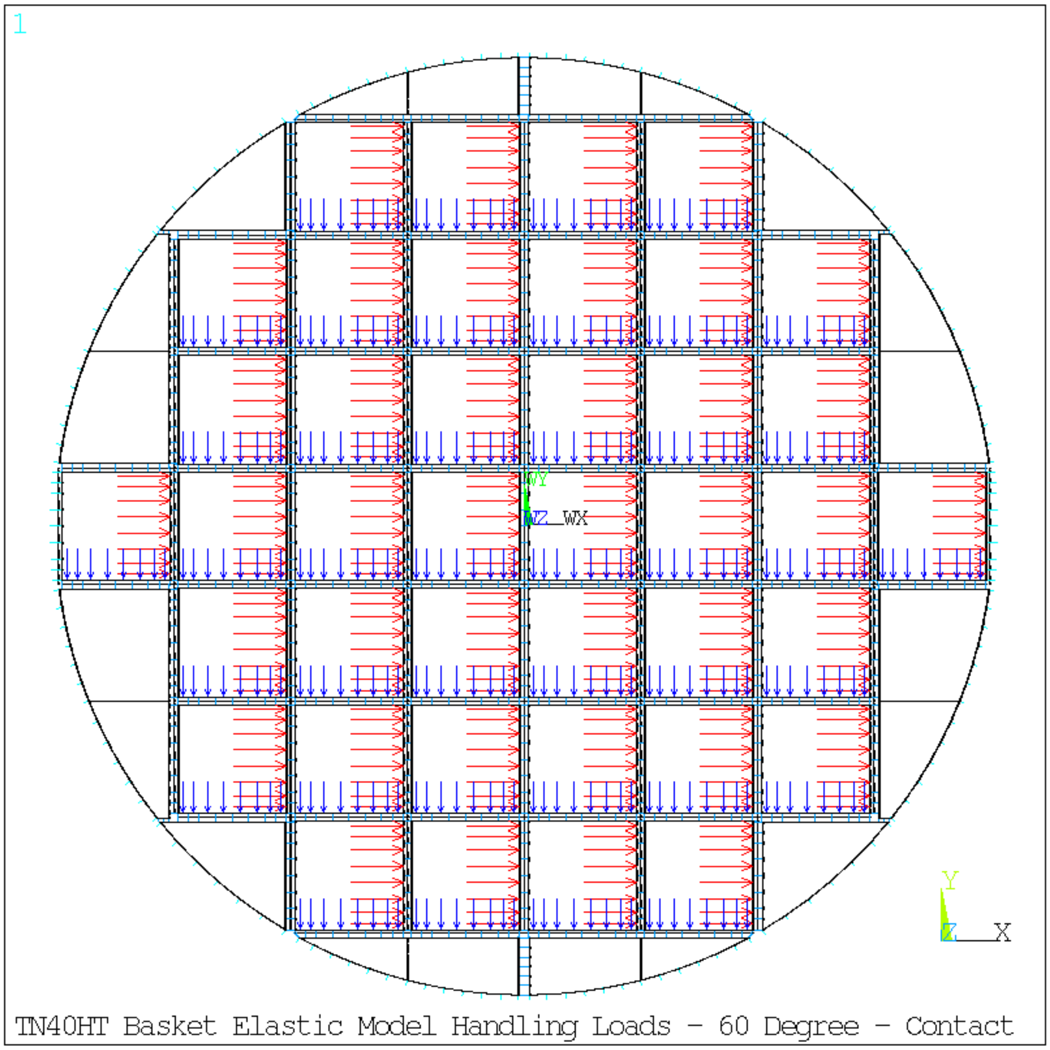

FIGURE A4B.1-11
BASKET FINITE ELEMENT MODEL APPLIED PRESSURES – 60° AZIMUTH

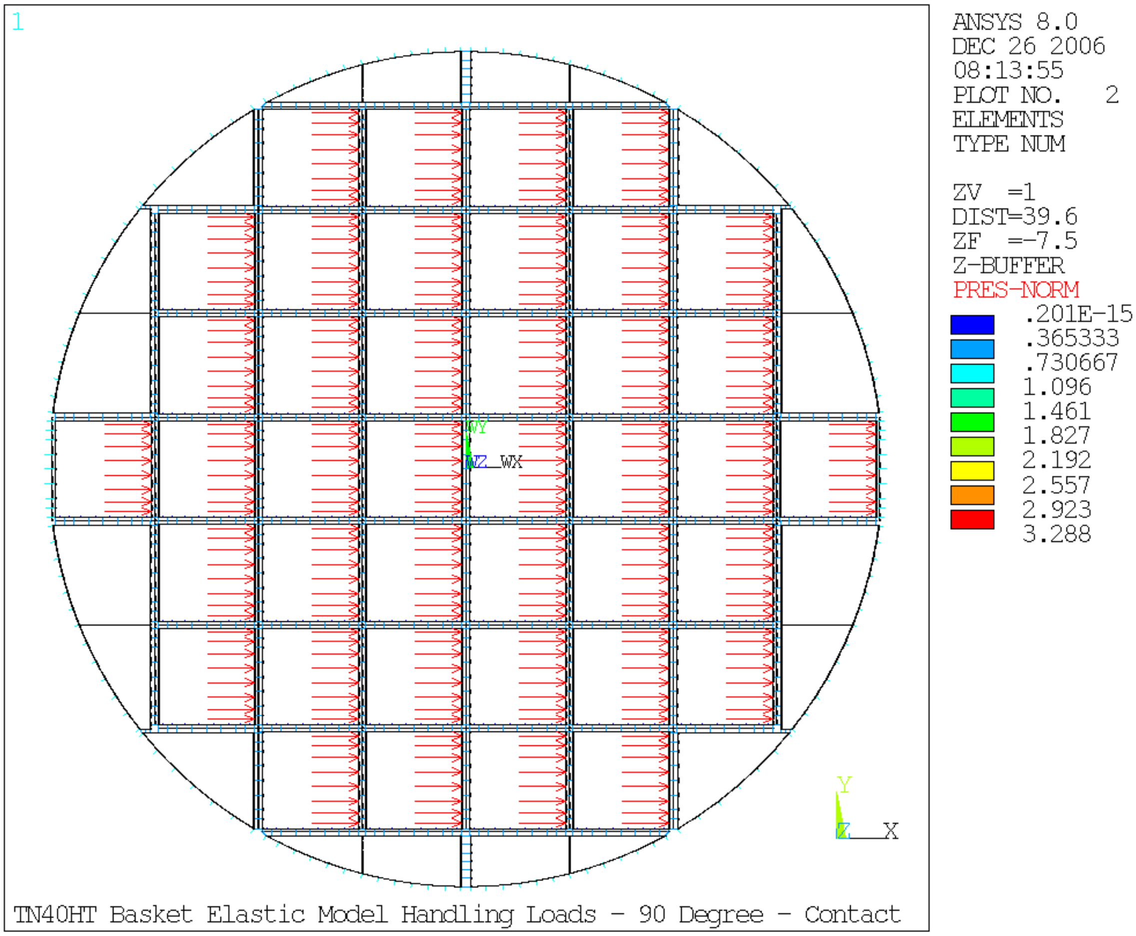

FIGURE A4B.1-12
BASKET FINITE ELEMENT MODEL APPLIED PRESSURES – 90° AZIMUTH

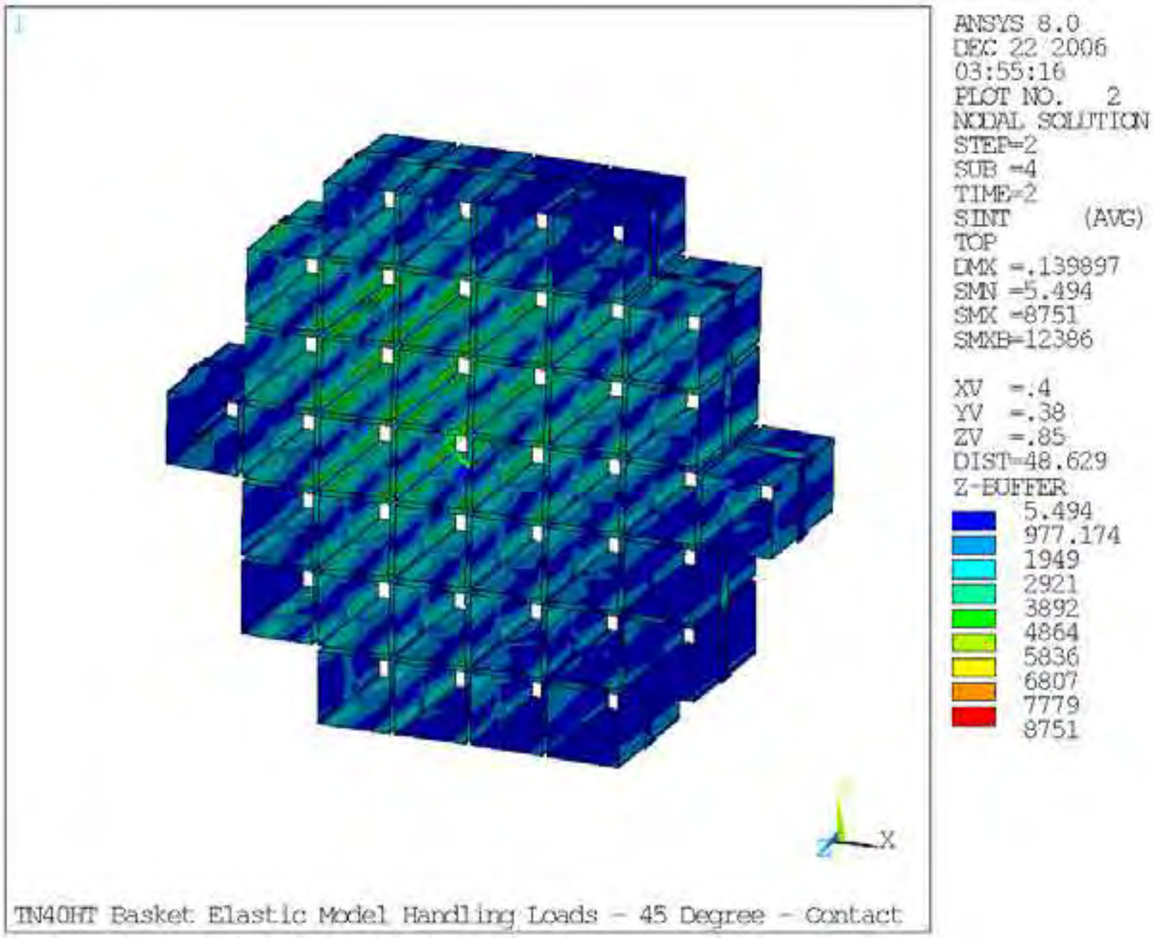

FIGURE A4B.1-13
NORMAL CONDITION 45° AZIMUTH LATERAL LOAD - FUEL COMPARTMENTS – TOP SURFACE MEMBRANE PLUS BENDING STRESS INTENSITY

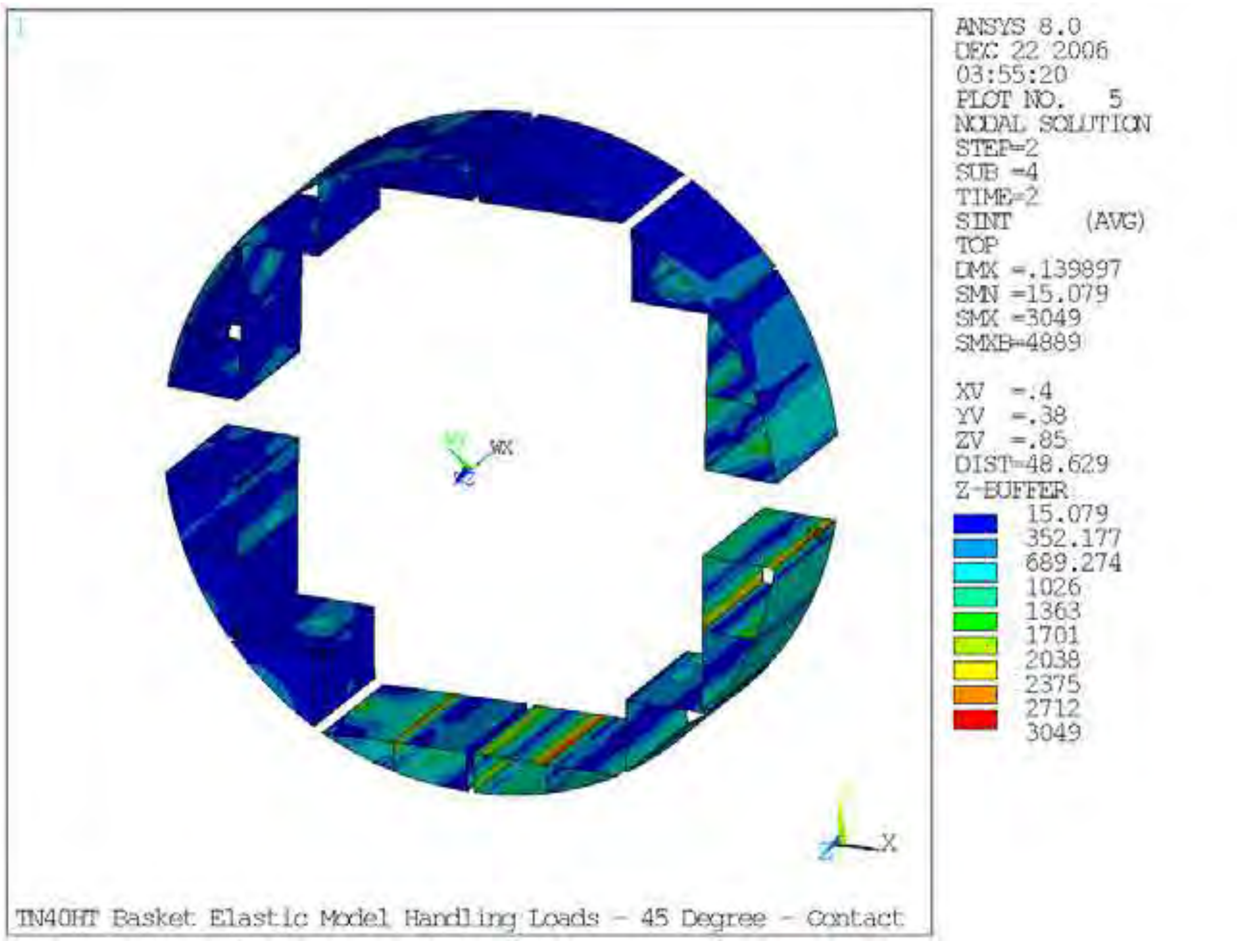

FIGURE A4B.1-14
NORMAL CONDITION 45° AZIMUTH LATERAL LOAD – PERIPHERAL RAILS TOP SURFACE MEMBRANE PLUS BENDING STRESS INTENSITY

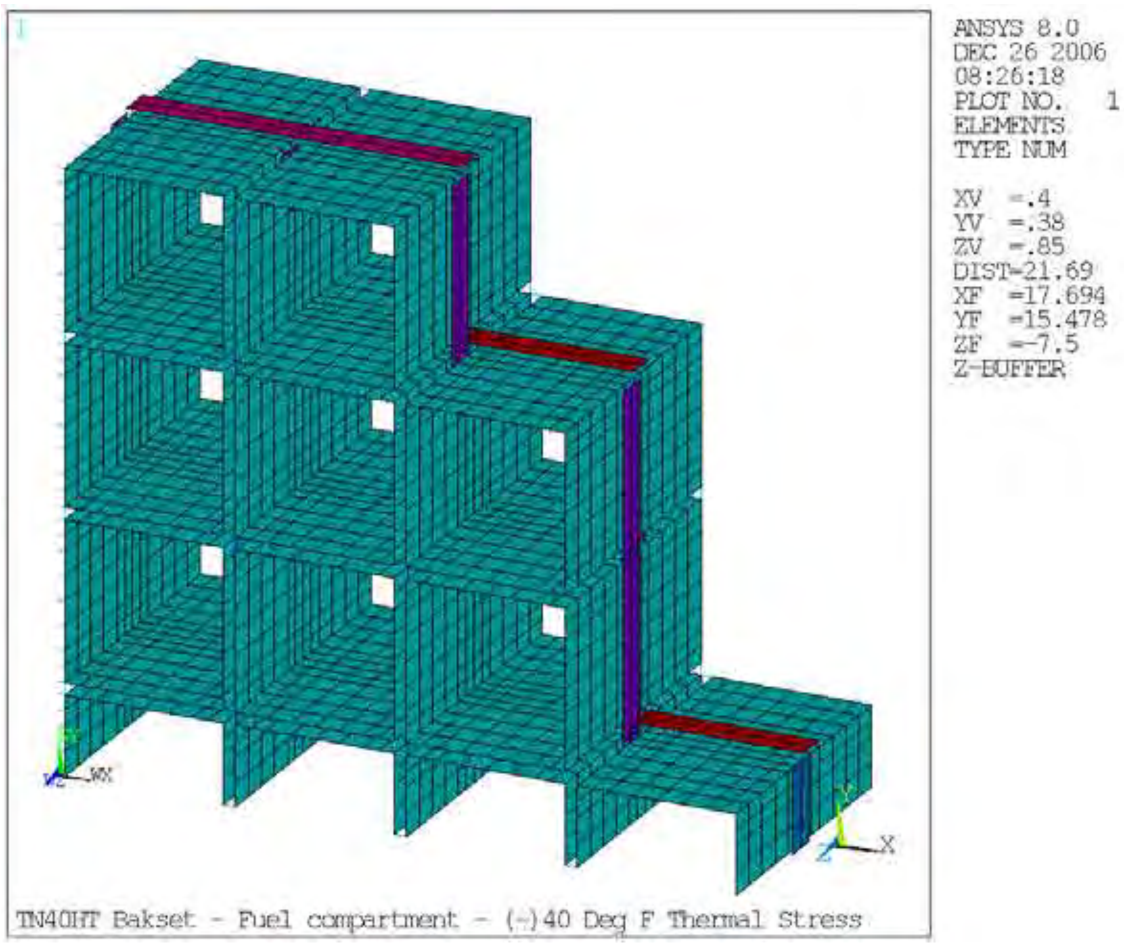

FIGURE A4B.1-15
THERMAL STRESS ANALYSIS FINITE ELEMENT MODEL - FUEL COMPARTMENT

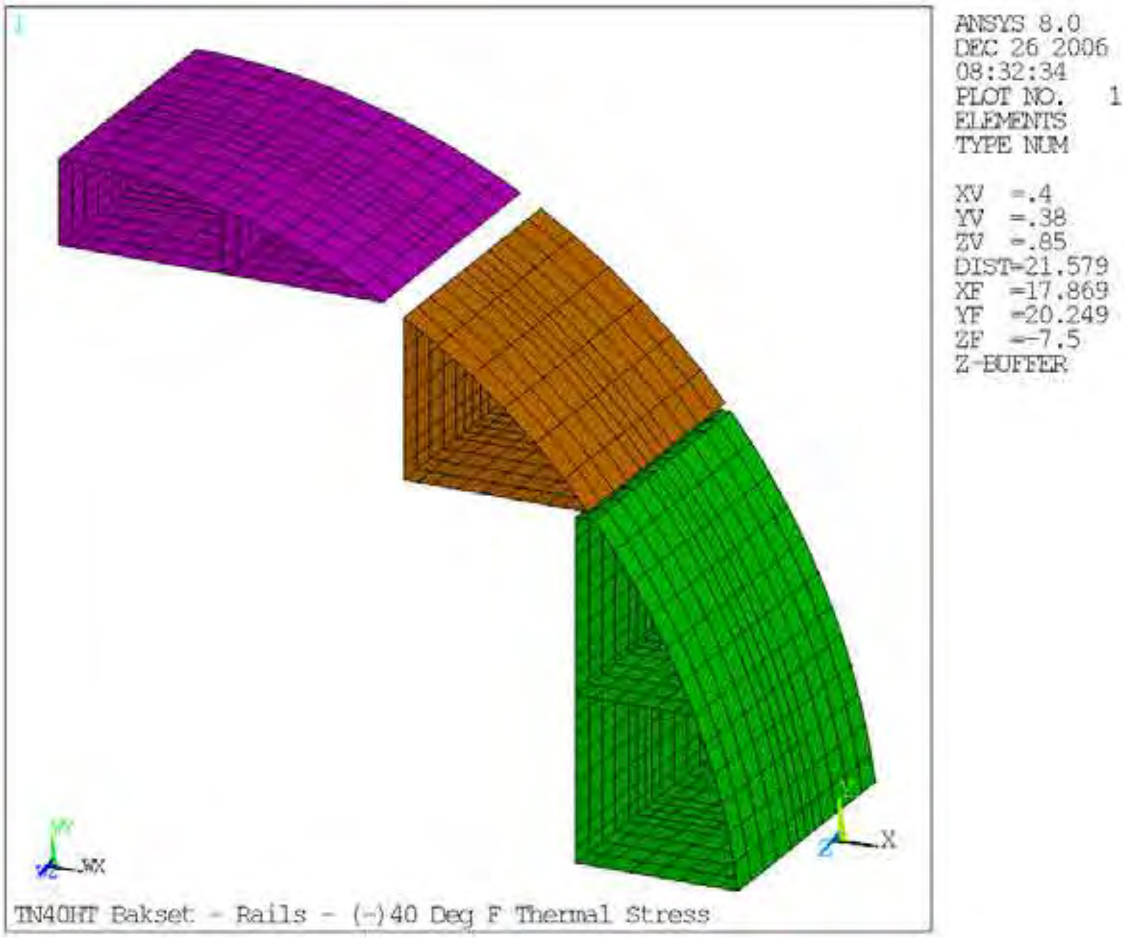

FIGURE A4B.1-16
THERMAL STRESS ANALYSIS FINITE ELEMENT MODEL - RAILS

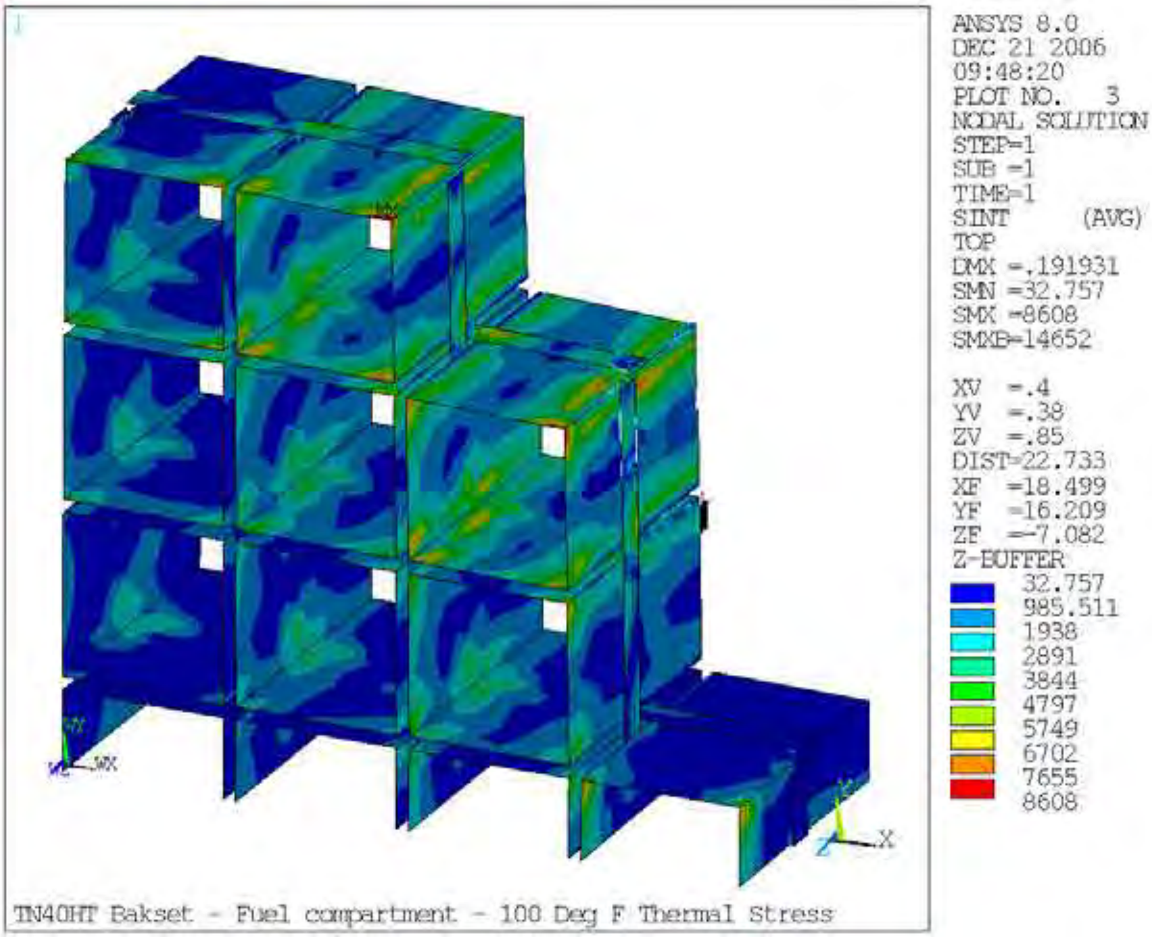

FIGURE A4B.1-17
THERMAL STRESS ANALYSIS – MAXIMUM FUEL COMPARTMENT STRESS INTENSITY FOR 100° F AMBIENT TOP SURFACE

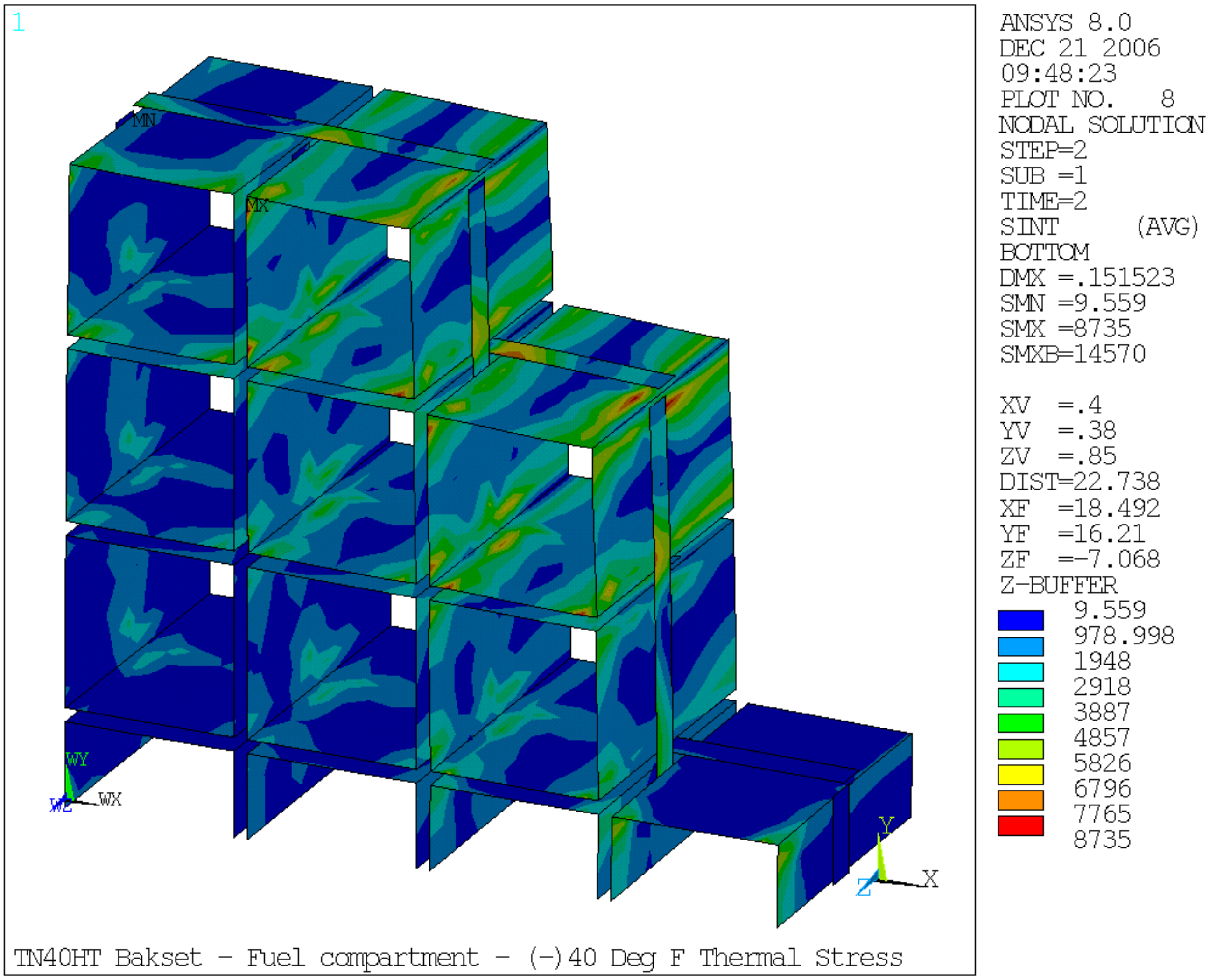

FIGURE A4B.1-18
THERMAL STRESS ANALYSIS – MAXIMUM FUEL COMPARTMENT STRESS INTENSITY FOR -40° F AMBIENT BOTTOM SURFACE

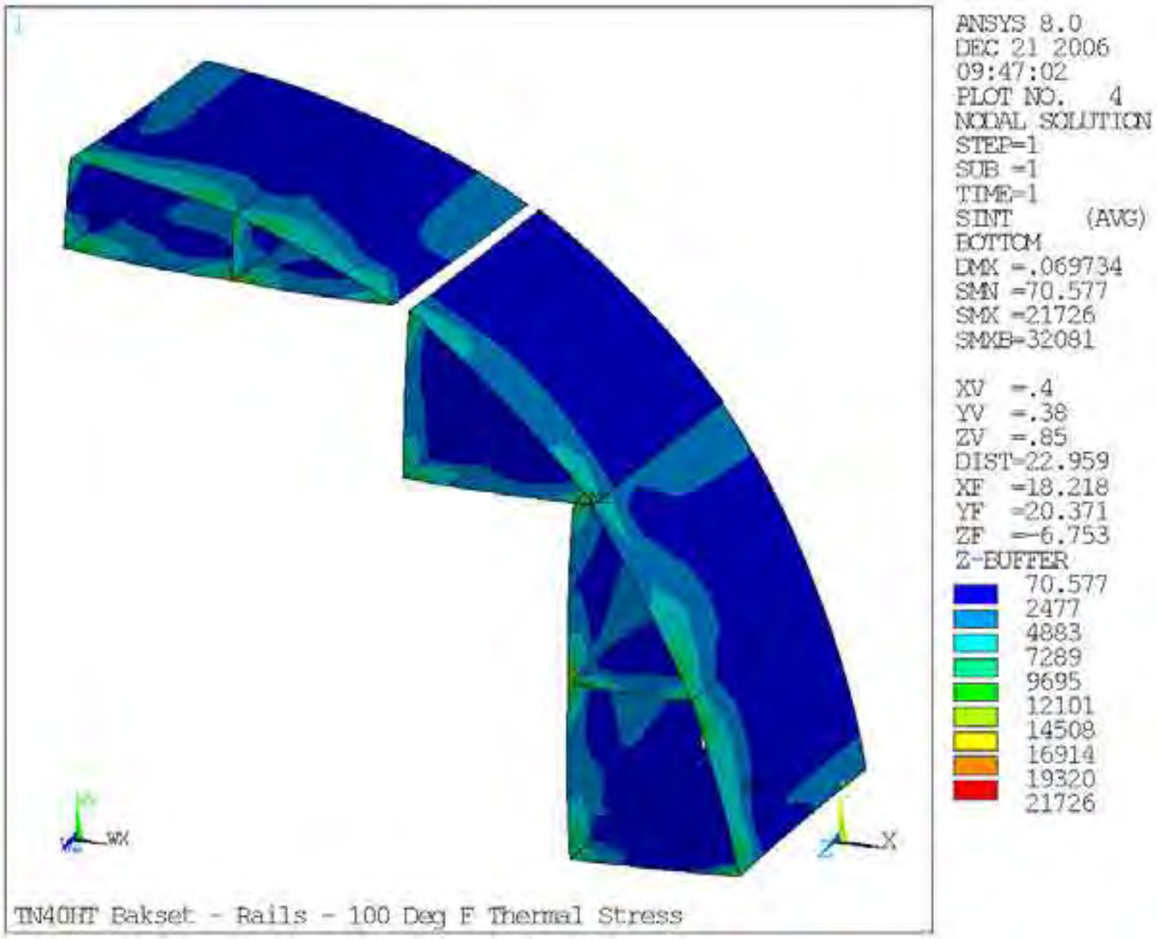

FIGURE A4B.1-19
THERMAL STRESS ANALYSIS – MAXIMUM RAILS STRESS INTENSITY FOR 100 °F AMBIENT BOTTOM SURFACE

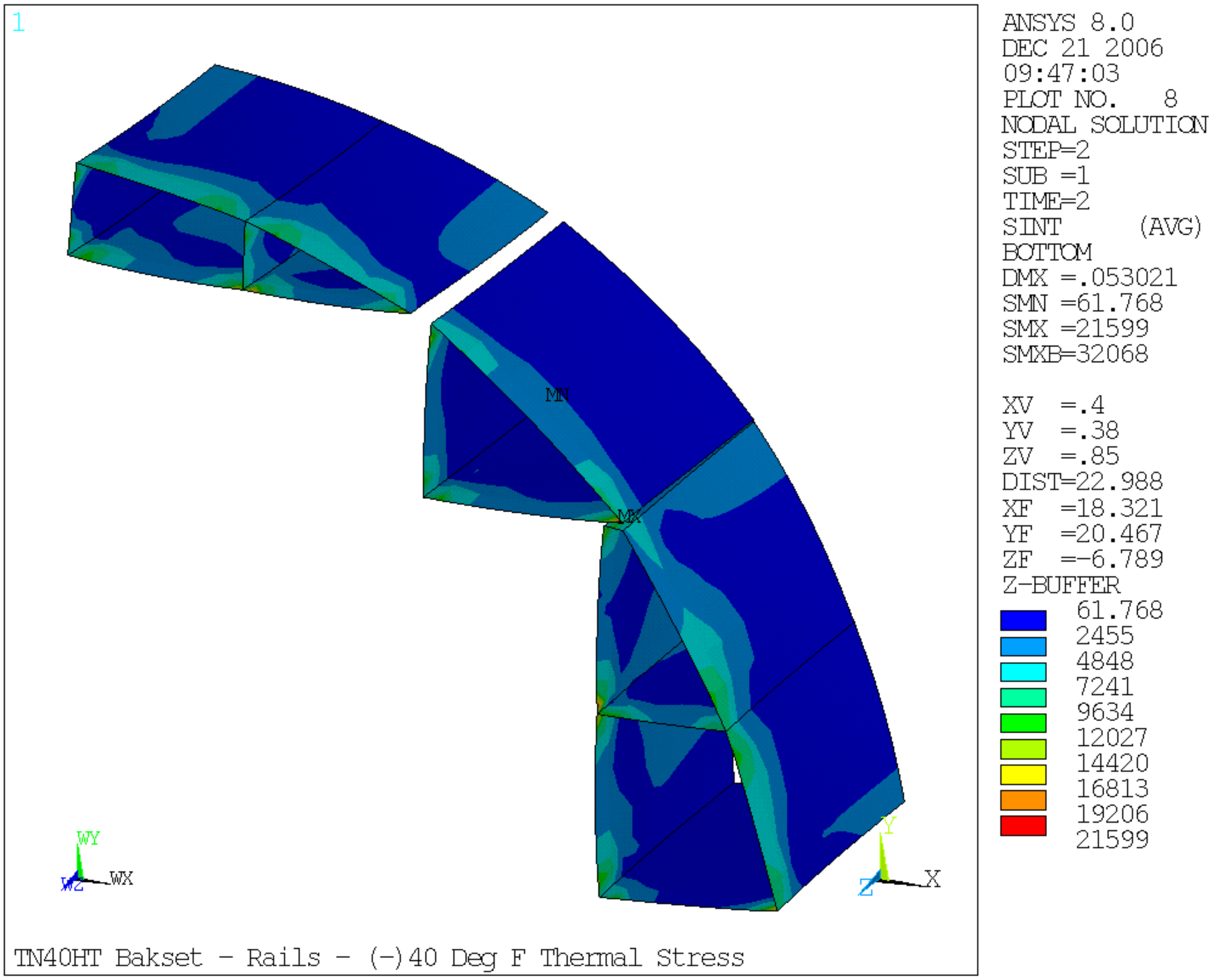

FIGURE A4B.1-20
THERMAL STRESS ANALYSIS – MAXIMUM RAILS STRESS INTENSITY
FOR -40 °F AMBIENT BOTTOM SURFACE

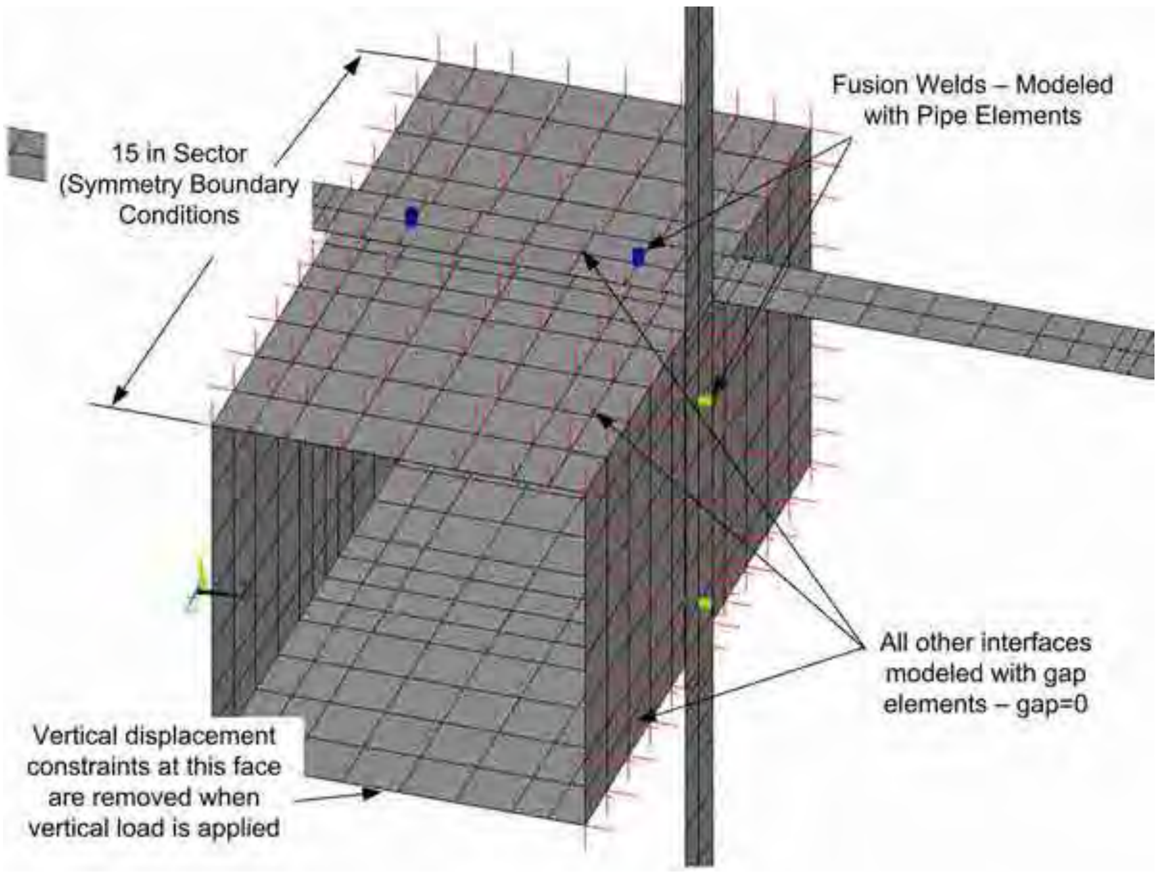

FIGURE A4B.1-21
INTERFACES FOR TYPICAL FUEL COMPARTMENT TUBE

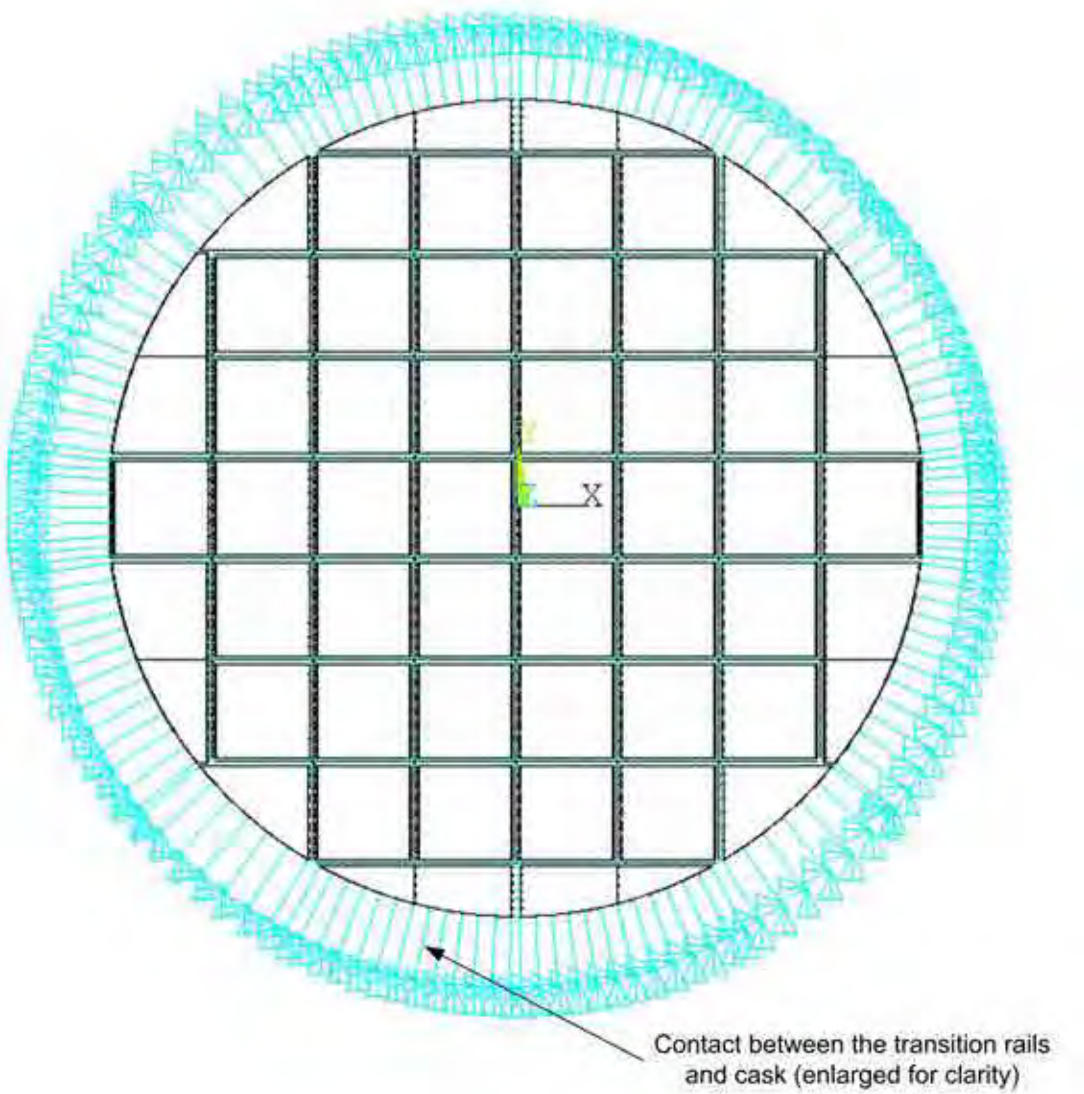

FIGURE A4B.1-22
BOUNDARY CONDITIONS FOR THE BASKET ANALYSIS
(SYMMETRY BOUNDARY CONDITIONS ARE NOT SHOWN FOR CLARITY)

SECTION A5

STORAGE SYSTEM OPERATIONS

A5.1 OPERATION DESCRIPTION

The TN-40HT cask was designed to use the same equipment as the TN-40 cask. As a consequence of this design objective, the operation of the TN-40 cask, as described in Section 5, is applicable to the operation of the TN-40HT cask. Therefore; rather than duplicating discussions and information already presented, the discussion of the TN-40HT storage system operation will be accomplished by referring to the appropriate section in Section 5 noting any necessary exceptions.

A5.1.1 NARRATIVE DESCRIPTION

The narrative of the storage system operation in Section 5.1.1 is applicable to the operation of the TN-40HT casks.

A5.1.2 FLOW SHEETS

The information outlined in Section 5.1.2 is applicable to the TN-40HT casks except for the location of the radiation exposure determination for the TN-40HT cask which is located in Section A7.

Note that the helium leak test of the “lid seals” includes all seals, e.g., the main lid seal, vent cover seal, and the drain cover seal.

A 5.1.3 IDENTIFICATION OF SUBJECTS FOR SAFETY AND RELIABILITY ANALYSIS

A5.1.3.1 CRITICALITY PREVENTION

The information in Section 5.1.3.1 is applicable to the TN-40HT casks except for the location of the criticality discussion which is located in Section A3.3.4.

A5.1.3.2 INSTRUMENTATION

The information in Section 5.1.3.2 is applicable to the TN-40HT casks except for the location of the description of the transmitters which is located in Section A3.3.3.

A5.1.3.3 MAINTENANCE TECHNIQUES

The information in Section 5.1.3.3 is applicable to the TN-40HT casks.

A5.2 CONTROL ROOM AND CONTROL AREAS

The information in Section 5.2 is applicable to the TN-40HT casks.

A5.3 SPENT FUEL ACCOUNTABILITY PROGRAM

The information in Section 5.3 is applicable to the TN-40HT casks.

A5.4 SPENT FUEL TRANSPORT TO ISFSI

The information in Section 5.4 is independent of cask design.

A5.5 SPENT FUEL TRANSFER TO TRANSPORT CASK

The information in Section 5.5 is applicable to the TN-40HT casks.

A5.6 REFERENCES

None.

SECTION A6

WASTE MANAGEMENT

A6.1 DESIGN

The information outlined in Section 6.1 is applicable to the TN-40HT casks except for the location of the decommissioning plan for the TN-40HT casks which is located in Section A4.6.

A6.2 REFERENCES

The references listed in Section 6.2 are also applicable to the TN-40HT casks and there are no additional references associated with Section A6.

SECTION A7

RADIATION PROTECTION

A7.1 ENSURING THAT OCCUPATIONAL RADIATION EXPOSURES ARE AS LOW AS REASONABLY ACHIEVABLE (ALARA)

A7.1.1 POLICY CONSIDERATIONS AND ORGANIZATION

The information in Section 7.1.1 is independent of cask design.

A7.1.2 DESIGN CONSIDERATIONS

The information in Section 7.1.2 is also applicable to the TN-40HT casks.

A7.1.3 OPERATIONAL CONSIDERATIONS

The information outlined in Section 7.1.3 is applicable to the TN-40HT casks except for the location of the description of the radiation protection design features is located in Section A7.3.

A7.2 RADIATION SOURCES

A7.2.1 CHARACTERIZATION OF SOURCES

There are five principal sources of radiation associated with cask storage that are of concern for radiation protection:

- Primary gamma radiation from spent fuel;
- Primary neutron radiation from spent fuel (both alpha-n reactions and spontaneous fission);
- Gamma radiation from activated fuel structural materials and fuel inserts;
- Capture gamma radiation produced by attenuation of neutrons by shielding material of the cask; and
- Neutrons produced by sub-critical fission in fuel.

The first three sources of radiation are evaluated using SAS2H/ORIGEN-S modules of the SCALE (Reference 1) code with the 44 group ENDF/B-V library. The capture gamma radiation and sub-critical multiplication are handled as part of the shielding analysis which is performed with MCNP5 (Reference 2).

The fuel assemblies acceptable for storage in the TN-40HT are listed in Table A3.1-1. The largest uranium loading results in the largest source term at the design basis enrichment and burnup. Table A7.2-1 provides additional fuel assembly design characteristics for the fuel designs.

The 14x14 Westinghouse standard is the design basis fuel for shielding purposes because it has the highest initial heavy metal loading (modeled as 0.410 Mtu), and therefore results in the highest radioactive source terms for a given irradiation history. Initial enrichment of 3.4 wt% U235, assembly average burnup of 60 GWd/MTU, and cooling time of 18 years complete the specification of the design basis fuel. A conservative two-cycle irradiation at a constant specific power of 20 MW/assy is utilized with a 20 day down time between each cycle to calculate the source terms for the design basis fuel.

The source terms are generated for the active fuel region, the plenum region, and each end region. Irradiation of the fuel assembly structural materials (including the fuel inserts, plenum, and end fittings) are included as an irradiation in the fuel zone with appropriate flux reduction factors as described below. The fuel assembly hardware materials and masses on a per assembly basis are listed in Table A7.2-2. Table A7.2-3 provides the material composition of fuel assembly hardware materials. Cobalt impurities are included in the SAS2H model. In particular, the cobalt impurities in Inconel-718, Zircaloy and Stainless Steel 304 are 0.469%, 0.001% and 0.08%, respectively.

Table A7.2-4 contains the masses of the various hardware materials present in the four principal regions of the fuel assembly. The masses for the materials in the top end fitting, the plenum, and the bottom fitting regions are multiplied by the activation ratios 0.1, 0.2 and 0.2, respectively (Reference 5), to correct for the spatial and spectral changes of the neutron flux outside of the active fuel zone.

As an example, the effective cobalt mass in the top end region is determined by taking the mass of the material listed in Table A7.2-4 times the cobalt impurity percentage listed above, which are also shown on Table A7.2-3. The resultant product is then adjusted by the above activation ratio:

Co = 6.30 kg (stainless steel, Table A7.2-4)*0.08% (Table A7.2-3) +
0.508 kg (Inconel Table A7.2-4)* 0.469% (Table A7.2-3) = 0.0074 kg
effective Co (after applying the 0.1 activation ratio) = 0.00074 kg

The material compositions of the fuel assembly hardware are included in the SAS2H/ORIGEN-S model on a per assembly basis. The cobalt content for each fuel assembly region utilized in the source term calculation is obtained from Table A7.2-4 reduced by the activation ratios.

Fuel Insert Thimble Plug Device (TPD)

The TPD materials and masses for each irradiation zone are listed in Table A7.2-5. The TPD is irradiated to an equivalent host assembly life burnup of 125 GWd/MTU. The model assumes that the TPD is irradiated in an assembly with an initial enrichment of 3.85 weight % U-235. The fuel assembly containing the TPD is burned for three cycles with a burnup of 15 GWd/MTU per cycle and a down time of 30 days between cycles. This is equivalent to an assembly life burnup of 45 GWd/MTU over the three cycles. The results are increased by a factor of 2.7778 to achieve the equivalent 125 GWD/MTU source. The source term for the TPD is taken at 16 years cooling time.

Fuel Insert Burnable Poison Rod Assembly (BPRA)

The BPRA materials and masses for each irradiation zone are also listed in Table A7.2-5. These materials are irradiated in the appropriate zone for two cycles of operation. The model assumes that the BPRA is irradiated in an assembly with an initial enrichment of 3.85 weight % U-235. The fuel assembly containing the BPRA is burned for two cycles with a burnup of 15 GWd/MTU per cycle and a down time of 30 days between cycles. This is equivalent to an assembly life burnup of 30 GWd/MTU over the three cycles. The source term for the BPRA is taken at 18 years cooling time.

Reactor Coolant System Boron Concentration

Soluble boron in the reactor coolant system is the primary reactivity control mechanism in a PWR. It is important to include boron in the depletion model because it is a thermal neutron absorber and its presence hardens the neutron spectrum. The presence of boron reduces thermal absorption in U-235 and as a second-order effect, increases epithermal absorption in U-238, increasing the buildup of actinides such as Cm-244, the major contributor to the neutron source term.

Typical cycle average boron concentration is on the order of 900 ppm. For modeling purposes in the current analysis, 600 ppm was chosen to be the average boron concentration for the first irradiation cycle, with the second having 95% of this value. Studies were performed showing that the use of a lower boron concentration leads to a tiny underproduction of decay heat, neutron and gamma source strength in the energy groups that contribute the most to casks dose rates. The under predictions are within 1% of those determined with the lower boron concentration and thus have essentially no effect on dose rates and cooling times.

The results of the fuel qualification sensitivity calculations with soluble boron concentration are shown in Table A7.2-12. Cases C1 through C8 are sensitivity calculations where the soluble boron concentration in Cases B1 through B7 on Table A7.2-11 was increased from 600 ppm to 1000 ppm. The results of these evaluations show that this increase in boron concentration results in an increase in the dose rate by approximately 1.5% and an increase in the decay heat by approximately 1%. The fuel qualification, however, ensures that the design basis fuel assembly, i.e. Case A7 on Table A7.2-11, utilized in the shielding calculations results in bounding dose rates even though the boron concentration utilized is lower than that of a typical cycle average value.

Reactor Coolant System Temperature

Moderator temperatures can vary between 500-600 ^{o}F. The long-term operating temperature affects the end-of-life reactivity (as a second order effect) and the total actinide inventory. Higher average moderator T_{av} reduces the average moderator density, which reduces neutron moderation during operation. This again results in increased epithermal absorption in U-238 which results in an increase in the actinide inventory in the fuel for a given total fuel burnup. A moderator density of 0.733 g/cc (which corresponds to 566ºF at an operating pressure of 2250 psia) is used in the SAS2H calculation.

The results of the fuel qualification sensitivity calculations with moderator temperature are shown in Table A7.2-12. Cases D1 through D8 are sensitivity calculations where the moderator temperature in Cases C1 through C7 on Table A7.2-12 was increased from 558 K (545ºF, representative of a core average moderator temperature) to 590 K (602ºF, representative of an average hot leg moderator temperature) and the moderator density was correspondingly reduced from 0.733 g/cm^3 to 0.690 g/cm^3. The results of these evaluations show that this increase in moderator temperature and boron concentration results in an increase (when compared to corresponding cases B1 through B7) in the dose rate by approximately 4% and an increase in the decay heat by approximately 2%. The fuel qualification, however, ensures that the design basis fuel assembly, i.e. Case A7 on Table A7.2-11, utilized in the shielding calculations results in bounding dose rates. In addition, the use of a moderator density of 0.733 g/cm^3 (which corresponds to a moderator temperature of 566ºF) for the design basis is justified because 566ºF is representative of a core average moderator temperature.

<u>Fuel and Cladding Temperature</u>

Representative temperatures of 840 K and 620 K were selected for the fuel and clad, respectively.

A7.2.2 AIRBORNE RADIOACTIVE SOURCES

In addition to the source terms generated for the shielding analysis, the SAS2H irradiation also provides the bounding radiological source terms for confinement. These results are provided in Table A7.2-6.

A7.2.3 AXIAL SOURCE DISTRIBUTION

Reference 4 provides axial PWR burnup profiles as a function of fuel assembly burnup ranges. For the Prairie Island high burnup fuel to be stored in the TN-40HT cask, the burnup profile for > 46 GWD/MTU was selected for use in this analysis. Figure A7.2-1 represents this profile.

The conservative axial profile containing 18 axial zones is utilized in the shielding evaluation. The axial zones are approximately equal and each zone represents between 5% and 6% of the total active fuel zone. The peaking factors range from a slightly more than 0.5 at the bottom and top, to a maximum of 1.11 just below the middle. The gamma source is directly proportional to the burnup and the neutron source is proportional to the fourth power of the burnup. This data is presented in Table A7.2-7 and shown in Figure A7.2-2. For the gamma distribution, the average value is around 1.0. However, for the neutron distribution, the average value of the distribution is greater than 1.0. The average value of the axial neutron distribution may be interpreted as the ratio of the true total neutron source in an assembly to the neutron source calculated by SAS2H/ORIGEN-S for an average assembly burnup. Therefore, to properly correct the magnitude of the neutron source, the neutron source per assembly, reported in Table A7.2-8, is multiplied by the average value of the neutron source distribution as reported in Table A7.2-7.

A7.2.4 GAMMA SOURCE

The gamma source terms for the 14x14 design basis fuel assembly are provided in Table A7.2-8. The gamma source spectra are presented in the 18-group structure consistent with the SCALE 27n-18γ cross section library. The conversion of the source spectra from the default ORIGEN-S energy grouping to the SCALE 27n-18γ energy grouping is performed directly through the ORIGEN-S code. The SAS2H/ORIGEN-S input file is provided in Appendix A7B.

The gamma source for the fuel assembly hardware is primarily from the activation of cobalt. This activation contributes primarily to SCALE Energy Groups 36 and 37.

For this analysis, it is assumed that the fuel insert source is a composite source; a BPRA in the core region and a TPD in the plenum and top fitting region. This bounds both types since the TPD does not extend into the core region but has a higher source term in the plenum and top fitting regions than a BPRA. The cumulative burnup of the fuel assembly(s) where the BPRA resided during reactor operation is assumed to be 30 GWd/MTU and the BPRA has cooled for 18 years. The cumulative burnup of the TPD host assemblies is assumed to be 125 GWD/MTU and the TPD has cooled for 16 years. The fuel insert source is shown in Table A7.2-9.

A7.2.5 NEUTRON SOURCE

Table A7.2-8 provides the total neutron source for the 14x14 design basis fuel assembly. The neutron source term consists primarily of spontaneous fission neutrons (largely from Cm-244) with (α,O-18) sources of lesser importance, both causing secondary fission neutrons. The overall spectrum is well represented by the Cm-244 fission spectrum. For the MCNP analyses, the default Cm-244 energy spectrum is utilized.

A7.2.6 FUEL QUALIFICATION

This section provides the basis for qualification of the design basis fuel chosen for the shielding analysis of the TN-40HT cask. The objective is to demonstrate that the fuel assemblies with the parameters corresponding to design basis fuel result in the highest calculated dose rate so that bounding shielding analysis can be performed by utilizing these design basis source terms. In order to determine the bounding spent fuel parameters (design basis fuel assembly), the candidate assembly parameters are ranked by their relative radiation source strengths. A simple 2-D shielding calculation based on a representation of the TN-40HT cask is performed and the radiation dose rates at 2m from the side surface are determined. The spent fuel parameters that yield the highest total dose rate (gamma + neutron) are considered the design basis for shielding calculations.

These analyses were carried out using the SAS2H depletion module from the SCALE (Reference 1) computer software and MCNP (Reference 2). For all SAS2H calculations the SCALE 44 group ENDF/B-V (44groupndf5) library was used. MCNP calculations used the default cross section libraries.

A simplified MCNP model was utilized to calculate a response function at 2 meters from the side surface of a cask. The response function is simply a source-to-dose conversion function and is representative of the TN-40HT cask shielding configuration. A representative response function is adequate for ranking the impact of burnup, enrichment and cooling time combination on dose rate. In essence the dose rate at 2 meters is calculated for each gamma energy group of the source as calculated by SAS2H. For neutrons, since a bounding energy spectrum is used, the response function calculated is just a total source to dose factor.

The response function is then utilized with SAS2H models to estimate the 2 meter side dose rate as a function of different burnup, enrichment and cooling time combinations. Other information, such as the decay heat per fuel assembly and the cooling time are also collected.

The response function is shown in Table A7.2-10. As described above, the response function for neutrons and secondary gamma is a total source to dose factor while that for the primary gamma is a function of the energy spectrum. Table A7.2-10 also provides the additional dose rate contribution from the active fuel portion of the BPRA. A comparison of the neutron, gamma and total dose rate results for the design basis fuel based on the response function and the calculational MCNP results (mid-plane average from Table A7A.5-2) indicates that the response function results are adequate (ratio of neutron to gamma) for the purpose of fuel qualification (relative comparison of source terms).

The response function is employed to determine the design basis spent fuel parameters from among seven limiting combinations of burnup and cooling time (BECT). These combinations are selected such that the resulting decay heat is greater than the maximum allowable decay heat of 800 watts per fuel assembly.

Four sets of calculations (A, B, C and D) are performed to determine the design basis spent fuel parameters by a comparison of the resulting response function dose rates for the combinations of spent fuel parameters.

The results of these calculations are shown in Table A7.2-11 and Table A7.2-12. Cases A1 through A7 show the results of the response function dose rate calculations for the seven limiting BECT combinations. These calculations show that Case A7 results in the highest dose rate. Cases B1 through B8 show the results of the response function dose rate calculations for eight BECT combinations with a decay heat of approximately 800 watts per fuel assembly. Cases B1 through B8 represent the actual BECT combinations (fuel that would more closely qualify for loading) while A1 through A7 represent conservative combinations. As expected, the dose rates for cases B1 through B7 are lower than those for cases A1 through A7. Based on the results of this evaluation, the design basis source terms for shielding are obtained conservatively from the Westinghouse 14x14 standard fuel assembly with an enrichment of 3.40 wt. % U-235, a burnup of 60,000 MWD/MTU and a cooling time of 18 years. Cases B9 and B10 represent BECT combinations at enrichments of 2.1 wt. % U-235 and 1.0 wt. % U-235. Their results are also bounded by A7.

The results of the sensitivity calculations – “C” and “D” cases are shown in Table A7.2-12. Cases C1 through C8 are sensitivity calculations where the soluble boron concentration is increased from 600 ppm to 1000 ppm. A boron concentration of 1000 ppm averaged over the entire depletion is a conservative representation of the boron concentration during actual depletion. The results of these evaluations show that the increase in boron concentration results in an increase in the dose rate by approximately 1.5% and an increase in the decay heat by approximately 1%.

Cases D1 through D8 are sensitivity calculations where the moderator temperature is increased from 558 K (545ºF) to 590 K (602ºF, representative of an average hot leg moderator temperature) and the moderator density is correspondingly reduced from 0.733 g/cm^3 to 0.690 g/cm^3. The soluble boron concentration is maintained at 1000 ppm, similar to that of the previous sensitivity evaluation. The results of these evaluations show that the increase in moderator temperature and soluble boron concentration results in an increase in the dose rate by approximately 4% and an increase in the decay heat by approximately 2%.

However, a comparison of the results from the A, B, C and D cases demonstrate that the highest calculated dose rate is obtained from Case A7. Therefore Case A7 represents the design basis case from a fuel qualification standpoint.

The calculated dose rate and decay heat along with the cooling time are then utilized to determine the bounding radiological source term. The final design basis radiological source term is generated by adding the fuel insert source term to the fuel/hardware source term.

The evaluation with the response function showed the design basis fuel assembly with parameters of 3.4 %wt U-235, 60 GWD/MTU burnup and cooled for 18 years to provide the appropriate bounding source terms. It is important to note that the decay heat for this bounding assembly is 845 watts which is in excess of the allowable limit as discussed in Section A3.

A7.2.7 RECONSTITUTED FUEL ASSEMBLIES

Reconstituted fuel assemblies are fuel assemblies that have replaced damaged fuel pins with either natural uranium dioxide replacement rods, Zirconium inert rods, or stainless steel rods. These replacement rods have the same dimensions as the damaged fuel pin being replaced. While lower enriched fuel rods will have a higher source term than higher enriched rods with the same burnup, and activated stainless steel rods will initially have a higher source than a fuel pin due to Cobalt-60, the source term of the design basis fuel described in Section A7.2.1 will bound reconstituted fuel assemblies for the following reasons:

Since the replacement rods will see at least one cycle of exposure less than the damage rods would have, the burnup of the natural uranium dioxide replacement pins will be at most 2/3 of the burnup that the damaged fuel pin would have seen. This difference is enough to ensure that the source term of the design basis fuel bounds reconstituted fuel assemblies with natural uranium dioxide replacement pin(s).

The source term due to activation of a Zirconium inert rod is much less than the source term would be for the fuel pin being replaced. Thus, the source term of a reconstituted fuel assembly with Zirconium inert rod(s) is bounded by the source term of the design basis fuel.

The source term (primarily Cobalt-60) for the activated steel pin is greater than what the replaced fuel pin would have been at time of discharge. The decay of the steel rod source term is much greater than the replaced rod. After the specified minimum cooling time of 12 years, the Cobalt-60 activity in the steel rod has decayed to less than ¼ of its original value. This decay is sufficient to ensure that the source term of the design basis fuel bounds reconstituted fuel assemblies with natural uranium replacement pin(s).

A7.3 RADIATION PROTECTION DESIGN FEATURES

A7.3.1 STORAGE SYSTEM DESIGN DESCRIPTION

The TN-40HT cask has a number of design features which ensure a high degree of integrity for the confinement of radioactive materials and reduction of direct radiation exposures to levels that are as low as practical.

- The casks are loaded, sealed, and decontaminated prior to transfer to the ISFSI.
- The fuel will not be unloaded nor will the casks be opened at the ISFSI.
- The fuel will be stored dry inside the casks, so that no radioactive liquid is available for leakage.
- The casks will be sealed with a helium atmosphere to preclude oxidation of the fuel.
- The casks will be heavily shielded to reduce external dose rates. The shielding design features are discussed below.
- No radioactive material will be discharged during storage.

Shielding for the TN-40HT cask is provided mainly by the thick-walled cask body. For neutron shielding, a borated polyester resin compound surrounds the cask body and a polypropylene disk covers the lid for storage. Additional shielding is provided by the steel shell surrounding the resin layer and by the stainless steel and aluminum/steel structure of the basket.

A7.3.2 SHIELDING

The design of the cask shielding, material of construction, and method of calculating shielding parameters are explained in Appendix A7A. No special features or remote handling of the casks in the ISFSI are proposed. Portable shielding may be used during cask maintenance, if appropriate.

A7.3.3 AREA RADIATION AND AIRBORNE RADIOACTIVITY MONITORING INSTRUMENTATION

As indicated in Section A3.3.5.3, there are no credible events associated with use of the TN-40HT casks which could result in releases of radioactive products or unacceptable increases in direct radiation. Area radiation and airborne radioactivity monitors are therefore not needed at the ISFSI; however, TLDs will be used to record dose rates along the outer (nuisance) fence boundary of the ISFSI

A7.4 ESTIMATED ONSITE COLLECTIVE DOSE ASSESSMENT

Table A7.4-1 shows the estimated design basis occupational exposures to ISFSI personnel during the loading, transport and emplacement of the storage casks. Dose rates utilized to determine occupational exposures to ISFSI personnel during the loading, transport and emplacement of the storage casks are conservatively estimated \from those reported in Appendix A7A.

Table A7.4-2 shows the estimated design basis annual exposure for surveillance and maintenance activities. Visual surveillance was based on a walkdown of each of the original two pads at a distance no closer than 2 meters to the casks. The dose rate for visual surveillance activities was increased to account for dose rate due to loaded casks already at the ISFSI and to account for short term activities close to the cask. 604000000330

To estimate dose rates for operability tests and calibration, the worker was assumed to be at the monitoring panel at the perimeter fence entrance and exposed to a dose rate of 4 mrem/hr. During instrumentation and surface defect repairs the worker is assumed to be exposed to a dose rate of 300 mrem/hr that is representative of high surface dose rates on the cask. For major maintenance work, the worker is assumed to be exposed to the 1 meter side dose rate.

Both Table A7.4-1 and Table A7.4-2 provide for each task the estimated time required for the task, number of personnel required, the design basis dose rates and the exposure. The purpose of these tables is to provide an estimated total dose and not to prescribe limits or restrictions on dose rates, times to complete tasks, or number of persons working on tasks. Actual loading and maintenance activities may deviate from those shown in the tables but will be conducted such that exposure is as low as reasonable achievable.

Localized regions of elevated dose rates should be anticipated and minimized with good ALARA practices. Such regions exist due primarily to radiation streaming, including for example, streaming through the vent and drain ports.

To evaluate the additional dose to station personnel from ISFSI operations, a dose rate analysis has been performed using the dose rate versus distance results given in Appendix A7A.7. The occupational dose calculation considers all workers at the Prairie Island Nuclear Generating Plant to be in buildings (however no credit is taken for shielding of personnel by buildings) or in the plant yard. This population includes a normal work force and contractor personnel as well as the increased staffing required during outages.

Table A7.4-3 provides a summary of staffing levels assumed at various site locations along with the distance from the center of the ISFSI. The locations designated on Table A7.4-3 are shown on Figure A7.4-A. This information is considered to be a general estimate of station staffing and does not necessarily reflect actual staffing at any given time. Changes in staffing levels and locations can be expected to occur in the future without affecting the general estimates contained in this section.

Distance dependent dose rates are provided in Table A7A.7-2. The data is based on loading 64 TN-40HT casks The first 48 casks are loaded over a 22 year period assuming 4 spent fuel casks are loaded every 2 years. The remaining 16 casks (for the ISFSI expansion) are assumed to begin loading immediately after the first 48 casks, so that the 16 casks are loaded over a 6-year period with 4 spent fuel casks loaded every 2 years. The dose rates in Table A7.4-3 were conservatively (using linear interpolation) calculated using the dose rate vs. distance data corresponding to the “corner” detectors. 604000000330

Table A7.4-4 summarizes the calculated total doses to full time and outage help at the various locations due to ISFSI operation. The collective onsite dose by location and the total onsite dose estimates are also shown on this table.

A7.5 OFFSITE COLLECTIVE DOSE ASSESSMENT

Figure 1.2-1 illustrates the Prairie Island Nuclear Generating Plant site boundary, which is also the boundary of the exclusion area as defined in 10CFR100.3. This exclusion area corresponds to the controlled area for the ISFSI as defined in 10CFR72.3.

In calculating the offsite collective dose, the entire permanent population within a 2 mile radius of the plant was conservatively taken to be at the location of the residence subject to the highest exposure, i.e. 0.45 miles NW of the ISFSI. In addition to the permanent population, there is a large transient population of persons employed at or visitors to the Treasure Island Hotel and Casino that is located within a 2 mile radius of the plant. For these calculations it is assumed that this entire transient population is located 0.8 miles from the ISFSI. The estimates of the population (both permanent and transient) within the 2 mile radius were taken from the Prairie Island Nuclear Generating Plant's evacuation time study (Reference 6). A description of the off-site locations considered in this evaluation, the relevant population data, distances and occupancy times are shown in Table A7.5-1.

The dose rate resulting from cask storage at the ISFSI as a function of distance is given in Table A7.5-2. For a distance of 0.45 mile (724 meters) in the corner direction, the total dose rate is 3.69 E-3 rem/year. This is the annual exposure at the nearest resident location.* 60400000330

Table A7.5-2 shows the total dose rates from the ISFSI at each of the assumed off-site locations. In addition, Table A7.5-2 also contains the information summarized in Table A7.5-1. For conservatism, the dose rates calculated at a distance of 1004 m from the "north-south" face of the ISFSI are utilized to determine the off-site exposures at distances greater than 0.8 miles (1280 m).

Table A7.5-2 summarizes the calculated total doses to the off-site population within a 2-mile radius due to the ISFSI operation. The total collective off-site dose is calculated to be 3.69 person-rem.

*Note that, for the purposes of demonstrating compliance with the requirements of 10 CFR 72.104(a), 40 CFR 190.10(a), and 10 CFR 20.1301(a), a more conservative value is calculated, including the dose contribution from other sources such as planned plant discharges, as discussed in Section A7A.7.2. 60400000330

A7.6 RADIATION PROTECTION PROGRAM

The information in Section 7.6 is independent of cask design.

A7.7 RADIOLOGICAL ENVIRONMENTAL MONITORING PROGRAM

The information in Section 7.7 is independent of cask design.

A7.8 REFERENCES

1. SCALE 4.4, "Modular Code System for Performing Standardized Computer Analyses for Licensing Evaluation for Workstations and Personal Computers," CCC-545, ORNL.

2. "MCNP/MCNPX – Monte Carlo N-Particle Transport Code System Including MCNP5 1.40 and MCNPX 2.5.0 and Data Libraries," CCC-730, Oak Ridge National Laboratory, RSICC Computer Code Collection, January 2006.

3. ORNL/TM-11018, "Standard- and Extended-Burnup PWR and BWR Reactor Models for the ORIGEN2 Computer Code," Oak Ridge National Laboratory, December 1989.

4. NUREG/CR-6801 (ORNL/TM-2001/273), March 2003, "Recommendations for Addressing Axial Burnup in PWR Burnup Credit Analysis."

5. Luksic, "Spent Fuel Assembly Hardware: Characterization and 10 CFR 61 Classification for Waste Disposal," PNL-6906, UC-85, June 1989.

6. Evacuation Time Estimate Study for the Prairie Island Nuclear Generating Plant Emergency Planning Zone, November 2012.

TABLE A7.2-1
PRAIRIE ISLAND FUEL ASSEMBLY DESIGN CHARACTERISTICS

Fuel Designations	Exxon Std (14x14)	Exxon Std High Burnup (14x14)	Exxon Toprod (14x14)	Westinghouse Standard (14x14)	Westinghouse OFA (including Vantage+) (14x14)
Max Length (in)	161.3	161.3	161.3	161.3	161.3
Max Width (in)	7.763	7.763	7.763	7.763	7.763
Fuel Density(1) (% Theoretical)	93.18	93.20	92.80	93.32	94.80
Rod Pitch (in)	0.556	0.556	0.556	0.556	0.556
No of Fueled Rods	179	179	179	179	179
Maximum Active Fuel Length (in)	144.0	144.0	144.0	144.0	144.0
Fuel Rod OD (in)	0.4240	0.4260	0.4170	0.4220	0.4000
Clad Thickness (in)	0.030	0.031	0.0295	0.0243	0.0243
Fuel Pellet OD (in)	0.3565	0.3565	0.3505	0.3659	0.3444
Clad Material	Zr-4	Zr-4	Zr-4	Zr-4	Zr-4/ZIRLO
Guide Tube OD (in)	0.541	0.541	0.541	0.539	0.528
Guide Tube Wall Thickness (Zr-4) (in)	0.017	0.017	0.017	0.017	0.019
Guide Tube #	16	16	16	16	16
Instrument Tube #	1	1	1	1	1
Instr. Tube OD (in)	0.424	0.424	0.424	0.422	0.4015
Instr. Tube Wall Thickness (Zr-4) (in)	0.025	0.025	0.025	0.0243	0.0258
Maximum MTU/assembly(2)	0.370	0.370	0.370	0.410	0.360
Free Gas Volume m^3 @STP	0.226	0.226	0.226	0.107	0.107
Fill Gas	He	He	He	He	He

Notes:

(1) The fuel density values are “as-built”, i.e., they incorporate the effect of the pellet dish and chamfer, as well as the theoretical density of the pellet. These densities were calculated from reload data provided by the fuel manufacturer, as follows:

As-built UO_2 density = total amount UO_2 in reload/ total volume of fuel in reload

Where fuel volume = (# fuel pins) (π/4) (pellet OD)^2 (active fuel length)

(2) The maximum MTU/assembly is calculated based on the theoretical density. The calculated value is higher than the actual value.

TABLE A7.2-2
WESTINGHOUSE 14X14 STANDARD FUEL ASSEMBLY HARDWARE CHARACTERISTICS

Item	Material	Average Mass (kg/assembly)
Fuel Zone		
Cladding	Zircaloy	83.4
Spacers	Inconel	5.37
Guide/Instrument Tube*	Stainless Steel	7.74
Fuel-Gas Plenum Zone		
Cladding	Zircaloy	4.13
Springs	Stainless Steel	5.68
Spacer	Inconel	0.68
Guide/Instrument Tube*	Stainless Steel	0.38
Top End Fitting Zone		
Top Nozzle	Stainless Steel	6.30
Hold Down Springs	Inconel	0.51
Bottom End Fitting Zone		
Bottom Nozzle	Stainless Steel	7.89
Total		122

* Conservatively assumed as stainless steel

TABLE A7.2-3
MATERIAL COMPOSITIONS FOR FUEL ASSEMBLY HARDWARE MATERIALS

Element	Atomic Number	Material Composition, grams per kg of material		
		Zircaloy-4	Inconel-718	Stainless Steel 304
H	1	1.30E-02	-	-
Li	3	-	-	-
B	5	3.30E-04	-	-
C	6	1.20E-01	4.00E-01	8.00E-01
N	7	8.00E-02	1.30E+00	1.30E+00
O	8	9.50E-01	-	-
F	9	-	-	-
Na	11	-	-	-
Mg	12	-	-	-
Al	13	2.40E-02	5.99E+00	-
Si	14	-	2.00E+00	1.00E+01
P	15	-	-	4.50E-01
S	16	3.50E-02	7.00E-02	3.00E-01
Cl	17	-	-	-
Ca	20	-	-	-
Ti	22	2.00E-02	7.99E+00	-
V	23	2.00E-02	-	-
Cr	24	1.25E+00	1.90E+02	1.90E+02
Mn	25	2.00E-02	2.00E+00	2.00E+01
Fe	26	2.25E+00	1.80E+02	6.88E+02
Co	27	1.00E-02	4.69E+00	8.00E-01
Ni	28	2.00E-02	5.20E+02	8.92E+01
Cu	29	2.00E-02	9.99E-01	-
Zn	30	-	-	-
Zr	40	9.79E+02	-	-
Nb	41	-	5.55E+01	-
Mo	42	-	3.00E+01	-
Ag	47	-	-	-
Cd	48	2.50E-04	-	-
In	49	-	-	-
Sn	50	1.60E+01	-	-
Gd	64	-	-	-
Hf	72	7.80E-02	-	-
W	74	2.00E-02	-	-
Pb	82	-	-	-
U	92	2.00E-04	-	-

TABLE A7.2-4
MATERIAL COMPOSITIONS FOR THE WESTINGHOUSE STANDARD 14X14 FUEL ASSEMBLY

Material Compositions for the Westinghouse Standard 14x14 Fuel Assembly

Fuel Zone	Height (cm)	Zircaloy (Kg)	UO_2 (Kg)	Inconel - 718 (Kg)	SS-304 (Kg)	Total (Kg)	Volume (cm^3)
Bottom	7.82				7.893	7.893	3.042E+03
Core	365.8	83.36	465.1	5.370	7.736	561.566	1.422E+05
Plenum	18.14	4.13		0.680	6.067	10.88	7.053E+03
Top	8.89			0.508	6.300	6.808	3.456E+03
Total		87.49	465.1	6.558	27.996	587.144	

Note: The PWR fuel assembly is modeled as a homogenized cuboid with a cross section area of 388.80 cm^2 (19.718 cm by 19.718 cm) or about 7.763″ by 7.763″. The assembly is conservatively assumed to contain 410 Kg Uranium.

TABLE A7.2-5
FUEL INSERTS - MATERIALS AND MASSES

Component	Region	Material	Mass (kg)
TPD	Top Fitting		
	Baseplate, yoke, hold down bar, etc.	Type 304 SS	2.5
	spring	Inconel 718	0.36
	Plenum		
	Thimble plugs	Type 304 SS	2.2
BPRA	Top Fitting		
	Baseplate, yoke, hold down bar, etc	Type 304 SS	2.5
	spring	Inconel 718	0.36
	Plenum		
	Cladding & liner	Type 304 SS	0.42
	Fuel Zone		
	Cladding & liner	Type 304 SS	7.96

TABLE A7.2-6
RADIOACTIVE INVENTORY FOR 14X14 DESIGN BASIS FUEL ASSEMBLY

Classification	Nuclide	14x14 W std
		(Ci/assembly)
gas	H3(1)	1.78E+02
fine	Pu238	3.02E+03
fine	Pu239	1.35E+02
fine	Pu240	2.67E+02
fine	Pu241	3.19E+04
fine	Am241	1.50E+03
fine	Am243	4.17E+01
fine	Cm244	5.28E+03
gas	Kr 85	1.78E+03
volatile	Sr 90	3.11E+04
fine	Y 90	3.11E+04
gas	I129	2.40E-02
volatile	Cs134	4.01E+02
volatile	Cs137	5.27E+04
fine	Ba137m	4.97E+04
fine	Pm147	6.53E+02
fine	Eu154	1.33E+03
fine	Np239	4.17E+01
	Total	**2.11E+05**
	SAS2H Results for all Isotopes(2)	
	Light Elements	1.44E+03
	Actinides	4.22E+04
	Fission Products	1.69E+05
	Total	**2.13E+05**

Notes:

1) The total of H3 from Light Elements and Fission Products.
2) A comparison of the total radioactive inventory indicates that the activity of the selected isotopes represents greater than 99.1% of the total.

TABLE A7.2-7
AXIAL SOURCE TERM PEAKING FACTOR

Fractional Core Height			Gamma Profile	Neutron Profile
0	to	0.0556	0.573	0.108
0.0556	to	0.111	0.917	0.707
0.111	to	0.167	1.066	1.291
0.167	to	0.222	1.106	1496
0.222	to	0.278	1.114	1.540
0.278	to	0.333	1.111	1.524
0.333	to	0.389	1.106	1.496
0.389	to	0.445	1.101	1.469
0.445	to	0.500	1.097	1.448
0.500	to	0.556	1.093	1.427
0.556	to	0.611	1.089	1.406
0.611	to	0.667	1.086	1.391
0.667	to	0.722	1.081	1.366
0.722	to	0.778	1.073	1.326
0.778	to	0.833	1.051	1.220
0.833	to	0.889	0.993	0.972
0.889	to	0.944	0.832	0.479
0.944	to	1.000	0.512	0.069
		Average:	1.00	1.15

TABLE A7.2-8
SOURCE DISTRIBUTION FOR 14X14 FUEL ASSEMBLY

			Gamma Source(1) (particles/sec/assembly)			
E_{min}, MeV	to	E_{max}, MeV	Bottom Nozzle	In-core	Plenum	Top Nozzle
0.00E+00	to	5.00E-02	4.6970E+10	1.1471E+15	6.4166E+10	2.8144E+10
5.00E-02	to	1.00E-01	5.8263E+09	2.2692E+14	7.4846E+09	3.4247E+09
1.00E-01	to	2.00E-01	1.4050E+09	1.5457E+14	2.0286E+09	8.2647E+08
2.00E-01	to	3.00E-01	6.9758E+07	4.6484E+13	1.0335E+08	4.1160E+07
3.00E-01	to	4.00E-01	9.1527E+07	3.0384E+13	1.7060E+08	5.3770E+07
4.00E-01	to	6.00E-01	5.7847E+06	3.8369E+13	1.1945E+09	3.3967E+06
6.00E-01	to	8.00E-01	2.0089E+06	1.6010E+15	1.5982E+09	3.6813E+08
8.00E-01	to	1.00E+00	7.9012E+07	2.4369E+13	1.0456E+09	3.9964E+08
1.00E+00	to	1.33E+00	1.7003E+12	7.4979E+13(2)	3.0819E+12(2)	1.6114+12(2)
1.33E+00	to	1.66E+00	4.8016E+11	1.5249E+13(2)	8.7003E+11(2)	4.5485+11(2)
1.66E+00	to	2.00E+00	1.6758E-06	7.8481E+10	2.9812E+01	2.4793E-03
2.00E+00	to	2.50E+00	1.1395E+07	4.4802E+09	1.4591E+07	6.6906E+06
2.50E+00	to	3.00E+00	1.7669E+04	4.4758E+08	2.2624E+04	1.0374E+04
3.00E+00	to	4.00E+00	1.5658E-14	7.9748E+07	2.7747E-11	1.0249E-11
4.00E+00	to	5.00E+00	0.00	2.6150E+07	0.0	0.0
5.00E+00	to	6.50E+00	0.00	1.0495E+07	0.0	0.0
6.50E+00	to	8.00E+00	0.00	2.0588E+06	0.0	0.0
8.00E+00	to	1.00E+01	0.00	4.3714E+05	0.0	0.0
Total Gamma:			2.2349E+12	3.3595E+15	4.0297E+12	2.0095E+12

			Neutron Source(1) (particles/sec/assembly)			
E_{min}, MeV	to	E_{max}, MeV	Bottom Nozzle	In-core	Plenum	Top Nozzle
1.00E-01	to	4.00E-01	0.00	2.89E+07	0.00	0.00
4.00E-01	to	9.00E-01	0.00	1.48E+08	0.00	0.00
9.00E-01	to	1.40E+00	0.00	1.35E+08	0.00	0.00
1.40E+00	to	1.85E+00	0.00	9.94E+07	0.00	0.00
1.85E+00	to	3.00E+00	0.00	1.75E+08	0.00	0.00
3.00E+00	to	6.43E+00	0.00	1.59E+08	0.00	0.00
6.43E+00	to	2.00E+01	0.00	1.41E+07	0.00	0.00
Total Neutrons(3) (n/sec/FA)			7.59E+8			

1. The design basis gamma source term correspond to the Westinghouse 14x14 Standard fuel assembly with 3.40 wt.% U-235 enrichment, 60,000 MWD/MTU burnup, 18 year cooling time with TPD/BPRA insert source term.
2. Total gamma source from the fuel assembly and the BPRA/ TPD source shown in Table A7.2-9.
3. The neutron source spectrum shown in the table is from the SAS2H run and thus shows the spectrum due to all spontaneous fissions as well as from the alpha-neutron reactions. For the shielding calculations, the neutron source spectrum is modeled as Cm-244 using the built-in MCNP distribution and the total neutron source.

TABLE A7.2-9
GAMMA SOURCE TERMS FOR FUEL INSERTS

Gamma Source from 125 GWD/MTU, 16 Yr Cooled TPD (gammas/sec/assembly)						
In-Core		**Plenum**		**Top End Fitting**		**Total**
1 - 1.33 MeV	1.33 - 1.66 MeV	1 - 1.33 MeV	1.33 - 1.66 MeV	1 - 1.33 MeV	1.33 - 1.66 MeV	
-	-	9.05E+11	2.55E+11	6.13E+11	1.73E+11	1.95E+12

Gamma Source from 30 GWD/MTU, 18 Yr Cooled BPRA (gammas/sec/assembly)						
In-Core		**Plenum**		**Top End Fitting**		**Total**
1 - 1.33 MeV	1.33 - 1.66 MeV	1 - 1.33 MeV	1.33 - 1.66 MeV	1 - 1.33 MeV	1.33 - 1.66 MeV	
3.10E+12	8.73E+11	-	-	-	-	3.97E+12

TABLE A7.2-10
RESPONSE FUNCTION FOR TN-40HT CASK

	Response Function ((mrem/hour) per particle) per cask
Neutron	5.38E-09
Secondary Gamma	2.32E-08

Primary Gamma Energy Range (MeV)	Response Function ((mrem/hour) per particle) per cask
0.40 to 0.60	8.11E-18
0.60 to 0.80	7.86E-16
0.80 to 1.00	5.39E-15
1.00 to 1.33	4.03E-14
1.33 to 1.66	1.84E-13
1.66 to 2.00	5.73E-13
2.00 to 2.50	1.57E-12
2.50 to 3.00	3.43E-12
3.00 to 4.00	7.32E-12

Dose Rate from BPRA	0.29 mrem/hour

Calculational Model	Neutron (mrem/hour)	Gamma (mrem/hour)	Total Dose (mrem/hour)
Response Function	13.52	11.07	24.59
Response Function (BPRA)	13.52	11.36	24.88
TN-40 HT Shielding (1)	10.10	9.10	19.20
Ratio	0.75	0.80	0.77

(1) The neutron, gamma and total dose rates are obtained as an average of the dose rates shown in Table A7A.5-2. The dose rates at axial height ranging from -22.9 cm to 27.8 cm are included in the average calculations.

TABLE A7.2-11
FUEL QUALIFICATION CALCULATIONS FOR TN-40HT CASK

Case	Burnup (GWD/MTU)	Enrichment (wt.% U-235)	Cooling Time (years)	Decay Heat (watts)	Dose Rate (mrem/hour) Neutron	Gamma	Total
	Design Basis Cases for Fuel Qualification						
A1	52	3.4	12.2	813	9.82	14.55	24.36
A2	53	3.4	12.8	817	10.31	14.09	24.40
A3	56	3.4	14.9	829	11.77	12.65	24.42
A4	57	3.4	15.6	835	12.25	12.27	24.52
A5	58	3.4	16.4	838	12.68	11.82	24.50
A6	59	3.4	17.2	841	13.10	11.43	24.53
A7	60	3.4	18.0	844	13.52	11.07	**24.59**
	Fuel Qualification for Decay Heat of 800 Watts/Assembly						
B1	52	3.4	12.7	798	9.63	13.80	23.43
B2	53	3.4	13.5	799	10.05	13.12	23.17
B3	56	3.4	16.1	803	11.25	11.36	22.62
B4	57	3.4	17.0	805	11.63	10.88	22.50
B5	58	3.4	18.1	801	11.90	10.28	22.18
B6	59	3.4	19.1	802	12.21	9.84	22.05
B7	60	3.4	20.2	800	12.45	9.37	21.83
B8	60	4.9	18.0	798	7.46	10.05	17.52
B9	44	2.1	12.0	687	10.03	14.39	24.42
B10	19	1.0	12.0	272	1.25	7.30	8.55

TABLE A7.2-12
FUEL QUALIFICATION SENSITIVITY CALCULATIONS FOR TN-40HT CASK

Case	Burnup (GWD/MTU)	Enrichment (wt.% U-235)	Cooling Time (years)	Decay Heat (watts)	Dose Rate (mrem/hour) Neutron	Gamma	Total
	Sensitivity - Soluble Boron Concentration of 1000 ppm						
C1	52	3.4	12.7	806	9.86	13.85	23.72
C2	53	3.4	13.5	806	10.27	13.18	23.45
C3	56	3.4	16.1	811	11.48	11.42	22.90
C4	57	3.4	17.0	812	11.85	10.94	22.79
C5	58	3.4	18.1	811	12.12	10.34	22.46
C6	59	3.4	19.1	811	12.42	9.90	22.32
C7	60	3.4	20.2	809	12.66	9.44	22.10
C8	60	4.9	18.0	806	7.65	10.16	17.81
	Sensitivity - Moderator Temperature of 590 K						
D1	52	3.4	12.7	818	10.26	14.01	24.27
D2	53	3.4	13.5	818	10.67	13.33	24.01
D3	56	3.4	16.1	824	11.87	11.57	23.45
D4	57	3.4	17.0	825	12.24	11.09	23.33
D5	58	3.4	18.1	823	12.50	10.49	22.99
D6	59	3.4	19.1	823	12.81	10.04	22.85
D7	60	3.4	20.2	821	13.04	9.58	22.62
D8	60	4.9	18.0	818	8.01	10.36	18.37

TABLE A7.4-1
OCCUPATIONAL EXPOSURES FOR CASK LOADING, TRANSPORT, AND EMPLACEMENT

Task Description	Dose Rate (mrem/hr)	Time Required (hrs)	No. of Persons (man)	Dose (man-rem)
Placement in Pool	2	2	3	0.012
Loading Process	2	5	5	0.050
Removal from Pool	32	5	5	0.800
Transfer to Decontamination Area	32	1	3	0.096
Processing of Cask	43	6.5	2	0.559
Helium Leak Test	43	2	2	0.172
Decontamination	66	2	3	0.396
Install Neutron Shield, Pressurize, Test	43	3	2	0.258
Preparation for Transport	30	1	3	0.090
Transfer of Cask to ISFSI	18	1	3	0.054
Final Cask Emplacement	63	2	5	0.630
TOTAL	**N/A**	**30.5**	**N/A**	**3.117**

TABLE A7.4-2
DESIGN BASIS ISFSI MAINTENANCE OPERATIONS ANNUAL EXPOSURES

Task Description	Dose Rate (mrem/hr)	Time Required (hrs)	No. of Persons (man)	Dose (man-rem)
Visual Surveillance of Casks	63	1	2	0.126
Instrumentation Operability Tests	4	1	2	0.008
Instrumentation Calibration	4	2	2	0.016
Instrumentation Repairs	300	1	2	0.600
Surface Defect Repair	300	1	2	0.600
Major Maintenance	32	32.5	3	3.120
TOTAL	**N/A**	**38.5**	**N/A**	**4.470**

TABLE A7.4-3
STATION PERSONNEL LOCATION AND DOSE RATES

Location #	Location	Distance (Feet From Center ISFSI)	Full Time (Personnel)	Outage (Personnel)	Dose Rate, mrem/hr
1	34 OCA Gatehouse (D-2)	978	2	0	3.71E-02
2	22 Receiving Warehouse (D-5) 55 13 P1ex Project Office (D-5) A 4 P1ex Project Office (D-5)	953	30	0	4.00E-02
3	24 NPD Building (E-6) 33 NPD Annex Building (E-5) Quality Assurance Modular Office (E-5)	1016	60	1	327E-02
4	42 Fabrication Shop (C-5) 25 Steam Generator Mock up Building (C-5) 48 Fabrication Shop (D-5)	1381	2	45	8.33E-03
5	30 Warehouse (C-5) 31 Multiuse Warehouse (C-5) 21 Warehouse -8 (C-6)	1650	0	2	3.38E-03
6	12 Substation, SBO Structures (B-6)	2236	0	2	5.96E-04
7	23 New Administration Building (D-6) 6 Security Building (D-6)	1496	287	25	4.83E-03
8	4 Turbine Building (D-7) 28 Warehouse -2 (E-7) 3 Auxiliary Building (E-7) 13 New Service Building (D-8) 11 D5/D6 DG Building (D-7) 79 Security DG Building (D-7)	1650	180	192	3.38E-03
9	Outage Trailers (E-7)	1322	5	40	I.02E-02
10	60 Fabrication Shop (E-7) 29 Main Plant Warehouse (E-7) 66 Maintenance Storage Building (E-7)	1557	23	45	425E-03
11	20 Environmental Lab (B-9)	2534	2	0	2.07E-04
12	Training Center	905	49	0	4.57E-02
13	38 Old Administration Building (D-7) 71 Administration Building Addition (D-7)	1745	68	0	2.50E-03
14	13 New Service Building (D-8)	1905	9	0	1.52E-03

604000000330

TABLE A7.4-4
STATION PERSONNEL COLLECTIVE DOSE

Location #	Location	Distance (Feet From Center ISFSI)	Full Time (person-rem)	Outage (person-rem)	Total Exposure, (person-rem)
1	34 OCA Gatehouse (D-2)	978	1.88E-01	0.00E+00	I.88E-01
2	22 Receiving Warehouse (D-5) 55 13 P1ex Project Office (D-5) A 4 P1ex Project Office (D-5)	953	3.01E+00	0.00E+00	3.01E+00
3	24 NPD Building (E-6) 33 NPD Annex Building (E-5) Quality Assurance Modular Office (E-5)	1016	4.90E+00	1.76E-02	4.92E+00
4	42 Fabrication Shop (C-5) 25 Steam Generator Mock up Building (C-5) 48 Fabrication Shop (D-5)	1381	4.34E-02	2.02E-01	2.46E-01
5	30 Warehouse (C-5) 31 Multiuse Warehouse (C-5) 21 Warehouse -8 (C-6)	1650	0.00E+00	3.66E-03	3.66E-03
6	12 Substation, SBO Structures (B-6)	2236	0.00E+00	6.43E·04	G.43E-04
7	23 New Administration Building (D-6) 6 Security Building (D-6)	1496	3.45+00	7.23E-02	3.53E+00
8	4 Turbine Building (D-7) 28 Warehouse -2 (E-7) 3 Auxiliary Building (E-7) 13 New Service Building (D-8) 11 D5/D6 DG Building (D-7) 79 Security DG Building (D-7)	1650	1.52E+00	3.47E-01	I.86E+00
9	Outage Trailers (E-7)	1322	1.30E-01	2.17E-01	3.47E-01
10	60 Fabrication Shop (E-7) 29 Main Plant Warehouse (E-7) 66 Maintenance Storage Building (E-7)	1557	2.46E-01	1.01 E-01	3.47E-01
11	20 Environmental Lab (B-9)	2534	1.34E-03	0.00E+00	1.34E-03
12	Training Center	905	5.59E+00	0.00E+00	5.59E+00
13	38 Old Administration Building (D-7) 71 Administration Building Addition (D-7)	1745	4.19E-01	0.00E+00	4.19E-01
14	13 New Service Building (D-8)	1905	2.89E-02	0.00E+00	2.89E-02
Total			1.95E+01	9.61E-0l	2.00E+01

* For full time employees, assume 2500 hours/year.
** For outage employees, assume 540 hours/year.

604000000330

TABLE A7.5-1
OFFISTE POPULATION: LOCATION, DISTANCE, OCCUPANCY TIME

Permanent population within 2 mile radius

Description	Population	Occupancy times	Distance
2 mile -radius	398	24 hr/day 365 day/yr	>0.45 mile

Transient Employee Population

Description	Population	Occupancy times	Distance
2 mile - PI community center, government center, and clinic	80	8 hr/ day, 5 day/wk, 50 wk/yr	0.8 mile
2 mile - Employees at Treasure Island Casino	435	At any give time; i.e. 24 hr/day 365 day/yr	0.8 mile

Transient recreational Population

Description	Population	Occupancy times	Distance
2 mile - Treasure Island Casino	5400, includes hotel occupants	24 hr/day, 365 day/yr	0.8 mile

Marina and RV Park

Description	Population	Occupancy times	Distance
2 mile - PI community center, government center, and clinic	450	8 hr/ day, 5 day/wk, 29 wk/yr	0.8 mile

TABLE A7.5-2
OFFSITE POPULATION: DOSE RATES AND COLLECTIVE DOSE

Offsite Population	Description	Distance	Occupancy times	Population	Dose Rate, (mrem/hr)	Collective Exposure, (person-rem)
Permanent* population within 2 mile radius	2 mile radius	>0.45 miles	8760	398	4.21E-04	1.47E+00
Transient Employee Population	2 mile -PI community center, government center, and clinic	0.8 mile	2000	80	4.81E-05	7.70E-03
	2 mile -Employees at Treasure Island Casino	0.8 mile	8760	435	4.81E-05	1.83E-01
Transient recreational population	2 mile -Treasure Island Casino	0.8 mile	8760	5400	4.81E-05	2.28E+00
Marina and RV Park	2 mile -PI community center, government center, and clinic	0.8 mile	1160	450	4.81E-05	2.51E-02
	Total Collective Within 2 Mile					**3.96E+00**

604000000330

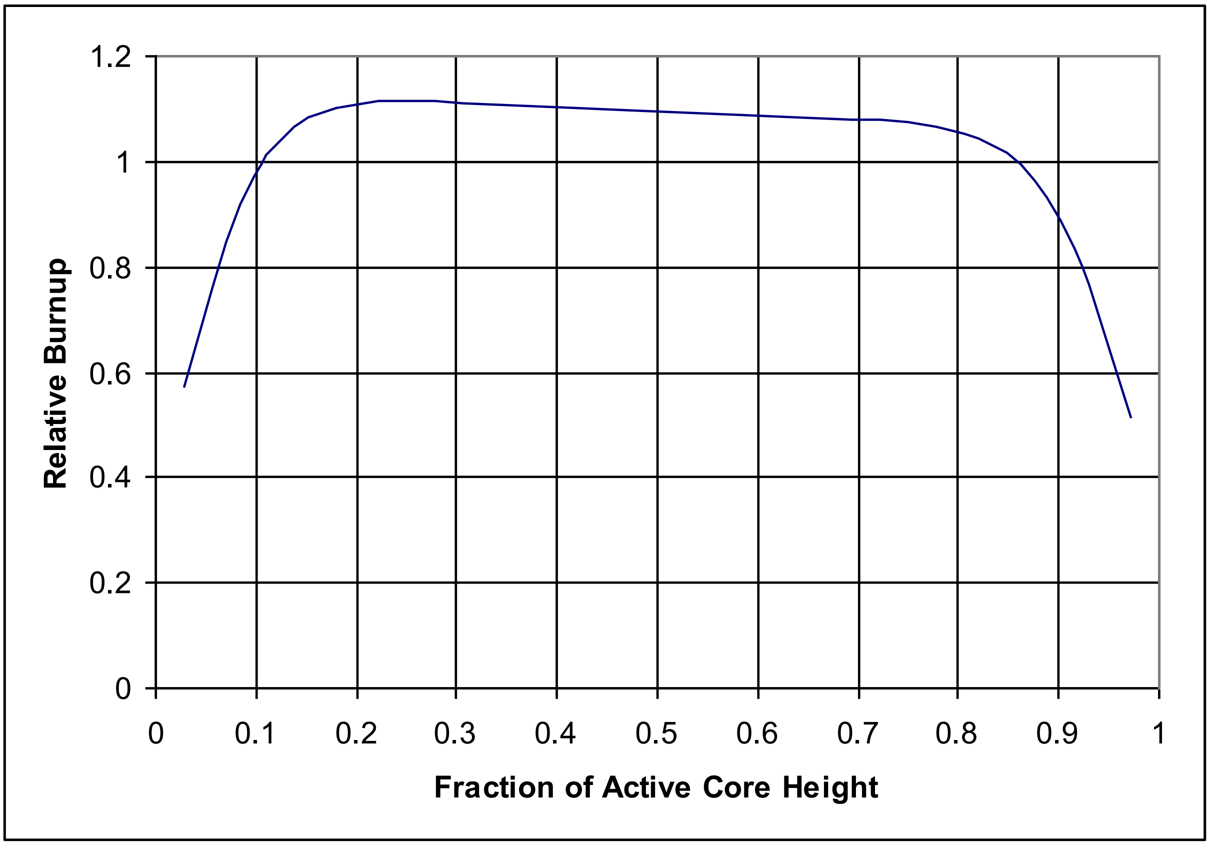

FIGURE A7.2-1
AXIAL BURNUP PROFILE FOR DESIGN BASIS FUEL

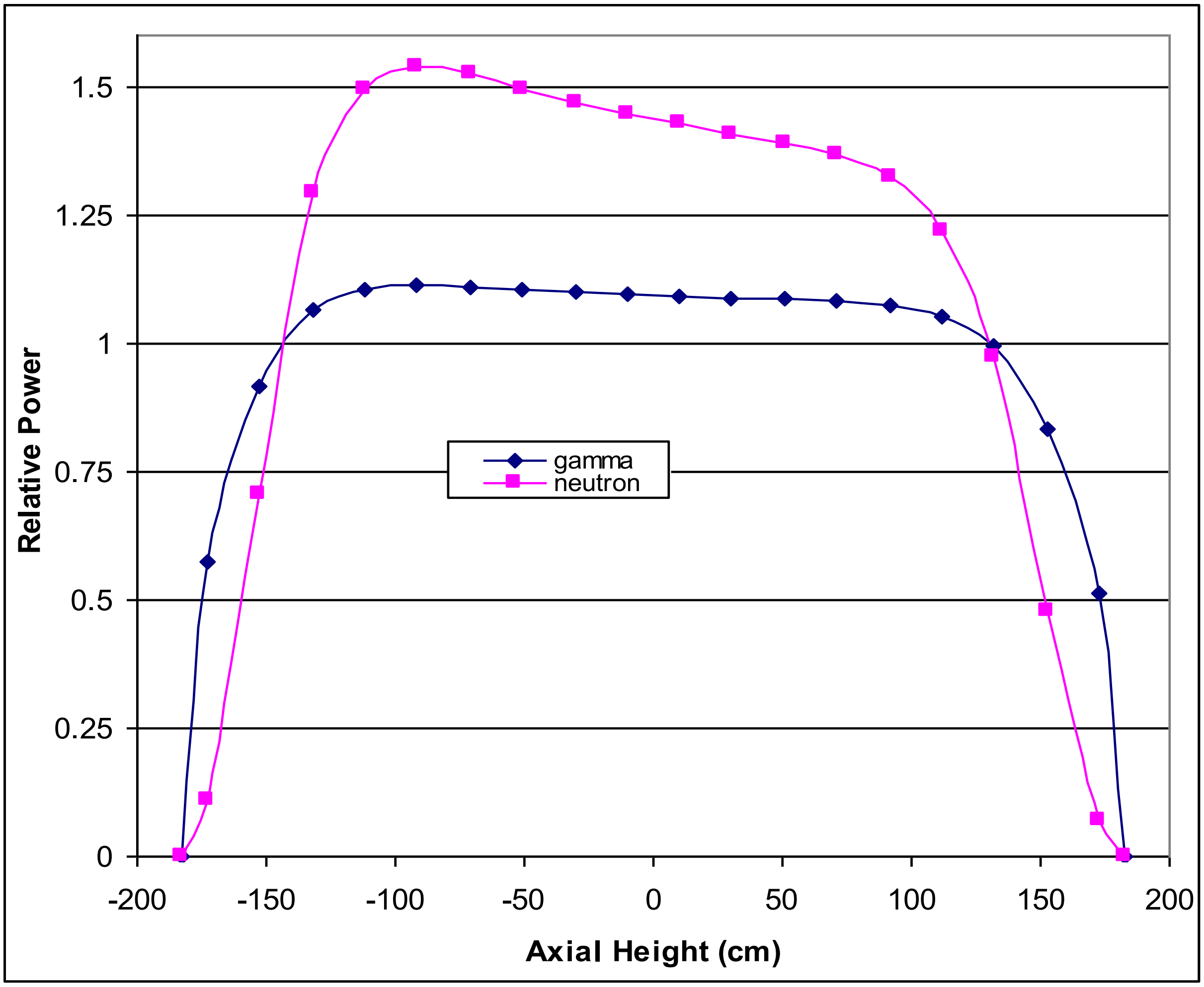

FIGURE A7.2-2
AXIAL NEUTRON AND GAMMA POWER PROFILES

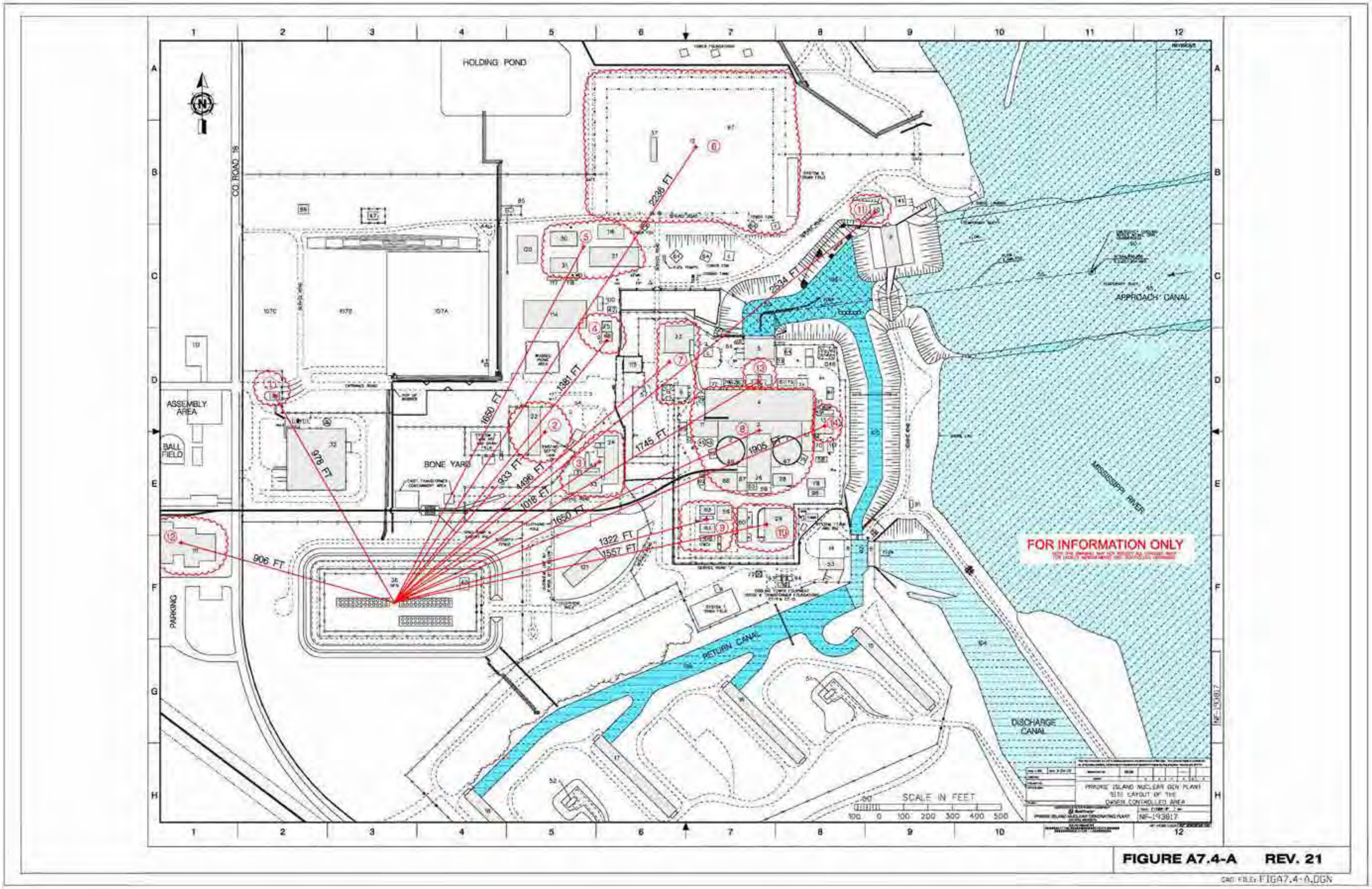

FIGURE A7.4-A REV. 21

CAD FILE: FIGA7.4-A.DGN

Appendix A7A

TN-40HT CASK DOSE ANALYSIS

A7A.1 SHIELDING DESIGN FEATURES

Shielding for the TN-40HT cask is provided mainly by the cask body. For the neutron shielding, a borated polyester resin compound surrounds the cask body and a polypropylene disk covers the lid. Additional shielding is provided by the steel shell surrounding the resin layer and by the steel and aluminum structure of the fuel basket.

Geometric attenuation, enhanced by air and ground attenuation, provides additional dose reduction for distant locations at the restricted area and site boundaries. Figure A7A.1-1 shows the configuration of shielding in the cask. Table A7A.1-1 lists the compositions of the shielding materials.

A7A.2 DISCUSSION AND SUMMARY OF RESULTS

The shielding evaluation presented in this section is performed utilizing as a design basis the source terms from the14x14 Westinghouse standard fuel assembly with fuel inserts. This fuel assembly is bounding because it contains the highest mass of fuel among the candidate fuel assemblies.

All shielding calculations are performed using the computer code MCNP (Reference 1) which uses a 3-dimensional Monte Carlo method. MCNP is a general-purpose Monte Carlo N-Particle code that can be used for neutron, photon, electron, or coupled neutron/photon/electron transport. The code treats an arbitrary three-dimensional configuration of materials in geometric cells bounded by first- and second-degree surfaces and some special fourth-degree surfaces. Point-wise (continuous energy) cross-section data are used. The MCNP code is selected because of its ability to handle thick, multi-layered shields as in the TN-40HT cask body using 3-D geometry.

For neutrons, all reactions given in a particular cross-section evaluation are accounted for in the cross section set. For photons, the code takes account of incoherent and coherent scattering, the possibility of fluorescent emission after photoelectric absorption, absorption in pair production with local emission of annihilation radiation, and bremsstrahlung. Important standard features that make MCNP very versatile and easy to use include a powerful general source; an extensive collection of cross-section data; and an extensive collection of variance reduction techniques that can be employed to track particles through very complex deep penetration problems. Mesh tallies capabilities were utilized in calculating dose rates distributed over and around the surface of the TN-40HT cask.

Normal and off-normal conditions are modeled with the TN-40HT cask intact. Average dose rates on the side, top and bottom of the TN-40HT cask are calculated. Maximum dose rates are also calculated above and below the radial neutron shield.

Accident conditions assume radially the neutron shield and steel outer shell are removed and axially the polypropylene disk and protective cover are removed. This evaluation bounds the accident conditions in Section A8.

The expected dose rates (for normal, off-normal, and accident conditions) from the TN-40HT cask are provided in Table A7A.2-1. The dose point locations are illustrated in Figure A7A.2-1.

The total (direct + skyshine) dose rates as a function of distance from the cask are presented in Table A7A.2-2.

The total ISFSI dose rate (from 64 casks all containing design basis fuel at the time of initial loading) as a function of distance from each location (N/S side, E/W side, or corner) is summarized in Table A7A.7-2.

.

A7A.3 METHODOLOGY

The methodology used in the shielding analysis of the TN-40HT cask is the 3-D MCNP code. MCNP allows for explicit 3-D modeling of any shielding configuration and reduces the number of approximations needed. The methodology used herein is summarized below.

1. Sources are developed for all fuel regions using the source term data from Section A7.2. Source regions include the active fuel region, bottom end fitting (including all materials below the active fuel region), plenum, and top end fitting (including all materials above the active fuel region).
2. Suitable shielding material densities are calculated for all regions modeled.
3. The 3-D Monte Carlo transport code MCNP is used to calculate dose rates on and around the TN-40HT cask.
4. For the cask, importance biasing is utilized for variance reduction for both the near and far field dose rate calculation. F4 type tallies are utilized for determining near field dose rates and far field dose rates.

A7A.4 MODEL SPECIFICATION

The neutron and gamma dose rates on the surface of the TN-40HT cask (Side, Top and Bottom surfaces) and at 1m and 2m from the side surface of the cask are evaluated with the 3-D Monte Carlo transport code MCNP (Reference 1). The flux-to-dose conversion factors specified by ANSI/ANS 6.1.1-1977 (Reference 2) are used and provided in Table A7A.4-1.

The cross-section data used is the continuous energy ENDF/B-VI provided with the MCNP code. The cross-section data allows coupled neutron/gamma-ray dose rate evaluation to be made to account for secondary gamma radiation (n,γ), if desired.

All of the near field dose rate calculations account for the dose rate due to secondary gamma radiation. For the far field (long distance) dose rate calculation, the dose rate contribution from the secondary gamma radiation is ignored because it is insignificant.

Figure A7A.4-1 is a plot of the TN-40HT cask MCNP model and shows the axial cross section of the cask. This shielding configuration is utilized to determine the radial (side surface) and axial (top and bottom surface) dose rates around the TN-40HT cask for normal, off-normal and accident conditions. This configuration is also utilized to determine the dose rates at long distances from the cask.

The following are key assumptions used in the development of the MCNP models:

- The condition of the cask during and after an accident assumes the side neutron shield and steel shell, the protective cover and the top neutron shield (polypropylene) are lost.
- The borated neutron absorber sheets in the TN-40HT basket are modeled as aluminum.
- Fuel is homogenized into 4 zones within the fuel assembly perimeter, although the TN-40HT basket is modeled explicitly.
- The basket is modeled as discrete stainless steel boxes surrounded by aluminum plates. The stainless steel support bars are conservatively neglected.
- The spatial distribution of the source is assumed to be uniform within each non-fuel hardware zone and within each axial burnup segment in the active fuel. Isotropic angular distribution is assumed for all sources.

A7A.4.1 MCNP MODEL FOR NORMAL AND OFF-NORMAL CONDITIONS

A single shielding configuration is utilized for the TN-40HT design for both normal and off-normal conditions of storage. The cask bottom dose rates are determined as a consequence of off-normal conditions since these become important only during loading and transfer. During normal conditions of storage the cask is upright and is firmly seated on the concrete pad. A three-dimensional MCNP model which includes a discrete fuel assembly model of the TN-40HT cask was developed for this purpose. In the MCNP model, the TN-40HT cask axis is modeled along the Z-direction. The X and Y axes in the MCNP model represent the cask in the radial direction. The cask is assumed to sit on a concrete pad (Z-direction).

The MCNP model for these shielding configurations is based on a discrete basket with the homogenized fuel assemblies (with an active height of 144 inches) positioned within fuel compartments. The MCNP model developed in this calculation is based on the design details from the TN-40HT cask drawings (within the limitations of the code geometry modeling options), shown in Section A1.5, except for some conservative representations. Table A7A.1-1 provides the cask material densities and thicknesses as designed and employed in the MCNP models. Figure A7A.1-1 is a sketch of the TN-40HT cask containing the modeled dimensions in the shielding evaluation models. Cells 2051 through 2133 represent the discrete basket and fuel assembly zones.

Figure A7A.4-1 is a Y-Z plot of the MCNP model of the TN-40HT cask (axial section view). All the major details of the cask model are shown in this figure. The fuel basket extends to 160″ in the axial direction from the bottom of the bottom fitting (-190.70 cm) to about 2” above the top of the fuel assembly (209.91 cm). The active fuel zone is 144″ long with the center at 0 (± 182.88 cm). A simple analog model is used for calculating the neutron dose. For the primary gamma dose rates, a multiple cell sub-layer model is used. The cask trunnions and the resin cutouts (flats) are modeled explicitly. The neutron resin boxes/radial neutron shield, top neutron shield and protective cover are also modeled explicitly.

The basket is modeled discretely using the advanced geometry features of MCNP. The fuel is modeled as a cuboid based on a 7.763″ square. The fuel compartment inside dimension is 8.05″ and is modeled with stainless steel with a thickness of 0.187″ surrounded by a 0.437″-thick basket aluminum plates. The Boral© (or any other poison material) plates were modeled as pure aluminum and the stainless steel strips (tie plates) were not modeled. The stainless steel and aluminum peripheral rails were modeled explicitly. A small air gap of 0.15″ (0.38 cm) was assumed between the basket and the cask shell. Figure A7A.4-2 is a radial cross section (X-Y plot) of the MCNP gamma model at Z=181 cm that shows the upper trunnions. Figure A7A.4-3 is also a radial cross section plot which shows one quarter of the basket and the rails.

Above the basket, the stainless steel fuel compartments and aluminum plates surrounding the fuel assembly are replaced by air (void).

The spatial distribution of the source is assumed to be uniform within each non-fuel hardware zone and within each axial burnup segment in the active fuel. Isotropic angular distribution is assumed for all sources.

Two MCNP models are developed for determining the normal and off-normal dose rates. The gamma model containing a detailed segmentation of the thicker cask steel body (for variance reduction purposes - implemented employing multiple cell sub-layers) is utilized to calculate the primary gamma dose rates. The neutron model is utilized to calculate the neutron and secondary gamma dose rates.

Tallies are based on the F4 type mesh tally feature of MCNP to provide the average flux in the defined volume. The radial tallies are located just off the cask surface, 1 m from cask outer surface and 2 m from cask outer surface. Similarly, axial tallies are located at the cask top (protective cover) and bottom which determine the average flux at the top and bottom surfaces, and 1m and 2m from the top surface.

A7A.4.2 MCNP MODEL FOR ACCIDENT CONDITIONS

The MCNP design basis model for accident conditions is almost identical to that of the normal (and off-normal) conditions except that all neutron shielding and the outer steel shell materials are replaced with void. This scenario is based on a cask drop accident that results in the complete removal of the neutron shielding materials including the polypropylene disk and the protective cover at the top. This is implemented in MCNP by replacing the appropriate materials in the MCNP models with void.

A7A.4.3 MCNP MODEL FOR LONG DISTANCES FROM THE CASK

The near field dose rate MCNP model described above is modified to determine the long distance dose rates. The near-field MCNP model is extended further to include additional volumetric detectors beyond the immediate vicinity of the cask and splitting cells are used to transport particles far from the cask (about 2000 m from the cask surface) to obtain dose rates at long distances. A schematic of the far field model is shown in Figure A7A.4-4. This modeling technique splits particles upwards and outwards to better simulate skyshine. At farther regions of the model, cones are used to split particles downward to the detector location.

The MCNP calculated dose rates at far distances consist of contributions from direct, air scatter (skyshine) and limited ground scatter (only in the immediate vicinity of the cask). Modifications (cell flagging) are also made to separate the direct and skyshine component. Any radiation that crosses an elevation of 20 feet (~1.5 meter above cask) is considered to be skyshine. This is a valid approximation for two main reasons. One, this height corresponds to the earth berm. Second, beyond this elevation it is highly probable the radiation will have to scatter back in order to reach far detectors.

Soil is modeled as the ground surface under and extending away from the cask. It is expected that the maximum contribution to the ground scatter component occurs at the immediate vicinity of the cask. A layer of soil more than 4 feet thick is adequate to account for “ground shine.” Actual soil depth modeled in MCNP models is about 6 feet. Axial splitting is not modeled in the soil.

The doses due to capture gamma sources are not calculated since they are insignificant at large distances in comparison to primary gamma and neutron sources.

The dose is calculated as F4 tallies (that calculate the volumetric dose rates) in an annular cylindrical detector, 20 cm thick and 3 feet high at about 6 feet off the ground. The dose rates are calculated at distances ranging from 10m to 2000m from the edge of the cask.

A7A.4.4 SHIELD REGIONAL DENSITIES

Table A7.2-4 shows the fuel assembly material composition for the four fuel assembly regions. Based on these material compositions and material densities, atom fractions for the fuel assembly regions are determined and provided in Table A7A.4-2. The mass of materials in each fuel assembly region is homogenized over the volume of the region (area = 60.26 in^2, based on a 7.763″ x 7.763″ cross-section). Table A7A.4-3 provide the shield regional densities for the TN-40HT cask. The actual fuel layout in the TN-40HT cask is an array of fuel assemblies inside stainless steel compartments surrounded by sheets of aluminum material.

The radial resin and aluminum boxes are discreetly modeled based on the material composition of the polyester resin and the aluminum.

A7A.5 NEAR FIELD DOSE RATE CALCULATIONS

Two basic three-dimensional MCNP models are employed for shielding analyses of the TN-40HT cask, one model for neutrons and the other for gammas. An additional two models are utilized for the accident configuration. The results of the near field dose rate calculations for normal and off-normal conditions are shown in Table A7A.5-1 and Table A7A.5-2. These results are also shown in Figure A7A.5-1 through Figure A7A.5-5. A sample MCNP input file listing is provided in Section A7B. Additional cask surface dose rate results above and below the neutron shield for normal and off-normal conditions are shown in Table A7A.5-3.

Figure A7A.2-1 shows the locations around the cask where the dose rates are calculated. As expected due to the reduced shielding, there is an increase in the dose rates at the surface above and below the neutron shield as shown in Table A7A.5-3 in comparison to the cask surface side dose rates shown in Table A7A.5-1.

For the TN-40HT cask an accident case is performed assuming the neutron shield and steel neutron shield jacket (outer skin) of each have been torn off and the top neutron shield and protective cover are gone. The results of the near field dose rate calculations for accident conditions are shown in Table A7A.5-4. These results are also shown in Figure A7A.5-6 through Figure A7A.5-9.

A7A.6 FAR FIELD DOSE RATE CALCULATIONS

MCNP models are developed to determine the far field dose rates as discussed above. The results of the far field dose rate calculations are shown in Table A7A.2-2 and Table A7A.6-1. These results are also shown in Figure A7A.6-1. The MCNP input file listing for neutron is shown in Section A7B.

A7A.7 OFFSITE DOSE RATE CALCULATIONS

This Section evaluates off-site dose rates assuming the original ISFSI consists of two (2) 2x12 array of TN-40HT casks, loaded in sets of four casks every two years, each loaded with design-basis fuel at the time of initial loading (i.e. total of 48 casks and credit for decay while the casks are on the ISFSI pads). This conservatively bounds the allowed storage on the original ISFSI of 48 casks and bounds operation with a mixture of TN-40 and TN-40HT casks. The ISFSI layout used in this evaluation is shown in Figure A7A.7-1. 60400000330

This Section also evaluates off-site dose rates assuming the southeast ISFSI pad consists of one (1) 2 x 8 array of TN-40HT casks, loaded in sets of four casks every two years, each loaded with design basis fuel at the time of initial loading (i.e., total of 16 casks and credit for decay while the casks are on the ISFSI pads). The southeast ISFSI pad location is conservatively modeled as being in the same location as the original ISFSI pad (although the southeast ISFSI pad actual location is farther from the location-specific dose points). This conservatively bounds the allowed storage on the southeast ISFSI pad of 16 casks and bounds operation with a mixture of TN-40 and TN-40HT casks. 60400000330

This evaluation determines the neutron and gamma-ray off-site dose rates including skyshine in the vicinity of the ISFSI. It provides results for distances ranging from 10 to 1,000 meters from the front, side and corner of the arrays. These results are used to determine the total normal operation radiation dose values at the nearest site boundary and at the nearest resident to show compliance with the requirements of 10 CFR 72.104(a), 40 CFR 190.10(a), and 10 CFR 20.1301(a). A co-ordinate transformation of these results is performed so that they may be reported as a distance from a common point, i.e., the center of the ISFSI. 60400000330

The Monte Carlo computer code MCNP (Reference 1) calculates the dose rates at the specified locations around the array of casks for the original ISFSI. An "MCNP Array" method is utilized to evaluate the dose rate as a function of distance from the original ISFSI. The MCNP results for the original ISFSI are scaled to determine the dose rate contribution from the southeast ISFSI. Direct scaling of the MCNP ISFSI dose versus distance information from the 48 cask ISFSI to obtain dose versus distance for the additional 16 cask (64 cask total) ISFSI is not accurate because the dose versus distance information takes credit for radiodecay due to scheduled ISFSI loading. Therefore, a decay factor is incorporated into the scaling factor used to determine the dose rate contribution from the southeast ISFSI in order to properly account for radiodecay and calculate accurate dose and dose rate values. 60400000330

60400000330

A7A.7.1 MCNP ARRAY AND SCALING METHOD – METHODOLOGY, MODEL AND ASSUMPTIONS

The ISFSI layout as illustrated in Figure A7A.7-1 is explicitly modeled in MCNP using advanced MCNP geometry. The gamma and neutron dose rates are determined as a function of distance from the ISFSI. All the doses are determined using F5 “detector” tallies.

The ISFSI array MCNP model consists of a two 2x12 arrays of TN40-HT casks. The cask array is modeled using advanced MCNP geometry to represent the ISFSI as shown in Figure A7A.7-1. Source specification is consistent with the loading “scheme” where four casks are loaded every two years. Due to the symmetry of the layout of the cask array and in the loading schedule, sources are only specified for the north-west row of casks (even-numbered casks 2 through 24 from Figure A7A.7-1). Even though, sources are not specified in the remaining 36 casks, the shielding configurations are identical and ensure that the resulting dose rate distribution around the ISFSI is symmetric. Tallies are constructed from small, spherical, F5 detectors providing for variance reduction capabilities. These detectors are positioned all around the ISFSI (all sides and corner locations) to determine the dose rates as a result of the source symmetry. These detector locations are shown in Table A7A.7-1.

Credit is taken for the ISFSI berm. The berm is modeled as an isosceles trapezoid with 14.02 and 2.44 meters bottom and top segments, respectively. The berm is assumed 6.25 meters height and made from soil. Based on the coordinate system depicted on Figure A7A.7-1 (the berm is not shown on the Figure), the planes of symmetry along the west and east sides of the berm are X=-114.30 and X=121.61 meters, respectively. Similarly, planes of symmetry along the north and south sides of the berm are at Y=-58.22 and Y=58.22 meters, respectively. -

Radiological sources from Bottom Nozzle, In-core, Plenum and Top Nozzle axial regions of the TN40 HT design basis fuel assembly are calculated for cooling times ranging from 18 to 40 years, with 2 years increments and shown in Table A7A.7-4. The SAS2H\ORIGEN-S models utilized in the design basis fuel source term calculations are also employed herein.

In order to simplify the source term specification in the MCNP models, the total gamma and neutron radiation source terms strength can be approximated with an exponential function as a function of decay time. The source strength at any cooling time is expressed as:

$$A_t = A_0 * e^{(-\lambda(t-18))}$$

where

A_t is the Source Strength at time t ($18 \le t \le 40$)

A_0 is the source strength at 18 years

λ is a decay constant

The decay constants are calculated based on the above equation using the source strengths obtained from the SAS2H calculations. Decay constants for calculating neutron, in-core gamma (active fuel region), and fittings (top and bottom nozzle and plenum regions) gamma radiation source terms strength are calculated to be equal to 0.0358 years^{-1} (corresponds to ~19.4 years half-life), 0.025 years^{-1} (corresponds to ~27.7 years half-life) and 0.1315 years^{-1} (corresponds to ~5.27 years half-life) respectively. These decay constants are calculated in such a way that exponential function produces source terms that match, within 1%, the source terms calculated using SAS2H\ORIGEN-S models.

For ease of input specification in the MCNP models, the total gamma source strength (4.8937e+18 gammas per second including contribution from BPRAs and TPDs.) is calculated utilizing the exponential functions. Spectrum due to the design basis fuel assembly is used to conservatively describe the spectral distribution of gamma radiation source terms in all the casks where source is specified.

For the neutron source specification, the total neutron source strength calculated directly (1.9253e+12 neutrons per second, including sub-critical multiplication and axial source profile) with the SAS2H\ORIGEN-S models are utilized. Spectral distribution of neutron radiation source terms is due to Cm-244. MCNP provides built-in parameters to describe this distribution in the calculational models.

The assumptions for the MCNP methodology are summarized below.

- Due to symmetry of the cask loading configurations, the source specification is simplified and considered only for 12 of the 48 casks while the detectors are positioned to obtain the results as a result of this simplified source specification.
- The "universe" is a sphere surrounding the ISFSI. The radius of this sphere (r=5.0 kilometers) is more than 20 mean free paths for neutrons and more than 20 mean free paths for gammas in energy groups that contribute the most to the gamma radiation dose rates. This ensures that the model is of a sufficient size to include all interactions affecting the dose rate at the detector locations.
- "Detectors" located at distances less than or equal to 45 meters are within the ISFSI berm perimeter. Dose rates points at larger distances are behind the berm. It is likely that the dose rates beyond the berm perimeter are almost entirely due to skyshine component.
- Dose rates include contribution due to primary gamma and neutron sources as well as due to the secondary gamma radiation from (n,g) interactions.

The dose rate contribution from the southeast ISFSI is determined by scaling the MCNP results for the original ISFSI, taking into account radiodecay due to the cask loading scheme of 4 loaded casks every 2 years. Since the source strength expression for the original ISFSI reduces the source strength as if all the different gammas and neutrons with their different half-lives and energies decay in unison at the specified rate, the dose rate is directly proportional to the gamma and neutron source strength and A_0 and A_t can be replaced by dose rates, D(0) and D(t). Given a gamma or neutron dose rate D(t) at a particular distance from the original ISFSI the contribution to the dose rate from any cask is determined by solving the following equation:

$$\begin{aligned} D(t)_{48} = {} & 4D(0) + 4D(0)e^{(-\lambda \times 2yr)} + 4D(0)e^{(-\lambda \times 4yr)} + 4D(0)e^{(-\lambda \times 6yr)} + 4D(0)e^{(-\lambda \times 8yr)} \\ & + 4D(0)e^{(-\lambda \times 10yr)} + 4D(0)e^{(-\lambda \times 12yr)} + 4D(0)e^{(-\lambda \times 14yr)} + 4D(0)e^{(-\lambda \times 16yr)} \\ & + 4D(0)e^{(-\lambda \times 18yr)} + 4D(0)e^{(-\lambda \times 20yr)} + 4D(0)e^{(-\lambda \times 22yr)} \end{aligned}$$

D(0) represents the dose rate for a cask with no radiodecay since the cask was placed on the ISFSI. The dose rate from any cask on the ISFSI is the product of D(0) and the exponent (which accounts for radiodecay for the specified number of years the cask has been on the ISFSI). The corresponding gamma or neutron dose rate from the southeast ISFSI is then calculated using the following equation:

$$D(t)_{16} = D(0) \times \left(4 + 4e^{(-\lambda \times 2yr)} + 4e^{(-\lambda \times 4yr)} + 4e^{(-\lambda \times 6yr)}\right)$$

Note that the gamma dose rate versus distance results for the original ISFSI include activation gammas; however, the activation gammas are treated as fission gammas in the above equations (i.e., only using a decay constant of 0.025 years-1). This is conservative since the effective half-life for the fission gammas (i.e., 27.7 years) is longer than that for the activation gammas (i.e., 5.27 years).

604000000330

A7A.7.2 MCNP ARRAY AND SCALING METHOD – DOSE RATE AS A FUNCTION OF DISTANCE 60400000330

The MCNP and scaling results provide the dose rate as a function of distance at all the locations (including sides and corner) around the ISFSI. The total and skyshine dose rate results for the N/S sides, E/W sides and the corners are shown in Table A7A.7-2. The skyshine doses are shown in Table A7A.7-3 only for comparison. Due to presence of the ISFSI berm, it is expected that the dose rates at distances greater than 100m are dominated by the skyshine component and these results serve to demonstrate this assertion. Co-ordinate transformation is performed such that the results reported in Table A7A.7-2 are based on the distance from the center of the ISFSI (with the southeast ISFSI pad modeled as being located at same location as the original ISFSI) .

The ISFSI dose rate as a function of distance results and the dose contribution due to other uranium fuel cycle operations conducted on the site are used to determine the total normal operation radiation dose values at the nearest site boundary and at the nearest resident to show compliance with the requirements of 10 CFR 72.104(a), 40 CFR 190.10(a), and 10 CFR 20.1301(a). The dose at the nearest site boundary due to other uranium fuel cycle operations is assumed to be negligible when compared to the radiation level associated with the ISFSI. The dose at the nearest resident due to other uranium fuel cycle operations is obtained from the 2017 Annual Radioactive Effluent Report. The dose at the nearest resident due to other uranium fuel cycle operations is 1.50E-02 mrem/yr.

Comparisons between normal operation radiation dose values and the dose limits of 10 CFR 72.104(a), 40 CFR 190.10(a), and 10 CFR 20.1301(a) are presented below: 60400000330

10 CFR 72.104(a) and), 40 CFR 190.10(a) Annual Dose (Nearest Resident)

Source	Total (mrem/yr)	Criteria (mrem/yr)	Margin (mrem/yr)
Original ISFSI (Fully Loaded)	4.34	25	20.66
Southeast ISFSI (16 Casks)			
Planned Discharges			

10 CFR 20.1301(a)(1) Annual Dose (Nearest Resident)

Source	Total (mrem/yr)	Criteria (mrem/yr)	Margin (mrem/yr)
Licensed Operation	4.34	100	95.66

10 CFR 20.1301(a)(2) Dose Rate (Site Boundary)

<table>
<tr><th>Source</th><th>Total (mrem/yr)</th><th>Criteria (mrem/yr)</th><th>Margin (mrem/yr)</th></tr>
<tr><td>Original ISFSI (Fully Loaded)</td><td rowspan="3">0.45</td><td rowspan="3">2</td><td rowspan="3">1.55</td></tr>
<tr><td>Southeast ISFSI (16 Casks)</td></tr>
<tr><td>Other Sources</td></tr>
</table>

604000000330

The calculated dose values at the nearest site boundary and at the nearest resident meet the acceptance criteria of 10 CFR 72.104(a), 40 CFR 190.10(a), and 10 CFR 20.1301(a). Note that this analysis does not establish any restrictions on cask placement. In other words, the analysis bounds any distribution of 64 TN-40HT (or TN-40) casks across the three ISFSI pads (e.g., 48 casks on the original ISFSI pads and 16 casks on the southeast pad, or 24 casks on the southeast pad and 40 casks on the original pads).

A7A.8 CONFINEMENT

A7A.8.1 CONTAINMENT BOUNDARY

The containment boundary consists of the inner shell and bottom plate, shell flange, lid outer plate, lid bolts, penetration cover plate and bolts and the inner portions of the lid seal and the two lid penetrations (vent and drain). The containment vessel prevents leakage of radioactive material from the cask cavity. It also maintains an inert atmosphere (helium) in the cask cavity. Helium assists in heat removal and provides a non-reactive environment to protect fuel assemblies against fuel cladding degradation.

A7A.8.2 SEALS AND WELDS

The containment boundary welds consist of the circumferential welds attaching the bottom closure and the top flange to the vessel shell. Also, the longitudinal weld(s) on the rolled plate, closing the cylindrical vessel shell, and the circumferential weld(s) attaching the rolled shells together are containment welds.

Double metal seals are utilized on the lid and the two lid penetrations. Helicoflex HND or equivalent seals may be used. The seals are shown in Figure A7A.8-1. The internal spring and lining maintain the necessary rigidity and sealing force, and provide some elastic recovery capability. The outer aluminum jacket provides a ductile material to seal against the sealing surfaces. The jacket also provides a connecting sheet between the inner outer seals.

Holes in this sheet allow for attachment screws and for communication between the overpressure system and the space between the seals. This sheet, which is about 0.020 in. thick, has insufficient strength to transmit radial forces great enough to overcome the axial compressive forces on the seals, which are over 1000 lb/in. of seal length. Additional information on the seals is provided in Section A3.3.2. The overpressure port seal is a single metal seal of the same design, Helicoflex HN200 or equivalent.

All TN-40HT surfaces which mate with the metal seals are stainless steel.

The use of a double seal system allows the TN-40HT cask to have a pressure monitoring of the interspace between the seals. This combined cover-seal pressure monitoring system always meets or exceeds the requirement of a double barrier closure which guarantees tight, permanent confinement. When the cask is placed in storage a pressure greater than the cavity pressure is set up in the gaps (interspace) between the double metal seals of the lid and the lid penetrations. A decrease in the pressure of the monitoring system would be signaled by a pressure transducer in the overpressure system.

The lid and penetration seals described above are contained in grooves. A high level of sealing over the storage period is assured by utilizing seals in a deformation-controlled design. The deformation of the seals is constant since bolt loads assure that the mating surfaces remain in contact. The seal deformation is set by the original diameter and the depth of the groove.

The nominal cross-section diameter of the lid seal is 0.26 in. and the nominal groove depth is 0.22 in. At 0.04 in. compression, the sealing force is 1,399 lb/inch (Reference 6). The total force of the double seal is 660,129 lb. The total minimum preload of the 48 lid bolts is 71,111 lb/bolt b, which is greater than the combined force of the seals and internal pressure, 23,175 lb/bolt (Appendix A4A.4).

The nominal cross-section diameter of the port seals is 0.161 in. and the nominal groove depth is 0.126 in. At .035 in. compression, the sealing force is 1,142 lb/inch. The total force of the double seal is 37,922 lb. The total minimum preload of the 8 cover bolts is 5,105 lb/bolt, which is greater than the combined force of the seals and internal pressure, 5,058 lb/bolt (Appendix A4A.5).

The maximum radial force on the seals is from the 5.5 atm abs overpressure system. This results in a force per unit seal length of about 15 lb./in., which is negligible compared to the compressive (axial) force of over 1000 lb/inch. Because the maximum pressure is between the two seals, the direction of this force is such that the seals are supported by the walls of the seal groove. However, the seals are designed to retain pressure in either direction.

Helicoflex metal seals are all capable of limiting leak rates to much less than 1×10^{-5} ref cm^3/s. After loading, all lid and cover seals are leak tested and the acceptable total cask leakage (both inner and outer seals combined) is 1×10^{-5} ref cm^3/s with a minimum test sensitivity of 5×10^{-6} atm-cc/sec.

A7A.8.3 CLOSURE

The containment vessel contains an integrally-welded bottom closure and a bolted and flanged top closure (lid). The lid plate is attached to the cask body with 48 bolts. The bolt torque required to seal the metal seals located in the lid and maintain confinement under normal and accident conditions is provided in Drawing TN40HT-72-1 in Section A1.5. The closure bolt analysis is presented in Section A4A.4.

The lid contains two penetrations which are sealed by flanged covers fastened to the lid by 8 bolts each. The bolt torque required to seal the metal seals in the penetration covers and maintain confinement under normal and accident conditions is provided in Drawing TN40HT-72-1 in Section A1.5. The penetration bolt analysis is presented in Section A4A.5.

A7A.8.4 MONITORING OF SYSTEM CONFINEMENT

An overpressure (OP) monitoring system is part of the TN-40HT design. The pressure in the monitoring system is greater than that of the cask cavity and ambient pressure. In this configuration, neither in-leakage of air nor out-leakage of cavity gas is possible.

If a leak existed in the seals, the design of the TN-40HT overpressure system is such that the leak will either be to the atmosphere or to the cask cavity. Leakage from the cask cavity past the higher pressure of the OP system is physically impossible.

The seals are collectively leak tested to 1 x 10^{-5} ref cm^3/s. Using the methodology of ANSI N14.5 (Reference 7), an equivalent maximum hole size is estimated based upon test conditions of equivalent air leaking from 1 atm abs to 0.01 atm abs in ambient temperature conditions (77 °F or 25 °C) and the maximum acceptable leak of 1 x 10^{-5} ref cm^3/s. The leakage hole length is assumed to be the same as the metal seal width, 0.5 cm. The equivalent maximum hole size is calculated below.

$$L_u = (F_c + F_m)(P_u - P_d)(P_a/P_u) \text{ cc/sec at } T_u, P_u$$

Other definitions:

L_u	= upstream volumetric leakage rate, cc/sec = 1 x 10^{-5} ref cm^3/s (Test Leak Rate)
F_c	= coefficient of continuum flow conductance per unit pressure, cc/atm-sec
F_m	= coefficient of free molecular flow conductance per unit pressure, cc/atm-sec
P_u	= fluid upstream pressure, atm abs = 1.0 atm abs
P_d	= fluid downstream pressure, atm abs = 0.01 atm abs
D	= leakage hole diameter, cm
a	= leakage hole length, cm = 0.5 cm (assuming leak path length is on the order of the metal seal width)
μ	= fluid viscosity, cP = 0.0185 cP (from ANSI N14.5, Table B.1)
T	= fluid absolute temperature, K = 298 K
M	= molecular weight, g/mol = 29.0 g/mol (from ANSI N14.5, Table B.1)
P_a	= average stream pressure = ½ ($P_u + P_d$), atm abs = 0.505 atm abs

$$L_u = (F_c + F_m)(P_u - P_d)(P_a/P_u) \text{ cc/sec}$$

where:

$$F_c = (2.49\text{x}10^6 \times D^4)/(a\mu) \text{ cc/atm-sec}$$
$$F_m = \{3.81\text{x}10^3 \times D^3 \times (T/M)^{0.5}\} / (aP_a) \text{ cc/atm-sec}$$

Substituting:

$F_c = (2.49x10^6 \times D^4)/(0.5 \times 0.0185) = 2.69 \times 10^8 D^4$
$F_m = \{3.81x10^3 \times D^3 \times (298/29.0)^{0.5}\} / \{0.5 \times 0.505) = 4.84 \times 10^4 D^3$

$L_u = (F_c + F_m)(P_u - P_d)(P_a/P_u)$ cc/sec
$1 \times 10^{-5} = (F_c + F_m)(1.0 - 0.01)(0.505 / 1.0)$
$F_c + F_m = 2 \times 10^{-5}$

Solving the simultaneous equations, the equivalent hole diameter, D, is 4.825×10^{-4} cm.

During operations, the OP system is initially back filled with 5.5 atm abs (66.2 psig) of helium at standard temperature.

The temperature of the helium in the OP tank at equilibrium is assumed to be 160 °F (71 °C)[1]. The pressure in the OP system at this temperature will be 6.349 atm abs (79 psig). Assuming the OP system is leaking to the atmosphere, the leak rate is defined using the equations of ANSI N14.5 (Reference 7):

$L_{u,He} = (F_c + F_m)(P_u - P_d)(P_a/P_u)$ cc/sec
$F_c = (2.49x10^6 \times D^4)/(a\mu)$ cc/atm-sec
$F_m = \{3.81x10^3 \times D^3 \times (T/M)^{0.5}\} / (aP_a)$ cc/atm-sec

Where:

$L_{u,He}$	= helium volumetric leakage rate
P_u	= 6.349 atm abs
P_d	= 1.0 atm abs
D	= 4.825×10^{-4} cm
a	= 0.5 cm
μ	= 0.0219 cP (for helium at 344 K)
T	= 344°K
M	= 4.0 g/mol
P_a	= ½ ($P_u + P_d$) = 3.674 atm abs

Substituting:

$F_c = \{2.49 \times 10^6 \times (4.825 \times 10^{-4})^4\}/(0.5 \times 0.0219) = 1.234 \times 10^{-5}$
$F_m = \{3.81 \times 10^3 \times (4.825 \times 10^{-4})^3 \times (344/4)^{0.5}\} / (0.5 \times 3.674) = 2.160 \times 10^{-6}$

$L_{u,He} = (F_c + F_m)(P_u - P_d)(P_a/P_u)$
$L_{u,He} = (1.234 \times 10^{-5} + 2.160 \times 10^{-6})(6.349 - 1.0)(3.674/6.349)$
$L_{u,He} = 4.489 \times 10^{-5}$ cc/sec of helium

[1] The assumed OP gas temperature is the average of the OP Tank and lid seal(s) temperatures.

Over the first year, the maximum volume leaked from the OP system is:

$V = 4.489 \times 10^{-5}$ cc/sec $\times$ (365 days/year $\times$ 24 hrs/day $\times$ 3600 sec/hr) = 1416 cc at T_u, P_u

The OP system tank consists of a 6 in. diameter schedule 80 pipe (27 in. long) and two 6 in. diameter schedule 80 end caps. The volume of the tank is 835 in^3. The volume of the OP system is increased to 900 in^3 (14,748 cc) to include the OP system tubing and the space between the metallic seals in the lid and penetrations. Correspondingly, the pressure is reduced by the following in the first year:

$$P_{OP\ released} = P_{OP\ Sys,\ Initial} \times \{V_{released} / V_{OP\ Sys}\}$$
$$P_{OP\ released} = 6.349\ \text{atm}\ (1416\text{cc} / 14748\text{cc}) = 0.609\ \text{atm}$$

The overpressure system pressure is also corrected for the corresponding drop in temperature over the first year. At the start of the second year, the overpressure system pressure is:

$$P_{OP\ start\ of\ second\ year} = (6.349\ \text{atm} - 0.609\ \text{atm})^{*}\ (339.6°\text{K}/344°\text{K}) = 5.666\ \text{atm abs}$$

These calculations are repeated every year for the 25 year period. Figure A7A.8-2 illustrates the pressure drop from the OP system to the atmosphere. Figure A7A.8-2 also illustrates the pressure drop in the cask cavity due to fuel cooling.

If a leak is to the cask cavity rather than the atmosphere, the pressure drop in the OP system is calculated using a downstream pressure the minimum cavity pressure of 1.37 atm abs (5.43 psig). Figure A7A.8-2 also illustrates the results of this analysis. In this scenario, the corresponding increase in the cask cavity pressure is negligible.

As shown above, the monitoring system pressure is greater than the cask cavity or atmospheric pressure assuming a leak based on the conservative initial acceptance test leak rate of 1×10^{-5} ref cm^3/s. Typically, Helicoflex metal seals result in joints with much lower leak rates than the acceptance criteria. Therefore, no leakage will occur from the cask cavity during the 25 year period.

The pressure in the overpressure system will be monitored over the lifetime of the cask. To allow time to diagnose and correct any problems, the OP monitoring system is set to alarm if the overpressure system drops below 2.89 atm abs (27.8 psig). This set point is based on the maximum off-normal cask cavity pressure (32.2 psia from Table A3.3-16) plus 0.7 atm for margin. It ensures that pressure decreases in the overpressure monitoring system are identified well before any potential out leakage from the cask cavity occurs. If needed during or after the 25 year period, the monitoring system is capable of being repressurized.

A7A.8.5 CONFINEMENT REQUIREMENTS FOR NORMAL CONDITIONS OF STORAGE

The TN-40HT dry storage cask is designed to provide storage of spent fuel. Since the containment vessel consists of a steel cylinder with an integrally-welded bottom closure, the cavity gas can escape only through the lid closure system. In order to ensure no release of radioactivity material, two systems are employed. First, all bolted closures are provided with double seals. Second, the interspace between the seals is pressurized to provide a positive pressure gradient. If the inner seals were to leak, helium would flow into the cask cavity and radioactive material would not be released. If the outer seals were to leak, helium would leak from the overpressure system to the exterior, and no radioactive material would be released.

The cask loadings for normal conditions of storage are given in Section A3.2.5. It is shown that the seals are not disturbed by any of the loadings and thus, the cask confinement is maintained.

A7A.8.6 CONFINEMENT REQUIREMENTS FOR HYPOTHETICAL ACCIDENT CONDITIONS

A7A.8.6.1 SOURCE TERMS FOR CONFINEMENT CALCULATIONS

Table A7.2-6 lists the activity representing the fission gases, volatiles, and fines contributing more than 0.1% of the activity contained in a design basis fuel, plus Iodine 129.

The releasable source term is first determined. The release fractions (References 8 and 9) applied to the source term are provided below.

Variable	Off-Normal Conditions	Accident Conditions
Fraction of crud that spalls off rods, f_C	0.15	1.0
Fraction of Rods that develop cladding breaches, f_B	0.10	1.0
Fraction of Gases that are released due to a cladding breach, f_G	0.3	0.3
Fraction of Fines that are released due to a cladding breach, f_F	3×10^{-6}*	3×10^{-6}*
Fraction of Volatiles that are released due to a cladding breach, f_V	2×10^{-4}	2×10^{-4}

* Per NUREG-1617, 3×10^{-5} of the fines are released during a cladding breach. Per SAND90-2406, (Reference 10), page IV-7, of the 3×10^{-5} of the fines released recommends that only 10% of the fuel fines ejected remain airborne.

The releasable source term also depends on the leak rate from the TN-40HT. Under off-normal conditions, it is assumed that the OP system is not functioning properly. In this case, the cask cavity gas is assumed to leak out at a rate of 1 x 10^{-5} std cc /sec. Assuming the cask cavity gas acts like helium (including the gases, volatiles, fines and crud), the leak rate is adjusted to a helium leak rate at cask cavity conditions using the equations of ANSI N14.5 (Reference 7). This calculation is shown below.

P_u = 2.42 atm abs , 20.9 psig (off-normal cask cavity pressure assuming 10% of the fuel rods have failed – Selected to be conservatively higher than value in Table A3.3-16)
P_d = 1.0 atm abs
D = 4.825 x 10^{-4} cm
a = 0.5 cm
μ = 0.0283 cP (for helium at 500K)
T = fluid absolute temp = average cavity gas temp = 456 °F = 508 K
M = 4.0
P_a = ½ (P_u + P_d) = 1.708 atm abs

Substituting:

F_c = 9.530E-06
F_m = 5.645E-06
$L_{u,he}$ = 1.518E-05 cc/sec of helium for off-normal conditions

Similarly, under hypothetical accident conditions, it is assumed that the OP system has stopped functioning and fire conditions exist.

P_u = 6.34 atm abs, 78.5 psig (cask cavity pressure following hypothetical fire and assuming 100% fuel rod failure – Selected to be conservatively higher than value in Table A3.3-16)
P_d = 1.0 atm abs
D = 4.825 x 10^{-4} cm a = 0.5 cm
μ = 0.0292 cP (for helium at 575 K)
T = fluid absolute temp = average cavity gas temp following fire = 592 °F = 584 K
M = 4.0
P_a = ½ (P_u + P_d) = 3.67 atm abs

Substituting in to the equations of ANSI N14.5:

F_c = 9.236E-06
F_m = 2.816E-06
$L_{u,he}$ = 3.725E-05 cc/sec of helium for hypothetical accident conditions.

The releasable contents from the TN-40HT during off-normal and hypothetical accident conditions are provided in Tables A7A.8-1 and A7A.8-2, respectively

A7A.8.6.2 RELEASE OF CONTENTS

Two scenarios are considered:

- Off-Normal Conditions – This condition exists over a 45 day period, seals are leaking at the test leak rate of 1 x 10^{-5} ref cm^3/s and the fraction of rods that have failed is 10%. Stability category D and a 5 m/s wind speed are used for this analysis. This scenario assumes one cask is in off-normal condition at the ISFSI. The 45 day exposure duration will serve as the bases for the allowed completion times for the Cask Interseal Pressure Technical Specification.

- Hypothetical Accident Conditions – This condition exists over a 30 day period, seals are leaking at the test leak rate of 1 x 10^{-5} ref cm^3/sec, the fraction of rods that have failed is 100%, and the temperature inside the cask is comparable to the fire accident conditions. Stability category F and 1 m/s wind speed is used for this analysis. This scenario assumes one cask is in the hypothetical accident condition at the ISFSI.

In the first scenario, the release is assumed to occur for more than a 20 minute period. The methodology of Reg Guide 1.145 (Reference 11) is applied. The atmospheric diffusion from a ground level point source at 110 meters is based on the following parameters.

Wind speed = 5 meter/second
σ_y = 9 meters (Reference 11, Figure 1)
σ_z = 5 meters (Reference 11, Figure 2)
M = 1.1, (Reference 11, Figure 3]
$\Sigma_y = M\sigma_y$ = 9.9 meters
A = cross sectional area of the TN-40HT = $9.1m^2$

Using the methodology of Reg Guide 1.145, $\{\chi/Q\}_{110\ meters}$ during off-normal conditions is 1.29E-03 sec/m^3. Similarly, the atmospheric diffusion for 700 meters which corresponds to the distance from the ISFSI to the nearest residence (700 meters is a conservative value, 724 meters is the distance from the center of the ISFSI to the nearest resident), during off-normal conditions is calculated using the following parameters.

Wind speed = 5 meter/second
σ_y = 50 meters
σ_z = 25 meters
M = 1.1
$\Sigma_y = M\sigma_y$ = 55 meters

During off normal conditions $\{\chi/Q\}_{700\ meters}$ is 4.63E-05 sec/m^3.

In the second scenario the release is assumed to be a short term ground level release (occurring, however, over a 30 day period) assuming the methodology of Regulatory Guide 1.25 (Reference 12). The atmospheric stability classification of F and a wind speed of 1 m/sec are used. The atmospheric diffusion from a ground level point source at 110 and 724 meters is taken from Table 8.2-1 and Table 2.3-2 to be:

$\chi/Q_{110\ meters}$ = 6.63E-03 sec/m^3 and

$\chi/Q_{0.45 miles}$ = 2.66E-04 sec/m^3

(nearest resident is 0.45 miles, about 724 meters from center of ISFSI)

A7A.8.6.2.1 DOSE CALCULATIONS

Dose components are calculated following the method of Regulatory Guide 1.109 (Reference 13) and utilizing dose conversion factors from EPA Federal Guidance Reports Numbers 11 and 12 (References 14 and 15). (Note: Two sets of dose conversion factors (DCFs) depending upon the chemical state of Sr-90 are reported in Federal Guidance Report Number 11. One set of DCF values is for Sr in the form of $SrTiO_3$ and the other set is for Sr in all other forms. The Sr-90 fission product should not form $SrTiO_3$ within the storage cask and therefore the DCF for this compound was not used.)

To determine the committed doses (from air inhalation), the following equation is used:

$$Dose_{inhalation} = R \times \chi/Q \times Q \times DCF_{inhalation} \times Time$$

Where:

R = Inhalation Rate = 8,000 m^3/year = 2.54E-04 m^3/sec (References 8 and13)

χ/Q = Short term average centerline value of atmospheric diffusion for a ground level release (sec/m^3)

Q = amount of material released (μCi/sec)

$DCF_{inhalation}$ = Exposure Dose Conversion Factor (mrem/μCi), from (Reference 14).

Time = Time of Exposure (Seconds)

To determine the deep doses (from air immersion), the following equation is used:

$$Dose_{air\ immersion} = \{\chi/Q \times Q \times DCF_{air\ immersion}\} \times Time$$

Where:

χ / Q = Short term average centerline value of atmospheric diffusion for a ground level release (sec/m^3)

Q = amount of material released (μCi/sec)

$DCF_{immersion}$ = Exposure Dose Conversion Factor (mrem/year per μCi/cm^3), (Reference 15)

Time = Time of Exposure (Seconds)

For off-normal conditions, the estimated 45 day airborne doses (internal and external) at 110 meters from a single TN-40HT cask are provided in Table A7A.8-3 and Table A7A.8-4. The sum of the deep dose (external) and the committed dose (internal) on an organ basis and total effective dose for distances of 110, and 700 meters are summarized below:

Target	Dose at 110 meters (mrem)	Dose at 700 meters (mrem)
Gonad	4.69E-02	1.69E-03
Breast	1.48E-02	5.34E-04
Lung	3.85E-01	1.39E-02
Red Marrow	3.32E-01	1.20E-02
Bone Surface	**2.90E+00**	**1.04E-01**
Thyroid	1.43E-02	5.15E-04
Remainder	1.26E-01	4.52E-03
Effective	**2.95E-01**	**1.06E-02**
Skin	1.73E-03	6.24E-05

The values presented in bold print above demonstrate that the criteria of 10CFR-72.104 are met under off-normal conditions.

For hypothetical accident conditions, the committed doses (internal) and the deep doses (external) at 110 meters from a single TN-40HT cask for a 30 day exposure are provided in Table A7A.8-5 and Table A7A.8-6. The total effective dose equivalent at 110 m and at 724 m from the TN-40HT cask is summarized in the table below.

Target	Dose at 110 meters (mrem/yr)	Dose at 724 meters (mrem/yr)
Gonad	3.88E+00	1.56E-01
Breast	9.79E-01	3.93E-02
Lung	2.75E+01	1.10E+00
Red Marrow	2.78E+01	1.11E+00
Bone Surface	2.44E+02	9.79E+00
Thyroid	9.66E-01	3.88E-02
Remainder	1.01E+01	4.04E-01
Effective (TEDE)	2.40E+01	9.63E-01
Skin	1.38E-01	5.54E-03
Lens Dose (Skin + TEDE)	2.41E+01	9.68E-01

The maximum 30-day TEDE value is 0.024 rem. The corresponding 10CFR 72.106 limit is 5 rem.

The maximum 30-day Lens Dose Equivalent value is 0.0241 rem. The corresponding 10CFR 72.106 limit is 15 rem.

The maximum 30-day dose to any organ/tissue is 0.244 rem and it occurs at the bone surface. The corresponding 10CFR 72.106 limit is 50 rem.

Therefore all the criteria of 72.106 are met at 110 m.

A summary of the doses at 110 m and their corresponding regulatory limits is shown below.

Off-Normal Conditions		
Organ	**10CFR72.104(a) Limit (mrem)**	**110 meter Dose (mrem)**
Whole Body (TEDE)	25	0.30
Thyroid	75	0.01
Other Critical Organ	25	2.90 (Bone Surface)
Accident Conditions		
Organ	**10CFR72.106(b) Limit (mrem)**	**110 meter Dose (mrem)**
Whole Body (TEDE)	5000	24.0
Organ (TODE)	50000	244 (Bone Surface)
Lens of Eye (LDE)	15000	24.1
Skin (SDE)	50000	0.14

A7A.8.6.3 LATENT SEAL FAILURE

By design the overpressure monitoring system does not immediately alarm if there is a leak in a seal or the overpressure system. The time period from when a leak begins to occur and when the overpressure system alarm is activated is dependent on the size of the leak. Two conditions which could exist within the TN-40HT confinement system are:

(1) The outer seal (or the overpressure system) is leaking to the atmosphere. In this case the inner seal is intact and there is no release of the contents of the cask cavity to the atmosphere.

(2) The inner seal is leaking (or the overpressure system is leaking into the cask cavity). In this case the outer seal is still intact and there is no release of the cask cavity contents to the atmosphere.

If a latent seal leak has occurred, the tables below provide some examples of the time to alarm based on assumed leakage rates.

Case 1 - Leakage of Overpressure System to the Atmosphere		
Leak Rate (ref cm^3/s)	**Estimated Time to Alarm (from Start of Latent Seal Failure)**	**Estimated Time to Loss of OP System Pressure (from Start of Latent Seal Failure)**
1×10^{-3}	19 days	34 days
1×10^{-4}	195 days	358 days
5×10^{-4}	1.2 year	6 years
1×10^{-5} (see Figure A7A.8-2)	9.5 years	over 40 years

Case 2 – Leakage of Overpressure System to Cask Cavity		
Leak Rate (ref cm^3/s)	**Estimated Time to Alarm (from Start of Latent Seal Failure)**	**Estimated Time to Equalize OP System Pressure with Cask Cavity Pressure (from Start of Latent Seal Failure)**
1×10^{-3}	19 days	28 days
1×10^{-4}	201 days	288 days
5×10^{-4}	1.4 years	13 years
1×10^{-5} (see Figure A7A.8-2)	9.5 years	over 40 years

As shown in the tables above, the alarm is set such that for any credible leak, there is time to evaluate the leaking condition and correct the condition provided that the overpressure system remains pressurized. This period can be extended by re-pressurizing the overpressure tank.

Another condition which has been considered is that a latent seal failure has occurred and the overpressure system is removed due to an accident.

(1) If the outer seal has the latent failure and the OP system is removed then there is no release of cask cavity contents to the atmosphere.

(2) If the inner seal has a latent failure and the OP system is removed then the table below provides the time before 10 CFR 72.106(b) limits will be exceeded.

Standard Leak Rate (ref cm^3/sec)	Time to exceed 10 CFR 72.106(b) Limits
1×10^{-3}	59 days
1×10^{-4}	602 days
5×10^{-5}	1213 days
1×10^{5}	6145 days

The times above demonstrate that a latent failure up to 100 times greater than the test value could occur and still allow recovery.

The time to reach the accident release limits is dependent on the size of the leak. Due to the reliability of the metal seals used in static applications, it is not considered credible that the inner seals could leak at a rate significantly higher than the test leak rate. The probability that a gross leak of an inner seal in combination with a gross leak in an outer seal or the overpressure system, such that the overpressure system could not hold pressure, is not considered a credible event.

A7A.9 REFERENCES

1. "MCNP/MCNPX – Monte Carlo N-Particle Transport Code System Including MCNP5 1.40 and MCNPX 2.5.0 and Data Libraries," CCC-730, Oak Ridge National Laboratory, RSICC Computer Code Collection, January 2006.

2. ANSI/ANS 6.1-1-1977, "Neutron and Gamma Ray Flux-to-Dose Rate Factors."

3. Title 10 Code of Federal Regulations Part 72, "Licensing Requirements for the Independent Storage of Spent Nuclear Fuel and High-Level Radioactive Waste."

4. Title 10 Code of Federal Regulations Part 20, "Standards for Protection Against Radiation."

5. Title 40 Code of Federal Regulations Part 190, "Environmental Radiation Protection Standards for Nuclear Power Operations."

6. Helicoflex Catalogue ET 507 E5930.

7. ANSI N14.5-1997, "Leakage Tests on Packages for Shipment," February 1998.

8. USNRC, Spent Fuel Project Office, Interim Staff Guidance No. 5, Revision 1.

9. NUREG-1617, "Standard Review Plan for Transportation Packages for Spent Nuclear Fuel, Draft Report for Comment," US Nuclear Regulatory Commission, March 1998.

10. SAND90-2406, "A Method for Determining the Spent Fuel Contribution to Transport Cask Containment Requirements," Sandia National Laboratories, November 1992.

11. USNRC Regulatory Guide 1.145,"Atmospheric Dispersion Models for Potential Accident Consequence Assessment at Nuclear Power Plants," Rev 1, 1983.

12. USNRC Regulatory Guide 1.25, "Assumptions Used for Evaluating the Potential Radiological Consequences of a Fuel Handling Accident in the Fuel Handling Storage Facility for Boiling and Pressurized Water Reactors."

13. USNRC Regulatory Guide 1.109, "Calculation of Annual Doses to Men from Routing Releases of Reactor Effluent for the Purpose of Evaluating Compliance with 10CFR50, Appendix I," Rev 1, 1977.

14. USEPA Federal Guidance Report No 11, "Limiting Values of Radionuclide Intake and Air Concentration and Dose Conversion Factors for Inhalation, Submersion and Ingestion," EPA-520/1-88-0202, September 1988.

15. USEPA Federal Guidance Report No 12, "External Exposure to Radionuclides in Air, Water, and Soil," EPA-402-R-93-081, September, 1983.

TABLE A7A.1-1
TN-40HT CASK SHIELD MATERIALS

Component	Material	Density (g/cm^3)	Thickness (inches)
Cask Body Wall	Carbon Steel	7.82	8.75
Lid	Carbon Steel	7.82	10.00
Bottom	Carbon Steel	7.82	8.75
Resin (1)	Polyester Resin Styrene Aluminum Hydrate Zinc Borate	1.58	5.00
Aluminum Box	Aluminum	2.7	0.12
Outer Shell	Carbon Steel	7.82	0.50
Basket (2)	Stainless Steel (Inserts)	7.94	0.19
	Stainless Steel (Strips)	7.94	0.44
	Aluminum Neutron Poison Material (3)	2.7	0.44
Protective Cover	Carbon Steel	7.82	0.38
Polypropylene Disc	Polypropylene	0.90	4.00

Notes:

(1) The neutron shielding is borated polyester resin compound with a density of 1.58 g/cc. The four major constituents are listed in the table.

(2) The stainless steel inserts of the basket are 0.19 inches thick. The intermittent stainless steel strips are not modeled.

(3) The neutron poison material is modeled as aluminum for shielding purposes.

TABLE A7A.2-1
SUMMARY OF AVERAGE DOSE RATES

	Average Dose Rates (mrem/hr) for Normal and Off-Normal Conditions							
	Side Above Shield[1]	Side Along Shield[5]	Side Below Shield[2]	Top Surface[3] (Protective Cover)	Side Surface[7]	Bottom Surface[4]	1 Meter from Side	2 Meter from Side
Gamma	61.3	32.7	52.9	18.5	35.5	272	12.8	7.61
Neutron	146	28.2	706	7.6	78.7	1515	18.9	10.6
Total	208	60.9	759	26.1	114	1790	31.7	18.2

	Average Dose Rates (mrem/hr) for Accident Conditions[6]							
				Top Surface[8] (Protective Cover)	Side Surface[7]	Bottom Surface	1 Meter from Side	2 Meter from Side
Gamma	-	-	-	63.4	116	-	50.6	31.0
Neutron	-	-	-	135	1980	-	785	444
Total	-	-	-	198	2095	-	835	475

Notes:

(1) Maximum surface dose rates above the neutron shield are 81.5 mrem/hr gamma and 189 mrem/hr neutron.

(2) Maximum surface dose rates below the neutron shield are 86.5 mrem/hr gamma and 928 mrem/hr neutron.

(3) Maximum surface dose rates on the protective cover are 45.5 mrem/hr gamma and 12.7 mrem/hr neutron.

(4) Maximum surface dose rates on the cask bottom are 804 mrem/hr gamma and 3980 mrem/hr neutron.

(5) Maximum surface dose rates on the cask side are 39.3 mrem/hr gamma and 34.8 mrem/hr neutron

(6) The radial neutron shield and outer shell are removed from the sides. The polypropylene disk and protective cover are removed from the top.

(7) Includes surfaces above and below the radial neutron shield.

(8) Top surface dose rate is on the Top Surface of the Cask Lid

Note: Maximum gamma and neutron dose rates may not occur at the same location.

TABLE A7A.2-2
DOSE RATES AT A DISTANCE FROM ONE TN-40HT CASK

Total Dose Rate Results

Distance (meter)	Gamma (mrem/hr)	Error	Neutron (mrem/hr)	Error
10	1.02E+00	0.0048	2.01E+00	0.0047
20	2.68E-01	0.0064	5.43E-01	0.0056
25	1.69E-01	0.0050	3.51E-01	0.0058
30	1.16E-01	0.0051	2.44E-01	0.0061
40	6.30E-02	0.0054	1.35E-01	0.0065
50	3.86E-02	0.0056	8.35E-02	0.0069
75	1.53E-02	0.0062	3.35E-02	0.0081
100	7.59E-03	0.0069	1.67E-02	0.0090
150	2.62E-03	0.0076	5.50E-03	0.0112
175	1.68E-03	0.0081	3.48E-03	0.0141
250	5.35E-04	0.0086	1.00E-03	0.0155
300	2.74E-04	0.0097	4.94E-04	0.0161
350	1.52E-04	0.0123	2.52E-04	0.0193
400	8.37E-05	0.0133	1.36E-04	0.0226
500	2.89E-05	0.0147	4.44E-05	0.0247
600	1.07E-05	0.0161	1.52E-05	0.0253
800	1.76E-06	0.0220	2.30E-06	0.0296
1,100	1.52E-07	0.0427	1.77E-07	0.0348
1,500	7.30E-09	0.1118	8.75E-09	0.0267
2,000	2.76E-10	0.2795	3.10E-10	0.0239

TABLE A7A.4-1
ANSI STANDARD-6.1.1-1977 FLUX-TO-DOSE FACTORS

Photon energy (MeV)	Response Function (rem/hr)/(γ/cm^2-s)	Neutron energy (MeV)	Response Function (rem/hr)/(n/cm^2-s)
0.01	3.96E-06	2.5E-08	3.67E-06
0.03	5.82E-07	1.0E-07	3.67E-06
0.05	2.90E-07	1.0E-06	4.46E-06
0.07	2.58E-07	1.0E-05	4.54E-06
0.10	2.83E-07	1.0E-04	4.18E-06
0.15	3.79E-07	1.0E-03	3.76E-06
0.20	5.01E-07	1.0E-02	3.56E-06
0.25	6.31E-07	1.0E-01	2.17E-05
0.30	7.59E-07	5.0E-01	9.26E-05
0.35	8.78E-07	1.0	1.32E-04
0.40	9.85E-07	2.5	1.25E-04
0.45	1.08E-06	5.0	1.56E-04
0.50	1.17E-06	7.0	1.47E-04
0.55	1.27E-06	10.0	1.47E-04
0.60	1.36E-06	14.0	2.08E-04
0.65	1.44E-06	20.0	2.27E-04
0.70	1.52E-06		
0.80	1.68E-06		
1.0	1.98E-06		
1.4	2.51E-06		
1.8	2.99E-06		
2.2	3.42E-06		
2.6	3.82E-06		
2.8	4.01E-06		
3.25	4.41E-06		
3.75	4.83E-06		
4.25	5.23E-06		
4.75	5.60E-06		
5.0	5.80E-06		
5.25	6.01E-06		
5.75	6.37E-06		
6.25	6.74E-06		
6.75	7.11E-06		
7.5	7.66E-06		
9.0	8.77E-06		
11.0	1.03E-05		
13.0	1.18E-05		
15.0	1.33E-05		

TABLE A7A.4-2
ATOMIC FRACTIONS FOR THE HOMOGENIZED DESIGN BASIS 14X14 FUEL

Nuclide ID	Element	Atomic Fraction
Active Fuel Region, Density = 3.949 g/cm^3		
8016	Oxygen	0.5453
92235	Uranium	0.0094
92238	Uranium	0.2631
40000	Zirconium	0.1420
24000	Chromium	0.0072
26000	Iron	0.0165
28000	Nickel	0.0125
Bottom Nozzle Region, Density = 2.595 g/cm^3		
14000	Silicon	0.0194
24000	Chromium	0.1995
25055	Manganese	0.0199
26000	Iron	0.6684
28000	Nickel	0.0884
Plenum Region, Density = 1.543 g/cm^3		
40000	Zirconium	0.2640
14000	Silicon	0.0164
24000	Chromium	0.1436
25055	Manganese	0.0131
26000	Iron	0.4465
28000	Nickel	0.1084
Top Nozzle Region, Density = 1.970 g/cm^3		
14000	Silicon	0.0216
24000	Chromium	0.1966
25055	Manganese	0.0184
26000	Iron	0.6245
28000	Nickel	0.1326

TABLE A7A.4-3
SHIELD REGIONAL DENSITIES FOR TN-40HT MCNP MODEL
(PAGE 1 OF 2)

			Carbon Steel(1)		**Stainless Steel 304(1)**		**Air(2)**		**Aluminum(1)**	
gram density (g/cc)			7.8212		7.94		1.23E-03		2.702	
atom density (atom/barn-cm)			0.08742		0.08759		0.00051		0.06031	
Element	Z	M	wt. %	at. %	wt. %	at. %	wt. %	at. %	wt. %	at. %
H	1	1.0								
C	6	12.0	1	4.486	0.08	0.364	0.014	0.017		
N	7	14.0					75.52	79.44		
O	8	16.0					23.18	21.08		
Al	13	27.0							100	100
Si	14	28.1			1	1.944				
P	15	31.0			0.045	0.079				
Ar	18	39.9					1.29	0.47		
Cr	24	52.0			19	19.949				
Ti	22	47.9								
Mn	25	54.9			2	1.987				
Fe	26	55.8	99	95.514	68.375	66.841				
Ni	28	58.7			9.5	8.836				
Zr	40	91.2								
Sn	50	118.7								
Hf	72	178.5								
		Total	100	100	100	100	100	100	100	100

Notes:

(1) – SCALE Standard Material Composition

(2) - ANSI/ANS-6.6.1, Dry Air

TABLE A7A.4-3
SHIELD REGIONAL DENSITIES FOR TN-40HT MCNP MODEL
(Page 2 of 2)

			Concrete(1)		Polyester Resin		Polypropylene(2)		Soil(3)	
gram density (g/cc)			2.32		1.58		0.9		1.625	
atom density (atom/barn-cm)			0.074447		0.106815		0.115918		0.068588	
Element	Z	M	wt. %	at. %	wt. %	at. %	wt. %	at. %	wt. %	at. %
H	1	1.0	0.56	10.427	5.05	44.631	14.37	66.667	2.10	29.73
C	6	12.0			35.13	26.054	85.63	33.333	1.60	1.90
Na	11	23.0	1.71	1.396						
O	8	16.0	49.83	58.449	41.73	23.234			57.70	51.46
Mg	12	24.3	0.24	0.185						
Al	13	27.0	4.56	3.172	14.93	4.929			5.00	2.64
Si	14	28.1	31.58	21.102					27.10	12.06
S	16	32.1	0.12	0.070						
K	19	39.1	1.92	0.922					1.30	0.47
Ca	20	40.1	8.26	3.868					4.10	1.46
Fe	26	55.8	1.22	0.410					1.10	0.28
B	5	10.8			1.05	0.865				
Zn	30	65.4			2.11	0.288				
		Total	100	100	100	100	100	100	100	100

Notes:

(1) - ANSI/ANS-6.4.3
(2) - Chemistry & Physics Handbook
(3) - Jacob, Radiation Protection Dosimetry 14, 299, 1986

TABLE A7A.5-1
TN-40HT NEAR FIELD DOSE RATES – NORMAL AND OFF-NORMAL CONDITIONS

Axial Location (cm)	Cask Side Surface (mrem/hr)		
	gamma	neutron	total
-205.3	19.4	484	503
-189.8	86.5	928	1014
-176.0	55.9	116	172
-164.0	72.1	43.2	115
-143.1	29.7	31.5	61.2
-113.3	33.5	34.1	67.6
-83.6	34.6	34.8	69.5
-53.8	35.6	31.0	66.6
-24.0	32.6	28.5	61.1
5.8	31.3	27.2	58.4
35.6	39.3	29.1	68.4
65.4	33.8	25.8	59.6
95.1	31.0	23.6	54.6
124.9	25.4	16.7	42.1
148.8	23.7	13.3	36.9
166.3	17.5	25.0	42.4
183.8	19.9	25.4	45.3
201.3	22.1	17.6	39.7
216.5	81.5	189	271
231.5	41.1	104	145
Average	**35.5**	**78.7**	**114**

Radial Location (cm)	Protective Cover (mrem/hr)			Top Neutron Shield (mrem/hr)			Cask Bottom (mrem/hr)		
	g	n	total	g	n	total	g	n	total
5.7	45.3	2.16	47.5	76.8	9.07	85.9	770	3979	4749
17.1	45.5	2.97	48.5	81.5	6.17	87.7	797	3905	4702
28.5	43.3	2.87	46.2	81.7	5.08	86.8	804	3670	4474
39.9	41.0	2.04	43.1	79.0	4.84	83.8	781	3446	4227
51.3	38.0	2.25	40.3	76.5	5.83	82.3	784	3119	3903
62.7	31.5	2.12	33.6	66.2	5.35	71.6	713	2686	3399
74.1	25.2	2.82	28.1	50.2	5.02	55.2	530	2261	2791
85.5	18.8	5.22	24.0	31.2	7.48	38.7	272	1724	1996
96.9	13.4	9.80	23.2	19.0	38.9	57.9	95.8	1104	1200
108.3	9.8	12.7	22.5	11.3	41.9	53.1	30.5	545	575
Average	**18.5**	**7.6**	**26.1**	**31.7**	**24.1**	**55.7**	**272**	**1515**	**1790**

TABLE A7A.5-2
TN-40HT NEAR FIELD DOSE RATES – NORMAL AND OFF-NORMAL CONDITIONS

Axial Location (cm)	1 M from cask side surface (mrem/hr)				2 M from cask side surface (mrem/hr)			
	gamma	neutron	total	error*	gamma	neutron	total	error*
-200.3	12.1	52.6	64.7	0.012	6.52	18.6	25.1	0.013
-175.0	12.6	46.8	59.4	0.012	7.30	18.8	26.1	0.013
-149.6	13.0	34.5	47.5	0.012	7.64	17.2	24.8	0.013
-124.3	13.7	26.6	40.3	0.014	7.98	15.7	23.6	0.013
-98.9	14.7	22.3	37.0	0.014	8.53	14.2	22.8	0.013
-73.6	15.4	19.1	34.4	0.013	8.87	12.8	21.7	0.013
-48.2	15.7	17.1	32.8	0.014	9.06	11.3	20.4	0.013
-22.9	15.7	16.4	32.2	0.014	9.17	11.0	20.2	0.014
2.5	15.7	14.6	30.3	0.014	9.16	10.0	19.2	0.013
27.8	15.7	13.7	29.4	0.015	9.15	9.2	18.4	0.014
53.2	15.2	12.4	27.6	0.014	8.92	8.8	17.7	0.014
78.5	14.4	11.5	25.9	0.018	8.53	8.3	16.8	0.014
103.9	13.3	11.8	25.1	0.024	7.98	8.1	16.1	0.015
129.2	11.9	10.4	22.3	0.016	7.59	7.7	15.3	0.015
154.6	10.8	9.6	20.4	0.016	7.00	7.4	14.4	0.015
179.9	10.1	10.3	20.4	0.016	6.54	6.9	13.4	0.015
205.3	9.9	11.8	21.8	0.016	6.18	7.0	13.2	0.016
230.6	10.1	12.9	23.0	0.020	5.83	6.8	12.6	0.017
256.0	8.9	12.4	21.3	0.017	5.43	6.6	12.0	0.021
281.3	6.5	12.0	18.5	0.020	4.84	6.4	11.2	0.018
Average	**12.8**	**18.9**	**31.7**		**7.61**	**10.6**	**18.3**	

Radial Location (cm)	1 M from Protective Cover (mrem/hr)				2 M from Protective Cover (mrem/hr)			
	gamma	neutron	total	error*	gamma	neutron	total	error*
5.7	17.9	1.91	19.8	0.046	8.99	0.52	9.51	0.060
17.1	17.4	1.87	19.2	0.030	8.59	1.40	10.0	0.050
28.5	17.2	1.37	18.6	0.024	8.69	1.19	9.88	0.038
39.9	16.4	1.57	18.0	0.022	8.34	1.28	9.61	0.032
51.3	15.0	1.94	17.0	0.022	7.90	1.34	9.24	0.029
62.7	13.6	1.45	15.0	0.019	7.34	1.59	8.93	0.033
74.1	12.6	2.27	14.9	0.022	7.07	1.20	8.27	0.028
85.5	10.9	2.71	13.6	0.022	6.44	1.60	8.04	0.028
96.9	9.5	3.36	12.9	0.025	6.00	1.78	7.78	0.028
108.3	8.4	3.34	11.7	0.025	5.77	1.98	7.75	0.030
Average	**10.7**	**2.79**	**13.5**		**6.44**	**1.67**	**8.11**	

* - fractional standard deviation

TABLE A7A.5-3
TN-40HT NEAR FIELD DOSE RATES – NORMAL AND OFF-NORMAL CONDITIONS
(DOSE RATES ABOVE AND BELOW THE RADIAL NEUTRON SHIELD)

Axial Location (cm)	Surface Dose (mrem/hr)				
	gamma	neutron	total	error*	
216.5	81.5	189	271	0.014	above N shield
231.5	41.1	104	145	0.017	
-205.3	19.4	484	503	0.018	below N shield
-189.8	86.5	928	1014	0.012	

* - fractional standard deviation

TABLE A7A.5-4
TN-40HT NEAR FIELD DOSE RATES – ACCIDENT CONDITIONS
(PAGE 1 OF 2)

Axial Location (cm)	Cask Surface (mrem/hr)			1 M from Cask Surface (mrem/hr)			2 M from Cask Surface (mrem/hr)		
	g	n	total	g	n	total	g	n	total
-200.3	36.4	650	687	33.9	642	676	21.6	384	406
-175.0	125	1396	1522	45.0	743	788	26.5	433	459
-149.6	137	2243	2381	54.7	863	917	30.5	479	509
-124.3	150	2919	3069	60.9	975	1036	34.1	522	556
-98.9	152	3276	3428	64.1	1077	1141	36.5	551	588
-73.6	152	3404	3556	65.6	1137	1202	38.2	573	611
-48.2	150	3347	3497	66.0	1178	1244	39.5	594	633
-22.9	135	3236	3372	65.8	1193	1259	40.4	597	637
2.5	110	3219	3319	66.7	1182	1249	40.4	590	630
27.8	188	3403	3592	67.3	1143	1210	40.2	581	621
53.2	162	3295	3457	67.0	1073	1140	39.0	552	591
78.5	146	2933	3079	64.7	974	1039	37.3	516	553
103.9	141	2417	2558	60.0	854	914	35.5	476	512
129.2	120	1741	1861	53.6	718	771	32.3	428	460
154.6	89.3	1062	1151	47.3	581	628	28.9	378	407
179.9	101	553	655	40.4	450	490	25.2	329	355
205.3	114	254	367	33.4	340	374	21.9	283	305
230.6	48.6	109	158	25.2	248	274	18.0	242	260
256.0	33.5	60.5	93.9	17.9	183	201	14.7	203	217
281.3	18.4	61.7	80.1	12.4	139	152	11.7	167	179
Average	116	1980	2095	50.6	785	835	30.6	444	475

TABLE A7A.5-4
TN-40HT NEAR FIELD DOSE RATES – ACCIDENT CONDITIONS
(PAGE 2 OF 2)

Radial Location (cm)	Lid Surface[1] (mrem/hr)			1 M from Lid (mrem/hr)			2 M from Lid (mrem/hr)		
	g	n	total	g	n	total	g	n	total
5.7	179	334	513	89.8	82.2	172	44.0	27.9	71.9
17.1	175	318	493	89.3	82.8	172	42.7	36.1	78.8
28.5	172	305	477	88.0	85.3	173	41.4	33.9	75.3
39.9	173	287	461	79.9	77.0	157	39.8	30.2	70.0
51.3	168	260	428	74.3	79.2	153	37.7	32.9	70.7
62.7	155	228	383	65.1	70.8	136	35.0	30.8	65.8
74.1	112	200	312	55.9	64.4	120	32.3	32.5	64.8
85.5	57.6	155	212	46.6	59.1	106	29.4	31.4	60.8
96.9	18.9	94.4	113	37.5	54.0	91.5	26.3	31.2	57.6
108.3	24.3	59.9	84.7	29.8	51.6	81.5	22.9	28.2	51.2
Average	63.4	135	198	44.9	59.0	104	28.4	30.6	59.1

Notes:

1. - Lid surface dose same as in normal conditions

TABLE A7A.6-1
TN-40HT - SINGLE CASK FARFIELD DOSE RATES

Skyshine Dose Rate Results						Direct Dose Rate Results		
Distance (meter)	**Gamma (mrem/hr)**	**Error***	**Neutron (mrem/hr)**	**Error***		**Distance (meter)**	**Gamma (mrem/yr)**	**Neutron (mrem/yr)**
10	1.17E-02	0.0072	1.29E-01	0.0052		10	1.01E+00	1.88E+00
20	9.35E-03	0.0057	9.30E-02	0.0041		20	2.59E-01	4.50E-01
25	8.36E-03	0.0054	7.91E-02	0.0041		25	1.61E-01	2.72E-01
30	7.52E-03	0.0055	6.73E-02	0.0040		30	1.09E-01	1.77E-01
40	6.09E-03	0.0053	4.89E-02	0.0040		40	5.69E-02	8.61E-02
50	4.99E-03	0.0052	3.68E-02	0.0053		50	3.36E-02	4.68E-02
75	3.19E-03	0.0057	1.93E-02	0.0079		75	1.21E-02	1.42E-02
100	2.10E-03	0.0058	1.10E-02	0.0085		100	5.49E-03	5.72E-03
150	1.02E-03	0.0065	4.19E-03	0.0110		150	1.61E-03	1.32E-03
175	7.19E-04	0.0073	2.79E-03	0.0150		175	9.56E-04	6.89E-04
250	2.80E-04	0.0081	8.68E-04	0.0154		250	2.55E-04	1.33E-04
300	1.57E-04	0.0102	4.38E-04	0.0148		300	1.17E-04	5.58E-05
350	9.40E-05	0.0137	2.29E-04	0.0181		350	5.84E-05	2.21E-05
400	5.39E-05	0.0147	1.27E-04	0.0217		400	2.98E-05	9.47E-06
500	1.99E-05	0.0117	4.20E-05	0.0220		500	8.98E-06	2.41E-06
600	7.72E-06	0.0129	1.42E-05	0.0230		600	2.97E-06	1.02E-06
800	1.35E-06	0.0130	2.19E-06	0.0261		800	4.07E-07	1.13E-07
1,100	1.20E-07	0.0191	1.73E-07	0.0331		1,100	3.14E-08	3.88E-09
1,500	5.91E-09	0.0408	8.72E-09	0.0266		1,500	1.39E-09	2.21E-11
2,000	1.91E-10	0.1226	3.1E-10	0.0234		2,000	8.52E-11	1.93E-12

- \- fractional standard deviation

TABLE A7A.7-1
TN-40HT ISFSI DETECTOR LOCATIONS FOR SITE DOSE EVALUATION

Distance (meters)	"North Detectors": Distance is measured from (X,Y)=(-548.64, 676.91) cm. "X" is constant. Tally F5.		"South Detectors": Distance is measured from (X,Y)=(-548.64, -128.27) cm. "X" is constant. Tally F15.		"West Detectors": Distance is measured from (X,Y)=(-7595.87, 274.32) cm. "Y" is constant. Tally F25.		"East Detectors": Distance is measured from (X,Y)=(6498.59, 274.32) cm. "Y" is constant. Tally F35.	
	Point Detector #	"Y" Coordinate, (meters)	Point Detector #	"Y" Coordinate, (meters)	Point Detector #	"X" Coordinate, (meters)	Point Detector #	"X" Coordinate, (meters)
0	1	6.77	14	-1.28	27	-75.96	40	64.99
10	2	16.77	15	-11.28	28	-85.96	41	74.99
45	3	51.77	16	-46.28	29	-120.96	42	109.99
100	4	106.77	17	-101.28	30	-175.96	43	164.99
200	5	206.77	18	-201.28	31	-275.96	44	264.99
300	6	306.77	19	-301.28	32	-375.96	45	364.99
400	7	406.77	20	-401.28	33	-475.96	46	464.99
500	8	506.77	21	-501.28	34	-575.96	47	564.99
600	9	606.77	22	-601.28	35	-675.96	48	664.99
700	10	706.77	23	-701.28	36	-775.96	49	764.99
800	11	806.77	24	-801.28	37	-875.96	50	864.99
900	12	906.77	25	-901.28	38	-975.96	51	964.99
1000	13	1006.77	26	-1001.28	39	-1075.96	52	1064.99

Distance (meters)	"North-West Detectors": Distance is measured from (X,Y)=(-7558.30, 639.34) cm. "X" is constant. Tally F45.			"North-East Detectors": Distance is measured from (X,Y)=(6461.02, 639.34) cm. "Y" is as in Tally F45. Tally F55.		"South-West Detectors": Distance is measured from (X,Y)=(-7558.30, -90.70) cm. "X" is constant. Tally F65.			"North-East Detectors": Distance is measured from (X,Y)=(6461.02, -90.70) cm. "Y" is as in Tally F65. Tally	
	Point Detector #	"X" Coord, (meters)	"Y" Coord, (meters)	Point Detector #	"X" Coord, (meters)	Point Detector #	"X" Coord, (meters)	"Y" Coord, (meters)	Point Detector #	"X" Coord, (meters)
10	53	-82.65	13.46	65	71.68	77	-82.65	-7.98	89	71.68
45	54	-107.40	38.21	66	96.43	78	-107.40	-32.73	90	96.43
100	55	-146.29	77.10	67	135.32	79	-146.29	-71.62	91	135.32
200	56	-217.00	147.81	68	206.03	80	-217.00	-142.33	92	206.03
300	57	-287.72	218.53	69	276.74	81	-287.72	-213.04	93	276.74
400	58	-358.43	289.24	70	347.45	82	-358.43	-283.75	94	347.45
500	59	-429.14	359.95	71	418.16	83	-429.14	-354.46	95	418.16
600	60	-499.85	430.66	72	488.87	84	-499.85	-425.17	96	488.87
700	61	-570.56	501.37	73	559.59	85	-570.56	-495.88	97	559.59
800	62	-641.27	572.08	74	630.30	86	-641.27	-566.59	98	630.30
900	63	-711.98	642.79	75	701.01	87	-711.98	-637.30	99	701.01
1000	64	-782.69	713.50	76	771.72	88	-782.69	-708.01	100	771.72

TABLE A7A.7-2
DOSE RATES AS A FUNCTION OF DISTANCE FROM THE ISFSI
(PAGE 1 OF 2)

From the ISFSI "North\South" Faces

Distance from the ISFSI Face (meters)	Distance from the ISFSI Center (meters)	Gamma Radiation Dose Rate (mrem/hr)	Neutron Radiation (mrem/hr)	Dose Rate, (mrem/hr)
0	4.03	7.84E+00	9.52E+00	1.74E+01
10	14.03	5.27E+00	6.83E+00	1.21E+01
45	49.03	1.60E+00	2.21E+00	3.80E+00
100	104.03	1.13E-01	3.32E-01	4.45E-01
200	204.03	2.79E-02	6.39E-02	9.18E-02
300	304.03	8.44E-03	1.63E-02	2.48E-02
400	404.03	2.83E-03	4.73E-03	7.56E-03
500	504.03	1.07E-03	1.52E-03	2.59E-03
600	604.03	4.44E-04	5.81E-04	1.03E-03
700	704.03	2.00E-04	2.18E-04	4.18E-04
800	804.03	9.83E-05	8.29E-05	1.81E-04
900	904.03	4.89E-05	4.14E-05	9.03E-04
1000	1004.03	2.47E-05	1.42E-05	3.89E-05

60400000330

From the ISFSI "East\West" Faces

Distance from the ISFSI Face (meters)	Distance from the ISFSI Center (meters)	Gamma Radiation Dose Rate (mrem/hr)	Neutron Radiation (mrem/hr)	Dose Rate, (mrem/hr)
0	70.47	4.85E+01	4.17E+01	9.02E+01
10	80.47	4.00E+00	6.43E+00	1.04E+01
45	115.47	9.20E-02	4.00E-01	4.91E-01
100	170.47	4.54E-02	1.52E-01	1.97E-01
200	270.47	1.12E-02	2.95E-02	4.07E-02
300	370.47	3.48E-03	7.63E-03	1.11E-02
400	470.47	1.20E-03	2.65E-03	3.84E-03
500	570.47	4.64E-04	8.11E-04	1.27E-03
600	670.47	2.21E-04	3.19E-04	5.41E-04
700	770.47	8.94E-05	1.15E-04	2.04E-04
800	870.47	4.15E-05	5.81E-05	9.96E-05
900	970.47	2.17E-05	2.22E-05	4.39E-05
1000	1070.47	1.20E-05	1.10E-05	2.30E-05

60400000330

TABLE A7A.7-2
DOSE RATES AS A FUNCTION OF DISTANCE FROM THE ISFSI
(PAGE 2 OF 2)

From ISFSI Corners

Distance from the ISFSI Face (meters)	Distance from the ISFSI Center (meters)	Gamma Radiation Dose Rate (mrem/hr)	Neutron Radiation (mrem/hr)	Dose Rate, (mrem/hr)
10	77.91	5.24E+00	7.12E+00	1.24E-01
45	107.91	7.15E-01	1.13E+00	1.84E+00
100	159.24	5.87E-02	1.76E+01	2.35E-01
200	256.49	1.61E-02	3.61E-02	5.22E-02
300	355.27	5.14E-03	9.67E-03	1.48E-02
400	454.58	1.96E-03	2.82E-03	4.78E-03
500	554.14	7.49E-04	1.03E-03	1.78E-03
600	653.84	3.18E-04	3.78E-04	6.96E-04
700	753.61	1.44E-04	1.49E-04	2.93E-04
800	853.44	7.30E-05	5.21E-05	1.25E-04
900	953.31	3.76E-05	2.55E-05	6.31E-05
1000	1053.20	2.09E-05	1.07E-05	3.16E-05

60400000330

TABLE A7A.7-3
SKYSHINE DOSE RATES AS A FUNCTION OF DISTANCE FROM THE ISFSI
(PAGE 1 OF 2)

From the ISFSI "North\South" Faces

Distance from the ISFSI Face (meters)	Distance from the ISFSI Center (meters)	Gamma Radiation Dose Rate (mrem/hr)	Neutron Radiation (mrem/hr)	Dose Rate, (mrem/hr)
0	4.03	6.80E+00	9.52E+00	1.63E+01
10	14.03	4.58E+00	6.82E+00	1.14E+01
45	49.03	1.38E+00	2.21E+00	3.59E+00
100	104.03	1.04E-01	3.32E-01	4.36E-01
200	204.03	2.59E-02	6.39E-02	8.98E-02
300	304.03	7.89E-03	1.63E-02	2.42E-02
400	404.03	2.65E-03	4.73E-03	7.37E-03
500	504.03	9.92E-04	1.52E-03	2.51E-03
600	604.03	4.11E-04	5.81E-04	9.92E-04
700	704.03	1.82E-04	2.18E-04	4.00E-04
800	804.03	8.92E-05	8.29E-05	1.72E-04
900	904.03	4.42E-05	4.14E-05	8.55E-05
1000	1004.03	2.19E-05	1.42E-05	3.61E-05

604000000330

From the ISFSI "East\West" Faces

Distance from the ISFSI Face (meters)	Distance from the ISFSI Center (meters)	Gamma Radiation Dose Rate (mrem/hr)	Neutron Radiation (mrem/hr)	Dose Rate, (mrem/hr)
0	4.03	4.14E+01	4.15E+01	8.29E+01
10	14.03	3.45E+00	6.43+00	9.88E+00
45	49.03	8.06E-02	4.00E-01	4.80E-01
100	104.03	4.11E-02	1.52E-01	1.93E-01
200	204.03	1.02E-02	2.95E-02	3.97E-02
300	304.03	3.17E-03	7.63E-03	1.08E-02
400	404.03	1.08E-03	2.65E-03	3.73E-03
500	504.03	4.18E-04	8.11E-04	1.23E-03
600	604.03	1.99E-04	3.19E-04	5.18E-04
700	704.03	7.85E-05	1.15E-04	1.93E-04
800	804.03	3.56E-05	5.81E-05	9.37E-05
900	904.03	1.84E-05	2.22E-05	4.06E-05
1000	1004.03	9.87E-06	1.10E-05	2.09E-05

604000000330

TABLE A7A.7-3
SKYSHINE DOSE RATES AS A FUNCTION OF DISTANCE FROM THE ISFSI
(PAGE 2 OF 2)

From ISFSI Corners

Distance from the ISFSI Face (meters)	Distance from the ISFSI Center (meters)	Gamma Radiation Dose Rate (mrem/hr)	Neutron Radiation (mrem/hr)	Dose Rate, (mrem/hr)
10	77.91	4.51E+00	7.10E+00	1.16E+01
45	107.91	6.17E-01	1.13E+00	1.75E+00
100	159.24	5.38E-02	1.76E-01	2.30E-01
200	256.49	1.50E-02	3.61E-02	5.11E-02
300	355.27	4.81E-03	9.67E-03	1.45E-02
400	454.58	1.84E-03	2.82E-03	4.66E-03
500	554.14	6.95E-04	1.03E-03	1.73E-03
600	653.84	2.93E-04	3.78E-04	6.71E-04
700	753.61	1.31E-04	1.49E-04	2.80E-04
800	853.44	6.59E-05	5.21E-05	1.18E-04
900	953.31	3.35E-05	2.55E-05	5.90E-05
1000	1053.20	1.86E-05	1.07E-05	2.93E-05

604000000330

TABLE A7A.7-4
SAS2H SOURCE TERMS AS A FUNCTION OF COOLING TIME

Decay Time	Source Strength (particles/sec)				
(years)	Bottom Nozzle	In-Core	Plenum	Top Nozzle	Neutron
18	2.235E+12	3.303E+15	2.870E+12	1.314E+12	7.59E+08
20	1.718E+12	3.142E+15	2.206E+12	1.010E+12	7.05E+08
22	1.321E+12	2.989E+15	1.696E+12	7.763E+11	6.54E+08
24	1.015E+12	2.843E+15	1.304E+12	5.967E+11	6.08E+08
26	7.805E+11	2.704E+15	1.002E+12	4.587E+11	5.65E+08
28	6.000E+11	2.573E+15	7.705E+11	3.527E+11	5.25E+08
30	4.613E+11	2.447E+15	5.923E+11	2.711E+11	4.88E+08
32	3.546E+11	2.328E+15	4.553E+11	2.084E+11	4.54E+08
34	2.726E+11	2.214E+15	3.500E+11	1.602E+11	4.22E+08
36	2.095E+11	2.106E+15	2.691E+11	1.232E+11	3.93E+08
38	1.611E+11	2.004E+15	2.068E+11	9.468E+10	3.65E+08
40	1.238E+11	1.906E+15	1.590E+11	7.278E+10	3.40E+08

TABLE A7A.8-1
TN-40HT RELEASABLE SOURCE TERM FOR OFF-NORMAL CONDITIONS – DESIGN BASIS 14X14 FUEL

Isotope	Activity (Ci/assembly)	Release Fraction	Concentration in Void Space of TN-40HT[1] (Ci/cm^3)	Material Released[2] Q (μCi/sec)
H 3	1.78E+02	0.30	3.80E-05	5.76E-04
Co60[(3)]	6.73E+00	1.50E-01	7.18E-06	1.09E-04
Pu238	3.02E+03	3.00E-06	6.44E-09	9.78E-08
Pu239	1.35E+02	3.00E-06	2.88E-10	4.37E-09
Pu240	2.67E+02	3.00E-06	5.70E-10	8.65E-09
Pu241	3.19E+04	3.00E-06	6.81E-08	1.03E-06
Am241	1.50E+03	3.00E-06	3.20E-09	4.86E-08
Am243	4.17E+01	3.00E-06	8.90E-11	1.35E-09
Cm244	5.28E+03	3.00E-06	1.13E-08	1.71E-07
Kr 85	1.78E+03	0.30	3.80E-04	5.77E-03
Sr 90	3.11E+04	2.00E-04	4.42E-06	6.72E-05
Y 90	3.11E+04	3.00E-06	6.64E-08	1.01E-06
I129	2.40E-02	0.30	5.12E-09	7.77E-08
Cs134	4.01E+02	2.00E-04	5.70E-08	8.66E-07
Cs137	5.27E+04	2.00E-04	7.50E-06	1.14E-04
Ba137m	4.97E+04	3.00E-06	1.06E-07	1.61E-06
Pm147	6.53E+02	3.00E-06	1.39E-09	2.12E-08
Eu154	1.33E+03	3.00E-06	2.84E-09	4.31E-08
Np239	4.17E+01	3.00E-06	8.90E-11	1.35E-09

1. Values are based on 10% failure of the fuel rods and cask free volume of 5.63 m^3.

2. Values are based on 1.518E-05 cm^3/sec helium leak from containment.

3. The Co-60 source is calculated using the methodology of Reference (Reference 8). It is based on a 14x14 PWR fuel assembly with surface area of 1300 cm^2/rod and a crud surface concentration of 140μCi /cm^2 (per Table 7.1 of Reference 8) at the time of discharge. (The value listed above includes a minimum cooling time of twelve years.)

Table A7A.8-2
TN-40HT RELEASABLE SOURCE TERM FOR ACCIDENT CONDITIONS – DESIGN BASIS 14X14 FUEL

Isotope	Activity (Ci/assembly)	Release Fraction	Concentration in Void Space of TN-40HT(1) (Ci/cm^3)	Material Released(2) Q (μCi/sec)
H3	1.78E+02	0.30	3.80E-04	1.41E-02
Co60(3)	6.73+00	1.00E-00	4.79E-05	1.78E-03
Pu238	3.02E+03	3.00E-06	6.44E-08	2.40E-06
Pu239	1.35E+02	3.00E-06	2.88E-09	1.07E-07
Pu240	2.67E+02	3.00E-06	5.70E-09	2.12E-07
Pu241	3.19E+04	3.00E-06	6.81E-07	2.54E-05
Am241	1.50E+03	3.00E-06	3.20E-08	1.19E-06
Am243	4.17E+01	3.00E-06	8.90E-10	3.31E-08
Cm244	5.28E+03	3.00E-06	1.13E-07	4.20E-06
Kr85	1.78E+03	0.30	3.80E-03	1.41E-01
Sr90	3.11E+04	2.00E-04	4.42E-05	1.65E-03
Y90	3.11E+04	3.00E-06	6.64E-07	2.47E-05
I129	2.40E-02	0.30	5.12E-08	1.91E-06
Cs134	4.01E+02	2.00E-04	5.70E-07	2.12E-05
Cs137	5.27E+04	2.00E-04	7.50E-05	2.79E-03
Ba137m	4.97E+04	3.00E-06	1.06E-06	3.95E-05
Pm147	6.53E+02	3.00E-06	1.39E-08	5.19E-07
Eu154	1.33E+03	3.00E-06	2.84E-08	1.06E-06
Np239	4.17E+01	3.00E-06	8.90E-10	3.31E-08

1. Values are based on 100% failure of the fuel rods and cask free volume of 5.63 m^3.

2. Values are based on 3.72E-05 cm^3/sec helium leak from containment.

3. The Co-60 source is calculated using the methodology of Reference (Reference 8). It is based on a 14x14 PWR fuel assembly with surface area of 1300 cm^2/rod and a crud surface concentration of 140 μCi / cm^2 at the time of discharge. (The value listed above includes a minimum cooling time of twelve years.)

TABLE A7A.8-3
OFF-SITE AIRBORNE DOSES FROM OFF-NORMAL CONDITIONS AT 110 M (INTERNAL + EXTERNAL)

Design Basis 14x14 Fuel, Committed Doses (Internal) + Deep Dose (External)
mrem for 45 days

Isotope	Gonad	Breast	Lung	R. Marrow	B. Surface	Thyroid	Remainder	Effective	Skin
H3	4.68E-05	4.68E-05	4.69E-05	4.68E-05	4.68E-05	4.68E-05	4.68E-05	4.68E-05	0.00E+00
Co60	2.69E-03	9.71E-03	1.77E-01	9.06E-03	7.28E-03	8.56E-03	1.87E-02	3.05E-02	2.93E-04
Pu238	1.29E-02	4.60E-07	1.47E-01	6.99E-02	8.73E-01	4.42E-07	3.23E-02	4.87E-02	7.40E-11
Pu239	6.53E-04	1.89E-08	6.64E-03	3.47E-03	4.34E-02	1.86E-08	1.55E-03	2.38E-03	1.51E-12
Pu240	1.29E-03	3.87E-08	1.31E-02	6.87E-03	8.58E-02	3.68E-08	3.07E-03	4.71E-03	6.27E-12
Pu241	3.31E-03	1.49E-07	1.54E-02	1.63E-02	2.04E-01	6.02E-08	6.36E-03	1.08E-02	2.24E-12
Am241	7.42E-03	6.11E-07	4.20E-03	3.97E-02	4.95E-01	3.66E-07	1.79E-02	2.74E-02	1.15E-09
Am243	2.07E-04	9.65E-08	1.13E-04	1.10E-03	1.38E-02	5.27E-08	4.91E-04	7.55E-04	6.87E-11
Cm244	1.28E-02	8.36E-07	1.55E-02	7.54E-02	9.40E-01	8.12E-07	3.84E-02	5.38E-02	1.24E-10
Kr85	1.25E-05	1.43E-05	1.22E-05	1.16E-05	2.35E-05	1.26E-05	1.16E-05	1.27E-05	1.41E-03
Sr90	8.33E-04	8.33E-04	1.18E-03	1.06E-01	2.29E-01	8.33E-04	1.81E-03	1.11E-01	1.14E-05
Y90	4.86E-08	4.92E-08	4.41E-05	1.32E-06	1.32E-06	4.86E-08	1.83E-05	1.08E-05	1.16E-06
I129	3.24E-08	7.73E-08	1.15E-07	5.14E-08	5.20E-08	5.70E-04	4.34E-08	1.71E-05	1.58E-09
Cs134	5.41E-05	4.53E-05	4.92E-05	4.92E-05	4.67E-05	4.64E-05	5.77E-05	5.21E-05	1.51E-06
Cs137	4.68E-03	4.19E-03	4.72E-03	4.44E-03	4.25E-03	4.24E-03	4.88E-03	4.62E-03	1.82E-05
Ba137m	8.40E-07	9.59E-07	8.34E-07	8.13E-07	1.38E-06	8.58E-07	7.98E-07	8.58E-07	1.11E-06
Pm147	2.16E-12	3.95E-12	7.69E-06	8.11E-07	1.01E-05	2.23E-12	5.85E-07	1.05E-06	3.17E-10
Eu154	2.42E-06	3.19E-06	1.61E-05	2.15E-05	1.06E-04	1.49E-06	2.29E-05	1.57E-05	6.61E-08
Np239	6.61E-10	3.22E-10	1.52E-08	1.48E-09	1.34E-08	2.36E-10	6.26E-09	4.50E-09	4.00E-10
Total	4.69E-02	1.48E-02	3.85E-01	3.32E-01	2.90E+00	1.43E-02	1.26E-01	2.95E-01	1.73E-03

TABLE A7A.8-4
OFF-SITE AIRBORNE DOSES FROM OFF-NORMAL CONDITIONS AT 110 M (EXTERNAL)

Design Basis14x14 Fuel, Deep Doses (External)
mrem for 45 days

Isotope	Gonad	Breast	Lung	R. Marrow	B. Surface	Thyroid	Remainder	Effective	Skin
H3	0.00E+00	0.00E+00	2.93E-08	0.00E+00	0.00E+00	0.00E+00	0.00E+00	3.53E-09	0.00E+00
Co60	2.48E-04	2.81E-04	2.50E-04	2.48E-04	3.59E-04	2.56E-04	2.42E-04	2.54E-04	2.93E-04
Pu238	1.19E-11	2.30E-11	1.92E-12	3.04E-12	1.68E-11	7.26E-12	3.60E-12	8.83E-12	7.40E-11
Pu239	3.92E-13	6.11E-13	2.14E-13	2.16E-13	7.66E-13	3.14E-13	2.31E-13	3.43E-13	1.51E-12
Pu240	1.02E-12	1.97E-12	1.74E-13	2.64E-13	1.48E-12	6.27E-13	3.14E-13	7.60E-13	6.27E-12
Pu241	1.37E-12	1.66E-12	1.24E-12	1.08E-12	4.19E-12	1.33E-12	1.16E-12	1.39E-12	2.24E-12
Am241	7.72E-10	9.62E-10	6.06E-09	4.68E-10	2.58E-09	7.04E-10	5.70E-10	7.36E-10	1.15E-09
Am243	5.47E-11	6.52E-11	4.80E-11	3.87E-11	1.87E-10	5.22E-11	4.47E-11	5.45E-11	6.87E-11
Cm244	2.18E-11	4.21E-11	2.24E-12	4.62E-12	2.79E-11	1.33E-11	5.73E-12	1.55E-11	1.24E-10
Kr85	1.25E-05	1.43E-05	1.22E-05	1.16E-05	2.35E-05	1.26E-05	1.16E-05	1.27E-05	1.41E-03
Sr90	9.67E-09	1.18E-08	8.00E-09	6.76E-09	2.83E-08	9.11E-09	7.59E-09	9.36E-09	1.14E-05
Y90	3.52E-09	4.10E-09	3.30E-09	3.02E-09	8.28E-09	3.49E-09	3.13E-09	3.54E-09	1.16E-06
I129	6.95E-10	9.58E-10	3.08E-10	2.36E-10	1.58E-09	5.55E-10	3.31E-10	5.47E-10	1.58E-09
Cs134	1.19E-06	1.35E-06	1.18E-06	1.15E-06	1.92E-06	1.21E-06	1.13E-06	1.21E-06	1.51E-06
Cs137	1.68E-08	2.04E-08	1.41E-08	1.20E-08	4.82E-08	1.59E-08	1.34E-08	1.63E-08	1.82E-05
Ba137m	8.40E-07	9.59E-07	8.34E-07	8.13E-07	1.38E-06	8.58E-07	7.98E-07	8.58E-07	1.11E-06
Pm147	2.93E-13	3.74E-13	2.13E-13	1.75E-13	8.53E-13	2.64E-13	2.06E-13	2.71E-13	3.17E-10
Eu154	4.78E-08	5.43E-08	4.78E-08	4.68E-08	7.52E-08	4.90E-08	4.58E-08	4.90E-08	6.61E-08
Np239	1.88E-10	2.18E-10	1.79E-10	1.62E-10	5.00E-10	1.88E-10	1.69E-10	1.92E-10	4.00E-10
Total	2.63E-04	2.97E-04	2.65E-04	2.62E-04	3.86E-04	2.71E-04	2.56E-04	2.69E-04	1.73E-03

TABLE A7A.8-5
OFF-SITE AIRBORNE DOSES FROM ACCIDENT CONDITIONS AT 110 M (INTERNAL)

Design Basis 14x14 Fuel, mrem/30 Days, Committed Doses (Internal)

Isotope	Gonad	Breast	Lung	R. Marrow	B. Surface	Thyroid	Remainder	Effective
H3	3.95E-03	3.95E-03	3.95E-03	3.95E-03	3.95E-03	3.95E-03	3.95E-03	3.95E-03
Co60	1.37E-01	5.30E-01	9.94E+00	4.96E-01	3.89E-01	4.67E-01	1.04E+00	1.70E+00
Pu238	1.09E+00	3.88E-05	1.24E+01	5.89E+00	7.37E+01	3.73E-05	2.72E+00	4.11E+00
Pu239	5.51E-02	1.60E-06	5.60E-01	2.93E-01	3.66E+00	1.56E-06	1.31E-01	2.01E-01
Pu240	1.09E-01	3.26E-06	1.11E+00	5.79E-01	7.23E+00	3.10E-06	2.59E-01	3.98E-01
Pu241	2.79E-01	1.25E-05	1.30E+00	1.38E+00	1.72E+01	5.08E-06	5.36E-01	9.13E-01
Am241	6.26E-01	5.14E-05	3.54E-01	3.35E+00	4.18E+01	3.08E-05	1.51E+00	2.31E+00
Am243	1.75E-02	8.14E-06	9.53E-03	9.26E-02	1.16E+00	4.44E-06	4.14E-02	6.37E-02
Cm244	1.08E+00	7.05E-05	1.31E+00	6.36E+00	7.93E+01	6.85E-05	3.24E+00	4.54E+00
Kr85	0.00E+00	0.00E+00	0.00E+00	0.00E+00	0.00E+00	0.00E+00	0.00E+00	0.00E+00
Sr90	7.03E-02	7.03E-02	9.93E-02	8.94E+00	1.93E+01	7.03E-02	1.53E-01	9.34E+00
Y90	3.80E-06	3.80E-06	3.72E-03	1.11E-04	1.11E-04	3.80E-06	1.54E-03	9.10E-04
I129	2.68E-06	6.44E-06	9.67E-06	4.31E-06	4.25E-06	4.81E-02	3.64E-06	1.44E-03
Cs134	4.46E-03	3.71E-03	4.05E-03	4.05E-03	3.77E-03	3.81E-03	4.77E-03	4.29E-03
Cs137	3.95E-01	3.54E-01	3.98E-01	3.74E-01	3.58E-01	3.58E-01	4.11E-01	3.89E-01
Ba137m	0.00E+00	0.00E+00	0.00E+00	0.00E+00	0.00E+00	0.00E+00	0.00E+00	0.00E+00
Pm147	1.58E-10	3.02E-10	6.49E-04	6.84E-05	8.55E-04	1.66E-10	4.94E-05	8.89E-05
Eu154	2.00E-04	2.65E-04	1.35E-03	1.81E-03	8.93E-03	1.22E-04	1.93E-03	1.32E-03
Np239	3.99E-08	8.73E-09	1.26E-06	1.11E-07	1.09E-06	4.08E-09	5.13E-07	3.63E-07
Total	3.86E+00	9.62E-01	2.75E+01	2.78E+01	2.44E+02	9.51E-01	1.00E+01	2.40E+01

TABLE A7A.8-6
OFF-SITE AIRBORNE DOSES FROM ACCIDENT CONDITIONS AT 110 M (EXTERNAL)

Design Basis 14x14 Fuel, mrem/30 Days, Deep Doses (External)

	Gonad	Breast	Lung	R. Marrow	B. Surface	Thyroid	Remainder	Effective	Skin
H3	0.00E+00	0.00E+00	2.47E-06	0.00E+00	0.00E+00	0.00E+00	0.00E+00	2.98E-07	0.00E+00
Co60	1.40E-02	1.58E-02	1.41E-02	1.40E-02	2.02E-02	1.44E-02	1.36E-02	1.43E-02	1.65E-02
Pu238	1.00E-09	1.94E-09	1.62E-10	2.56E-10	1.42E-09	6.12E-10	3.04E-10	7.45E-10	6.24E-09
Pu239	3.30E-11	5.15E-11	1.81E-11	1.82E-11	6.46E-11	2.65E-11	1.95E-11	2.89E-11	1.27E-10
Pu240	8.58E-11	1.66E-10	1.47E-11	2.23E-11	1.25E-10	5.29E-11	2.65E-11	6.41E-11	5.29E-10
Pu241	1.16E-10	1.40E-10	1.05E-10	9.08E-11	3.53E-10	1.13E-10	9.82E-11	1.17E-10	1.89E-10
Am241	6.51E-08	8.11E-08	5.11E-07	3.95E-08	2.18E-07	5.94E-08	4.81E-08	6.20E-08	9.71E-08
Am243	4.62E-09	5.50E-09	4.05E-09	3.27E-09	1.57E-08	4.41E-09	3.77E-09	4.60E-09	5.80E-09
Cm244	1.84E-09	3.55E-09	1.89E-10	3.90E-10	2.35E-09	1.12E-09	4.83E-10	1.31E-09	1.04E-08
Kr85	1.05E-03	1.21E-03	1.03E-03	9.81E-04	1.98E-03	1.06E-03	9.81E-04	1.07E-03	1.19E-01
Sr90	8.15E-07	9.95E-07	6.75E-07	5.70E-07	2.39E-06	7.68E-07	6.40E-07	7.89E-07	9.64E-04
Y90	2.97E-07	3.46E-07	2.78E-07	2.55E-07	6.98E-07	2.94E-07	2.64E-07	2.99E-07	9.81E-05
I129	5.86E-08	8.08E-08	2.60E-08	1.99E-08	1.33E-07	4.68E-08	2.79E-08	4.61E-08	1.33E-07
Cs134	1.00E-04	1.14E-04	9.96E-05	9.72E-05	1.62E-04	1.02E-04	9.54E-05	1.02E-04	1.28E-04
Cs137	1.41E-06	1.72E-06	1.19E-06	1.01E-06	4.07E-06	1.34E-06	1.13E-06	1.37E-06	1.53E-03
Ba137m	7.09E-05	8.09E-05	7.04E-05	6.86E-05	1.16E-04	7.24E-05	6.73E-05	7.24E-05	9.37E-05
Pm147	2.47E-11	3.16E-11	1.80E-11	1.47E-11	7.20E-11	2.23E-11	1.74E-11	2.29E-11	2.68E-08
Eu154	4.03E-06	4.58E-06	4.03E-06	3.95E-06	6.34E-06	4.14E-06	3.87E-06	4.13E-06	5.57E-06
Np239	1.59E-08	1.84E-08	1.51E-08	1.37E-08	4.22E-08	1.59E-08	1.43E-08	1.62E-08	3.37E-08
Total	1.52E-02	1.72E-02	1.53E-02	1.51E-02	2.25E-02	1.57E-02	1.48E-02	1.55E-02	1.38E-01

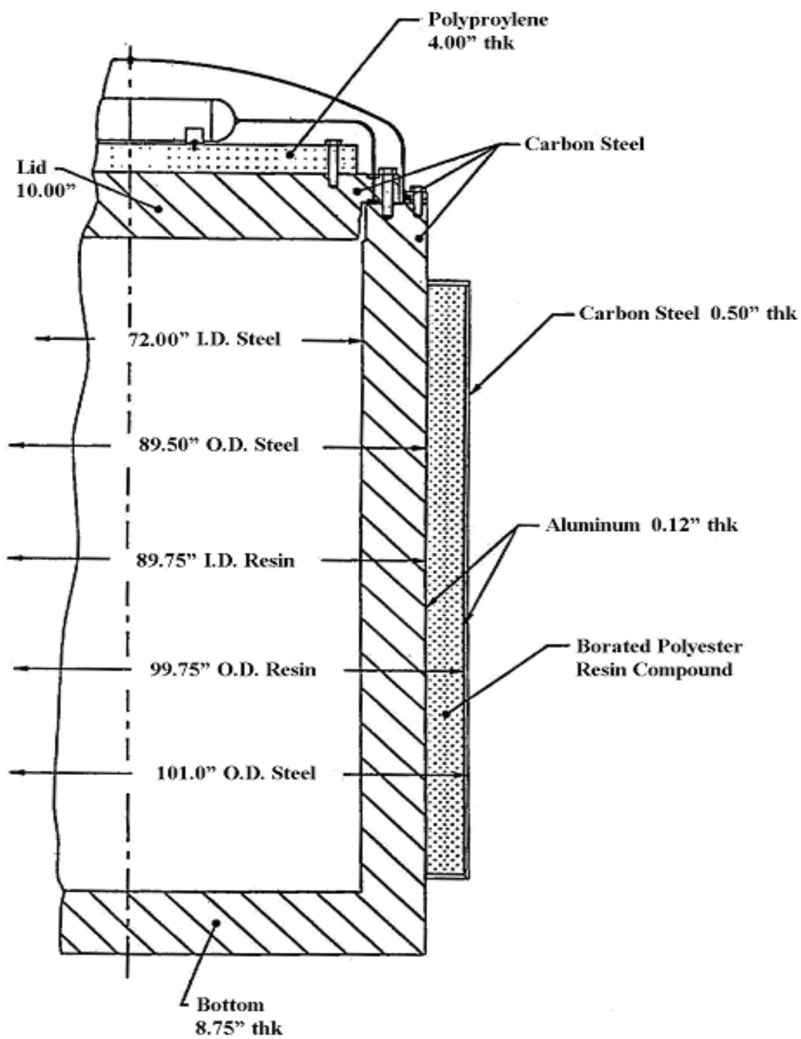

FIGURE A7A.1-1
TN-40HT CASK SHIELDING CONFIGURATION

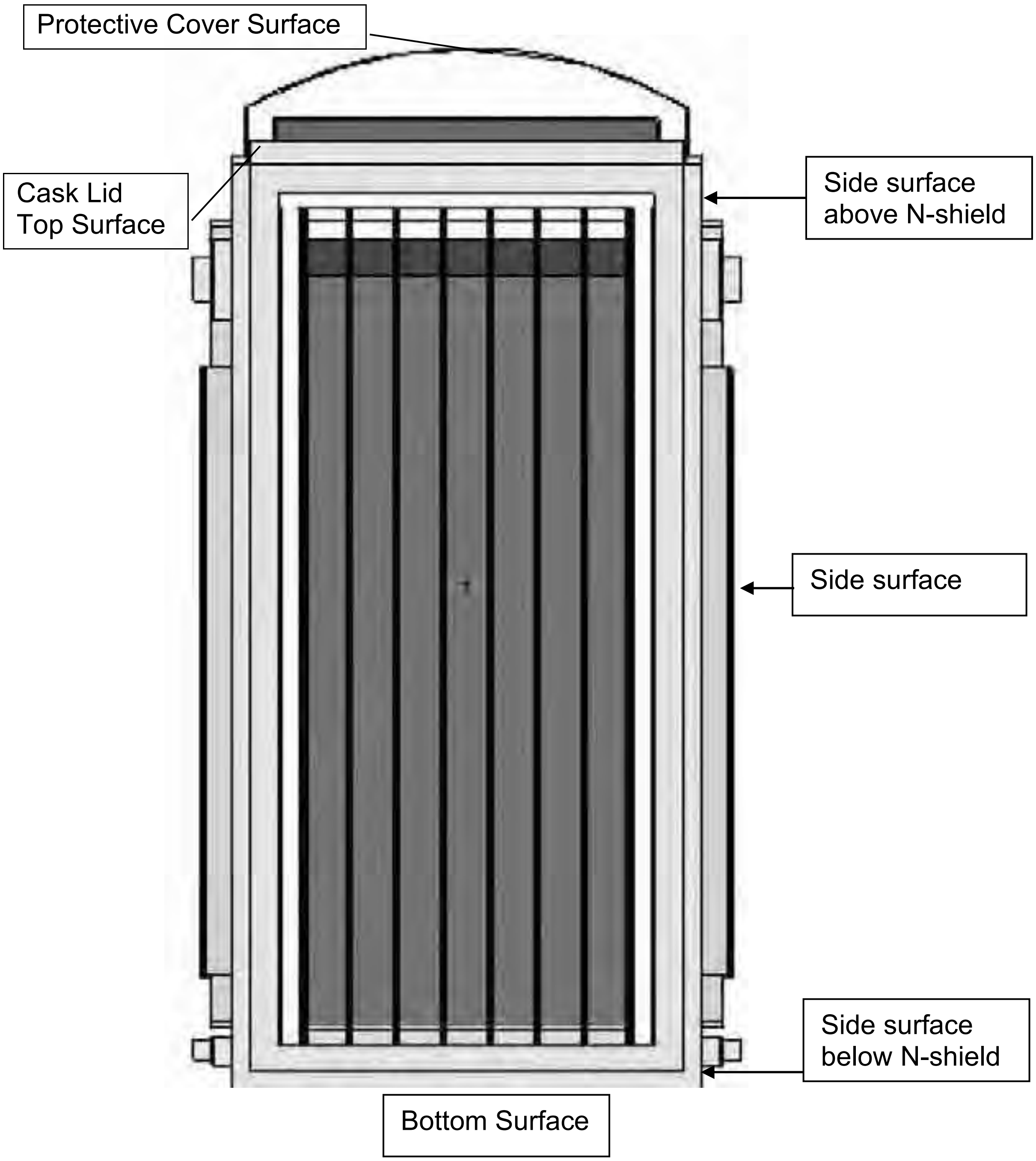

FIGURE A7A.2-1
TN-40HT NORMAL CONDITIONS DOSE POINT LOCATIONS

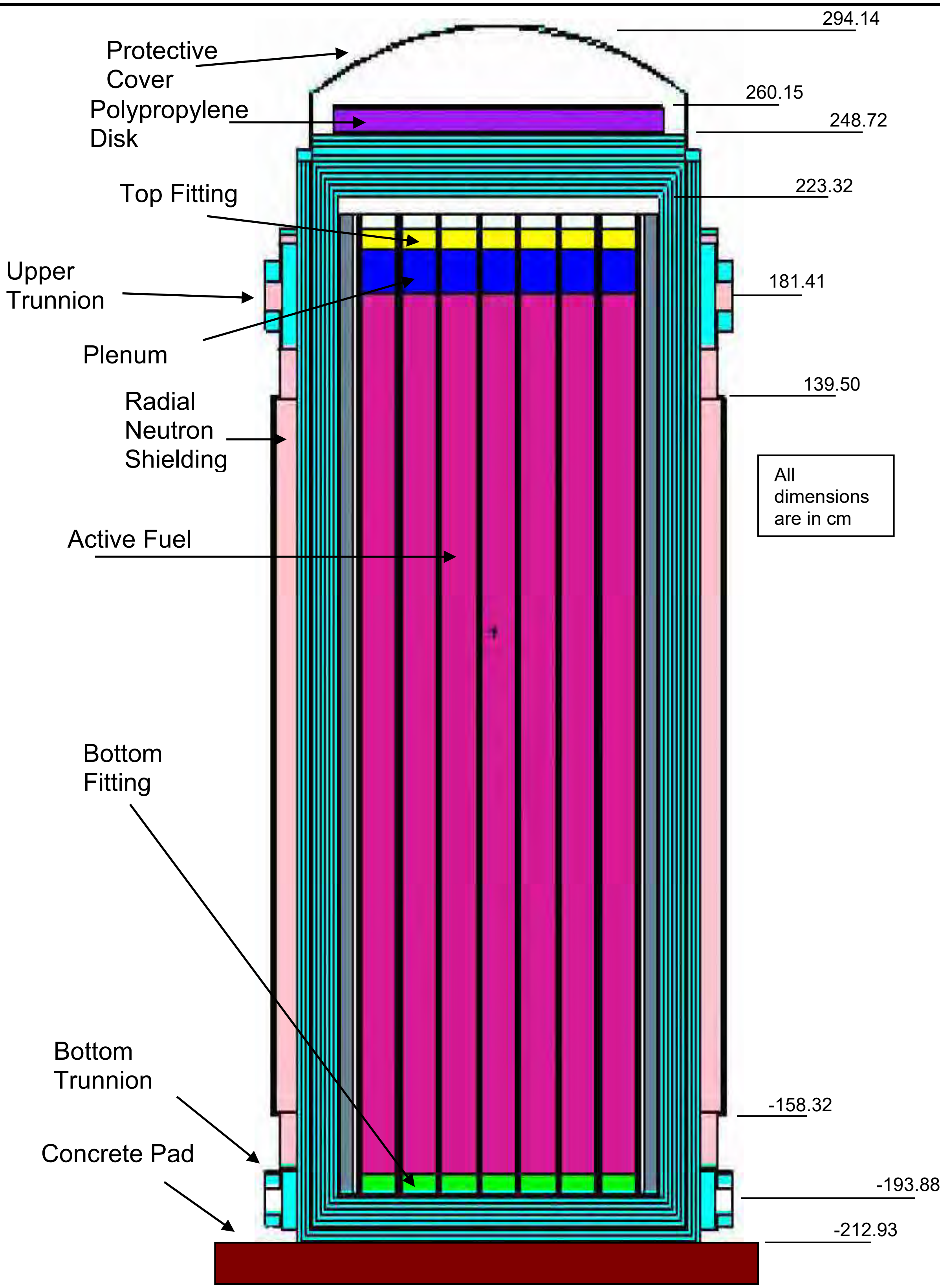

FIGURE A7A.4-1
TN-40HT MCNP GAMMA MODEL YZ PLOT

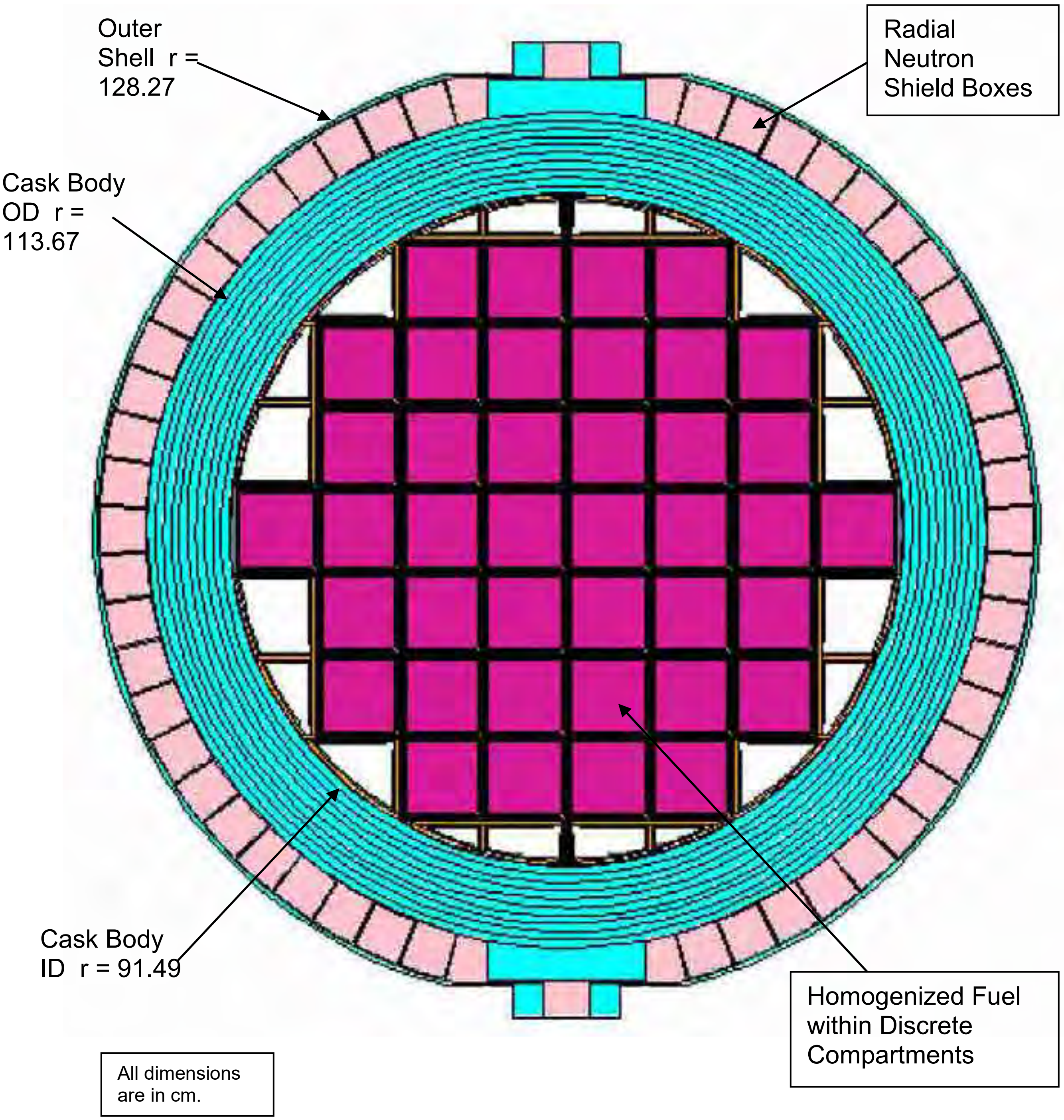

FIGURE A7A.4-2
TN-40HT MCNP GAMMA MODEL – XY PLOT AT Z=181 CM

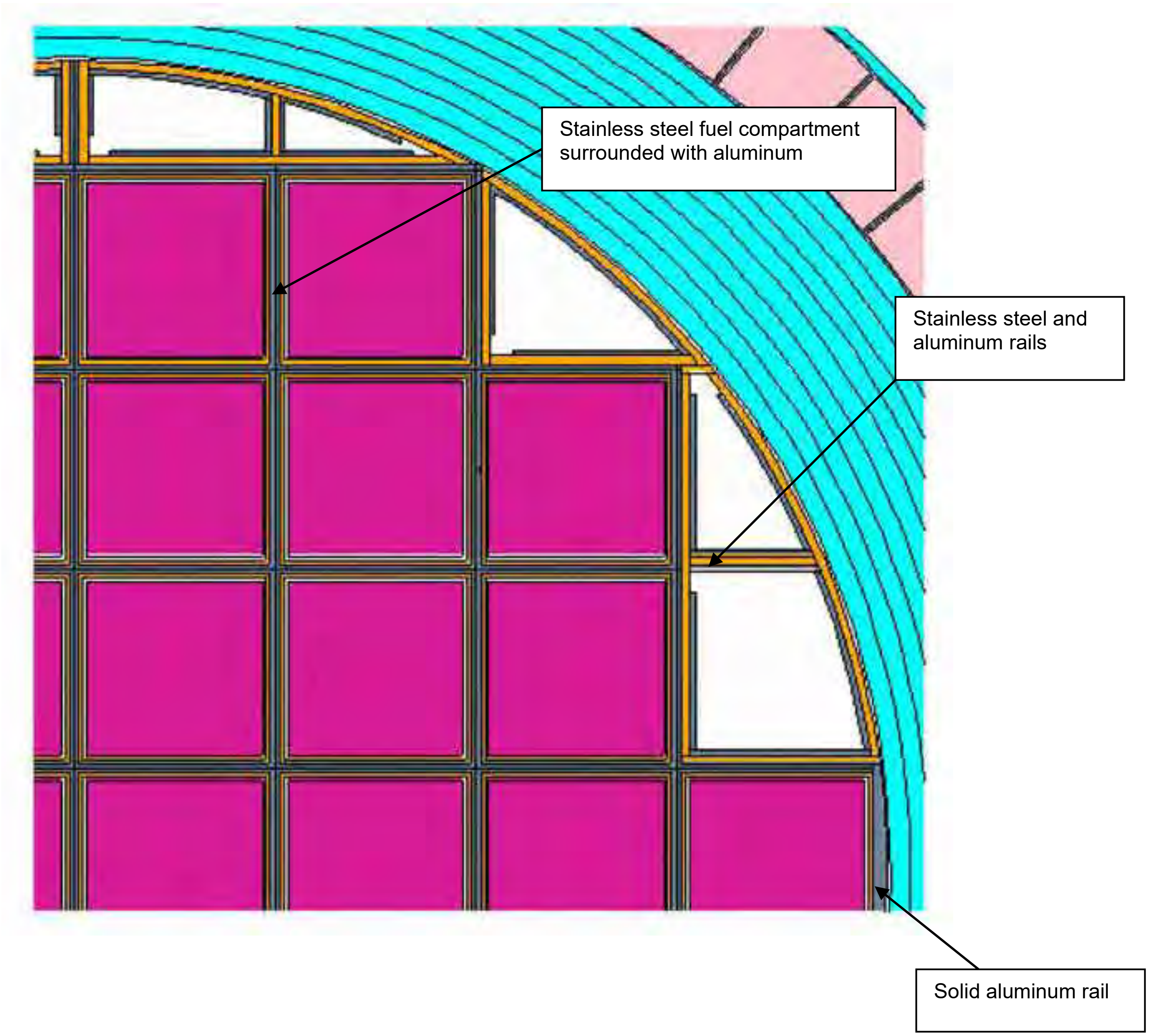

FIGURE A7A.4-3
TN-40HT MCNP QUARTER GAMMA MODEL – XY PLOT AT Z=0 CM

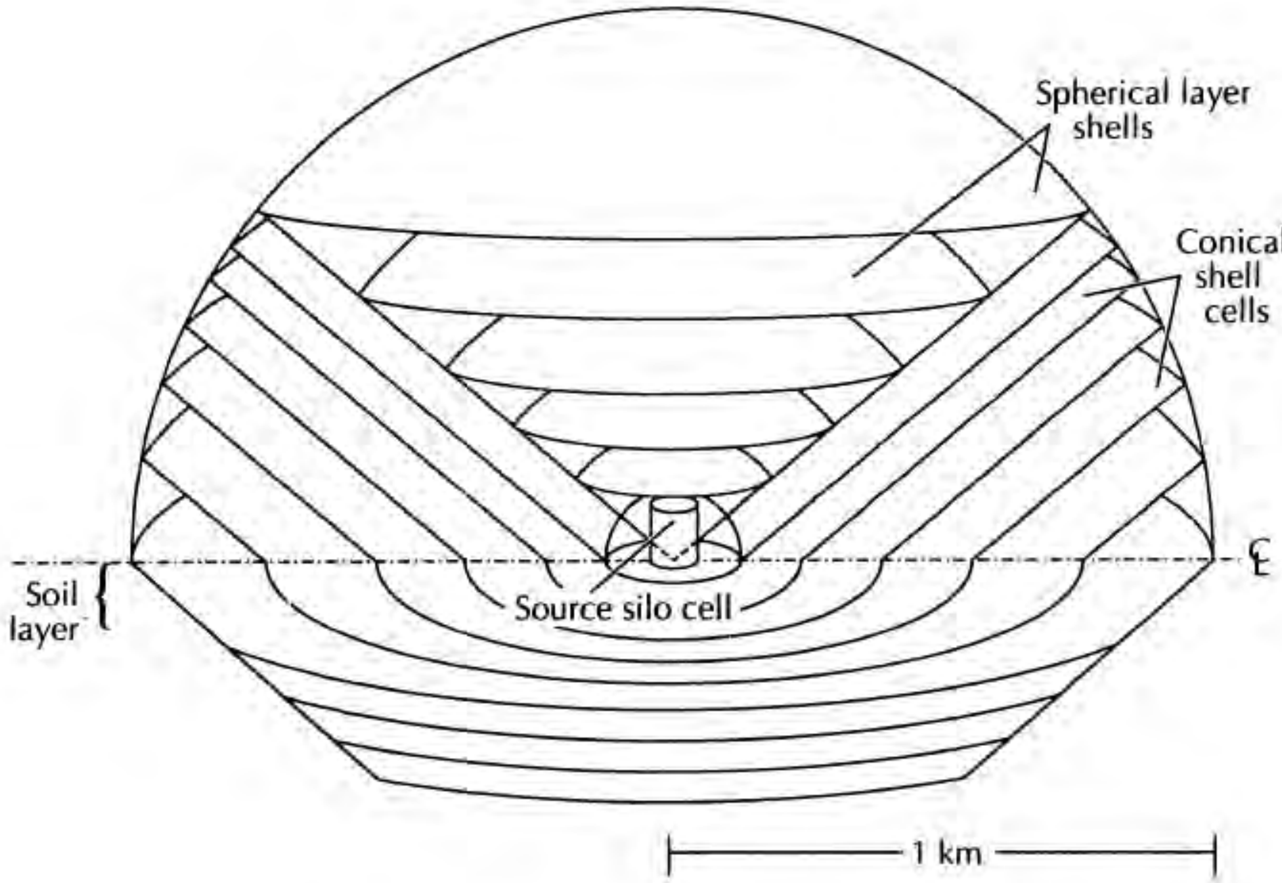

FIGURE A7A.4-4
TN-40HT FAR FIELD MCNP MODEL

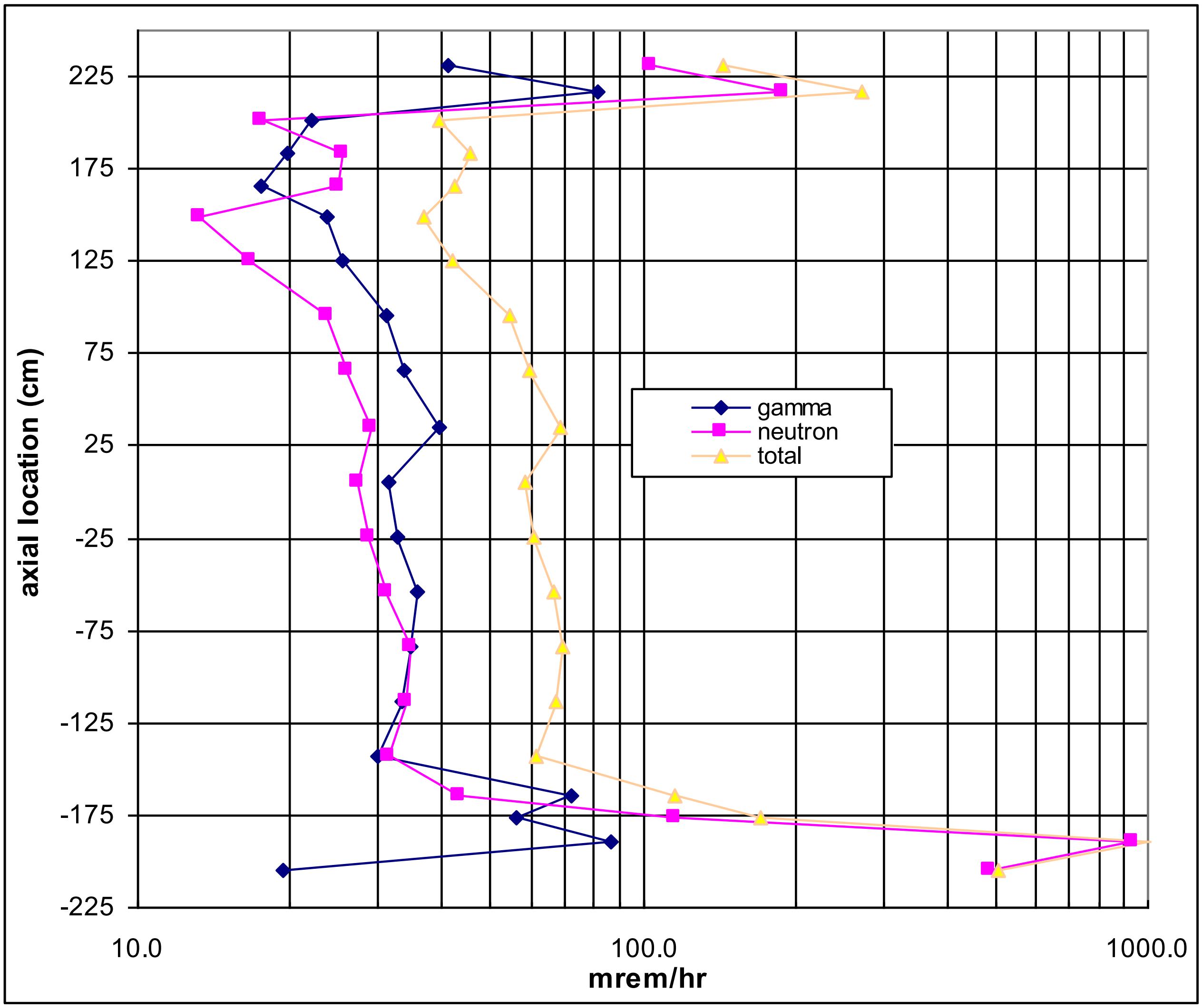

Note: 0.0 is the center line of the active fuel

FIGURE A7A.5-1
TN-40HT CASK SIDE SURFACE DOSE RATES
NORMAL AND OFF-NORMAL CONDITIONS

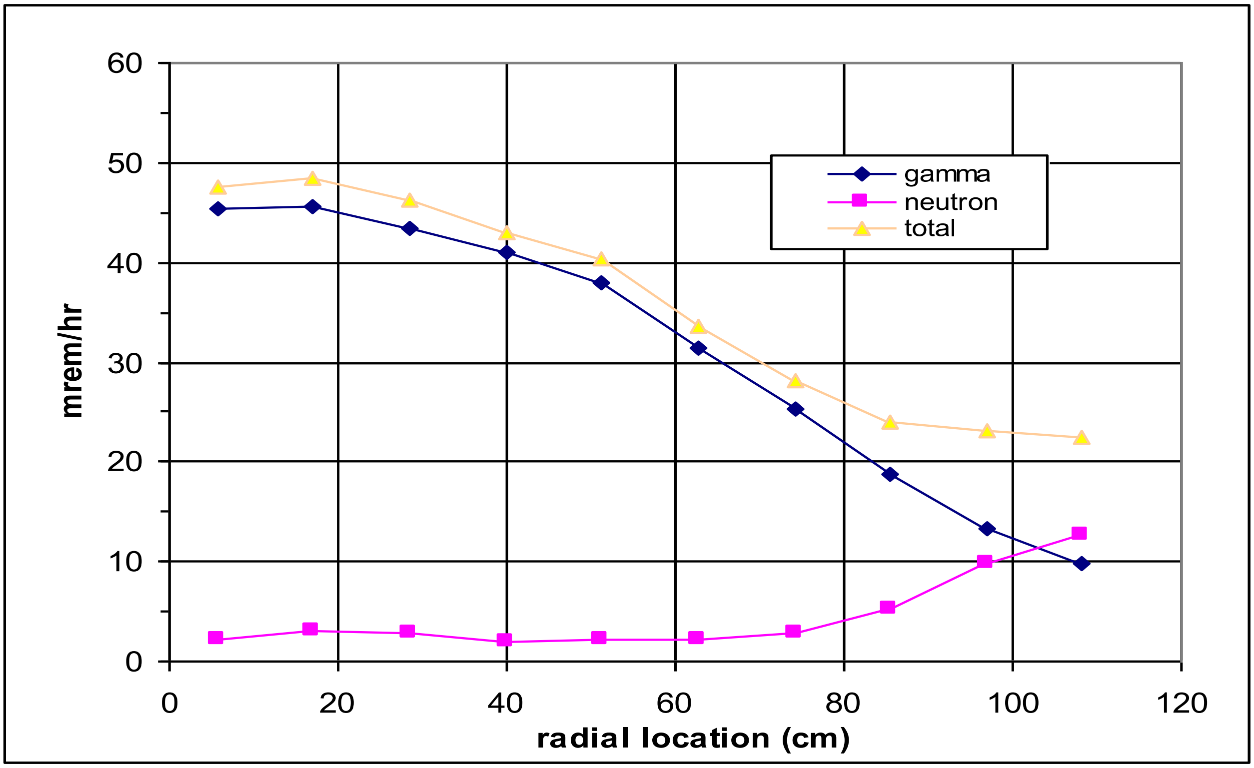

FIGURE A7A.5-2
TN-40HT CASK PROTECTIVE COVER SURFACE DOSE RATES
NORMAL AND OFF-NORMAL CONDITIONS

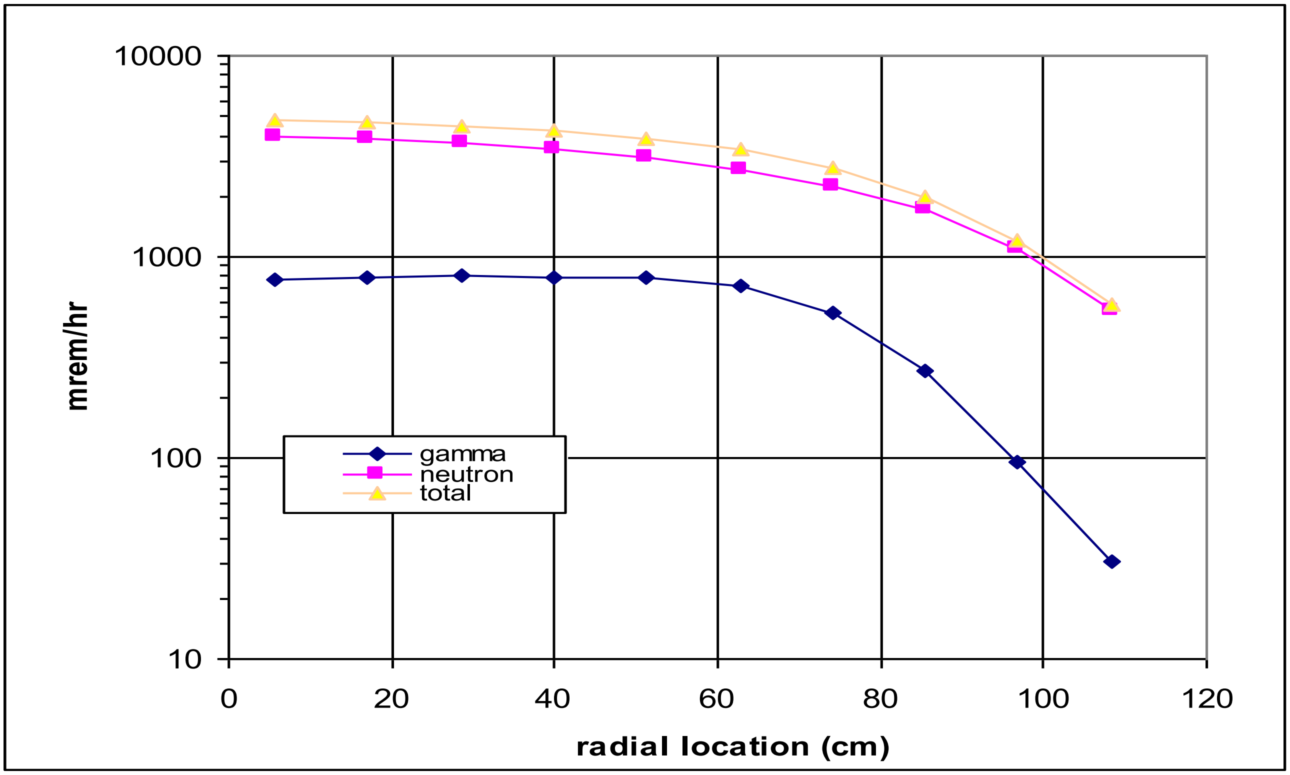

FIGURE A7A.5-3
TN-40HT CASK BOTTOM SURFACE DOSE RATES
NORMAL AND OFF-NORMAL CONDITIONS

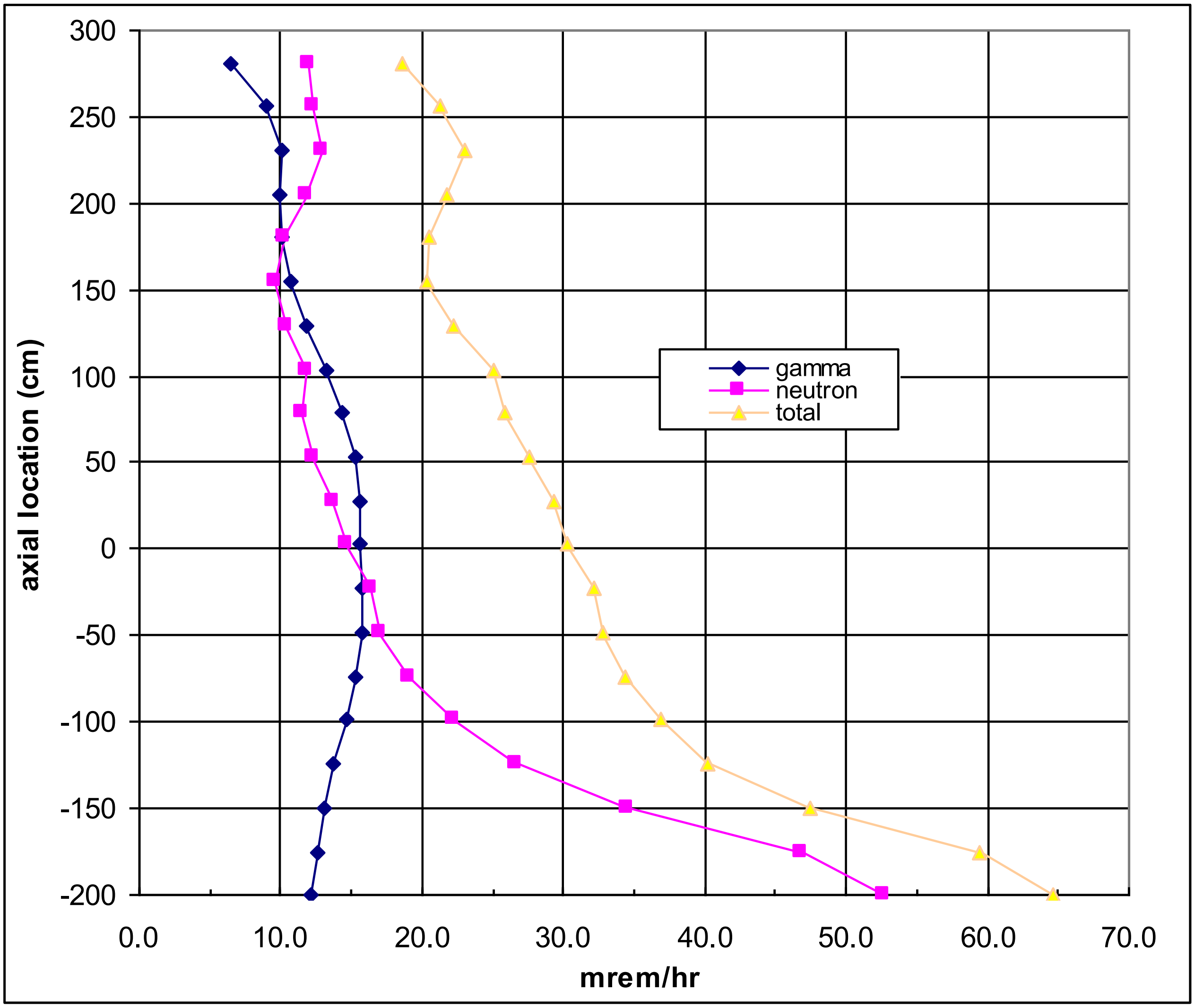

FIGURE A7A.5-4
TN-40HT CASK DOSE RATES 1 M FROM SIDE SURFACE
NORMAL AND OFF-NORMAL CONDITIONS

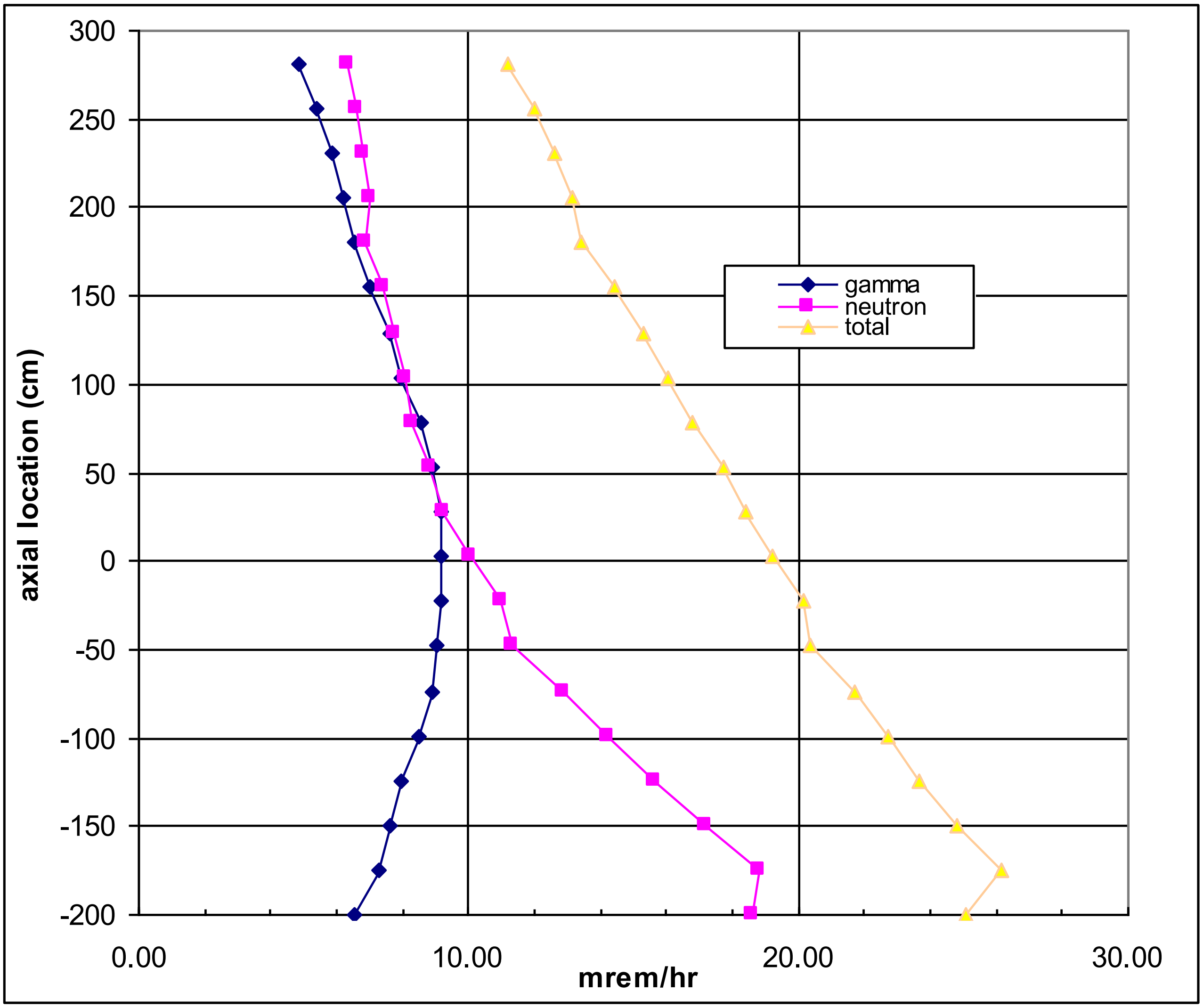

FIGURE A7A.5-5
TN-40HT CASK DOSE RATES 2 M FROM SIDE SURFACE
NORMAL AND OFF-NORMAL CONDITIONS

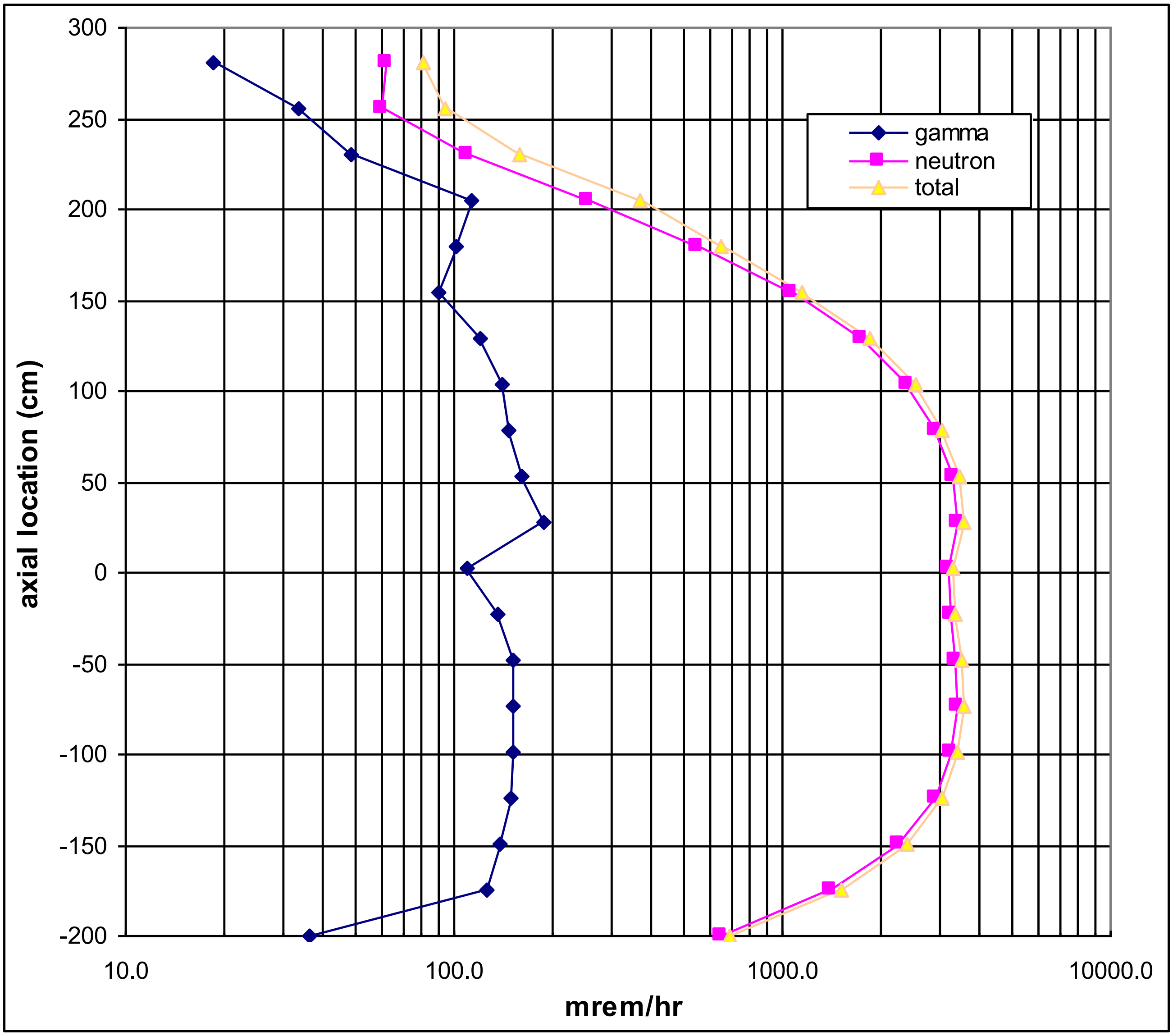

FIGURE A7A.5-6
TN-40HT CASK SIDE SURFACE DOSE RATES – ACCIDENT CONDITIONS

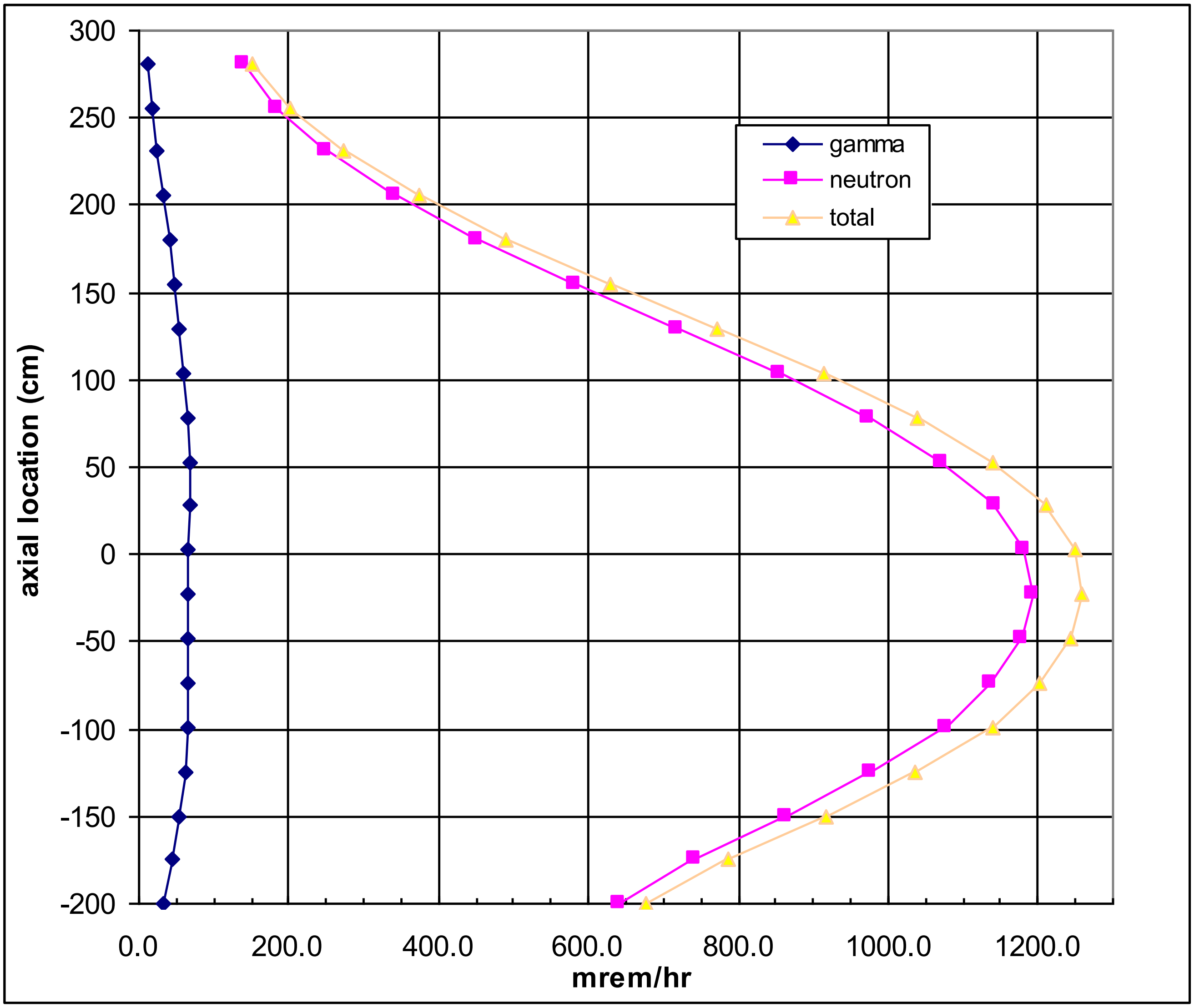

FIGURE A7A.5-7
TN-40HT CASK DOSE RATES 1 M FROM SIDE SURFACE – ACCIDENT CONDITIONS

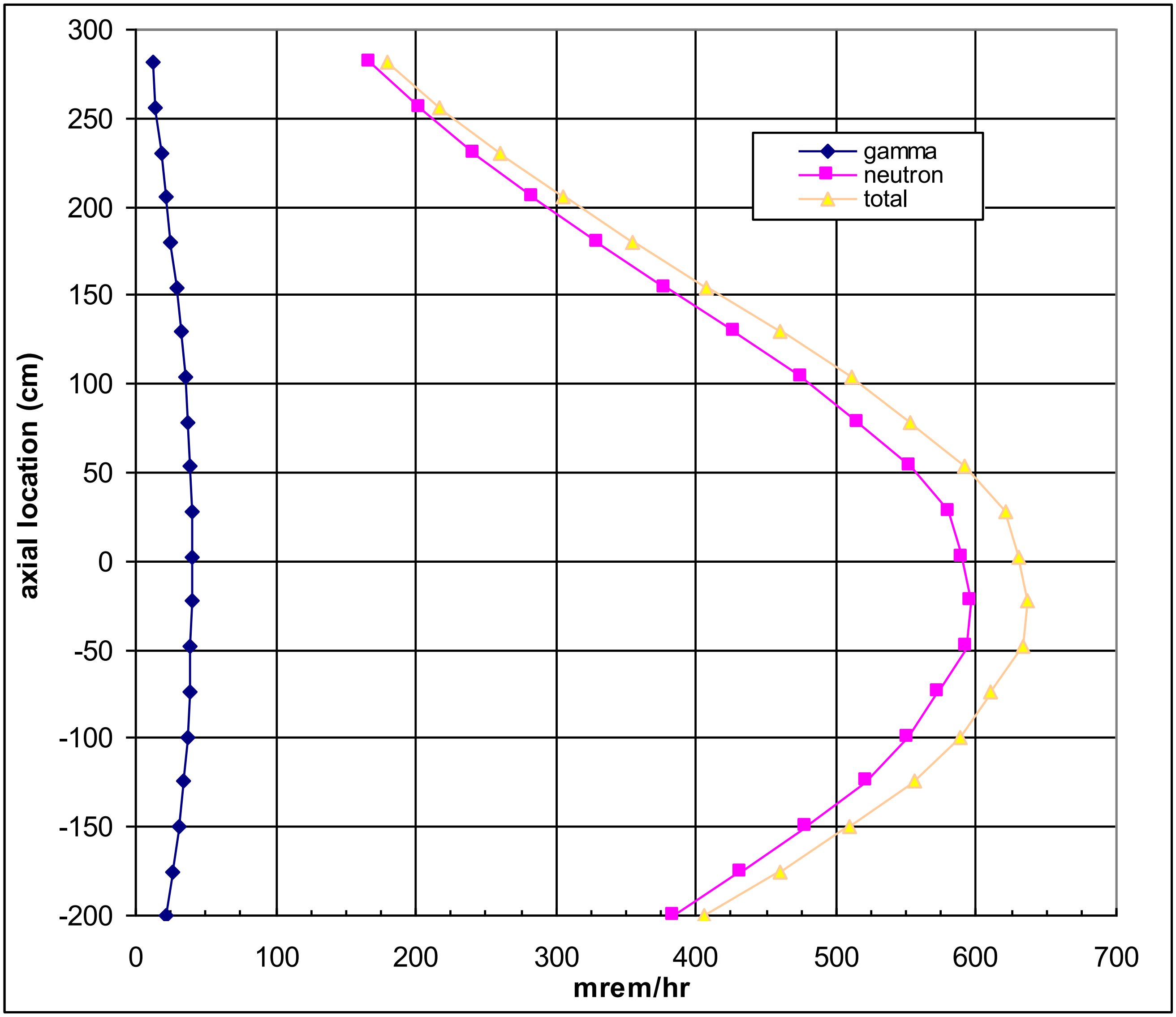

FIGUREA7A.5-8
TN-40HT CASK DOSE RATES 2 M FROM SIDE SURFACE – ACCIDENT CONDITIONS

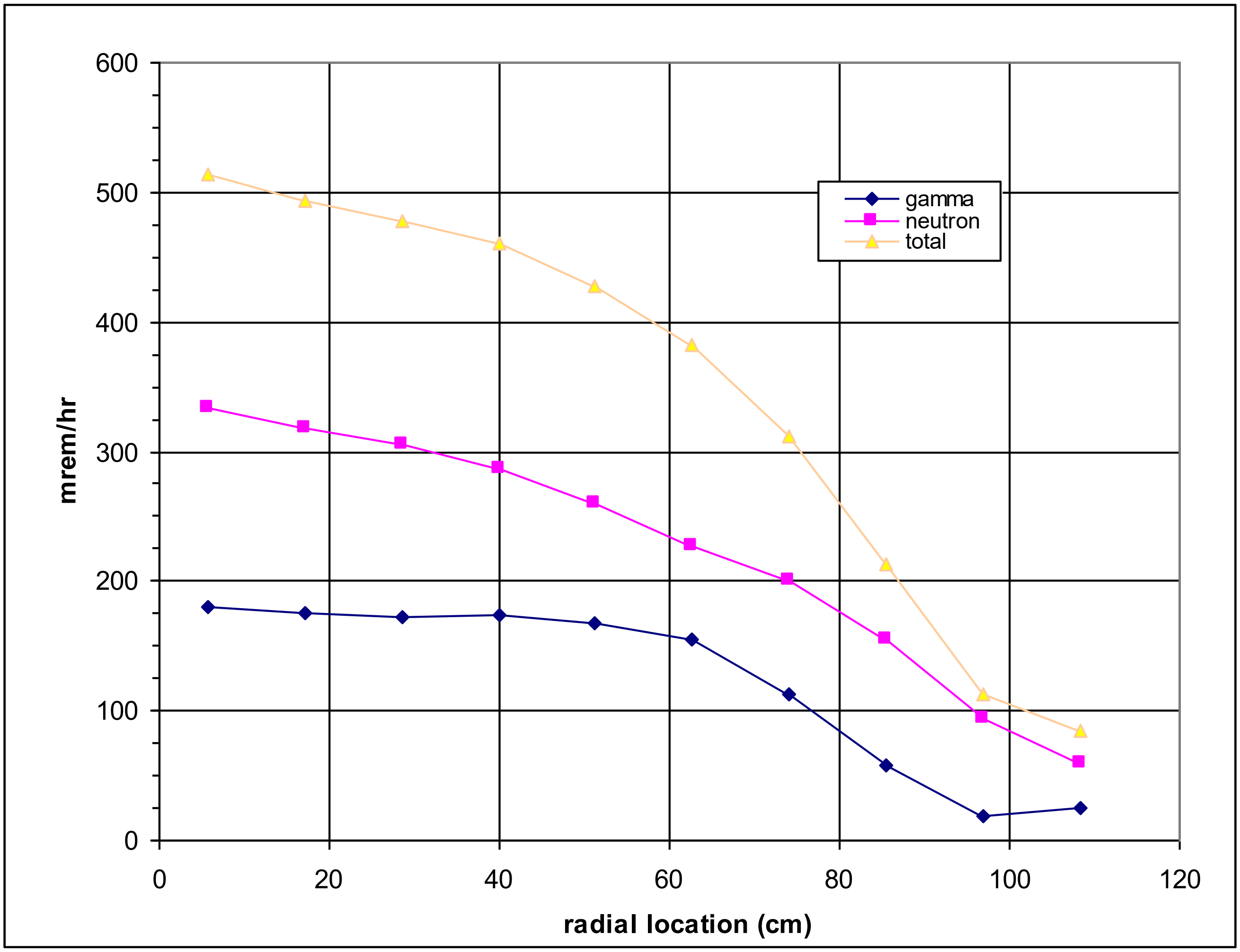

FIGURE A7A.5-9
TN-40HT CASK LID SURFACE DOSE RATES – NORMAL AND ACCIDENT CONDITIONS

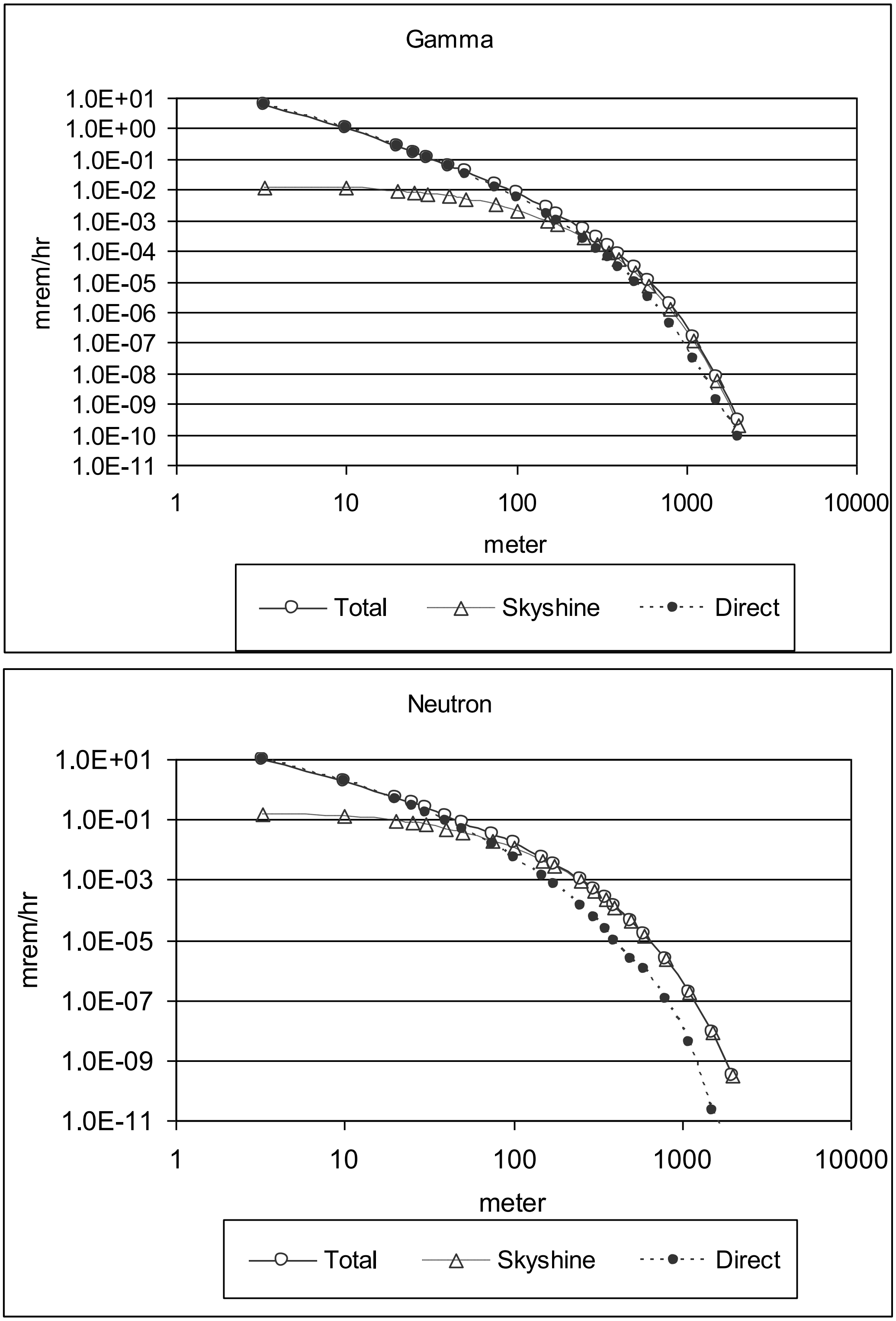

FIGURE A7A.6-1
TN-40HT CASK – DOSE RATE AS A FUNCTION OF DISTANCE

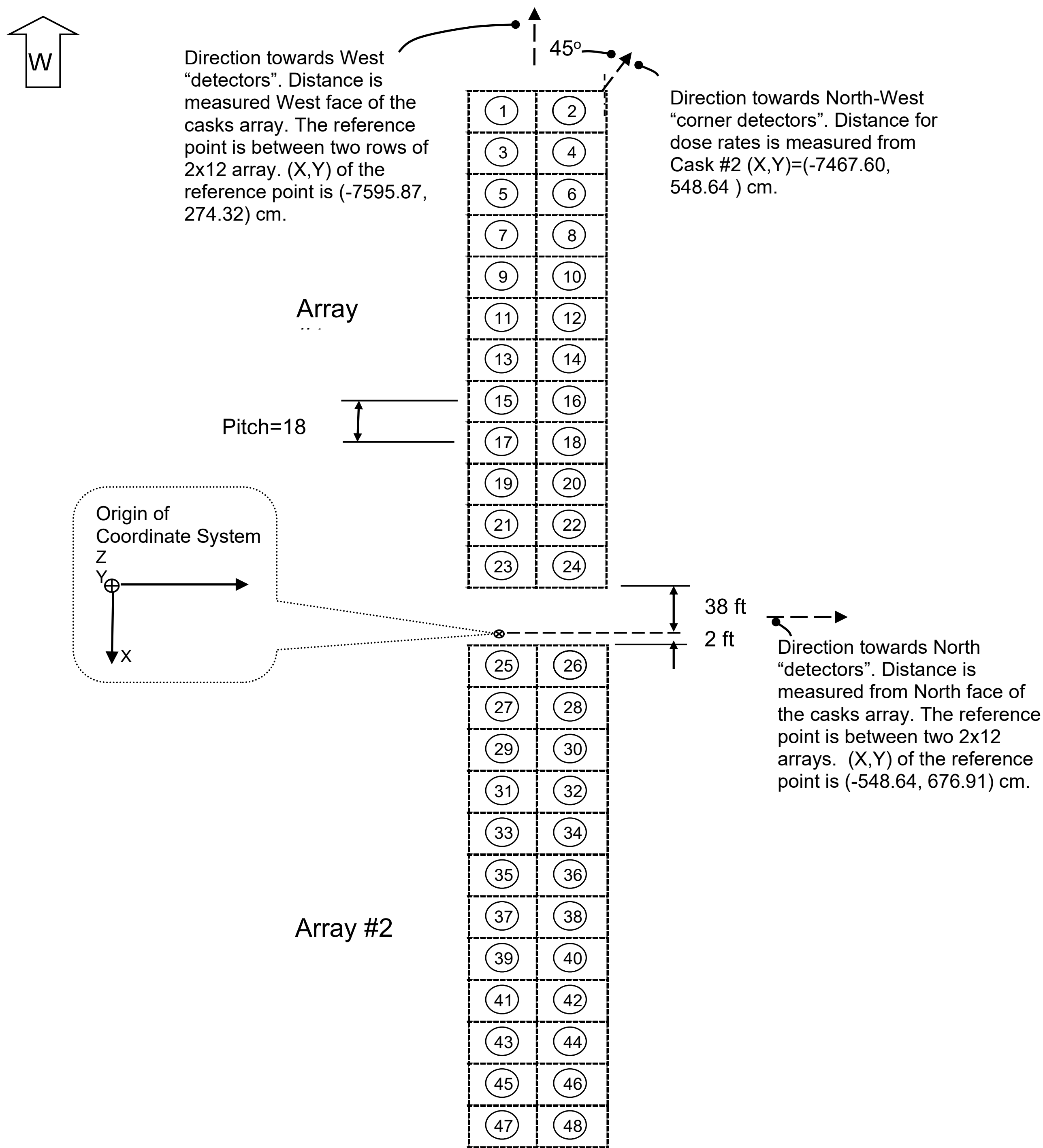

FIGURE A7A.7-1
ARRANGEMENT OF CASKS AND "DETECTORS" IN MCNP CALCULATION MODEL FOR ISFSI DOSE RATE ESTIMATES

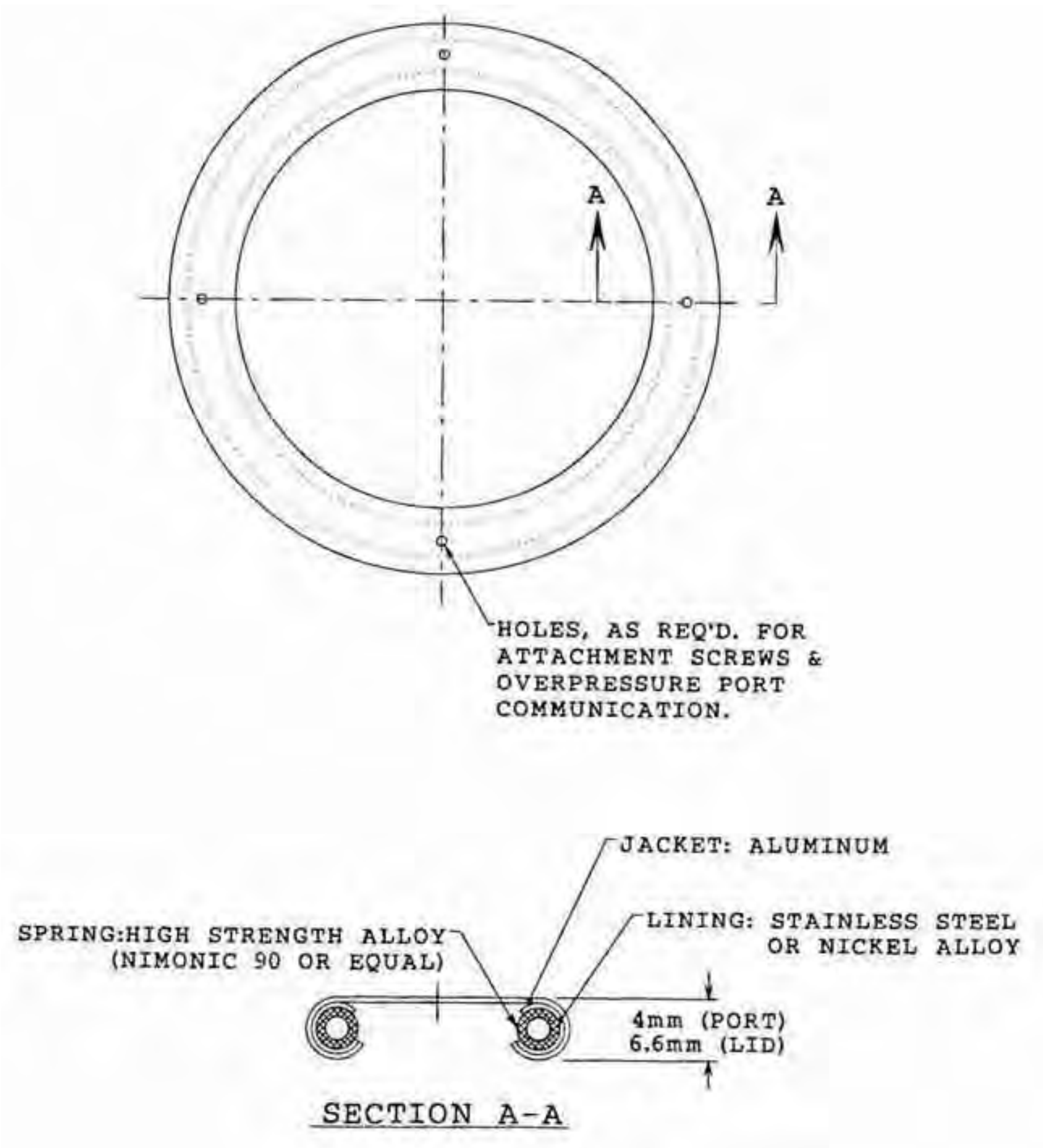

FIGURE A7A.8-1
LID, VENT PORT AND DRAIN PORT METAL SEALS

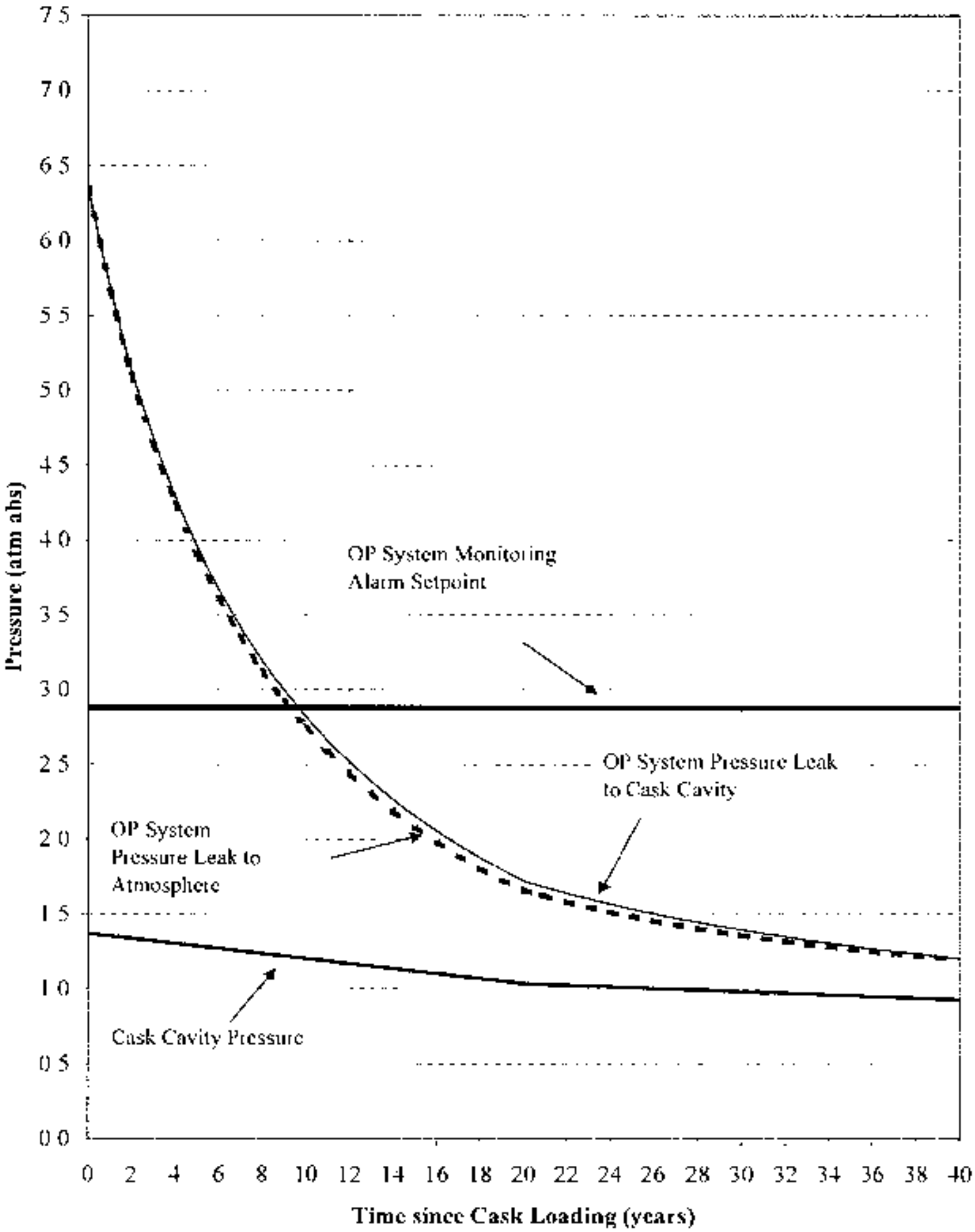

FIGURE A7A.8-2
OVERPRESSURE MONITORING SYSTEM PRESSURE DROP WITH TIME

Appendix A7B

TN-40HT SHIELDING EVALUATION COMPUTER INPUT

A7B SAMPLE SHIELDING INPUT FILES

This Section provides representative input files for the computer codes, SAS2H and MCNP, utilized to calculate the source terms and dose rates for the TN-40HT Cask. A listing of the file names and a brief description are provided below, followed by the files themselves.

Section #	File Name	Description
A7B.1	I_6034.in	SAS2H Input File for Design Basis Fuel (In-core zone)
A7B.2	htgnfn	MCNP Input for Primary Gamma Dose (Near Field, Normal and Off-Normal Storage Conditions)
A7B.3	Htgnfa	MCNP Input for Primary Gamma Dose (Near Field, Accident Storage Conditions)
A7B.4	gfwd2_	MCNP Input for Gamma Dose (Far Field)

A7B.1 SAS2H INPUT FILE FOR DESIGN BASIS FUEL (IN-CORE ZONE)

I_6043.in

PROPRIETARY - TRADE SECRET INFORMATION WITHHELD PURSUANT TO 10 CFR 2.390

PROPRIETARY - TRADE SECRET INFORMATION
WITHHELD PURSUANT TO 10 CFR 2.390

PROPRIETARY - TRADE SECRET INFORMATION
WITHHELD PURSUANT TO 10 CFR 2.390

A7B.2 MCNP INPUT FOR PRIMARY GAMMA DOSE (NEAR FIELD, NORMAL AND OFF-NORMAL STORAGE CONDITIONS)

htgnfn

PROPRIETARY - TRADE SECRET INFORMATION
WITHHELD PURSUANT TO 10 CFR 2.390

**PROPRIETARY - TRADE SECRET INFORMATION
WITHHELD PURSUANT TO 10 CFR 2.390**

PROPRIETARY - TRADE SECRET INFORMATION
WITHHELD PURSUANT TO 10 CFR 2.390

PROPRIETARY - TRADE SECRET INFORMATION
WITHHELD PURSUANT TO 10 CFR 2.390

PROPRIETARY - TRADE SECRET INFORMATION
WITHHELD PURSUANT TO 10 CFR 2.390

PROPRIETARY - TRADE SECRET INFORMATION
WITHHELD PURSUANT TO 10 CFR 2.390

PROPRIETARY - TRADE SECRET INFORMATION
WITHHELD PURSUANT TO 10 CFR 2.390

**PROPRIETARY - TRADE SECRET INFORMATION
WITHHELD PURSUANT TO 10 CFR 2.390**

**PROPRIETARY - TRADE SECRET INFORMATION
WITHHELD PURSUANT TO 10 CFR 2.390**

PROPRIETARY - TRADE SECRET INFORMATION
WITHHELD PURSUANT TO 10 CFR 2.390

**PROPRIETARY - TRADE SECRET INFORMATION
WITHHELD PURSUANT TO 10 CFR 2.390**

PROPRIETARY - TRADE SECRET INFORMATION
WITHHELD PURSUANT TO 10 CFR 2.390

**PROPRIETARY - TRADE SECRET INFORMATION
WITHHELD PURSUANT TO 10 CFR 2.390**

PROPRIETARY - TRADE SECRET INFORMATION
WITHHELD PURSUANT TO 10 CFR 2.390

**PROPRIETARY - TRADE SECRET INFORMATION
WITHHELD PURSUANT TO 10 CFR 2.390**

PROPRIETARY - TRADE SECRET INFORMATION
WITHHELD PURSUANT TO 10 CFR 2.390

PROPRIETARY - TRADE SECRET INFORMATION
WITHHELD PURSUANT TO 10 CFR 2.390

**PROPRIETARY - TRADE SECRET INFORMATION
WITHHELD PURSUANT TO 10 CFR 2.390**

A7B.3 MCNP INPUT FOR PRIMARY GAMMA DOSE (NEAR FIELD, ACCIDENT STORAGE CONDITIONS)

Htgnfa

**PROPRIETARY - TRADE SECRET INFORMATION
WITHHELD PURSUANT TO 10 CFR 2.390**

PROPRIETARY - TRADE SECRET INFORMATION
WITHHELD PURSUANT TO 10 CFR 2.390

PROPRIETARY - TRADE SECRET INFORMATION
WITHHELD PURSUANT TO 10 CFR 2.390

**PROPRIETARY - TRADE SECRET INFORMATION
WITHHELD PURSUANT TO 10 CFR 2.390**

PROPRIETARY - TRADE SECRET INFORMATION
WITHHELD PURSUANT TO 10 CFR 2.390

**PROPRIETARY - TRADE SECRET INFORMATION
WITHHELD PURSUANT TO 10 CFR 2.390**

PROPRIETARY - TRADE SECRET INFORMATION
WITHHELD PURSUANT TO 10 CFR 2.390

PROPRIETARY - TRADE SECRET INFORMATION
WITHHELD PURSUANT TO 10 CFR 2.390

PROPRIETARY - TRADE SECRET INFORMATION
WITHHELD PURSUANT TO 10 CFR 2.390

PROPRIETARY - TRADE SECRET INFORMATION
WITHHELD PURSUANT TO 10 CFR 2.390

PROPRIETARY - TRADE SECRET INFORMATION
WITHHELD PURSUANT TO 10 CFR 2.390

**PROPRIETARY - TRADE SECRET INFORMATION
WITHHELD PURSUANT TO 10 CFR 2.390**

PROPRIETARY - TRADE SECRET INFORMATION
WITHHELD PURSUANT TO 10 CFR 2.390

PROPRIETARY - TRADE SECRET INFORMATION
WITHHELD PURSUANT TO 10 CFR 2.390

**PROPRIETARY - TRADE SECRET INFORMATION
WITHHELD PURSUANT TO 10 CFR 2.390**

PROPRIETARY - TRADE SECRET INFORMATION
WITHHELD PURSUANT TO 10 CFR 2.390

PROPRIETARY - TRADE SECRET INFORMATION
WITHHELD PURSUANT TO 10 CFR 2.390

A7B.4 MCNP INPUT FOR GAMMA DOSE (FAR FIELD)

gfwd2

**PROPRIETARY - TRADE SECRET INFORMATION
WITHHELD PURSUANT TO 10 CFR 2.390**

PROPRIETARY - TRADE SECRET INFORMATION
WITHHELD PURSUANT TO 10 CFR 2.390

PROPRIETARY - TRADE SECRET INFORMATION
WITHHELD PURSUANT TO 10 CFR 2.390

**PROPRIETARY - TRADE SECRET INFORMATION
WITHHELD PURSUANT TO 10 CFR 2.390**

PROPRIETARY - TRADE SECRET INFORMATION
WITHHELD PURSUANT TO 10 CFR 2.390

PROPRIETARY - TRADE SECRET INFORMATION
WITHHELD PURSUANT TO 10 CFR 2.390

PROPRIETARY - TRADE SECRET INFORMATION
WITHHELD PURSUANT TO 10 CFR 2.390

PROPRIETARY - TRADE SECRET INFORMATION
WITHHELD PURSUANT TO 10 CFR 2.390

PROPRIETARY - TRADE SECRET INFORMATION
WITHHELD PURSUANT TO 10 CFR 2.390

**PROPRIETARY - TRADE SECRET INFORMATION
WITHHELD PURSUANT TO 10 CFR 2.390**

**PROPRIETARY - TRADE SECRET INFORMATION
WITHHELD PURSUANT TO 10 CFR 2.390**

PROPRIETARY - TRADE SECRET INFORMATION
WITHHELD PURSUANT TO 10 CFR 2.390

**PROPRIETARY - TRADE SECRET INFORMATION
WITHHELD PURSUANT TO 10 CFR 2.390**

**PROPRIETARY - TRADE SECRET INFORMATION
WITHHELD PURSUANT TO 10 CFR 2.390**

**PROPRIETARY - TRADE SECRET INFORMATION
WITHHELD PURSUANT TO 10 CFR 2.390**

**PROPRIETARY - TRADE SECRET INFORMATION
WITHHELD PURSUANT TO 10 CFR 2.390**

**PROPRIETARY - TRADE SECRET INFORMATION
WITHHELD PURSUANT TO 10 CFR 2.390**

PROPRIETARY - TRADE SECRET INFORMATION
WITHHELD PURSUANT TO 10 CFR 2.390

PROPRIETARY - TRADE SECRET INFORMATION
WITHHELD PURSUANT TO 10 CFR 2.390

**PROPRIETARY - TRADE SECRET INFORMATION
WITHHELD PURSUANT TO 10 CFR 2.390**

PROPRIETARY - TRADE SECRET INFORMATION
WITHHELD PURSUANT TO 10 CFR 2.390

**PROPRIETARY - TRADE SECRET INFORMATION
WITHHELD PURSUANT TO 10 CFR 2.390**

PROPRIETARY - TRADE SECRET INFORMATION
WITHHELD PURSUANT TO 10 CFR 2.390

SECTION A8

ACCIDENT ANALYSIS

A8.1 OFF-NORMAL OPERATIONS

Off-normal operations are design events of the second type (Design Event II) as defined in ANSI/ANS 57.9 (Reference 1). Design Event II consists of that set of events that, although not occurring regularly, can be expected to occur with moderate frequency or on the order of once during a calendar year of ISFSI operation.

Of the various types of Design Event II conditions described in Reference 1, only the loss of external power supply for a limited duration is considered to be applicable and credible to ISFSI operations. Loss of electric power as an off-normal condition is analyzed below.

A8.1.1 LOSS OF ELECTRICAL POWER

A total loss of ac power is postulated to occur in the feeder cabling which supplies power to the ISFSI. The failure could be either an open or a short to ground circuit, or any other mechanism capable of producing an interruption of power.

A8.1.1.1 POSTULATED CAUSE OF THE EVENT

A loss of power to the ISFSI may occur as a result of natural phenomena, such as lightning or extreme wind, or as a result of undefined disturbances in the non-safety-related portion of the electric power system of the Prairie Island Nuclear Generating Plant (PINGP).

If electric power is lost, the following systems could be de-energized and rendered nonfunctional:

- Area lighting
- Area receptacles
- Cask pressure monitoring instrumentation

A8.1.1.2 DETECTION OF EVENTS

A loss of power at the PINGP site would be indicated and/or alarmed in the main control room. If the loss of power were localized at the ISFSI site, this would be detected during periodic surveillance by noting that area lighting is not operational.

A8.1.1.3 ANALYSIS OF EFFECTS AND CONSEQUENCES

This event has no safety or radiological consequences because a loss of power will not affect the integrity of the storage casks, jeopardize the safe storage of the fuel, or result in radiological releases. None of the systems whose failure could be caused by this event are necessary for the accomplishment of the safety function of the ISFSI. The lighting system functions merely for convenience and visual monitoring, and the instrumentation monitors the long-term performance of the storage casks with respect to the cask seals. None of these parameters are expected to change rapidly and their status is not dependent upon electric power.

A8.1.1.4 CORRECTIVE ACTION

Following a loss of electric power to the ISFSI, plant maintenance personnel will be informed and will isolate the fault and restore service by conventional means. Such an operation is straightforward and routine for the maintenance personnel of an electric utility.

A8.1.2 RADIOLOGICAL IMPACT FROM OFF-NORMAL OPERATIONS

No radiological impact from off-normal operations is postulated.

A8.2 ACCIDENTS

Accidents are design events of the third and fourth type (Design Events III and IV) as defined in ANSI/ANS 57.9 (Reference 1). Design Event III consists of that set of infrequent events that could reasonably be expected to occur during the lifetime of the ISFSI.

Design Event IV consists of the events that are postulated because their consequences may result in the maximum potential impact on the immediate environs. Their consideration establishes a conservative design basis for certain systems with important confinement features.

A8.2.1 EARTHQUAKE

A8.2.1.1 CAUSE OF ACCIDENT

The design earthquake (DE) is postulated to occur as a design basis extreme natural phenomenon.

A8.2.1.2 ACCIDENT ANALYSIS

Cask response to a seismic event is evaluated in Sections A3.2.3 and A4.2.3. Results of these analyses show that the cask does not tip over or slide and that the containment vessel stresses resulting from the seismic loads are below ASME code allowable stresses for accident conditions. The integrity of the cask is not compromised. No damage to the cask is postulated. The basket stresses are also low and do not result in deformations that would prevent fuel from being unloaded from the cask.

A8.2.1.3 ACCIDENT DOSE CALCULATIONS

The DE does not damage the cask. Hence, no radioactivity is released and there is no associated dose increase due to this event.

A8.2.2 EXTREME WIND

A8.2.2.1 CAUSE OF ACCIDENT

The extreme winds due to passage of the design tornado as defined in Section A3.2.1 are postulated to occur as an extreme natural phenomenon.

A8.2.2.2 ACCIDENT ANALYSIS

In Section A3.2.1, it is shown that extreme winds do not result in a cask tip over or sliding of the cask. The pressure due to high winds on the surface of the cask is bounded by the assumed external pressure of 25 psig. The stresses in the cask resulting from this external pressure are presented in Appendix A4A. High winds have no effect on the integrity of the cask, and do not result in damage to the cask. High winds do not affect the basket or the ability to retrieve the spent fuel from the cask. The effect of tornado missiles hitting the cask has been evaluated in Section A3.2.1. These analyses show that the stresses in the cask as a result of missile impact are well below the ASME Code allowable stresses for Accident (Level D) conditions. It is also shown in Section A3.2.1 that the tornado missile impact will not result in a cask tip over. Local damage to the neutron shield may result from the tornado missile impact.

A8.2.2.3 ACCIDENT DOSE CALCULATIONS

Extreme winds are not capable of overturning the casks nor of damaging the cask seals. The overpressure system and the neutron shielding may be damaged.

To determine the bounding dose rate, loss of neutron shielding (322 mrem from Section A8.2.5) is combined with the total effective dose equivalent (TEDE) from the loss of one confinement barrier and 100% fuel cladding failure (24 mrem from Section A8.2.9). The resulting site boundary accident dose, 346 mrem, is below the 5 rem TEDE limit as specified in 10 CFR 72.106(b) (Reference 2).

A8.2.3 FLOOD

A8.2.3.1 CAUSE OF ACCIDENT

The probable maximum flood has been calculated to reach a level of 703.6 ft., with wave action to a maximum level of 706.7 ft.

A8.2.3.2 ACCIDENT ANALYSIS

The casks are designed to withstand the forces developed by the probable maximum flood without damage to cask integrity or tipping of the casks. The height of the cask seals will be above the level of the probable maximum flood and associated wave action. Accordingly no fuel damage or criticality is postulated to occur as a result of flooding. Analyses are contained in Section A3.2.2.

A8.2.3.3 ACCIDENT DOSE CALCULATIONS

The probable maximum flood is not capable of overturning the casks or of damaging their seals. Therefore, no resultant doses are projected.

A8.2.4 EXPLOSION

A8.2.4.1 CAUSE OF ACCIDENT

A munition barge explosion has been postulated to occur at a location approximately 2600 feet from the ISFSI. This occurrence is described in detail in Section 2.2. The pressure wave of 2.25 psi is estimated to occur at the ISFSI.

A8.2.4.2 ACCIDENT ANALYSIS

The TN-40HT cask is designed for an external pressure of 25 psig as described in Appendix A4A.

A8.2.4.3 ACCIDENT DOSE CALCULATIONS

The cask will not tip as a result of the postulated pressure wave. Accordingly, no cask damage or release of radioactivity is postulated. Since no radioactivity is released, no resultant dose increase is associated with this event.

A8.2.5 FIRE

A8.2.5.1 CAUSE OF ACCIDENT

The only combustible materials in the ISFSI are in the form of insulation on instrumentation wiring and paint on the outside surface of the storage casks. In addition, the transport vehicle will contain a small amount of gasoline or diesel fuel. No other combustible or explosive materials are allowed to be stored on the ISFSI slabs. The ISFSI area is cleared of trees. The entire area surrounding the Equipment Storage Building and concrete pad within the perimeter road is covered with crushed rock. In addition, other equipment in the area is adequately separated from the ISFSI slabs. Therefore, no fires other than small electrical fires are considered credible at the ISFSI. 60400000330

However, a hypothetical fire accident is evaluated for the TN-40HT cask based on a fuel fire, the source of fuel being that from a ruptured fuel tank of the wheeled cask transporter tow vehicle or tracked cask transporter. The bounding capacity of the fuel tank is 200 gallons and the bounding hypothetical fire is an engulfing fire around the cask.

A8.2.5.2 ACCIDENT ANALYSIS

The evaluation of the hypothetical fire event is presented in Section A3.3.2.2.2. The fire thermal evaluation is performed primarily to demonstrate the containment integrity of the TN-40HT cask. This is assured as long as the metal lid seals remain below 536 °F and the cavity pressure is less than 100 psig.

Based on the thermal analyses for the fire accident conditions, the TN-40HT cask can withstand the hypothetical fire accident event without compromising its containment integrity. No melting of the metallic cask components occurs. Peak cask component temperatures are summarized in Table A3.3-6. The maximum seal temperature is well below the temperature limit of the metal seals. Table A3.3-15 and Table A3.3-16 show that at the elevated temperatures corresponding to the hypothetical fire, the cask cavity pressure remains below the analyzed pressure of 100 psig.

A8.2.5.3 ACCIDENT DOSE CALCULATIONS

Local damage to the neutron shielding may result from the fire. This is bounded by removal of all the neutron shielding which is evaluated in Appendix A7A. Even with this conservative assumption, the site boundary accident dose rates are below 5 rem to the whole body or any organ as specified in 10CFR72.106(b) (Reference 2).

The off-site doses are evaluated for the following accident condition:

1) loss of radial neutron shielding and
2) loss of the protective cover and top neutron shield.

For accident conditions, the following assumptions are made:

a) the nearest postulated site boundary is 100 meters distant from the cask
b) the accident involves a single cask
c) the accident duration is 30 days
d) a person remains at the postulated site boundary 24 hours per day for the entire duration

The normal condition total dose rates at 100 meters are scaled by the ratio of accident to normal surface dose rates as shown in the following table. All units are mrem/hr.

	Normal Dose Rate 100 m Table A7A.2-2	**Accident, Surface Table A7A.2-1**	**Average, Surface Table A7A.2-1**	**Accident, 100 m mrem/hr**
Gamma	7.59E-03	116	35.5	2.48E-02
Neutron	1.67E-02	1980	78.7	4.20E-01
			Total:	4.45E-01

The total dose over 30 days would be 320 mrem. The background from the rest of the ISFSI would be less than 1/12 of the 25 mrem/year limit (10 CFR 72.104) (Reference 2), or 2 mrem. The combined total accident dose would be 322 mrem. There is no activity release from the cask containment.

A8.2.6 INADVERTENT LOADING OF A NEWLY DISCHARGED FUEL ASSEMBLY

A8.2.6.1 CAUSE OF ACCIDENT

The possibility of a spent fuel assembly, with a heat generation rate greater than 0.8 kw, being erroneously selected for storage in a cask has been considered. The cause of this accident is postulated to be an error during the loading operations, e.g., wrong assembly picked by the fuel handling crane, or a failure in the administrative controls governing the fuel handling operations.

A8.2.6.2 ACCIDENT ANALYSIS

The fuel assemblies require several years of storage in the spent fuel pool before the heat generation decays to a rate below 0.8 kw. This accident scenario postulates the inadvertent loading of an assembly not intended for storage in the storage canister, with a heat generation rate in excess of the design basis specified in Section A3.1.1.

In order to preclude this accident from going undetected, and to ensure that appropriate rectification actions can take place prior to the sealing of the casks, a final verification of the assemblies loaded into the casks and a comparison with fuel management records will be performed to ensure that the loaded assemblies do not exceed any of the specified limits.

These administrative controls and the records associated with them will be included in the procedures described in Section A9 and will comply with the applicable requirements of the Quality Assurance Program described in Section A11.

Therefore, appropriate and sufficient actions will be taken to ensure that an erroneously loaded fuel assembly does not remain undetected. In particular, the storage of a fuel assembly with a heat generation in excess of 0.8 kw is not considered credible in view of the multiple administrative controls.

A8.2.6.3 ACCIDENT DOSE CALCULATIONS

The inadvertent loading of a fuel assembly not intended for storage in a storage cask is not considered to be a credible occurrence. Therefore, no doses are postulated.

A8.2.7 CASK SEAL LEAKAGE

The storage casks feature redundant seals in conjunction with an extremely rugged body design. Additional barriers to the release of radioactivity are presented by the sintered fuel pellet matrix and the Zircaloy cladding which surrounds the fuel pellets. Furthermore, the interseal gaps are pressurized in excess of the cask cavity. As a result, no credible mechanisms that could result in leakage of radioactive products have been identified. Nevertheless, a loss of the storage cask confinement capability is postulated in Section A8.2.9, and the results found to be negligible.

A8.2.8 HYPOTHETICAL CASK DROP ACCIDENT

A8.2.8.1 CAUSE OF ACCIDENT

The stability of the TN-40HT storage cask in the upright position on the ISFSI concrete storage pad is demonstrated in Section A3.2. The effects of tornado wind and missiles, flood water and earthquakes are described in Sections A3.2.1, A3.2.2 and A3.2.3, respectively. It is shown in those sections that the cask will not tip over under the most severe natural phenomena specified in the Prairie Island Updated Safety Analysis Report.

The cask is lifted at Prairie Island using a single failure proof crane. The upper trunnions are designed to meet the requirements of NUREG-0612 (Reference 5) for non-redundant lifting fixture. This is accomplished by evaluating the trunnions to the stress design factors required by ANSI N14.6 (Reference 3), i.e. capable of lifting 6 times and 10 times the cask weight without exceeding the yield and ultimate strengths of the material, respectively. The loaded cask will be handled by the transport vehicle in a vertical orientation and not lifted higher than 18 in.

However section of the SAR considers design events of the third and fourth types (includes accidents) as defined in ANSI/ANS 57.9. The third type of events are those that could reasonably be expected to occur over the lifetime of the ISFSI (does not include dropping of the cask). The fourth type of event includes severe natural phenomena (described in Section A8.2.1 through A8.2.5) and man-induced low probability events postulated because their consequences could result in the maximum potential impact on the immediate environs. Therefore the cask is examined for a dropping accident which is an impact event that is extremely unlikely to occur.

A8.2.8.2 ACCIDENT ANALYSIS

In this section the cask is evaluated under bottom end impact on the ISFSI storage pad after a drop from a height of 18 in. The storage pad is the hardest concrete surface outside of the containment building. The cask is always oriented vertically and is never lifted higher than 18 in. once it leaves the containment building. Therefore this case is an upper bound drop event since impact onto a softer surface would result in lower cask deceleration and a lower impact force.

A8.2.8.2.1 DYNAMIC IMPACT LOADS

The peak decelerations in the cask and basket during the 18 inch end drop were calculated by a dynamic nonlinear analysis described in Section A4A.10. The analysis showed a maximum acceleration in the TN40HT cask body of 44.1g. This occurred in the bottom plate. The highest acceleration in the basket and fuel was 28.8g. However, since the basket and fuel were not modeled explicitly, the maximum acceleration (28.8g) must be multiplied by the dynamic load factor of 1.52 resulting in a maximum loading of 43.8g.

To bound as-built conditions, an additional cask end drop accident analysis was performed using a bounding concrete strength of 7,500 psi. The analysis was performed using the same input files for the LS-DYNA model that was created for the original analysis (described in Section A4A.10). The analysis confirmed that an 18 in. end drop of the TN-40HT cask onto the ISFSI pad remains bounded by an end drop resulting in a 50 g deceleration.

A8.2.8.2.2 CASK BODY ANALYSIS

The cask is analyzed conservatively for a 50 g vertical load simulating the end drop. The evaluation is presented in Section A4.2.3.4. All calculated stresses meet code allowables.

A8.2.8.2.3 LID BOLT ANALYSIS

During a bottom end drop, the rim of the lid is forced against the flange of the cask body. The lid is initially seated against the flange by preloading (torquing) the bolts. The bolt preload will not be affected if compressive yielding of the contact bearing area does not occur.

The evaluation of the cask presented in Section A4.2.3.4 shows that during a drop cask accident the maximum stresses in the lid outer plate and the shell flange are less than the yield stress. Thus the bolt preload will not be affected by the bottom drop. Therefore, this hypothetical accident case will not affect the bolts.

A8.2.8.2.4 BASKET ANALYSIS

The basket is analyzed conservatively for a 50 g vertical load simulating the end drop. The evaluation is presented in, Section A4.2.3.4. All calculated stresses meet code allowables.

A8.2.8.3 ACCIDENT DOSE CALCULATIONS

Cask drop will not breach the cask confinement barrier. No radioactivity will be released and no resultant doses will occur.

However, a bounding dose can be determined. The loss of neutron shielding (322 mrem from Section A8.2.5) is combined with the total effective dose equivalent (TEDE) from the loss of one confinement barrier and 100% fuel cladding failure (24 mrem from Section A8.2.9). The resulting site boundary accident dose, 346 mrem, is below the 5 rem TEDE limit as specified in 10 CFR 72.106(b) (Reference 2).

A8.2.9 LOSS OF CONFINEMENT BARRIER

A8.2.9.1 CAUSE OF ACCIDENT

A combined event of failure of one of the seals in addition to a failure of the pressure monitoring system is assessed. This could also be a failure of the pressure boundary of the overpressure system.

A8.2.9.2 ACCIDENT ANALYSIS

Analysis has been performed in Appendix A4A to show that the bolts will be able to maintain the seal under accident conditions. Thus the leak rate is limited to the test leak rate of 1 $x10^{-5}$ ref cm^3/s.

A description of the three possible leaks which could occur is presented below:

- <u>In any of the inner containment seals (lid seal, inner vent seal or inner drain seal)</u>

  The lid and lid penetration cover bolts and seals are designed to prevent leakage during all postulated accident events. Therefore, this is a very unlikely event.

  In this case the overpressure system, which has a higher pressure than the cask cavity, would leak helium into the cask cavity. Since the pressure is higher in the overpressure tank, it would prevent leakage of radioactive materials out of the cask cavity until the pressure between the overpressure tank and the cask cavity equalized. This would take several years, depending on the size of the leak. At the test leak rate, the overpressure system pressure would always exceed the cask cavity pressure, as shown in Appendix A7A. Therefore no leakage of radioactive material can occur, even if the alarm were to fail. Appendix A7A also demonstrates that even if the inner seal has experienced a latent seal failure there is ample time for identifying the leak through routine surveillances.

- <u>In any of the outer seals (lid, overpressure port cover, vent cover or drain cover)</u>

  The lid and lid penetration cover bolts and seals are designed to prevent leakage during all postulated accident events. Therefore, this is a very unlikely event.

  In this case, leakage out of the interspace to the atmosphere would occur. This would not result in release of radioactive material from the cask cavity since the inner seal is intact. Again, as demonstrated in Appendix A7A, a latent seal failure of the outer seals would not result in a release of any radioactive material to the environment. There is also ample time for identifying the leak through routine surveillances.

- <u>A leak in the overpressure system</u>

  This is the most likely cause of a leak.

  In this case two scenarios could exist:

  - The overpressure system is not functioning and the inner seal is intact. In this case there is no release of radioactive material to the environment; or

  - The overpressure system is not functioning and the inner seal is leaking at some rate.

In this latter case, leakage out of the interspace to the atmosphere and the cask cavity could occur. This would not result in release of radioactive material from the cask cavity until the pressure fell to the cask cavity pressure.

At the test leak rate of 1 x 10^{-5} ref cm^3/s, this would not occur during a 25 year storage period. However, a leak of this magnitude in combination with a loss of the over pressure system has been evaluated in Appendix A7A.

A8.2.9.3 ACCIDENT DOSE CALCULATIONS

The results of the calculations in Appendix A7A assuming accident conditions indicated that at the site boundary (110m from the cask), for a 30 day release, the total effective dose equivalent is 24 mrem. The total organ dose equivalent to any individual organ (the critical organ in this case is the bone surface) is 244 mrem for a 30 day release. The lens dose equivalent to the lens of the eye is 24.1 mrem for a 30 day release. These values are well below the limiting off site doses defined in 10 CFR 72.106(b).

Another accident condition under consideration is that the overpressure system is not functioning and the inner seal has experienced a latent seal failure. This analysis is presented in Appendix A7A. This accident analysis demonstrates that a latent failure up to 100 times greater that the test value could occur and there is ample time for recovery before the limiting off site doses in 10 CFR 72.106(b) are met. The probability that a gross leak of an inner seal in combination with a gross leak in the outer seal is not considered a credible event.

A8.3 SITE CHARACTERISTICS AFFECTING SAFETY ANALYSIS

Site characteristics have been considered in the formation of the bases for these safety analyses. Conservative assumptions concerning meteorology were used in the determination of χ/Q. The characteristics of extreme winds and their contribution to maximum flood level were considered. Regional and site seismology and geology were used to help define the design earthquake acceleration value and analyze for liquefaction potential. Population distribution and other demographic data were used to determine radiation doses.

Other site characteristics affecting safety analyses include the proximity to the Mississippi River to the ISFSI assumptions concerning barge traffic was used to develop the bases for the explosion (Section A8.2.4).

A8.4 REFERENCES

1. American Nuclear Society, ANSI/ANS-57.9, Design Criteria for an Independent Spent Fuel Storage Installation (Dry Storage Type), 1992.

2. 10 CFR Part 72, “Licensing Requirements for the Independent Storage of Spent Nuclear Fuel and High-Level Radioactive Waste.”

3. American National Standards Institute, ANSI N14.6, Special Lifting Devices for Shipping Containers Weighing 10,000 pounds or More, 1986.

4. “Structural Design of Concrete Storage Pads for Spent Fuel Casks”, EPRI NP-7551, August 1991 by Rashid, Nickel and James.

5. NUREG-612 “Control of Heavy Loads at Nuclear Power Plants”, July 1980

SECTION A9

CONDUCT OF OPERATIONS

A9.1 ORGANIZATIONAL STRUCTURE

A9.1.1 CORPORATE ORGANIZATION

A9.1.1.1 CORPORATE FUNCTIONS, RESPONSIBILITIES AND AUTHORITIES

The information in Section 9.1.1.1 is independent of cask design.

A9.1.1.2 ISFSI PROJECT ORGANIZATION

The information in Section 9.1.1.2 is independent of cask design.

A9.1.1.3 RELATIONSHIP WITH CONTRACTORS AND SUPPLIERS

The information in Section 9.1.1.3 is independent of cask design.

A9.1.1.4 TECHNICAL STAFF

The information in Section 9.1.1.4 is independent of cask design.

A9.1.2 OPERATING ORGANIZATION, MANAGEMENT AND ADMINISTRATIVE CONTROL SYSTEM

A9.1.2.1 ONSITE ORGANIZATION

The information in Section 9.1.2.1 is independent of cask design.

A9.1.2.2 PERSONNEL FUNCTIONS, RESPONSIBILITIES AND AUTHORITIES

The information in Section 9.1.2.2 is independent of cask design.

A9.1.3 PERSONNEL QUALIFICATION REQUIREMENTS

A9.1.3.1 MINIMUM QUALIFICATION REQUIREMENTS

The information in Section 9.1.3.1 is independent of cask design.

A9.1.3.2 QUALIFICATIONS OF PERSONNEL

The information in Section 9.1.3.2 is independent of cask design.

A9.1.4 LIAISON WITH OUTSIDE ORGANIZATIONS

The information in Section 9.1.4 is independent of cask design.

A9.2 STARTUP TESTING AND OPERATION

A9.2.1 ADMINISTRATIVE PROCEDURES FOR CONDUCTING TEST PROGRAM

The information in Section 9.2.1 is independent of cask design.

A9.2.2 TEST PROGRAM DESCRIPTION

A9.2.2.1 PHYSICAL FACILITIES

The information in Section 9.2.2.1 is independent of cask design.

A9.2.2.2 OPERATIONS

The information in Section 9.2.2.2 is independent of cask design.

A9.2.3 TEST DISCUSSION

The information in Section 9.2.3 is independent of cask design.

A9.2.4 COMPLETION OF PRE-OPERATIONAL TEST PROGRAM

The information in Section 9.2.4 is independent of cask design.

A9.3 TRAINING PROGRAM

The information in Section 9.3 is independent of cask design.

A9.4 NORMAL OPERATIONS

A9.4.1 PROCEDURES

The information in Section 9.4.1 is independent of cask design.

A9.4.1.1 ADMINISTRATIVE PROCEDURES

The information in Section 9.4.1.1 is independent of cask design.

A9.4.1.2 ANNUNCIATOR RESPONSE GUIDES

The information in Section 9.4.1.2 is independent of cask design.

A9.4.1.3 RADIATION PROTECTION PROCEDURES

The information in Section 9.4.1.3 is independent of cask design.

A9.4.1.4 MAINTENANCE PROCEDURES

The information in Section 9.4.1.4 is independent of cask design.

A9.4.1.5 OPERATING PROCEDURES

The information in Section 9.4.1.5 is independent of cask design.

A9.4.1.6 TEST PROCEDURES

The information in Section 9.4.1.6 is independent of cask design.

A9.4.1.7 PREOPERATIONAL TEST PROCEDURES

The information in Section 9.4.1.7 is independent of cask design.

A9.4.1.8 QUALITY ASSURANCE PROCEDURES

The information in Section 9.4.1.8 is independent of cask design.

A9.4.2 RECORDS

The information in Section 9.4.2 is independent of cask design.

A9.5 EMERGENCY PLANNING

The information in Section 9.5 is independent of cask design.

A9.6 PHYSICAL SECURITY PLAN

The information in Section 9.6 is independent of cask design.

A9.7 ADDITIONAL FABRICATION TESTING AND INSPECTIONS

A9.7.1 CHARPY IMPACT TESTING

The base metals for the TN-40HT shield shell and bottom shield shall be subject to Charpy impact testing in accordance with ASME Code (Reference 4) NF-2320 at -20°F during cask fabrication. The acceptance standard shall be a minimum energy absorption of 18 ft-lb.

The weld filler material and Heat Affected Zone (HAZ) shall be subject to Charpy impact testing per ASME Code NF-2431.1(a) through (d), except that:

a) In lieu of the base materials specified for weld test assemblies in the governing weld material specification (SFA), the weld test assemblies for Charpy impact testing shall be prepared using the same base metals that are used for the shield shell and bottom shield.
b) Charpy impact testing shall be performed for both the weld filler material and the heat affected zone of each base metal.
c) The acceptance standard shall be a minimum energy absorption of 18 ft-lb.

A9.7.2 WELDING REQUIREMENTS AND INSPECTIONS

Qualification of welding procedures and welders shall be determined using Section IX of the ASME Code, Reference 4.

The ASME Code qualified materials (i.e. containment boundary) used in the construction of the TN-40HT shall be examined following the requirements of ASME Code Section II. Section V of the ASME Code shall be used in producing Non-destructive examination (NDE) specifications and procedures. NDE requirements for welds are specified on the drawings provided in Chapter A1. Acceptance criteria are as specified by the governing code. NDE personnel shall be qualified in accordance with SNT-TC-1A, Reference 5.

The confinement welds on the TN40HT shall be inspected in accordance with ASME Code Subsection NB including alternatives to ASME Code specified in SAR Section A3.5.

Non-confinement welds shall be inspected in accordance with ASME Code Subsection NF including alternatives to the Code as specified in SAR Section A3.5.

Basket welds shall be inspected to the NDE acceptance criteria of ASME Code Subsection NG as described on the drawings in Section A1. Alternatives to the ASME Code are specified in SAR Section A3.5.

A9.7.3 NEUTRON ABSORBER REQUIREMENTS

The neutron absorber used for criticality control in the TN-40HT basket may consist any of the following types of material:

(a) Boron-aluminum alloy (borated aluminum)

(b) Boron carbide / aluminum metal matrix composite (MMC)

(c) Boral®

The TN-40HT safety analyses do not rely upon the tensile strength of these materials. The radiation and temperature environment in the cask is not sufficiently severe to damage these metallic/ceramic materials.

To assure performance of the neutron absorber's design function only visual inspections, thermal conductivity testing, and the presence / uniformity of B10 need to be verified with testing requirements specific to each material.

References to metal matrix composites throughout this chapter are not intended to refer to borated aluminum or Boral®.

A9.7.3.1 BORON ALUMINUM ALLOY (BORATED ALUMINUM)

Description

The material is produced by direct chill (DC) or permanent mold casting with boron precipitating as a uniform fine dispersion of discrete aluminum diboride (AlB_2) or Titanium diboride (TiB_2) particles in the matrix of aluminum or aluminum alloy. For extruded products, the TiB_2 form of the alloy shall be used. For rolled products, the AlB_2, the TiB_2, or a hybrid may be used.

Boron is added to the aluminum in the quantity necessary to provide the specified minimum B10 areal density in the final product. The boron may have the natural isotopic distribution or may be enriched in B10.

The criticality calculations take credit for 90% of the minimum specified B10 areal density of borated aluminum. The basis for this credit is the B10 areal density acceptance testing, which shall be as specified in Section A9.7.4.3.

Requirements

The boron content in the aluminum or aluminum alloy shall not exceed 5% by weight.

The neutron absorbers shall be 100% visually inspected in accordance with the inspection requirements described in Section A9.7.4.1.

The thermal conductivity of the material shall be tested in accordance with the testing requirements in Section A9.7.4.2.

The minimum B10 areal density specified in Table A3.3-17 shall be confirmed via neutron transmission testing as described in Section A9.7.4.3.

A9.7.3.2 BORON CARBIDE / ALUMINUM METAL MATRIX COMPOSITES (MMC)

Description

The material is a composite of fine boron carbide particles in an aluminum or aluminum alloy matrix. The material shall be produced by either direct chill casting, permanent mold casting, powder metallurgy, or thermal spray techniques. It is a low-porosity product, with a metallurgically bonded matrix.

The criticality calculations take credit for 90% of the minimum specified B10 areal density of MMCs. The basis for this credit is the B10 areal density acceptance testing, which is specified in Section A9.7.4.3.

Requirements

For non-clad MMC products, the boron carbide content shall not exceed 40% by volume. The boron carbide content for MMCs with an integral aluminum cladding shall not exceed 50% by volume.

Non-clad MMC products shall have a density greater than 98% of theoretical density, with no more than 0.5 volume % interconnected porosity. For MMC with an integral cladding, the final density of the core shall be greater than 97% of theoretical density, with no more than 0.5 volume % interconnected porosity of the core and cladding as a unit of the final product.

Boron carbide particles for the products considered here typically have an average size in the range 10-40 microns, although the actual specification may be by mesh size, rather than by average particle size. No more than 10% of the particles shall be over 60 microns.

The neutron absorbers shall be 100% visually inspected in accordance with the inspection requirements described in Section A9.7.4.1.

The thermal conductivity of the material shall be tested in accordance with the testing requirements in Section A9.7.4.2.

The minimum B10 areal density specified in Table A3.3-17 shall be confirmed via neutron transmission testing as described in Section A9.7.4.3.

The MMCs material shall be qualified in accordance with the requirements specified in Section A9.7.5, and shall subsequently be subject to the process controls specified in Section A9.7.6.

A9.7.3.3 BORAL®

Description

This material consists of a core of aluminum and boron carbide powders between two outer layers of aluminum, mechanically bonded by hot-rolling an "ingot" consisting of an aluminum box filled with blended boron carbide and aluminum powders. The core, which is exposed at the edges of the sheet, is slightly porous. The average size of the boron carbide particles in the finished product is approximately 50 microns after rolling.

The criticality calculations take credit for 75% of the minimum specified B10 areal density of Boral®.

Requirements

The nominal boron carbide content shall be limited to 65% (+ 2% tolerance limit) of the core by weight.

The neutron absorbers shall be 100% visually inspected in accordance with the inspection requirements described in Section A9.7.4.1.

The thermal conductivity of the material shall be tested in accordance with the testing requirements in Section A9.7.4.2.

The minimum B10 areal density specified in Table A3.3-17 shall be confirmed via chemical analysis and by certification of the B10 isotopic fraction for the boron carbide powder, or by neutron transmission testing described in Section A9.7.4.3. Areal density testing shall be performed on a coupon taken from the sheet produced from each ingot. If the measured areal density is below that specified, all the material produced from that ingot will be either rejected, or accepted only on the basis of alternate verification of B10 areal density for each of the final pieces produced from that ingot.

A9.7.4 NEUTRON ABSORBERS ACCEPTANCE TESTING

A9.7.4.1 VISUAL INSPECTIONS OF NEUTRON ABSORBERS

For borated aluminum and MMCs, visual inspections shall follow the recommendations in Aluminum Standards and Data (Reference 6), Chapter 4 “Quality Control, Visual Inspection of Aluminum Mill Products and Castings”. Local or cosmetic conditions such as scratches, nicks, die lines, inclusions, abrasion, isolated pores, or discoloration are acceptable. Widespread blisters, rough surface, or cracking shall be treated as non-conforming. Inspection of MMCs with an integral aluminum cladding shall also include verification that the matrix is not exposed through the faces of the aluminum cladding and that solid aluminum is not present at the edges.

For Boral®, visual inspection shall verify that there are no cracks through the cladding, exposed core on the face of the sheet, or solid aluminum at the edge of the sheet.

A9.7.4.2 THERMAL CONDUCTIVITY TESTING OF NEUTRON ABSORBERS

Testing shall conform to ASTM E1225 (Reference 7), ASTM E1461 (Reference 8), or equivalent method, performed at room temperature on coupons taken from the rolled or extruded production material. Previous testing of borated aluminum and metal matrix composite, Table A9.7-1, shows that thermal conductivity increases slightly with temperature. Initial sampling shall be one test per lot, defined by the heat or ingot, and may be reduced if the first five tests meet the specified minimum thermal conductivity.

If a thermal conductivity test result is below the specified minimum, at least four additional tests shall be performed on the material from that lot. If the mean value of those tests, including the original test, falls below the specified minimum the associated lot shall be rejected. 01424752

After twenty five tests of a single type of material, with the same aluminum alloy matrix, the same boron content, and the same primary boron phase, e.g., B_4C, TiB_2, or AlB_2, if the mean value of all the test results less two standard deviations meets the specified thermal conductivity, no further testing of that material is required. This exemption may also be applied to the same type of material if the matrix of the material changes to a more thermally conductive alloy (e.g., from 6000 to 1000 series aluminum), or if the boron content is reduced without changing the boron phase.

The thermal analysis in Chapter A3.3.2.2 considers a dual plate basket construction base model with 0.125" thick neutron absorber with a 0.312" thick aluminum 1100 plate. This model gives the bounding values for the maximum component temperatures. Either a dual plate basket construction or an alternate single plate (borated aluminum or MMC) construction basket may be utilized. For the dual plate construction, the specified thickness of the neutron absorber may vary, and the thermal conductivity acceptance criterion for the neutron absorber will be based on the nominal thickness specified. In either construction type, to maintain the thermal performance of the basket, the minimum thermal conductivity shall be such that the total thermal conductance (sum of conductivity * thickness) of the neutron absorber and the aluminum 1100 plate shall at least equal the conductance assumed in the thermal analysis, 3.55 BTU/hr-deg F. Samples of the acceptance criteria for various neutron absorber thicknesses are highlighted in Table A9.7-2.

The aluminum 1100 plate does not need to be tested for thermal conductivity; the material may be credited with the values published in the ASME Code Section II part D. The neutron absorber material need not be tested for thermal conductivity if the nominal thickness of the aluminum 1100 plate is 0.320 inch or greater.

01424752

A9.7.4.3 NEUTRON TRANSMISSION TESTING OF NEUTRON ABSORBERS

Neutron Transmission acceptance testing procedures shall be subject to approval by Transnuclear . Test coupons shall be removed from the rolled or extruded production material at locations that are systematically or probabilistically distributed throughout the lot. Test coupons shall not exhibit physical defects that would not be acceptable in the finished product, or that would preclude an accurate measurement of the coupon's physical thickness.

A lot is defined as all the pieces produced from a single ingot or heat or from a group of billets from the same heat. If this definition results in a lot size too small to provide a meaningful statistical analysis of results, an alternate larger lot definition may be used, so long as it results in accumulating material that is uniform for sampling purposes.

The sampling rate for neutron transmission measurements shall be such that there is at least one neutron transmission measurement for each 2000 square inches of final product in each lot.

The B10 areal density is measured using a collimated thermal neutron beam of up to 1 inch diameter.

The neutron transmission through the test coupons is converted to B10 areal density by comparison with transmission through calibrated standards. These standards are composed of a homogeneous boron compound without other significant neutron absorbers. For example, boron carbide, zirconium diboride or titanium diboride sheets are acceptable standards. These standards are paired with aluminum shims sized to match the effect of neutron scattering by aluminum in the test coupons. Uniform but non-homogeneous materials such as metal matrix composites may be used for standards, provided that testing shows them to provide neutron attenuation equivalent to a homogeneous standard. Standards will be calibrated, traceable to nationally recognized standards, or by attenuation of a monoenergetic neutron beam correlated to the known cross section of boron 10 at that energy.

Alternatively, digital image analysis may be used to compare neutron radioscopic images of the test coupon to images of the standards. The area of image analysis shall be up to 0.75 sq. inch.

The minimum areal density specified shall be verified for each lot at the 95% probability, 95% confidence level or better. If a goodness-of-fit test demonstrates that the sample comes from a normal population, the one-sided tolerance limit for a normal distribution may be used for this purpose. Otherwise, a non-parametric (distribution-free) method of determining the one-sided tolerance limit may be used. Demonstration of the one-sided tolerance limit shall be evaluated for acceptance in accordance with Transnuclear 's QA procedures.

The following illustrates one acceptable method and is intended to be utilized as an example. The acceptance criterion for individual plates is determined from a statistical analysis of the test results for their lot. The B10 areal densities determined by neutron transmission are converted to volume density, i.e., the B10 areal density is divided by the thickness at the location of the neutron transmission measurement or the maximum thickness of the coupon. The lower tolerance limit of B10 volume density is then determined as the mean value of B10 volume density for the sample less K times the standard deviation, where K is the one-sided tolerance limit factor with 95% probability and 95% confidence (Reference 9).

Finally, the minimum specified value of B10 areal density is divided by the lower tolerance limit of B10 volume density to arrive at the minimum plate thickness which provides the specified B10 areal density.

Any plate which is thinner than the statistically derived minimum thickness or the minimum design thickness, whichever is greater, shall be treated as non-conforming, with the following exception. Local depressions are acceptable, so long as they total no more than 0.5% of the area on any given plate, and the thickness at their location is not less than 90% of the minimum design thickness.

Non-conforming material shall be evaluated for acceptance in accordance with Transnuclear 's QA procedures.

A9.7.5 QUALIFICATION TESTING OF METAL MATRIX COMPOSITES

A9.7.5.1 APPLICABILITY AND SCOPE

Prior to initial use in a spent fuel dry storage system, new MMCs shall be subjected to qualification testing that will verify that the product satisfies the design function. Key process controls shall be identified per Section A9.7.6 so that the production material is equivalent to or better than the qualification test material. Changes to key processes shall be subject to qualification before use of such material in a spent fuel dry storage system.

ASTM methods and practices are referenced below for guidance. Alternative methods may be used with the approval of Transnuclear .

A9.7.5.2 DURABILITY

There is no need to include accelerated radiation damage testing in the qualification. Metals and ceramics do not experience measurable changes in mechanical properties due to fast neutron fluences typical over the lifetime of spent fuel storage.

Thermal damage and corrosion (hydrogen generation) testing shall be performed unless such tests on materials of the same chemical composition have already been performed and found acceptable. The following paragraphs illustrate two cases where such testing is not required.

Thermal damage testing is not required for unclad MMCs consisting only of boron carbide in an aluminum 1100 matrix, because there is no reaction between aluminum and boron carbide below 842 °F (Reference 10), well above the basket temperature under normal conditions of storage or transport.

Corrosion testing is not required for MMCs (clad or unclad) consisting only of boron carbide in an aluminum 1100 matrix, because testing on one such material has already been performed by Transnuclear (Reference 11).

A9.7.5.3 DELAMINATION TESTING OF CLAD MMC

Clad MMCs shall be subjected to thermal damage testing following water immersion to ensure that delamination does not occur under normal conditions of storage.

A9.7.5.4 REQUIRED TESTS AND EXAMINATIONS TO DEMONSTRATE MECHANICAL INTEGRITY

At least three samples, one each from approximately the two ends and middle of the test material production run shall be subjected to:

a) room temperature tensile testing (ASTM- B557 (Reference 12)) demonstrating that the material:

- has a 0.2% offset yield strength no less than 1.5 ksi;
- has an ultimate strength no less than 5.0 ksi; and
- has minimum elongation in two inches no less than 0.5%.

As an alternative to the elongation requirement, ductility may be demonstrated by bend testing per ASTM E290 (Reference 13). The radius of the pin or mandrel shall be no greater than three times the material thickness, and the material shall be bent at least 90 degrees without complete fracture.

b) testing by ASTM-B311 (Reference 14) to verify more than 98% theoretical density for non-clad MMCs and 97% for the matrix of clad MMCs. Testing or examination for interconnected porosity on the faces and edges of unclad MMC, and on the edges of clad MMC shall be performed by a method to be approved by Transnuclear. The maximum interconnect porosity is 0.5 volume %.

And for at least one sample,

c) for MMCs with an integral aluminum cladding, thermal durability testing demonstrating that after a minimum 24 hour soak in either pure or borated water, then insertion into a preheated oven at approximately 825°F for a minimum of 24 hours, the specimens are free of blisters and delamination and pass the mechanical testing requirements described in test ‘a’ of this section.

A9.7.5.5 REQUIRED TESTS AND EXAMINATIONS TO DEMONSTRATE B10 UNIFORMITY

Uniformity of the boron distribution shall be verified either by:

(a) Neutron radioscopy or radiography (ASTM E94 (Reference 15), E142 (Reference 16), and E545 (Reference 17)) of material from the ends and middle of the test material production run, verifying no more than 10% difference between the minimum and maximum B10 areal density, or

(b) Quantitative testing for the B10 areal density, B10 density, or the boron carbide weight fraction, on locations distributed over the test material production run, verifying that one standard deviation in the sample is less than 10% of the sample mean. Testing may be performed by a neutron transmission method similar to that specified in Section A9.7.4.3, or by chemical analysis for boron carbide content in the composite.

A9.7.5.6 APPROVAL OF PROCEDURES

Qualification procedures shall be subject to approval by Transnuclear.

A9.7.6 PROCESS CONTROLS FOR METAL MATRIX COMPOSITES

This section provides process controls to ensure that the material delivered for use is equivalent to the qualification test material.

A9.7.6.1 APPLICABILITY AND SCOPE

Key processing changes shall be subject to qualification prior to use of the material produced by the revised process. Transnuclear shall determine whether a complete or partial re-qualification program per Section A9.7.5 is required, depending on the characteristics of the material that could be affected by the process change.

A9.7.6.2 DEFINITION OF KEY PROCESS CHANGES

Key process changes are those which could adversely affect the uniform distribution of the boron carbide in the aluminum, reduced density, reduced corrosion resistance, or reduce the mechanical strength or ductility of the MMC.

A9.7.6.3 IDENTIFICATION AND CONTROL OF KEY PROCESS CHANGES

The manufacturer shall provide Transnuclear with a description of materials and process controls used in producing the MMC. Transnuclear and the manufacturer shall identify key process changes as defined in Section A9.7.6.2.

An increase in nominal boron carbide content over that previously qualified shall always be regarded as a key process change.

The following are examples of other changes that are established as key process changes, as determined by Transnuclear's review of the specific applications and production processes:

(a) Changes in the boron carbide particle size specification that increase the average particle size by more than 5 microns, or that increase the amount of particles larger than 60 microns from the previously qualified material by more than 5% of the total distribution but less than the 10% limit;

(b) Change of the billet production process, e.g., from vacuum hot pressing to cold isostatic pressing followed by vacuum sintering;

(c) Change in the nominal matrix alloy;

(d) Changes in mechanical processing that could result in reduced density of the final product, e.g., for powder metallurgy or thermal spray MMCs that were qualified with extruded material, or a change to direct rolling from the billet;

(e) For MMCs using a magnesium-alloyed aluminum matrix, changes in the billet formation process that could increase the likelihood of magnesium reaction with the boron carbide, such as an increase in the maximum temperature or time at maximum temperature;

(f) Changes in powder blending or melt stirring processes that could result in less uniform distribution of boron carbide, e.g., change in duration of powder blending; and

(g) For MMCs with an integral aluminum cladding, a change greater than 25% in the ratio of the nominal aluminum cladding thickness (sum of two sides of cladding) and the nominal matrix thickness could result in changes in the mechanical properties of the final product.

A9.7.7 RADIAL NEUTRON SHIELDING TESTS

The shielding performance of the radial polyester resin can be verified adequately by chemical analysis and verification of density. Uniformity is assured by installation process control.

Testing Requirements

Chemical analysis shall be performed on the first batch mixed with a given set of components, and thereafter whenever a new lot of one of the major components is introduced. The acceptance values for the chemical composition of the polyester resin are listed in the following table. Note that the chemical composition used in the shielding models (i.e. listed in Table A7A.4-3) are included in the following table for comparison.

Table A7A.4-3 values		Acceptance Testing Values		
Element	nominal wt %	Element	wt %	acceptance range (wt %)
H	5.05	H	5.05	-10 / +20
B	1.05	B	1.05	± 20
C	35.13	C	35.13	± 20
Al	14.93	Al	14.93	± 20
O	41.73	O+Zn (balance)	43.84	± 20
Zn	2.11			
Total	100.0%		100%	

A density measurement shall be performed on every mixed batch of the polyester resin. The minimum polymer density measured shall be greater than 1.547 g/cm^3.

Process Controls

Qualification tests of the personnel and procedure used for mixing and pouring the polyester resin shall be performed. Qualification testing shall include verification that the chemical composition and density is achieved, and the process is performed in such a manner as to prevent voids.

A9.7.8 FABRICATION LEAK TEST REQUIREMENTS

A9.7.8.1 LID, VENT PORT COVER, AND DRAIN PORT COVER

The lid, vent port cover, and drain port cover shall be helium leak tested at the fabricator in accordance with ANSI N14.5-1997, with an acceptance criterion of 1E-7 ref cc/s.

A9.7.8.2 CONFINEMENT SHELL

The confinement shell, bottom plate, flange, and associated welds, shall be helium leak tested at the fabricator in accordance with ANSI N14.5-1997, with an acceptance criterion of 1E-7 ref cc/s.

A9.7.8.3 LID, VENT, AND DRAIN PORT SEALS

The main lid seal along with the vent and drain port seals shall be helium leak tested at the fabricator in accordance with ANSI N14.5-1997. The combined leak rate of all seals including inner and outer seals shall be less than 1E-5 ref cc/s.

A9.8 Aging Management

A9.8.1 Aging Management Review

The information in Section 9.8.1 is applicable to the TN-40HT casks.

A9.8.2 ISFSI Inspection and Monitoring Activities Program

The information in Section 9.8.2 is applicable to the TN-40HT casks.

A9.8.3 Time-Limited Aging Analyses

A review of time-limited aging analyses (TLAA) involving the TN-40HT cask design and spent fuel assemblies stored in a TN-40HT cask was performed as a part of the ISFSI license renewal. TLAAs are defined as those licensee calculations or analyses that have all of the attributes listed in Section 9.8.3.

No TLAAs were identified for the spent fuel assemblies stored in a TN-40HT cask. Two analyses for the TN-40HT cask design were identified as having all six attributes of a TLAA. The first TLAA is an analysis of the basket aluminum components deadweight compressive stresses taking into account the effects of material creep. The second TLAA is an evaluation of neutron damage of the cask metallic components due to fast neutron irradiation. 01505901

The evaluation of basket aluminum components for long term storage deadweight is documented in Section A4B.1.5.6. The evaluation of the effect of fast neutron irradiation of the metals inside a TN-40HT cask is documented in Section A4.2.3.5. These sections demonstrate that the TLAAs are valid for the period of extended operation.

A9.8.4 High Burnup Fuel Monitoring Program

The Aging Management Review of the high burnup fuel spent fuel assemblies in a dry inert environment did not identify any aging effects/mechanisms that could lead to a loss of intended function. However, it is recognized that there has been relatively little operating experience, to date, with dry storage of high burnup fuel. Therefore, a High Burnup Fuel Monitoring Program will be used to confirm that the high burnup fuel assemblies' intended function(s) are maintained during the period of extended operations.

The High Burn up Fuel Monitoring Program relies upon the joint Electric Power Research Institute (EPRI) and Department of Energy (DOE) "High Burnup Dry Storage Cask Research and Development Project" (HDRP) (Reference 20) or an alternative program meeting the guidance to Interim Staff Guidance (ISG) 24, Reference 21, as a surrogate program to monitor the condition of high burn up spent fuel assemblies in dry storage.

01505901

Formal evaluations of the aggregate feedback from the HDRP and other sources of information will be performed at the specific points in time during the period of extended operation delineated in the table below. These evaluations will include an assessment of the continued ability of the high burn up fuel assemblies to continue to perform their intended function(s) at each point.

Toll Gate	Year*	Assessment
1	2028	Evaluate information obtained from the HDRP loading and initial period of storage along with other available sources of information. If the HDRP non-destructive examination (NDE) (i.e., cask gas sampling, temperature data) has not been obtained at this point and no other information is available then NSPM has to provide evidence to the NRC that no more than 1% of the high burnup fuel (HBF) has failed.
2	2038	2.a - (i) Evaluate information obtained from the destructive (DE) and non-destructive (NDE) examination of the fuel placed into storage in the HDRP along with other available sources of information and provide the evaluation to the NRC with simultaneous copies to the Prairie Island Indian Community. (ii) If the aggregate of this information indicates that the high burnup fuel assemblies will not perform "intended function(s)"- as that term is used in NRC regulations - NSPM will submit a License Amendment Request to NRC with its proposed actions to address the issues indicated by the evaluation and to continue safe storage of high burnup fuel. (iii) If the aggregate of this information confirms the ability of the high burn up fuel assemblies to continue to perform intended function(s) for the remainder of the period of extended operations, subsequent assessments may be cancelled. 2.b If by January 1, 2033 it becomes evident that the HDRP DE of the fuel will not be completed in time to support the assessment required by Toll Gate 2.a, NSPM will submit a License Amendment Request to the NRC outlining its plans to obtain evidence to demonstrate that the fuel performance acceptance criteria 1-4 in element 6 continue to be met. This License Amendment Request will be submitted to the NRC for approval no later than December 31 , 2033. The evaluation using this evidence will be completed by 2038.
3	2048	Evaluate any other new information.

*Assessments are due by April 4 of the year identified in the table

01505901

The above assessments are not, by definition, stopping points. No particular action other than performing an assessment is required to continue cask operation. To proceed, an assessment of aggregated available operating experience (both domestic and international), including data from monitoring and inspection programs, NRC-generated communications, and other information will be performed. The evaluation will include an assessment of the ability of the high burnup fuel assemblies to continue to perform their intended function(s). 01505901

A9.9 REFERENCES

01505901

The references 1 through 3 listed in Section 9.7 are independent of cask design. The new references associated with Section A9 are:

4. American Society of Mechanical Engineers, ASME Boiler And Pressure Vessel Code, Sections II, III, V, and IX, 2004 edition including 2006 addenda.

5. SNT-TC-1A, “American Society for Nondestructive Testing, Personnel Qualification and Certification in Nondestructive Testing,”.

6. “Aluminum Standards and Data, 2003” The Aluminum Association.

7 ASTM E1225, “Thermal Conductivity of Solids by Means of the Guarded-Comparative-Longitudinal Heat Flow Technique”

8. ASTM E1461, “Thermal Diffusivity of Solids by the Flash Method”

9. Natrella, “Experimental Statistics,” Dover, 2005.

10. Pyzak and Beaman, “Al-B-C Phase Development and Effects on Mechanical Properties of B4C/Al Derived Composites,” J. Am. Ceramic Soc., 78[2], 302-312 (1995)

11. “Hydrogen Generation Analysis Report for TN-68 Cask Materials,” Test Report No. 61123-99N, Rev 0, Oct 23, 1998, National Technical Systems.

12. ASTM B557, “Standard Test Methods of Tension Testing Wrought and Cast Aluminum- and Magnesium-Alloy Products”

13. ASTM E290, “Standard Test Methods for Bend Testing of Material for Ductility”

14. ASTM B311, “Test Method for Density Determination for Powder Metallurgy (P/M) Materials Containing Less Than Two Percent Porosity”

15. ASTM E94, “Recommended Practice for Radiographic Testing”

16. ASTM E142, “Controlling Quality of Radiographic Testing”

17. ASTM E545, “Standard Method for Determining Image Quality in Thermal Neutron Radiographic Testing”

18. Thermal Conductivity Measurements of Boron Carbide/Aluminum Specimens, Oct 1998, testing by Precision Measurements and Instruments Corp. for Transnuclear, Inc., Purchase Order Number 98037

19. Eagle Picher Report AAQR06, “Qualification of Thermal Conductivity, Borated Aluminum 1100”, May 2001

20. High Burnup Dry Storage Cask Research and Demonstration Project Final Test Plan, February 27, 2014, DOE Contract No.: DE-NE-0000593.

21. NRC Interim Staff Guidance 24, "The Use of a Demonstration Program as a Surveillance Tool for Confirmation of Integrity for Continued Storage of High Burn up Fuel Beyond 20 Years," Revision 0, July 11, 2014.

01505901

Table A9.7-1
THERMAL CONDUCTIVITY FOR SAMPLE NEUTRON ABSORBERS

Temperature	Material			
°C	1	2	3	4
20	193	170	194	194
100	203	183	207	201
200	208	-	-	
250	-	201	218	206
300	211	204	220	203
314	-	-	-	202
342	-	-	-	202

Units: W/mK

Materials:
1) Boralyn® MMC, aluminum 1100 with 15% B_4C
2) Borated aluminum 1100, 2.5% boron as TiB_2
3) Borated aluminum 1100, 2.0% boron as TiB_2
4) Borated aluminum 1100, 4.3% boron as AlB_2

Sources:
References 18 and 19

TABLE A9.7-2
SAMPLE DETERMINATION OF THERMAL CONDUCTIVITY ACCEPTANCE CRITERION

Single Plate Model	Al 1100	n absorber	total
thickness (inch)	0	0.437	0.437
conductivity at 70°F (Btu/hr-in-°F)	n/a	**8.12**	n/a
conductance (Btu/hr-°F)	0	3.55	3.55

Dual Plate Construction	Al 1100	n absorber	total	
thickness (inch)	0.312	0.125	0.437	as modeled
conductivity at 70°F (Btu/h-.in-°F)	11.09	**0.68**	n/a	
conductance (Btu/hr-°F)	3.46	0.09	3.55	

thickness (inch)	0.187	0.250	0.437	thicker neutron absorber
conductivity at 70°F (Btu/hr-in-°F)	11.09	**5.90**	n/a	
conductance (Btu/hr-°F)	2.07	1.48	3.55	

thickness (inch)	0.320	0.117	0.437	thinner neutron absorber
conductivity at 70°F (Btu/hr-in-°F)	11.09	*	n/a	
conductance (Btu/hr-°F)	3.55	n/a	3.55	

The acceptance criterion is identified by boldface type for each thickness.
* The "*" value for neutron absorber conductivity indicates that the required total conductance value can be met solely by the aluminum plate and the neutron absorber material need not be tested.

01424752

SECTION A10

OPERATING CONTROLS AND LIMITS

The operating controls and limits associated with the TN-40HT cask are located in the Prairie Island ISFSI Technical Specifications.

SECTION A11

QUALITY ASSURANCE

A11.1 QUALITY ASSURANCE PROGRAM DESCRIPTION

10 CFR 72.140 requires that a quality assurance (QA) program be established and implemented. The previously approved QA program described in Section 11 will be applied to activities, systems and components of the TN-40HT cask commensurate with their importance to safety. This is the same previously approved NSPM QA Program which satisfies applicable criteria of 10 CFR 50, Appendix B.

Since NSPM is currently licensed under 10 CFR 50 to operate nuclear power facilities, a quality assurance program meeting the requirements of 10 CFR 50, Appendix B, is already in place. The governing document for this program is “Northern States Power Company-Minnesota, Quality Assurance Topical Report,” (QATR) (Reference 1 in Section 11.3) which has been reviewed and approved by the NRC. The QATR is applied to the “important to safety” activities associated with the TN-40HT cask, as allowed by 10 CFR 72.140.d. This program is implemented through directives, instructions, and procedures. The objective of the company QATR is to comply with the criteria as expressed in 10 CFR 50, Appendix B, as amended, and with the quality assurance program requirements for nuclear power plants as referenced in the Regulatory Guides and industry standards. This program will be applied to those activities associated with the TN-40HT cask.

Those major components of the TN-40HT cask which are important to safety are listed in Table A4.5-1. As such, the QATR delineates the requirements for engineering, procurement, fabrication, and inspection of this equipment.

The procurement documents (specifications, requisitions, etc.) of the TN-40HT casks will be reviewed technically prior to use to ensure that the proper criteria have been specified. During the cask design phase, vendor information (drawings, specifications, procedures, etc.) will be reviewed to ensure compliance with technical requirements. During cask fabrication, NSPM representatives will visit the vendor’s shop to ensure compliance with requirements and to witness parts of the cask fabrication and testing. Until NSPM is satisfied that the cask meets the technical requirements, the vendor may not ship the cask.

Each of the 18 criteria of 10 CFR 50, Appendix B and their applicability to the TN-40HT storage casks and associated activities are described in Sections A11.1.1 through A11.1.18.

A11.1.1 ORGANIZATION

The information in Section 11.1.1 is independent of cask design.

A11.1.2 QUALITY ASSURANCE PROGRAM

The information in Section 11.1.2 is independent of cask design.

A11.1.3 DESIGN CONTROL

The information in Section 11.1.3 is independent of cask design.

A11.1.4 PROCUREMENT DOCUMENT CONTROL

The information in Section 11.1.4 is independent of cask design.

A11.1.5 INSTRUCTIONS, PROCEDURES AND DRAWINGS

The information in Section 11.1.5 is independent of cask design.

A11.1.6 DOCUMENT CONTROL

The information in Section 11.1.6 is independent of cask design.

A11.1.7 CONTROL OF PURCHASED MATERIALS, EQUIPMENT AND SERVICES

The information in Section 11.1.7 is independent of cask design.

A11.1.8 IDENTIFICATION AND CONTROL OF MATERIALS, PARTS AND COMPONENTS

The information in Section 11.1.8 is independent of cask design.

A11.1.9 CONTROL OF SPECIAL PROCESSES

The information in Section 11.1.9 is independent of cask design.

A11.1.10 INSPECTION

The information in Section 11.1.10 is independent of cask design.

A11.1.11 TEST CONTROL

The information in Section 11.1.11 is independent of cask design.

A11.1.12 CONTROL OF MEASURING AND TEST EQUIPMENT

The information in Section 11.1.12 is independent of cask design.

A11.1.13 HANDLING, STORAGE AND SHIPPING

The information in Section 11.1.13 is independent of cask design.

A11.1.14 INSPECTION, TEST AND OPERATING STATUS

The information in Section 11.1.14 is independent of cask design.

A11.1.15 NON-CONFORMING MATERIALS, PARTS OR COMPONENTS

The information in Section 11.1.15 is independent of cask design.

A11.1.16 CORRECTIVE ACTION

The information in Section 11.1.16 is independent of cask design.

A11.1.17 QUALITY ASSURANCE RECORDS

The information in Section 11.1.17 is independent of cask design.

A11.1.18 AUDITS

The information in Section 11.1.18 is independent of cask design.

A11.2 QUALITY ASSURANCE PROGRAM – CONTRACTORS

A11.2.1 ARCHITECT-ENGINEER

The information in Section 11.2.1 is independent of cask design.

A11.2.2 CASK SUPPLIER

As described in the QATR, NSPM has the ultimate responsibility for ensuring that the manufacture of important to safety components is done in accordance with the plan. In accordance with the plan, the cask manufacturer must do work under the approved NSPM QA Program.

A11.2.3 CONCRETE STORAGE PAD CONTRACTOR

The references listed in Section 11.2.3 are independent of cask design and there are no additional references associated with Section A11.

A11.3 REFERENCES

The references listed in Section 11.3 are independent of cask design and there are no additional references associated with Section A11.